

Modal Analysis and Controls Laboratory  
Mechanical Engineering Department  
University of Massachusetts at Lowell  
Lowell, Massachusetts

## **Gemini South 8m Optical Telescope**

### **Final Report**

**MACL Report # 05-08570-001**

October 2000

Approved By: \_\_\_\_\_

Date: \_\_\_\_\_





## **Intent of Report**

This report addresses aspects of testing and analysis performed for the Gemini South 8m Optical Telescope in Cerro Pachon, Chile.







## Table of Contents

### 1.0 Introduction

- 1.1. Purpose of Test and Analysis
- 1.2. Scope of the Report
- 1.3. Personnel Involved in Test and Analysis Efforts
- 1.4. Institutional Participants

### 2.0 Test Description and Strategy

### 3.0 Theoretical Basis

- 3.1 Applicable Modal Theory
- 3.2 Applicable Measurement Theory
- 3.3 Typical Impact Measurement
- 3.4 Typical Operating Measurement

### 4.0 Summary of Testing and Analysis Performed

- 4.1 Experimental Modal Impact Testing
- 4.2 Operating Tests
- 4.3 Analysis of Design of Experiments
- 4.4 Data Coherence with Accelerometers
- 4.5 Coherence with Wind Speed
- 4.6 Correlation of Operating Shapes with Experimental Modal Shapes

### 5.0 Conclusions

### 6.0 References

### 7.0 Description of CD Contents





Table of Contents (continued)

Attachments to the Report

- A. Gemini South 8m Optical Telescope Test Setup Report,  
MACL Report # 05-08570-002, dated October 2000
- B. Gemini South 8m Optical Telescope Data Cleansing Report,  
MACL Report # 05-08570-003, dated October 2000
- C. Gemini South 8m Optical Telescope Modal Test Report,  
MACL Report # 05-08570-004, dated October 2000
- D. Gemini South 8m Optical Telescope Operating Test Report,  
MACL Report # 05-08570-005, dated October 2000
- E. Gemini South 8m Optical Telescope Correlation Report,  
MACL Report # 05-08570-006, dated October 2000
- F. Gemini South 8m Optical Telescope DoE and Wind Data Report,  
MACL Report # 05-08570-007, dated October 2000
- G. Avitabile, P., "Overview of Modal Analysis using the Frequency  
Response Method", dated July 1997





## **1.0 Introduction**

### **1.1 Purpose of Test and Analysis**

The purpose of the test and analysis described herein was to investigate the structural response of a large optical telescope in a variety of wind loading conditions. The data from the test are to be used in improving the operations of existing 8m class telescopes as well as in the design of the next generation of very large (>30m diameter) telescopes.

To accomplish this, the test had to provide the data necessary to allow for:

- 1) Validation of existing FE models of the telescope structure.
- 2) Measurement of the actual wind forcing profile on the primary mirror in a variety of wind loading conditions, and comparison of this profile with both computed values and simulations in wind/water tunnels with scale models of the structure.
- 3) Simultaneous measurement of the actual structural response, including both the primary mirror figure and secondary mirror position, in these wind loading conditions.
- 4) Measurement of local wind conditions in the immediate vicinity of the telescope structure.





A series of tests were conducted on the Gemini South 8m optical telescope located on Cerro Pachon in Chile to accomplish these goals. The Gemini South telescope was the ideal instrument for this test. This telescope is a large optical telescope, and is located in a unique enclosure which allows wind loading conditions that vary from nearly fully protected to nearly fully exposed. Additionally, Gemini South was an ideal choice because the telescope had reached a point in construction in which it was capable of controlled motion but the primary mirror had not yet been installed. The "dummy" mirror cell provided a location for direct mounting of pressure transducers while maintaining approximately the same mass and stiffness as the final mirror. The absence of the final optics also enabled a risk-free impact test of the structure to provide good modal characterization, which can ultimately be used to validate or improve finite element models used for design of the structure. Finally, the Gemini telescope design was subjected to an intensive modeling and testing effort during its design phase, so there is a substantial set of analytical and scale-model data which could be compared in the future with these experimental results.





## 1.2 Scope of the Report

This final report is broken down into separate individual reports [1-8] that address various aspects of the test and analysis performed for the Gemini South telescope. This final report expands upon the findings of the preliminary report issued in June 2000 [9].

This report presents the testing conditions and configurations, the theory behind the data reduction methods, the mode shapes of the structure, the operating shapes of the structure, and the correlation between the modal and operating shapes. Additionally, the coherence between the wind pressure measurements and both the accelerometers and the wind speed measurements is presented here. Since the testing parameter space was covered statistically, the results of the analysis of this experimental approach are also presented, in order to guide future testing efforts. Typical cases are presented in the report body, in order to demonstrate the methods used and the most important results.

The attachments to this report contain all the detailed test and analysis performed for the telescope. These attachments are identified below as well as listed in the references.

- Test Setup Report
- Data Cleansing Report
- Modal Test Report
- Operating Test Report
- Correlation Report
- DoE and Wind Data Report
- CD containing all related data





The Test Setup Report [2] discusses all of the details pertaining to the setup of the test of the telescope. Information pertinent to the data acquisition system and instrumentation used is presented in the report, together with items relevant to the tests performed. The Data Cleansing Report [3] details the data channels that required filtering or processing to remove unwanted measurement effects. The Modal Test Report [4] discusses the development of the frequency response functions and generation of mode shapes from these computed functions. Discussion of methodologies for generation of parameters is also presented. The Operating Test Report [5] discusses the development of the cross spectra used for the creation of operating deflection shapes. Additionally, techniques for assessment of reference locations for this analysis are presented in this report. The Correlation Report [6] presents the comparison of the experimental modal impact mode shapes and the operating shapes. The DoE and Wind Data Report [7] discusses the reduction of the operating data of the telescope along with the pressure measurements made. The attached CD [8] contains all of the test reports and related data acquired; animations of the experimental modal impact mode shapes and operating mode shapes are also contained on the CD, together with universal files of these shapes.





### 1.3 Personnel involved in the Test and Analysis Efforts

David R. Smith (formerly of MACL)  
MERLAB, PC  
Mechanical Engineering Research Laboratory  
309 S. McDonough St.  
Decatur, GA 30030

Peter Avitabile, Johann Teutsch, Keith Weech  
Modal Analysis & Controls Laboratory (MACL)  
University of Massachusetts Lowell  
1 University Avenue  
Lowell, MA 01854

Geoff Gwaltney  
Keweenaw Research Center (KRC)  
Route 1-94D Airport Road  
Calumet, MI 49913

### 1.4 Institutional Participants

Mike Sheehan, Gemini Observatory  
Myung Cho, University of Arizona





## **2.0 Test Description and Strategy**

In order to determine the operating deformation and modal characteristics for the Gemini South Optical Telescope, two types of tests were conducted. The operating data were taken under a variety of telescope and enclosure configurations using the wind as the structural disturbance. The modal data were taken at zenith pointing in maximally quiet conditions using an instrumented impact hammer to put a controlled input into the structure.

The response of the telescope varies widely with the wind loading conditions. Even the modal frequencies of the telescope may vary slightly with the elevation angle. As a result, it was impossible to cover the full testing parameter space in the time available for testing. Rather, the number of tests was reduced.

The impact tests were conducted only with the telescope pointed to zenith. Since the purpose of the impact tests is to provide the data necessary for the eventual FE model validation, this can be done in a single elevation angle. To ensure the best data for the impact tests, these measurements were made during periods of minimal activity around the structure.

The operating data tests could not be taken at a single configuration, because the goal of the test was not only to determine the worst-case wind loading, but also to characterize the effects of the wind under a range of conditions. As a result, the following parameters were varied for the test:





1. Wind azimuth angle of attack (AoA)
2. Telescope elevation angle (El)
3. Upwind vent gate position (UVG)
4. Downwind vent gate position (DVG)

Additionally, one test was performed with the lower wind screen raised into position.

Due to the number of possible test configurations, the tests could not cover the entire parameter space with the time allocated for the testing. Instead, a statistical approach was used to test the telescope using standard design of experiments (DoE) techniques [16]. Using this approach, fewer tests are required to obtain the desired information. In this way, better resolution in each of the parameters with fewer tests was obtained.





### 3.0 Theoretical Basis

For the generation of operating and modal data, several commonly used frequency spectra related functions are required. A brief discussion on the theoretical basis of the operating deflection and modal characterization are described herein. Some of the applicable modal theory is presented followed by some applicable measurement theory; these set the underlying theory that is utilized. Next a brief discussion on some of the steps taken to obtain the required measurements is provided. Two short descriptions are provided on impact measurements and operating measurements development. A much more detailed description of modal theory is presented in [14].

#### 3.1 Applicable Modal Theory

The equation of motion for a multiple degree of freedom system can be written in matrix form as

$$[M] \{\ddot{x}\} + [C] \{\dot{x}\} + [K] \{x\} = \{F(t)\}$$

If these equations are transformed into the Laplace domain, then

$$[[M]s^2 + [C]s + [K]]\{X(s)\} = \{F(s)\}$$

which can be written as

$$[B(s)]\{x(s)\} = \{F(s)\} \quad \Rightarrow \quad [B(s)]^{-1} = \frac{\{x(s)\}}{\{F(s)\}}$$

The inverse of the system matrix  $[B(s)]$  gives the System Transfer Matrix

$$[B(s)]^{-1} = [H(s)] = \frac{\text{Adj}[B(s)]}{\det[B(s)]} = \frac{[A(s)]}{\det[B(s)]}$$





The system transfer function can be written in matrix form in terms of the poles and residues of a system in partial fraction form as

$$[H(s)] = \sum_{k=1}^m \frac{[A_k]}{(s - p_k)} + \frac{[A_k^*]}{(s - p_k^*)}$$

or as an individual input/output 'ij' term as

$$h_{ij}(s) = \sum_{k=1}^m \frac{a_{ijk}(s)}{(s - p_k)} + \frac{a_{ijk}^*(s)}{(s - p_k^*)}$$

When the system transfer function is evaluated at  $s=j\omega$ , then the resulting function is called the *Frequency Response Function* (FRF) and is given by

$$[H(s)]_{s=j\omega} = [H(j\omega)] = \sum_{k=1}^m \frac{[A_k]}{(j\omega - p_k)} + \frac{[A_k^*]}{(j\omega - p_k^*)}$$

or as an individual input/output 'ij' term as

$$h_{ij}(s)_{s=j\omega} = h(j\omega) = \sum_{k=1}^m \frac{a_{ijk}}{(j\omega - p_k)} + \frac{a_{ijk}^*}{(j\omega - p_k^*)}$$

In essence, the frequency response function is made up of a collection of single degree of freedom systems summed up over all of the modes of the systems.

Now the system transfer function can be evaluated for a given system pole and can be broken down, through singular valued decomposition techniques, to give

$$[H(s)]_{s=p_k} = \{u_k\} \frac{q_k}{s - p_k} \{u_k\}^T$$





Considering all of the modes of the system, we can write

$$[H(s)] = \sum_{k=1}^m \frac{q_k \{u_k\} \{u_k\}^T}{(s - p_k)} + \frac{q_k \{u_k^*\} \{u_k^*\}^T}{(s - p_k^*)}$$

Notice that from this we can write a relationship between the residue matrix and the mode shapes of the system. This directly implies that the mode shapes of the system are contained within the residue matrix.

The process of experimental modal analysis is to decompose the frequency response functions into their characteristic poles (frequency and damping) and residues (mode shapes) is a complicated process. The estimation of modal parameters is generally performed over frequency bands of the measured data as shown in Figure 3.1.

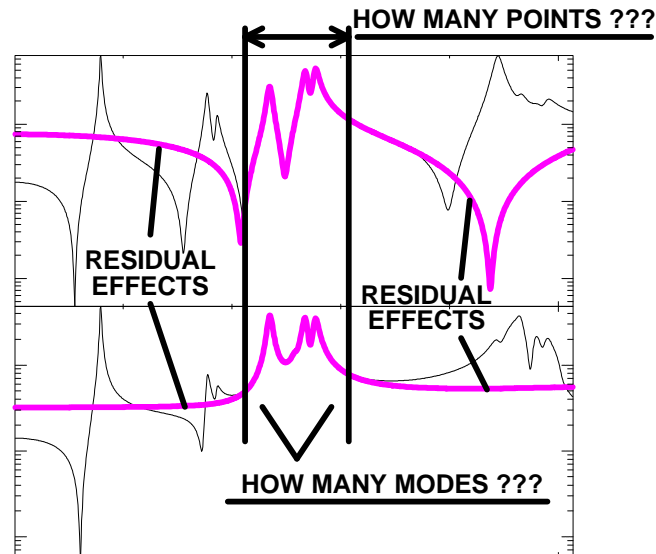


Fig 3.1 Conceptual Overview of the Modal Parameter Estimation Process





The process of curvefitting essentially attempts to decompose the frequency response function shown in Figure 3.2 into the summation of a set of single degree of freedom frequency responses.

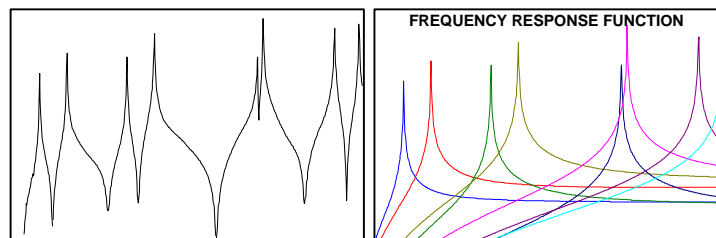


Fig 3.2 Modal Decomposition of the Frequency Response Function

The frequency, damping and residues or mode shapes can be extracted from every frequency response function. The complete set of frequency response functions are used to extract mode shapes as illustrated in Figures 3.3.

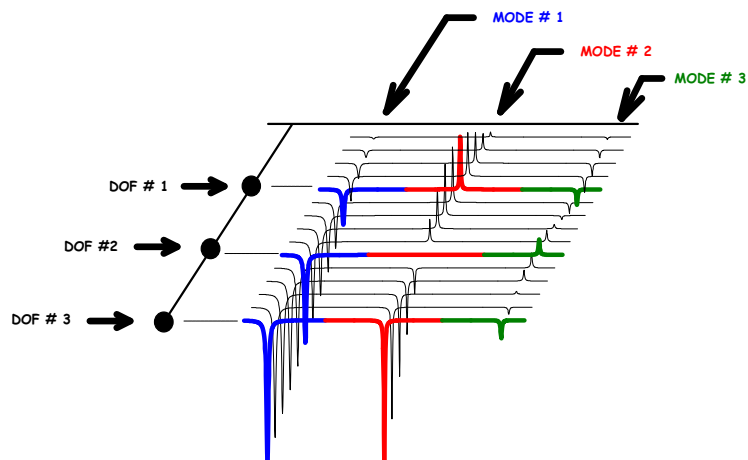


Fig 3.3 Schematic of Mode Shape Estimation from Measured Data



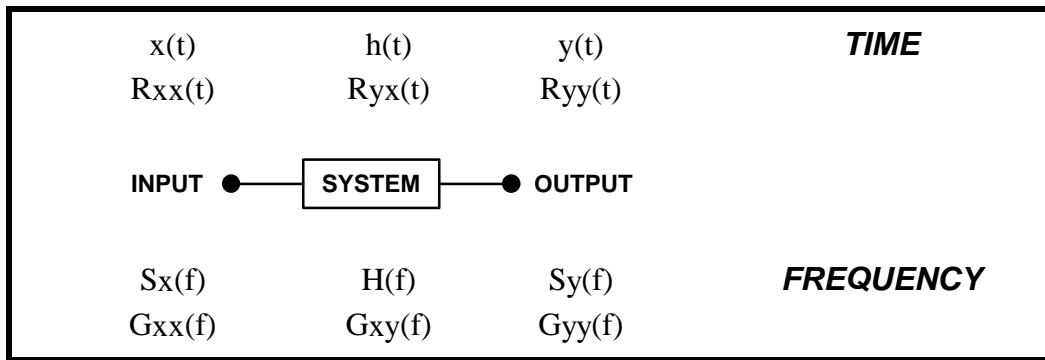


### 3.2 Applicable Measurement Theory

From a measurement standpoint, the estimation of either operating data or frequency response data requires response data and reference data. With these linear spectra, averaged functions can be acquired necessary to form the cross power spectra required for the generation of operating data and for frequency response data required for the generation of modal data. One commonly used form of the frequency response function is

$$S_y = H S_x \quad S_y S_x^* = H S_x S_x^* \Rightarrow H = \frac{G_{yx}}{G_{xx}}$$

The input/output model and definition of linear and square law relationships is shown schematically in Figure 3.4.



where

- |   |   |
|---|---|
| <ul style="list-style-type: none"> <li><math>x(t)</math> - time domain input to the system</li> <li><math>S_x(f)</math> - linear Fourier spectrum of <math>x(t)</math></li> <li><math>H(f)</math> - system transfer function</li> <li><math>R_{xx}(t)</math> - autocorrelation of the input signal <math>x(t)</math></li> <li><math>G_{xx}(f)</math> - autopower spectrum of <math>x(t)</math></li> <li><math>G_{yx}(f)</math> - cross power spectrum of <math>y(t)</math> and <math>x(t)</math></li> </ul> | <ul style="list-style-type: none"> <li><math>y(t)</math> - time domain output to the system</li> <li><math>S_y(f)</math> - linear Fourier spectrum of <math>y(t)</math></li> <li><math>h(t)</math> - system impulse response</li> <li><math>R_{yy}(t)</math> - autocorrelation of the output signal <math>y(t)</math></li> <li><math>G_{yy}(f)</math> - autopower spectrum of <math>y(t)</math></li> <li><math>R_{yx}(t)</math> - cross correlation of <math>y(t)</math> and <math>x(t)</math></li> </ul> |
|---|---|

Fig 3.4 Definition of Input/Output Measurements





The overall measurement process is not described in detail herein. However, the overview of the process is shown schematically in Figure 3.5. In essence, the analog data is digitized and transformed from the time to the frequency domain (with windows if necessary) to form the linear spectra of the input and output. These functions are used to compute averaged power spectra (auto and cross) to be used to form the frequency response functions and coherence.

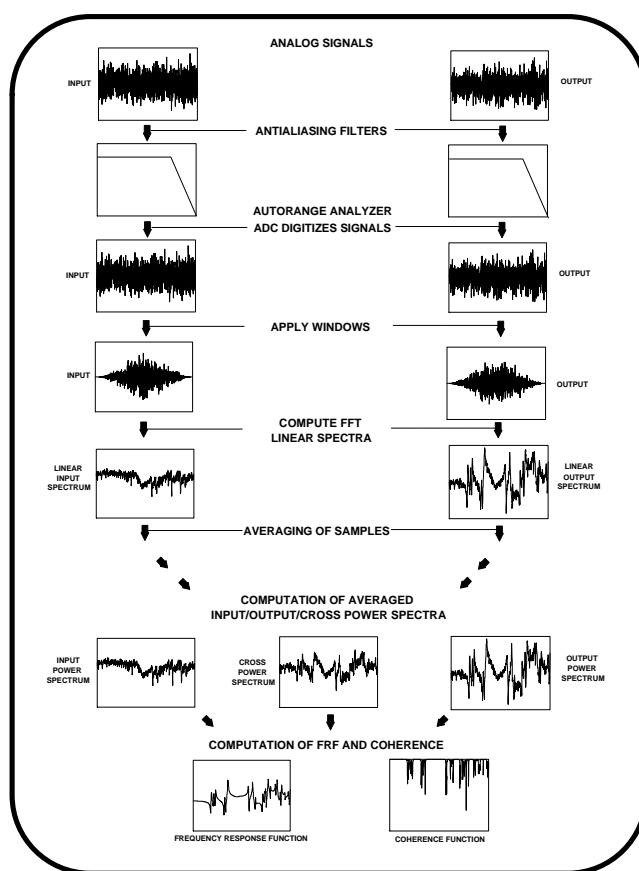


Fig 3.5 The Overall Measurement Process





For the development of a modal model, the measurement of the input excitation and response of the system due to that excitation is necessary. This allows for the development of an averaged frequency response function. Using these frequency response functions, modal parameter estimation algorithms are used to extract the characteristic modal information. An overview of the process is shown schematically in Figure 3.6.

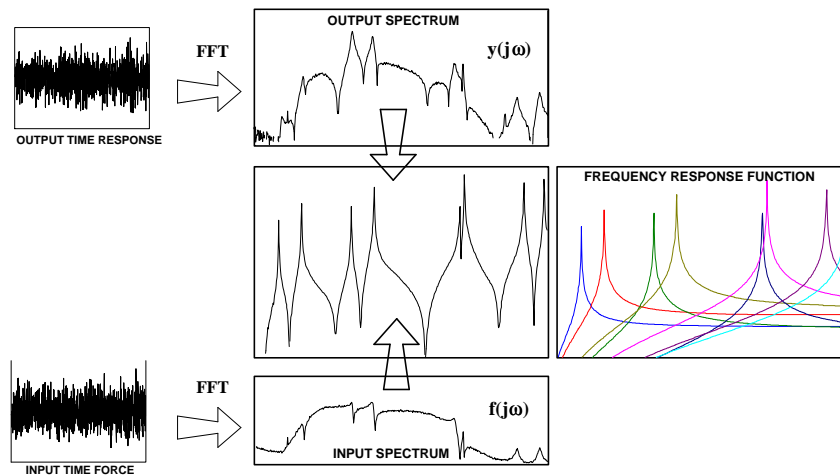


Fig 3.6 Overview of Measurement Development

For the generation of operating data, only the output response of the system is necessary. However, in order to obtain averaged spectra to help eliminate unwanted noise, cross power spectra must be measured relative to some specified reference location. From the schematic in Figure 3.6, the frequency response function acts like a filter to amplify and attenuate the input excitation on a frequency basis. In the collection of operating data, the input excitation is not measured or estimated and the frequency response functions are not available. However, it is clear that the cross power spectrum will contain information pertaining to the modal characteristics of the system.





### 3.3 Typical Impact Measurement

Using the acquired time data, trigger levels for the impact channel are specified in order to determine the start of each sample along with a specified duration time for each sample. The entire set of time data is then used to form 25 averages for the development of a normal frequency response measurement. Basically, the time signals are transformed from the time to the frequency domain using the FFT algorithm. These linear spectra are used to form auto and cross power spectra, which are then averaged. These averaged power spectra are then used to formulate the frequency response function and the coherence. These FRFs are then used in the modal parameter estimation process to extract modal information. Typical data used is shown in Figure 3.7.

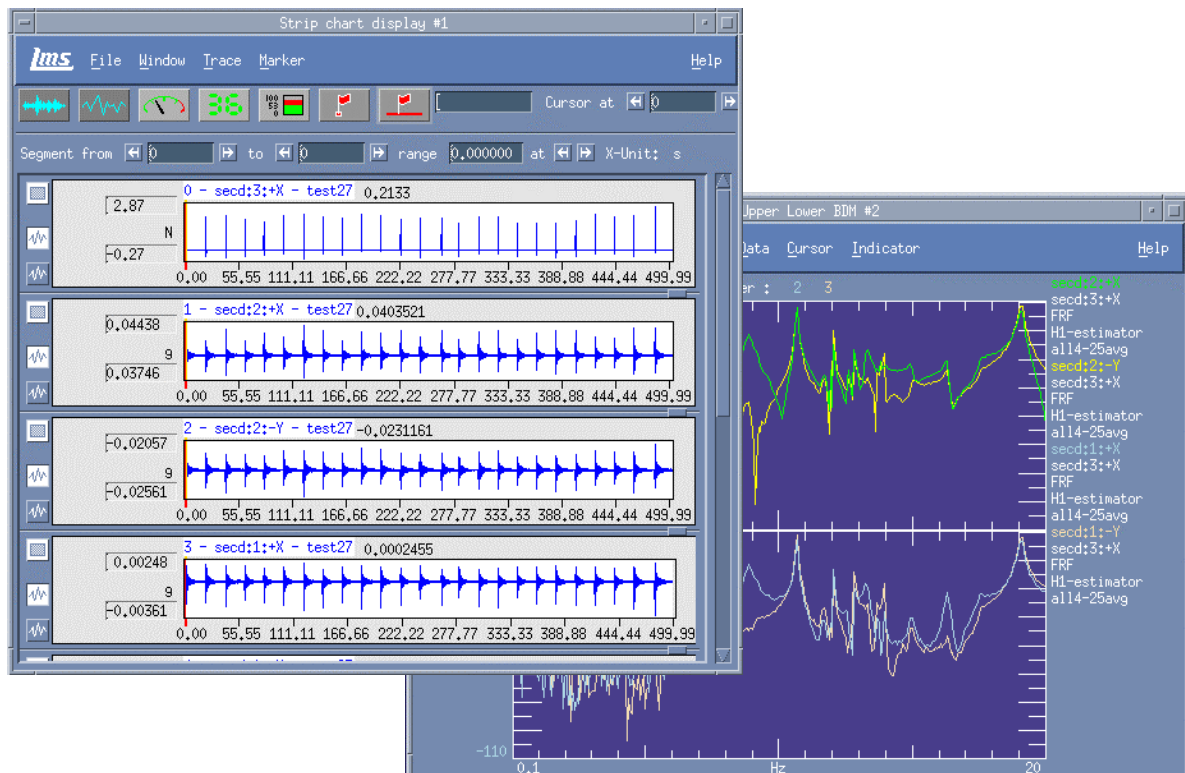


Fig 3.7 Typical Impact Measurement Data Development





### 3.4 Typical Operating Measurement

Using the acquired time data, spectral processing is performed. Basically, the time signals are transformed from the time to the frequency domain using the FFT algorithm. The linear spectra are computed using block size, averaging, overlap and windows parameters specified. These linear spectra are used to form auto and cross power spectra, which are then averaged using a specified reference channel for the computation. These averaged power spectra are then used for operating data assessment. A peak pick methodology is used for the determination of operating deflection patterns. Typical data used is shown in Figure 3.8.

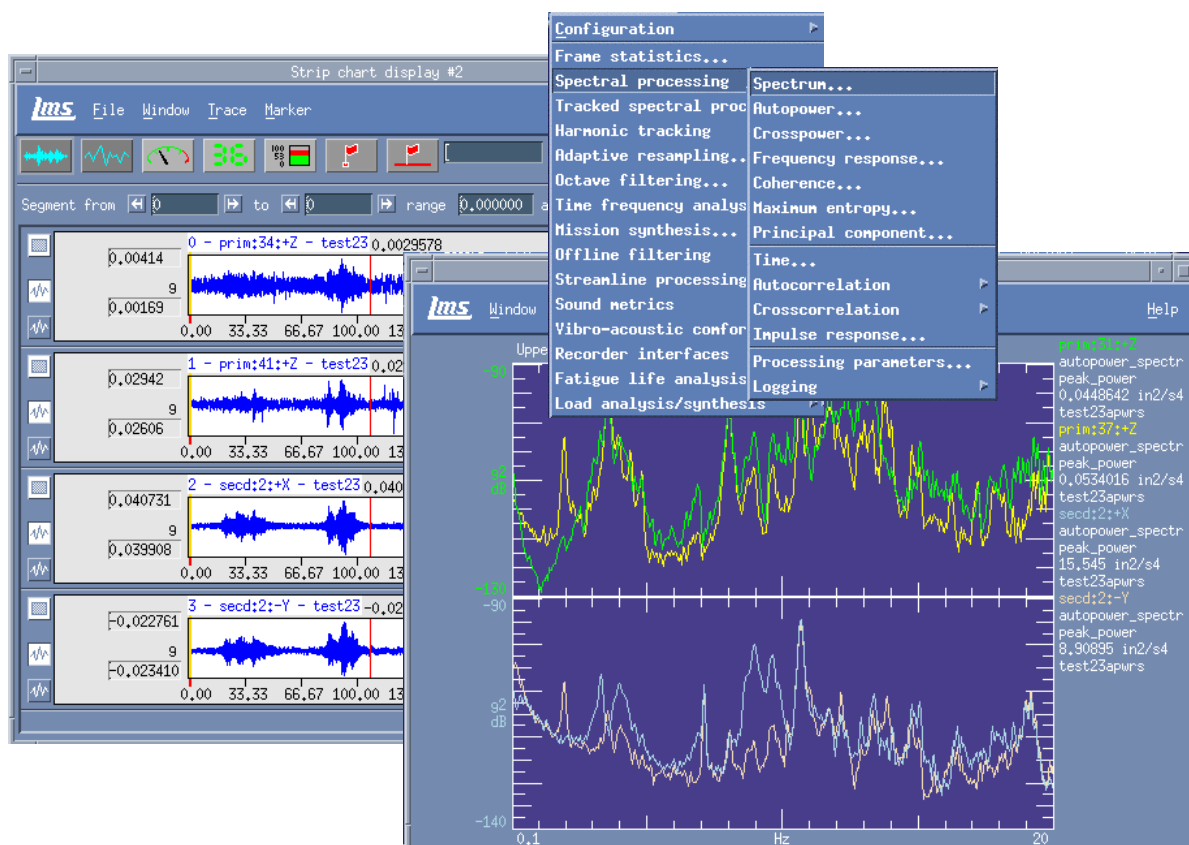


Fig 3.8 Typical Operating Measurement Data Development





## 4.0 Summary of Testing and Analysis Results

The results of the various analyses discussed in the referenced reports are summarized herein.

### 4.1 Experimental Modal Impact Test

Impact testing was performed for the Gemini telescope for the purpose of development of modal parameters. The telescope was instrumented with 75 accelerometers and excitation was applied to the structure using a calibrated impact hammer. The detailed specification of the instrumentation used, location of accelerometers and other pertinent information is contained in the Test Setup Report [2]. The geometry used for the test acquisition is shown in Figure 4.1.

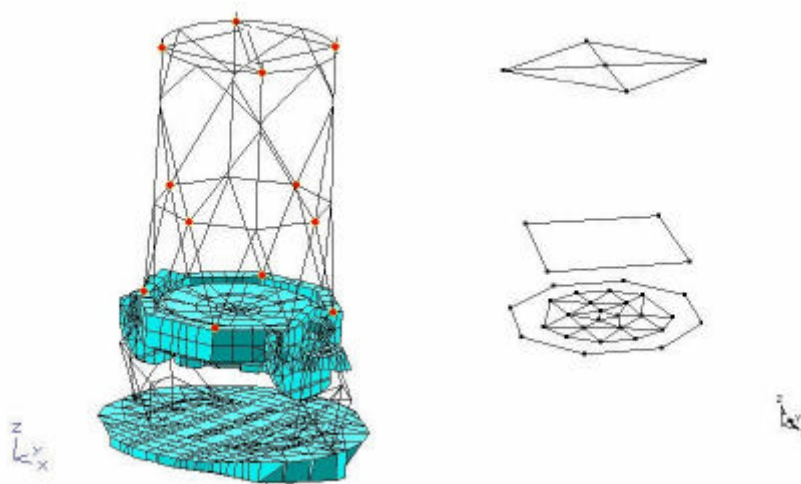


Figure 4.1 Test Schematic and Transducer Layout





Several impact tests were performed but only four tests were utilized for the generation of frequency response functions. The time data was processed to obtain frequency response functions. The frequency response functions were then used in the modal parameter estimation process in order to extract modal parameters. The details of the development of the frequency response functions and the reduction of the data is contained in the Modal Test Report [4].

The modal analysis of the telescope revealed consistent modal parameters for the tests evaluated relative to each of the references utilized. A list of the lower order mode frequencies together with a description of the corresponding mode shapes is shown in Table 4.1.

The natural frequencies for the structure, from 0-30Hz, are summarized in the Table 4.2. (Plots of these mode shapes are contained in the Modal Test report [4] and animations are available on the attached CD-ROM [8].) In reviewing the animations, note that most of the measurements the primary mirror itself are in the Z direction only. Thus, the animations show no lateral motion of most of the primary. This is not an indication that the primary moves laterally independently of the weldment, but is merely a reflection of the measured degrees of freedom.





Table 4.1 – Lower Order Modal Frequencies

Mode Shape	Frequency (Hz)	Description
1	1.82	All – Nodding about the x-axis
2	3.24	Weldment – shifting along the x-axis
3	4.13	All – torsion about the z-axis
4	7.08	Secondary – motion along the x-axis Weldment – flexing out of x-y plane
5	7.74	Primary – piston motion along the z-axis
6	8.88	All – Nodding about the y-axis Midplane – nodding out of phase

Table 4.2 – Modal Frequencies from Impact Tests

Mode	Frequency (Hz)	Damping (%)	Mode	Frequency (Hz)	Damping (%)
1	1.82	2.12	17	16.32	0.42
2	3.24	1.14	18	17.56	1.33
3	4.13	0.25	19	19.08	0.46
4	7.08	0.10	20	20.88	0.68
5	7.74	0.49	21	23.28	0.27
6	8.88	1.36	22	23.49	0.20
7	10.69	0.28	23	23.62	0.12
8	11.05	0.46	24	24.58	0.16
9	0.63	0.15	25	24.77	0.20
10	12.07	0.12	26	24.51	0.11
11	12.84	0.08	27	26.51	0.20
12	13.26	0.69	28	27.12	0.20
13	13.67	0.28	29	28.10	0.22
14	13.79	0.25	30	28.22	0.35
15	13.94	0.17	31	28.31	0.29
16	14.95	0.75	32	28.44	0.23





## 4.2 Operating Tests

Operating data was collected for the Gemini telescope for the purpose of development of in-service operating deformations due to the wind effects. The telescope was instrumented with 62 accelerometers to measure the response of the system. The detailed specification of the instrumentation used, location of accelerometers and other pertinent information is contained in the Test Setup Report [2].

Numerous operating tests were performed for the telescope due to a variety of different configurations. The time data was processed to obtain auto-spectra for all the measured channels collected. These spectra were then evaluated to determine the energy distribution in the major sections of the telescope. This data was used to assist in the selection of a reference for the computation of cross-spectra. Using the computed cross-spectra, operating mode shapes are estimated using simple peak picking techniques for the extraction of parameters. The details of the development of the spectra and the reduction of the data is contained in the Operating Test Report [5]. Plots of these operating shapes are also available in that report, and animations are available on the attached CD-ROM [8].

The operating data analysis extracted the frequency bands at which discernable amplitudes were found in the 0 to 30 Hz frequency range. A list of these typical operating bandwidths is shown in table 4.3.





Table 4.3 - Frequency Bands of Significant Response

1.6 – 1.9 Hz	20.7 – 21.0 Hz
3.2 – 4.1 Hz	21.8 – 22.0 Hz
7.0 – 7.2 Hz	23.2 – 23.6 Hz
8.0 – 8.2 Hz	24.4 – 24.8 Hz
9.0 – 9.2 Hz	24.9 – 25.1 Hz
10.5 – 10.7 Hz	25.3 – 25.5 Hz
11.0 – 11.2 Hz	25.8 – 26.0 Hz
12.1 – 12.9 Hz	26.4 – 26.6 Hz
13.2 – 14.0 Hz	27.1 – 27.4 Hz
14.9 – 15.1 Hz	27.6 – 27.8 Hz
16.1 – 16.3 Hz	28.0 – 28.6 Hz
17.2 – 18.0 Hz	29.1 – 29.4 Hz
19.0 – 19.2 Hz	

The operating analysis suggests that for similar configurations, operating shapes and frequencies compare favorably. Also, the analysis suggests that for significantly different telescope configurations a frequency shift corresponding to similar operating shapes occurs. Wind direction and vent gate position had little effect on the frequencies at which deformation patterns were observed, but did have an effect on which of the operating shapes were excited and the strength of those responses. Complete details pertaining to the operating tests and data reduction are contained in the Operating Test Report [5].





### 4.3 Analysis of Design of Experiments (DoE)

As outlined in Section 2.0, it was impossible to cover every combination of the four telescope configuration factors: Azimuth angle of Attack (AoA), Elevation angle (El), and the positions of the Upwind and Downwind vent gates (UVG and DVG). Instead, we used Design of Experiments (DoE) techniques [16] to obtain optimal statistical coverage of the testing conditions. A full discussion of the results is provided in the attached DoE report [7], with the dominant effects summarized below.

#### 4.3.1 Metric #1: Wind Pressure RMS

This metric was calculated by calculating the RMS of each pressure channel, and then combining the individual RMS values as a root-sum-squared (RSS). Using this metric, the significant effects revealed by the DoE analysis are (in order of importance):

1. Position of the Upwind Vent Gate (UVG)
2. Interaction of changing the AoA and the UVG simultaneously
3. Position of the Downwind Vent Gate (DVG)
4. AoA
5. Interaction between the UVG and DVG

The worst case configuration predicted by the experiments for this metric occurs in the configuration: AoA=45, El=45, UVG open, and DVG half-open. Surprisingly, however, the Elevation angle of the telescope did not have any statistically significant impact on the pressure RMS on the primary.





#### 4.3.2 Metric #2: Accelerometer RMS

This metric was formed by taking the combined RMS of the accelerometers on the primary mirror. In this case, the only significant effects revealed were:

1. Position of the Downwind Vent Gate (DVG)
2. Position of the Upwind Vent Gate (UVG)

These are both, however, only marginally significant. The reason for the difference between the results using the two metrics appears to be due to the ambient level of excitation in the accelerometers due to operational activities at the telescope.

#### 4.4 Data Coherence with Accelerometers

As detailed in the attached report [7], the experiments showed no statistically significant coherence between the acceleration of the primary mirror and individual pressure transducers. Similarly, there was a lack of coherence between pairs of pressure transducers, with the possible exception of the most closely-spaced pairs. This suggests that for analysis and modeling purposes they can be treated as independent random inputs.

#### 4.5 Coherence with Wind Speed

As detailed in the attached report [7], calculations of the coherence between the wind speed sensors revealed no significant coherence between either the wind speed measurements and the surface pressures or even between two different wind speed measurements. Additionally, there are no peaks visible in the power spectrum above the noise for the test. This suggests that on-site wind





measurements are of limited utility in determining the instantaneous wind speed at other locations on the structure.

#### 4.6 Correlation of Operating Shapes with Experimental Modal Shapes

Correlation analysis was performed to compare the experimental modal impact shapes with the operating deflection shapes. The details of the study are contained in the Correlation Report [6]. The description of the experimental modal impact shapes is contained in the Modal Test Report [4] and the corresponding operating shapes are contained in the Operating Test Report [5]. Many different correlation studies were conducted and are too numerous to present here but some summarizing statements can be made.

In general, the mode sets correlated best when the operating modes were obtained in a geometric configuration which is most similar to the configuration used for the experimental modal tests (vertical upright). The correlation tends to degrade gradually as the geometric configuration changes from the vertical upright configuration. The correlation also degrades gradually as the telescope pointing direction varies relative to the direction of the wind.





## **5.0 Conclusions**

The tests at the Gemini South 8m Optical Telescope have provided a large database of information about the structure and its response in a variety of wind conditions. This report and the related companion reports identify all the testing and analysis performed. Several reports address the conduct of the test, collection of the data and reduction of the data which are necessary routine operations. The balance of the reports address specific analyses that were performed.

The Modal Test Report identified the generation of frequency response functions for the extraction of modal parameters. These mode shapes were used in the studies herein for the comparison to the operating shapes. Additionally, these shapes will be extremely useful for further studies beyond the scope of this report, including correlation and validation of the finite element model.

The Operating Test Report presents the development of operating deformation shapes from frequency spectra. The report also assesses the energy distribution in various components of the telescope for assessment of response characteristics. Most importantly, however, the operating shapes which have been extracted, contain critical information regarding the actual wind-induced deformations of the telescope.





The Correlation Report shows the comparison of the experimental modal impact mode shapes with the operating mode shapes. This information is important to determining which modes of the structure are significantly involved in the telescope response due to wind loadings. This study helps to identify the major modes of the structure that affect system performance.

The DoE and Wind Data Test Report evaluated the operating frequency spectra and pressure data to provide insight into the effects of the dome configurations. This data is useful for determination of optimal dome configuration to minimize the effects on system performance, and is also helpful in designing future tests.





## **6.0 References**

1. Gemini South 8m Optical Telescope Final Report, MACL Report # 05-08570-001, dated October 2000
2. Gemini South 8m Optical Telescope Test Setup Report, MACL Report # 05-08570-002, dated October 2000
3. Gemini South 8m Optical Telescope Data Cleansing Report, MACL Report # 05-08570-003, dated October 2000
4. Gemini South 8m Optical Telescope Modal Test Report, MACL Report # 05-08570-004, dated October 2000
5. Gemini South 8m Optical Telescope Operating Report, MACL Report # 05-08570-005, dated October 2000
6. Gemini South 8m Optical Telescope Correlation Report, MACL Report # 05-08570-006, dated October 2000
7. Gemini South 8m Optical Telescope DoE and Wind Data Report, MACL Report # 05-08570-007, dated October 2000
8. CD containing all pertinent test data and reports
9. Preliminary Data Assessment of Gemini South Optical Telescope Operating and Modal Data Report, dated June 2000
10. LMS Cada-X 3.4 Test and Analysis Software (TMON, FMON, Modal Analysis, Matrix Toolbox), Leuven Measurement Systems, Detroit Michigan
11. LMS Cada-X 3.5C Test and Analysis Software (TMON, FMON, Modal Analysis), Leuven Measurement Systems, Detroit Michigan
12. LMS Road Runner Data Acquisition System, Leuven Measurement Systems, Detroit Michigan
13. MEspoe VES Version 2.0, Vibrant Technologies, Jamestown, CA
14. Avitabile, P., "Overview of Modal Analysis using the Frequency Response Method", July 1997
15. Box, George E.P., Hunter, J. Stuart, and Hunter, William G., *Statistics for Experimenters: An Introduction to Design, Data Analysis, and Model Building*, Wiley, 1978.
16. Shina, Sammy G., *Concurrent Engineering and Design for Manufacture of Electronic Products*, Van Nostrand Reinhold, 1991.





## **7.0 Description of CD Contents**

The attached CD-ROM contains electronic versions of these reports as well as the raw test data, universal files of the mode shape and operating shape analyses for all analyses referenced in the reports; animations (AVI files) of all of the experimental modal impact mode shapes and several of the more important operating deflection shapes extracted from the operating data are also included. The CD contains 'README.TXT' files in the various directories that exist on the CD and explain the nature of the material in that particular directory. The important categories of information are listed below.

The **REPORT** directory contains a PDF file of the final report that has been issued. The PDF file contains the main report and all the associated referenced reports. The PDF file has BOOKMARKS to easily navigate to different reports referenced. The Acrobat PDF viewer must be used to read these files ([www.adobe.com](http://www.adobe.com) for free viewer)

The **UNIVERSAL\_FILES** directory contains the analysis shapes in SDRC universal file format. There are the experimental modal impact mode shapes which are named 'MODAL.unv'. There are operating mode shapes for every test evaluated which are named 'ODS\_Txx.unv' (where the xx is associated with the particular TEST ##). These files can be used for further analysis with any software package which supports universal file format. Please note that these files were written using the LMS CADA-X NT software – there may be slight differences in the implementation of the SDRC file format depending on the particular software package used.

The **ANIMATIONS** directory contains AVI files that contain the the mode shapes for the experimental modal impact mode shapes and the operating deflection mode shapes for Test 7 and Test 21. Any Windows based AVI player can be used to view these files.

- The animated experimental mode shapes are named 'ms\_##p##.avi' so that the frequency of the mode is easily identified from the file name (for instance, the mode shape at 1.82Hz – ms\_01p82.avi).
- The animated operating deflection shape files are named 'txx\_##p##.avi' so that the test number and frequency are easily interpreted from the name (for instance, Test 21 operating shape at 28.42 Hz – t21\_28p42.avi)



Modal Analysis and Controls Laboratory  
Mechanical Engineering Department  
University of Massachusetts at Lowell  
Lowell, Massachusetts

## **Gemini South 8m Optical Telescope**

### **Test Setup Report**

**MACL Report # 05-08570-002**

October 2000

Approved By: \_\_\_\_\_

Date: \_\_\_\_\_





## **Intent of Report**

This report addresses aspects pertaining to the test setup for modal and operating testing of the Gemini South 8m Optical Telescope in Cerro Pachon, Chile.







## Table of Contents

- 1.0 Administrative Data
  - 1.1 Purpose of Test
  - 1.2 Drawing
  - 1.3 Test Log
  - 1.4 Dates of Tests
  - 1.5 Tests Conducted By
- 2.0 Test Description
  - 2.1 Test Requirement
  - 2.2 Test Setup
  - 2.3 Testing Details
- 3.0 Testing Configurations
- 4.0 Test Equipment List
- 5.0 Test Schematic and Geometry
- 6.0 References





## **1.0 Administrative Data**

### **1.1 Purpose of Test**

Testing was conducted on the Gemini South 8m telescope at Cerro Pachon in Chile to obtain modal data of the structure and operating data of the structural response excitations due primarily to wind.

### **1.2 Drawing**

Drawings and schematics of test configuration are available in Section 5.0.

### **1.3 Test Log**

A logbook containing documentation of equipment used, transducer information, and test details for all tests conducted, is on file at the Modal Analysis and Controls Laboratory.

### **1.4 Testing Dates**

May 8-12, 2000

### **1.5 Tests Conducted By**

Peter Avitabile  
Geoff Gwaltney  
David Smith  
Johann Teutsch





## **2.0 Test Description**

### **2.1 Test Requirement**

The data acquisition included 80-96 channels of simultaneous vibration, pressure, and system voltage measurements. MACL provided the necessary data acquisition system, accelerometers, signal conditioning, and accelerometer cabling required for the vibration measurements. Gemini Observatory provided the wind measurement and pressure transducers and any associated cabling. Additional signals of interest, such as controller voltages, etc., that are made available to the data acquisition system were also recorded. The number and type of transducers for the tests and the channel identification is found in Section 4.0 of this report.

### **2.2 Test Setup**

The equipment was set up for testing in the Gemini South 8m Optical Telescope facilities of Cerro Pachon located in Chile.

#### **2.2.1 Test Conditions**

The testing was performed at ambient observatory conditions. The various telescope configurations are identified in Section 4.0 of this report.

#### **2.2.2 Test Mounting/Orientation**

Accelerometers were used to measure structural response. The accelerometers were connected to the data acquisition equipment primarily through the use of BNC cabling. The BNC cabling was cut to length and spliced into the junction blocks. The BNC cabling was routed along the perimeter of the telescope and secured to the telescope via Duct-tape. The accelerometers were attached using either Bondo or Hot-glue. The





accelerometers on the primary of the telescope (accelerometer numbers 40-63) and the accelerometers on the weldment (accelerometer numbers 28-39) were attached using Bondo. The remaining accelerometers (accelerometer numbers 1-27) were attached via hot glue. (Accelerometers are identified in Section 4.0, Test Equipment List)

A general test setup is shown in Figure 5.2 (see Section 5.0). The telescopes x, y, and z axis's were used to orient the accelerometers.

### 2.2.3 Test Monitoring

The telescope was monitored using a multichannel data acquisition system [12]. During modal testing, the input to the structure was measured via a force transducer mounted on an impact hammer. The response of the telescope for both modal and operating tests was measured using 75 channels of accelerometers located on the structure as seen in Section 5.0 of this report. Wind pressure on the “dummy” primary measured with 24 pressure transducers.

Refer to Section 4.0 of this report for individual transducer specification.

### 2.2.4 Test Excitation

This section contains the method of excitation for both types of tests performed, modal and operating.

#### Modal Test Excitation:

An impact hammer was used to apply input excitation at each predetermined input location. The impact hammer was outfitted with a soft tip used to excite the telescope in a low frequency band.





### Operating Test Excitation:

The wind was used as the input excitation to the telescope. The excitation of the telescope was regulated by various configurations of the telescopes angle of attack and elevation angle and by the dome's upwind vent gate, downwind vent gate and shutter.

## 2.3 Testing Details

This section contains the details of modal testing and operating testing data acquisition.

### 2.3.1 Modal Tests

Eight impact tests were performed on the structure. The impact tests are Test 2, Test 4, and Tests 25-30. The structure's configuration is found in Section 3.0 of this report. Force was inputted into the structure at timed intervals and at a particular point per test. The time response of the input force along with the time response of the accelerometers was recorded for each of the impact tests. Details of the modal tests are contained in the Modal Test Report [4].

### 2.3.2 Operating Tests:

Forty-five operating tests were conducted on the structure. The various configurations and conditions are found in Section 3.0 of this report. The time response of the accelerometers was recorded for each test. Details of the modal tests are contained in the Operating Test Report [5].





### 3.0 Testing Configurations

The following table identifies all of the different telescope configurations tested.

ID	Elevation	Zenith	AoA	Upwind Gate	Downwind Gate	Fs (Hz)	Time (s)
Test 01	90	0	N/A	Closed	Closed	200	200
Test 02	90	0	N/A	Closed	Closed	200	30
Test 03	60	30	0	Closed	Closed	200	300
Test 04	90	0	N/A	Closed	Closed	200	250
Test 05	90	0	30?	Open	Open	200	300
Test 06	60	30	0-45	Closed	Closed	200	300
Test 07	60	30	0	Open	Open	200	300
Test 08	60	30	0	Closed	Closed	200	300
Test 09	60	30	45	Open	Closed	200	300
Test 10	60	30	45	Closed	Open	200	300
Test 11	30	60	45	Closed	Closed	200	300
Test 12	30	60	45	Open	Open	200	300
Test 13	30	60	0	Open	Closed	200	300
Test 14	30	60	0	Closed	Open	200	300
Test 15	30	60	0	Closed	Closed	200	300
Test 16	30	60	90	Half	Half	200	300
Test 17	30	60	180	Open	Open	200	300
Test 18	45	45	180	Closed	Half	200	300
Test 19	45	45	90	Open	Closed	200	300
Test 20	45	45	0	Half	Open	200	300
Test 21	60	30	0	Closed	Closed	200	300
Test 22	60	30	0	Closed	Half	200	300
Test 23	60	30	90	Closed	Open	200	300
Test 24	60	30	180	Half	Closed	200	300
Test 25	90	0	NA	Closed	Closed	200	500
Test 26	90	0	NA	Closed	Closed	200	500
Test 27	90	0	NA	Closed	Closed	200	500





### 3.0 Testing Configurations (continued)

ID	Elevation	Zenith	AoA	Upwind Gate	Downwind Gate	Fs (Hz)	Time (s)
Test 27	90	0	NA	Closed	Closed	200	500
Test 28	90	0	NA	Closed	Closed	200	500
Test 29	90	0	NA	Closed	Closed	200	250
Test 30	90	0	NA	Closed	Closed	200	250
Test 31	60	30	0	Open	Open	200	300
Test 33	60	30	0	Closed	Open	200	300
Test 34	60	30	45	Closed	Closed	200	300
Test 35	60	30	45	Open	Open	200	300
Test 36	30	60	45	Open	Closed	200	300
Test 37	30	60	0	Closed	Open	200	300
Test 38	30	60	0	Closed	Closed	200	300
Test 39	30	60	0	Open	Open	200	300
Test 40	75	15	45	Closed	Closed	200	300
Test 41	75	15	90	Half	Half	200	300
Test 42	75	15	135	Open	Open	200	300
Test 43	45	45	135	Closed	Half	200	300
Test 44	45	45	90	Open	Closed	200	300
Test 45	45	45	90	Open	Half	200	300
Test 46	45	45	90	Open	Open	200	300
Test 47	45	45	45	Half	Open	200	300
Test 48	30	60	45	Open	Half	200	300
Test 49	30	60	90	Closed	Open	200	300





## 4.0 Test Equipment List

The following sections identify all of the equipment used for testing.

### 4.1 Data Acquisition Equipment

1Skalar Roadrunner 32 Mainframe and Roadrunner 4 Expansion Mainframe, Serial # 990031
2Gemini South PC-based DAS, no information given

### 4.2 Accelerometers

Sensor Number	Point #	Model #	Serial #	Channel	Direction	Calibration (mV/g)	+/- (g)	Resolution (g)
1	1	336C31	8814	1G4	+X	1026.84	4	0.001
2	1	336C31	8816	1G5	-Y	1019.22	4	0.001
3	1	336C31	8865	1G6	+Z	1011.62	4	0.001
4	2	336C31	8717	1G1	+X	993.99	4	0.001
5	2	336C31	8724	1G2	-Y	972.91	4	0.001
6	2	336C31	8728	1G3	+Z	980.75	4	0.001
7	3	336C31	9060	2B6	+X	984.18	4	0.001
8	3	336C31	9065	2B7	-Y	983.83	4	0.001
9	3	336C31	9066	2B8	+Z	988.54	4	0.001
10	4	336C31	9052	2B3	+X	1006.45	4	0.001
11	4	336C31	9053	2B4	-Y	995.36	4	0.001
12	4	336C31	9057	2B5	+Z	975.34	4	0.001
13	5	336C31	9070	2C1	+X	1013.73	4	0.001
14	5	336C31	9073	2C2	+Y	1004.14	4	0.001
15	5	336C31	9075	2C3	+Z	999.66	4	0.001
16	6	336C31	8673	1F6	+X	979.64	4	0.001
17	6	336C31	8687	1F7	-Y	1009.22	4	0.001
18	6	336C31	8695	1F8	+Z	1007.41	4	0.001
19	7	336C31	9038	2A8	+X	967.30	4	0.001
20	7	336C31	9042	2B1	-Y	995.51	4	0.001
21	7	336C31	9046	2B2	+Z	984.99	4	0.001
22	8	336C31	8978	1G7	+X	983.33	4	0.001
23	8	336C31	8987	1G8	-Y	991.67	4	0.001
24	8	336C31	8989	2A1	+Z	988.30	4	0.001
25	9	336C31	8999	2A2	+X	989.05	4	0.001
26	9	336C31	9003	2A3	+Y	992.40	4	0.001
27	9	336C31	9021	2A4	+Z	991.03	4	0.001





#### 4.2 Accelerometers (continued)

Sensor Number	Point #	Model #	Serial #	Channel	Direction	Calibration (mV/g)	+/- (g)	Resolution (g)
28	10	356A18	6684	1E1	+X	954.46	5	0.00006
				1E2	+Y	960.83	5	0.00006
				1E3	+Z	998.68	5	0.00006
29	11	356A18	6683	1D6	+X	1009.86	5	0.00006
				1D7	+Y	914.04	5	0.00006
				1D8	+Z	997.14	5	0.00006
30	12	356A18	6682	1D3	+X	1006.30	5	0.00006
				1D4	+Y	1002.68	5	0.00006
				1D5	+Z	951.20	5	0.00006
31	13	XT352M85	13915	1E5	+X	987.62	5	0.00007
32	13	XT352M85	13916	1E6	+Y	1047.68	5	0.00007
33	13	XT352M85	13917	1E7	+Z	1013.76	5	0.00007
34	14	356A18	5602	* 1C2	+X	991.00	5	0.00006
				* 1C3	+Y	1064.00	5	0.00006
				* 1C4	+Z	1007.00	5	0.00006
35	15	356A18	5603	* 1C5	+X	926.00	5	0.00006
				* 1C6	+Y	1020.00	5	0.00006
				* 1C7	+Z	950.00	5	0.00006
36	16	336C31	9030	* 2A5	+X	980.97	4	0.001
37	16	336C31	9033	* 2A6	+Y	993.03	4	0.001
38	16	336C31	9037	* 2A7	+Z	978.96	4	0.001
39	17	356A18	5604	* 1C8	+X	977.00	5	0.00006
				* 1D1	+Y	952.00	5	0.00006
				* 1D2	+Z	1044.00	5	0.00006
40	31	393M25	1587	1A6	+Z	1343.73	0.5	0.000001
41	31	333A50	7795	1E4	+Y	977.32	5	0.00008
42	32	393M25	1586	1A5	+Z	1295.72	0.5	0.000001
43	33	U393C	5829	1B6	+Z	1119.96	2.5	0.0001
44	33	U393C	3659	1B7	+X	1063.60	2.5	0.0001
45	34	308B02	31219	1F3	+Z	995.92	5	0.0005
46	35	U393C	5830	1B3	+Z	1145.82	2.5	0.0001
47	36	393B	6282	1B1	+Z	1003.38	2.5	0.0001
48	36	393B	6063	1B2	+Y	1118.98	2.5	0.0001
49	37	393C	2895	1B4	+Z	1046.36	2.5	0.0001
50	38	U393C	4124	1B8	+Z	1084.35	2.5	0.0001
51	38	333A50	7794	1A1	+X	949.38	5	0.00008
52	39	308B02	31211	1E8	+Z	994.87	5	0.0005
53	40	393M25	1593	1A8	+Z	1244.58	2.5	0.000001
54	41	308B02	31237	1F5	+Z	996.73	5	0.0005
55	42	U393C	1193	1C1	+Z	1179.21	2.5	0.0001
56	43	308B02	31218	1F2	+Z	1002.29	5	0.0005
57	44	U393C	2896	1B5	+Z	1012.09	2.5	0.0001





#### 4.2 Accelerometers (continued)

Sensor Number	Point #	Model #	Serial #	Channel	Direction	Calibration (mV/g)	+/- (g)	Resolution (g)
58	45	308B02	31232	1F4	+Z	1013.44	5	0.0005
59	46	393M25	1588	1A7	+Z	812.13	2.5	0.000001
60	47	393B31	4064	1A4	+Z	9720.24	0.5	0.000001
61	48	393B31	4061	1A2	+Z	9814.70	0.5	0.000001
62	49	393B31	4062	1A3	+Z	7840.82	0.5	0.000001
** 63	NA	308B02	31213	1F1	+Z	1001.68	5	0.0005

#### 4.3 Impact Hammer

64	roving	288ED01	1062	1F1	roving	98.60 mV/lb	50	0.002
----	--------	---------	------	-----	--------	-------------	----	-------

#### 4.4 Pressure Sensors

##### Tests 9-54

65	101	(No information given)	2C5	+Z	20 Pa/V	50	0.002Pa
66	102		2C6	+Z			
67	103		2C7	+Z			
68	104		2C8	+Z			
69	105		2D1	+Z			
70	106		2D2	+Z			
71	107		2D3	+Z			
72	108		2D4	+Z			
73	109		2D5	+Z			
74	110		2D6	+Z			
75	111		2D7	+Z			
76	112		2D8	+Z			

##### Tests 30-54

77	113	(No information given)	1C2	+Z	20 Pa/V	50	0.002Pa
78	114		1C3	+Z			
79	115		1C4	+Z			
80	116		1C5	+Z			
81	117		1C6	+Z			
82	118		1C7	+Z			
83	119		2A5	+Z			
84	120		2A6	+Z			
85	121		2A7	+Z			
86	122		1C8	+Z			
87	123		1D1	+Z			
88	124		1D2	+Z			

\* Channels pulled for addition of pressure transducers

\*\* Mounted but not used for measurements due to loss of cable





## 5.0 Test Schematic and Geometry

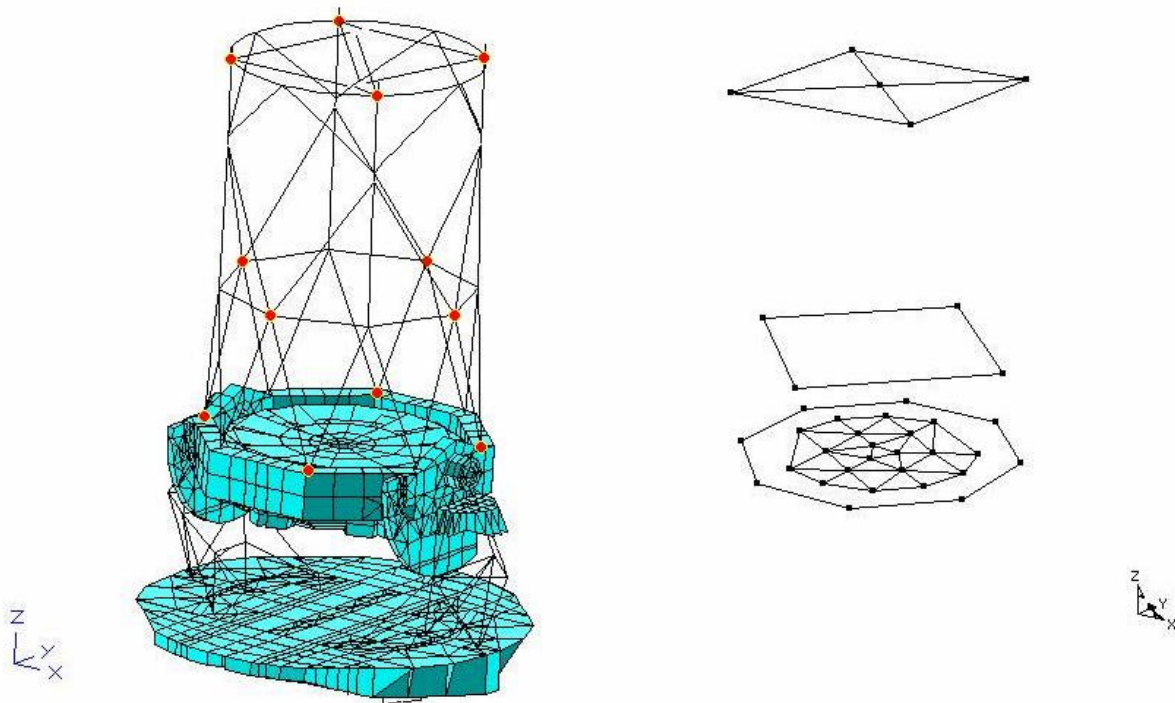


Figure 5.1 General Test Schematic



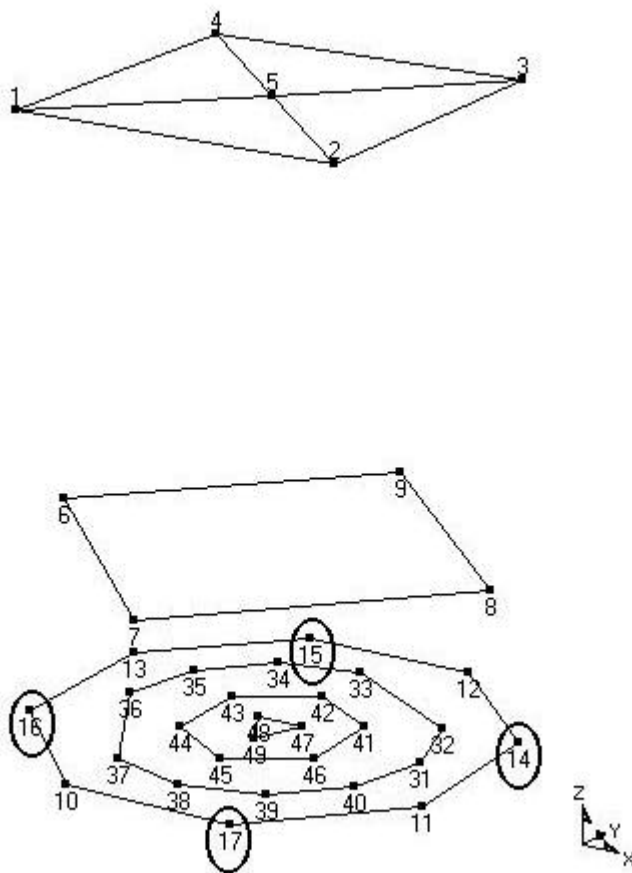


Figure 5.2 Accelerometer Location Numbering



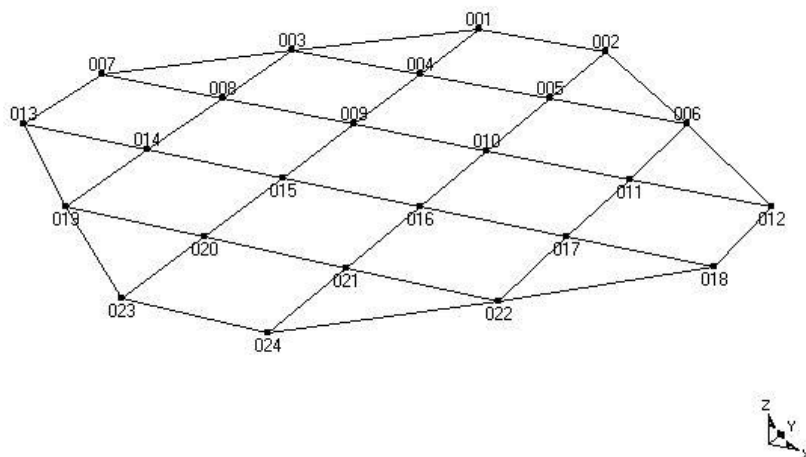


Figure 5.3 Pressure Transducer Location Numbering

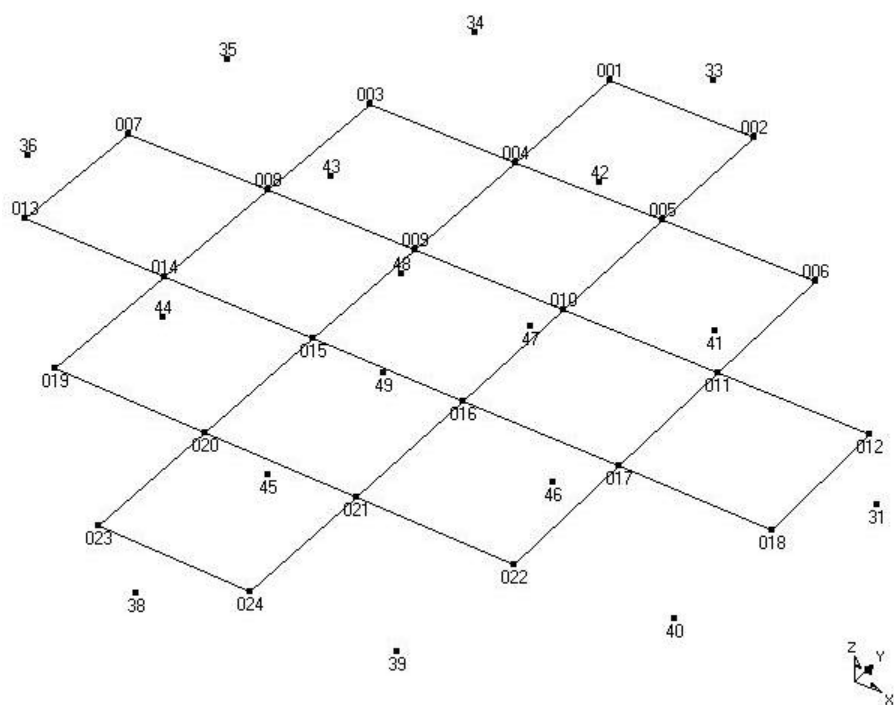


Figure 5.4 "Dummy" Primary Transducer Location Numbering





Table 5.1 Transducer Location Geometry

### Accelerometers

Point #	X (m)	Y (m)	Z (m)	Location Name
1	-4.11	-4.11	15.24	Top End
2	4.11	-4.11	15.24	Top End
3	4.11	4.11	15.24	Top End
4	-4.11	4.11	15.24	Top End
5	0.00	0.00	15.24	Secondary
6	-5.79	0.00	4.57	Mid-plane
7	0.00	-5.79	4.57	Mid-plane
8	5.79	0.00	4.57	Mid-plane
9	0.00	5.79	4.57	Mid-plane
10	-2.21	-5.33	0.00	Weldment
11	5.33	-2.21	0.00	Weldment
12	2.21	5.33	0.00	Weldment
13	-5.33	2.21	0.00	Weldment
14	5.33	2.21	0.00	Weldment
15	-2.21	5.33	0.00	Weldment
16	-5.33	-2.21	0.00	Weldment
17	2.21	-5.33	0.00	Weldment
31	3.99	0.00	0.00	Primary
32	3.46	2.00	0.00	Primary
33	0.00	3.99	0.00	Primary
34	-2.00	3.46	0.00	Primary
35	-3.46	2.00	0.00	Primary
36	-3.99	0.00	0.00	Primary
37	-2.00	-3.46	0.00	Primary
38	0.00	-3.99	0.00	Primary
39	2.00	-3.46	0.00	Primary
40	3.46	-2.00	0.00	Primary
41	1.83	1.14	0.00	Primary
42	0.00	2.29	0.00	Primary
43	-1.83	1.14	0.00	Primary
44	-1.83	-1.14	0.00	Primary
45	0.00	-2.29	0.00	Primary
46	1.83	-1.14	0.00	Primary
47	0.61	0.38	0.00	Primary
48	-0.61	0.38	0.00	Primary
49	0.00	-0.76	0.00	Primary

### Pressure Transducers

Point #	X (m)	Y (m)	Z (m)	Location Name
001	-0.70	3.51	0.00	Primary
002	0.70	3.51	0.00	Primary
003	-2.13	2.13	0.00	Primary
004	-0.70	2.13	0.00	Primary
005	0.70	2.13	0.00	Primary
006	2.13	2.13	0.00	Primary
007	-3.51	0.70	0.00	Primary
008	-2.13	0.70	0.00	Primary
009	-0.70	0.70	0.00	Primary
010	0.70	0.70	0.00	Primary
011	2.13	0.70	0.00	Primary
012	3.51	0.70	0.00	Primary
013	-3.51	-0.70	0.00	Primary
014	-2.13	-0.70	0.00	Primary
015	-0.70	-0.70	0.00	Primary
016	0.70	-0.70	0.00	Primary
017	2.13	-0.70	0.00	Primary
018	3.51	-0.70	0.00	Primary
019	-2.13	-2.13	0.00	Primary
020	-0.70	-2.13	0.00	Primary
021	0.70	-2.13	0.00	Primary
022	2.13	-2.13	0.00	Primary
023	-0.70	-3.51	0.00	Primary
024	0.70	-3.51	0.00	Primary





## 6.0 References

1. Gemini South 8m Optical Telescope Final Report, MACL Report # 05-08570-001, dated October 2000
2. Gemini South 8m Optical Telescope Test Setup Report, MACL Report # 05-08570-002, dated October 2000
3. Gemini South 8m Optical Telescope Data Cleansing Report, MACL Report # 05-08570-003, dated October 2000
4. Gemini South 8m Optical Telescope Modal Test Report, MACL Report # 05-08570-004, dated October 2000
5. Gemini South 8m Optical Telescope Operating Report, MACL Report # 05-08570-005, dated October 2000
6. Gemini South 8m Optical Telescope Correlation Report, MACL Report # 05-08570-006, dated October 2000
7. Gemini South 8m Optical Telescope DoE and Wind Data Report, MACL Report # 05-08570-007, dated October 2000
8. CD containing all pertinent test data and reports
9. Preliminary Data Assessment of Gemini South Optical Telescope Operating and Modal Data Report, dated June 2000
10. LMS Coda-X 3.4 Test and Analysis Software (TMON, FMON, Modal Analysis, Matrix Toolbox), Leuven Measurement Systems, Detroit Michigan
11. LMS Coda-X 3.5C Test and Analysis Software (TMON, FMON, Modal Analysis), Leuven Measurement Systems, Detroit Michigan
12. LMS Road Runner Data Acquisition System, Leuven Measurement Systems, Detroit Michigan
13. MEScopia VES Version 2.0, Vibrant Technologies, Jamestown, CA
14. Avitabile, P., "Overview of Modal Analysis using the Frequency Response Method", July 1997
15. Box, George E.P., Hunter, J. Stuart, and Hunter, William G., *Statistics for Experimenters: An Introduction to Design, Data Analysis, and Model Building*, Wiley, 1978.
16. Shina, Sammy G., *Concurrent Engineering and Design for Manufacture of Electronic Products*, Van Nostrand Reinhold, 1991.



Modal Analysis and Controls Laboratory  
Mechanical Engineering Department  
University of Massachusetts at Lowell  
Lowell, Massachusetts

## **Gemini South 8m Optical Telescope**

### **Data Cleansing Report**

**MACL Report # 05-08570-003**

October 2000

Approved By: \_\_\_\_\_

Date: \_\_\_\_\_





## **Intent of Report**

This report addresses aspects of data cleansing performed on the operating and modal data for the Gemini South 8m Optical Telescope in Cerro Pachon, Chile.







## Table of Contents

1.0 Administrative Data
1.1 Purpose of Cleansing
1.2 Plots and Figures
1.3 Test Log
1.4 Data Cleansers
2.0 Data Cleansing Description
2.1 Operating Data
2.2 Modal Data
3.0 Summary of Data Channels
4.0 Figures
5.0 References





## **1.0 Administrative Data**

### **1.1 Purpose of Cleansing**

The purpose of cleansing the data is to fully utilize the data from Gemini South vibration tests by addressing the quality of the test data.

### **1.2 Plots and Figures**

Figures of various data channels are available in Section 4.0 of this report.

### **1.3 Test Log**

A logbook containing documentation of equipment used, transducer information, and test details for all tests conducted, is on file at the Modal Analysis and Controls Laboratory.

### **1.4 Data Cleansed by:**

Johann Teutsch  
Keith Weech





## **2.0 Data Cleansing Description**

This section contains the detailed description of how the raw time data was adjusted prior to analysis.

### **2.1 Operating Data**

Each recorded channel of data, for each test, was passed into LMS Coda-X TMON [11] for examination. Before any spectral processing took place, the DC bias off set was removed by defining a new mean value in TMON. This process reduced all the channel responses to the same mean value, namely zero, so as to not effect further data processing. The autopower spectrum was calculated and plotted for graphical examination of channel quality. Each channel of data that exhibited a  $1/f$  characteristic drop was labeled a dead, bad, channel. On a number of the tests, an unexplainable phenomenon occurred. At a common time in all the channel traces a sudden change in voltage occurred. This 'spike' as shown, for example, in Figure 2.1, corrupted the data to such an extent that it made analysis of the entire time data trace impossible. To overcome this setback, tests that exhibited these spikes were analyzed using the largest non-corrupted segment of the time trace. For Tests 15 and 18 multiple spikes in the time domain left an inadequate segment to be processed and so were removed from further analysis. The bad channels observed per test are listed in table 3-1 of Section 3.0.



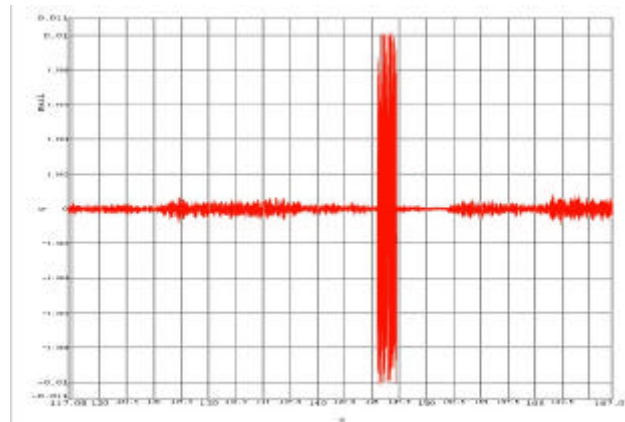


Figure 2.1 Anomalies in Time Trace

## 2.2 Modal Data

The time domain of Test 4 and Tests 25-30, the impact tests, was examined for each channel for each test. The channels that exhibited bit noise, severe distortion, or were devoid of data were labeled as bad channels and were removed from the tests. Channels that exhibited slight drift were labeled as questionable. These questionable channels were used in the final analysis, after cleansing, with no appreciable effect. The bad channels and questionable channels were the same throughout the impact tests. (A listing of the bad and questionable channels can be found in Section 3.0)

The impact data was cleansed, first removing the DC bias from each channel for each test. The DC bias was removed setting the mean of each channel individually to zero. Data drift was resolved by removing the drifting segment of the test (see Figures 2.2 and 2.3). This reduced the number of possible averages, but resulted in much better overall coherence per impact test. The five best concurrent impacts, and corresponding responses, per impact test were used for analysis. This elevated the effects of drift while allowing for averaging to reduce the effects of background noise and provide a better coherence calculation.



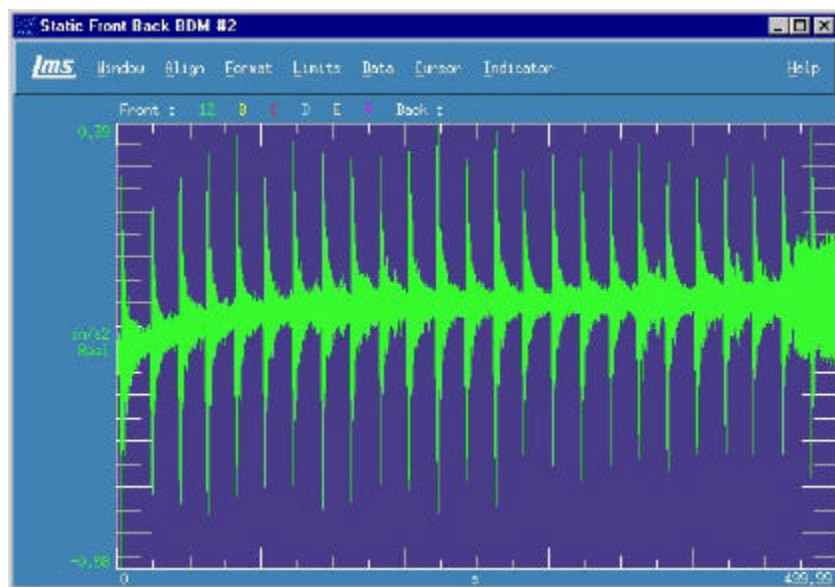


Figure 2.2 Impact response time trace (0-500s)

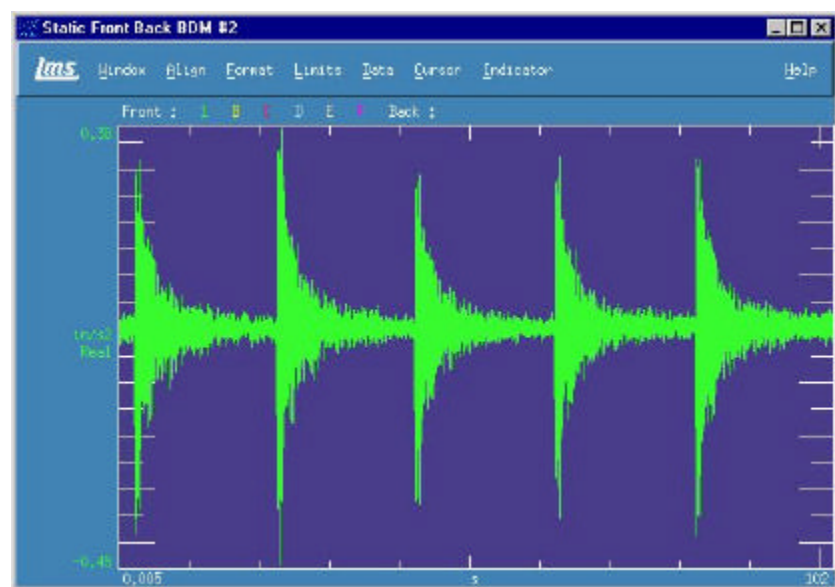


Figure 2.3 Reduced impact response time trace (240-342s)





### 3.0 Summary of Data Channels

This section contains the table of bad channels for each of the tests performed.

Table 3.1

Test ID	Bad Channels
Test 1	BAD TEST
Test 2	Used to set-up the equipment and was not used for analysis.
Test 3	1z,2xyz,5xz,6xyz,7xyz,9xz,14x
Test 4	Used to check test setup and was not used for analysis.
Test 5	BAD TEST
Test 6	BAD TEST
Test 7	1z,5z,6xyz,7xyz,9x,14x
Test 8	Test 8 data set was unintentionally destroyed (Test 4 data was written to this data set).
Test 9	1z,6xz,14x,16z
Test 10	1yz,6xyz,14xy,38x
Test 11	1z,6xy,14x
Test 12	1z,6x,8z,14x,16z,41z
Test 13	1yx,2xyz,6x,13xyz,14xy,41z,43z
Test 14	1z,6x,14x
Test 15	BAD TEST
Test 16	1z,6x,8z,14x
Test 17	1z,6x
Test 18	BAD TEST
Test 19	1z,6x,8z
Test 20	1z,6x,8z
Test 21	1z,6x,33x
Test 22	1z,6x,33x
Test 23	1z,6x,13xyz,33x,40z
Test 24	1z,6x,13xyz,33x,40z
Test 25	Bad(1z,33z,40z,41z,46z) Questionable(6xyz,16xyz,33x,35z,36yz,37z,38z,42z,43z,44z)
Test 26	Bad(1z,33z,40z,41z,46z) Questionable(6xyz,16xyz,33x,35z,36yz,37z,38z,42z,43z,44z)
Test 27	Bad(1z,33z,40z,41z,46z) Questionable(6xyz,16xyz,33x,35z,36yz,37z,38z,42z,43z,44z)
Test 28	Bad(1z,33z,40z,41z,46z) Questionable(6xyz,16xyz,33x,35z,36yz,37z,38z,42z,43z,44z)
Test 29	Bad(1z,33z,40z,41z,46z) Questionable(6xyz,16xyz,33x,35z,36yz,37z,38z,42z,43z,44z)
Test 30	Bad(1z,33z,40z,41z,46z) Questionable(6xyz,16xyz,33x,35z,36yz,37z,38z,42z,43z,44z)





Table 3.1 (continued)

Test ID	Bad Channels
Test 31	1z,42z,46z
Test 33	1z,42z,46z
Test 34	1z,13xyz,42z,46z
Test 35	1z,6xyz,8z,13y,42z,46z
Test 36	1z,6x,42z,46z
Test 37	1z,6xyz,8z,13y,42z,46z
Test 38	1z,6xyz,42z,46z
Test 39	1z,42z,46z
Test 40	1z,13xyz,42z,46z
Test 41	1z,8z,13xyz,42z,46z
Test 42	1z,8z,42z,46z
Test 43	1z,13xyz,42z,43z,45z,46z
Test 44	1z,8z,13xyz,42z,46z
Test 45	1z,8z,13xyz,42z,46z
Test 46	1z,3z,8z,13xyz,42z,46z
Test 47	1z,,8z,13xyz,42z,46z
Test 48	1z,8z,42z,46z
Test 49	1z,13xyz,42z,46z
Test 50	1z,42z,46z
Test 51	1z,8z,42z,46z
Test 52	1z,8z,33z,42z,46z
Test 53	1z,8z,33z,42z,46z
Test 54	1z,8z,33z,42z,46z





## 4.0 Figures

This section contains figures of various bad data channels.

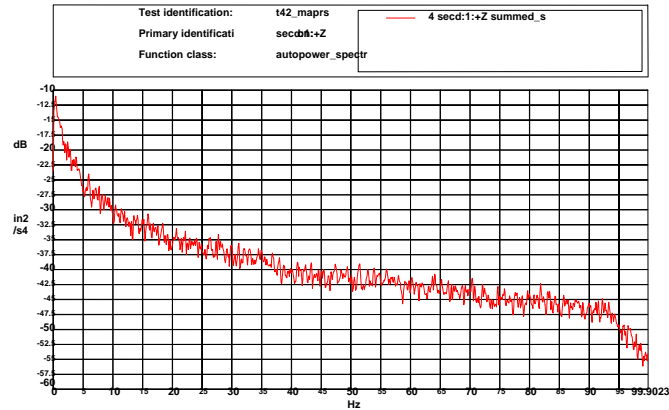


Figure 4.1 – Frequency domain of 1Z from Test 42

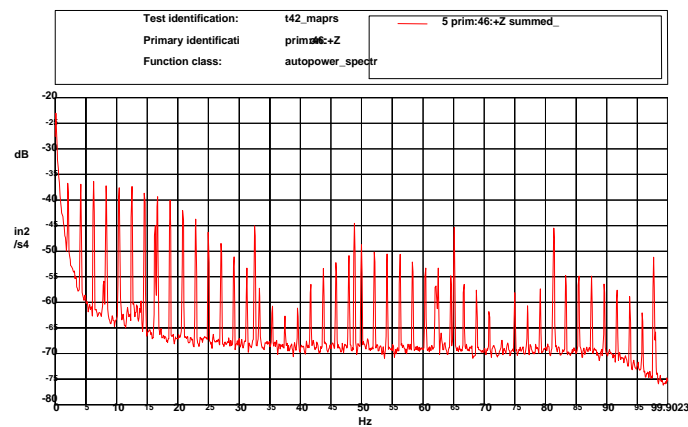


Figure 4.2 – Frequency domain of 46Z from Test 42





## 5.0 **References**

1. Gemini South 8m Optical Telescope Final Report, MACL Report # 05-08570-001, dated October 2000
2. Gemini South 8m Optical Telescope Test Setup Report, MACL Report # 05-08570-002, dated October 2000
3. Gemini South 8m Optical Telescope Data Cleansing Report, MACL Report # 05-08570-003, dated October 2000
4. Gemini South 8m Optical Telescope Modal Test Report, MACL Report # 05-08570-004, dated October 2000
5. Gemini South 8m Optical Telescope Operating Report, MACL Report # 05-08570-005, dated October 2000
6. Gemini South 8m Optical Telescope Correlation Report, MACL Report # 05-08570-006, dated October 2000
7. Gemini South 8m Optical Telescope DoE and Wind Data Report, MACL Report # 05-08570-007, dated October 2000
8. CD containing all pertinent test data and reports
9. Preliminary Data Assessment of Gemini South Optical Telescope Operating and Modal Data Report, dated June 2000
10. LMS Coda-X 3.4 Test and Analysis Software (TMON, FMON, Modal Analysis, Matrix Toolbox), Leuven Measurement Systems, Detroit Michigan
11. LMS Coda-X 3.5C Test and Analysis Software (TMON, FMON, Modal Analysis), Leuven Measurement Systems, Detroit Michigan
12. LMS Road Runner Data Acquisition System, Leuven Measurement Systems, Detroit Michigan
13. MEScopia VES Version 2.0, Vibrant Technologies, Jamestown, CA
14. Avitabile, P., "Overview of Modal Analysis using the Frequency Response Method", July 1997
15. Box, George E.P., Hunter, J. Stuart, and Hunter, William G., *Statistics for Experimenters: An Introduction to Design, Data Analysis, and Model Building*, Wiley, 1978.
16. Shina, Sammy G., *Concurrent Engineering and Design for Manufacture of Electronic Products*, Van Nostrand Reinhold, 1991.



Modal Analysis and Controls Laboratory  
Mechanical Engineering Department  
University of Massachusetts at Lowell  
Lowell, Massachusetts

## **Gemini South 8m Optical Telescope**

### **Modal Test Report**

**MACL Report # 05-08570-004**

October 2000

Approved By: \_\_\_\_\_

Date: \_\_\_\_\_





## **Intent of Report**

This report addresses aspects of modal testing and analysis performed for the Gemini South 8m Optical Telescope in Cerro Pachon, Chile.







## Table of Contents

1.0 Administrative Data	
1.1 Purpose of Analysis	
1.2 Drawing	
1.3 Test Reference Identification	
1.4 Test Log	
1.5 Dates of Tests	
1.6 Tests Conducted By	
1.7 Analysis Performed By	
2.0 Description of Test and Analysis	
2.1 Test/Analysis Requirement	
2.2 Test Setup	
2.3 Testing Details	
2.4 Test Identification Table	
2.5 Measurement Development	
2.6 Modal Parameter Estimation	
3.0 Summary of Test Results	
4.0 Test Schematic	
5.0 Figures	
5.1 Test 4 (Test8)	
5.2 Test 25	
5.3 Test 26	
5.4 Test 27	
5.5 Test 28	
5.6 Test 29	
5.7 Test 30	
6.0 FRF Calculation Parameters	
6.1 Test 4	
6.2 Test 25	
6.3 Test 26	
6.4 Test 27	
6.5 Test 28	
6.6 Test 29	
6.7 Test 30	
7.0 References	
8.0 Mode Shape Plots	





## **1.0 Administrative Data**

### **1.1 Purpose of Analysis**

The purpose of the analysis performed herein was to compute frequency response functions from acquired time data and extract modal parameters.

### **1.2 Drawing**

Drawings and schematics of test configuration are available in Section 5.0.

### **1.3 Test Reference Identification**

All tests performed are specified in the Test Setup [2].

The particular tests for modal testing are: Test 2 (-7Y), Test 4 (-7Y), Test 8 (-7Y), Test 25 (+4X), Test 26 (4+Y), Test 27 (+3X), Test 28 (-3Y), Test 29 (-36Z), and Test 30 (-31Z)

### **1.4 Test Log**

A logbook containing documentation of equipment used, transducer information, and test details for all tests conducted, is on file at the Modal Analysis and Controls Laboratory.

### **1.5 Dates of Tests**

May 8-12, 2000





1.6 Tests Conducted By

Peter Avitabile

Geoff Gwaltney

David Smith

Johann Teutsch

1.7 Analysis Performed By

Johann Teutsch





## **2.0 Description of Test and Analysis**

### **2.1 Test/Analysis Requirement**

The purpose of the analysis described herein was to estimate frequency response functions from the acquired impact modal data collected on the Gemini South 8m Optical Telescope and to determine modal parameters.

### **2.2 Test Setup**

A detailed description of the test setup is contained in the Test Setup Report [2].

#### **2.2.1 Test Conditions**

The testing was performed at ambient observatory conditions with the dome shutter, upper vent gate, and lower vent gate closed.

#### **2.2.2 Test Mounting/Orientation**

Details of the test mounting and orientation used for testing are contained in the Test Setup Report [2].

#### **2.2.3 Test Monitoring**

The telescope was monitored using a Road Runner digital data acquisition system. The input to the structure was measured via a force transducer mounted on the impact hammer while the response was monitored using 75 channels of accelerometers. Details of the transducer number and location used for testing are contained in the Test Setup Report [2].

#### **2.2.4 Test Excitation**

An impact hammer was used to apply input excitation at each predetermined input location. The impact hammer was outfitted with a soft tip used to excite the telescope in a low frequency band.





## 2.3 Testing Details

Eight impact tests were performed on the structure. The impact tests are Test 2, Test 4, Test 8, and Tests 25-30. Impacts to the structure were performed at timed intervals and at a particular point per test. The time response of the input force along with the time response of the accelerometers was recorded for each of the impact tests.

### 2.3.1 Test 2

Impacts were made at point number 7 in the -Y direction (see Figure 5.2). Time data was recorded for 30s, allowing for 25 impacts spaced at approximately 2s each. Test 2 was a preliminary test used to set-up the equipment and was not used for analysis.

### 2.3.2 Test 4

Impacts were made at point number 7 in the -Y direction (see Figure 5.2). Time data was recorded for 250s, allowing for 25 impacts spaced at approximately 10s each. Test 4 was used to check test setup and was not used for analysis.

### 2.3.3 Test 8

Test 8 data set was unintentionally destroyed (Test 4 data was written to this data set). No further discussion of this data set will be addressed in this report.

### 2.3.4 Test 25

Impacts were made at point number 4 in the +X direction (see Figure 5.2). Time data was recorded for 500s, allowing for 25 impacts spaced at approximately 20s each.





#### 2.3.5 Test 26

Impacts were made at point number 4 in the -Y direction (see Figure 5.2). Time data was recorded for 500s, allowing for 25 impacts spaced at approximately 20s each.

#### 2.3.6 Test 27

Impacts were made at point number 3 in the +X direction (see Figure 5.2). Time data was recorded for 500s, allowing for 25 impacts spaced at approximately 20s each.

#### 2.3.7 Test 28

Impacts were made at point number 3 in the -Y direction (see Figure 5.2). Time data was recorded for 500s, allowing for 25 impacts spaced at approximately 20s each.

#### 2.3.8 Test 29

Impacts were made at point number 31 in the -Z direction on the dummy mirror surface (see Figure 5.2). Time data was recorded for approximately 260s, allowing for 13 impacts spaced at approximately 20s each. This test was cut short due to excessive background/electrical noise that caused channel overload so no further reduction or manipulation of this data was performed.

#### 2.3.9 Test 30

Impacts were made at point number 36 in the -Z direction on the dummy mirror surface (see Figure 5.2). Time data was recorded for approximately 270s, allowing for 13 impacts spaced at approximately 20s each. This test was cut short due to excessive background/electrical noise that caused channel overload so no further reduction or manipulation of this data was performed.





## 2.4 Test Identification Table

Table 2.1 Impact Test Identification Table

ID	Impact Location	Elevation Angle	Zenith Angle	Vent Gate Upwind	Vent Gate Downwind	Fs (Hz)	Time (s)
Test 2	-7Y	90	0	Closed	Closed	200	30
Test 4	-7Y	90	0	Closed	Closed	200	250
Test 8*	-7Y	90	0	Closed	Closed	200	250
Test 25	+4X	90	0	Closed	Closed	200	500
Test 26	-4Y	90	0	Closed	Closed	200	500
Test 27	+3X	90	0	Closed	Closed	200	500
Test 28	-3Y	90	0	Closed	Closed	200	500
Test 29	-31Z	90	0	Closed	Closed	200	260
Test 30	-36Z	90	0	Closed	Closed	200	270

\*Refer to Section 2.3.3 of this report.

## 2.5 Measurement Development

All data reduction, including modal parameter estimation, was performed using LMS Cada-X [11] software.

The recorded time data for each test was passed into TMON [11] to check for bad channels and data cleansing. Details of data cleansing are presented in the Data Cleansing Report [3].

The time data was organized per test such that the input channel was listed first followed by the good response channels. The five impacts and the corresponding responses, that occurred from 240s to 342s in the time trace, were used to calculate the frequency response functions (see Figures 2.5.1 and 2.5.2). This provided five impacts for calculating the frequency response functions (FRFs). Once in this format the time data was passed into FMON (Acquisition Throughput Monitor) [11] to compute the FRF of each of the output/input combinations for each test. The FRFs, coherence of the FRFs, and the auto-power spectrum of the input per each test was stored for modal parameter analysis. Specific parameters used for FRF computation are contained in Section 6.0 of this report.



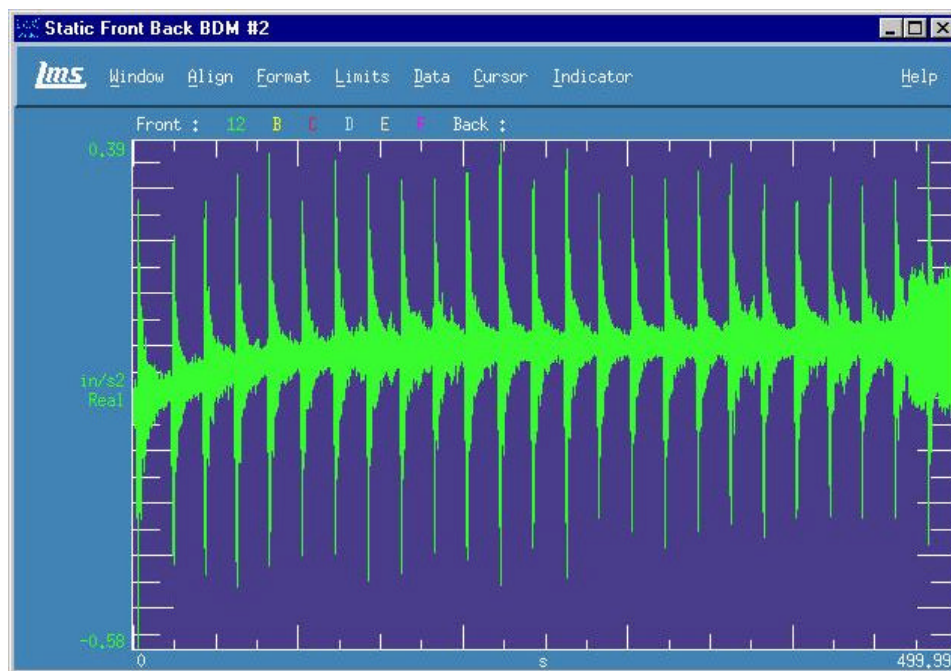


Figure 2.5.1 Impact response time trace

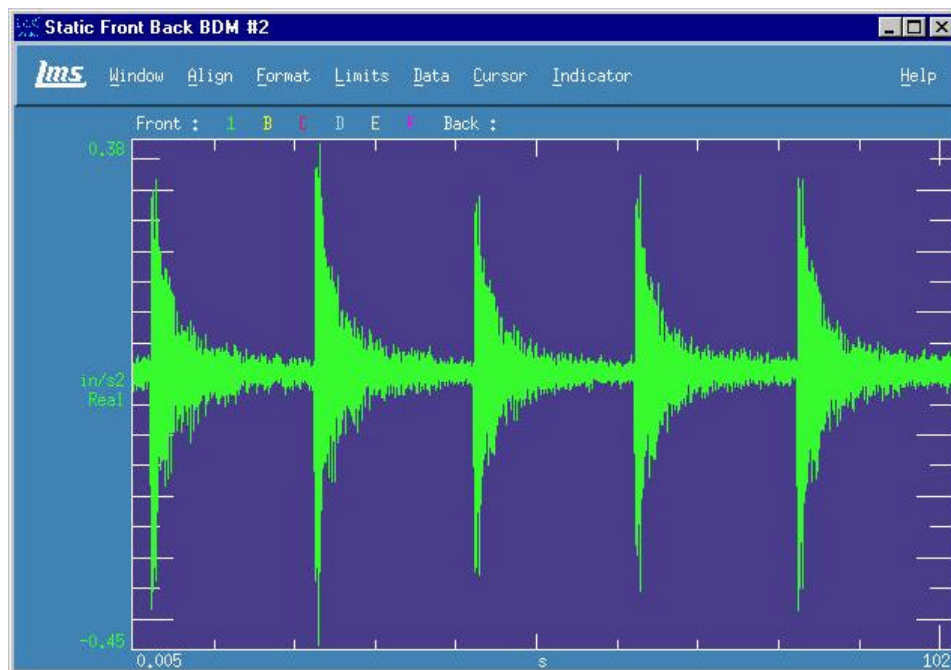


Figure 2.5.2 Reduced impact response time trace





## 2.6 Modal Parameter Estimation

Using the calculated FRFs from Tests 25-28, Cada-X Modal Analysis [11] was used for pole and residue extraction. Tests 4, 8, 29, and 30 were not used for further analysis due to poor measurement quality. (See Figures 6.1.1, 6.6.3, and 6.7.3 in Section 6 of this report)

### 2.6.1 Single Degree of Freedom (SDOF)

The single degree of freedom (SDOF) technique was used as a preliminary assessment for determining the modes of the telescope with the cleansed data.

The data from Test 25 and Test 27, both with references in the X-direction, was passed into Cada-X Modal Analysis for pole extraction. The single degree of freedom (SDOF) technique was used separately for both tests. Within the SDOF, a peak picking technique was used.

The data from Test 26 and Test 28, both with references in the Y-direction, was passed into Cada-X Modal Analysis for pole extraction. The single degree of freedom technique was used separately for both tests.

### 2.6.2 Multiple Degree of Freedom (MDOF)

The multiple degree of freedom (MDOF) technique was also used to extract the modal parameters of the telescope.

The data from Test 25 and Test 27, both with references in the X-direction, was passed into Cada-X Modal Analysis for pole extraction. The multiple degree of freedom technique was used for both tests.

The data from Test 26 and Test 28, both with references in the Y-direction, was passed into Cada-X Modal Analysis for pole extraction. The multiple degree of freedom technique was used for both tests.





### 2.6.3 Final Modal Parameters

The data from Tests 25-28 was passed into Cada-X Modal Analysis for pole extraction. The multiple degree of freedom technique was used for all four tests at once, except for the 1.82Hz peak and the 8.88Hz peak.

Test 26 and Test 28, with references in the Y-direction, were used for modal parameter extraction for the 1.82Hz which has a mode shape in the Y-direction. Test 25 and Test 27, with references in the X-direction, were used for modal parameter extraction for the 8.88Hz which has a mode shape in the X-direction. Test 26 and Test 28 with references in the Y-direction do not see the peak in the peak at 8.88Hz. (See Figure 2.6.3)

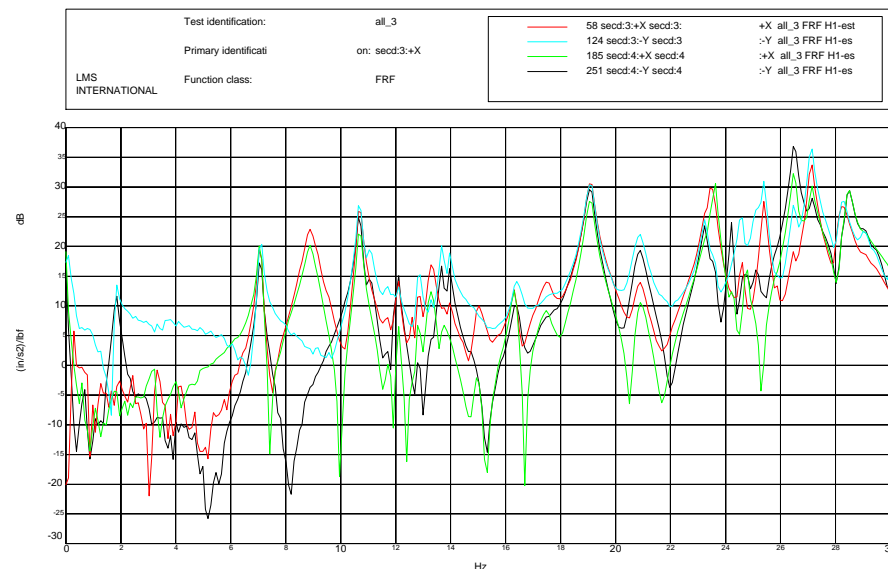


Figure 2.6.3 Drive-point Measurements of Tests 25- 28

Bands were chosen about predominant peaks of the Summed FRF spectrum. Double R2 bands were used to examine the modal peaks seen





in the summation of the FRFs. Table 2.3 displays the bands used to check for pole stability and solving for residues.

The mode indicator function (MIF) along with the stability diagram was used to determine the poles of the system. (See Figure 2.6.4)

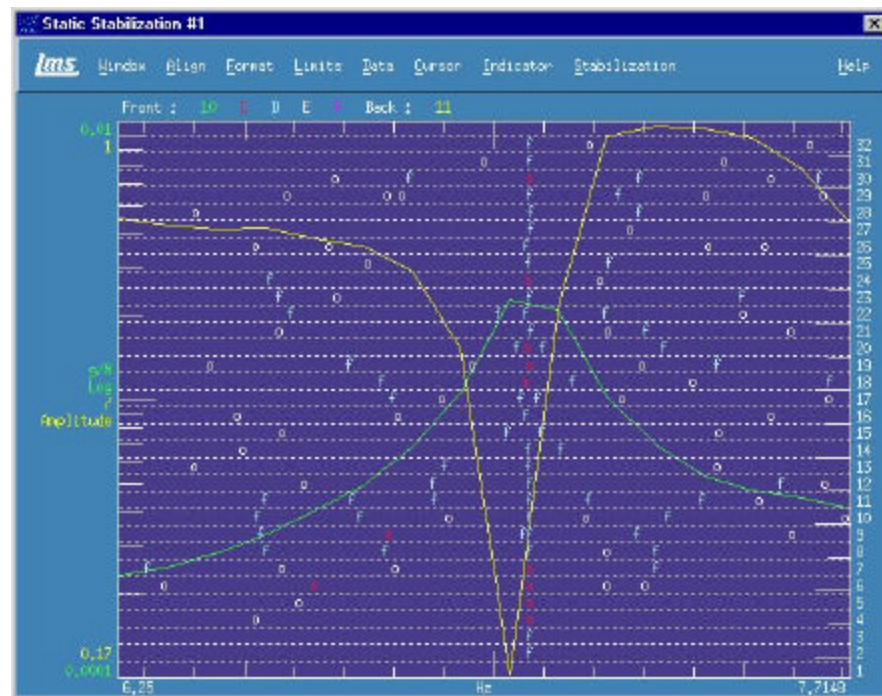


Figure 2.6.4 Typical Stability Diagram

The stability diagram is a graphical method used to determine the poles from FRFs. The stability of a pole refers to the repeatability of information over the selected FRFs in a particular frequency band. A pole is stable when the frequency is within 1%, the damping is less than 5%, and the frequency is repeatable over all of the measurements. All of the poles extracted from 0-30Hz are stable.

Once the poles of a given double R2 band are determined, the residues are extracted over that band. See summary of results, Section 3.0 for a listing of the poles and residues (mode shapes).





The results of the MDOF analyses are located in Table 2.3 below.

Table 2.3

Frequency Band	Pole Hz	Damping %	Frequency Band	Pole Hz	Damping %
1.367 to 4.395	1.82	2.12	15.723 to 21.875	16.32	0.42
	3.24	1.14		17.56	1.33
3.613 to 5.078	4.13	0.25		19.08	0.46
6.641 to 9.668	7.08	0.10		20.88	0.68
	7.74	0.49	22.754 to 25.781	23.28	0.27
	8.88	1.36		23.49	0.20
9.375 to 12.402	10.69	0.28		23.62	0.12
	11.05	0.46		24.58	0.16
	0.63	0.15		24.77	0.20
	12.07	0.12		24.51	0.11
12.402 to 15.430	12.84	0.08	26.070 to 29.100	26.51	0.20
	13.26	0.69		27.12	0.20
	13.67	0.28		28.10	0.22
	13.79	0.25		28.22	0.35
	13.94	0.17		28.31	0.29
	14.95	0.75		28.44	0.23

The modeshapes determined from the poles listed in Table 2.3 were checked for accuracy by synthesizing the FRFs. The synthesized FRFs overlaid on the original FRFs graphically display the accuracy of the extracted parameters. (See Figures 2.6.5 and 2.6.6)



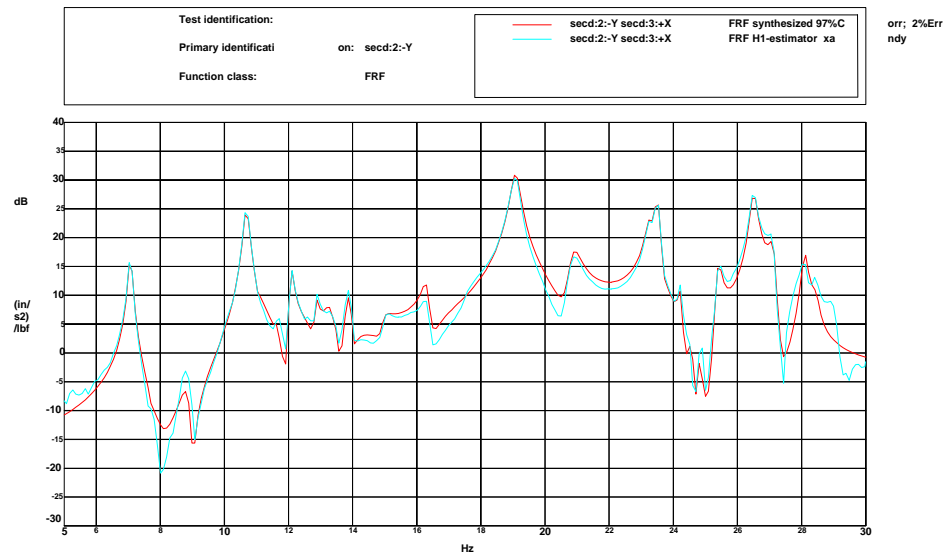


Figure 2.6.5 Synthesized FRF of 2Y (97% correct) overlaid on measured FRF of 2Y

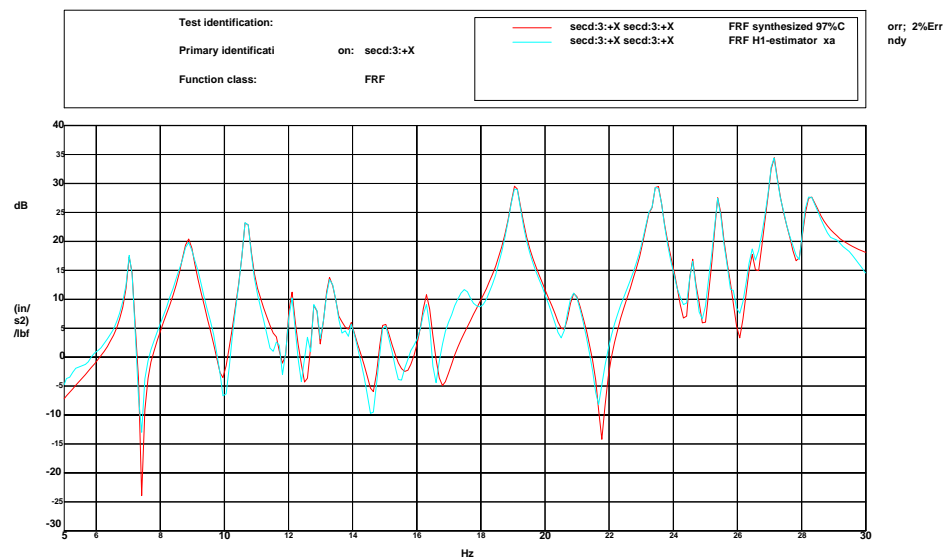


Figure 2.6.6 Synthesized FRF of 3X (97% correct) overlaid on measured FRF of 3X





### 3.0 Summary of Test Results

The summary of the modal parameter estimates is shown in the attached table.

Table 3.1

Mode	Frequency (Hz)	Damping (%)	Mode	Frequency (Hz)	Damping (%)
1	1.82	2.12	17	16.32	0.42
2	3.24	1.14	18	17.56	1.33
3	4.13	0.25	19	19.08	0.46
4	7.08	0.10	20	20.88	0.68
5	7.74	0.49	21	23.28	0.27
6	8.88	1.36	22	23.49	0.20
7	10.69	0.28	23	23.62	0.12
8	11.05	0.46	24	24.58	0.16
9	0.63	0.15	25	24.77	0.20
10	12.07	0.12	26	24.51	0.11
11	12.84	0.08	27	26.51	0.20
12	13.26	0.69	28	27.12	0.20
13	13.67	0.28	29	28.10	0.22
14	13.79	0.25	30	28.22	0.35
15	13.94	0.17	31	28.31	0.29
16	14.95	0.75	32	28.44	0.23





## 4.0 Test Schematic

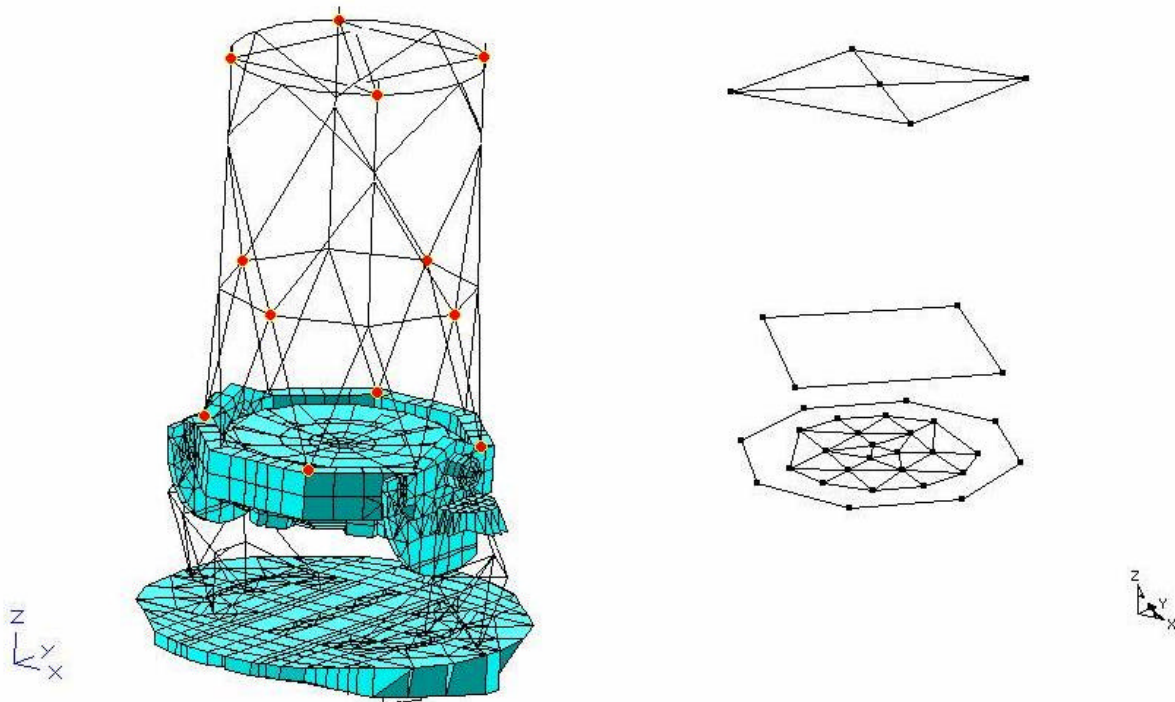


Figure 4.1 General Test Schematic



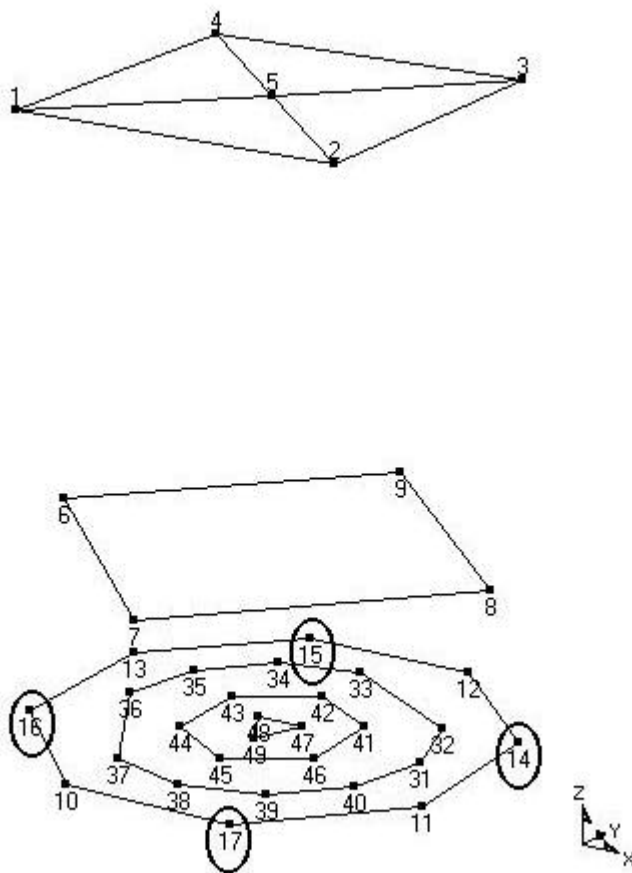


Figure 4.2 Transducer Location Numbering





## 5.0 Figures

This section contains figures of from the various modal tests of this report.

### 5.1 Test 4 (Test 8)

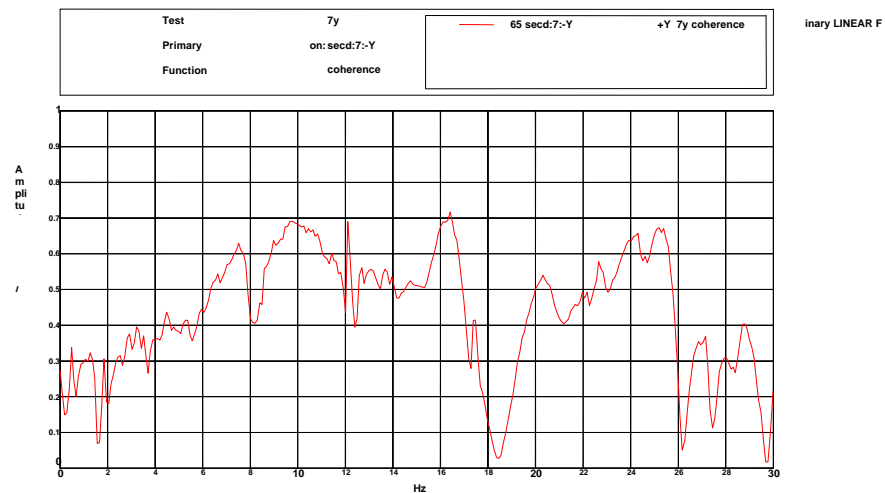


Figure 5.1.1 Typical coherence of Test 4 and Test 8

### 5.2 Test 25

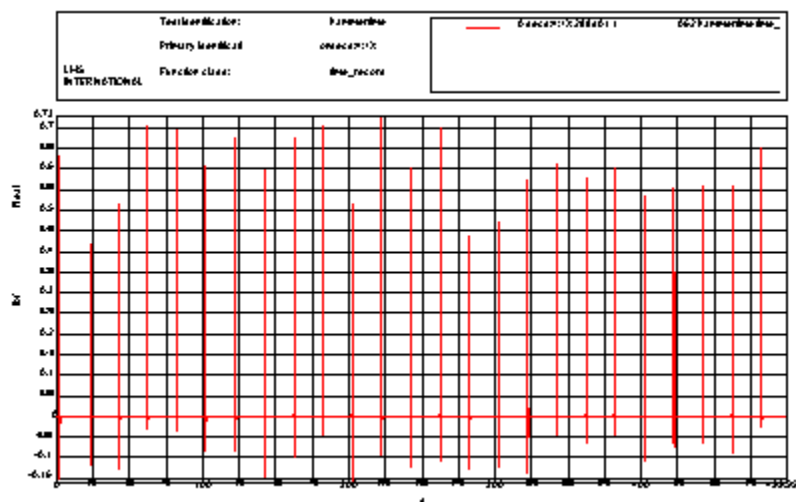


Figure 5.2.1 Input Time Data from Test 25





## 5.2 Test 25 (continued)

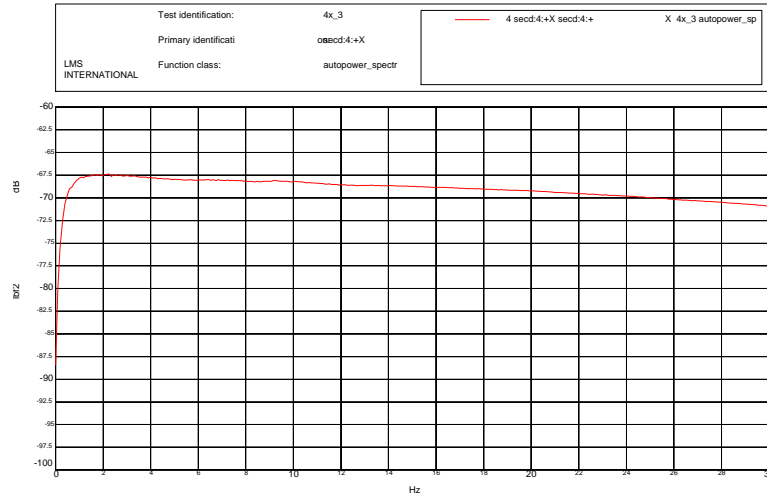


Figure 5.2.2, Input Frequency Data from Test 25

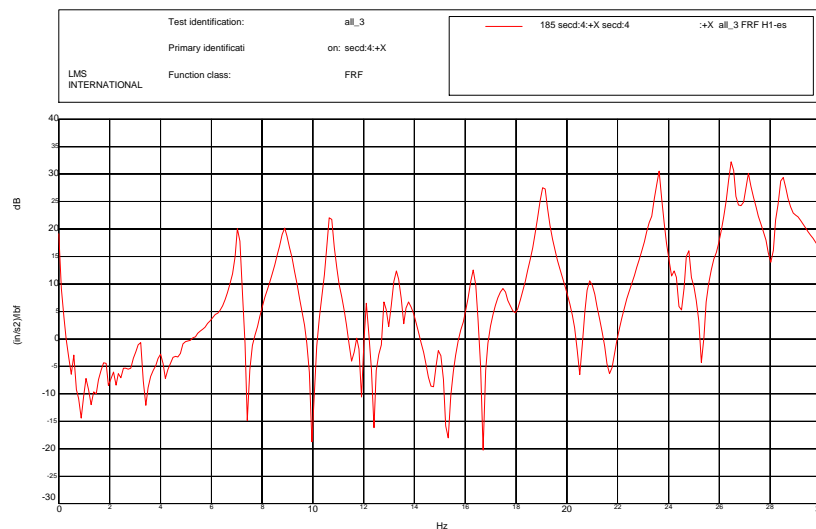


Figure 5.2.3, Frequency Response of 4x from Test 25 (drive-point)





## 5.2 Test 25 (continued)

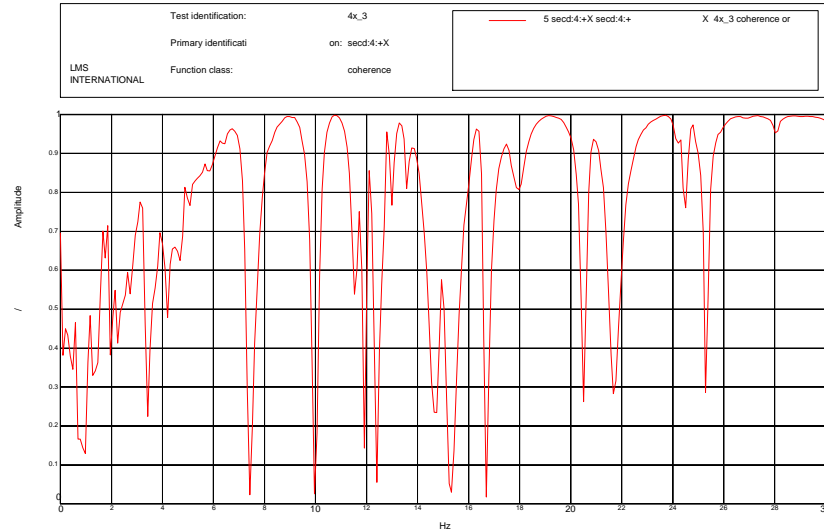


Figure 5.2.4, Coherence of 4x from Test 25 (drive-point)





### 5.3 Test 26

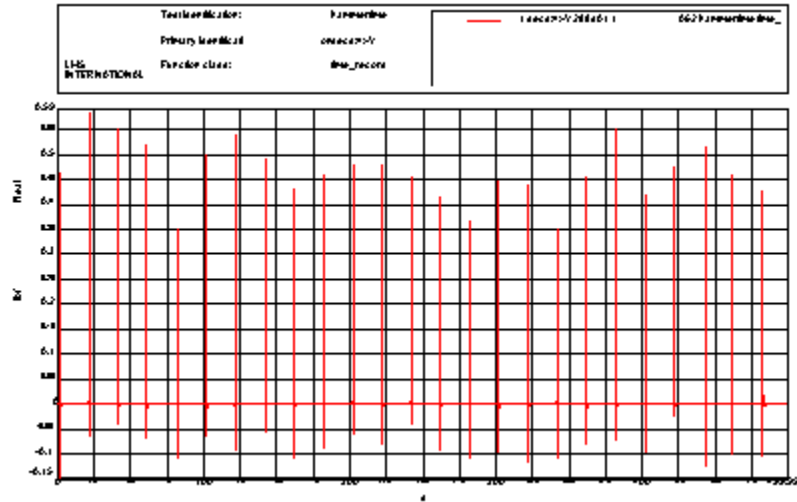


Figure 5.3.1, Input Time Data from Test 26

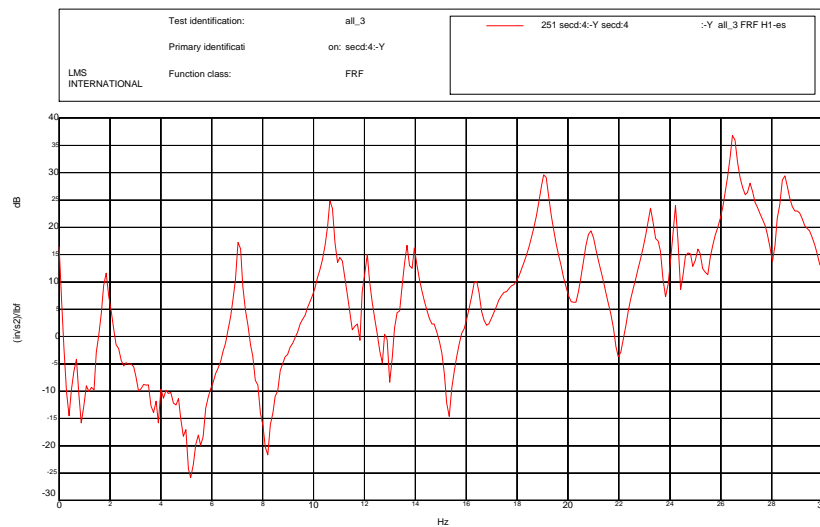


Figure 5.3.2, Frequency Response of 4y from Test 26 (drive-point)





### 5.3 Test 26 (continued)

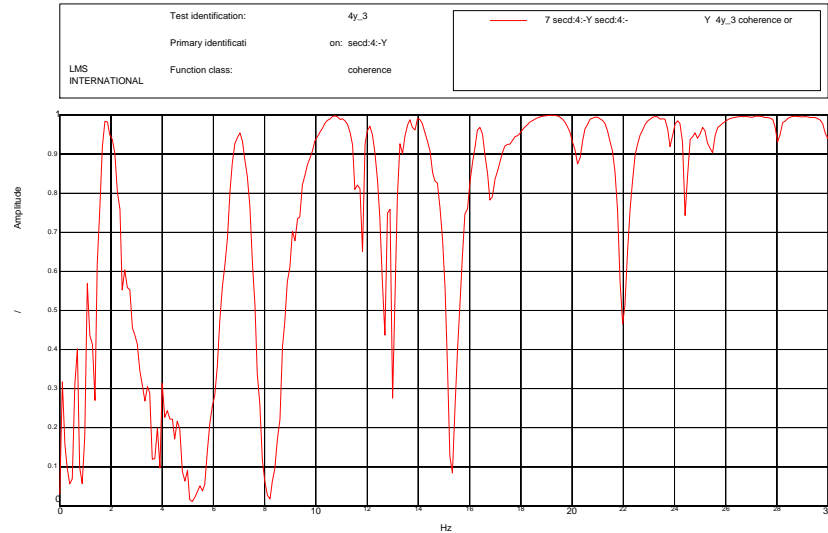


Figure 5.3.3, Coherence of 4y from Test 26 (drive-point)



Figure 5.3.4, Input Frequency Data from Test 26





## 5.4 Test 27

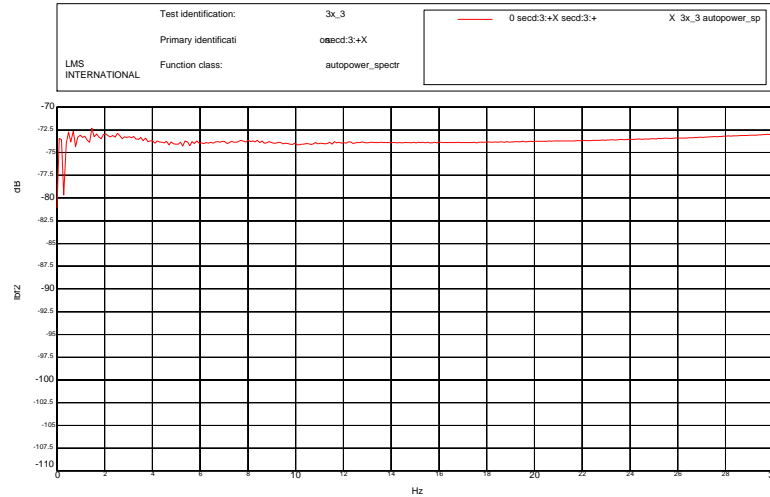


Figure 5.4.1, Input Frequency Data from Test 27

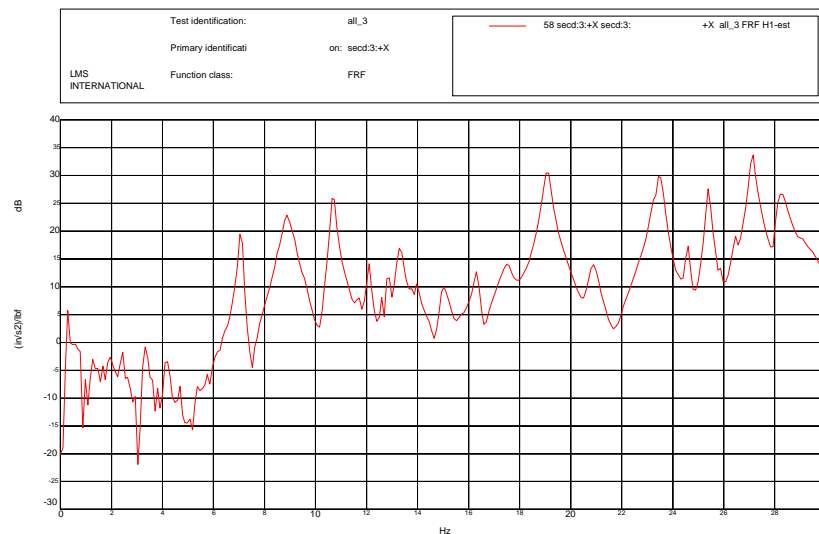


Figure 5.4.2, Frequency Response of 3x from Test 27 (drive-point)





## 5.4 Test 27 (continued)

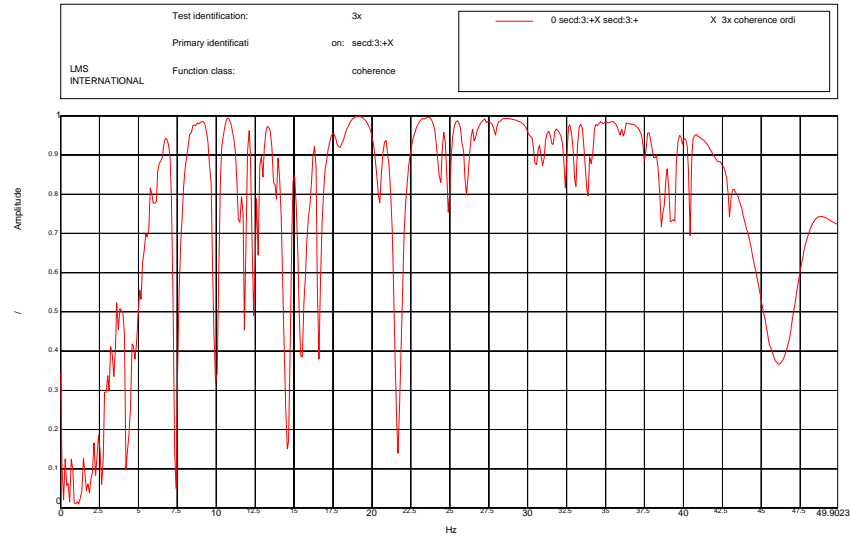


Figure 5.4.3, Coherence of 3x from Test 27 (drive-point)





## 5.5 Test 28

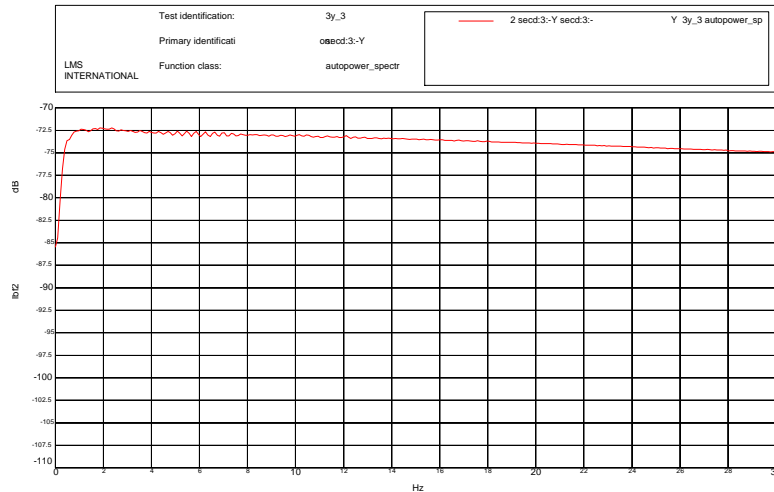


Figure 5.5.1, Input Frequency Data from Test 28

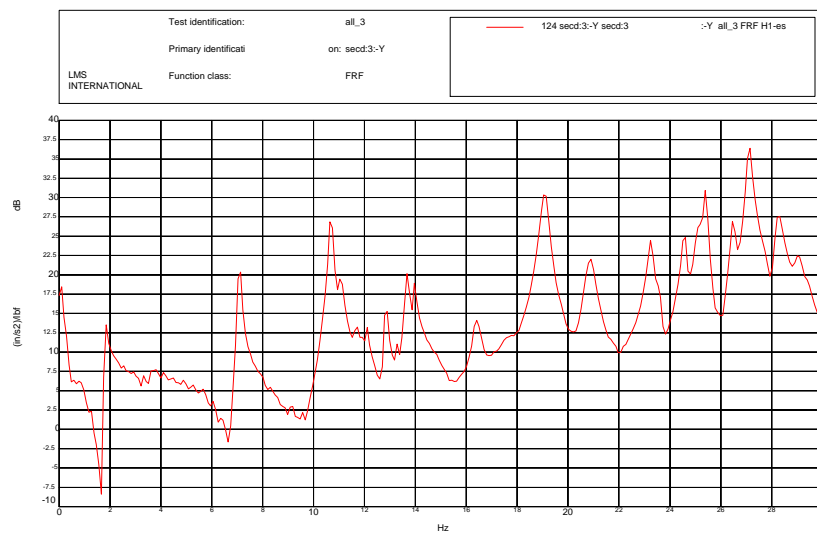


Figure 5.5.2, Frequency Response of 3y from Test 28 (drive-point)





## 5.5 Test 28 (continued)

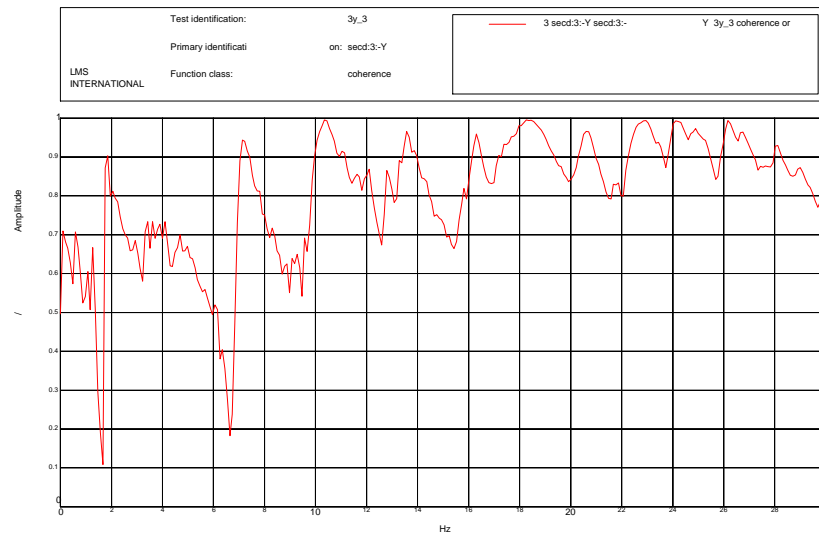


Figure 5.5.3, Coherence of 3y from Test 28 (drive-point)





## 5.6 Test 29

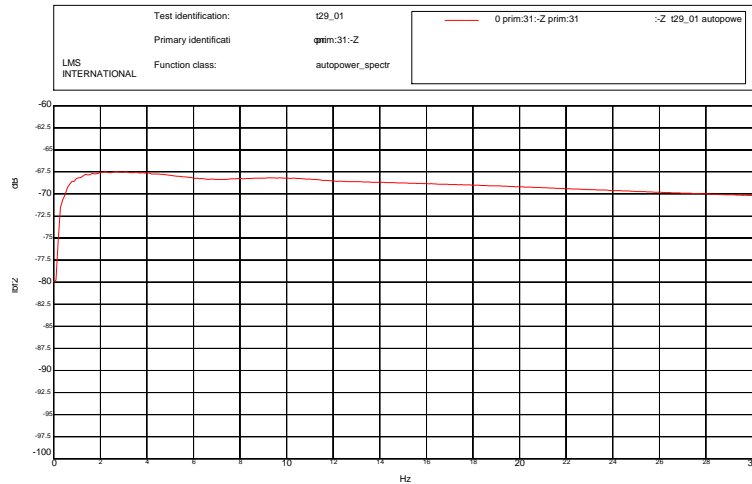


Figure 5.6.1, Input Frequency Data from Test 29

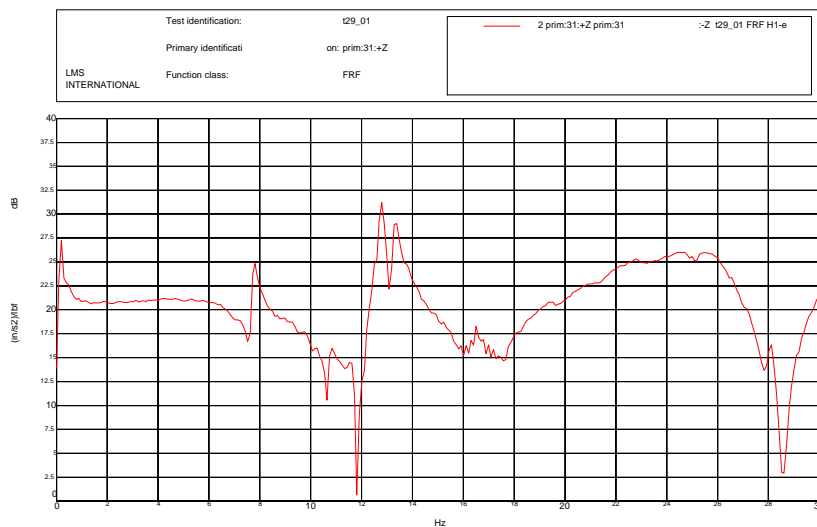


Figure 5.6.2, FRF of 31z from Test 29 (drive-point)





## 5.6 Test 29 (continued)

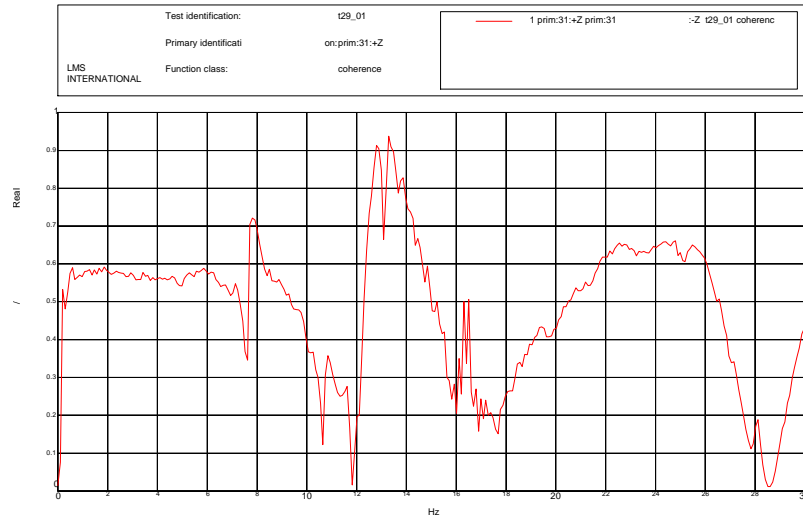


Figure 5.6.3, Coherence of 31z from Test 29 (drive-point)





## 5.7 Test 30

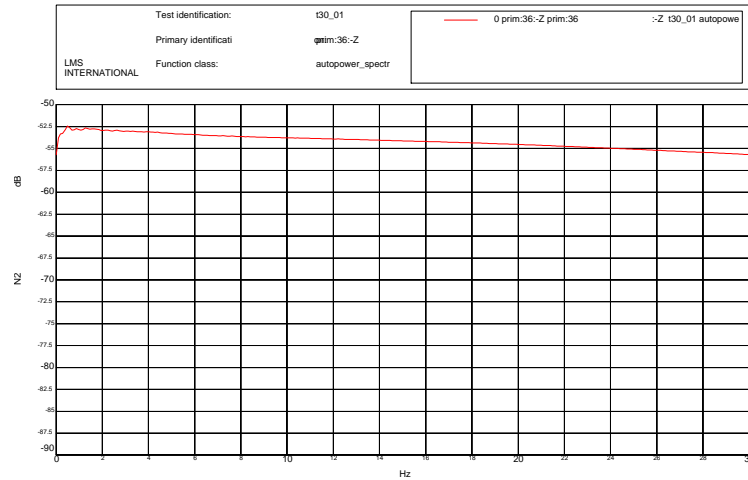


Figure 5.7.1, Input Frequency Data from Test 30

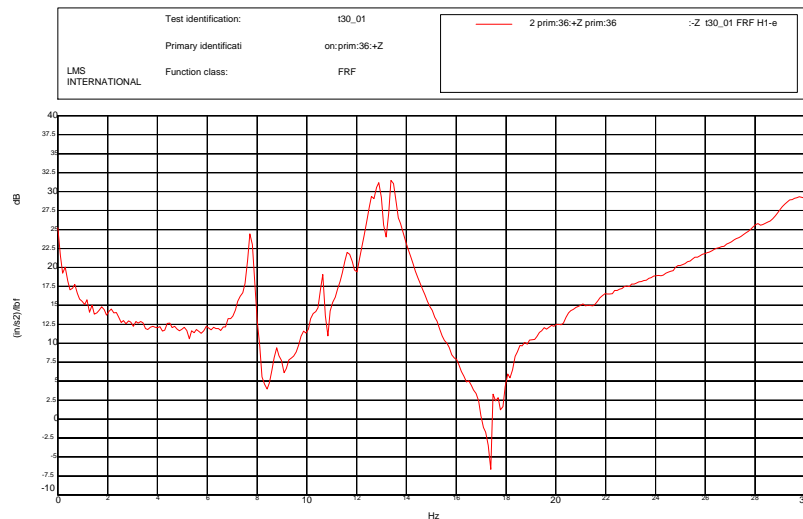


Figure 5.7.2, FRF of 36z from Test 30 (drive-point)





## 5.7 Test 30 (continued)

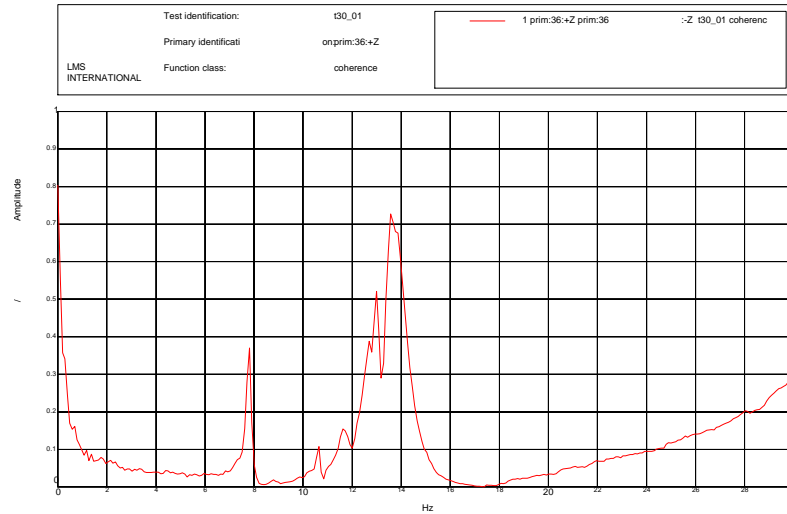


Figure 5.7.3, Coherence of 36z from Test 30 (drive-point)





## 6.0 FRF Calculation Parameters

This section contains the FRF calculation parameters used in calculating the frequency response functions from the cleansed time data [3].

### 6.1 Test 4

FMON frequency response calculation:

Frequency Band: 0 to 50Hz

Trigger Level: 15%

Trigger Offset: none

Windows:

Input: Uniform

Output: Exponential (5%)

Resolution: 512 lines (0.0976Hz)

Averages: 5

### 6.2 Test 25

FMON frequency response calculation:

Frequency Band: 0 to 50Hz

Trigger Level: 15%

Trigger Offset: none

Windows:

Input: Uniform

Output: Exponential (5%)

Resolution: 512 lines (0.0976Hz)

Averages: 5





### 6.3 Test 26

FMON frequency response calculation:

Frequency Band: 0 to 50Hz

Trigger Level: 15%

Trigger Offset: none

Windows:

Input: Uniform

Output: Exponential (5%)

Resolution: 512 lines (0.0976Hz)

Averages: 5

### 6.4 Test 27

FMON frequency response calculation:

Frequency Band: 0 to 50Hz

Trigger Level: 15%

Trigger Offset: none

Windows:

Input: Uniform

Output: Exponential (5%)

Resolution: 512 lines (0.0976Hz)

Averages: 5





### 6.5 Test 28

FMON frequency response calculation:

Frequency Band: 0 to 50Hz

Trigger Level: 15%

Trigger Offset: none

Windows:

Input: Uniform

Output: Exponential (5%)

Resolution: 512 lines (0.0976Hz)

Averages: 5

### 6.6 Test 29

FMON frequency response calculation:

Frequency Band: 0 to 50Hz

Trigger Level: 15%

Trigger Offset: none

Windows:

Input: Uniform

Output: Exponential (5%)

Resolution: 512 lines (0.0976Hz)

Averages: 5





### 6.7 Test 30

FMON frequency response calculation:

Frequency Band: 0 to 50Hz

Trigger Level: 15%

Trigger Offset: none

Windows:

Input: Uniform

Output: Exponential (5%)

Resolution: 512 lines (0.0976Hz)

Averages: 5





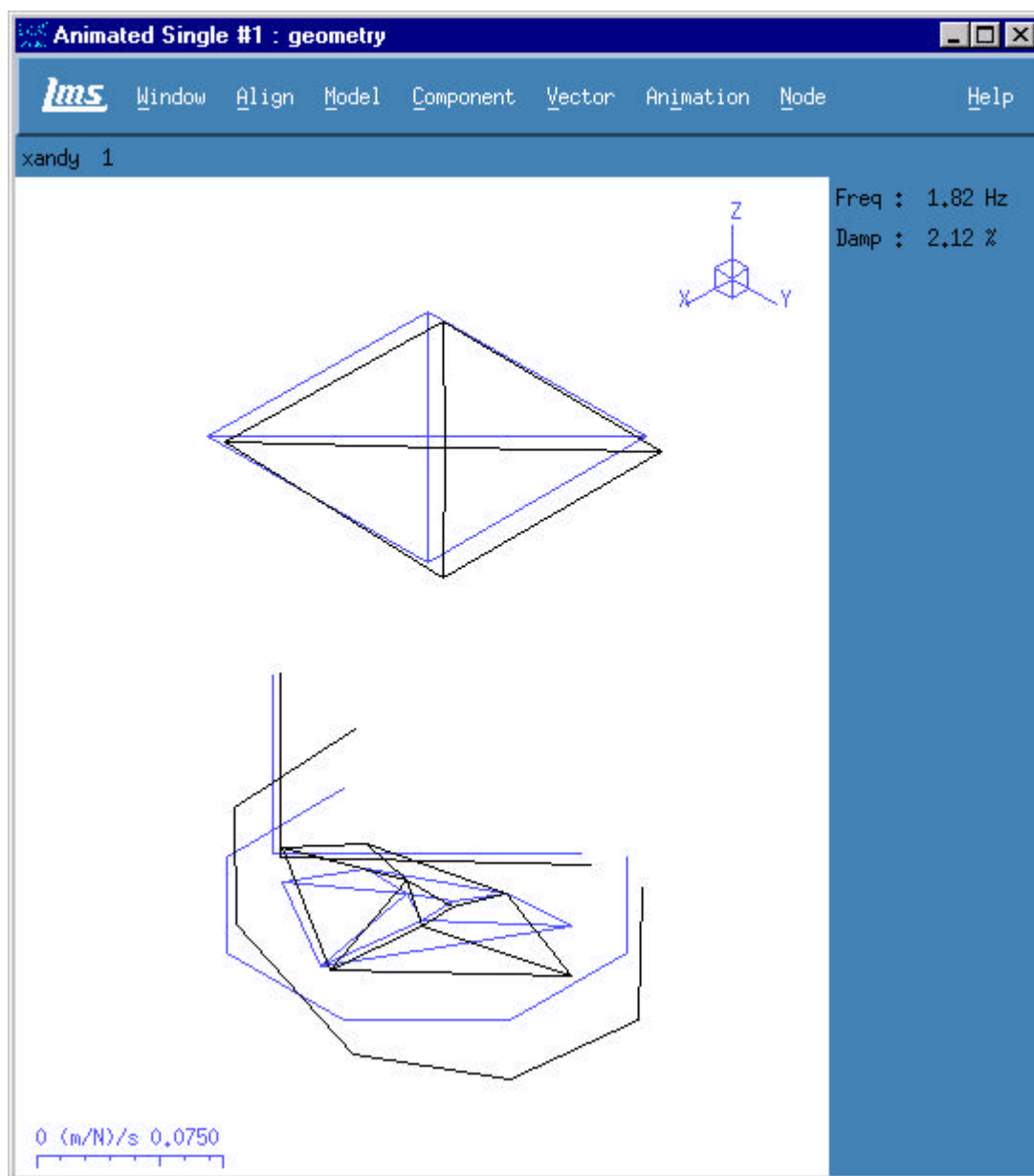
## 7.0 References

1. Gemini South 8m Optical Telescope Final Report, MACL Report # 05-08570-001, dated October 2000
2. Gemini South 8m Optical Telescope Test Setup Report, MACL Report # 05-08570-002, dated October 2000
3. Gemini South 8m Optical Telescope Data Cleansing Report, MACL Report # 05-08570-003, dated October 2000
4. Gemini South 8m Optical Telescope Modal Test Report, MACL Report # 05-08570-004, dated October 2000
5. Gemini South 8m Optical Telescope Operating Report, MACL Report # 05-08570-005, dated October 2000
6. Gemini South 8m Optical Telescope Correlation Report, MACL Report # 05-08570-006, dated October 2000
7. Gemini South 8m Optical Telescope DoE and Wind Data Report, MACL Report # 05-08570-007, dated October 2000
8. CD containing all pertinent test data and reports
9. Preliminary Data Assessment of Gemini South Optical Telescope Operating and Modal Data Report, dated June 2000
10. LMS Coda-X 3.4 Test and Analysis Software (TMON, FMON, Modal Analysis, Matrix Toolbox), Leuven Measurement Systems, Detroit Michigan
11. LMS Coda-X 3.5C Test and Analysis Software (TMON, FMON, Modal Analysis), Leuven Measurement Systems, Detroit Michigan
12. LMS Road Runner Data Acquisition System, Leuven Measurement Systems, Detroit Michigan
13. MEScopia VES Version 2.0, Vibrant Technologies, Jamestown, CA
14. Avitabile, P., "Overview of Modal Analysis using the Frequency Response Method", July 1997
15. Box, George E.P., Hunter, J. Stuart, and Hunter, William G., *Statistics for Experimenters: An Introduction to Design, Data Analysis, and Model Building*, Wiley, 1978.
16. Shina, Sammy G., *Concurrent Engineering and Design for Manufacture of Electronic Products*, Van Nostrand Reinhold, 1991.





## 8.0 Mode Shape Plots

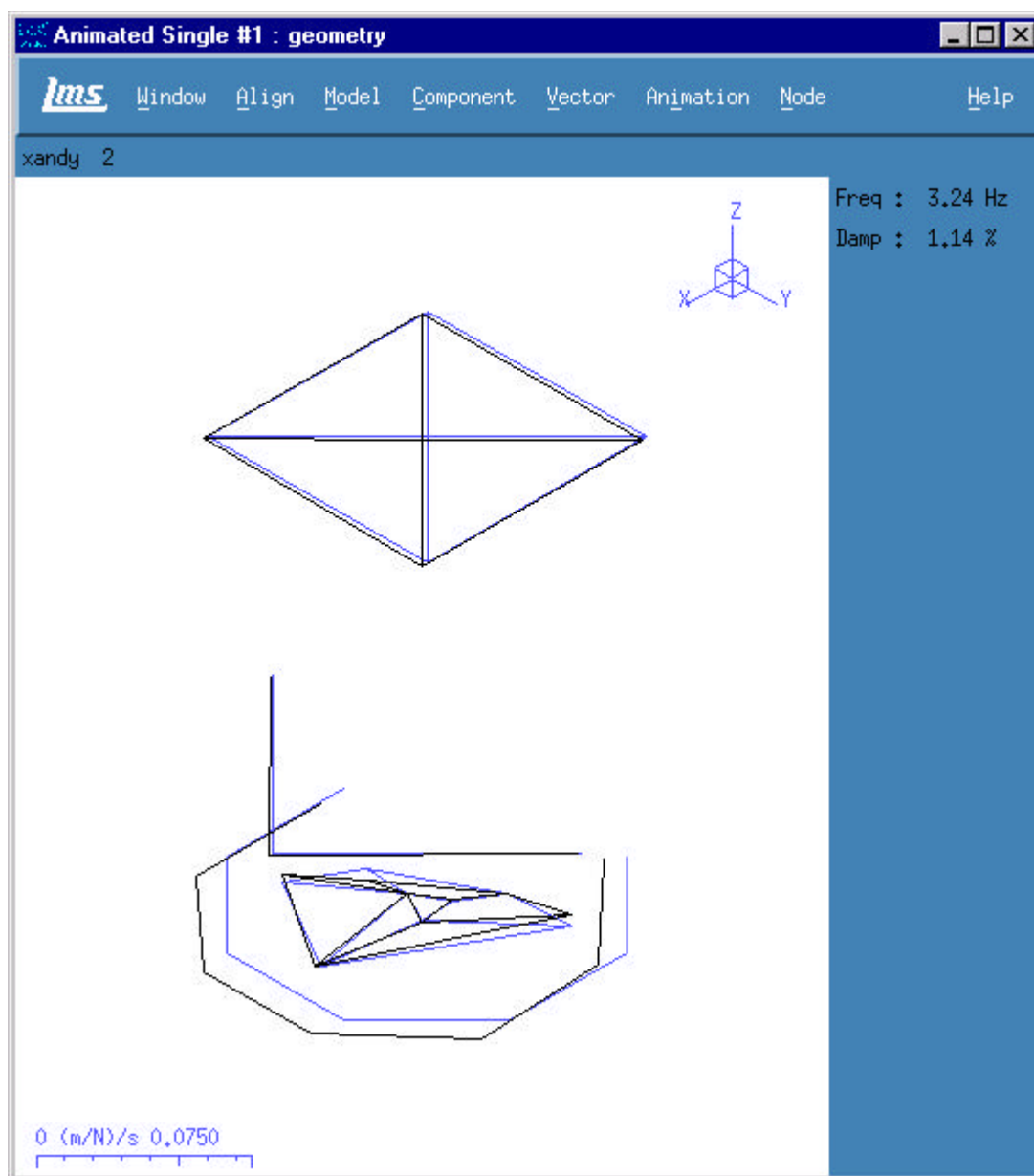


Mode Shape : 1.82Hz





## 8.0 Mode Shape Plots

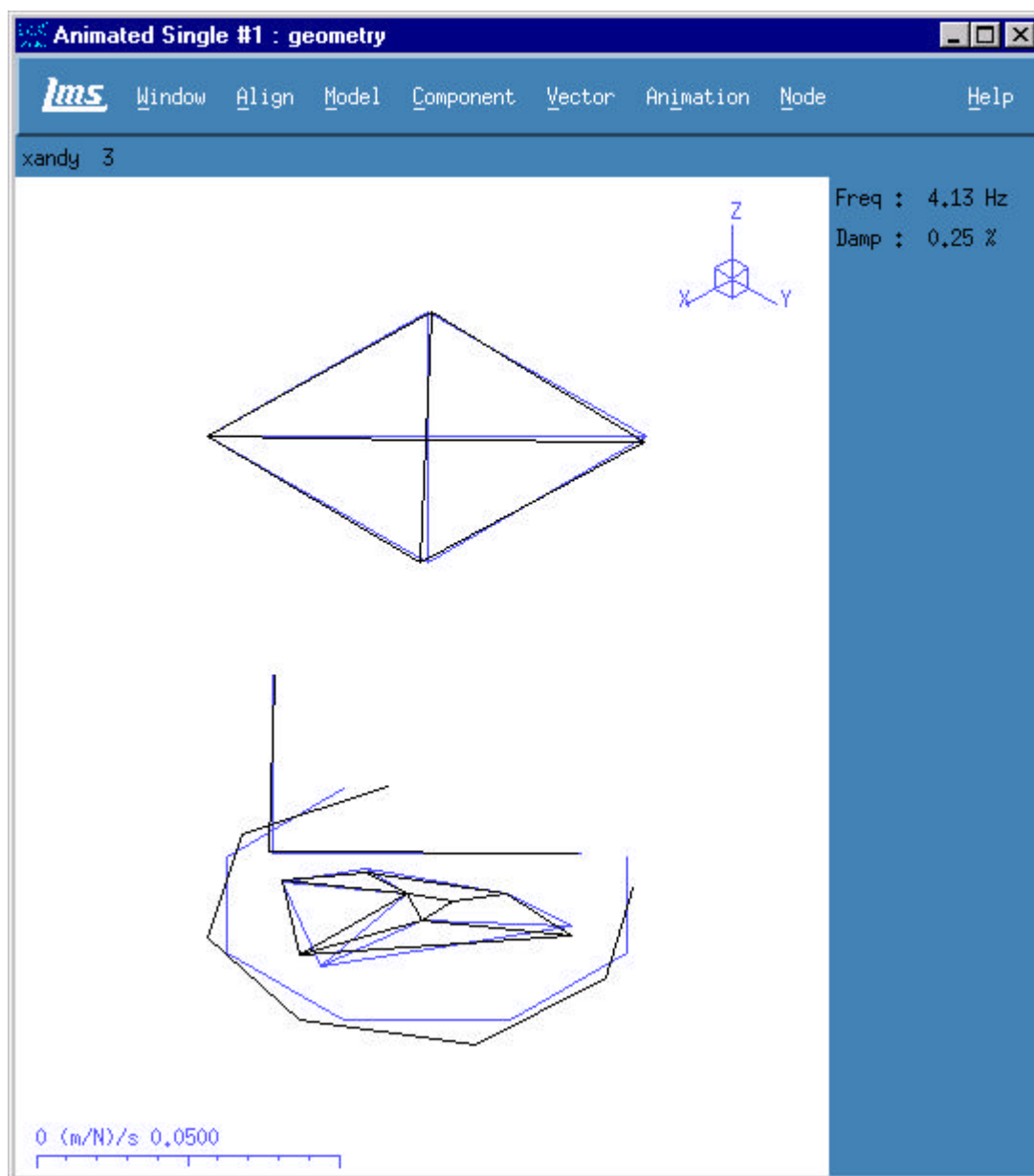


Mode Shape : 3.24Hz





## 8.0 Mode Shape Plots

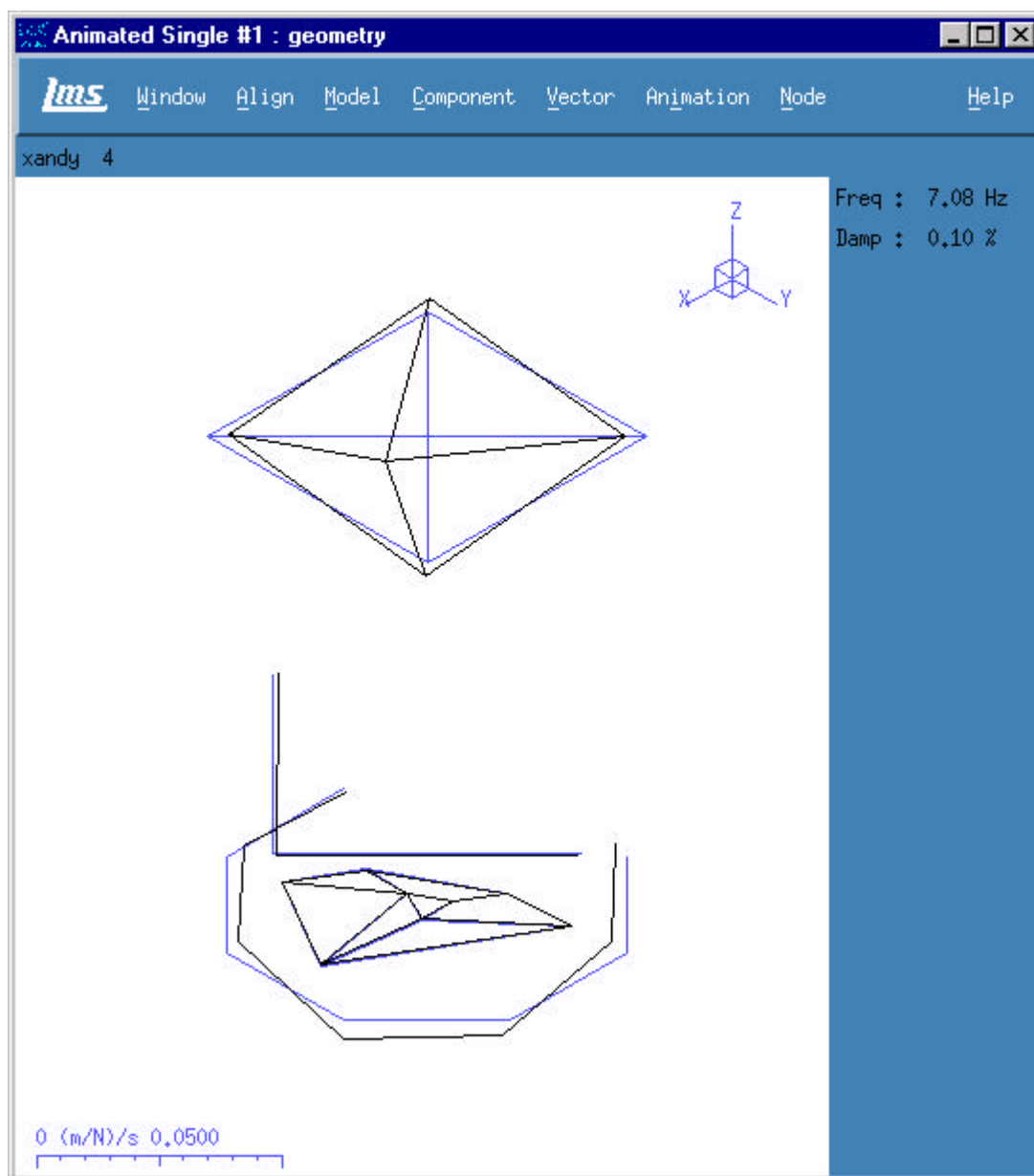


Mode Shape : 4.13Hz





## 8.0 Mode Shape Plots

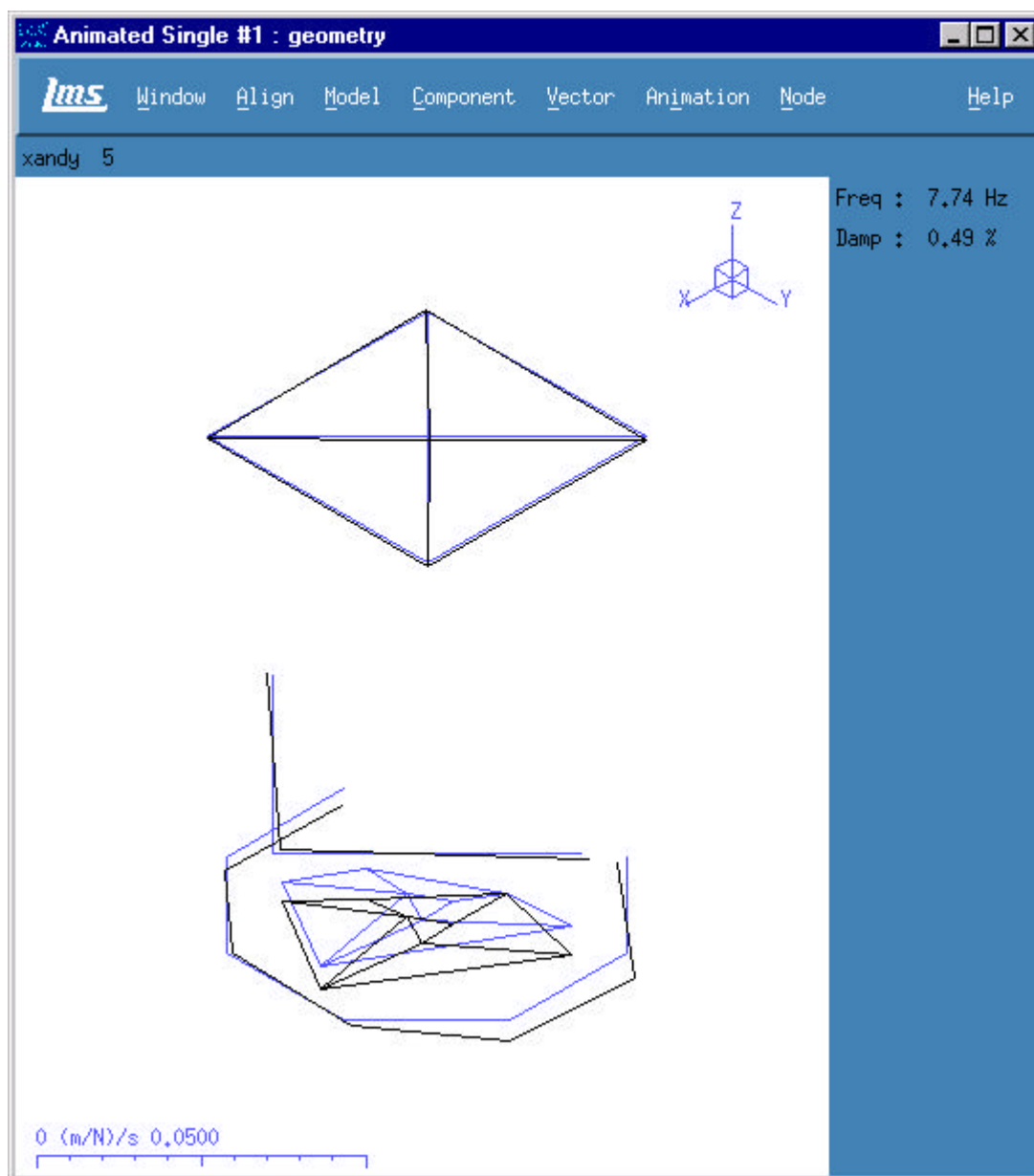


Mode Shape : 7.08Hz





## 8.0 Mode Shape Plots

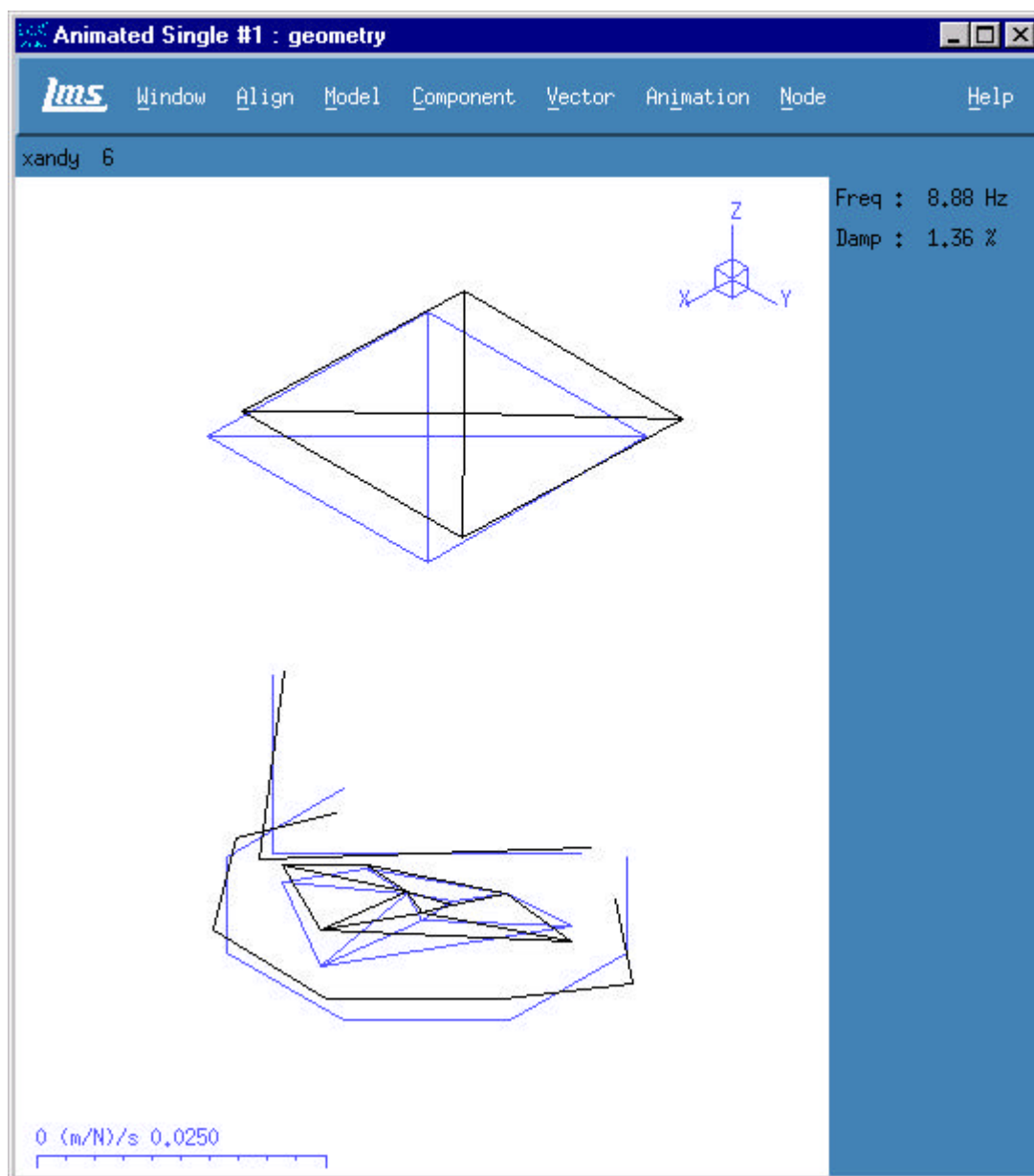


Mode Shape : 7.74Hz





## 8.0 Mode Shape Plots

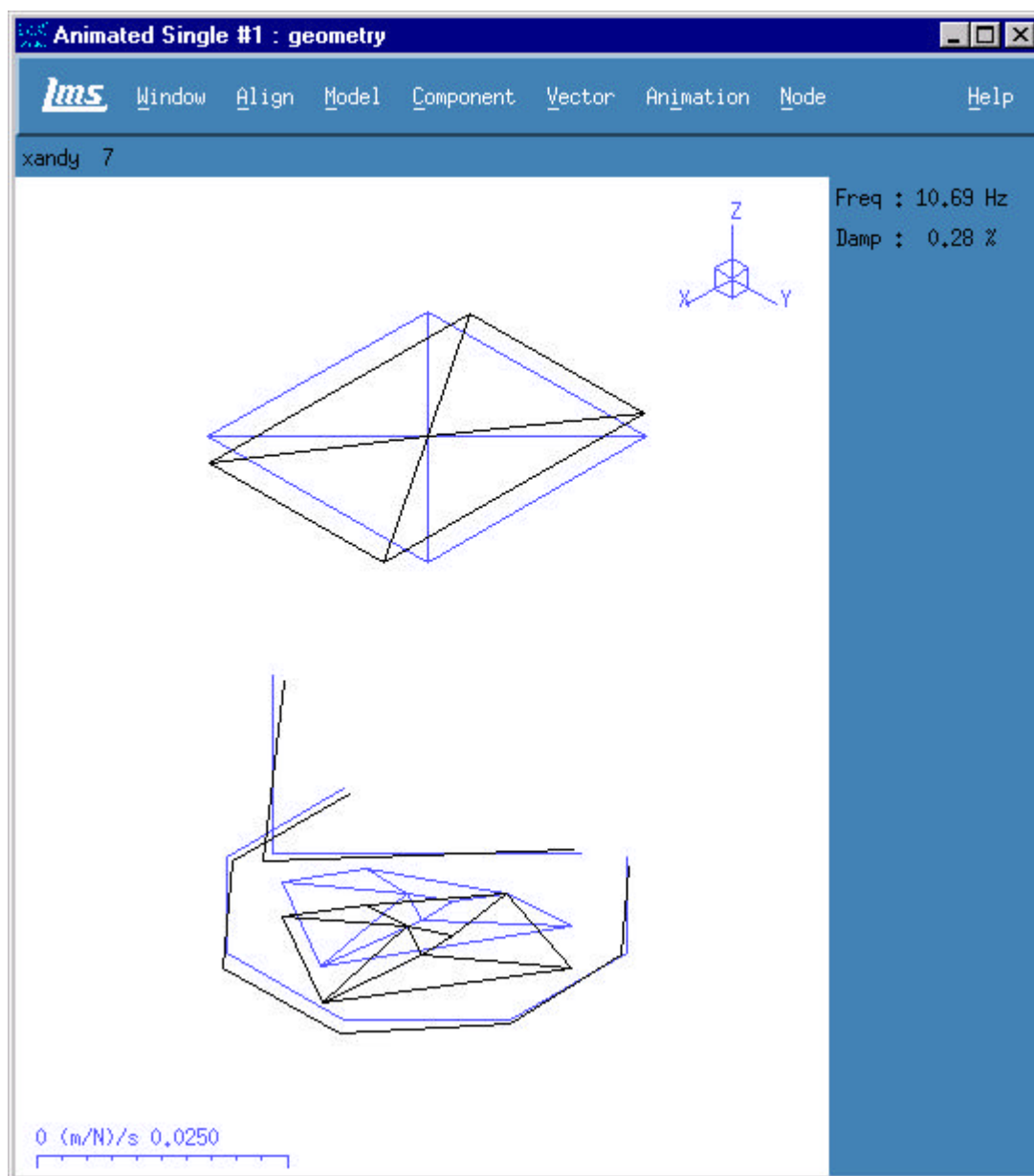


Mode Shape : 8.88Hz





## 8.0 Mode Shape Plots

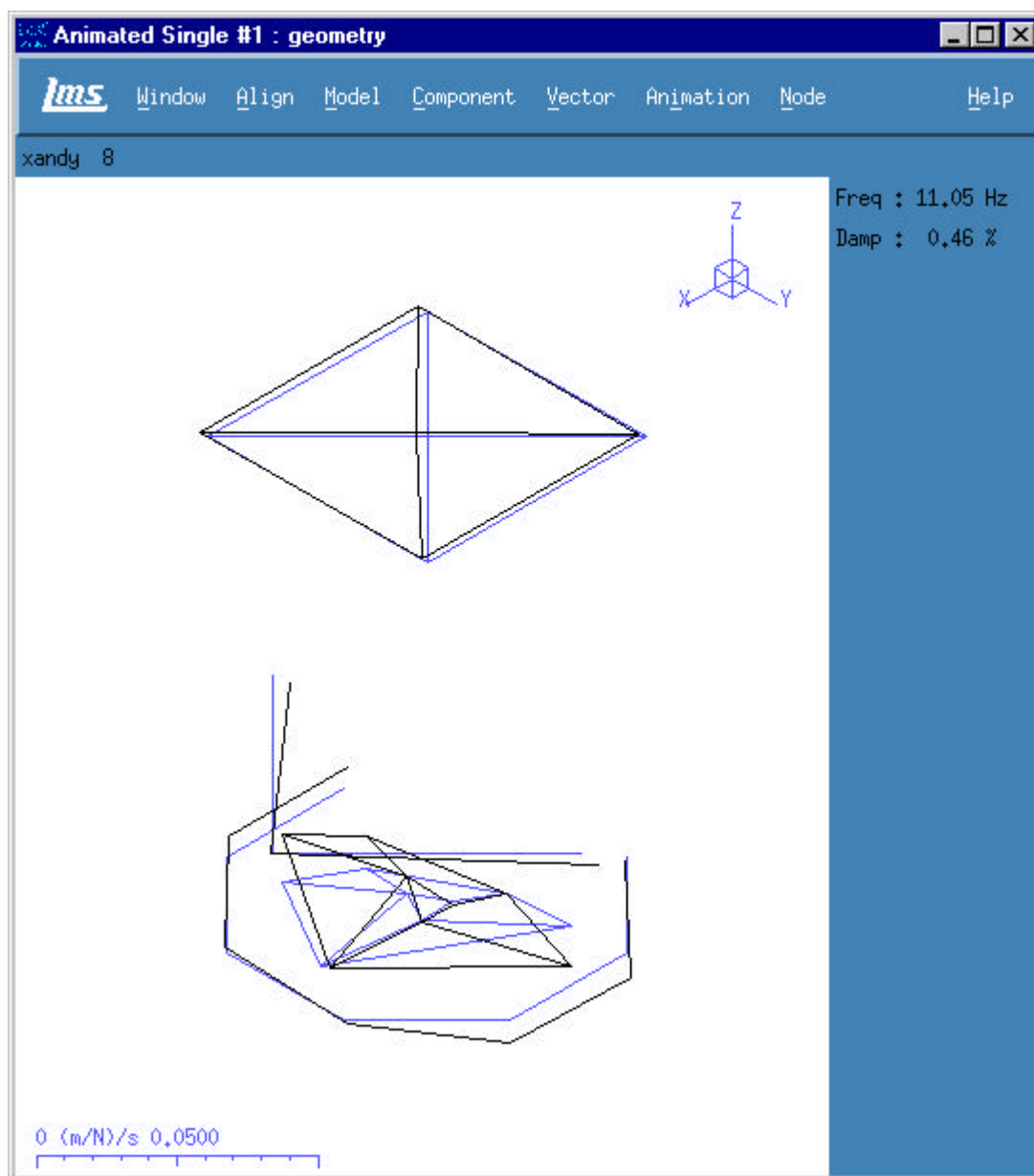


Mode Shape : 10.69Hz





## 8.0 Mode Shape Plots

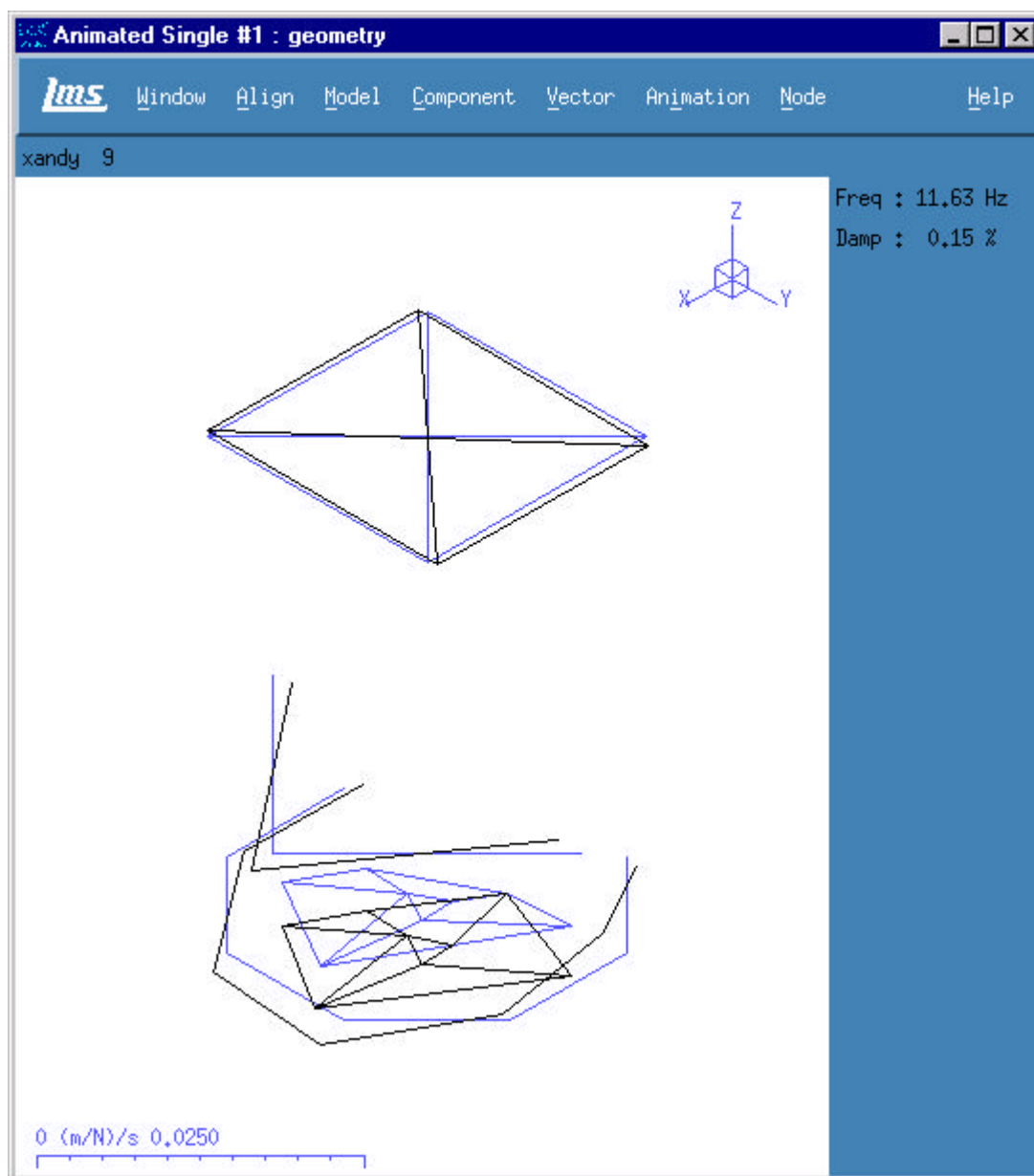


Mode Shape : 11.05Hz





## 8.0 Mode Shape Plots

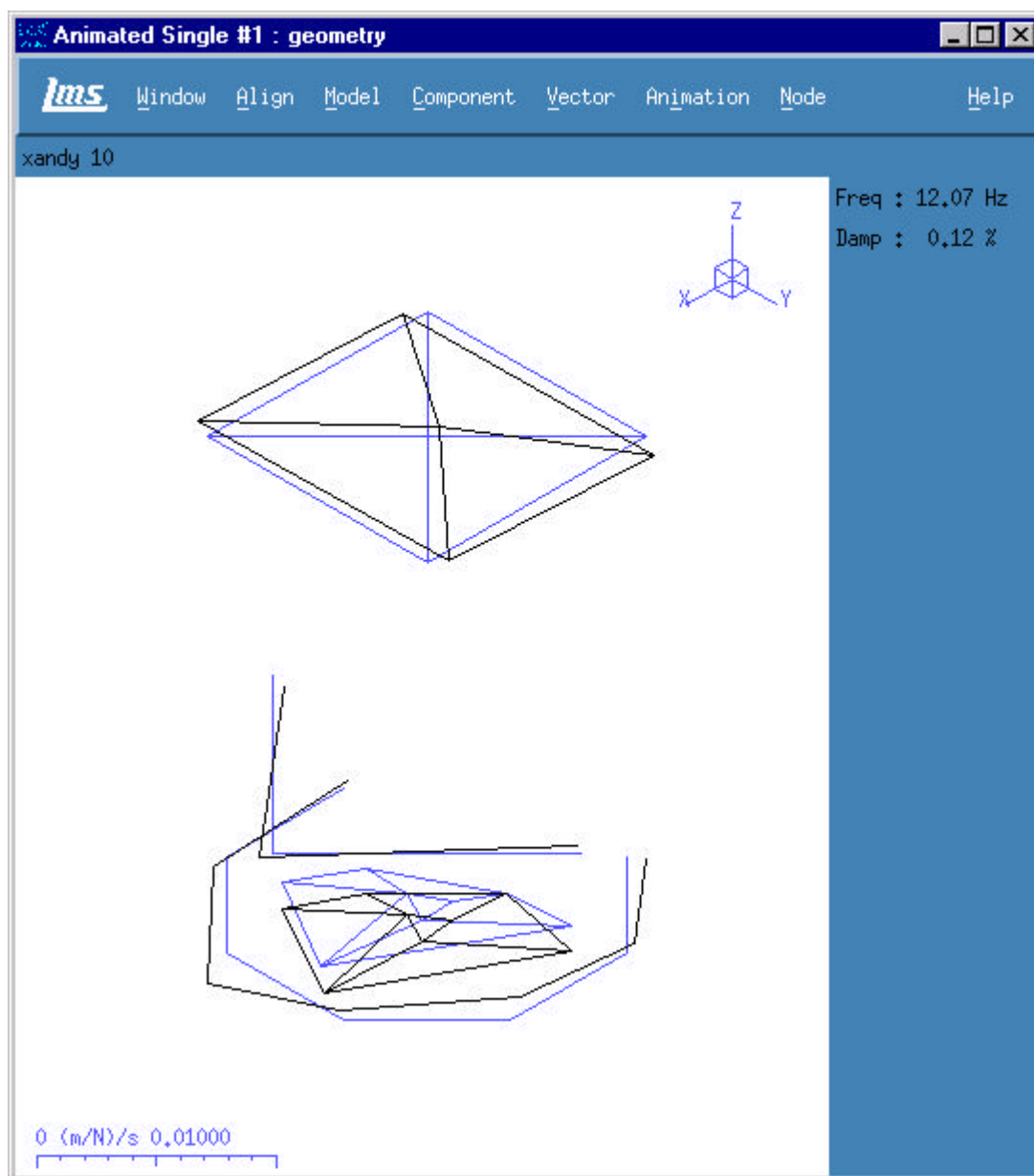


Mode Shape : 11.63Hz





## 8.0 Mode Shape Plots

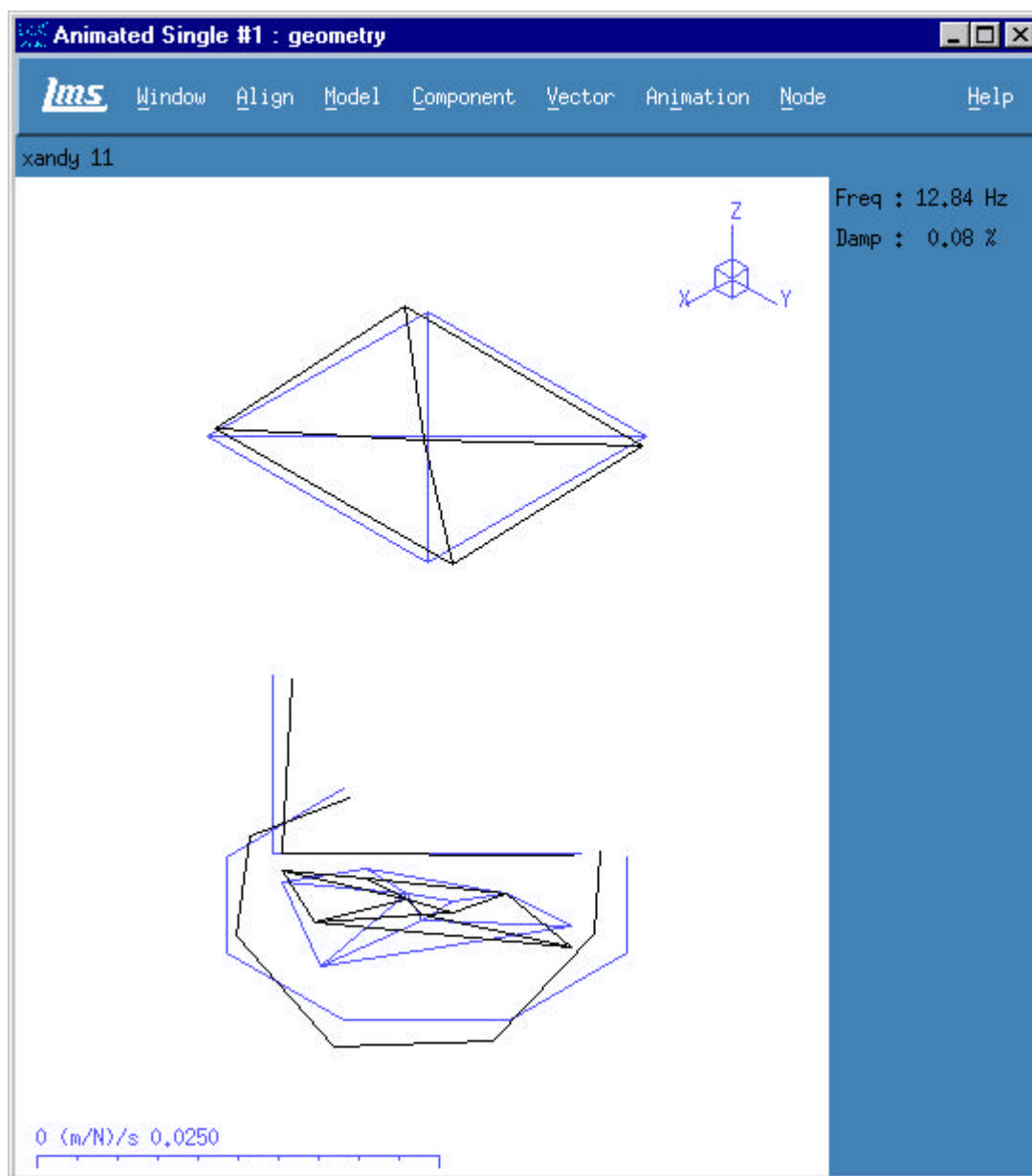


Mode Shape : 12.07Hz





## 8.0 Mode Shape Plots

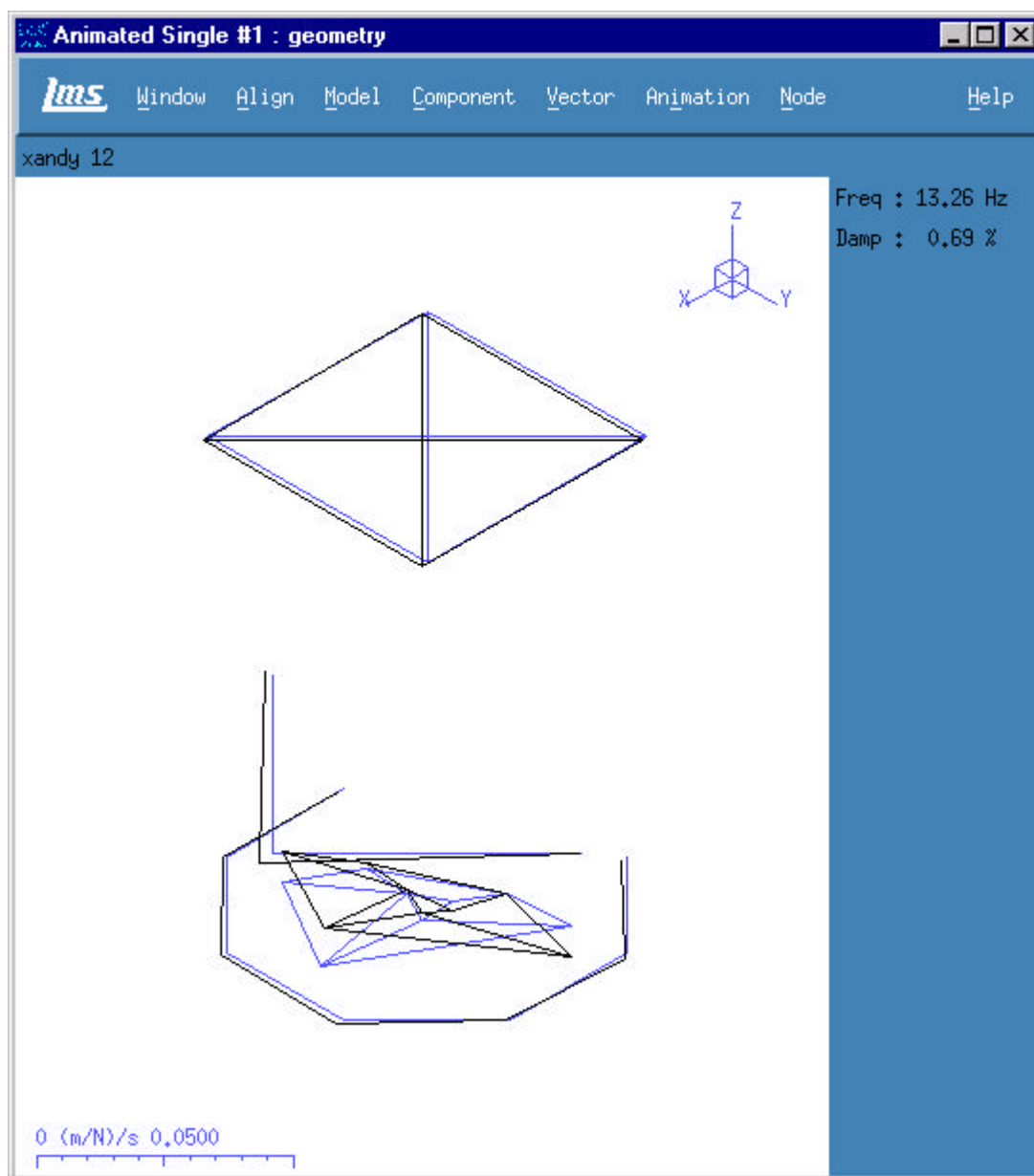


Mode Shape : 12.84Hz





## 8.0 Mode Shape Plots

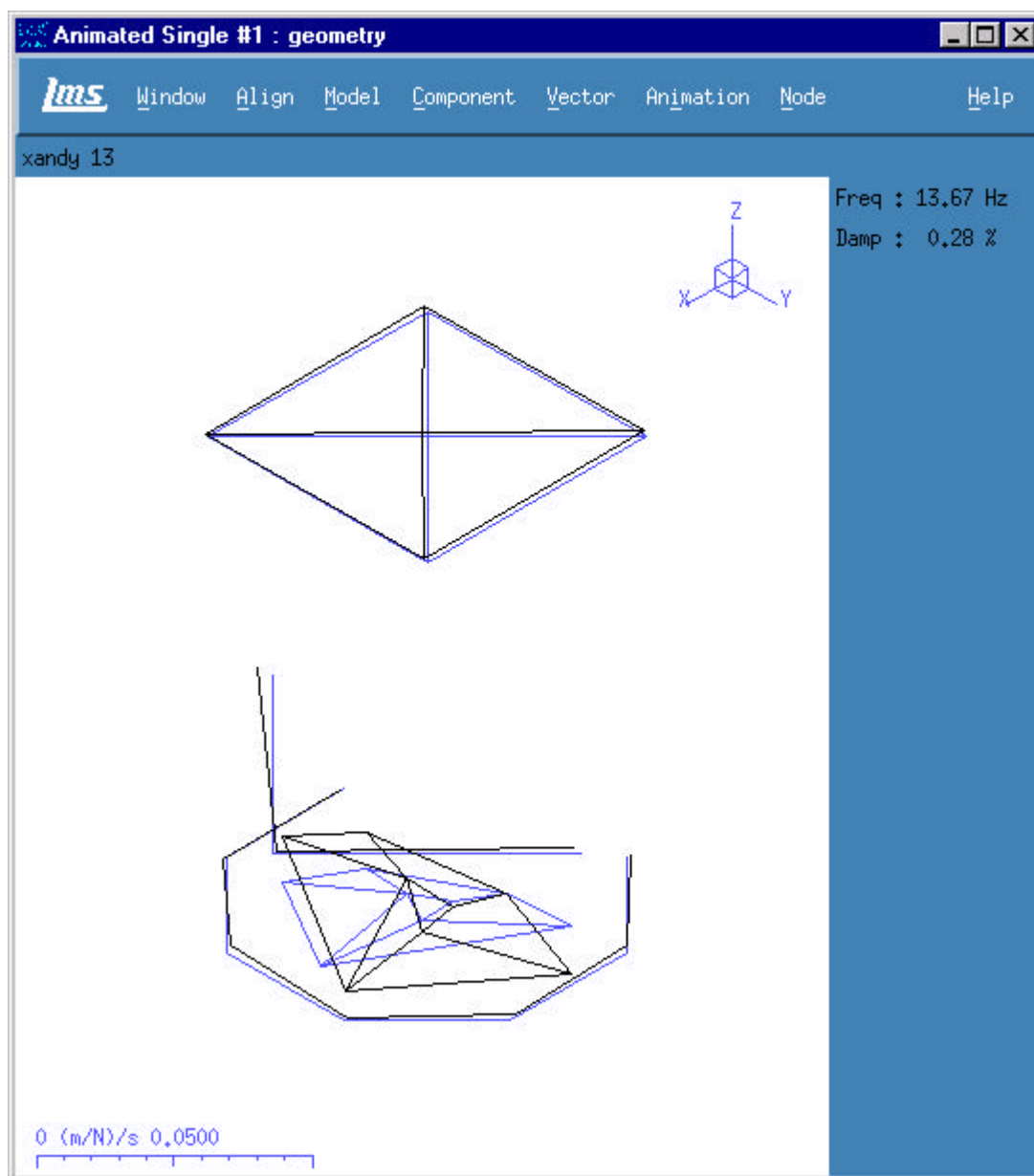


Mode Shape : 13.26Hz





## 8.0 Mode Shape Plots

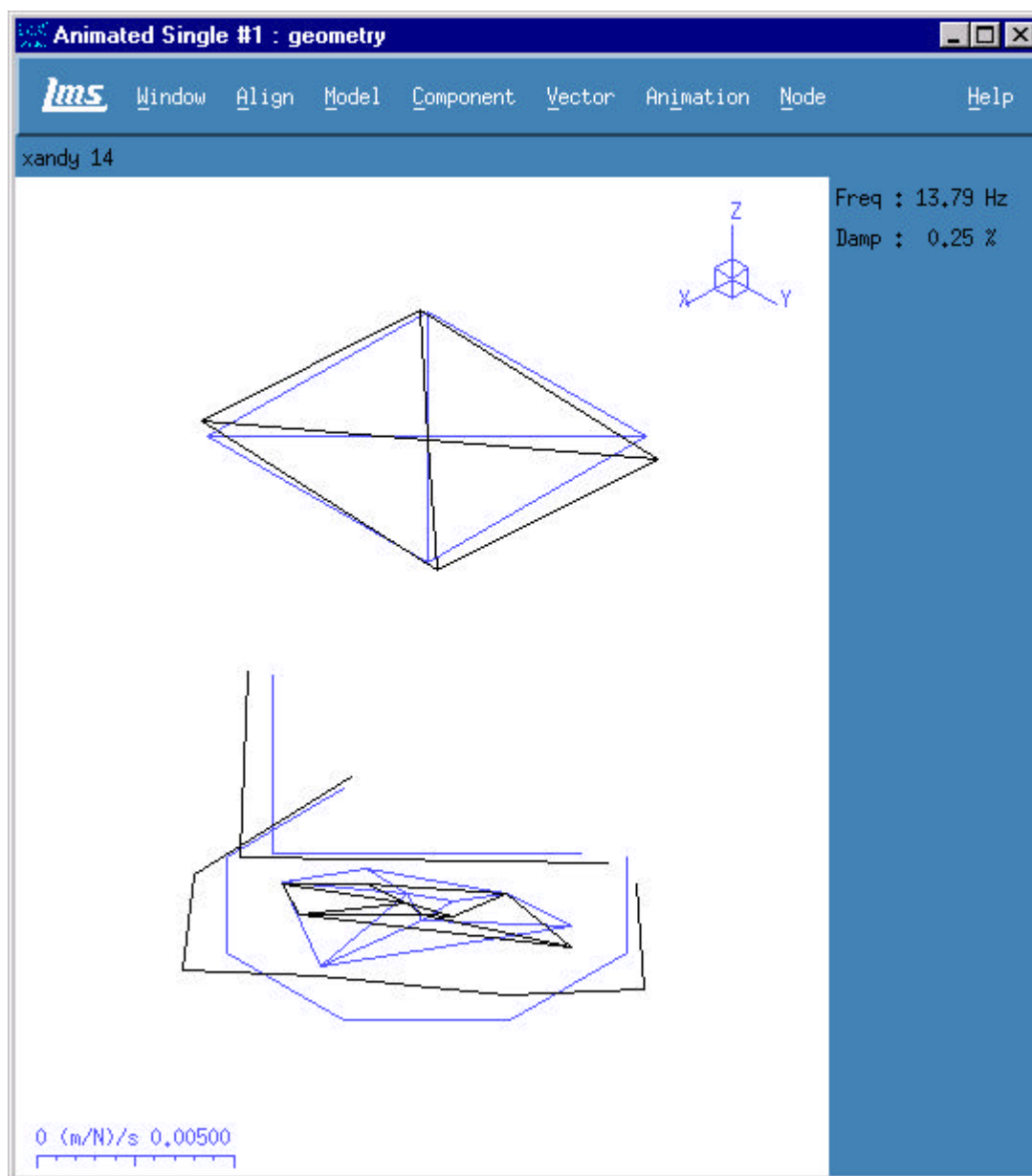


Mode Shape : 13.67Hz





## 8.0 Mode Shape Plots

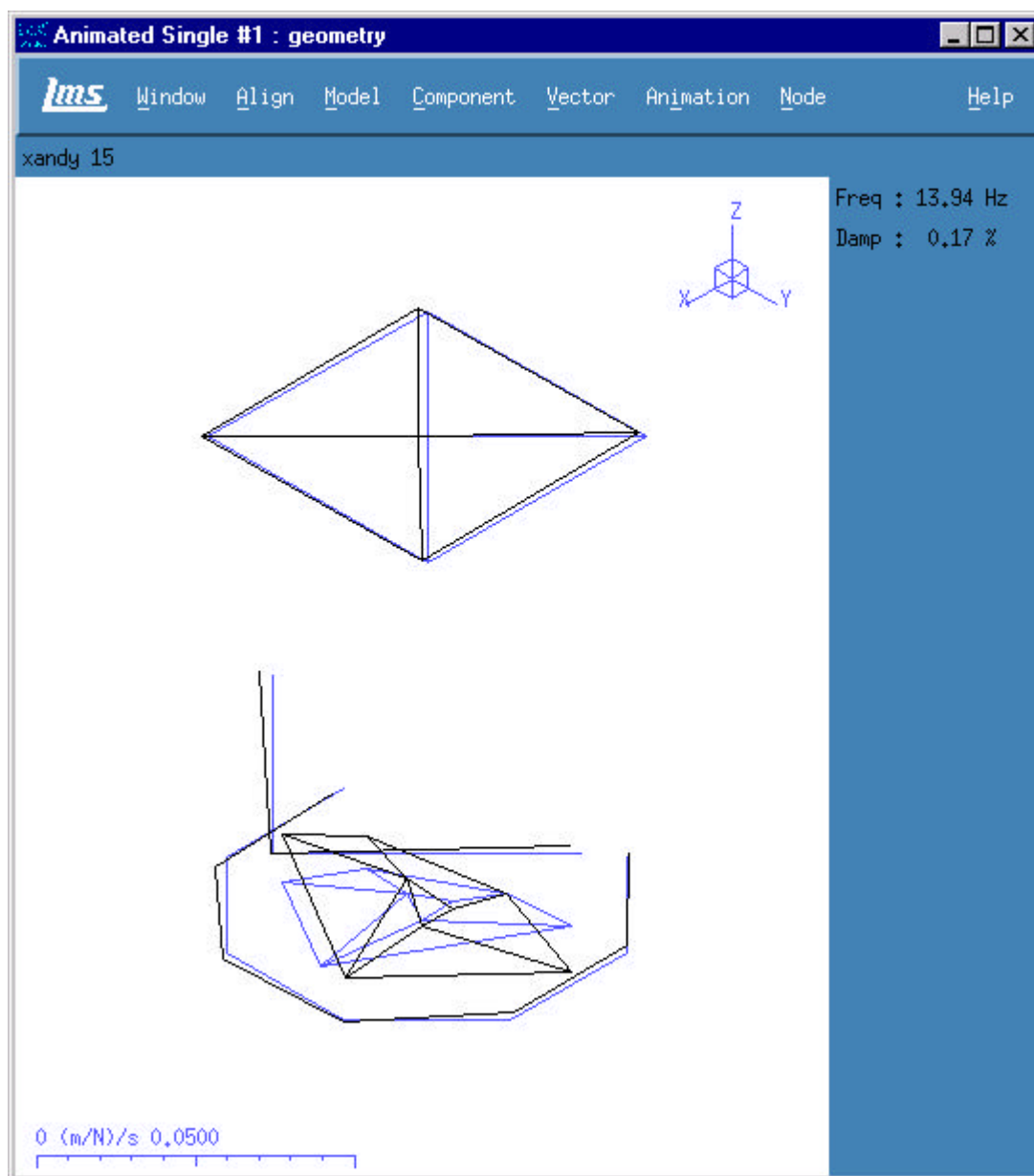


Mode Shape : 13.79Hz





## 8.0 Mode Shape Plots

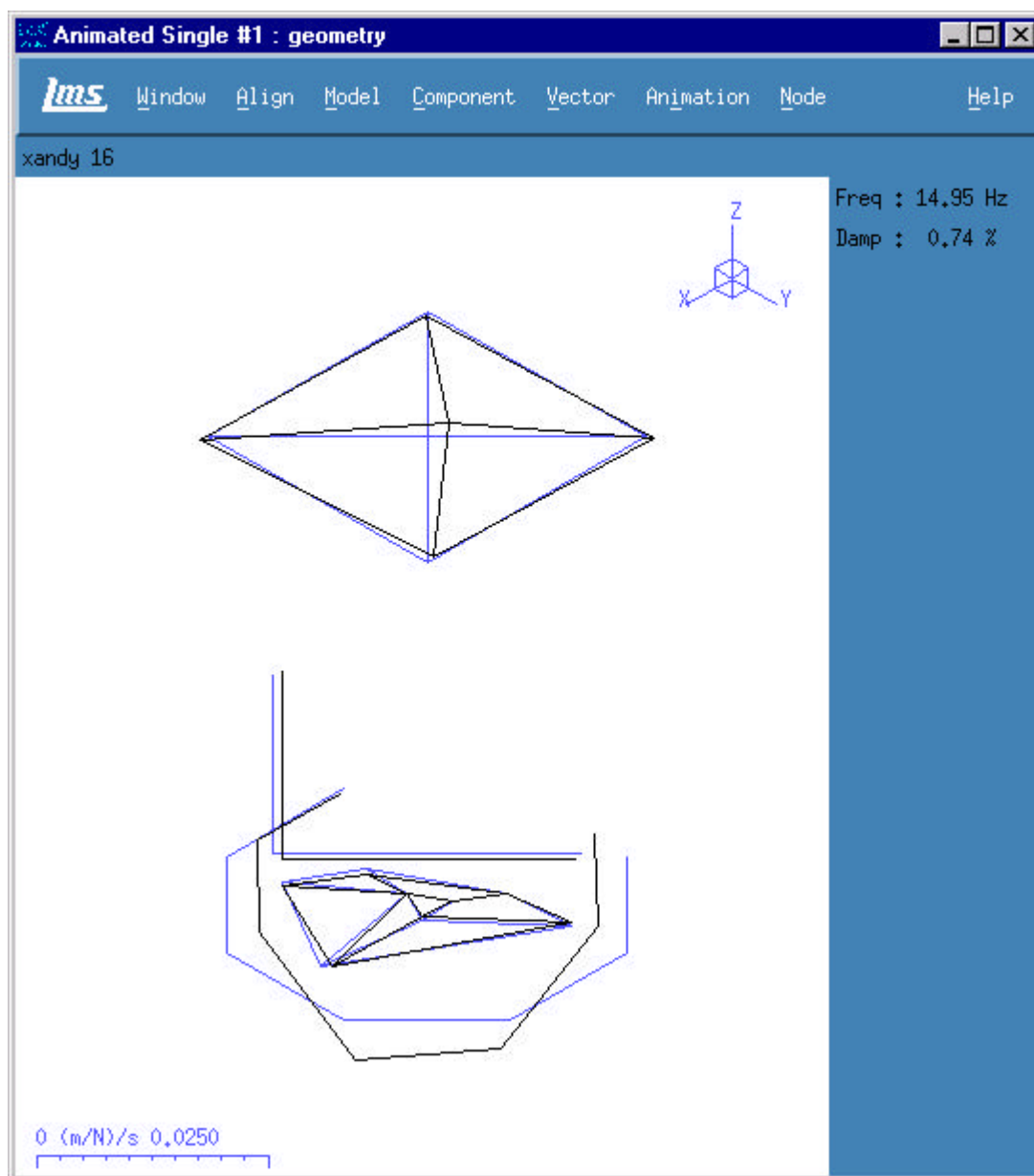


Mode Shape : 13.94Hz





## 8.0 Mode Shape Plots

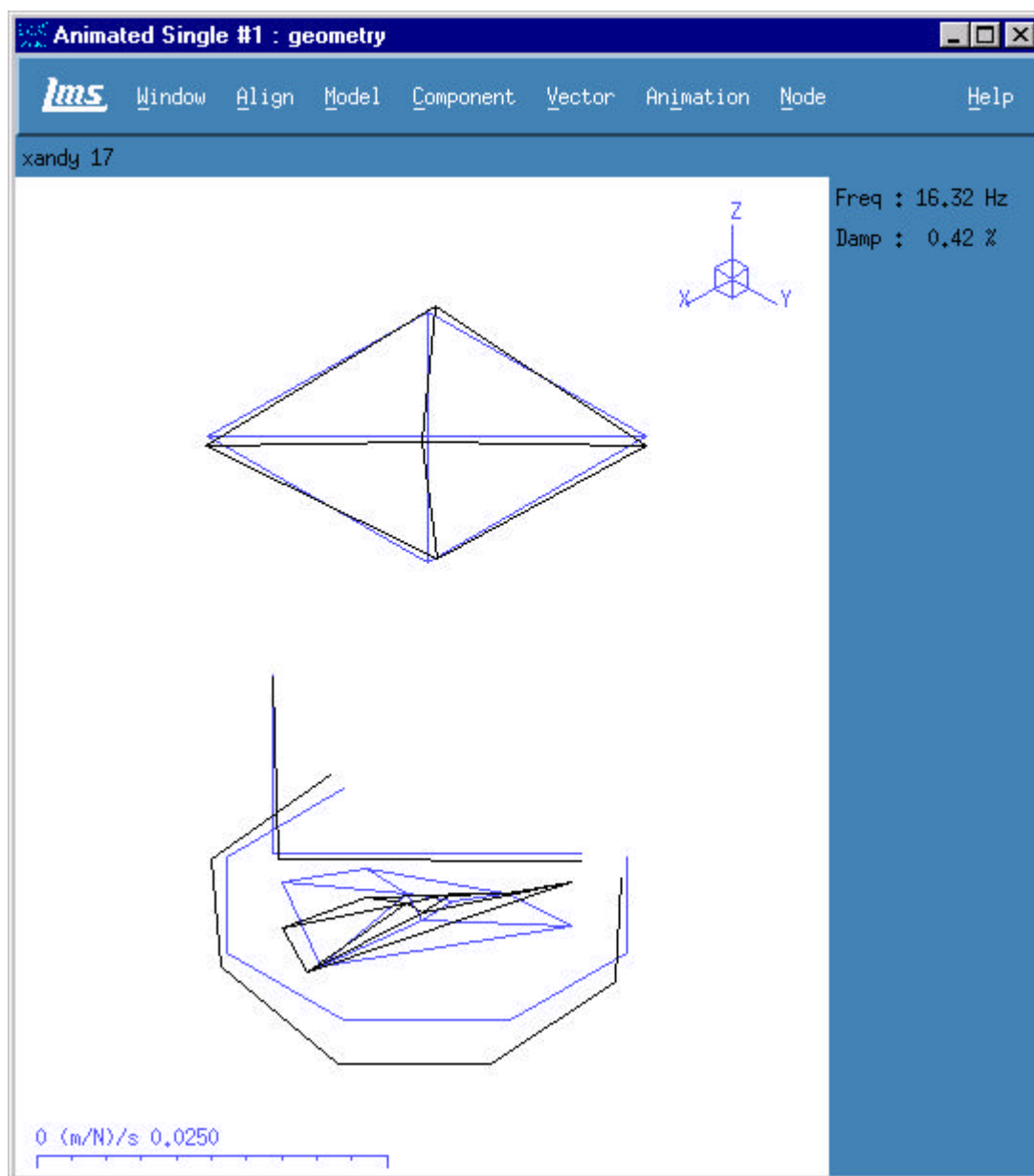


Mode Shape : 14.95Hz





## 8.0 Mode Shape Plots

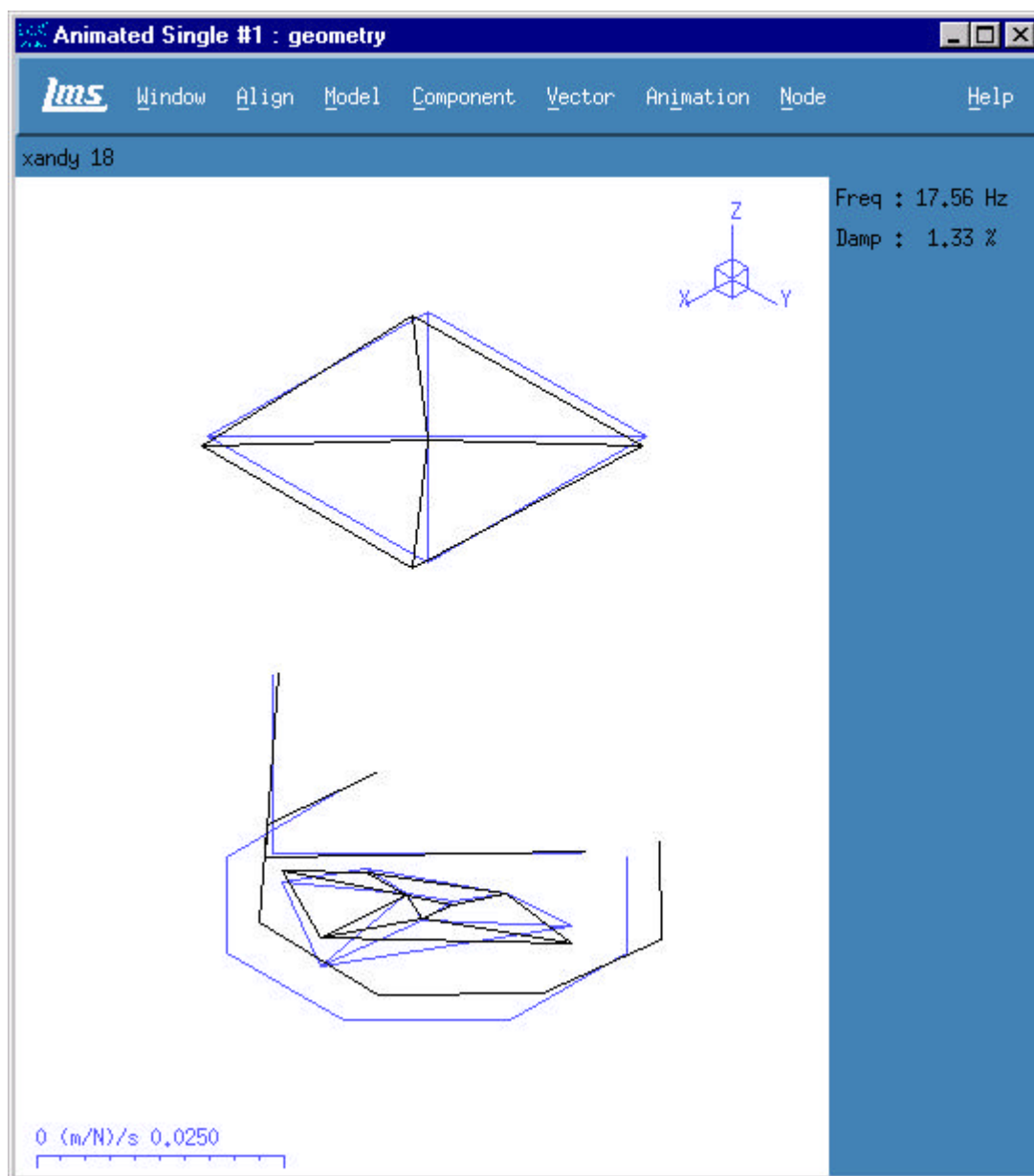


Mode Shape : 16.32Hz





## 8.0 Mode Shape Plots

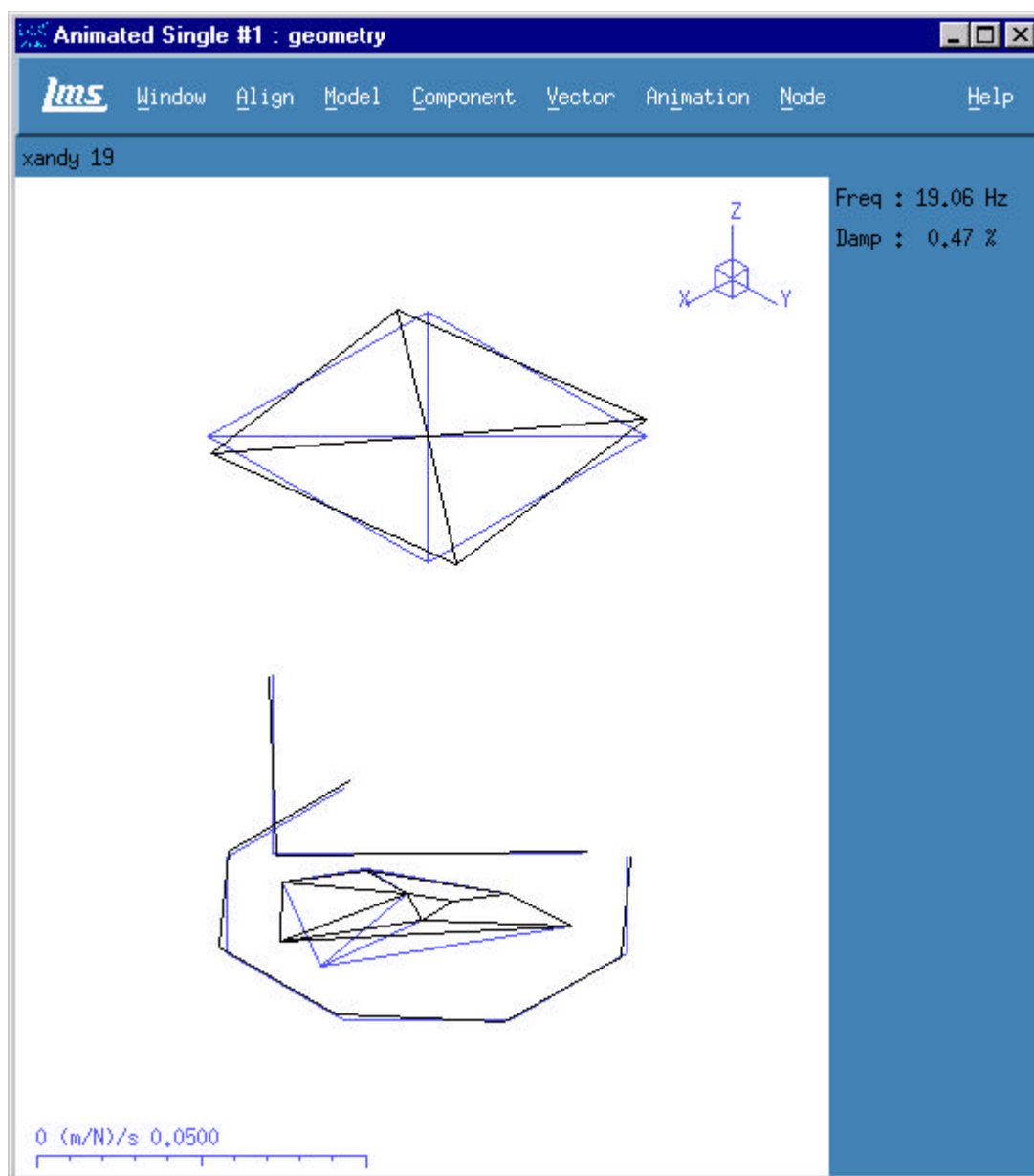


Mode Shape : 17.56Hz





## 8.0 Mode Shape Plots

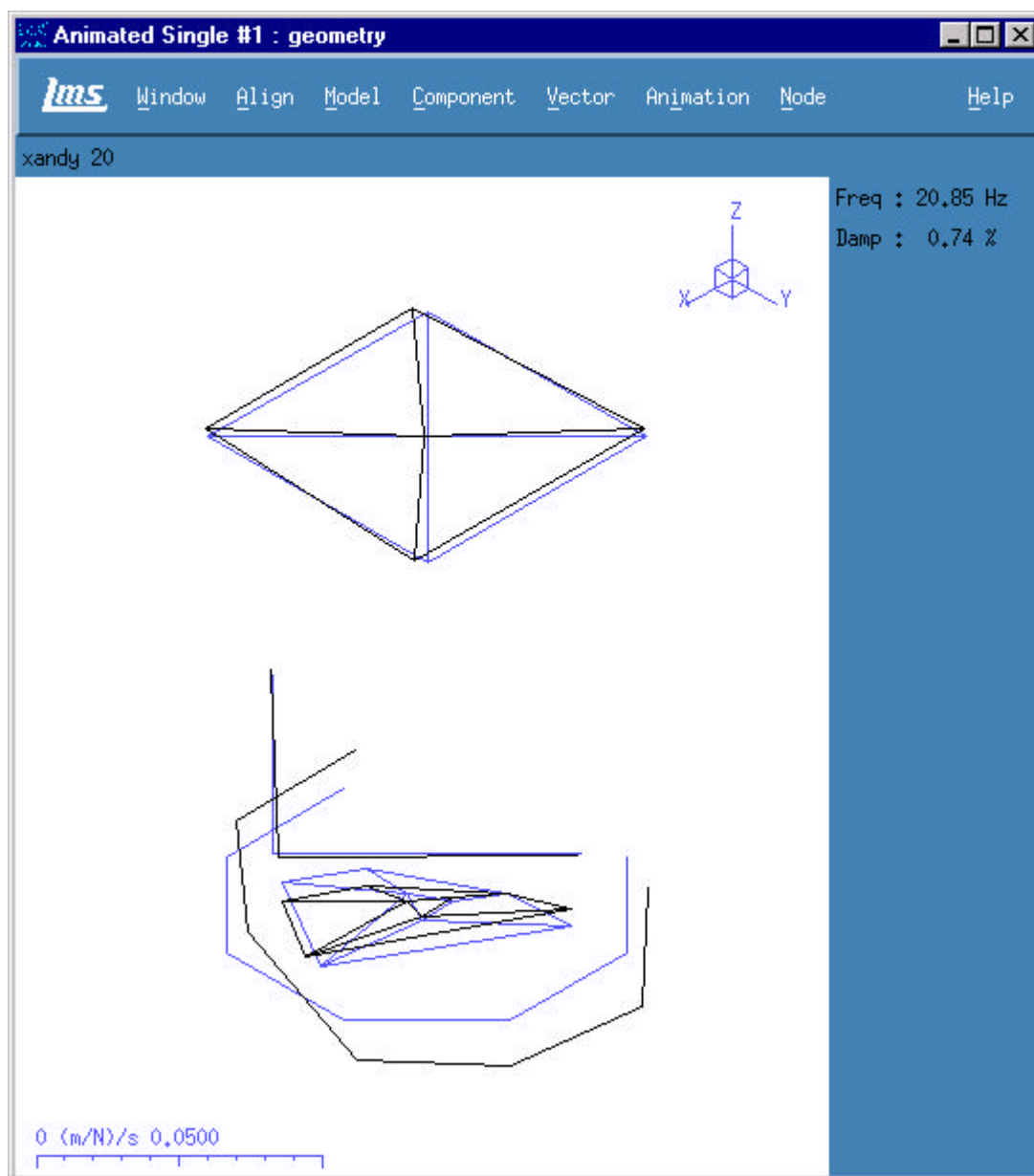


Mode Shape : 19.06Hz





## 8.0 Mode Shape Plots

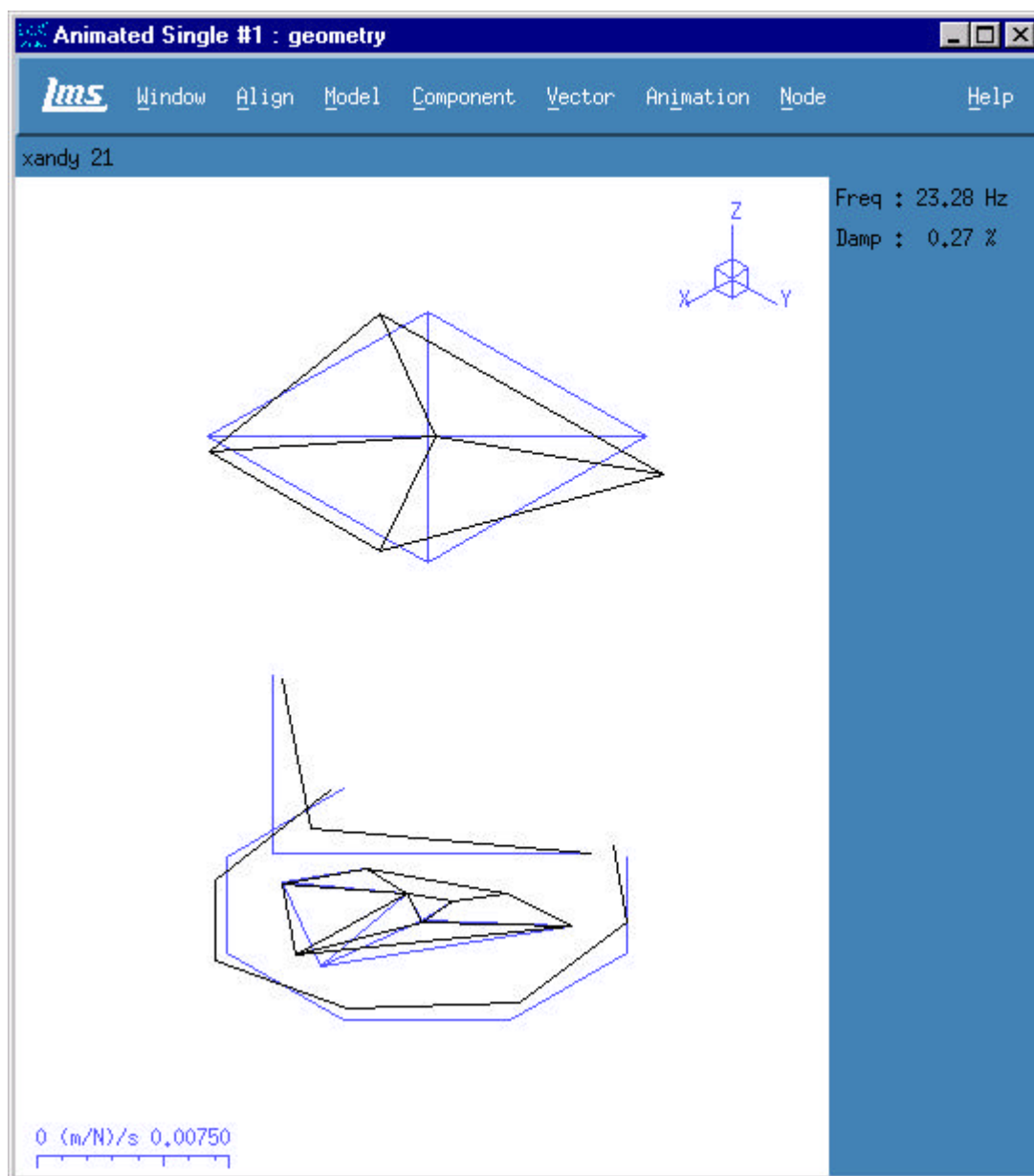


Mode Shape : 20.85Hz





## 8.0 Mode Shape Plots

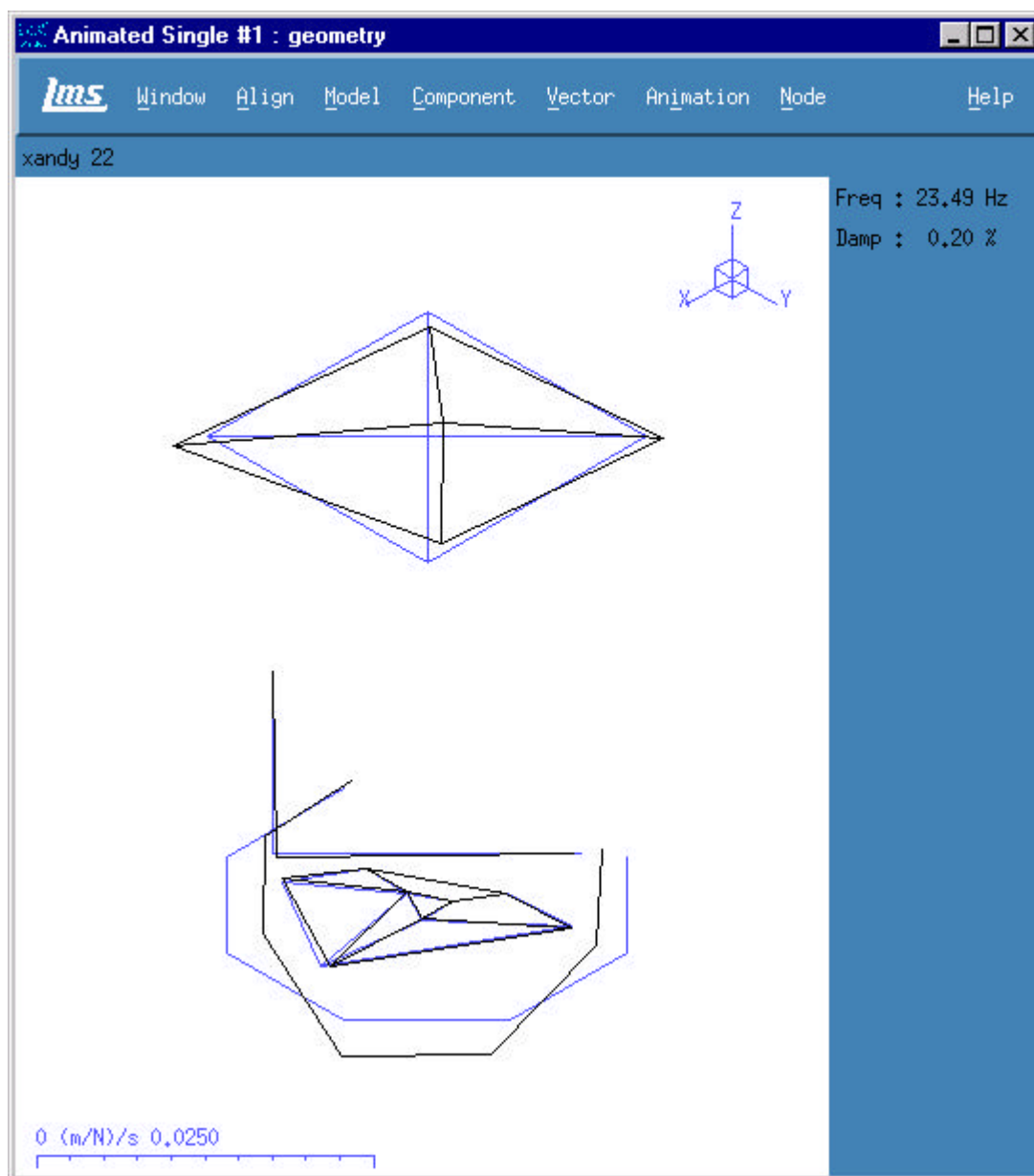


Mode Shape : 23.28Hz





## 8.0 Mode Shape Plots

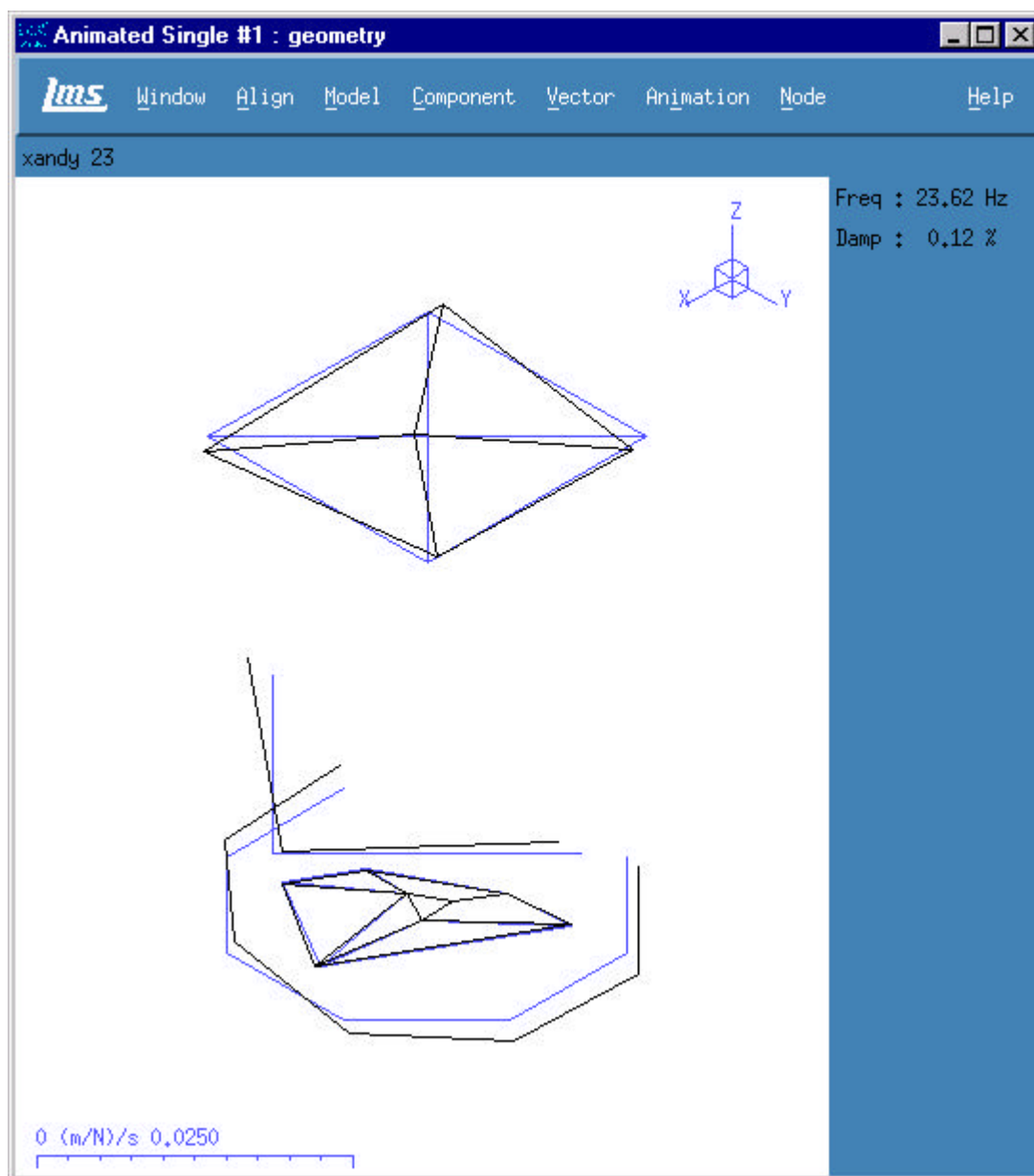


Mode Shape : 23.49Hz





## 8.0 Mode Shape Plots

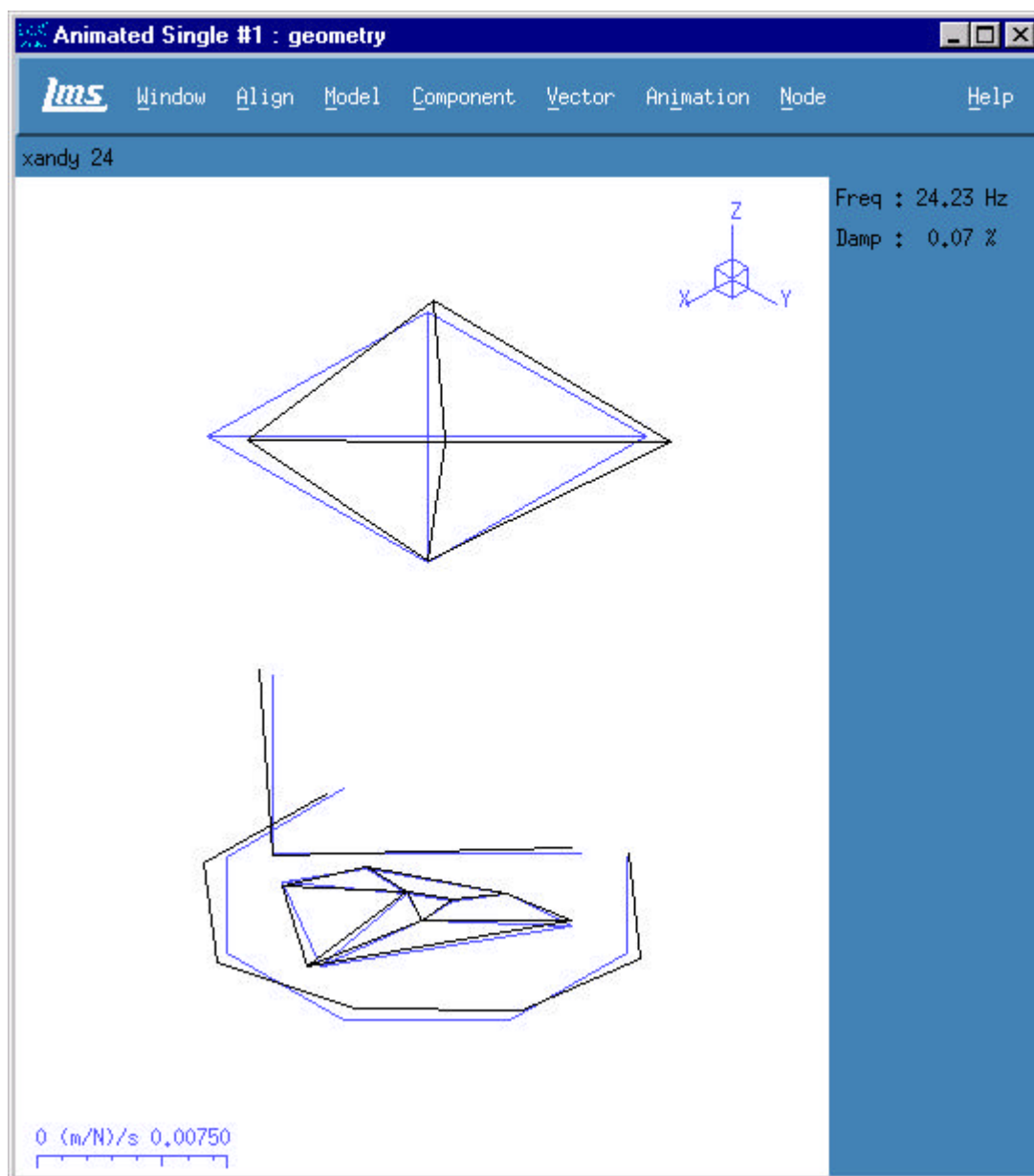


Mode Shape : 23.62Hz





## 8.0 Mode Shape Plots

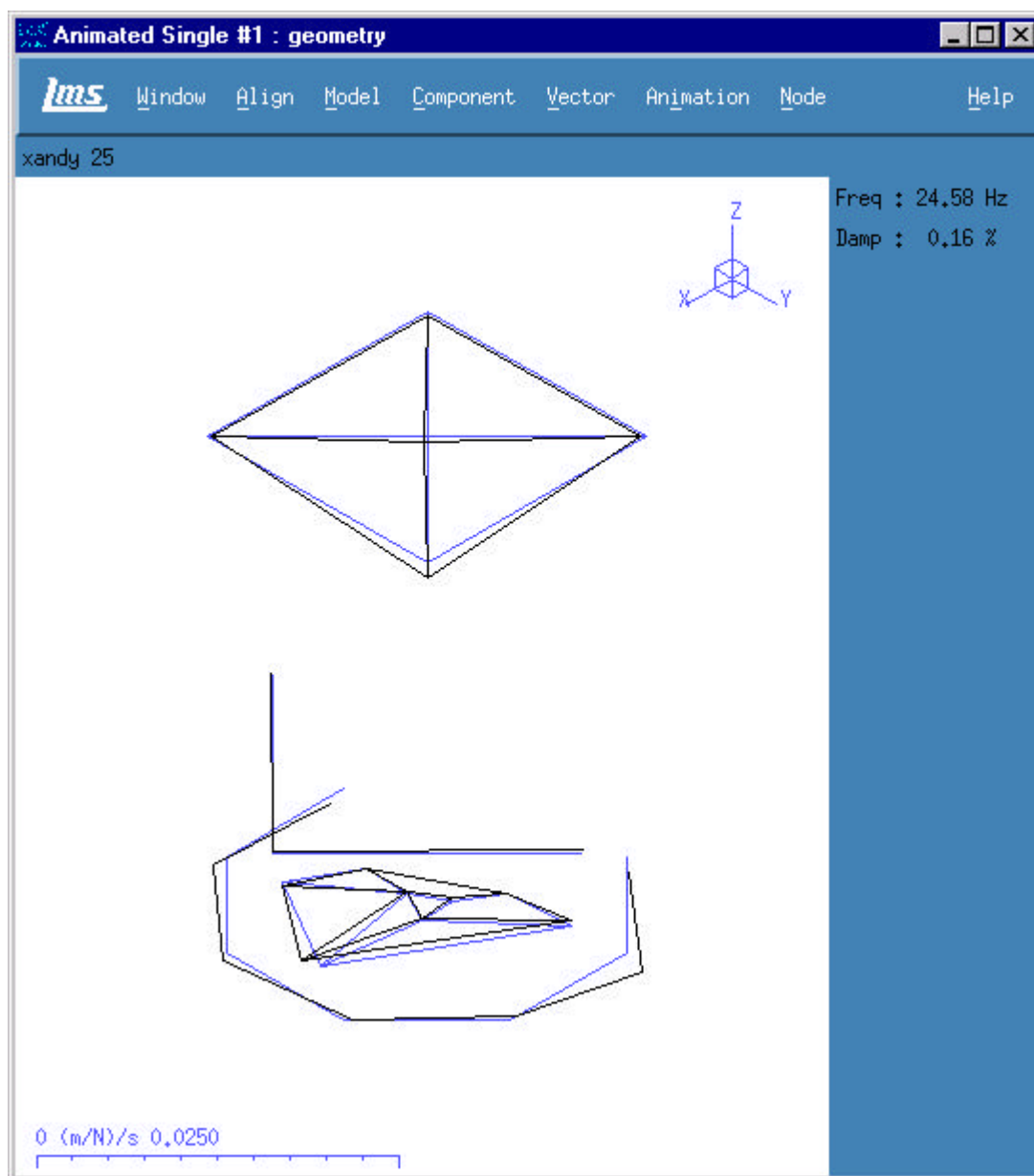


Mode Shape : 24.23Hz





## 8.0 Mode Shape Plots

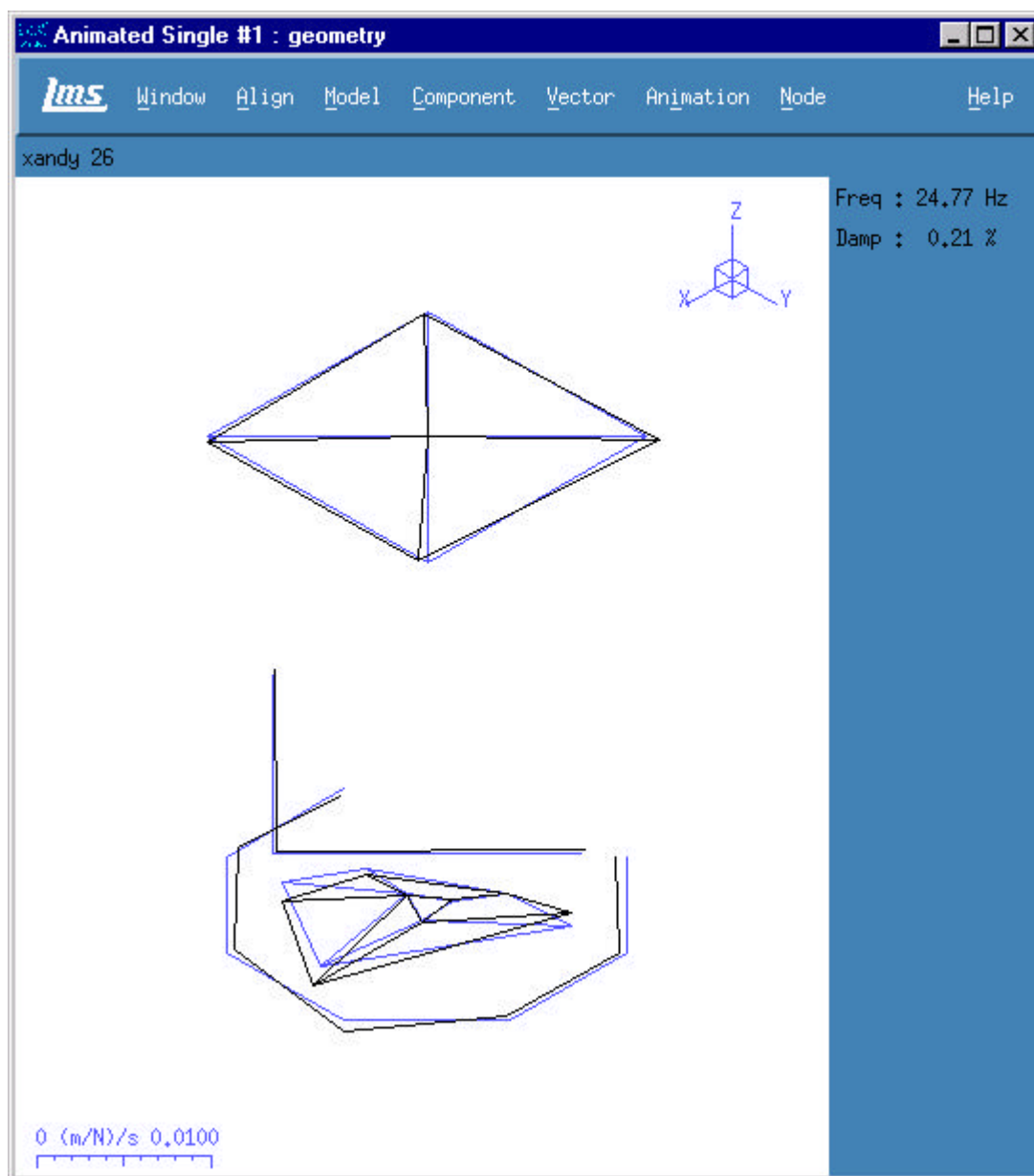


Mode Shape : 24.58Hz





## 8.0 Mode Shape Plots

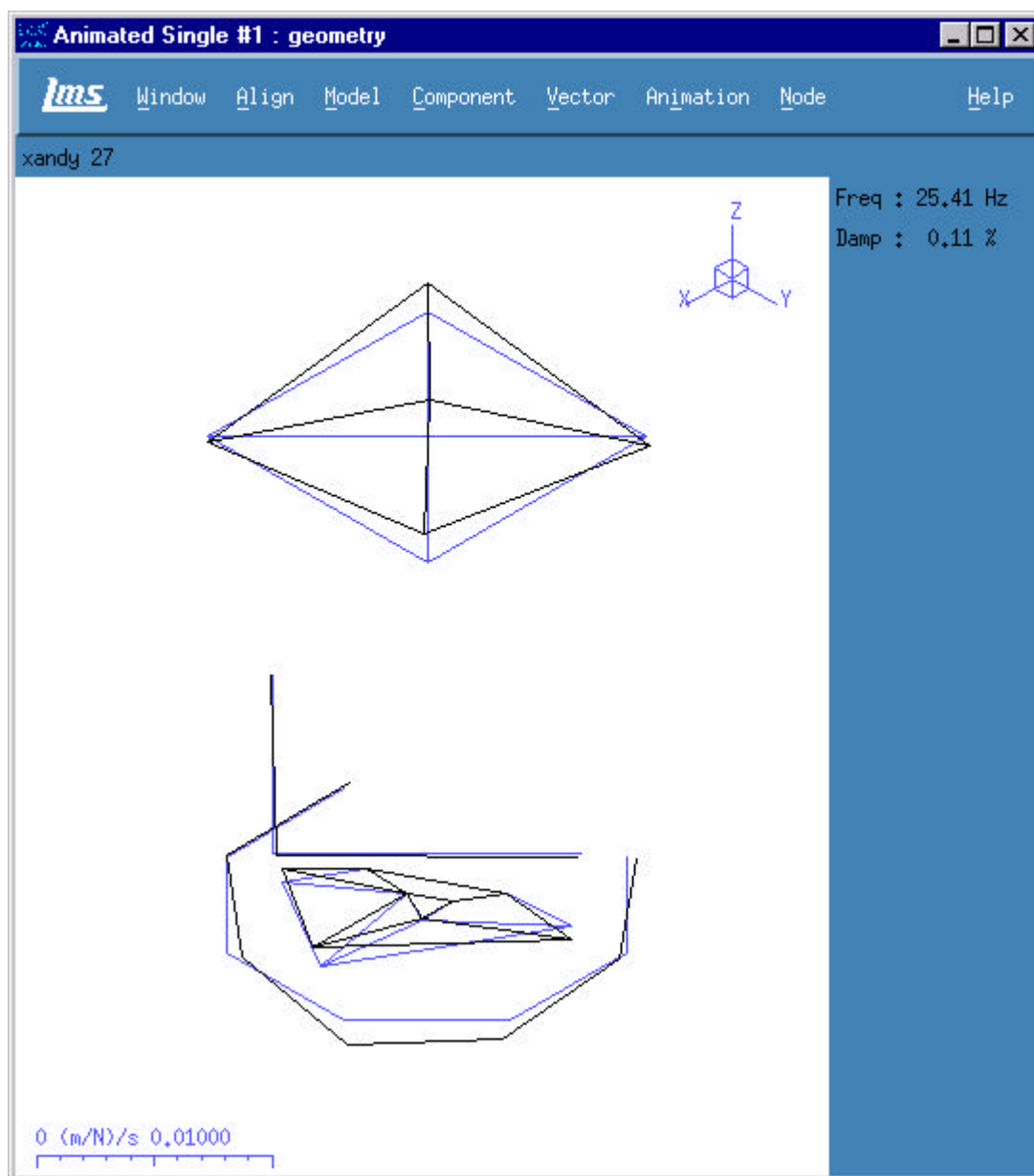


Mode Shape : 24.77Hz





## 8.0 Mode Shape Plots

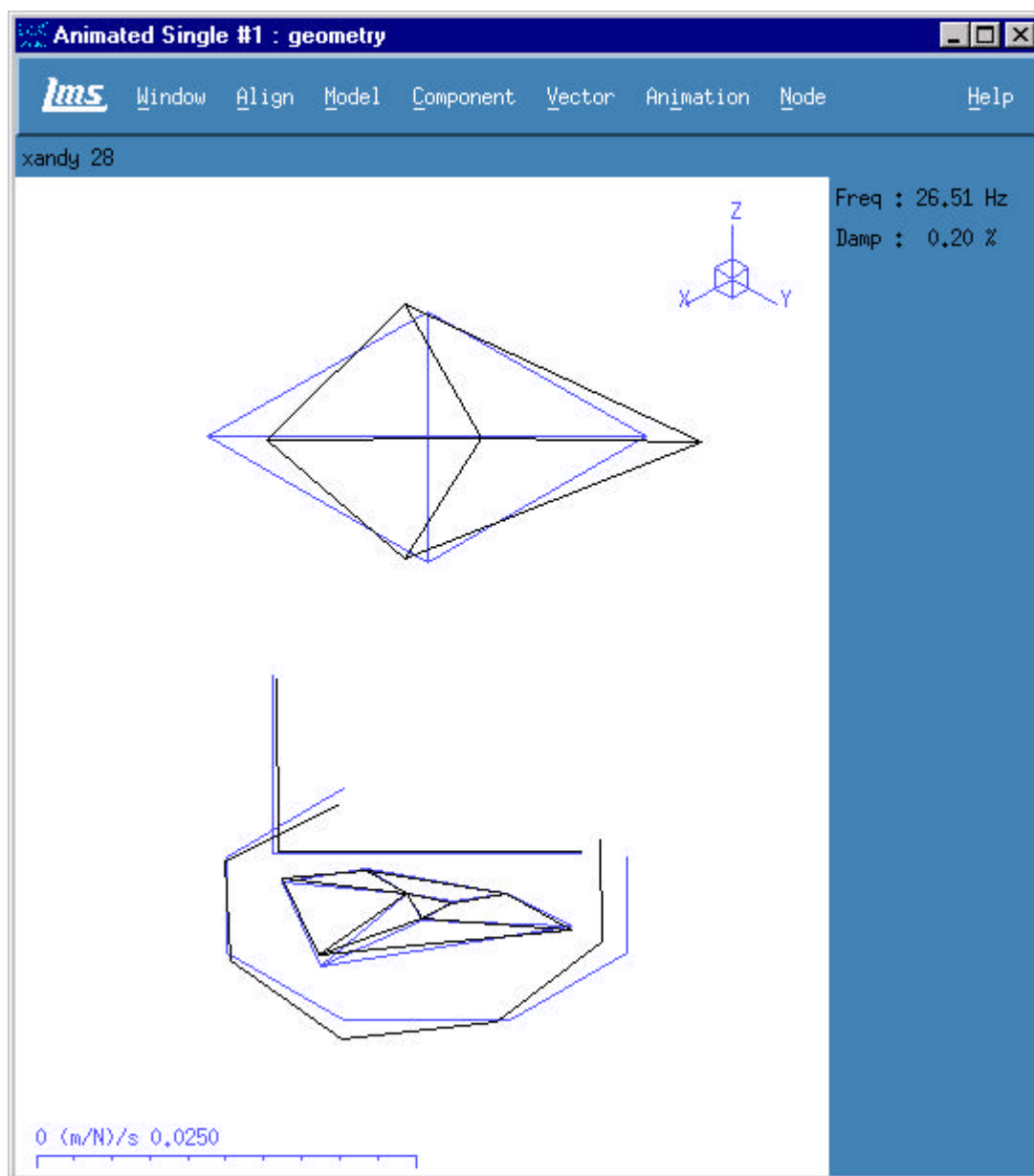


Mode Shape : 25.41Hz





## 8.0 Mode Shape Plots

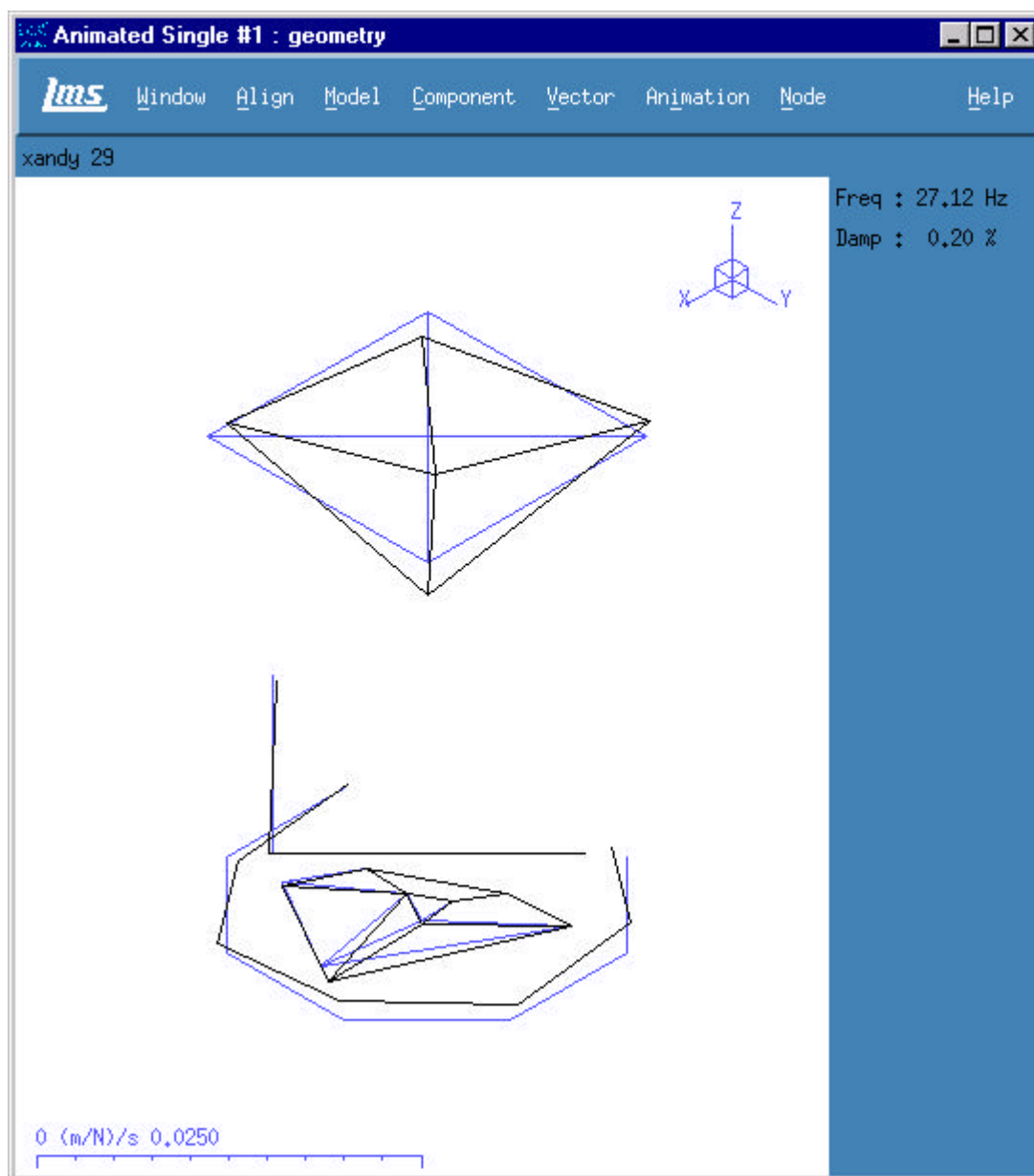


Mode Shape : 26.51Hz





## 8.0 Mode Shape Plots

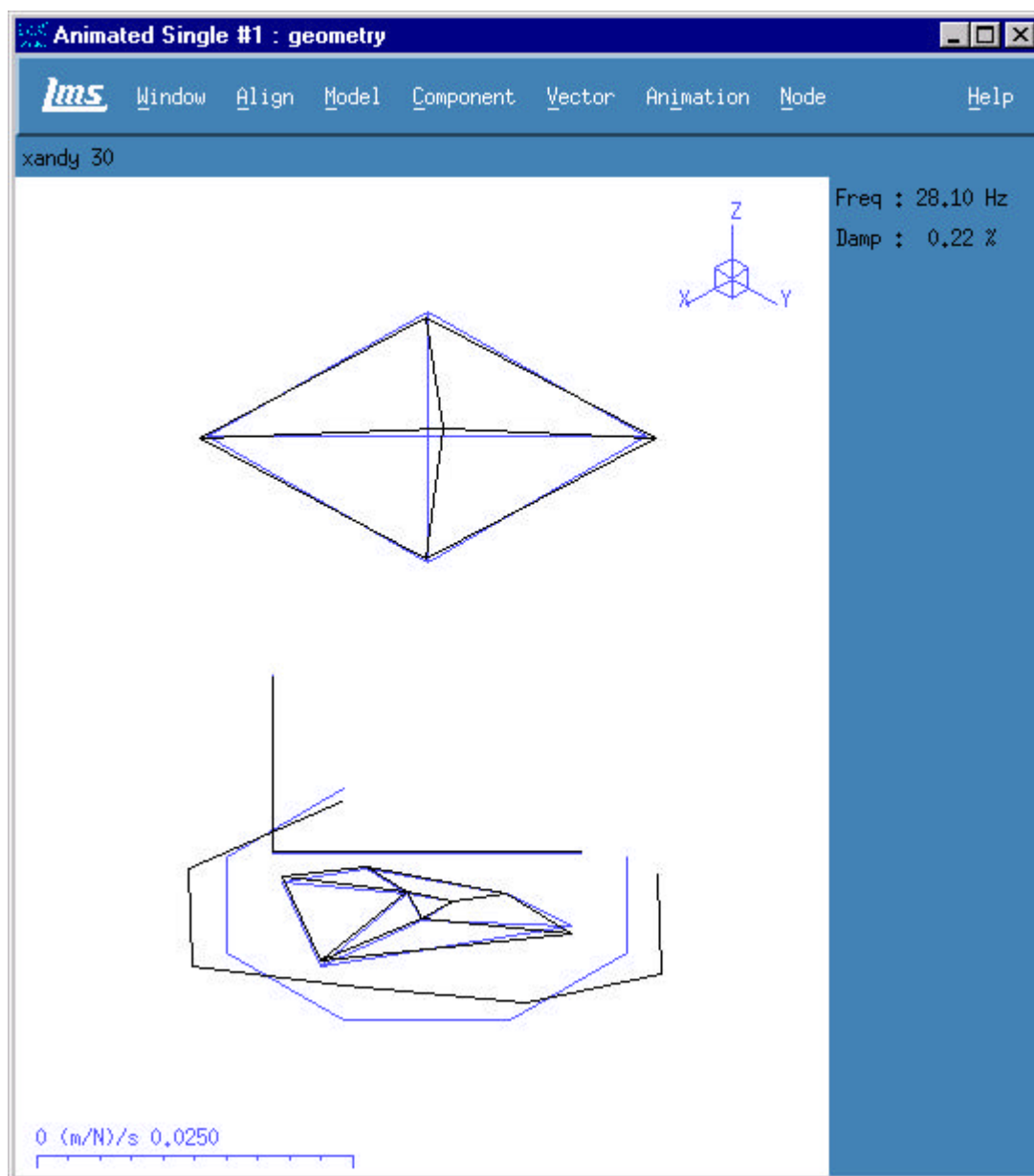


Mode Shape : 27.12Hz





## 8.0 Mode Shape Plots

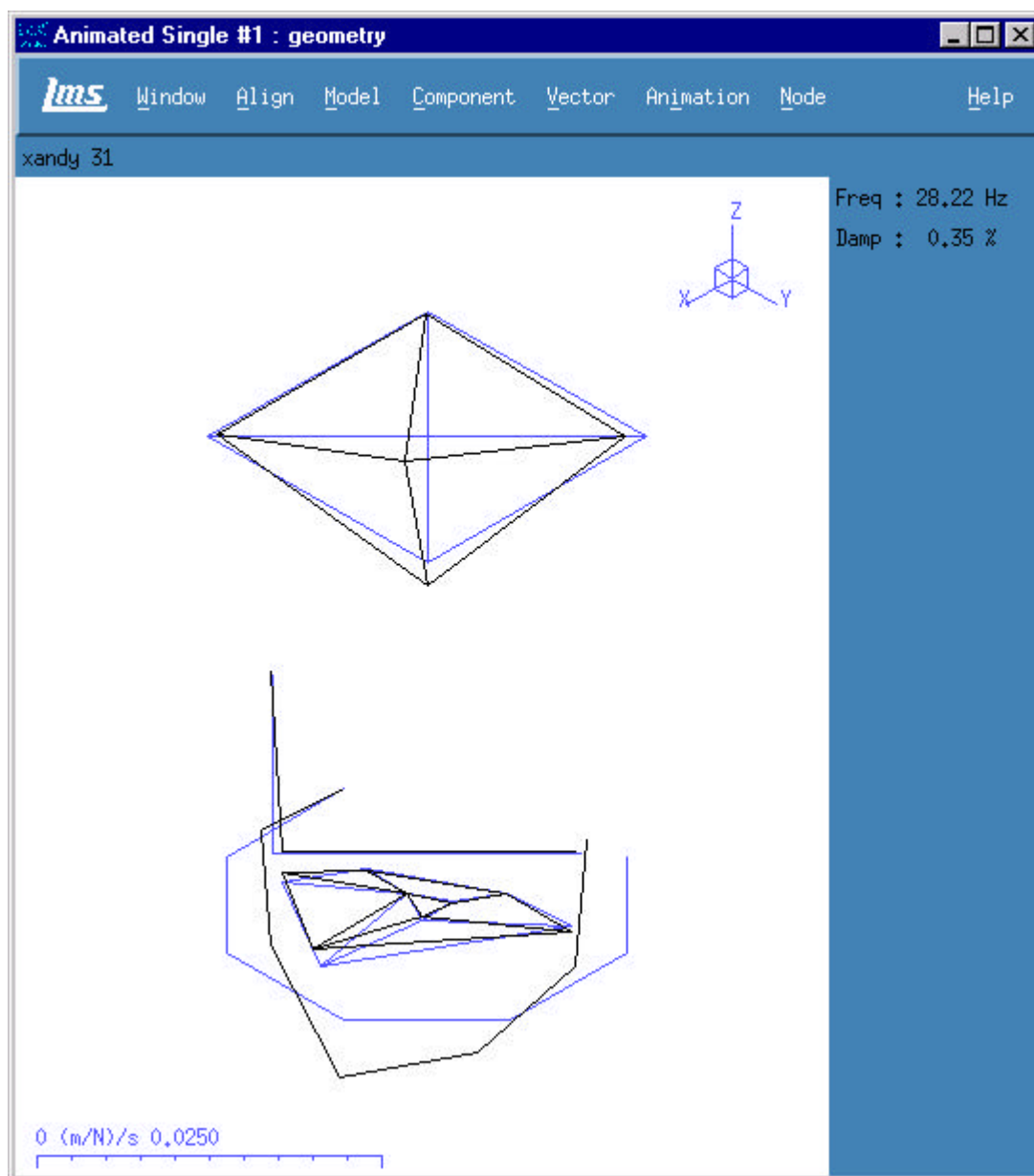


Mode Shape : 28.10Hz





## 8.0 Mode Shape Plots

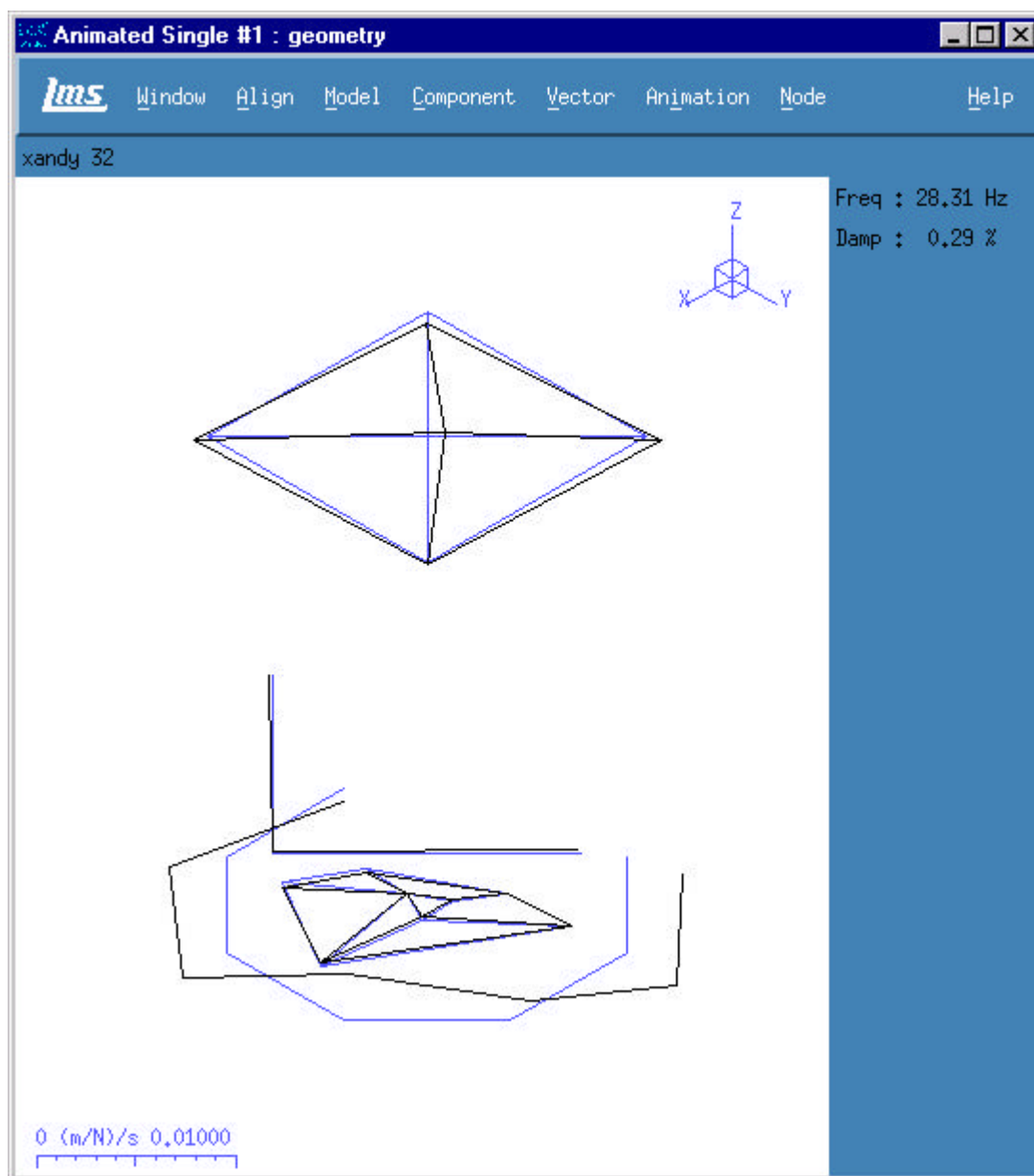


Mode Shape : 28.22Hz





## 8.0 Mode Shape Plots

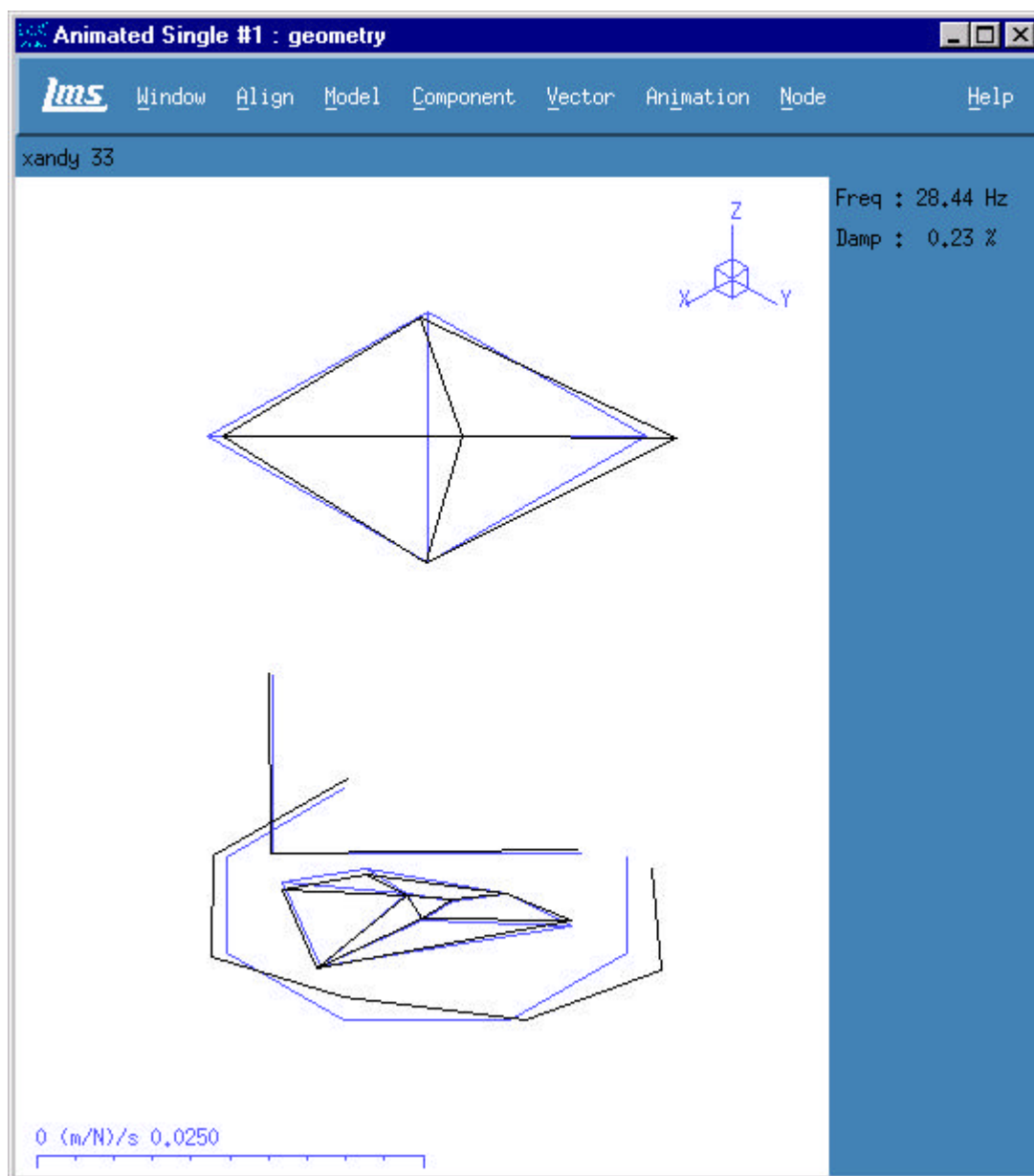


Mode Shape : 28.31Hz





## 8.0 Mode Shape Plots



Mode Shape : 28.44Hz



Modal Analysis and Controls Laboratory  
Mechanical Engineering Department  
University of Massachusetts at Lowell  
Lowell, Massachusetts

## **Gemini South 8m Optical Telescope**

### **Operating Test Report**

**MACL Report # 05-08570-005**

October 2000

Approved By: \_\_\_\_\_

Date: \_\_\_\_\_





## **Intent of Report**

This report addresses aspects of the analysis of the operating tests performed for the Gemini South 8m Optical Telescope in Cerro Pachon, Chile.







## Table of Contents

1.0 Administrative Data	
1.1 Purpose of Report	
1.2 Drawings	
1.3 Relevant Tests	
1.4 Test Log	
1.5 Dates of Test	
1.6 Tests Conducted By	
1.7 Analysis Performed By	
2.0 Summary of Testing	
3.0 Data Preparation	
4.0 Frequency Identification	
5.0 Reference Identification	
6.0 Operating Deflection Shape Analysis	
7.0 Results	
8.0 Data	
8.1 Drawings and Schematics	8.21 Test 36
8.2 Test 3	8.22 Test 37
8.3 Test 7	8.23 Test 38
8.4 Test 9	8.24 Test 39
8.5 Test 11	8.25 Test 40
8.6 Test 12	8.26 Test 41
8.7 Test 13	8.27 Test 42
8.8 Test 14	8.28 Test 43
8.9 Test 16	8.29 Test 44
8.10 Test 17	8.30 Test 45
8.11 Test 19	8.31 Test 46
8.12 Test 20	8.32 Test 47
8.13 Test 21	8.33 Test 48
8.14 Test 22	8.34 Test 49
8.15 Test 23	8.35 Test 50
8.16 Test 24	8.36 Test 51
8.17 Test 31	8.37 Test 52
8.18 Test 33	8.38 Test 53
8.19 Test 34	8.39 Test 54
8.20 Test 35	
9.0 References	
10.0 Operating Mode Shape Plots	





## **1.0 Administrative Data**

This section contains relevant information pertaining to the administration of the Operating Test Report.

### **1.1 Purpose of Report**

This report covers the detailed analysis of the operating data tests from the testing of the Gemini South 8m Optical Telescope on Cerro Pachon in Chile. Specifically, the report covers identification of dominant driven frequencies, selection of an appropriate reference, and extraction of characteristic operating deformation patterns.

### **1.2 Drawings**

Drawings and schematics of telescope and accelerometer locations are available in the Data Section 8.0 of this report.

### **1.3 Relevant Tests**

The tests used in this report and their configurations are compiled in Table 2.1. Testing geometry and other details for each of these is available in the Test Setup Report [2].

### **1.4 Test Log**

A logbook containing documentation of equipment used, transducer information, and test details for all tests conducted, is on file at the Modal Analysis and Controls Laboratory.





1.5 Dates of Tests

May 8-12, 2000

1.6 Tests Performed By

Peter Avitabile

Geoff Gwaltney

David Smith

Johann Teutsch

1.7 Analysis Conducted By

Keith Weech

Johann Teutsch





## **2.0 Summary of Testing**

The purpose of this analysis was to identify the characteristic operating frequencies and associated deformation patterns under typical operating conditions. This was accomplished by collecting accelerometer data of the Gemini South 8m telescope in a variety of configurations and wind loading. In all cases, operating data was collected from the accelerometers at a sample rate of 200Hz for an intended time of five minutes. The excitation of the structure is due to wind, external machinery, and other disturbances, and is not controlled. The resulting operating data provides detailed information about the actual deformations of the telescope structure in response to these excitations.

Only 38 tests of the total number possible of 44 tests have been analyzed here in this report. These tests, together with the corresponding wind angle of attack, telescope elevation angle, and position of the vent gates are summarized in Table 2.1. A complete listing of tests and configurations can be found in the Test Setup report [2]. The remaining 6 operating data tests were eliminated from the analysis, as described in the next section.





Table 2.1  
Test Configurations

ID	Elevation	Zenith	AoA	Upwind Gate	Downwind Gate	Fs (Hz)	Time
Test 03	60	30	0	Closed	Closed	200	300
Test 07	60	30	0	Open	Open	200	300
Test 09	60	30	45	Open	Closed	200	300
Test 11	30	60	45	Closed	Closed	200	300
Test 12	30	60	45	Open	Open	200	300
Test 13	30	60	0	Open	Closed	200	300
Test 14	30	60	0	Closed	Open	200	300
Test 16	30	60	90	Half	Half	200	300
Test 17	30	60	180	Open	Open	200	300
Test 19	45	45	90	Open	Closed	200	300
Test 20	45	45	0	Half	Open	200	300
Test 21	60	30	0	Closed	Closed	200	300
Test 22	60	30	0	Closed	Half	200	300
Test 23	60	30	90	Closed	Open	200	300
Test 24	60	30	180	Half	Closed	200	300
Test 31	60	30	0	Open	Open	200	300
Test 33	60	30	0	Closed	Open	200	300
Test 34	60	30	45	Closed	Closed	200	300
Test 35	60	30	45	Open	Open	200	300
Test 36	30	60	45	Open	Closed	200	300
Test 37	30	60	0	Closed	Open	200	300
Test 38	30	60	0	Closed	Closed	200	300
Test 39	30	60	0	Open	Open	200	300
Test 40	75	15	45	Closed	Closed	200	300
Test 41	75	15	90	Half	Half	200	300
Test 42	75	15	135	Open	Open	200	300
Test 43	45	45	135	Closed	Half	200	300
Test 44	45	45	90	Open	Closed	200	300
Test 45	45	45	90	Open	Half	200	300
Test 46	45	45	90	Open	Open	200	300
Test 47	45	45	45	Half	Open	200	300
Test 48	30	60	45	Open	Half	200	300
Test 49	30	60	90	Closed	Open	200	300
Test 50	30	60	135	Half	Closed	200	300
Test 51	30	60	45	Open	Open	200	300
Test 52	45	45	45	Open	Open	200	300
Test 53	60	30	45	Open	Open	200	300
Test 54	75	15	45	Open	Open	200	300





Due to the 200 Hz sample rate, the data contains information about frequencies up to 100 Hz. However, for this report only frequencies less than 30 Hz have been examined. Higher frequencies, while clearly visible in the data, correspond to displacements that are insignificant to the performance of the telescope.

The data was collected in two sets. The first set of tests was taken before the impact testing, and consists of 74 channels of accelerometers. For the second set of tests, the acquisition system was reconfigured, eliminating four tri-axial measurements at the outer weldment to allow measurement of some external pressure transducers. This reduced the number of accelerometers to 62 output channels.





### **3.0    Data Preparation**

The original time data sets were modified using the techniques discussed in the Data Cleansing Report [3]. These time data sets were then transformed to the frequency domain by calculating the auto power spectrum for each channel in each of the tests. The auto powers were calculated utilizing a Hanning window, with 50% overlap of sample blocks. Each time data record was divided into 2048 block size samples of 10.24 seconds in length; this provided a frequency resolution of 0.098Hz. With this block size and the full number of 60000 samples, 57 separate averages can be obtained. This will reduce the effects of random noise and enable better identification of the resonant frequencies of the telescope.

The frequency domain representation allowed an additional examination of data quality. A number of channels were revealed to exhibit a behavior dominated by a  $1/f$  frequency response or no input. These bad channels were identified for each test and are noted in the Data Cleansing Report [3]. These bad channels were not used in further analyses. For several tests (Tests 1, 10, 5, and 6), there were a substantial number of bad channels (greater than 30%). These tests were eliminated from further analysis because they did not contain enough relevant degrees of freedom to allow meaningful comparison with other tests

An unusual and unexplainable event happened on a number of tests. A spike or sudden change in voltage is seen in the time trace. This spike is at a consistent time for all response channels of the effected tests. Some of the tests that were identified with these spikes were used in the analysis. The tests with spikes that were used (Tests 12, 35, 42, 44, 53 and 54) contained enough good data (over two thirds of the entire time trace) that a sufficient number of averages could be obtained to reduce the noise effects while retaining the frequency resolution





desired (0.098Hz). Two of the affected tests (Test 15 and 18) were eliminated due to multiple spikes in the time traces. These tests, that would have had fewer than thirty averages, have been eliminated from analysis here to provide the most consistent comparison of data.





## 4.0 Frequency Identification

For each test, the set of good auto power spectra was divided into the significant components of the telescope structure. These components include:

1. The upper ring of the secondary support structure (nodes 1 – 9)
2. The primary mirror (points 31 - 49)
3. The octagonal outer weldment (nodes 10 - 17).

The frequency responses from these separate components were summed together. The summed spectrum was then examined for peaks throughout the 0 to 30Hz bandwidth. A list of the dominant peaks for the secondary structure and the primary mirror components for each test is listed in the Data Section 8.0 of this report. The number of peaks observed in the summed spectra of the tests varies due to different configuration and input wind energy. However, certain frequencies of large output were evident in all components and all tests. A list of these dominant frequency bands is listed in Table 4.1.

Table 4.1  
Frequency Bands of Significant Deformation

1.6 – 1.9 Hz	20.7 – 21.0 Hz
3.2 – 4.1 Hz	21.8 – 22.0 Hz
7.0 – 7.2 Hz	23.2 – 23.6 Hz
8.0 – 8.2 Hz	24.4 – 24.8 Hz
9.0 – 9.2 Hz	24.9 – 25.1 Hz
10.5 – 10.7 Hz	25.3 – 25.5 Hz
11.0 – 11.2 Hz	25.8 – 26.0 Hz
12.1 – 12.9 Hz	26.4 – 26.6 Hz
13.2 – 14.0 Hz	27.1 – 27.4 Hz
14.9 – 15.1 Hz	27.6 – 27.8 Hz
16.1 – 16.3 Hz	28.0 – 28.6 Hz
17.2 – 18.0 Hz	29.1 – 29.4 Hz
19.0 – 19.2 Hz	





## 5.0 Reference Identification

In order to analyze the operating responses of the telescope, deformation patterns of the structure under typical operating conditions are necessary. To accomplish this, the output spectra must be compared to some common reference to show the relative displacement and phase between the measurement points. A complete method of pursuing this would be to use every output as reference and to treat the test as a multiple input test with the number of inputs equal to the number of responses. However, such an analysis is unwieldy and unnecessary.

The data in this analysis has many nearly redundant responses that show the same peaks in the data. To reduce the amount of computational time required to analyze the data, several tests were examined in detail to find a common reference that displayed the dominant peaks for all channels of those tests. This was done by choosing a set of typical responses from a number of channels about the structure. The reference response channels that were used in the selection process are listed in Table 5.1.

Table 5.1  
List of Predicted Good Reference Channels

3xy
4xy
5xyz
11xyz
38xz

The full response matrix of the channel's responses was generated using the Matrix Toolbox from LMS CADA-X [10]. The cross power matrix was decomposed by means of a singular value decomposition (SVD) to show the predominate peaks at common frequencies throughout this set of channels. The full response matrix for this set of channels was then processed as described next.





This process was accomplished by removing sets of references and responses from the full set of channels, and subsequently performing singular value decomposition (SVD) on the resulting reduced order matrices. The greatest singular value responses of these matrices were then compared to each other. The goal of this process was to find a single reference choice that could represent all of the peaks observed from the auto power analysis. When such a channel is removed from the matrix, it results in the ‘loss’ of one or more peaks from the response. A typical graph of the reference selection process is shown below in Figure 5.1.

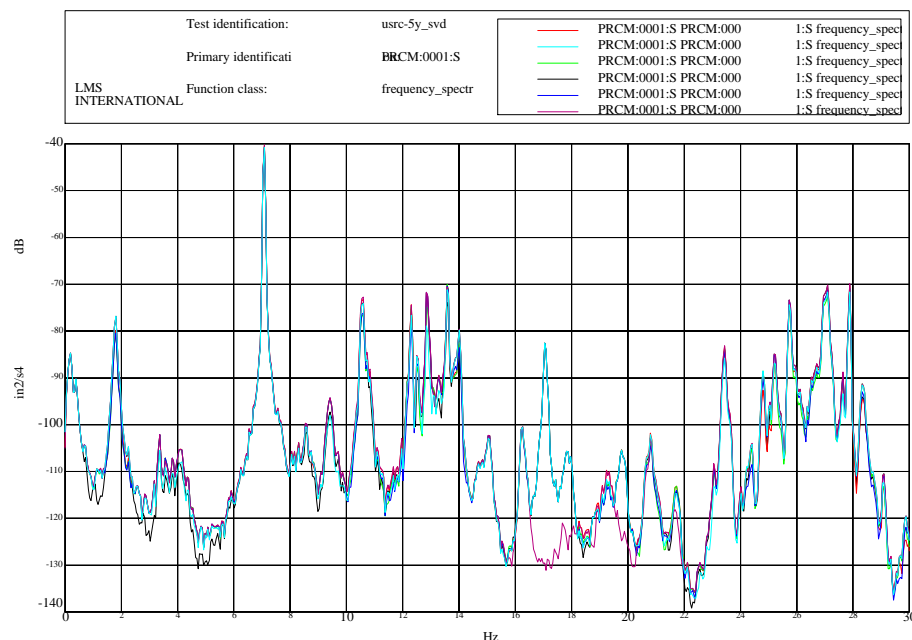


Figure 5.1 - Singular Values of Reduced Matrices

From this analysis, the response from the secondary support tube (node #5) was found to show all of the dominant peaks in the zero to 30 Hz range found in the auto power analysis. In particular, the Z direction in this point displayed obvious peaks in the frequency ranges as seen in the auto power analysis as well as those predicted as modes from the modal impact tests [4]. As a result, this reference





was used for a reference for most of the tests. However, for some of the tests (Tests 3, 7 and 21), this channel was found to be of poor quality (bad channel or extremely low response), a secondary reference was chosen from the predicted set of good references to generate useful cross power spectra to analyze the shapes of these peaks in the frequency domain. The reference channel and configuration for each test is included in the Data Section 8.0 of this report.





## **6.0 Operating Deflection Shape Analysis**

Using the chosen single reference (node 5 in the Z direction or secondary choice), the tests were processed using the Time Domain Test Monitor [11] analysis package from LMS. The cross power spectra were generated to define operating shapes of the structure at the peaks shown in the auto power frequency domain as well as modes from the Modal Test Report [4]. For each test, a list of poles used to calculate the shapes is provided in the Data section of this report. These analyses were then compared to other operating tests of varying configurations.

The following is list of observations of shapes at peak frequencies in sequential order.

- The lowest operational deformation shape seen throughout all the tests for all configurations was a nodding mode or first bending in the y direction of the entire structure in the range of 1.7 to 2 Hz
- A hopping motion of the weldment and primary surface was seen in the 3.2 to 3.6 Hz range
- A hopping motion of the weldment and primary surface with an added rocking component in the X was observed in the 4 to 4.2 Hz range.
- One of the more dominant operating responses occurs at the 7-8 Hz band. This shape is localized in the upper secondary (nodes 1 – 5) and appears to be flexing shape (top diamond-ing back and forth) of the upper secondary with a translation in the X direction of the center (node 5). This deformation pattern is seen in all of the tests analyzed.





- A similar diamond shape flexing of the lower secondary (nodes 6-9) in the 8.5 to 8.9 Hz range.
- In the 10.8 to 11 Hz range, the observed deformation pattern is characterized by a rocking of the primary surface about the X-axis (in the Y direction).
- A similar shape but with the primary rocking about the Y-axis (X direction) was found about 12.2 Hz.
- The next set of shapes are tightly packed in the 13 to 15 Hz frequency range. The shapes appear to be closely related. These shapes are difficult to describe but in general have a rocking and platter rolling of the primary surface and an expansion flexing of the secondary structure characterize these deformation patterns.
- A strong response at the 17.1 Hz range corresponds to a pistoning shape of the primary and weldment (in phase) and a pistoning of the upper secondary counter to the lower structure ( $180^\circ$  out of phase).
- In the 17.8Hz area a similar pistoning of the upper secondary and weldment ( $180^\circ$  out of phase) and rocking of the primary about an axis rotated  $45^\circ$  clockwise from the X-axis.
- Another pistoning deformation pattern in the 18.7 to 18.9 Hz frequency band. This deformation is characterized by the upper secondary and the





primary moving (up and down) in phase while the weldment is  $180^\circ$  out of phase.

- A torsional deformation pattern of the secondary (the upper secondary twisting about the Z axis) was observed in the 19 to 19.2 Hz band with a translation of the primary moving up and down.
- The shape observed was a rocking of the weldment at 20.6 Hz.
- The next group of shapes was found in the range greater than 22 Hz upper to the 30 Hz limit. These shapes, while distinct peaks were shown, are difficult to separate and appear as combinations of lower frequency operating shape due to the lack of spatial resolution. These shapes could be better identified and characterized if more responses were taken during the time of the testing.

A list of the poles for each test analyzed is include in Data Section 8.0 at the end of this report.





## **7.0 Results**

The operating shapes extracted from this analysis have identified the more predominate deformation patterns of the telescope in the 0 to 30Hz bandwidth. The operating analysis suggests that for similar configurations, operating shapes and frequencies compare favorably. Also, that for significantly different configurations of the telescope that a frequency shift corresponding to similar operating shapes would occur. Wind direction and vent gate position had little affect on the frequencies at which deformation patterns were observed, but did have an affect on which of the operating shapes would be excited and the strength of those responses.





## 8.0 Data

The following is a list of the results for each of the test analyzed. For a list of bad channels for each test refer to the Data Cleansing Report attached [3].

### 8.1 Telescope Schematic

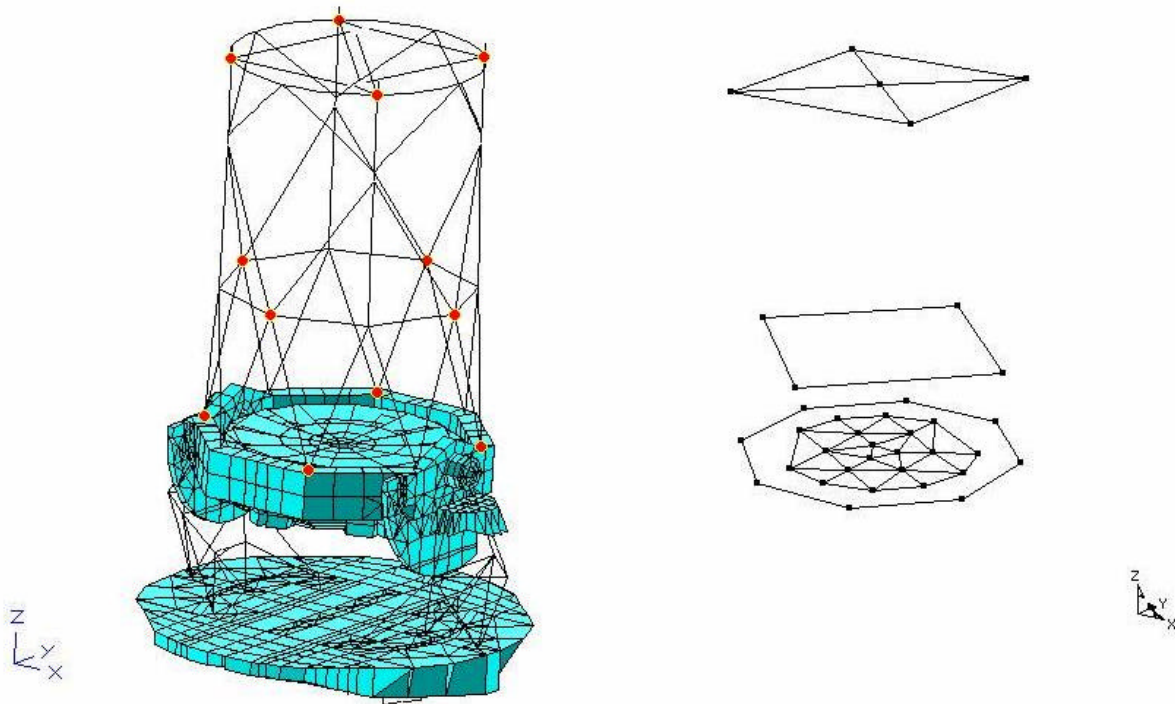


Figure 8.1  
Diagram of Gemini Telescope  
and the  
Accelerometer Locations

## Key to Test Code

(Reference Channel / Elevation / Zenith / Angle of Attack / Upwind Gate / Downwind Gate)





8.2 Test #3 – (5y / 60° / 30° / 0° / Closed / Closed)  
(Reference Channel / Elevation / Zenith / Angle of Attack / Upwind Gate / Downwind Gate)

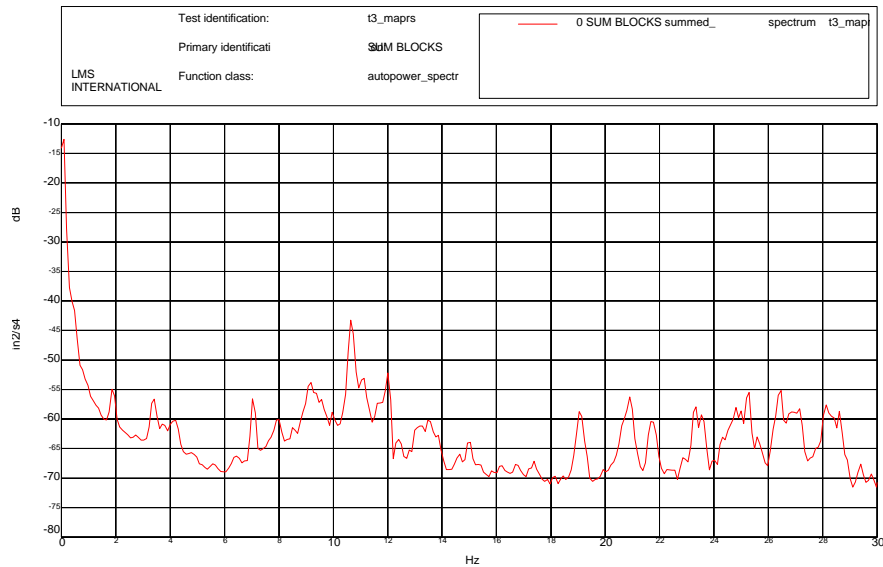


Figure 8.2.1  
Test #3 - Summed Auto Powers of the Secondary

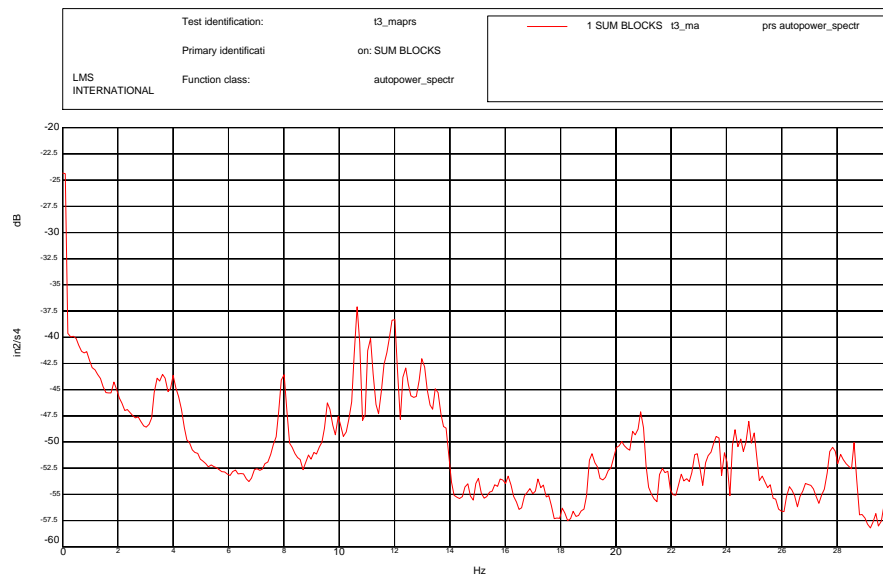


Figure 8.2.2  
Test #3 - Summed Auto Powers of the Primary





Table 8.2.1  
Test #3 - Peaks in the Auto Power Summation by Component

Secondary	Primary	Secondary	Primary	Secondary	Primary
1.855	1.855	13.867			22.949
3.418	3.418	14.648	14.648	23.34	
	3.613	15.039	15.039	23.535	
3.711			16.113		23.633
	4.004	16.211			23.926
4.199		16.699		24.023	
7.031			16.895	24.316	24.316
8.008	8.008		17.188		24.512
8.496		17.383		24.805	24.805
9.18			18.066	25	
9.57	9.57	19.043		25.293	
9.961	9.961		19.141	25.586	
10.645	10.645		20.215		26.27
11.133	11.133		20.605	26.465	
12.012	12.012	20.898	20.898		26.855
12.402	12.402	21.68	21.68	27.148	
	12.989		21.875		27.832
13.281			22.363	28.125	28.125
13.477		22.852		28.613	28.613

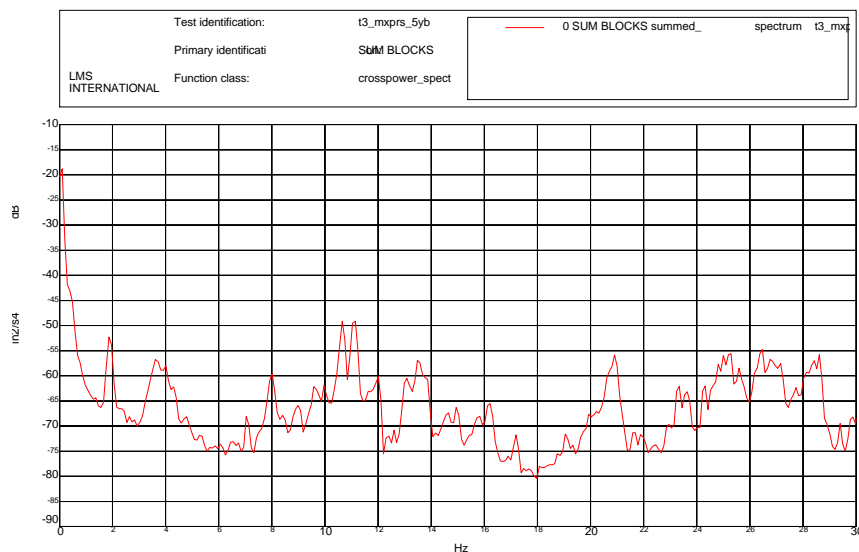


Figure 8.2.3  
Test #3 - Summed Cross Powers





Table 8.2.2  
Test #3 - Peaks in Cross Power

Frequency (Hz)	
1.86	23.34
3.61	23.63
4.0	24.32
8.01	24.8
10.64	25.0
11.13	25.29
13.48	25.59
14.94	26.46
16.21	26.76
17.19	27.15
19.04	28.42
20.9	28.61





### 8.3 Test #7 – (5y / 60° / 30° / 0° / Open / Open) (Reference Channel / Elevation / Zenith / Angle of Attack / Upwind Gate / Downwind Gate)

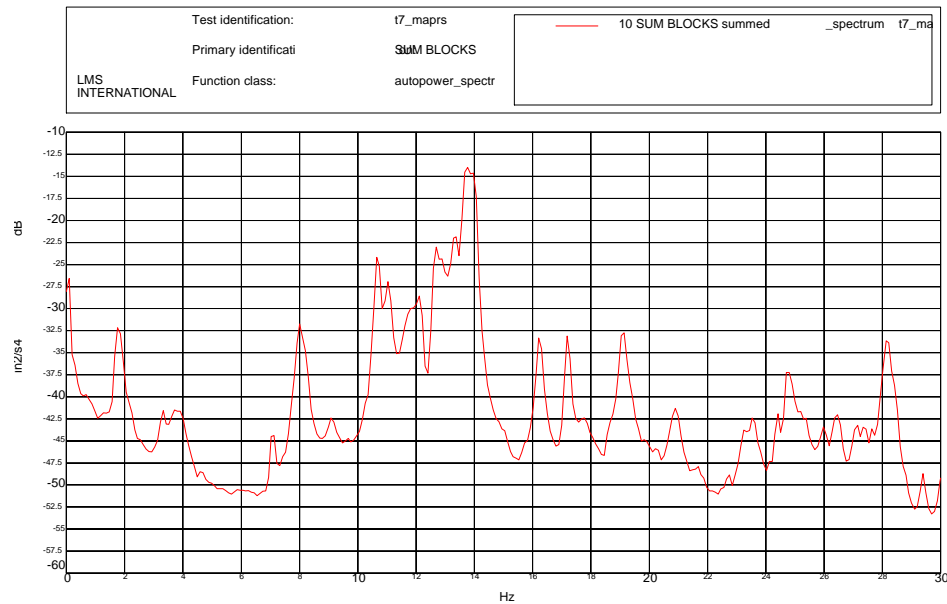


Figure 8.3.1  
Test #7 - Summed Auto Power of the Secondary

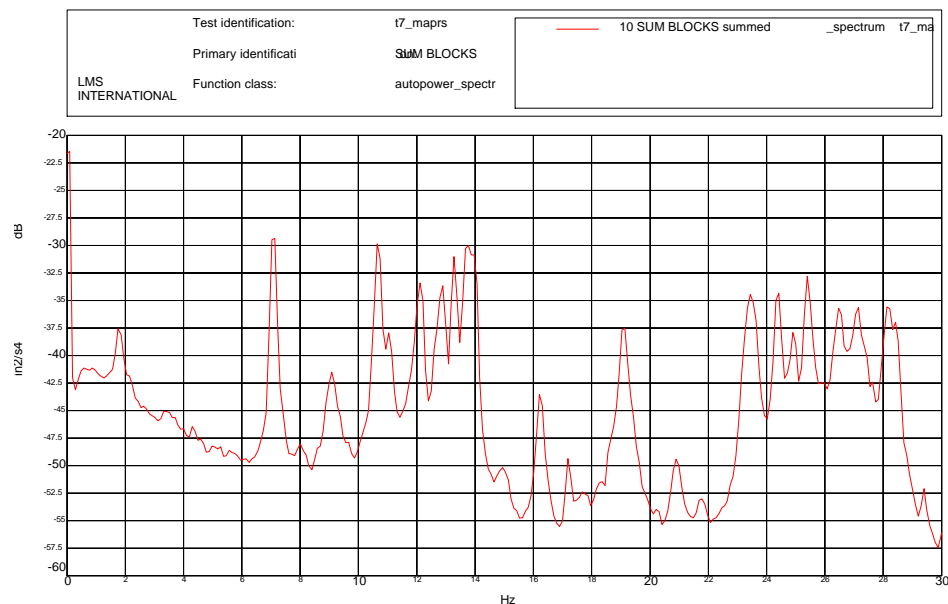


Figure 8.3.2  
Test #7 - Summed Auto Powers of the Primary





Table 8.3.1  
Test #7 - Peaks in the Auto Power Summation by Component

Secondary	Primary	Secondary	Primary	Secondary	Primary
1.758	1.758		13.379		24.707
3.32	3.32	13.77	13.77	24.902	
	3.711		13.965		25.195
3.906	3.906	14.941		25.391	25.391
7.129	7.129	16.211	16.211	25.977	25.977
8.008	8.008	17.188	17.188	26.465	26.465
9.082	9.082	19.141	19.141	27.148	27.148
10.645	10.645	20.898	20.898	27.344	27.344
11.035	11.035	21.77			27.637
12.109	12.109		23.242	28.125	28.125
	12.695	23.438		28.418	
12.891	12.891		23.535	29.395	29.395
13.281		24.414	24.414		

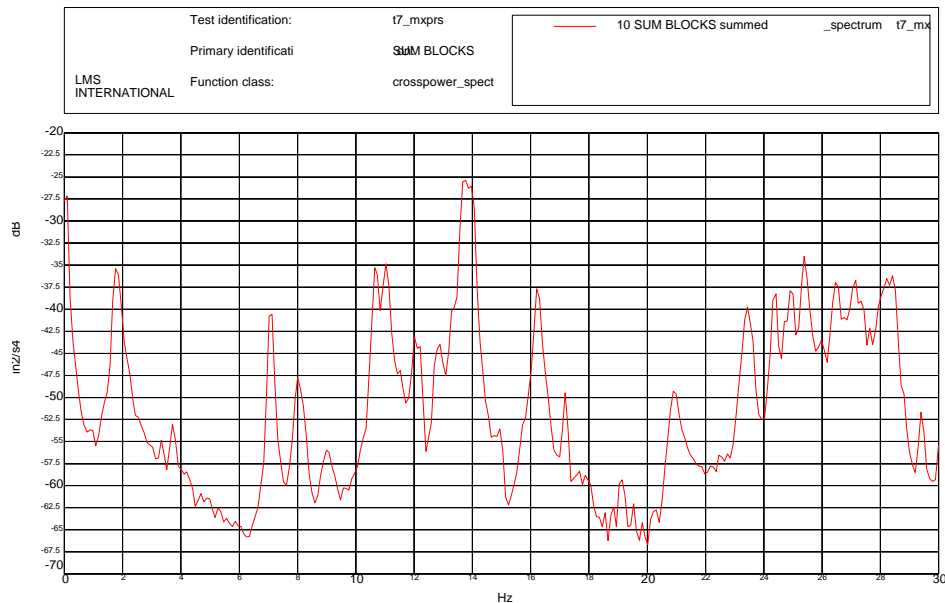


Figure 8.3.3  
Test #7 - Summed Cross Powers





Table 8.3.2  
Test #7 – Peaks in Cross Power

Frequency (Hz)	
1.76	16.21
3.32	17.19
3.71	19.14
7.13	20.90
8.01	23.44
8.98	24.41
10.64	24.9
11.04	25.39
12.01	26.46
12.21	27.15
12.89	28.22
13.77	28.42
13.96	29.39
14.94	





#### 8.4 Test #9 – (5z / 60° / 30° / 45° / Open / Closed) (Reference Channel / Elevation / Zenith / Angle of Attack / Upwind Gate / Downwind Gate)

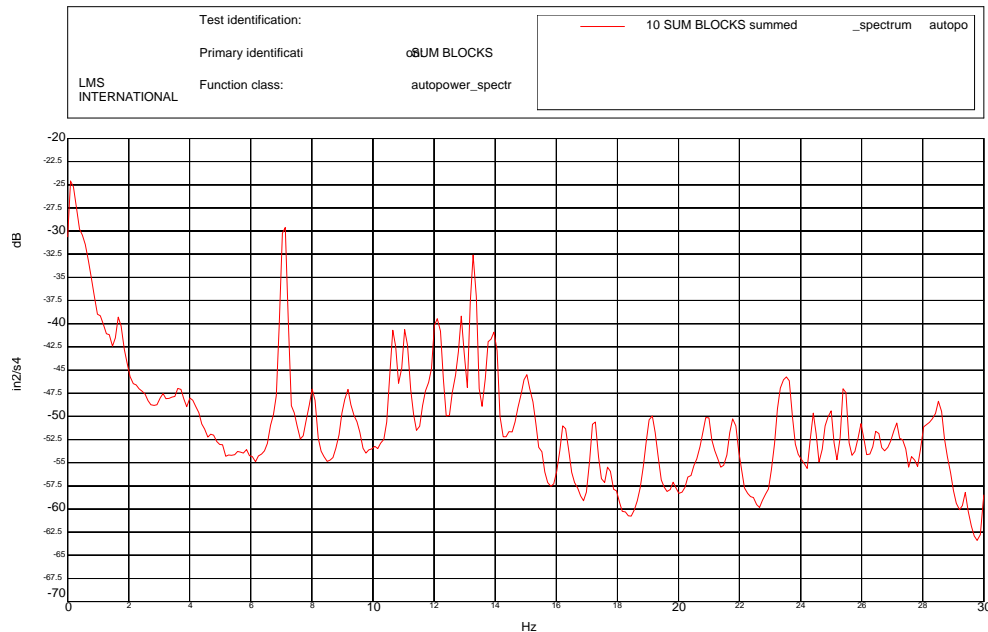


Figure 8.4.1  
Test #9 - Summed Auto Power of the Secondary

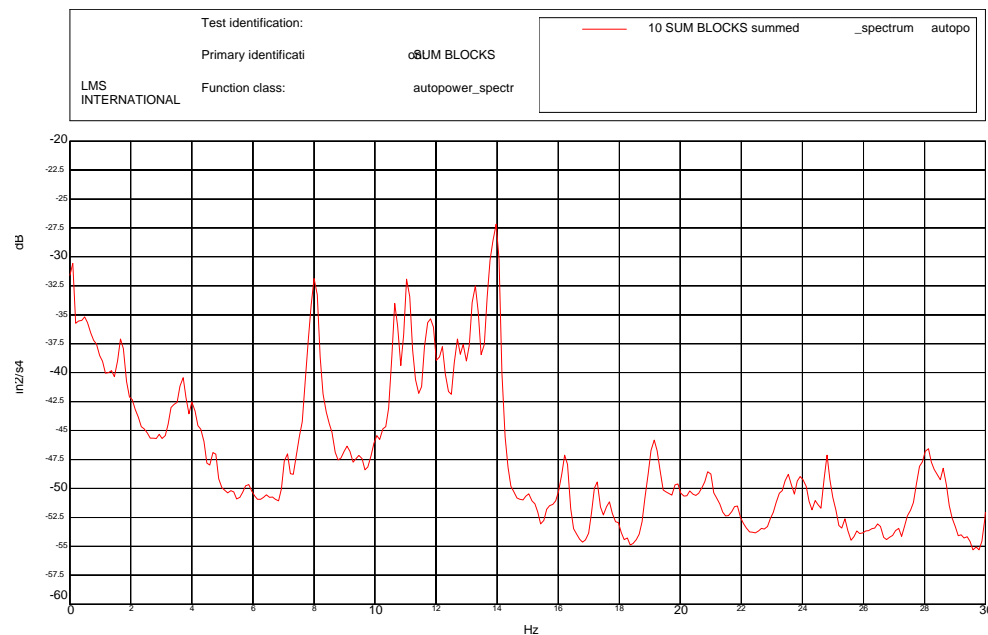


Figure 8.4.2  
Test #9 - Summed Auto Powers of the Primary





Table 8.4.1  
Test #9 - Peaks in the Auto Power Summation by Component

Secondary	Primary	Secondary	Primary	Secondary	Primary
1.709	1.709	13.281	13.281		24.805
3.32	3.32	13.818	13.818	24.951	24.951
	3.662	14.014	14.014	25.439	25.439
	3.76	14.99	14.99	25.83	
4.004	4.004		16.211	26.514	
	4.102	16.26		27.148	
4.15		17.236		27.393	27.393
7.08	7.08	17.725		27.686	
8.008	8.008	17.969		28.076	28.076
9.18	9.18	19.043		28.223	28.223
10.645	10.645	20.947	20.947	28.516	
11.035	11.035	21.826	21.826		28.613
	11.768	23.438	23.438	29.395	
	11.865	23.584	23.584		
	12.158	24.414	24.414		

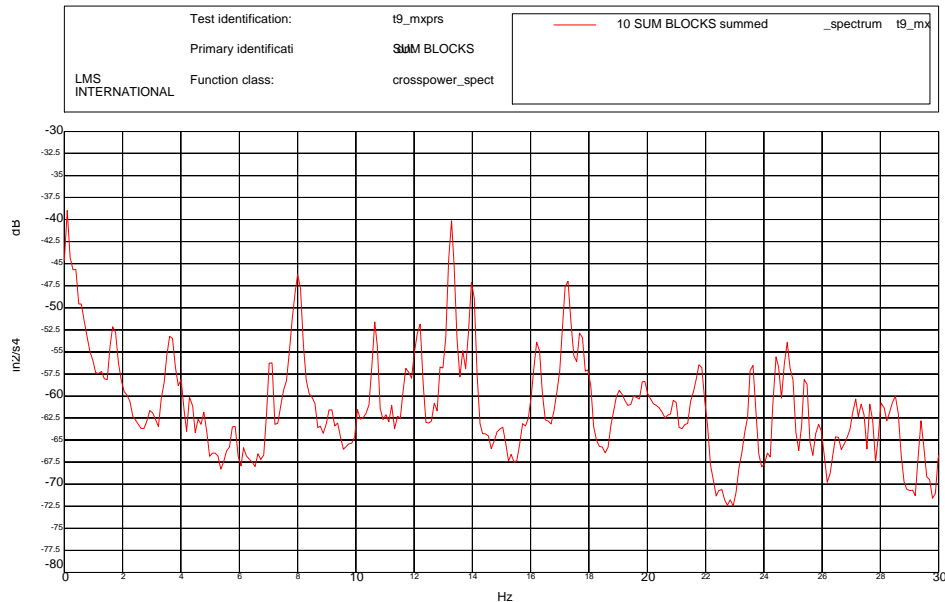


Figure 8.4.3  
Test #9 - Summed Cross Powers





Table 8.4.2  
Test #9 – Peaks in Cross Power

Frequency (Hz)	
1.66	17.68
2.93	19.04
3.61	19.53
4.00	19.92
4.3	20.90
4.79	21.78
5.86	23.63
7.13	24.41
8.01	24.80
9.18	25.39
10.06	25.88
10.64	26.46
11.72	27.15
12.21	27.34
13.28	27.64
13.96	28.03
15.04	28.52
16.21	29.39
17.29	





8.5 Test #11 – (5z / 30° / 60° / 45° / Closed / Closed)  
(Reference Channel / Elevation / Zenith / Angle of Attack / Upwind Gate / Downwind Gate)

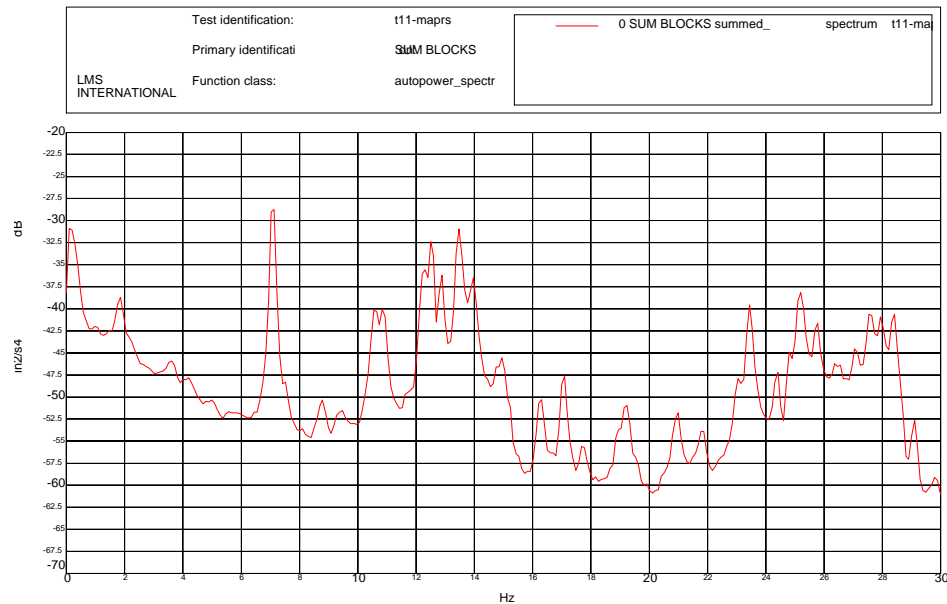


Figure 8.5.1  
Test #11 - Summed Auto Power of the Secondary

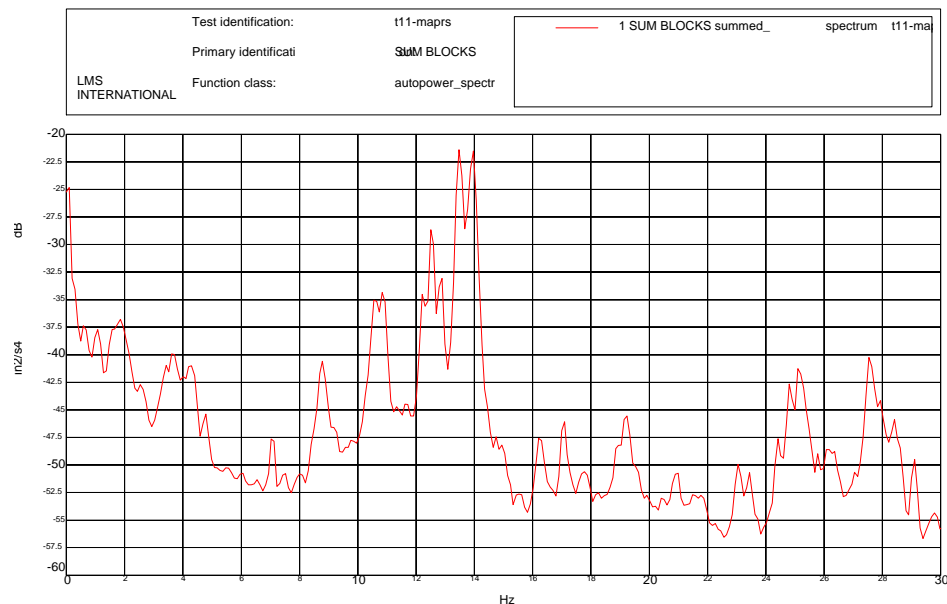


Figure 8.5.2  
Test #11 - Summed Auto Powers of the Primary





Table 8.5.1  
Test #11 - Peaks in the Auto Power Summation by Component

Secondary	Primary	Secondary	Primary	Secondary	Primary	Secondary	Primary
1.855	1.855		12.207	19.189		25.586	
	3.418	12.305		19.58	19.58	25.732	25.732
	3.662	12.549	12.549		20.459		25.928
	4.199	12.842	12.842	20.801		26.074	
	4.346	13.086	13.086		20.85	26.172	
7.08	7.08	13.477	13.477	20.996	20.996	26.318	26.318
	8.008	13.623			21.631	26.562	
	8.789	13.965	13.965		21.826	26.709	
	9.229	14.258		22.705		27.051	27.051
	9.521	14.697		23.096	23.096	27.148	
	9.766		14.746	23.438	23.438	27.295	27.295
	10.059	14.941	14.941	23.828		27.539	27.539
10.547	10.547	15.527		24.072			27.686
10.645	10.645		16.26	24.219		27.93	27.93
	10.84	16.309		24.365			28.125
10.889		16.699			24.414	28.369	
11.084		17.09	17.09	24.854	24.854		28.418
11.621	11.621	18.848			25.098		28.613
11.865		18.994	18.994	25.244		29.102	29.102

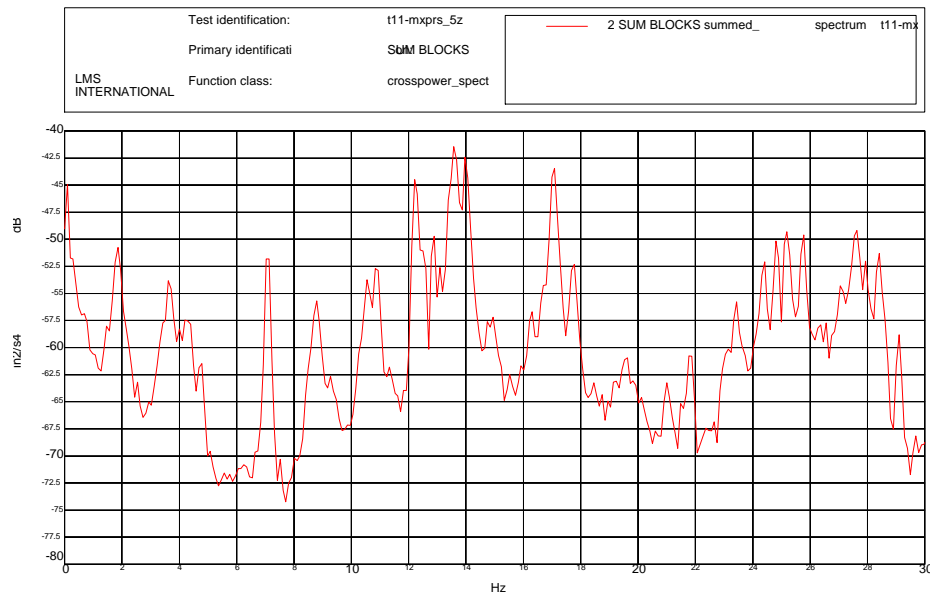


Figure 8.5.3  
Test #11 - Summed Cross Powers





Table 8.5.2  
Test #11 – Peaks in Cross Power

Frequency (Hz)	
1.855	17.09
3.613	17.773
4.004	19.629
4.199	20.996
7.031	21.777
8.789	23.438
10.547	24.414
10.84	24.805
12.207	25.195
12.891	25.781
13.086	27.051
13.574	27.637
13.965	27.93
14.746	28.418
14.941	29.102
16.309	





8.6 Test #12 – (5z / 30° / 60° / 45° / Open / Open)  
(Reference Channel / Elevation / Zenith / Angle of Attack / Upwind Gate / Downwind Gate)

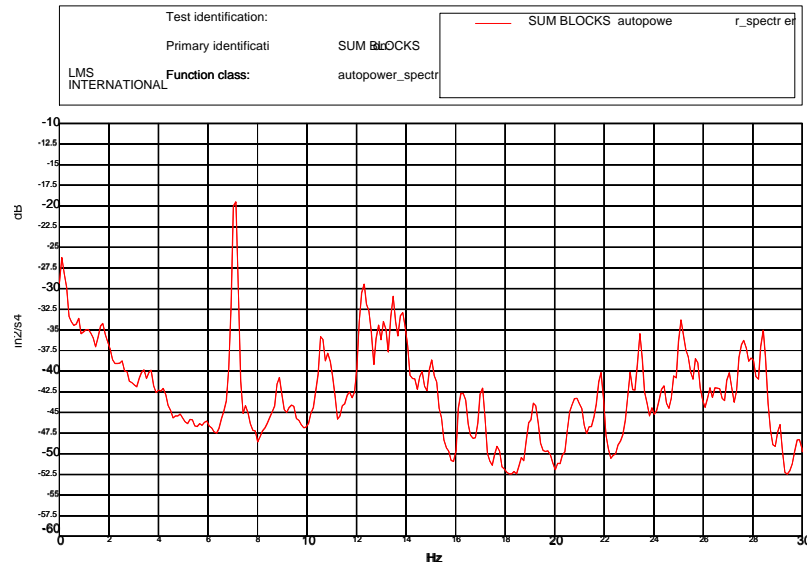


Figure 8.6.1  
Test #12 - Summed Auto Power of the Secondary

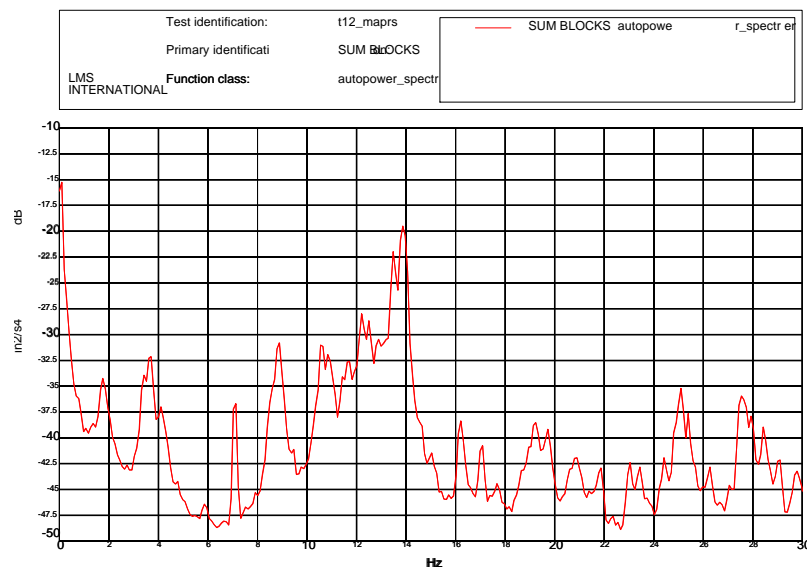


Figure 8.6.2  
Test #12 - Summed Auto Power of the Primary





Table 8.6.1  
Test #12 - Peaks in the Auto Power Summation by Component

Secondary	Primary	Secondary	Primary	Secondary	Primary
1.758	1.758		12.5	23.047	23.047
3.418	3.418	12.891	12.891	23.438	23.438
3.711	3.711	13.086			24.414
4.199		13.477	13.477	25.098	25.098
	4.102	13.867	13.867		25.391
	5.859	14.648		25.684	
7.129	7.129	15.039	15.039	27.051	
8.887	8.887	16.211	16.211		26.27
9.375		17.09	17.09		27.539
10.547	10.547	17.676	17.676	27.637	
10.84	10.84	19.141			27.93
	11.426		19.238	28.418	28.418
11.719	11.719		19.727	29.102	29.102
	12.207	20.898	20.898		
12.305		21.875	21.875		

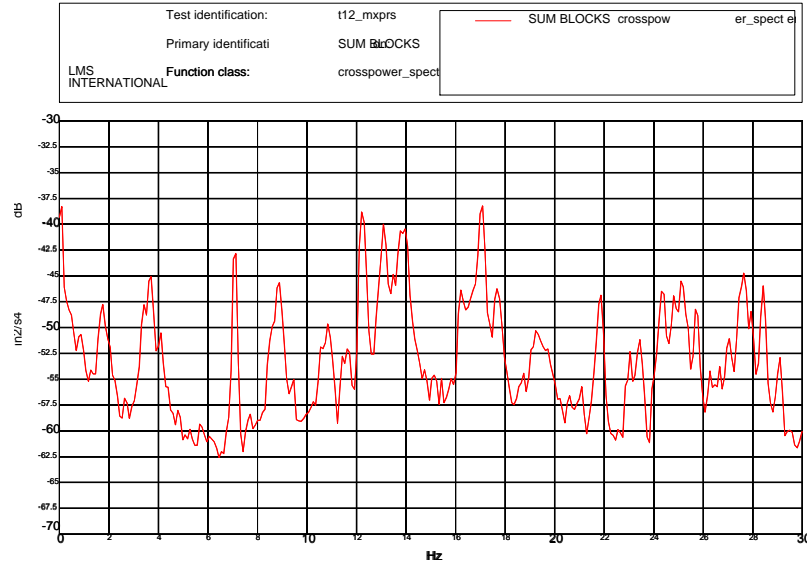


Figure 8.6.3  
Test #12 - Summed Cross Powers





Table 8.6.2  
Test #12 – Peaks in Cross Power

Frequency (Hz)	
1.758	17.676
3.711	19.238
7.129	21.875
8.887	23.438
10.547	24.316
12.207	24.805
13.086	25.098
13.769	25.684
13.965	27.637
16.211	28.418
17.09	29.102





8.7 Test #13 - (5z / 30° / 60° / 0° / Open / Closed)  
(Reference Channel / Elevation / Zenith / Angle of Attack / Upwind Gate / Downwind Gate)

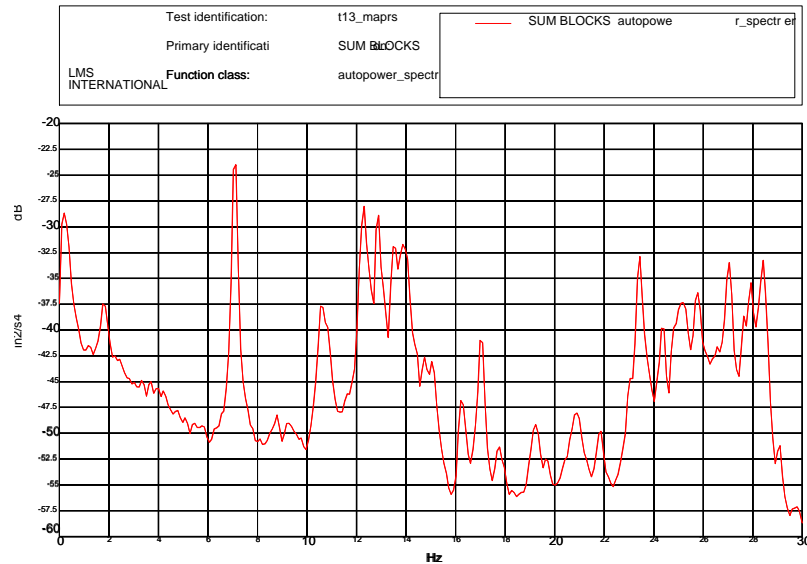


Figure 8.7.1  
Test #13 - Summed Auto Power of the Secondary

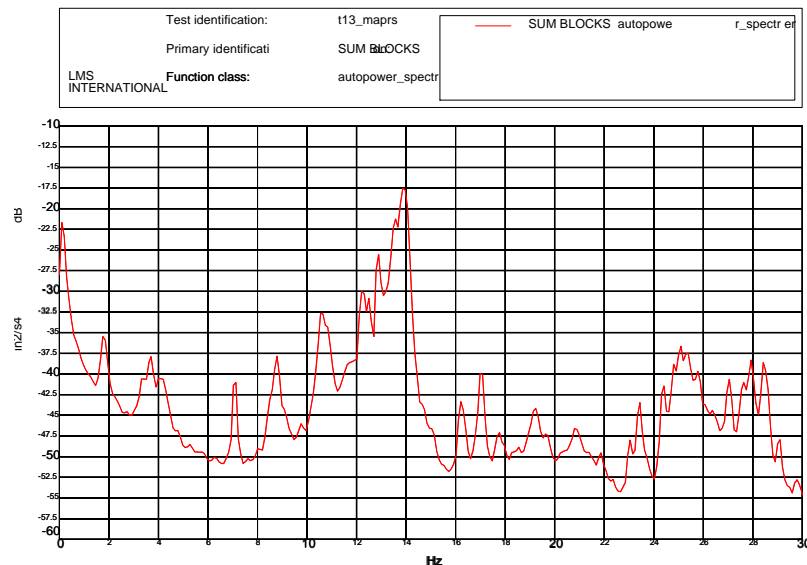


Figure 8.7.2  
Test #13 - Summed Auto Powers of the Primary





Table 8.7.1  
Test #13 - Peaks in the Auto Power Summation by Component

Secondary	Primary	Secondary	Primary	Secondary	Primary
1.758			12.852		20.459
	1.807	13.184		20.85	20.85
	3.369		13.232	22.754	21.875
	3.662	13.477	13.477	22.998	
	4.004	13.574	13.574		23.047
	4.15	13.818	13.818	23.438	23.438
7.08	7.08		13.916	24.365	24.365
	8.545	13.965		24.805	24.805
	8.74		14.697	25.049	25.049
		14.746		25.244	
	9.131				
9.229					25.342
	9.766	15.039		25.732	
10.596	10.596	16.211	16.211		25.83
10.791	10.791	17.041	17.041	26.562	
	11.67	17.725	17.725	27.051	27.051
	11.865		17.969		
			18.311	27.637	27.637
	12.207		18.506		27.93
12.305	12.305	18.994	18.994	28.418	28.418
12.512	12.5	19.189	19.189		
12.842		19.629	19.678	29.053	29.053

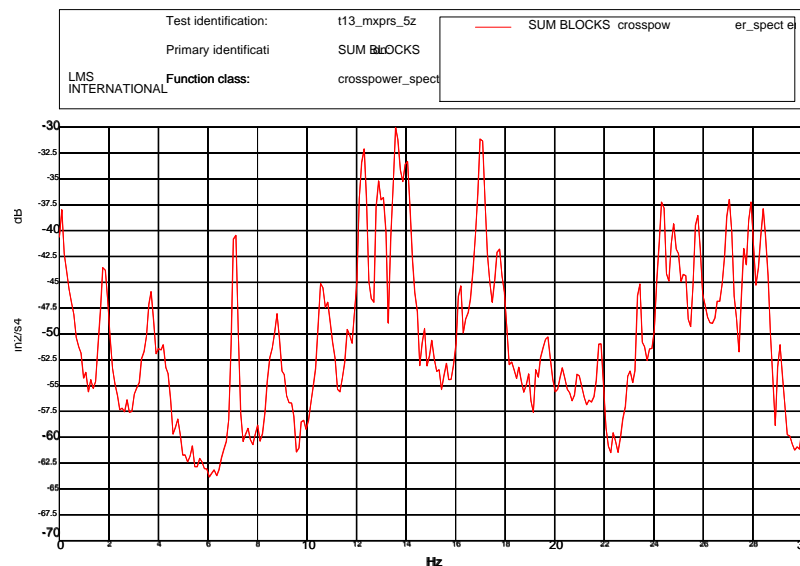


Figure 8.7.3  
Test #13 - Summed Cross Powers





Table 8.7.2  
Test #13 – Peaks in Cross Power

Frequency (Hz)	
1.758	16.211
3.711	16.992
4.004	17.773
4.199	19.727
7.129	21.875
8.789	23.438
10.547	24.316
10.84	24.805
11.621	25.195
12.305	25.781
12.891	27.051
13.086	27.637
13.574	27.93
14.062	28.418
14.746	29.102
15.039	





8.8 Test #14 - (5z / 30° / 60° / 0° / Closed / Open)  
(Reference Channel / Elevation / Zenith / Angle of Attack / Upwind Gate / Downwind Gate)

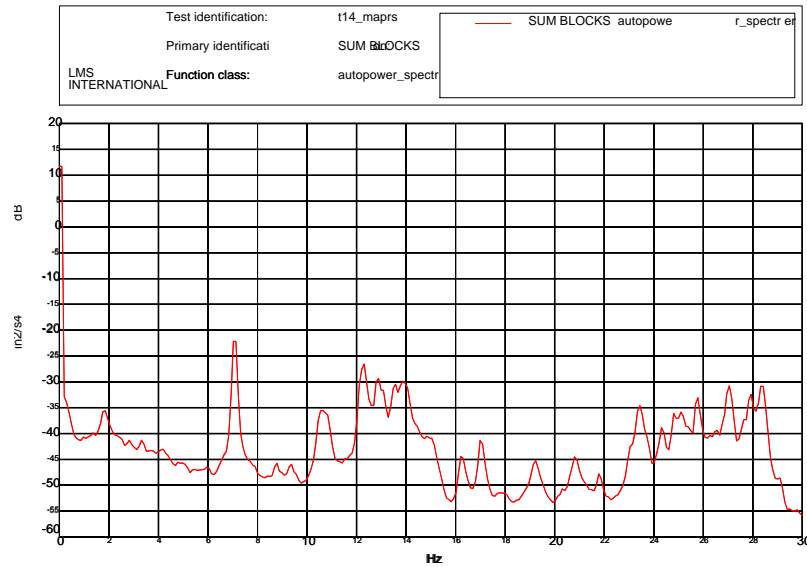


Figure 8.8.1  
Test #14 - Summed Auto Power of the Secondary

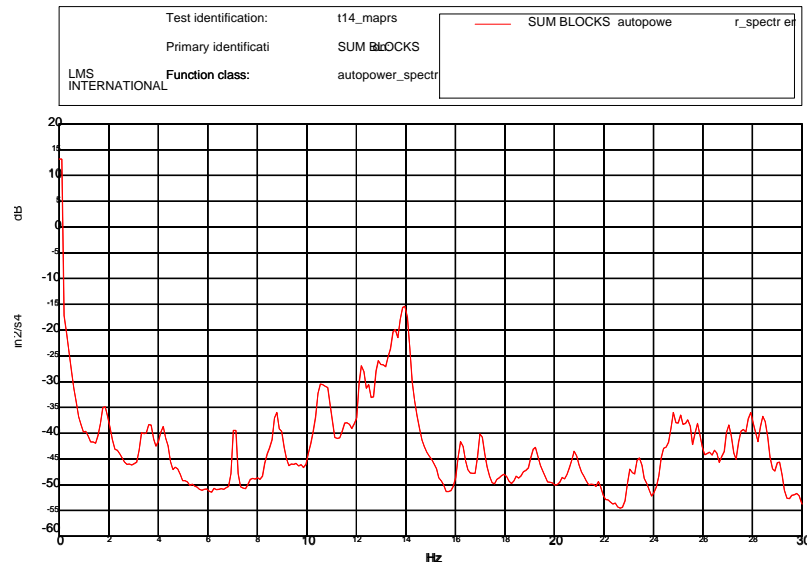


Figure 8.8.2  
Test #14 - Summed Auto Powers of the Primary





Table 8.8.1  
Test #14 - Peaks in the Auto Power Summation by Component

Secondary	Primary	Secondary	Primary	Secondary	Primary
1.807	1.807	12.5	12.5		23.145
2.832		12.842		23.389	23.389
3.271			12.891	23.682	
3.326		13.037		24.365	
	3.369		13.086		24.414
	3.662	13.281	13.281		24.561
3.76			13.477	24.805	24.805
	4.199		13.574		25.049
7.08	7.08	13.623		25.195	
	8.398	13.818			25.293
8.789	8.789		13.867		25.439
	8.984	13.965	13.965	25.732	25.732
	10.254	16.26	16.26	26.562	
10.547		17.041	17.041	27.051	27.051
	10.596	17.676		27.637	27.637
10.84	10.791	18.896		27.881	27.881
11.23	11.23	19.189	19.189	28.369	
	11.523	19.58			28.418
	11.67	20.801	20.801		29.053
	12.207		21.777	29.102	
12.305	12.305	23.047	23.047		23.145

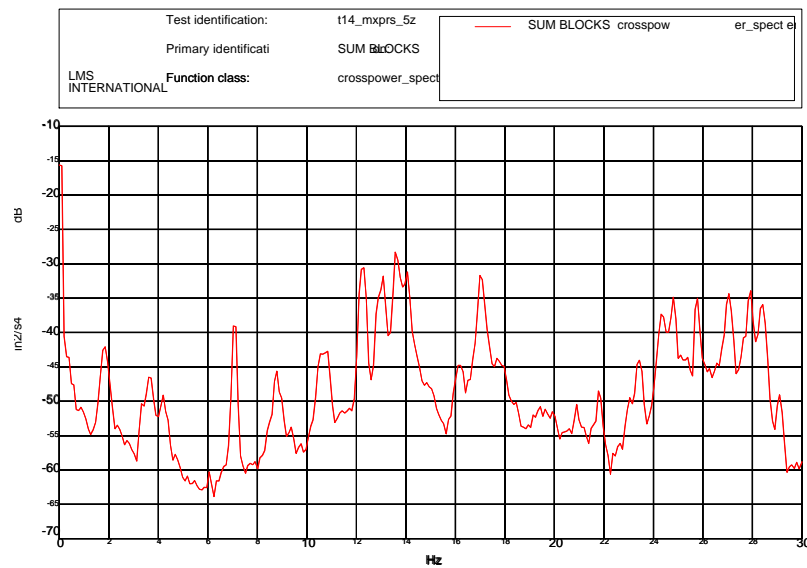


Figure 8.8.3  
Test #14 - Summed Cross Powers





Table 8.8.2  
Test #14 – Peaks in Cross Power

Frequency (Hz)	
1.855	19.434
3.32	19.629
3.613	19.922
4.199	20.898
7.031	21.777
8.789	23.047
10.547	23.438
10.84	24.316
12.305	24.805
13.086	25.098
13.574	25.391
14.062	25.781
16.211	27.051
16.992	27.93
17.676	28.418
18.457	29.102
19.141	





8.9 Test #16 - (5z / 30° / 60° / 90° / Half / Half)  
(Reference Channel / Elevation / Zenith / Angle of Attack / Upwind Gate / Downwind Gate)

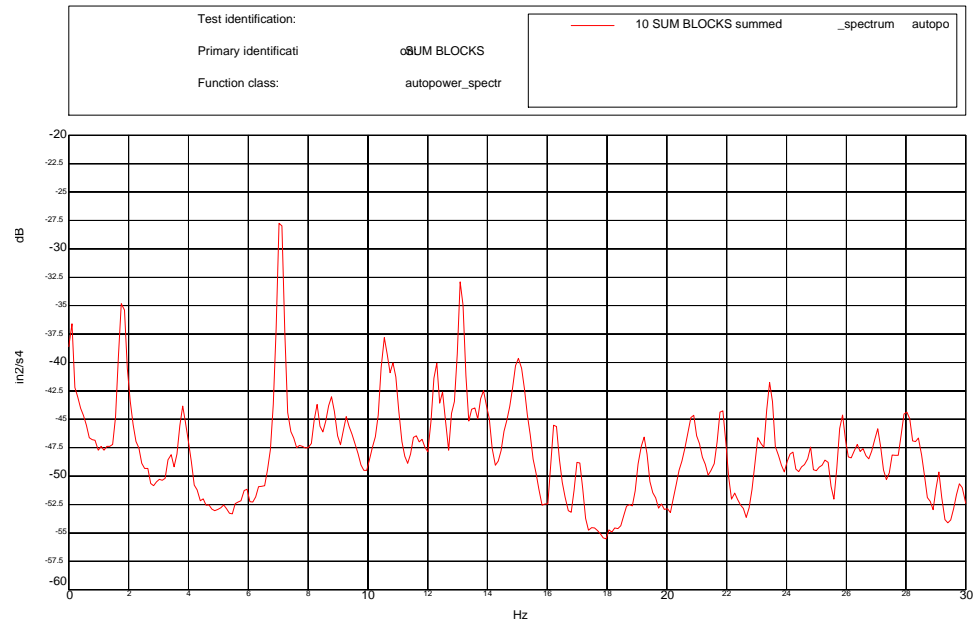


Figure 8.9.1  
Test #16 - Summed Auto Power of the Secondary

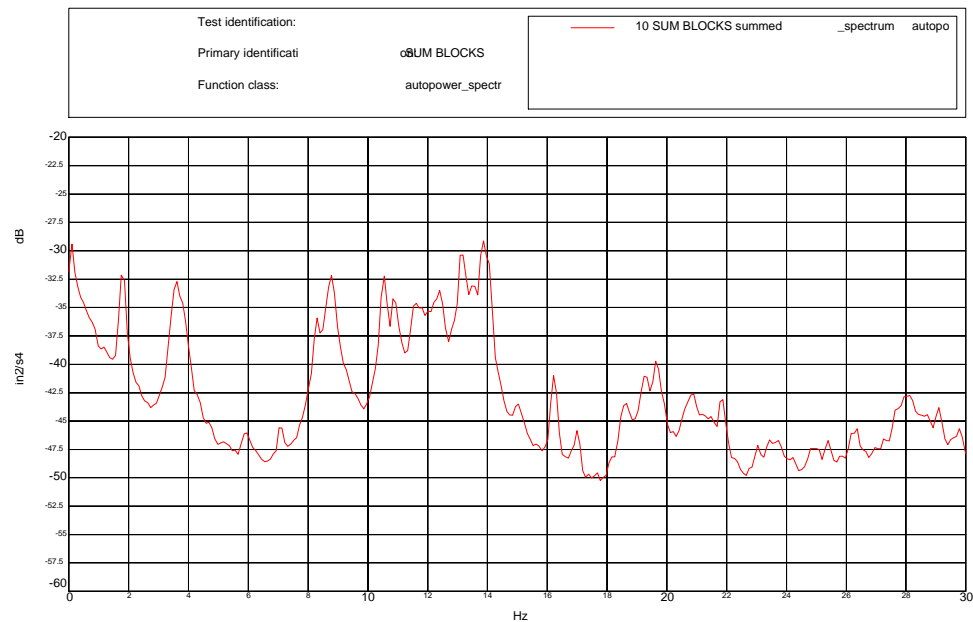


Figure 8.9.2  
Test #16 - Summed Auto Powers of the Primary





Table 8.9.1  
Test #16 - Peaks in the Auto Power Summation by Component

Secondary	Primary	Secondary	Primary	Secondary	Primary	Secondary	Primary
1.807	1.807	9.277	9.277	13.818	13.818		23.633
3.369		9.424		14.014	14.014		23.779
	3.564		9.521	14.6		24.414	
	3.76	9.619	9.619	14.99	14.99	24.805	24.805
3.875	3.857	9.814			16.211	25.098	25.098
4.297		10.547	10.547	16.26		25.244	
4.834	4.834	10.84		17.041	17.041		25.391
4.98			10.889	17.822		25.732	
	5.176	11.475		19.238		26.172	26.172
5.225			11.572		19.287		26.367
	5.518		12.061	19.58		26.562	
5.664			12.256		19.678		26.953
	5.811	12.305		20.41		27.051	27.051
5.859			12.402		20.605		27.295
	5.957	12.5		20.85	20.85	27.686	27.686
7.08	7.08	12.842	12.842	21.094		27.93	27.93
7.715			13.086		21.533		28.174
7.91		13.135		21.826	21.826	28.418	
8.252		13.232	13.232		22.266		28.564
8.643			13.428	23.047	23.047		28.711
8.789	8.789	13.574	13.574	23.438	23.438	29.102	29.102

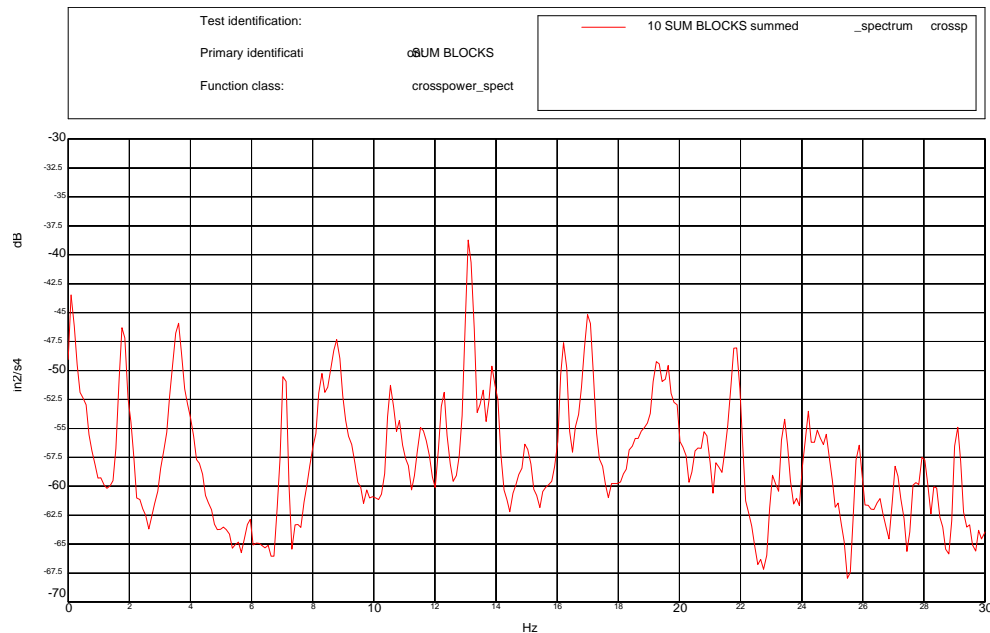


Figure 8.9.3  
Test #16 - Summed Cross Powers





Table 8.9.2  
Test #16 – Peaks in Cross Power

Frequency (Hz)	
1.758	19.629
3.613	20.801
7.031	21.191
8.301	21.777
8.789	23.047
10.547	23.438
10.84	24.219
11.523	24.512
12.305	24.805
13.086	25.879
13.574	26.562
13.867	27.051
14.941	27.93
16.211	28.418
16.992	29.102
19.238	





8.10 Test #17 - (5z / 30° / 60° / 180° / Open / Open)  
(Reference Channel / Elevation / Zenith / Angle of Attack / Upwind Gate / Downwind Gate)

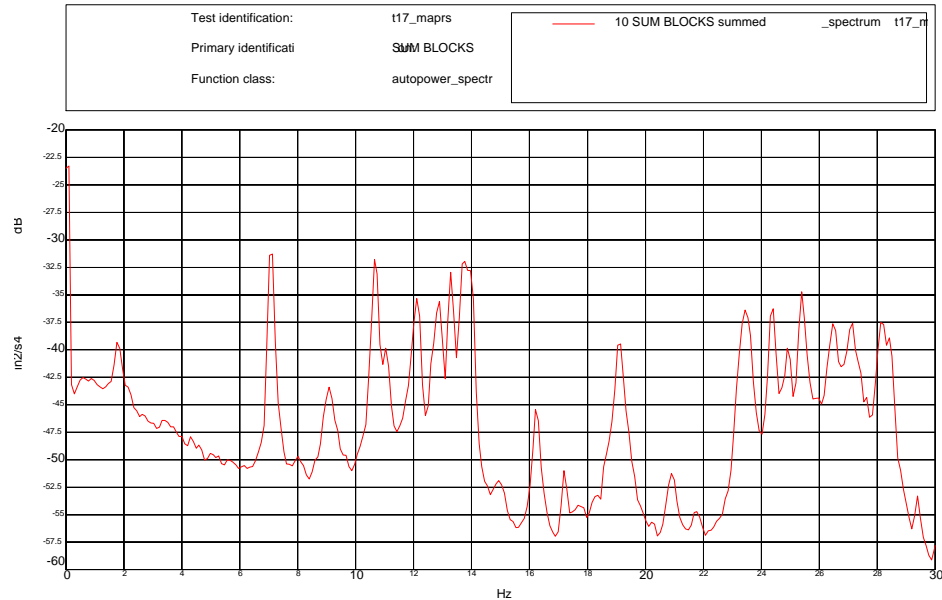


Figure 8.10.1  
Test #17 - Summed Auto Power of the Secondary

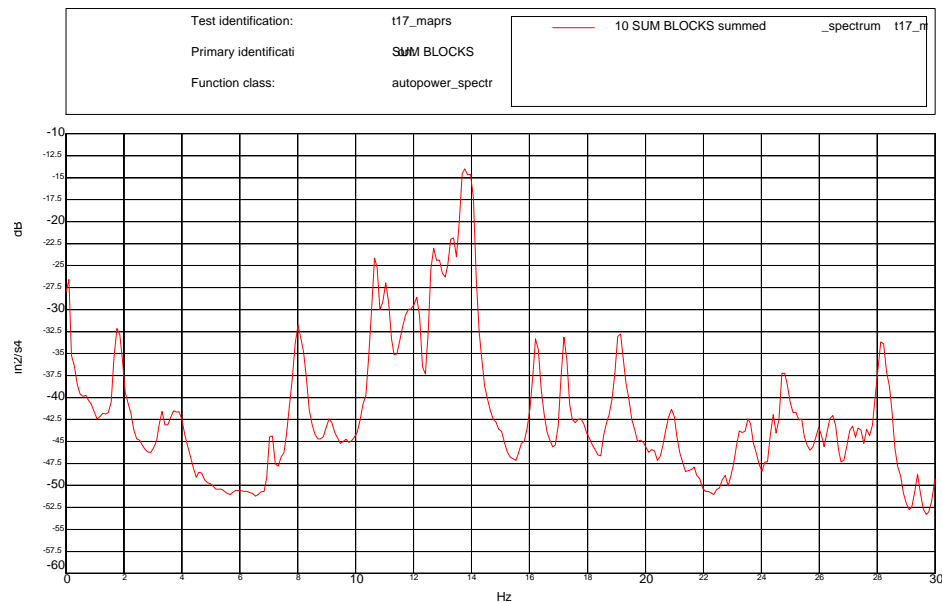


Figure 8.10.2  
Test #17 - Summed Auto Powers of the Primary





Table 8.10.1  
Test #17 - Peaks in the Auto Power Summation by Component

Secondary	Primary	Secondary	Primary	Secondary	Primary	Secondary	Primary
1.807	1.807		8.545	13.867			21.875
3.174		8.594		14.014	14.014	23.047	
3.369	3.369	8.74		15.039		23.438	23.438
3.564	3.564		9.08		16.211	24.365	
3.809		9.668	9.668	16.26			24.756
4.053	4.053		9.863	17.041	17.041	24.805	
4.15			10.547		17.432	25.049	25.049
4.541	4.541	10.596		17.822		25.195	
	4.736	10.742			17.92		25.244
	5.127		10.791	17.969		25.732	
5.322		10.84		18.896			25.781
	5.371	11.084		19.092		27.1	27.1
	5.859		12.207	19.238		27.637	27.637
5.908		12.305		19.336	19.336	27.881	27.881
7.08	7.08	12.5	12.5	19.775	19.775	28.32	28.32
	7.812	12.842			20.703	29.102	
8.057			12.891	20.801	20.801		
8.154	8.154	13.281			21.289		
8.301		13.574		21.729			

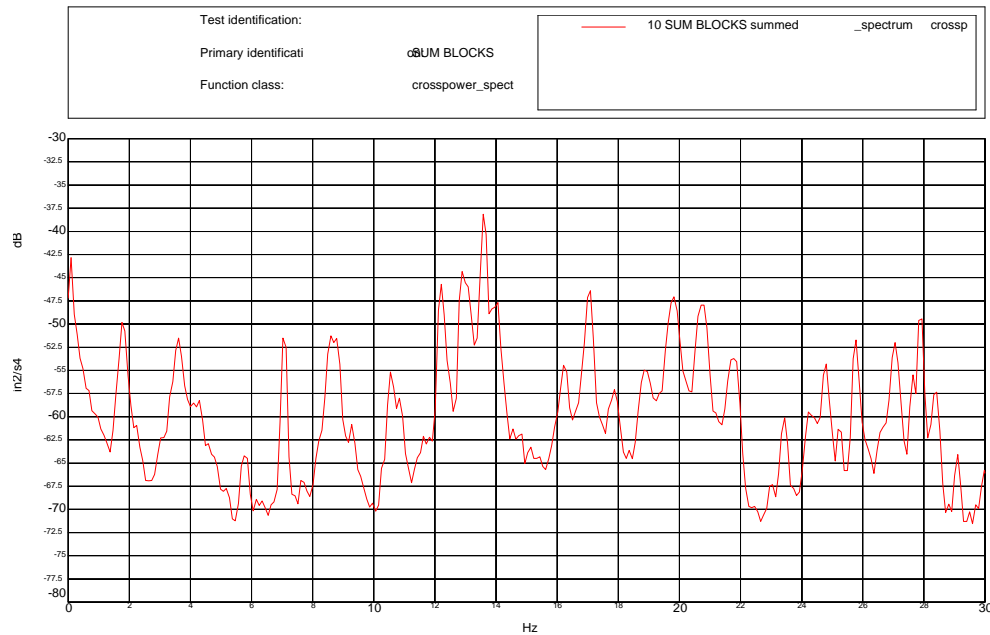


Figure 8.10.3  
Test #17 - Summed Cross Powers





Table 8.10.2  
Test #17 – Peaks in Cross Power

Frequency (Hz)	
1.758	18.848
3.613	19.043
4.102	19.336
5.762	19.727
7.031	20.605
8.594	20.801
8.789	21.875
10.547	23.438
12.207	24.219
12.891	24.414
13.086	24.805
13.574	25.781
13.867	27.051
14.062	27.637
16.211	27.93
17.09	28.32
17.871	29.102





8.11 Test #19 - (5z / 45° / 45° / 90° / Open / Closed)  
(Reference Channel / Elevation / Zenith / Angle of Attack / Upwind Gate / Downwind Gate)

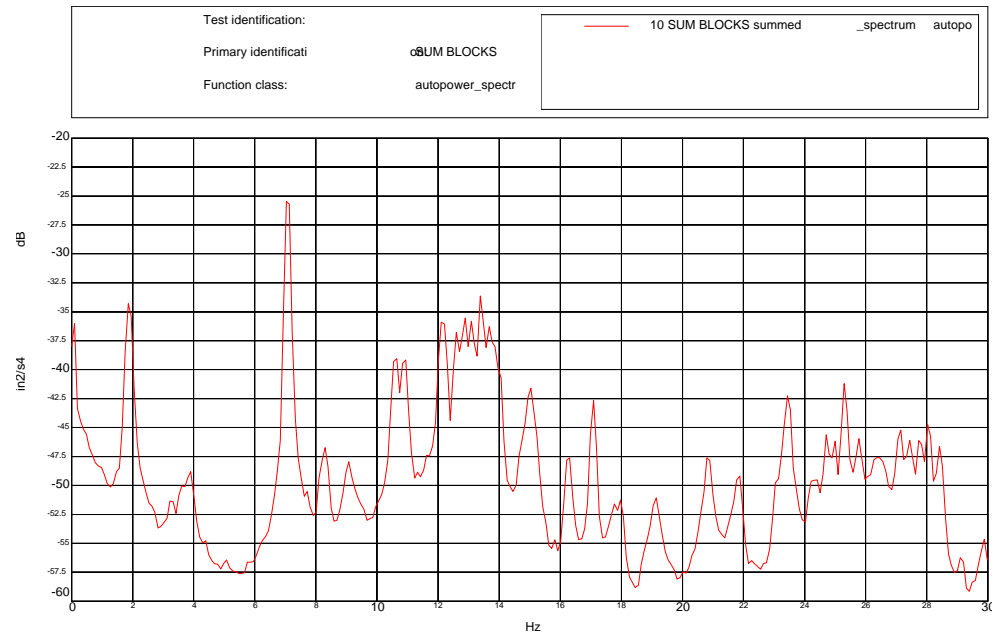


Figure 8.11.1  
Test #19 - Summed Auto Power of the Secondary

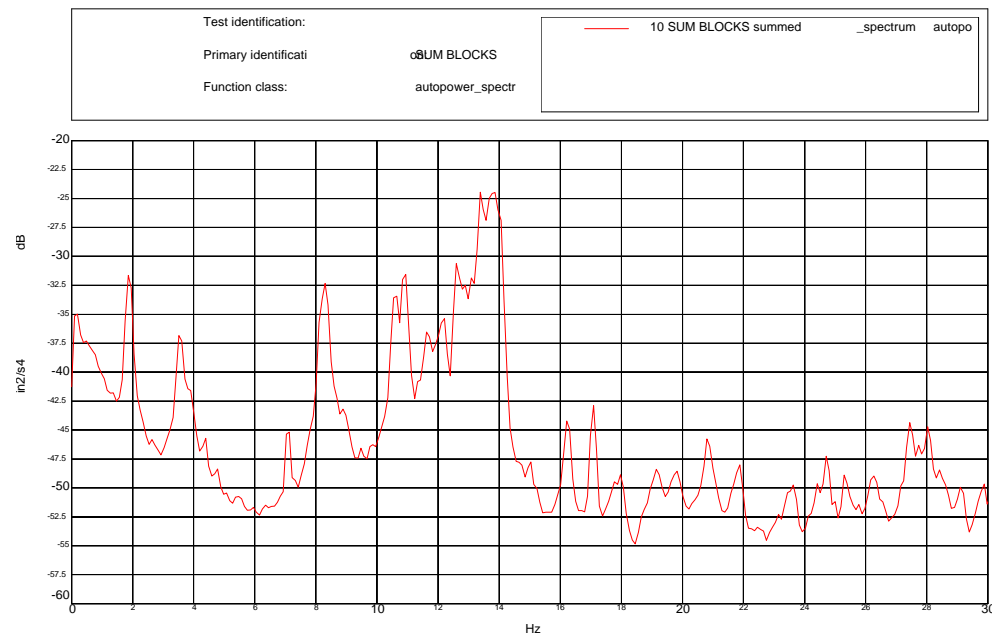


Figure 8.11.2  
Test #19 - Summed Auto Powers of the Primary





Table 8.11.1  
Test #19 - Peaks in the Auto Power Summation by Component

Secondary	Primary	Secondary	Primary	Secondary	Primary	Secondary	Primary
1.904	1.904		12.109	19.141	19.141	25.293	25.293
2.1		12.207	12.207		19.824	25.781	25.781
3.271	3.271	12.598	12.598	20.85	20.85	25.635	
	3.564	12.842	12.842	21.338			26.172
3.857	3.857	13.135	13.135	21.484		26.318	26.318
	5.127	13.379	13.379		21.68	26.514	
	5.469	13.672	13.672	21.826	21.826	27.148	27.148
7.08	7.08	13.818	13.818		22.9	27.441	
	7.91	14.014	14.014	23.096	23.096		27.49
8.301	8.301	15.039	15.039	23.438			27.734
	8.936	15.234			23.486	27.783	
	10.107	16.26	16.26		23.633	28.076	28.076
10.596	10.596	17.09	17.09		23.975	28.467	28.467
10.889	10.889		17.125		24.17		28.613
	11.621	17.725		24.414	24.414	29.15	29.15
	11.768	17.969	17.969	24.756	24.756		
	11.963		18.994	25	25		

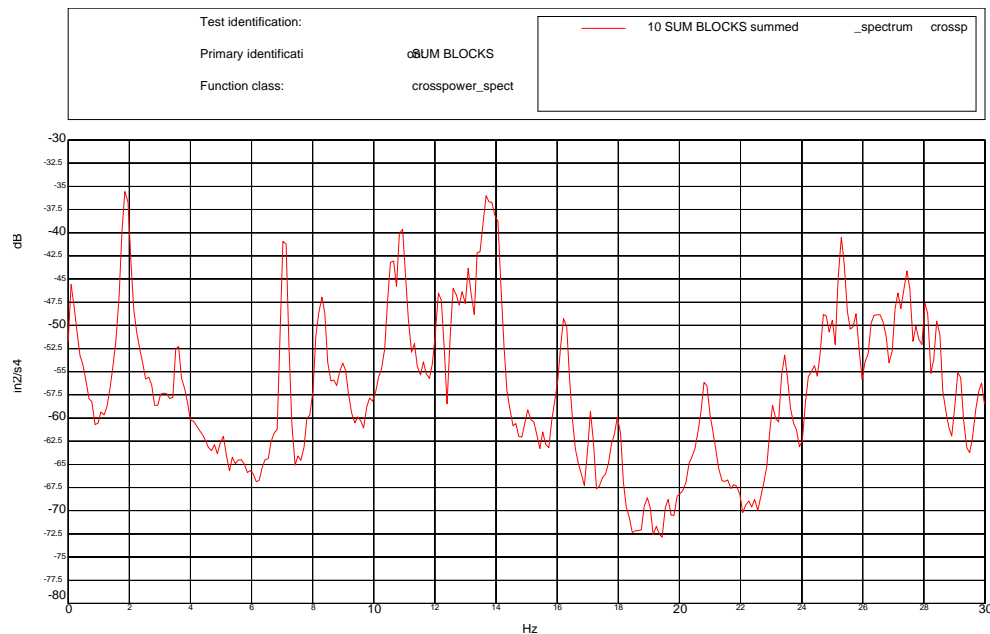


Figure 8.11.3  
Test #19 - Summed Cross Powers





Table 8.11.2  
Test #19 – Peaks in Cross Power

Frequency (Hz)	
1.855	19.141
3.516	19.727
4.395	20.801
7.031	21.875
8.301	23.438
10.547	24.219
10.938	24.414
11.621	24.707
12.207	25.293
13.086	25.781
13.379	27.148
13.672	27.441
15.039	27.734
16.211	28.027
17.09	28.418
17.773	29.102
17.969	





8.12 Test #20 - (5z / 45° / 45° / 0° / Half / Open)  
(Reference Channel / Elevation / Zenith / Angle of Attack / Upwind Gate / Downwind Gate)

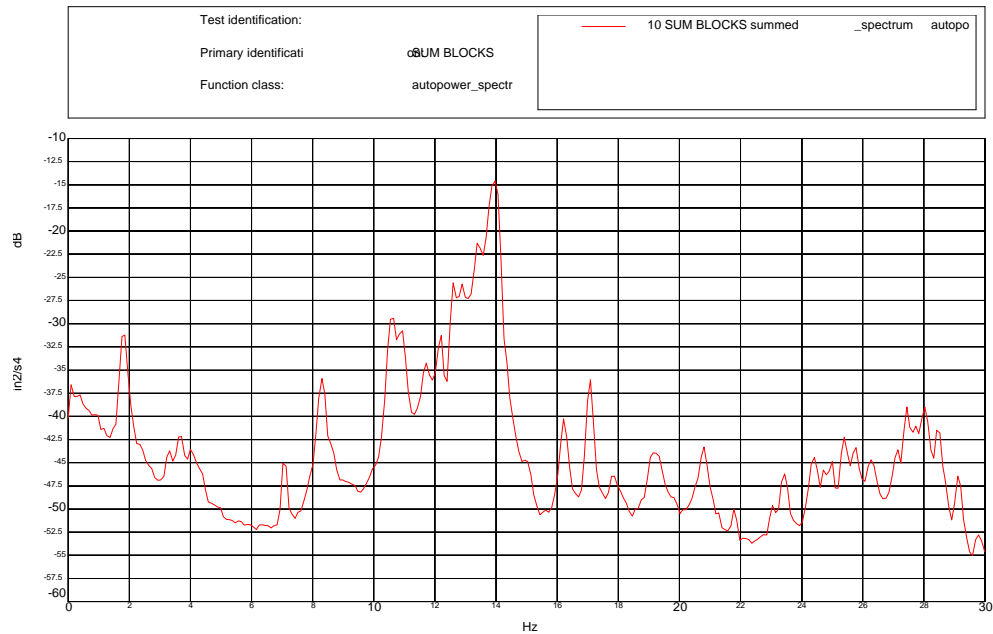


Figure 8.12.1  
Test #20 - Summed Auto Power of the Secondary

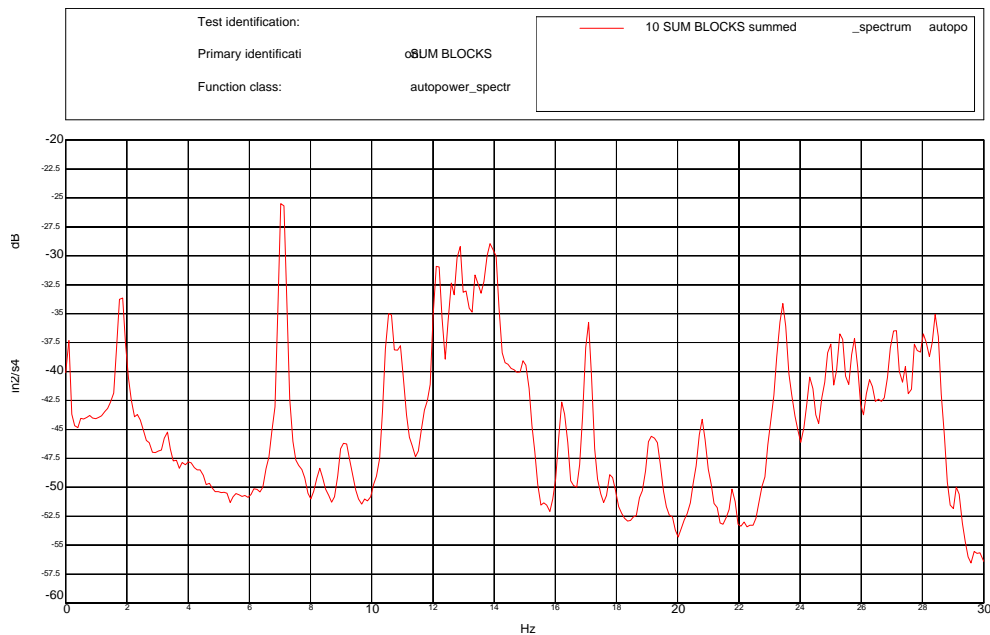


Figure 8.12.2  
Test #20 - Summed Auto Powers of the Primary





Table 8.12.1  
Test #20 - Peaks in the Auto Power Summation by Component

Secondary	Primary	Secondary	Primary	Secondary	Primary	Secondary	Primary
1.807	1.807	9.766			15.576	25.293	
2.051		10.156	10.156	16.211	16.211		25.391
2.393	2.393	10.547	10.547		16.553	25.732	
3.271	3.271		10.645	16.65			25.781
	3.662	10.889	10.889	16.895	16.895	26.221	26.221
	4.004		11.377	17.09	17.09	26.367	26.367
6.787			11.865	17.773	17.773	26.611	
7.08	7.08	12.207	12.207	19.092		27.1	
	7.324	12.598	12.598	19.238			27.148
	7.568	12.842		20.85		27.441	27.441
7.617			12.891	23.096	23.096		27.686
	7.764	13.086	13.086	23.438	23.438	27.783	
	8.301	13.379	13.379	24.316			28.027
8.484		13.867	13.867		24.365	28.076	
	8.545	14.014	14.014	24.609		28.418	
	8.643	14.355			24.756		28.467
	8.936	14.648		24.854		28.662	
9.131	9.131	14.941	14.941		24.951		29.102
	9.375	15.039		25.098		29.15	

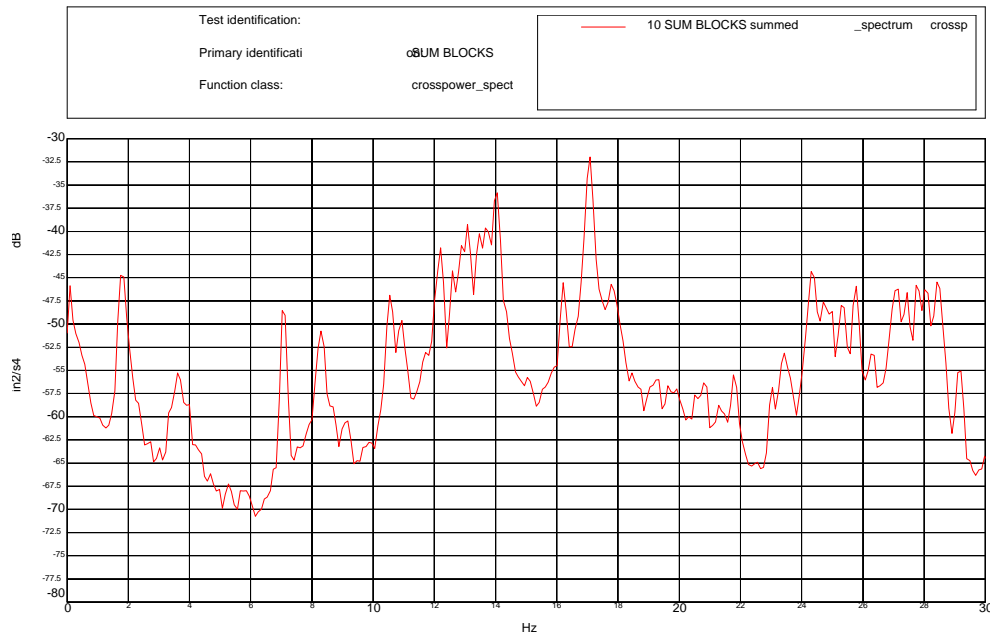


Figure 8.12.3  
Test #20 - Summed Cross Powers





Table 8.12.2  
Test #20 – Peaks in Cross Power

Frequency (Hz)	
1.758	21.777
3.613	23.047
7.031	23.438
8.301	24.316
10.547	24.707
10.938	25
12.207	25.293
12.598	25.781
12.891	26.27
13.086	27.148
13.477	27.441
13.672	27.734
14.062	28.027
16.211	28.418
17.09	29.199
17.773	





8.13 Test #21 - (5y / 60° / 30° / 0° / Closed / Closed)  
(Reference Channel / Elevation / Zenith / Angle of Attack / Upwind Gate / Downwind Gate)

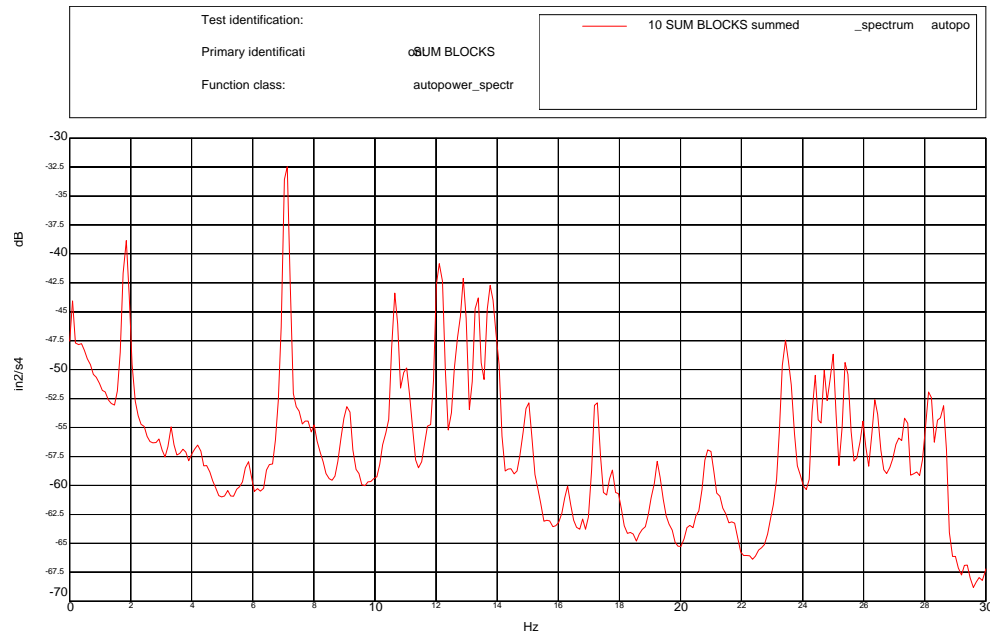


Figure 8.13.1  
Test #21 - Summed Auto Power of the Secondary

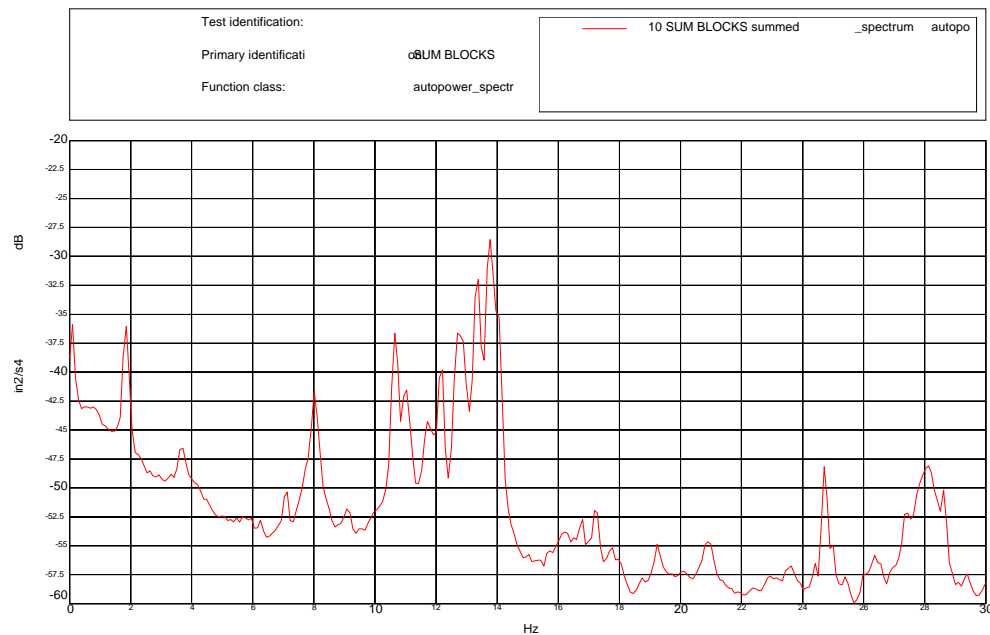


Figure 8.13.2  
Test #21 - Summed Auto Powers of the Primary





Table 8.13.1  
Test #21 - Peaks in the Auto Power Summation by Component

Secondary	Primary	Secondary	Primary	Secondary	Primary	Secondary	Primary
1.855	1.855	7.52		12.695	12.695	23.438	23.438
2.246		7.715		12.891	12.891	23.564	
2.686		7.812	7.812	13.33	13.33	24.414	24.414
2.93		8.008	8.008	13.77		24.707	24.707
3.32	3.32		8.447	14.014	14.014	25	25
3.662	3.662		8.984		15.039	25.391	25.391
	4.004	9.131	9.131	16.162		25.977	25.977
4.15			9.424		16.309	26.367	26.367
	4.248	10.645		16.748		27.393	27.393
5.469		10.986		17.236	17.236	27.539	
5.713		11.377		17.773		27.832	
5.908			11.645	18.018		28.027	
6.25		11.719		18.75		28.174	28.174
7.08	7.08		11.986	19.238	19.238	28.613	28.613
7.227			12.061	20.85	20.85	29.346	
	7.471	12.158	12.158	20.996	20.996		29.395

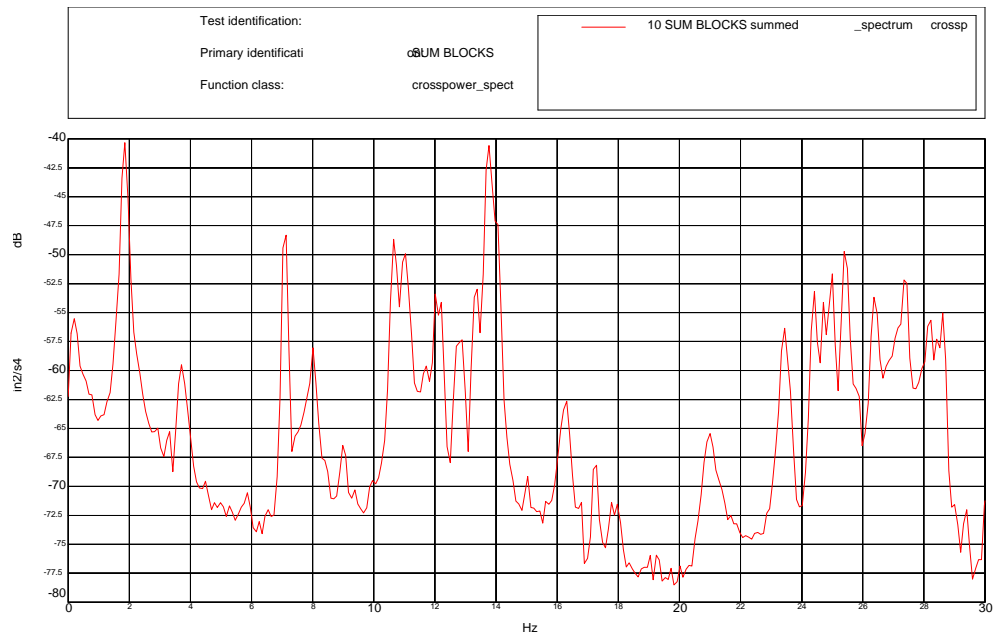


Figure 8.13.3  
Test #21 - Summed Cross Powers





Table 8.13.2  
Test #21 – Peaks in Cross Power

Frequency (Hz)	
1.855	17.285
3.711	17.773
5.859	17.969
7.129	19.043
8.008	19.238
8.984	20.996
10.645	23.438
11.035	24.414
11.719	24.707
12.012	25
12.207	25.391
12.891	26.367
13.379	27.344
13.77	28.223
15.039	28.418
16.309	29.395





8.14 Test #22 - (5z / 60° / 30° / 0° / Closed / Half)  
(Reference Channel / Elevation / Zenith / Angle of Attack / Upwind Gate / Downwind Gate)

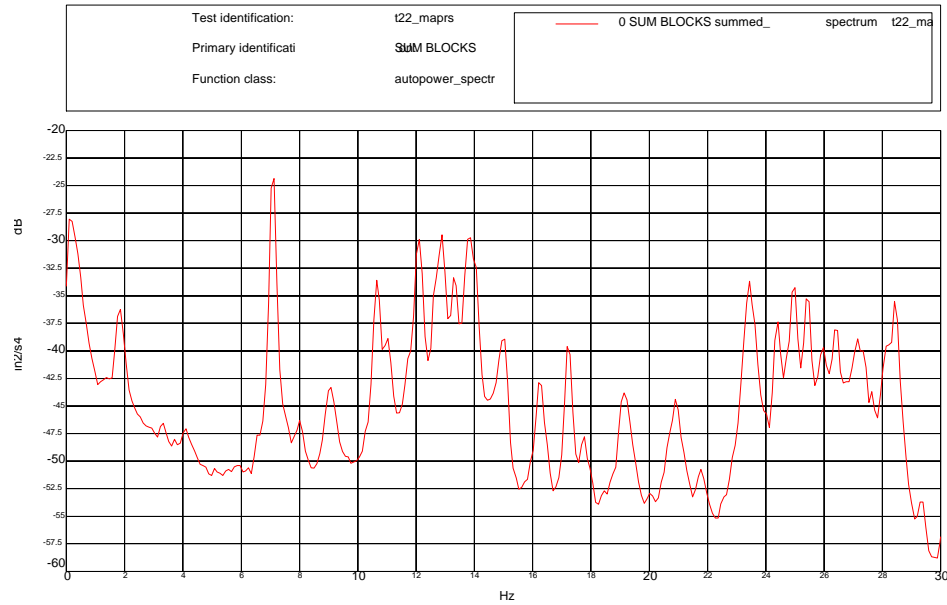


Figure 8.14.1  
Test #22 - Summed Auto Power of the Secondary

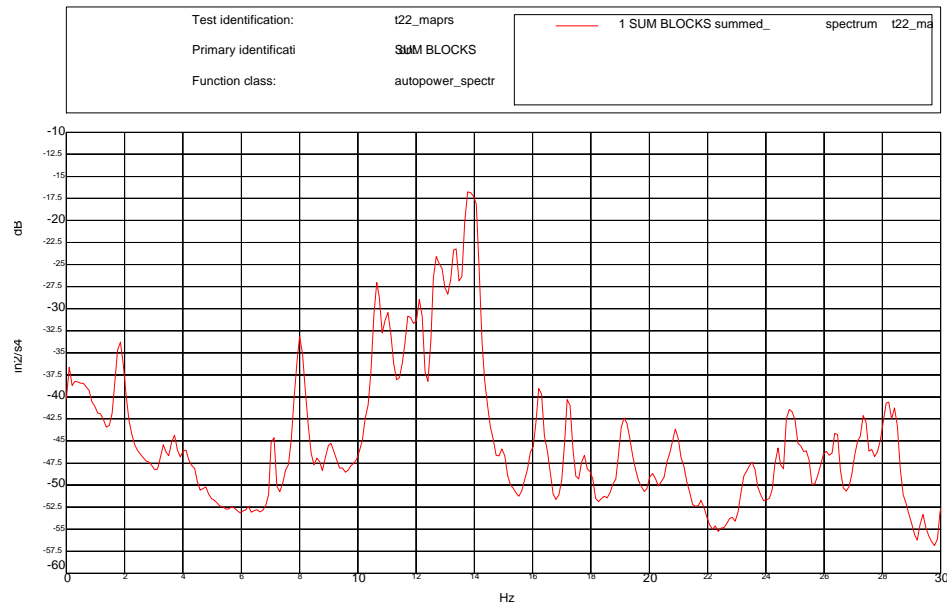


Figure 8.14.2  
Test #22 - Summed Auto Powers of the Primary





Table 8.14.1  
Test #22 - Peaks in the Auto Power Summation by Component

Secondary	Primary	Secondary	Primary	Secondary	Primary
1.855	1.855		12.793		23.584
	3.32	12.891		24.414	24.414
	3.662	13.33	13.33		24.756
	4.004	13.818	13.818	24.951	24.951
	4.102	14.014		25.439	25.439
7.08	7.08		14.941		25.928
	8.008	15.039		26.416	26.416
9.033	9.033		15.918	27.148	27.148
9.131	9.131	16.26	16.26	27.344	
10.645	10.645	17.236	17.236		27.393
10.986	10.986	19.092		27.637	27.637
11.768	11.768		19.238	28.174	28.174
	12.109		20.068		28.418
12.158		20.898		28.467	
12.695	12.695	23.438	23.438		

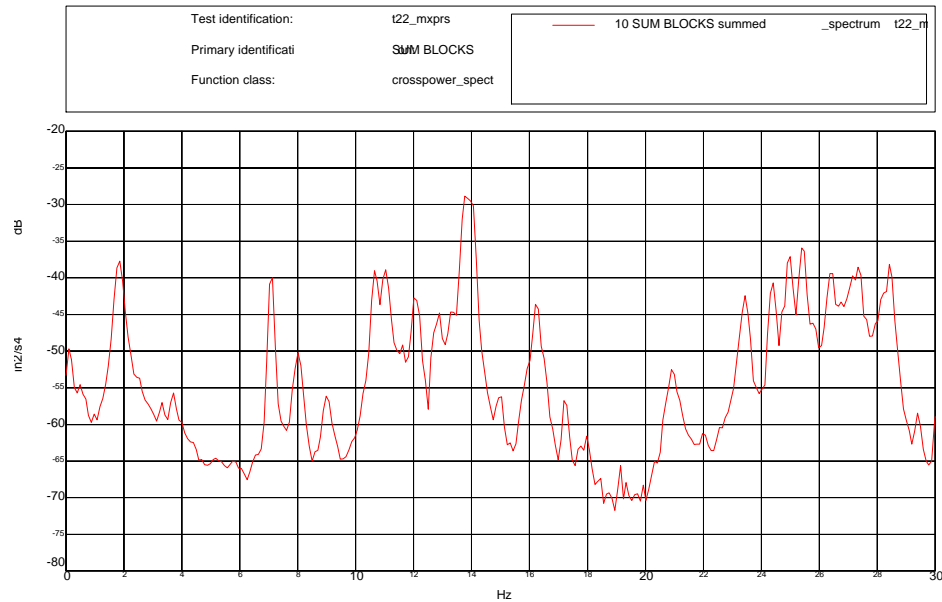


Figure 8.14.3  
Test #22 - Summed Cross Powers





Table 8.14.2  
Test #22 – Peaks in Cross Power

Frequency (Hz)	
1.855	17.773
3.516	20.117
3.711	20.898
7.129	21.777
7.52	23.535
8.008	24.414
8.984	24.707
10.644	24.902
11.719	25.391
12.109	25.879
12.695	26.465
12.891	27.148
13.281	27.344
13.672	27.637
14.062	28.223
14.941	28.418
16.211	29.395
17.188	





8.15 Test #23 - (5z / 60° / 30° / 90° / Closed / Open)  
(Reference Channel / Elevation / Zenith / Angle of Attack / Upwind Gate / Downwind Gate)

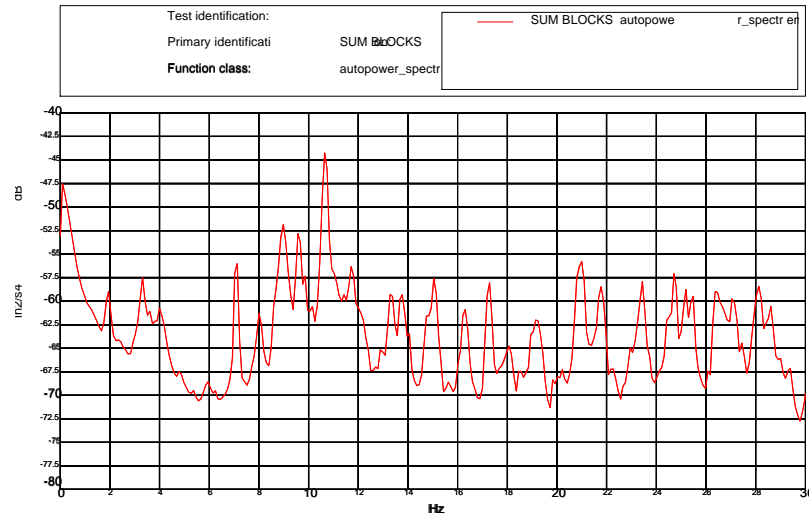


Figure 8.15.1  
Test #23 - Summed Auto Power of the Secondary

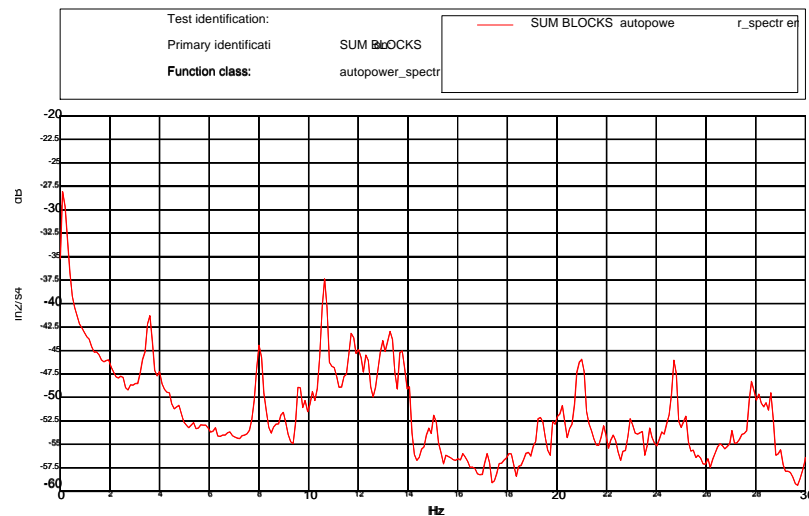


Figure 8.15.2  
Test #23 - Summed Auto Powers of the Primary





Table 8.15.1  
Test #23 - Peaks in the Auto Power Summation by Component

Secondary	Primary	Secondary	Primary	Secondary	Primary
1.953			12.354	21.729	
3.32			12.988	23.291	
3.564	3.564		13.232	23.438	
4.004		13.33	13.33	24.414	
7.08		13.721		24.756	24.756
	8.057		13.818	25.195	25.195
8.984		14.014	14.014	25.439	
	8.963	14.795		26.416	
9.619	9.619	15.039		26.514	
	10.156	16.26		27.1	
	10.645		15.088		27.832
10.693		17.236		28.027	
	10.896	18.994			28.125
11.719		19.189		28.174	
	11.768	19.336			28.418
	12.061	20.85	20.85	28.613	28.613
12.158		21.045			

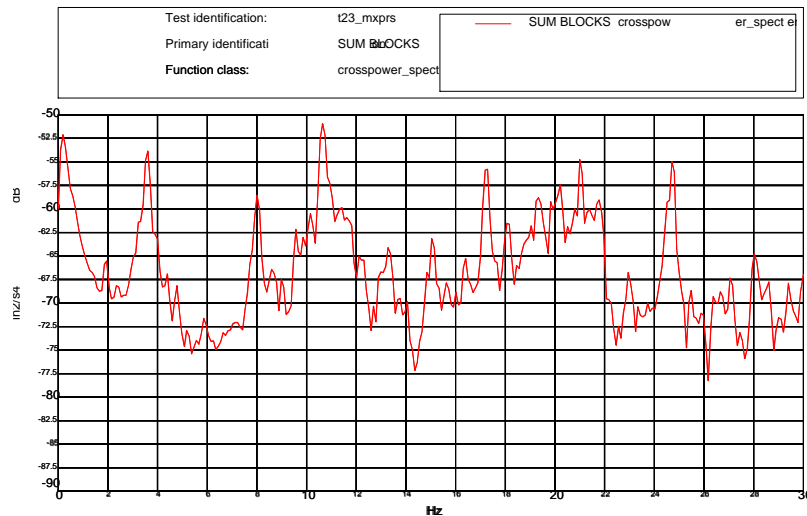


Figure 8.15.3  
Test #23 - Summed Cross Powers





Table 8.15.2  
Test #23 – Peaks in Cross Power

Frequency (Hz)	
1.953	19.336
3.613	20.215
8.008	20.996
10.644	21.777
11.426	24.707
13.281	28.027
15.039	27.051
17.285	28.613
18.066	29.395





8.16 Test #24 - (5z / 60° / 30° / 180° / Half / Closed)  
(Reference Channel / Elevation / Zenith / Angle of Attack / Upwind Gate / Downwind Gate)

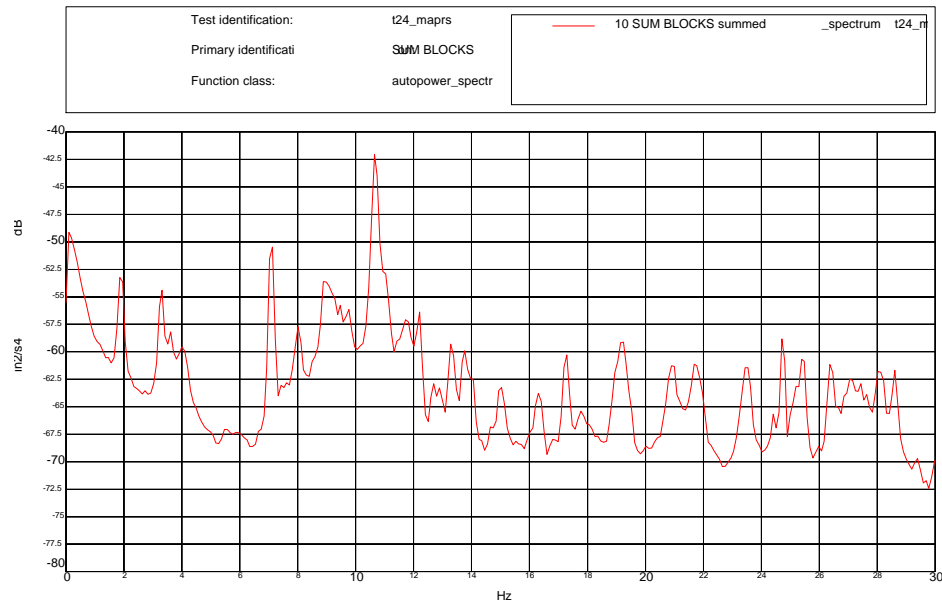


Figure 8.16.1  
Test #24 - Summed Auto Power of the Secondary

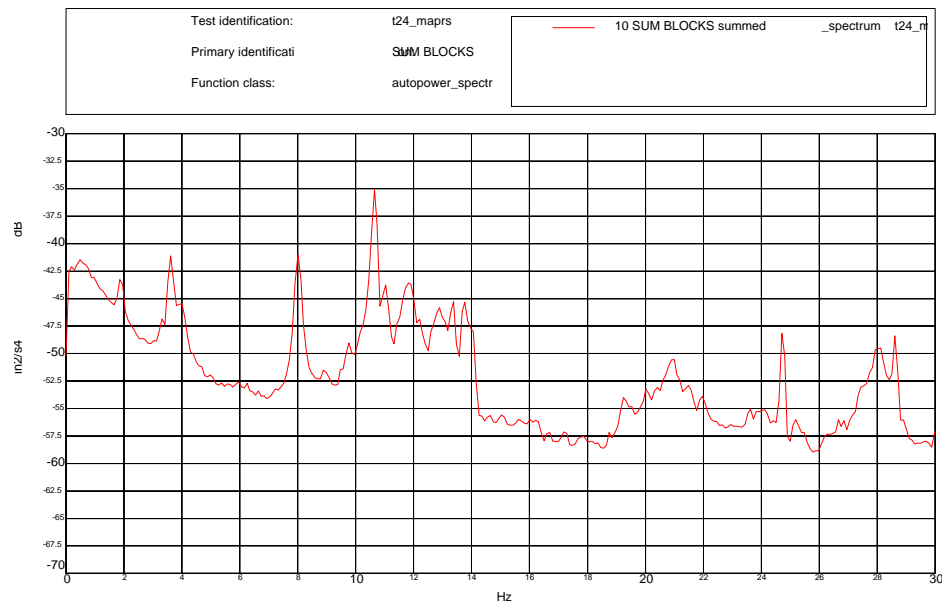


Figure 8.16.2  
Test #24 - Summed Auto Powers of the Primary





Table 8.16.1  
Test #24 - Peaks in the Auto Power Summation by Component

Secondary	Primary	Secondary	Primary	Secondary	Primary
1.904		12.646			20.85
3.32	3.32	12.646		20.947	20.947
3.613	3.613	12.891	12.891	23.438	
4.053		13.329		24.414	
7.08		13.721	13.721	24.756	24.756
	8.008		14.014	25.439	
8.936		14.99		26.416	
9.131		15.088		27.051	
9.277		16.357		27.393	
10.645	10.645	17.236		28.076	
	11.035	17.822			28.125
	11.768	18.945		28.613	28.613
12.207	12.207	19.189			20.85

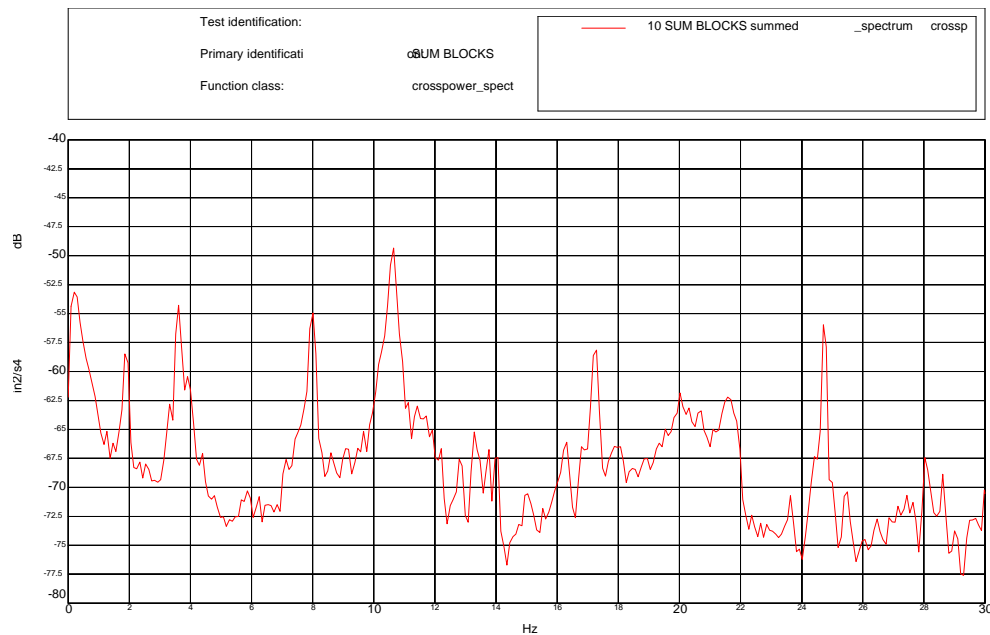


Figure 8.16.3  
Test #24 - Summed Cross Powers





Table 8.16.2  
Test #24 – Peaks in Cross Power

Frequency (Hz)	
1.855	16.309
3.613	17.285
3.906	18.945
7.129	20.02
8.008	20.312
10.644	21.68
11.133	24.707
11.426	25.488
12.207	26.465
13.281	27.441
13.769	28.027
14.062	28.613
15.039	29.004





8.17 Test #31 - (5z / 60° / 30° / 0° / Open / Open)  
(Reference Channel / Elevation / Zenith / Angle of Attack / Upwind Gate / Downwind Gate)

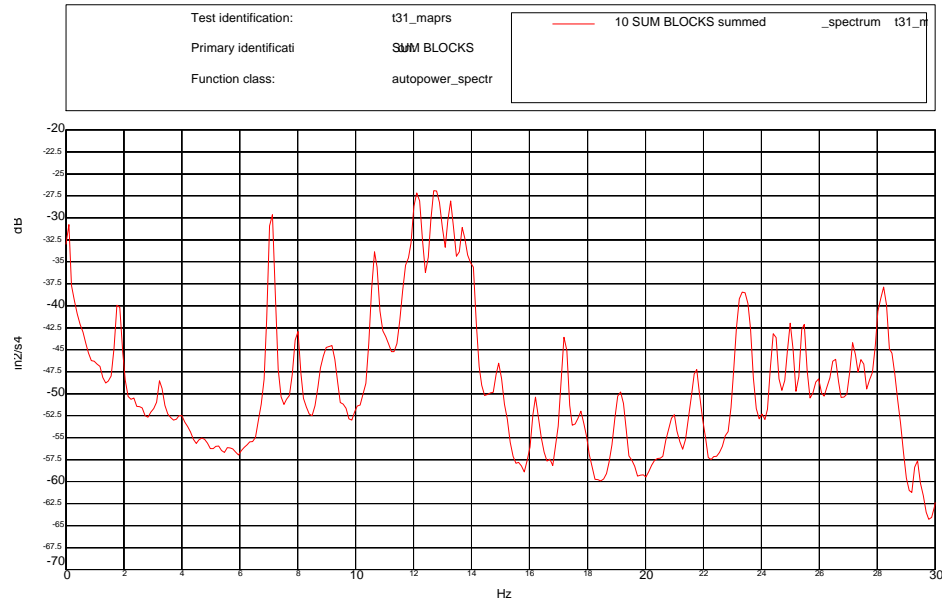


Figure 8.17.1  
Test #31 - Summed Auto Power of the Secondary

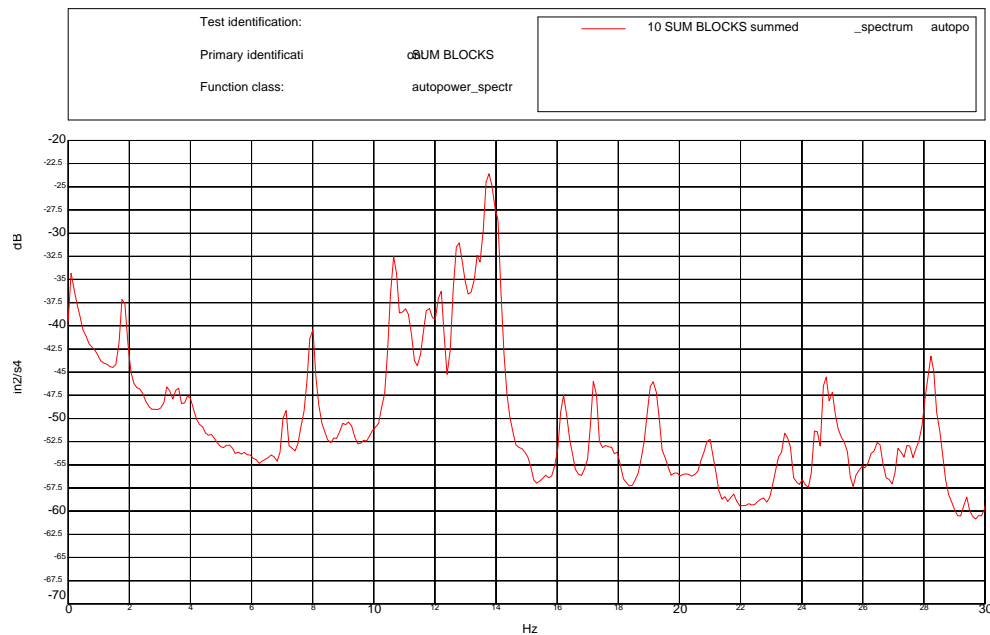


Figure 8.17.2  
Test #31 - Summed Auto Powers of the Primary





Table 8.17.1  
Test #31 - Peaks in the Auto Power Summation by Component

Secondary	Primary	Secondary	Primary	Secondary	Primary
1.807	1.807	12.027		19.141	19.141
	3.223		12.208	20.947	20.947
	3.564		12.844		23.242
	3.955	12.939		23.438	23.438
7.08	7.08	13.379	13.379		23.584
	7.959	13.672	13.672	24.463	24.463
8.936		13.818	13.818		24.756
9.131		14.014	14.014	25	25
10.645	10.645	14.941		25.439	
	11.035	16.211	16.211	26.465	
11.084		17.236	17.236	27.148	
	11.719	17.725		28.223	28.223

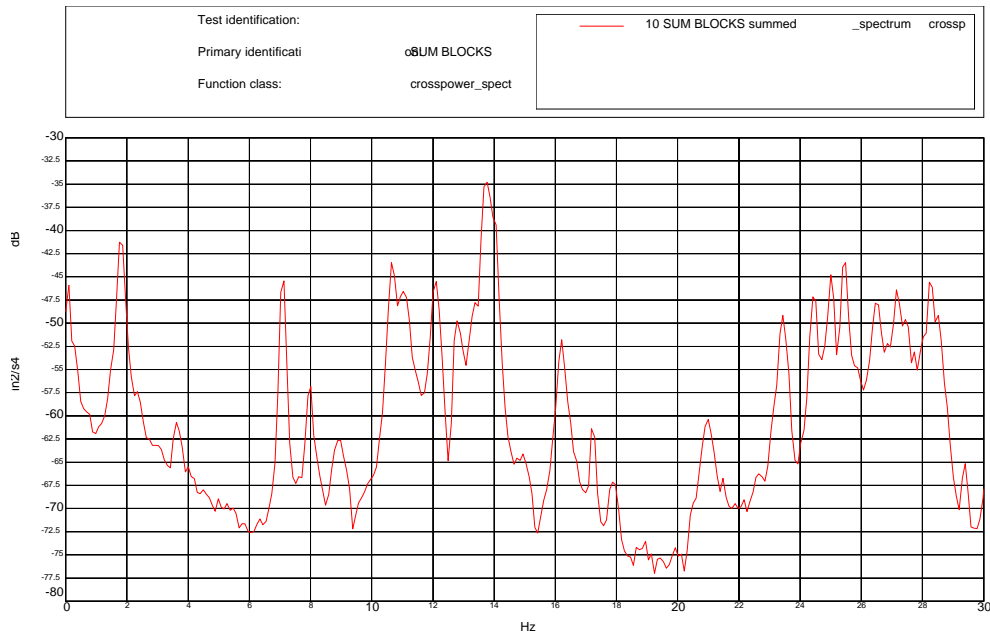


Figure 8.17.3  
Test #31 - Summed Cross Powers





Table 8.17.2  
Test #31 – Peaks in Cross Power

Frequency (Hz)	
1.758	17.773
3.613	19.043
7.129	21.777
8.008	23.633
10.645	24.512
12.207	25
12.891	25.488
13.281	25.879
13.477	26.465
13.672	27.148
14.062	27.734
14.941	28.223
16.211	29.395
17.188	





8.18 Test #33 - (5z / 60° / 30° / 0° / Closed / Open)  
(Reference Channel / Elevation / Zenith / Angle of Attack / Upwind Gate / Downwind Gate)

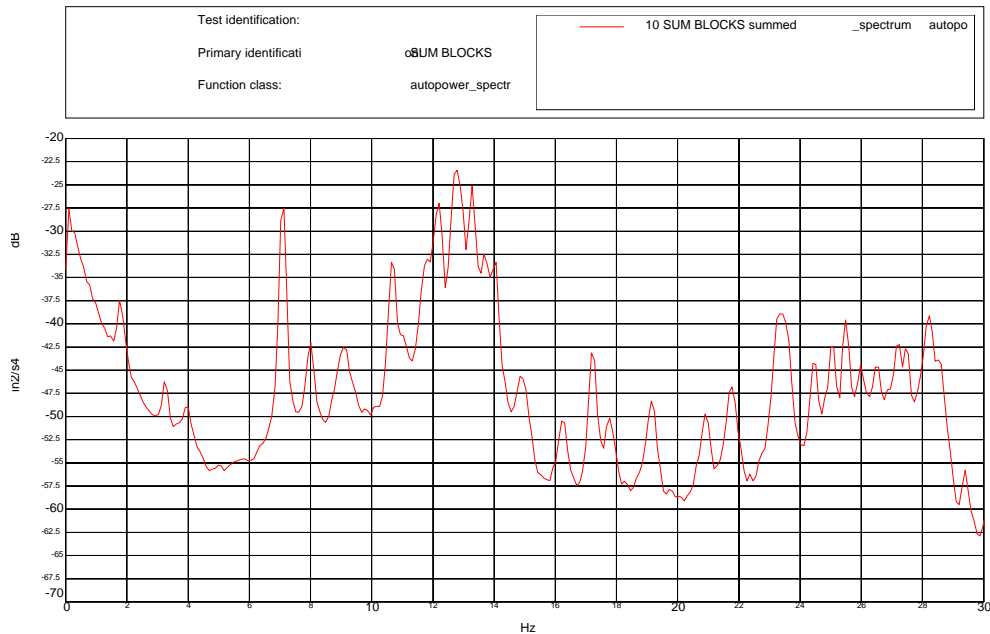


Figure 8.18.1  
Test #33 - Summed Auto Power of the Secondary

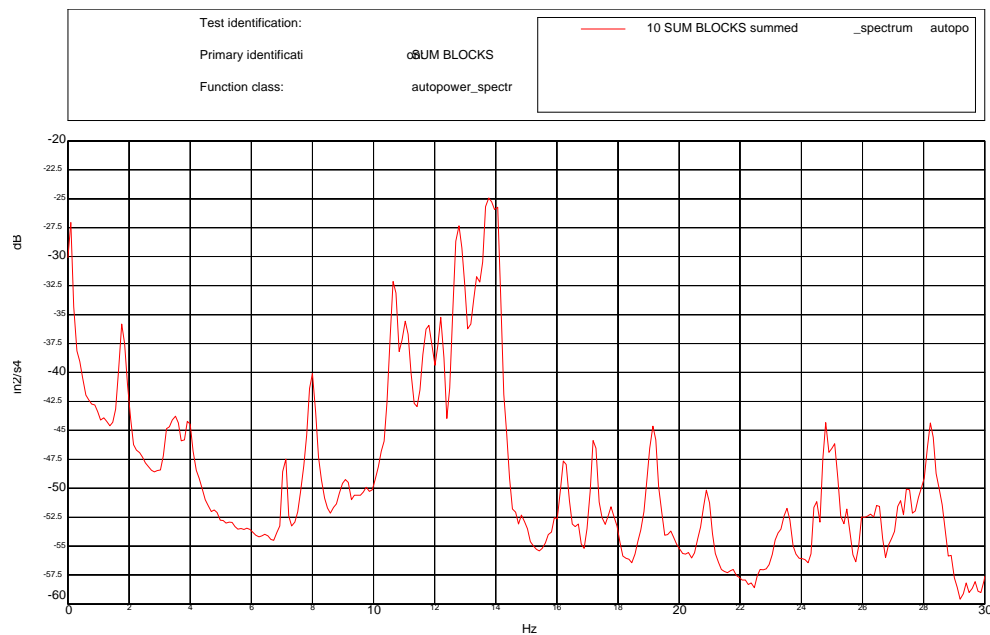


Figure 8.18.2  
Test #33 - Summed Auto Powers of the Primary





Table 8.18.1  
Test #33 - Peaks in the Auto Power Summation by Component

Secondary	Primary	Secondary	Primary	Secondary	Primary
1.758	1.758	12.939			23.584
	3.271	13.379			24.463
	3.467		13.428	24.512	
	3.955	13.721	13.721		24.805
7.08	7.08	13.867	13.867	25.049	25.049
	7.959	14.014	14.014	25.488	25.488
8.936		14.893			26.514
9.131		16.26	16.26	25.977	
10.693	10.693	17.236	17.236	26.514	
10.938			17.725	27.197	27.197
11.035	11.035	17.729		27.49	27.49
	11.719	19.189	19.189	27.783	
	11.816		20.898		28.223
12.207	12.207	20.947		28.271	
	12.744	23.486	23.486	28.564	

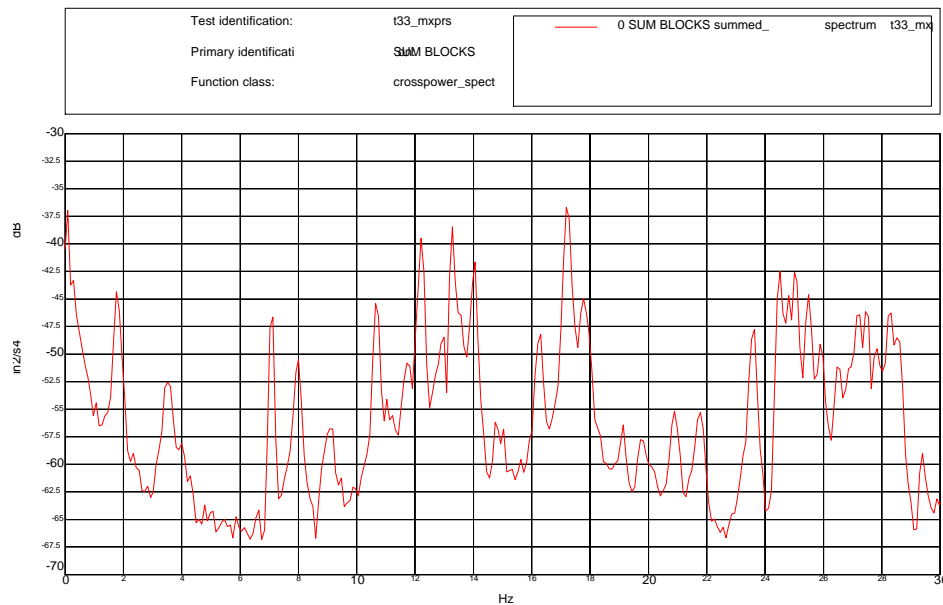


Figure 8.18.3  
Test #33 - Summed Cross Powers





Table 8.18.2  
Test #33 – Peaks in Cross Power

Frequency (Hz)	
1.758	19.141
3.516	19.727
7.129	20.898
8.008	21.777
9.082	23.633
10.645	24.512
11.035	24.805
11.23	25
11.719	25.488
12.207	25.879
12.988	26.465
13.281	27.246
14.062	27.441
14.746	27.832
15.039	28.32
16.309	28.516
17.188	29.395
17.773	29.883





8.19 Test #34 - (5z / 60° / 30° / 45° / Closed / Closed)  
(Reference Channel / Elevation / Zenith / Angle of Attack / Upwind Gate / Downwind Gate)

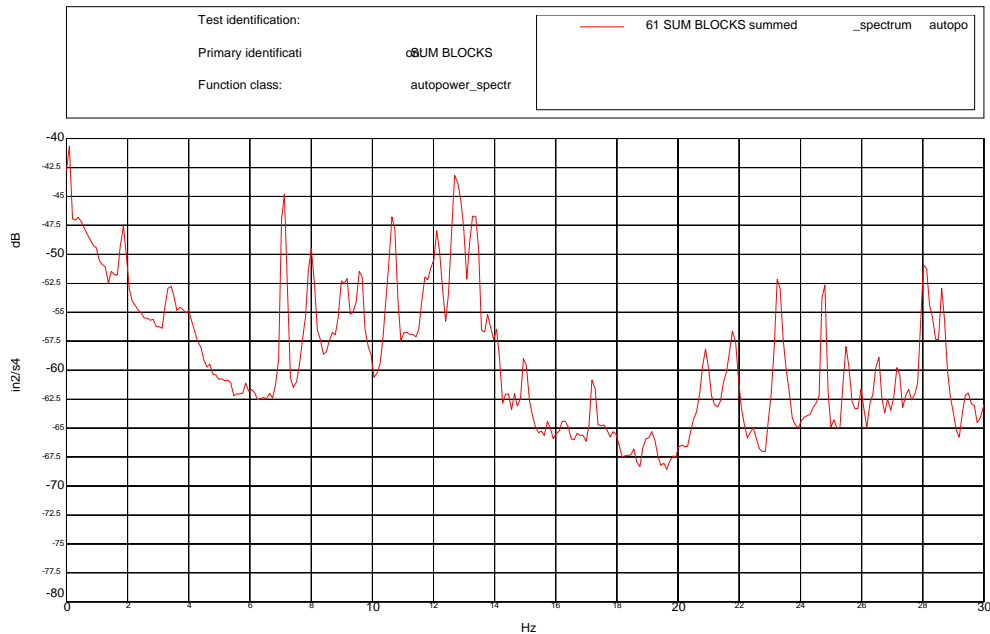


Figure 8.19.1  
Test #34 - Summed Auto Power of the Secondary

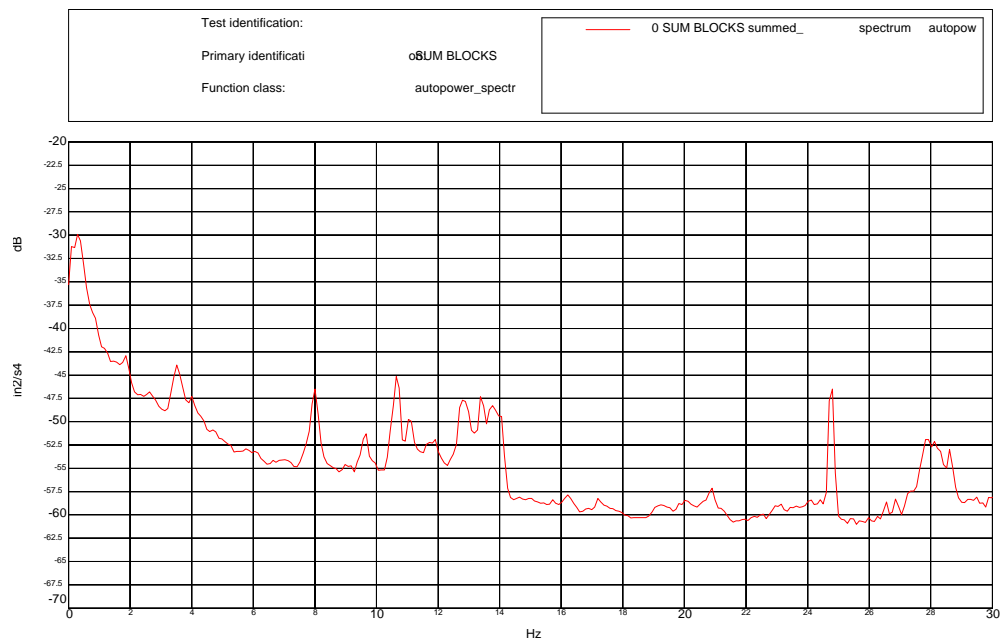


Figure 8.19.2  
Test #34 - Summed Auto Powers of the Primary





Table 8.19.1  
Test #34 - Peaks in the Auto Power Summation by Component

Secondary	Primary	Secondary	Primary	Secondary	Primary
1.855	1.855		11.914	23.242	
3.418		12.109		24.805	24.805
	3.516	12.695		25.488	
3.711			12.793	25.977	
4.004	4.004	13.379	13.379	26.562	26.562
5.859		13.77	13.77		26.855
7.129		14.062		27.148	
8.008	8.008	14.941			27.344
8.984			16.211		27.93
9.18		17.188	17.188	28.027	
9.57		19.141			28.125
	9.668		19.238	28.613	28.613
10.645	10.645		20.02	29.492	29.492
11.035	11.035	20.898	20.898		
11.719		21.77			

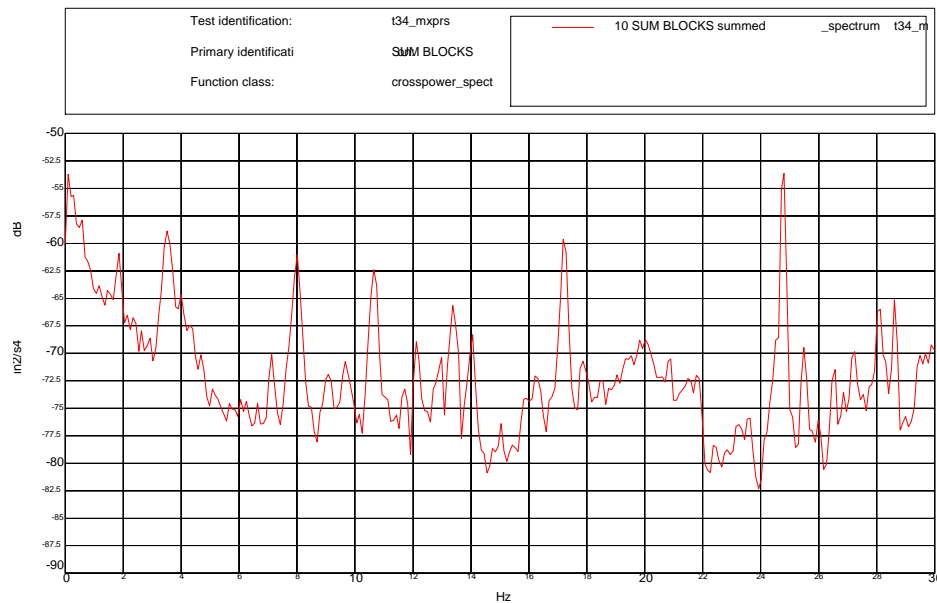


Figure 8.19.3  
Test #34 - Summed Cross Powers





Table 8.19.2  
Test #34 – Peaks in Cross Power

Frequency (Hz)	
1.855	16.211
3.516	17.188
4.004	17.871
7.129	19.824
8.008	20.02
9.082	24.805
9.668	25.488
10.644	26.562
12.109	27.246
12.988	28.125
13.379	28.613
14.062	





## 8.20 Test #35 - (5z / 60° / 30° / 45° / Open / Open)

(Reference Channel / Elevation / Zenith / Angle of Attack / Upwind Gate / Downwind Gate)

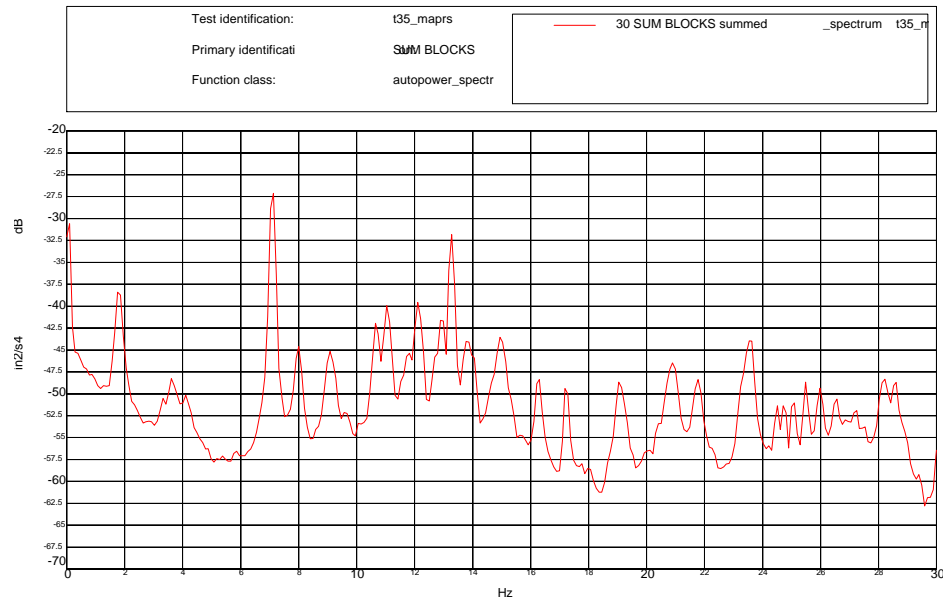


Figure 8.20.1  
Test #35 - Summed Auto Power of the Secondary

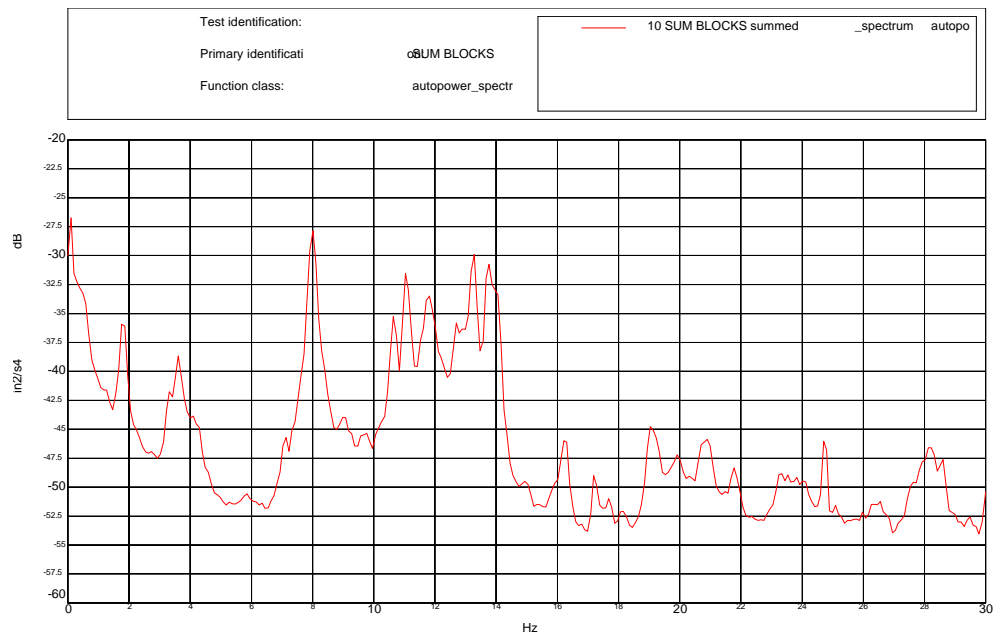


Figure 8.20.2  
Test #35 - Summed Auto Powers of the Primary





Table 8.20.1  
Test #35 - Peaks in the Auto Power Summation by Component

Secondary	Primary	Secondary	Primary	Secondary	Primary
1.758			12.695	20.898	
	1.807	12.988		21.777	21.777
3.32	3.32	13.281	13.281	23.438	
	3.613	13.77	13.77	24.512	
4.162		14.941		25.098	
7.129	7.129		16.211	25.488	
8.008	8.008	16.309		26.522	
9.082	9.082	17.188	17.188	27.246	
10.645	10.645		17.676		27.707
11.035	11.035	19.043	19.043		28.125
	11.816		19.922	28.223	
12.207			20.898	28.613	28.613

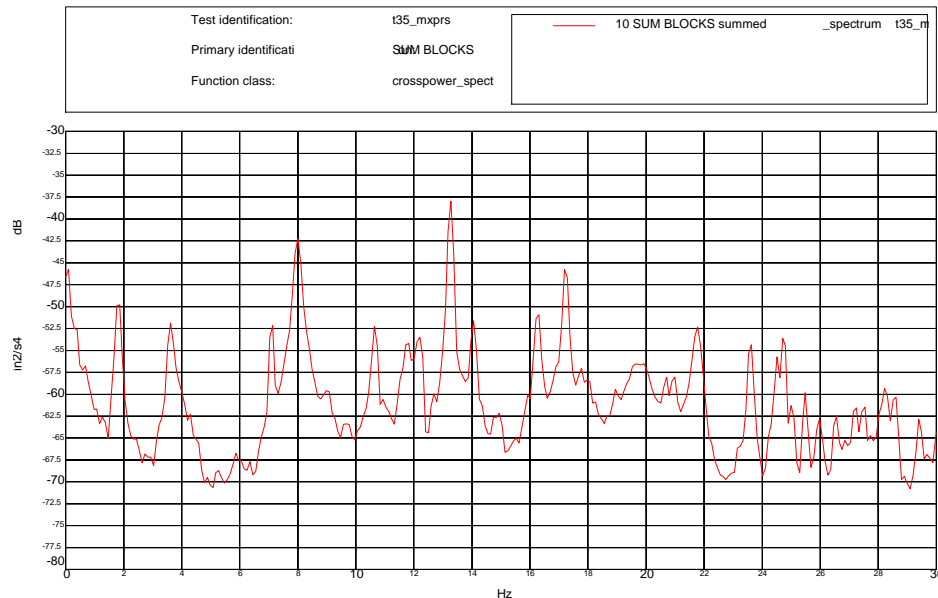


Figure 8.20.3  
Test #35 - Summed Cross Powers





Table 8.20.2  
Test #35 – Peaks in Cross Power

Frequency (Hz)	
1.855	19.922
3.613	21.777
7.129	23.633
8.008	24.512
10.644	24.707
11.816	25.488
12.207	25.977
13.281	26.562
14.062	27.246
16.309	27.539
17.188	28.223
17.773	28.613
19.629	29.395





8.21 Test #36 - (5z / 30° / 60° / 45° / Open / Closed)  
(Reference Channel / Elevation / Zenith / Angle of Attack / Upwind Gate / Downwind Gate)

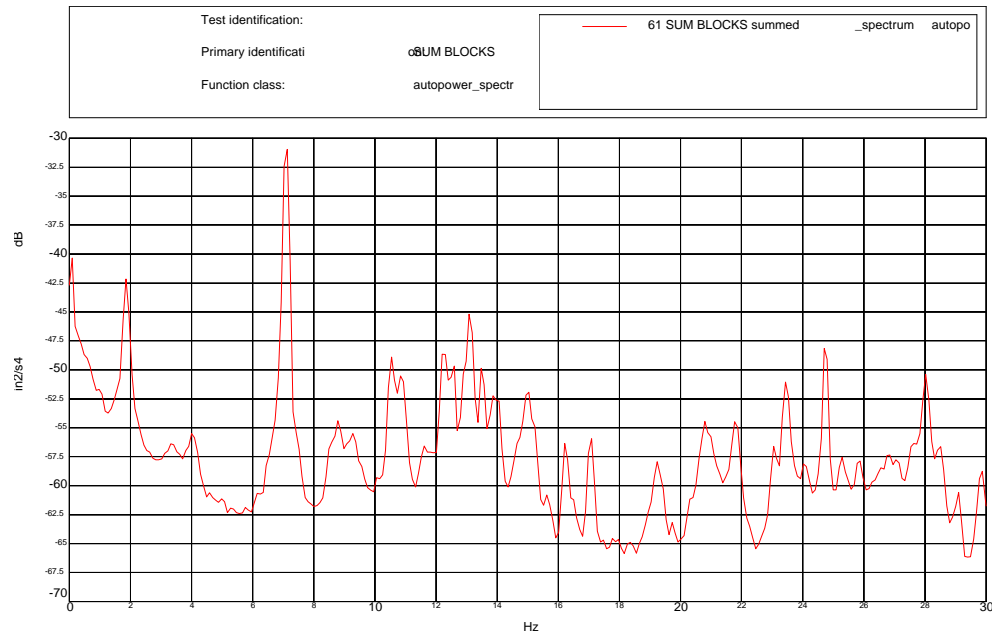


Figure 8.21.1  
Test #36 - Summed Auto Power of the Secondary

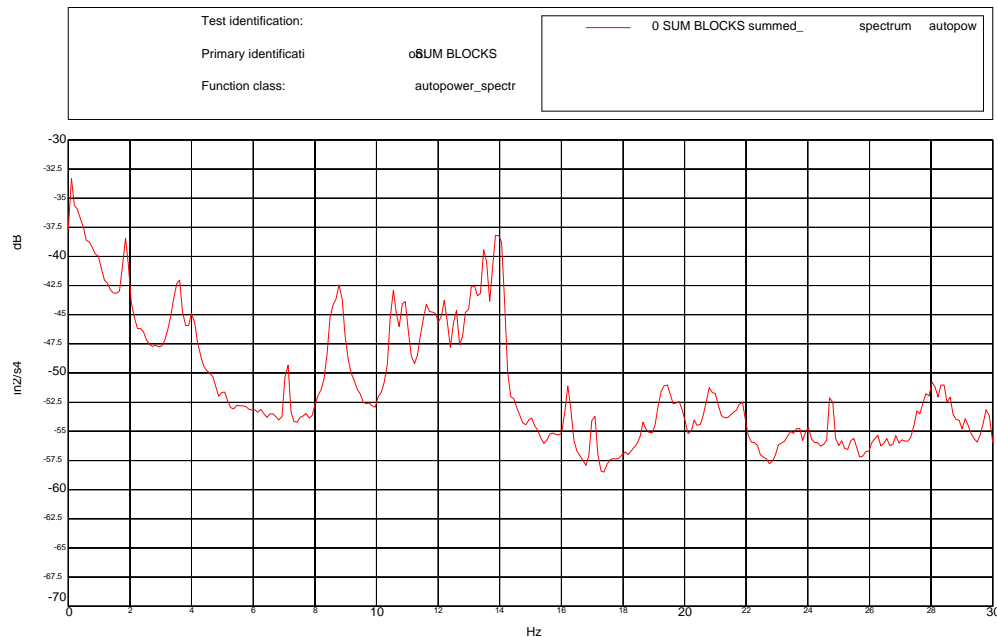


Figure 8.21.2  
Test #36 - Summed Auto Powers of the Primary





Table 8.21.1  
Test #36 - Peaks in the Auto Power Summation by Component

Secondary	Primary	Secondary	Primary	Secondary	Primary
1.855	1.855	12.549	12.549	21.826	21.826
3.418		12.891	12.891	23.047	
	3.564		13.086	23.438	
	4.007	13.184		24.463	
4.102			13.232	24.756	24.756
7.089	7.089	13.525	13.525	25.244	
	8.595	13.867	13.867	25.781	
8.838	8.838	14.014	14.014	26.807	
9.131		14.99	14.99	27.051	
9.326		16.211	16.211	27.588	
10.547	10.547		17.041	28.027	
10.84		17.09			28.076
	10.889		18.652		28.369
	11.572	19.238	19.238	28.467	
	11.914		19.434	28.613	28.613
	12.207		19.824	29.102	
12.354		20.801	20.801		29.785

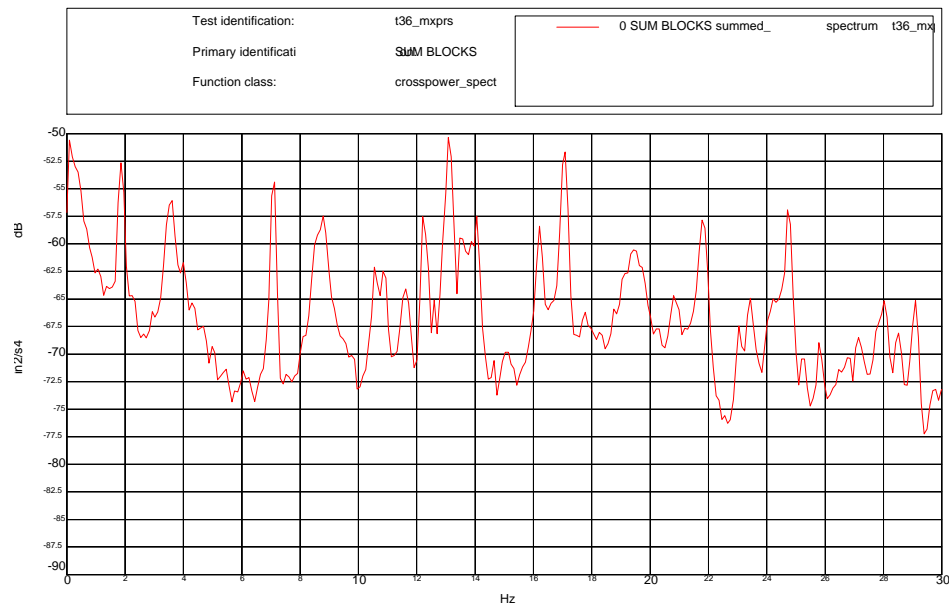


Figure 8.21.3  
Test #36 - Summed Cross Powers





Table 8.21.2  
Test #36 – Peaks in Cross Power

Frequency (Hz)	
1.855	17.09
3.613	19.434
4.004	20.801
7.129	21.777
8.789	23.047
10.547	23.438
10.84	24.219
11.621	24.707
12.207	25.293
12.598	25.781
13.086	27.148
13.477	28.027
13.867	28.516
14.062	29.102
16.211	





8.22 Test #37 - (5z / 30° / 60° / 0° / Closed / Open)  
(Reference Channel / Elevation / Zenith / Angle of Attack / Upwind Gate / Downwind Gate)

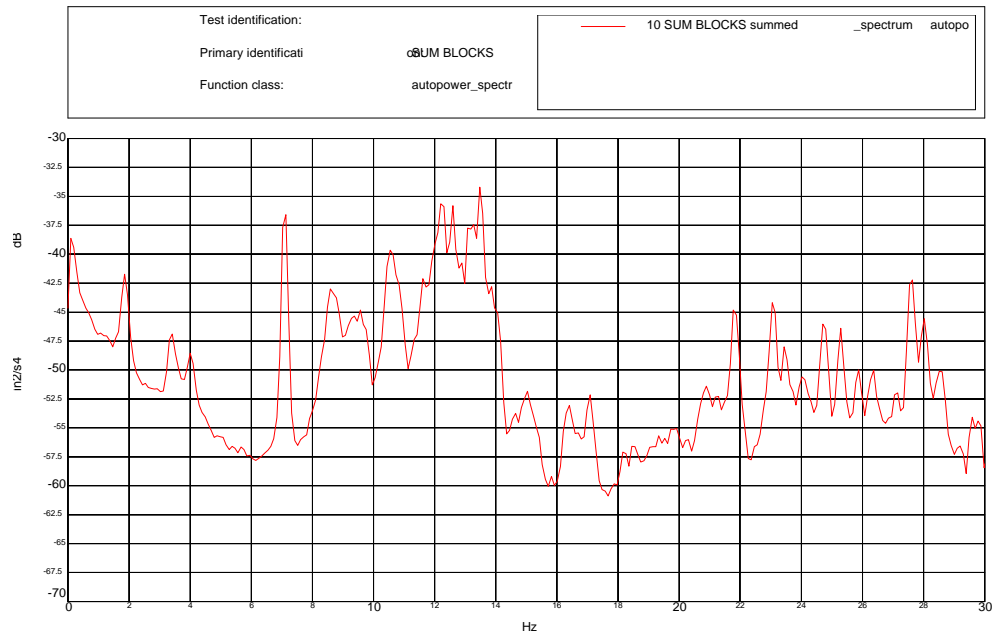


Figure 8.22.1  
Test #37 - Summed Auto Power of the Secondary

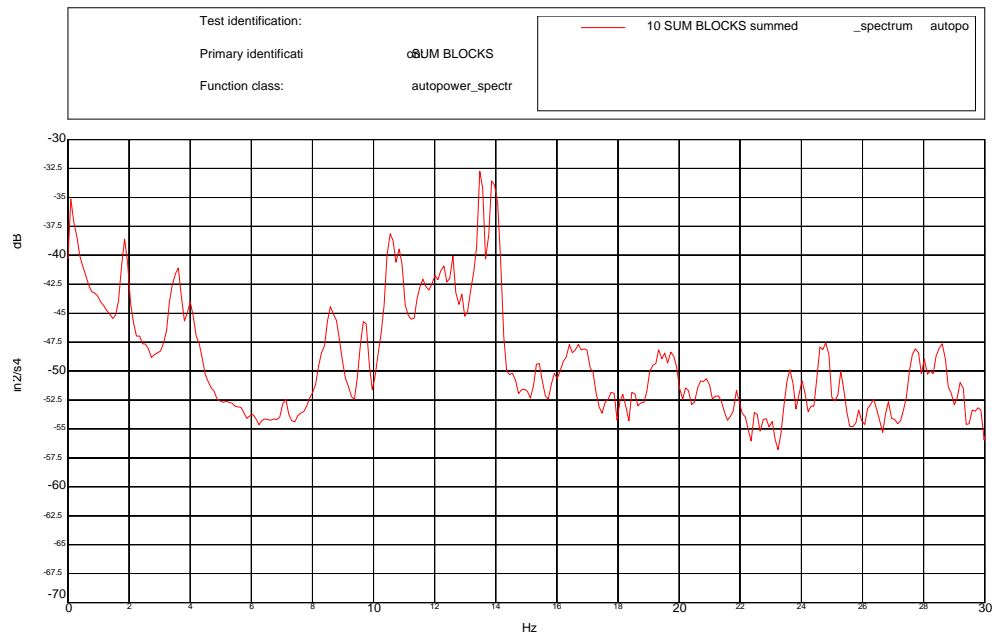


Figure 8.22.2  
Test #37 - Summed Auto Powers of the Primary





Table 8.22.1  
Test #37 - Peaks in the Auto Power Summation by Component

Secondary	Primary	Secondary	Primary	Secondary	Primary	Secondary	Primary
1.855	1.855		12.891	18.457	18.457		24.609
3.418		13.086		19.336	19.336	24.707	
	3.613	13.281			19.531		24.805
4.004	4.004	13.477	13.477	19.727	19.727	25.293	25.293
7.129	7.129	13.867	13.867	19.922		25.879	25.879
8.594	8.594	14.645			20.215	26.367	26.367
9.375		15.039			20.703		26.855
9.57			15.43	20.898	20.898	27.148	
	9.668	15.82		21.289	21.289	27.637	
10.547	10.547		15.918	21.777			27.734
	10.84	16.406	16.406		22.461	28.027	28.027
11.621	11.621		16.699		22.852	28.516	
	12.012		16.89	23.047	23.047		28.613
12.207		17.09		23.438		29.199	29.199
	12.305		17.773		23.633	29.59	29.59
12.598	12.598	18.164	18.164	24.023	24.023	29.785	29.785

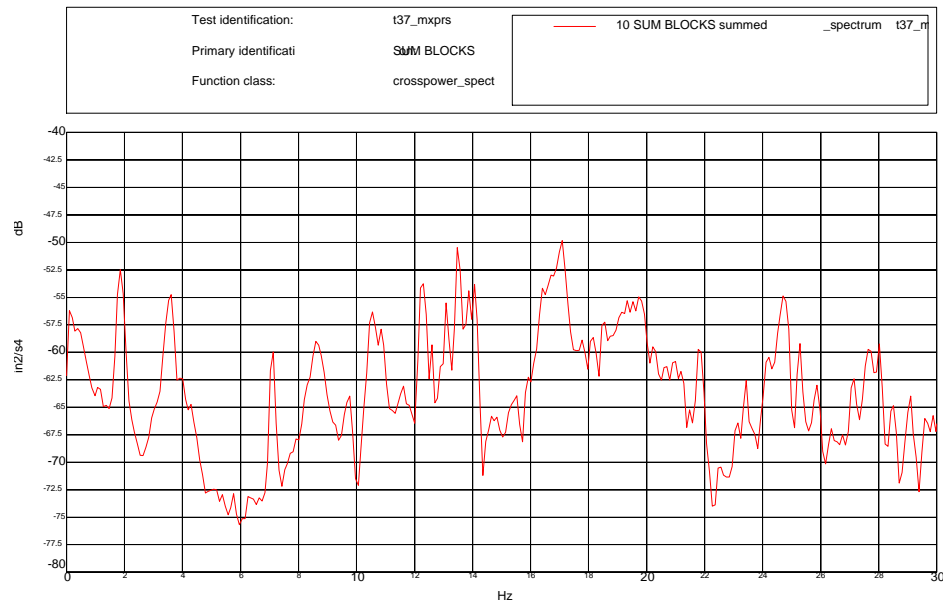


Figure 8.22.3  
Test #37 - Summed Cross Powers





Table 8.22.2  
Test #37 – Peaks in Cross Power

Frequency (Hz)	
1.855	19.141
3.613	19.434
4.004	20.898
7.129	21.777
8.594	23.438
9.766	24.316
10.547	24.805
10.84	25.293
12.305	25.781
12.598	26.367
13.086	27.148
13.477	27.637
13.867	28.027
14.062	28.516
16.211	29.102
17.09	





8.23 Test #38 - (5z / 30° / 60° / 0° / Closed / Closed)  
(Reference Channel / Elevation / Zenith / Angle of Attack / Upwind Gate / Downwind Gate)

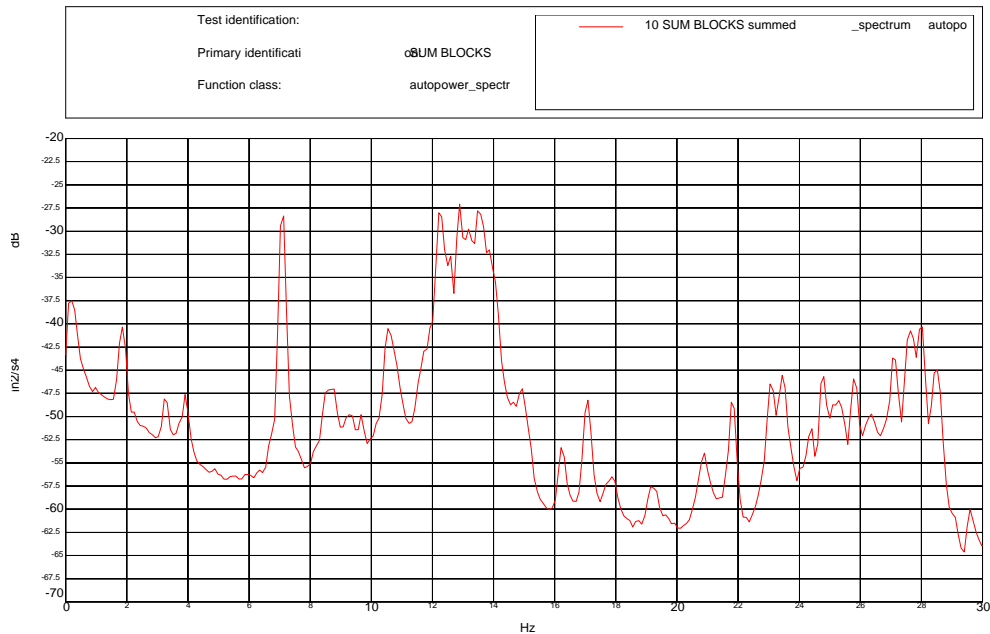


Figure 8.23.1  
Test #38 - Summed Auto Power of the Secondary

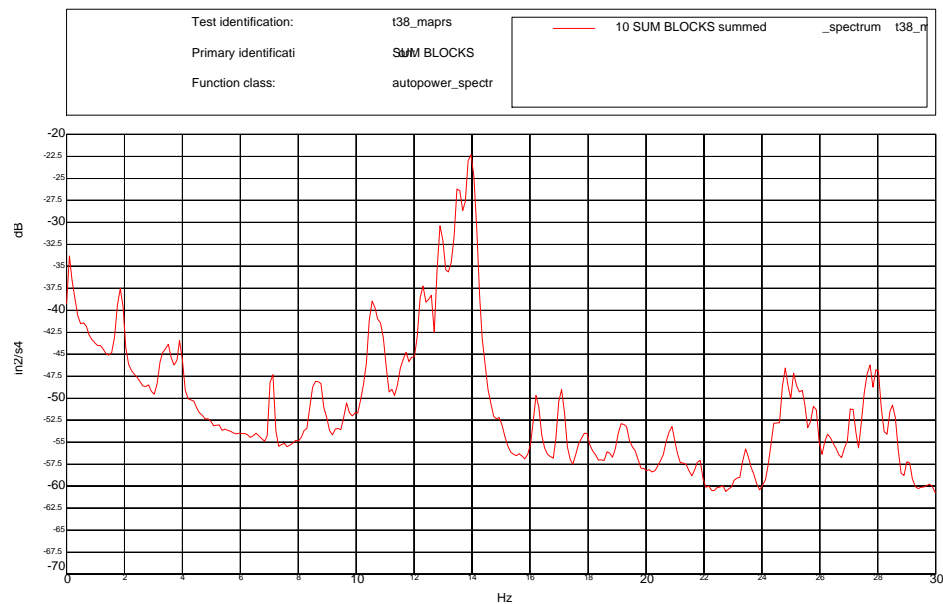


Figure 8.23.2  
Test #38 - Summed Auto Powers of the Primary





Table 8.23.1  
Test #38 - Peaks in the Auto Power Summation by Component

Secondary	Primary	Secondary	Primary	Secondary	Primary
1.855	1.855	13.477	13.477	24.805	
3.223		13.867		25.098	25.098
	3.516		13.965	25.293	
3.906	3.906	14.648			25.391
7.129	7.129	14.941	14.941	25.781	25.781
	8.594	16.211	16.211		26.27
8.789		17.09	17.09	26.367	
9.277		17.871	17.871	27.051	27.051
9.668	9.668		18.652	27.637	
10.547	10.547	19.141	19.141		27.734
	11.719	20.898	20.898		27.93
12.207		21.777		28.027	
	12.305		21.875	28.516	28.516
12.598	12.598	23.047			29.004
12.891	12.891	23.438	23.438	29.59	
13.184		24.414			29.785

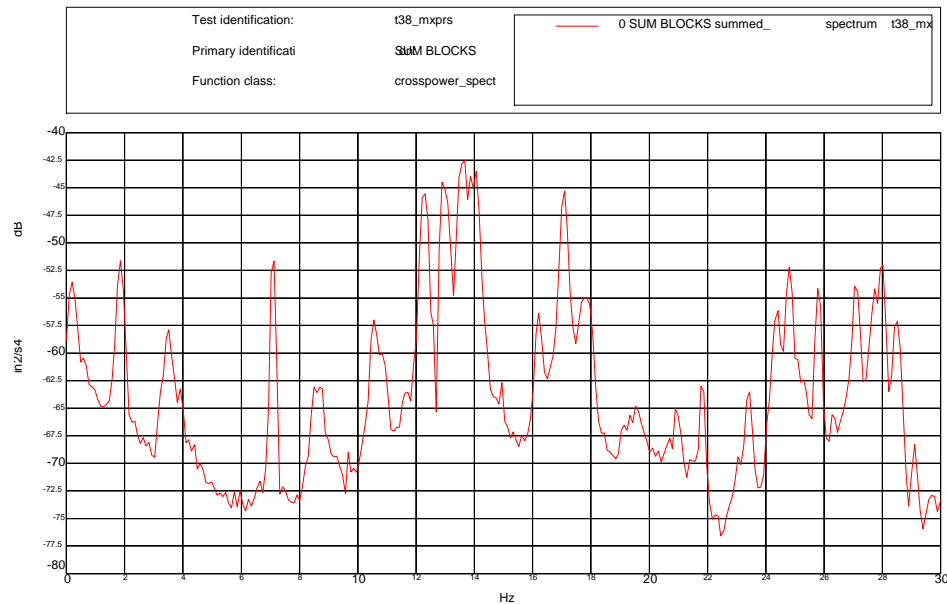


Figure 8.23.3  
Test #38 - Summed Cross Powers





Table 8.23.2  
Test #38 – Peaks in Cross Power

Frequency (Hz)	
1.855	19.141
3.516	19.336
3.906	19.531
7.129	20.898
8.496	21.777
8.691	23.438
10.547	24.414
12.305	24.805
12.891	25.781
13.672	26.27
13.867	27.051
14.062	27.734
14.941	28.027
16.211	28.516
17.09	29.102
17.773	





8.24 Test #39 - (5z / 30° / 60° / 0° / Open / Open)  
(Reference Channel / Elevation / Zenith / Angle of Attack / Upwind Gate / Downwind Gate)

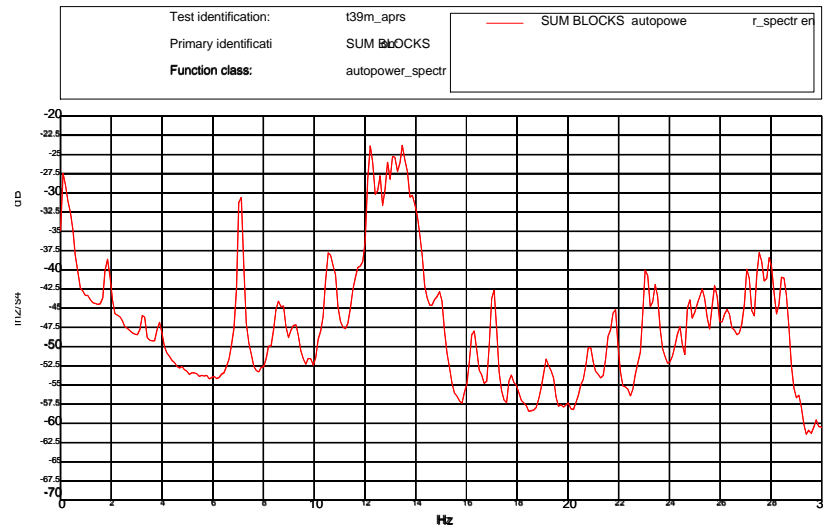


Figure 8.24.1  
Test #39 - Summed Auto Power of the Secondary

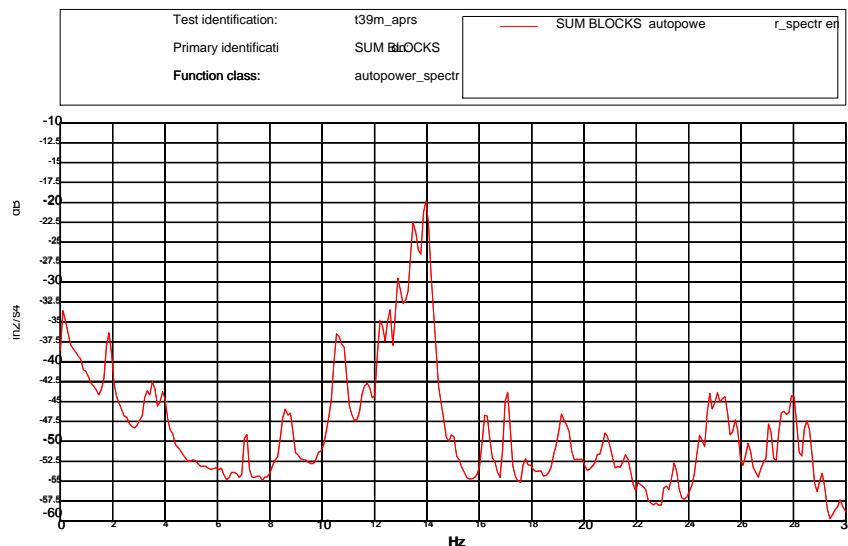


Figure 8.24.2  
Test #39 - Summed Auto Powers of the Primary





Table 8.24.1  
Test #39 - Peaks in the Auto Power Summation by Component

Secondary	Primary	Secondary	Primary	Secondary	Primary
1.855	1.855	12.549			21.582
	3.271		12.598	23.096	
	3.564	12.891	12.891	23.438	23.438
	3.906	13.477	13.477	24.414	24.414
7.08	7.08	13.623		24.805	24.805
	8.545	13.965	13.965		25.098
	8.643	14.99		25.244	
	8.789	16.26	16.26	25.781	25.781
9.326		17.041	17.041		26.27
10.596	10.596	17.725		27.1	27.1
10.791			17.773	27.93	
	11.768	19.141	19.141		27.979
	12.207		19.922		28.516
12.305		20.85	20.85		29.102

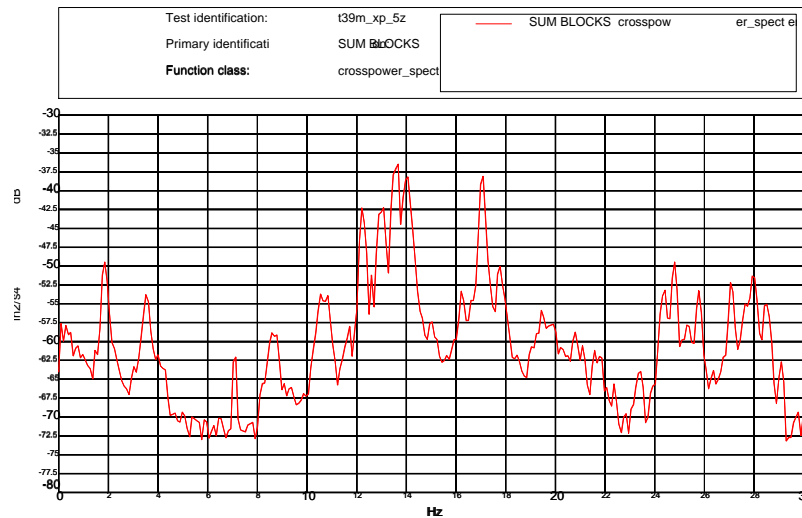


Figure 8.24.3  
Test #39 - Summed Cross Powers





Table 8.24.2  
Test #39 – Peaks in Cross Power

Frequency (Hz)	
1.855	16.211
3.516	17.09
4.004	17.773
7.129	19.434
8.594	19.922
8.789	24.414
10.547	24.805
10.84	25.293
12.207	25.781
12.598	27.051
13.086	27.637
13.672	27.93
14.062	28.516
15.039	29.102





8.25 Test #40 - (5z / 75° / 15° / 45° / Closed / Closed)  
(Reference Channel / Elevation / Zenith / Angle of Attack / Upwind Gate / Downwind Gate)

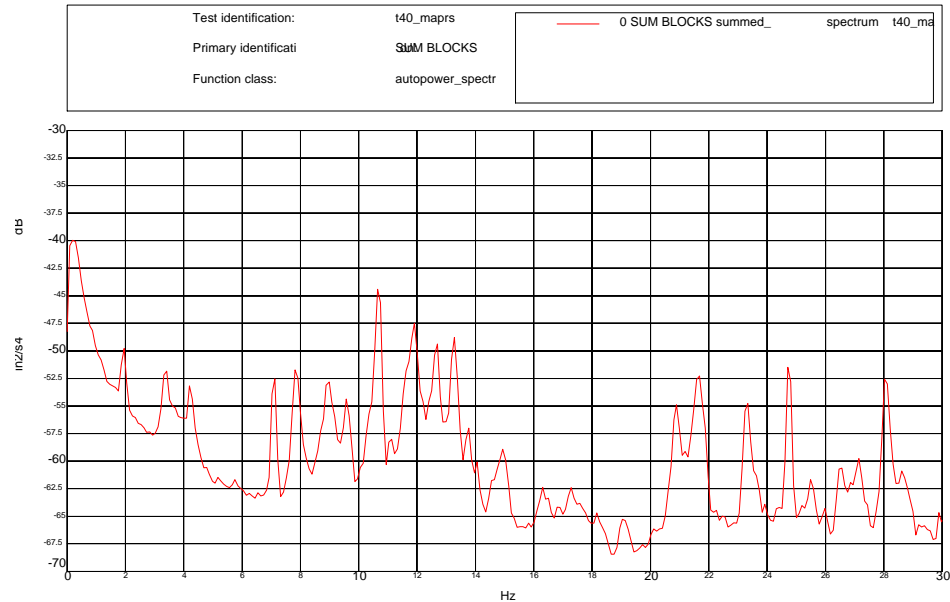


Figure 8.25.1  
Test #40 - Summed Auto Power of the Secondary

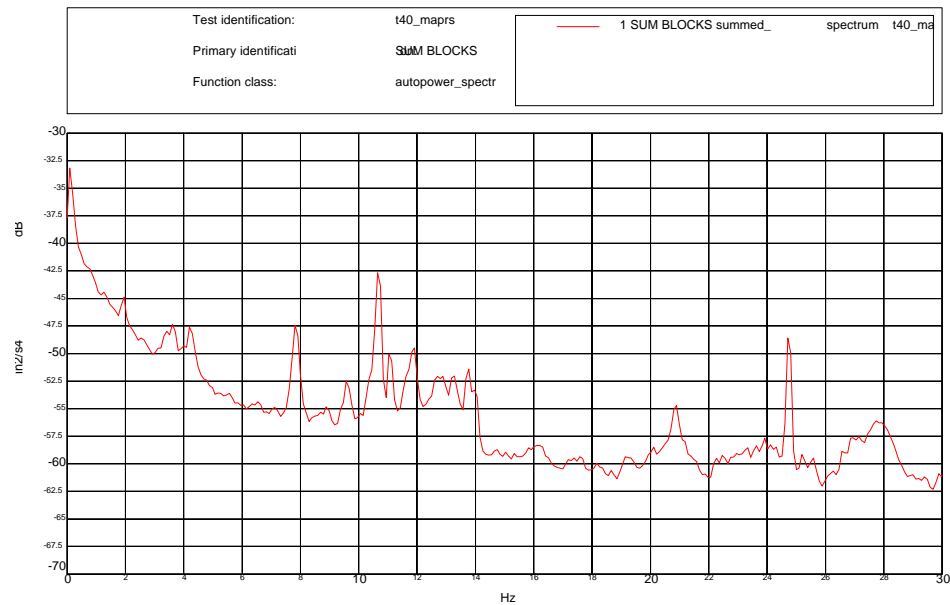


Figure 8.25.2  
Test #40 - Summed Auto Powers of the Primary





Table 8.25.1  
Test #40 - Peaks in the Auto Power Summation by Component

Secondary	Primary	Secondary	Primary	Secondary	Primary
1.953	1.953	13.281	13.281		20.117
3.418	3.418	13.77	13.77	20.898	20.898
	3.613	14.062		21.68	
4.199	4.199	14.941		23.34	23.34
7.129			16.211		23.926
7.812	7.812	16.309		24.707	24.707
	8.887	16.504			25.195
8.984		16.797		25.488	
9.57	9.57		17.188		25.586
10.645	10.645	17.285		25.977	
	11.035		17.383	26.562	26.562
11.133			17.578	27.148	
11.914	11.914	18.164	18.164		27.734
12.695	12.695	19.043		28.027	
	12.891		19.141	28.613	

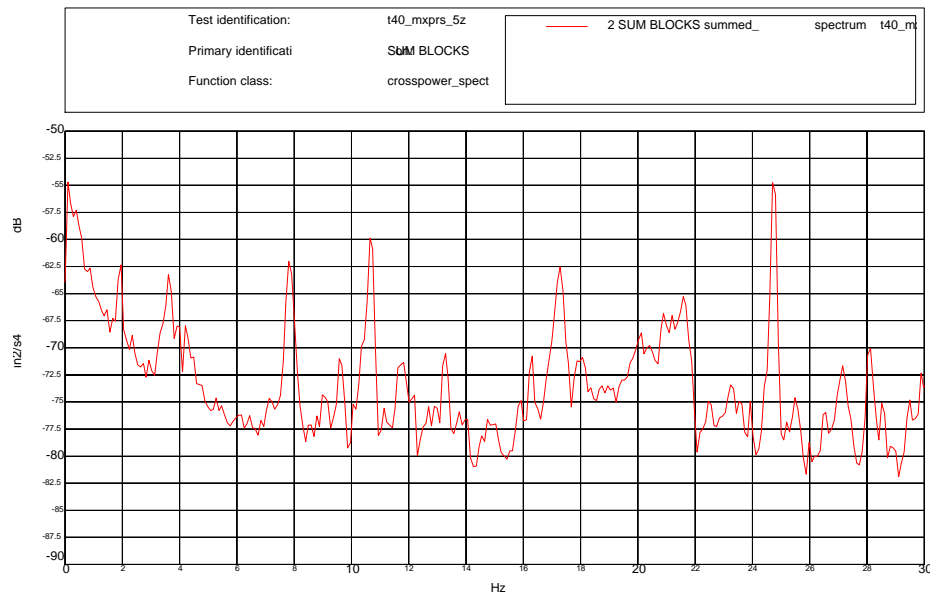


Figure 8.25.3  
Test #40 - Summed Cross Powers





Table 8.25.2  
Test #40 – Peaks in Cross Power

Frequency (Hz)	
1.953	17.871
3.613	18.066
3.906	20.117
4.199	20.41
7.129	20.898
7.813	21.191
9.57	21.582
10.645	22.461
11.133	23.242
11.816	23.535
12.207	23.926
12.695	24.707
12.891	25.488
13.281	27.148
15.918	28.125
16.309	28.516
17.285	29.492





8.26 Test #41 - (5z / 75° / 15° / 90° / Half / Half)  
(Reference Channel / Elevation / Zenith / Angle of Attack / Upwind Gate / Downwind Gate)

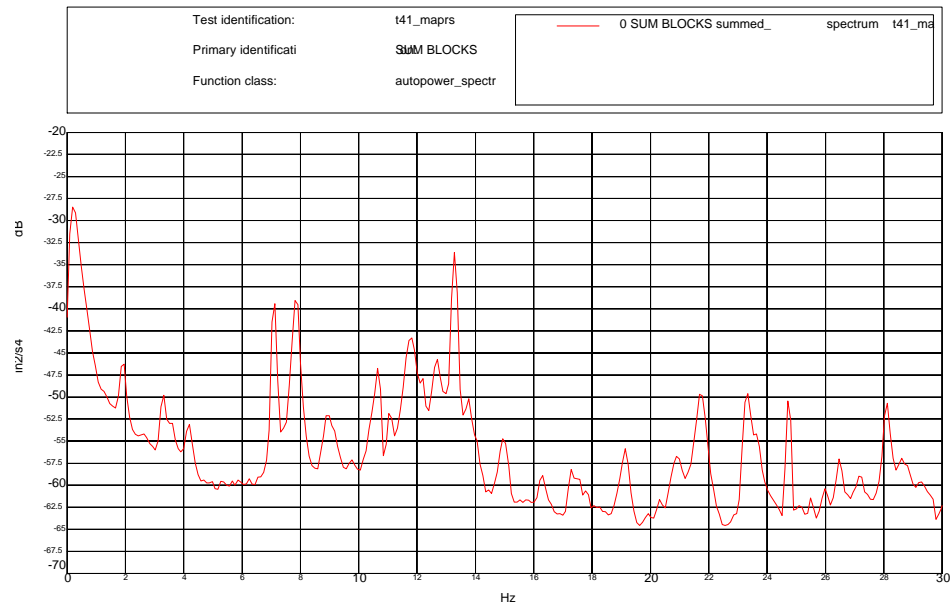


Figure 8.26.1  
Test #41 - Summed Auto Power of the Secondary

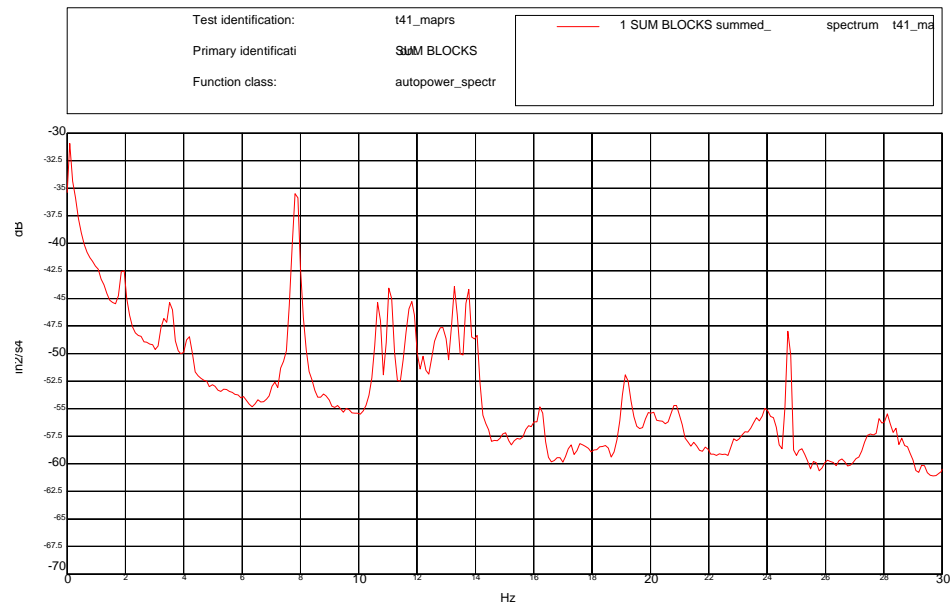


Figure 8.26.2  
Test #41 - Summed Auto Powers of the Primary





Table 8.26.1  
Test #41 - Peaks in the Auto Power Summation by Component

Secondary	Primary	Secondary	Primary	Secondary	Primary
1.953	1.953	13.77	13.77	23.34	
3.32	3.32		14.062	23.633	
	3.516	14.941			23.928
3.613			15.039	24.707	24.707
4.199	4.199		15.82		25.195
7.129			16.211	25.488	
7.812	7.812	16.309		25.977	
8.984		17.285	17.285	26.465	
9.68			17.578	27.148	
10.645	10.645	17.773			27.539
11.035	11.035	19.141	19.141		27.832
11.816	11.816		19.922	28.125	28.125
12.207	12.207		20.117		28.418
12.695		20.312		28.613	28.613
13.281	12.891	20.898	20.898	29.297	
	13.281	21.68			

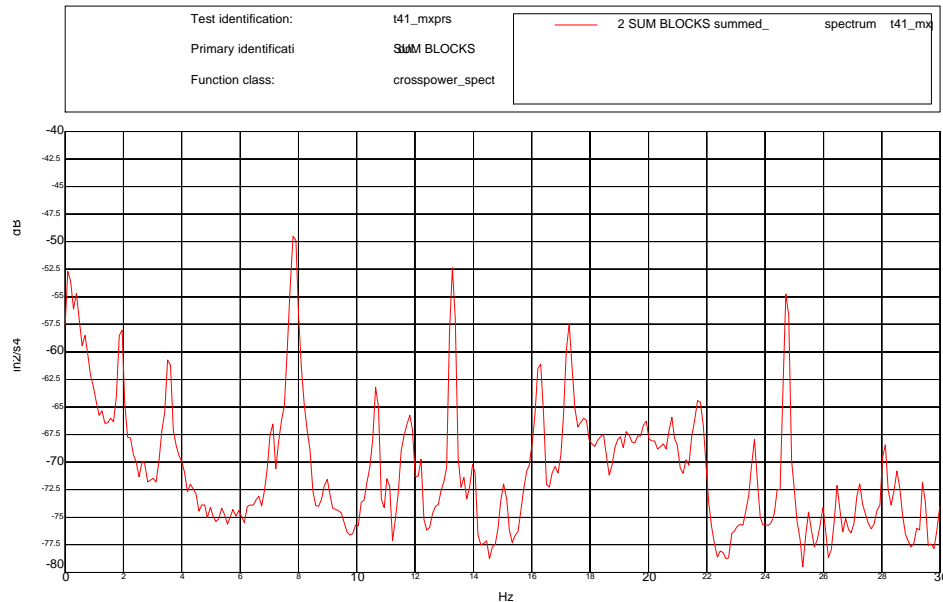


Figure 8.26.3  
Test #41 - Summed Cross Powers





Table 8.26.2  
Test #41 – Peaks in Cross Power

Frequency (Hz)	
1.953	17.285
3.516	19.922
7.129	20.801
7.813	21.68
8.984	23.633
10.645	24.707
11.035	25.488
11.816	25.977
12.207	26.465
13.281	27.246
13.672	28.125
13.965	28.516
15.039	29.395
16.309	





8.27 Test #42 - (5z / 75° / 15° / 135° / Open / Open)  
(Reference Channel / Elevation / Zenith / Angle of Attack / Upwind Gate / Downwind Gate)

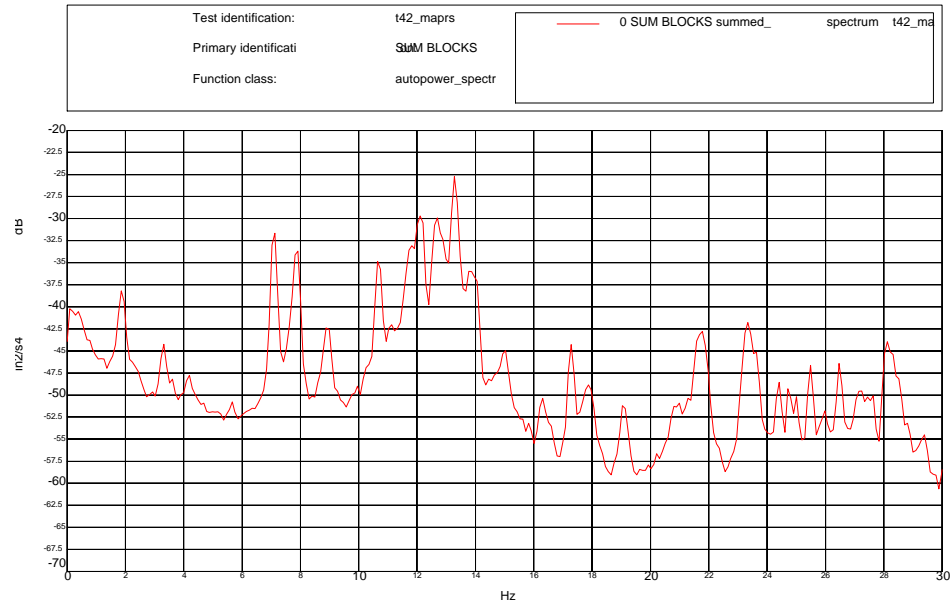


Figure 8.27.1  
Test #42 - Summed Auto Power of the Secondary

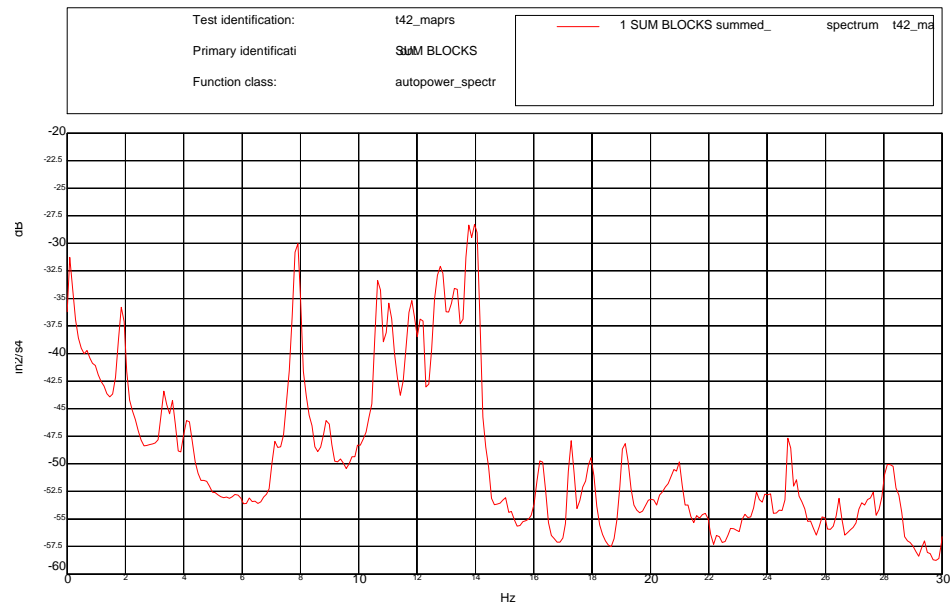


Figure 8.27.2  
Test #42 - Summed Auto Powers of the Primary





Table 8.27.1  
Test #42 - Peaks in the Auto Power Summation by Component

Secondary	Primary	Secondary	Primary	Secondary	Primary
1.855	1.855	12.939		21.631	
3.32	3.32	13.379	13.379	23.438	
	3.613	13.77			23.633
4.15	4.15	13.867		24.414	
7.08		14.014	14.014	24.756	24.756
	7.129	14.746			24.951
7.861	7.861	14.893		25	
8.984	8.984	15.039		25.488	
	10.449		16.211	26.465	26.465
10.693	10.693	16.26		27.148	
11.035		17.285	17.285		27.246
	11.084	17.871			
	11.816	17.898		27.637	27.637
12.158	12.158		17.969	28.125	
	12.685	19.092	19.092		28.174
	12.793	20.801		27.32	28.32
	12.871	20.996	20.996	28.516	

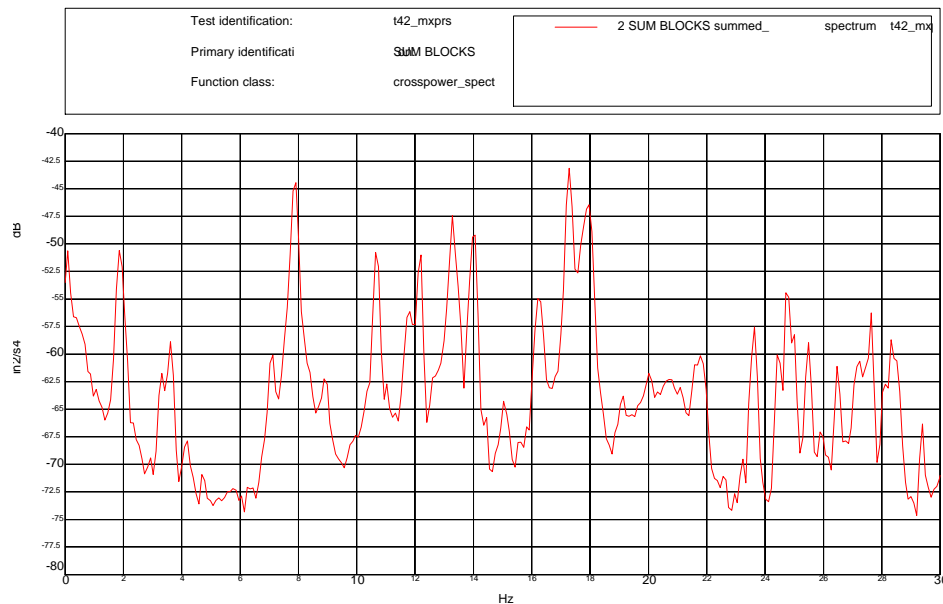


Figure 8.27.3  
Test #42 - Summed Cross Powers





Table 8.27.2  
Test #42 – Peaks in Cross Power

Frequency (Hz)	
1.855	17.969
3.32	19.141
3.613	20.02
7.129	20.703
7.91	21.777
8.887	23.633
10.645	24.414
11.816	24.707
12.207	25.488
13.281	26.465
14.062	27.246
15.039	27.637
16.211	28.32
17.285	29.395





8.28 Test #43 - (5z / 45° / 45° / 135° / Closed / Half)  
(Reference Channel / Elevation / Zenith / Angle of Attack / Upwind Gate / Downwind Gate)

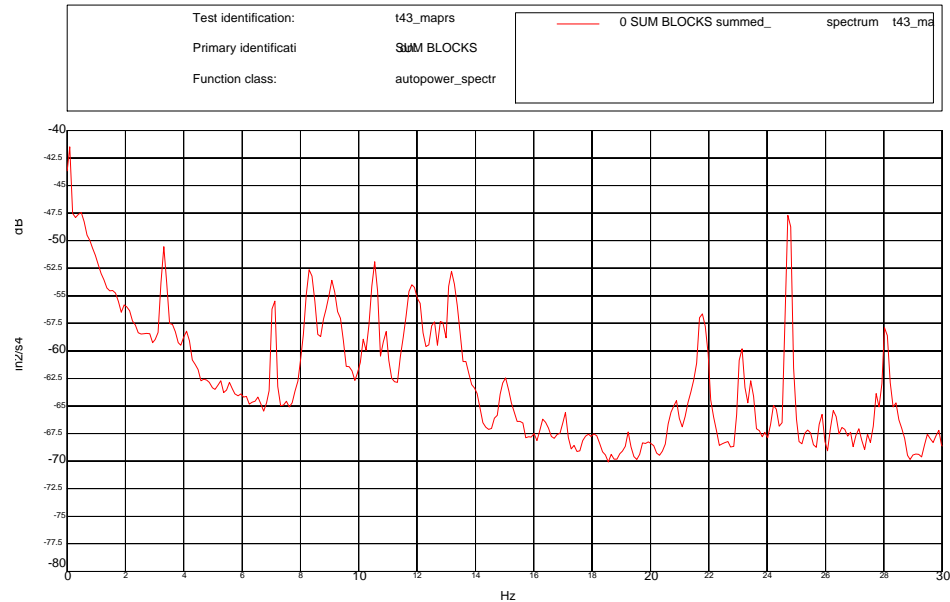


Figure 8.28.1  
Test #43 - Summed Auto Power of the Secondary

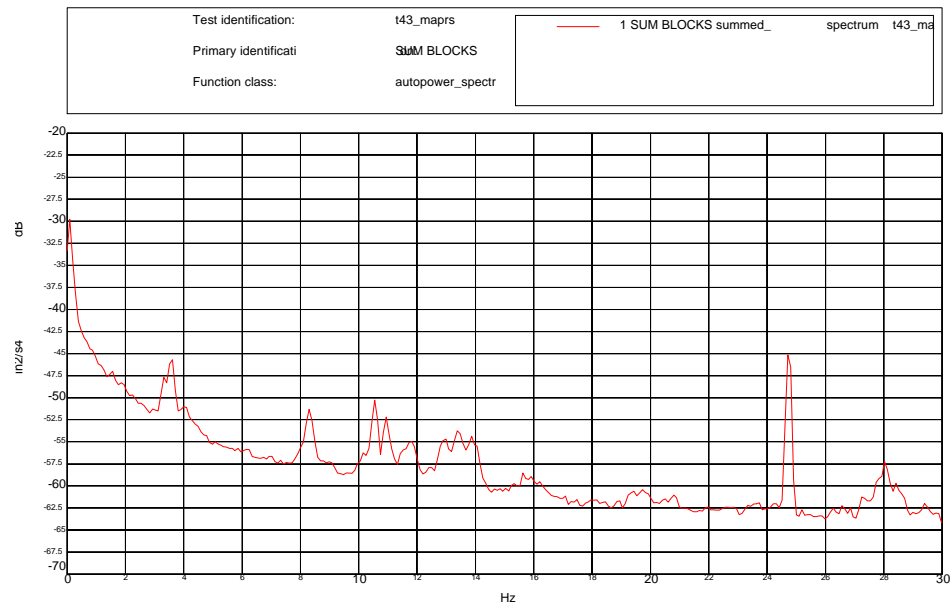


Figure 8.28.2  
Test #43 - Summed Auto Powers of the Primary





Table 8.28.1  
Test #43 - Peaks in the Auto Power Summation by Component

Secondary	Primary	Secondary	Primary	Secondary	Primary
3.32	3.32		13.379	23.438	
	3.613		13.867	24.219	
	4.004	15.039		24.707	24.707
4.102			15.629	25.391	
7.129			15.918	25.879	
8.301	8.301	16.039	19.434	26.27	26.27
9.082		17.09			26.562
10.156	10.156	17.871		27.148	
10.547	10.547	18.066			27.246
10.938	10.938	19.238		27.734	
11.816	11.816	19.727	19.727	28.027	28.027
	12.402	19.922		28.418	28.418
12.516			20.801		29.395
12.793		20.898		29.492	
	12.898	21.777		29.883	
13.184		23.148			

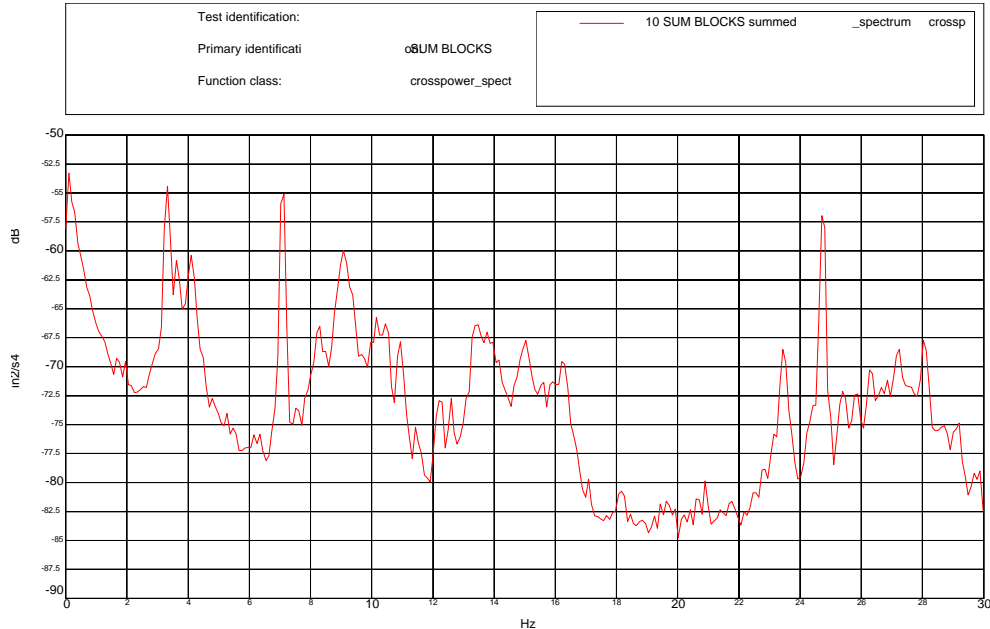


Figure 8.28.3  
Test #43 - Summed Cross Powers





Table 8.28.2  
Test #43 – Peaks in Cross Power

Frequency (Hz)	
3.32	14.16
3.613	15.039
4.102	16.211
7.129	17.09
8.301	18.164
9.082	20.898
10.156	23.438
10.449	24.707
10.937	25.391
11.426	25.879
12.207	26.27
12.598	27.246
13.477	28.027
13.77	29.199
13.965	





8.29 Test #44 - (5z / 45° / 45° / 90° / Open / Closed)  
(Reference Channel / Elevation / Zenith / Angle of Attack / Upwind Gate / Downwind Gate)

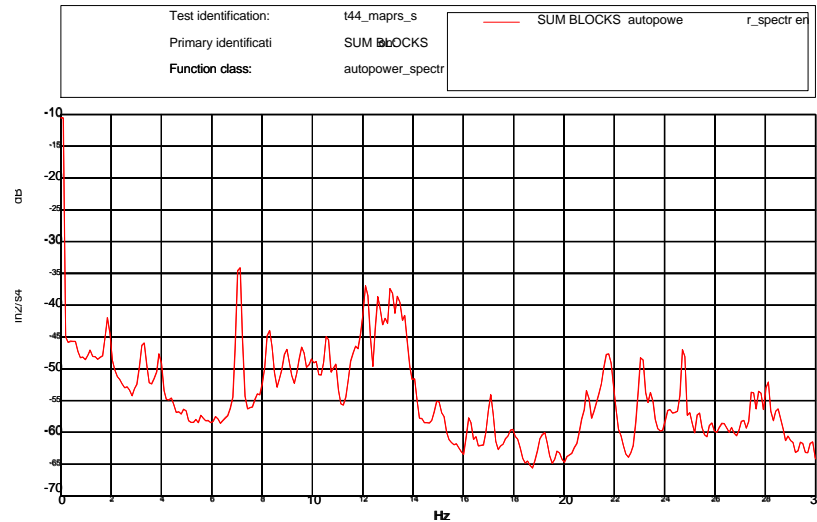


Figure 8.29.1  
Test #44 - Summed Auto Power of the Secondary

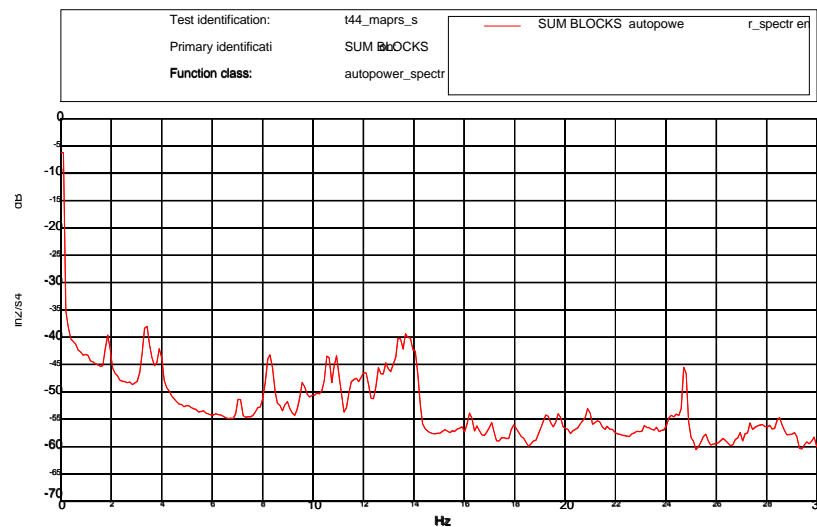


Figure 8.29.2  
Test #44 - Summed Auto Powers of the Primary





Table 8.29.1  
Test #44 - Peaks in the Auto Power Summation by Component

Secondary	Primary	Secondary	Primary	Secondary	Primary	Secondary	Primary
1.855	1.855	10.938		17.09	17.09	23.145	
	3.32	11.523			17.773		23.438
3.369		11.768		17.92		24.268	
3.516		11.963			17.969	24.414	24.414
3.906	3.906		12.256		19.043	24.756	24.756
7.08	7.08	12.646		19.189	19.189		25
8.252		12.891	12.891	19.287			25.342
8.936		13.428	13.428	19.385			25.781
	8.984	13.672	13.672	19.727			27.1
9.57	9.57		13.818		20.752	27.344	
9.961	9.961	13.867		20.898	20.898		28.076
10.107		14.062	14.062	21.289		28.467	
10.596	10.596		14.941	21.68			28.516
	10.889	16.26	16.26		23.096		29.102

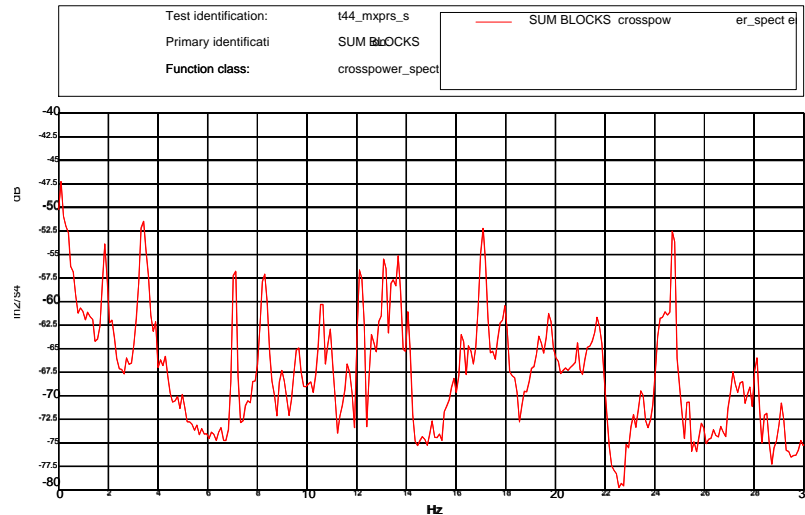


Figure 8.29.3  
Test #44 - Summed Cross Powers





Table 8.29.2  
Test #44 – Peaks in Cross Power

Frequency (Hz)	
1.855	17.969
3.418	19.336
7.129	19.727
8.301	20.898
10.644	21.68
12.109	24.414
13.086	24.707
13.477	27.148
13.672	28.125
16.211	29.102
17.09	





8.30 Test #45 - (5z / 45° / 45° / 90° / Open / Half)  
(Reference Channel / Elevation / Zenith / Angle of Attack / Upwind Gate / Downwind Gate)

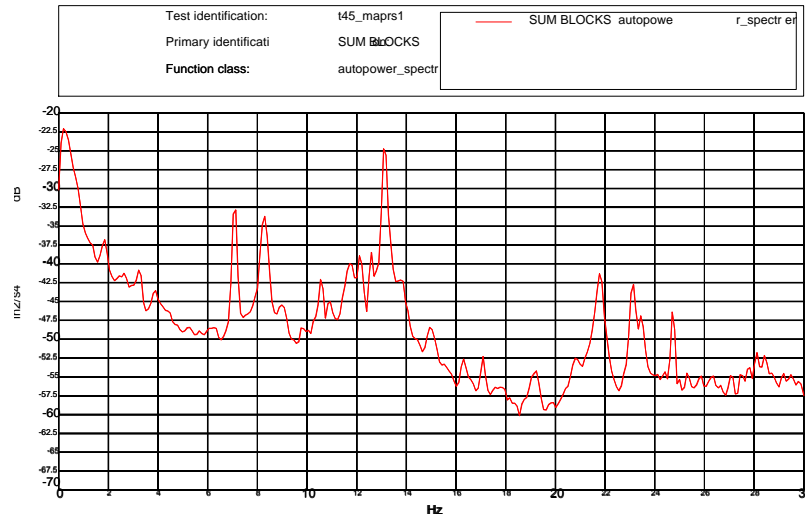


Figure 8.30.1  
Test #45 - Summed Auto Power of the Secondary

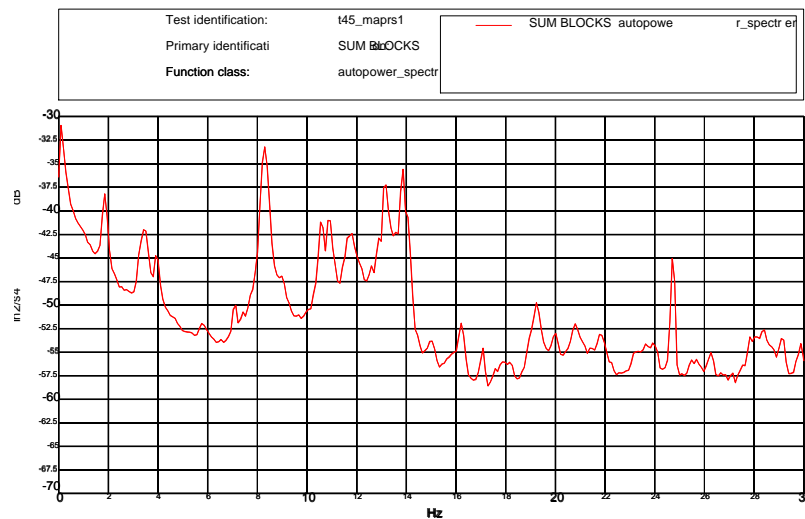


Figure 8.30.2  
Test #45 - Summed Auto Powers of the Primary





Table 8.30.1  
Test #45 - Peaks in the Auto Power Summation by Component

Secondary	Primary	Secondary	Primary	Secondary	Primary
1.855	1.855	12.207		23.096	
3.271	3.271	12.598	12.598	23.438	
	3.467	12.891	12.891		23.626
3.955	3.955	13.135	13.135	24.365	
	5.762	13.867	13.867	24.756	24.756
7.08	7.08		14.062	25	
8.301	8.301	14.941	14.941	25.342	
8.838	8.838		15.039	25.781	
9.033	9.033		16.211	26.367	
9.131		16.26		26.66	
9.521		17.09	17.09	27.1	
9.814		17.773		27.539	
10.059		19.092		27.832	
10.596	10.596	19.238	19.238	28.076	28.369
10.889	10.889		19.971	28.516	
	11.67	20.752	20.752	29.15	
	11.816	21.777			

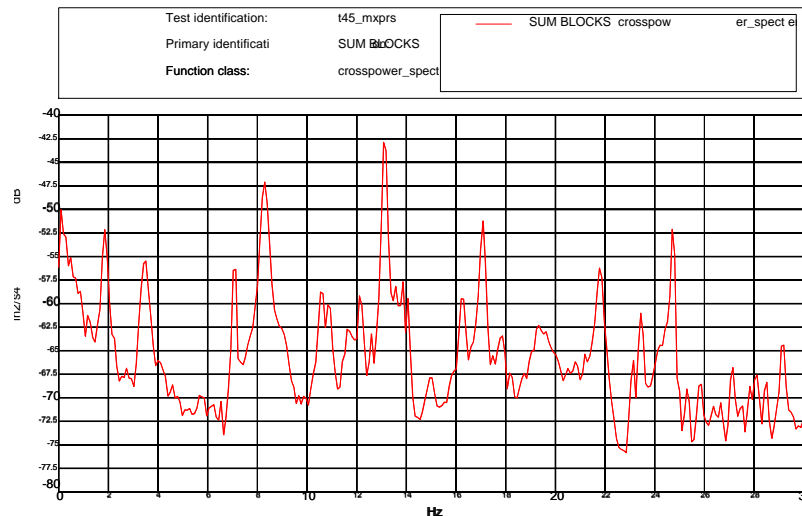


Figure 8.30.3  
Test #45 - Summed Cross Powers





Table 8.30.2  
Test #45 – Peaks in Cross Power

Frequency (Hz)	
1.172	16.211
1.855	17.09
3.516	17.48
4.004	17.871
7.129	19.336
8.301	19.629
10.547	21.777
10.84	23.145
12.109	23.438
13.086	24.707
13.574	27.148
13.867	28.125
14.062	29.199
14.941	





8.31 Test #46 - (5z / 45° / 45° / 90° / Open / Open)  
(Reference Channel / Elevation / Zenith / Angle of Attack / Upwind Gate / Downwind Gate)

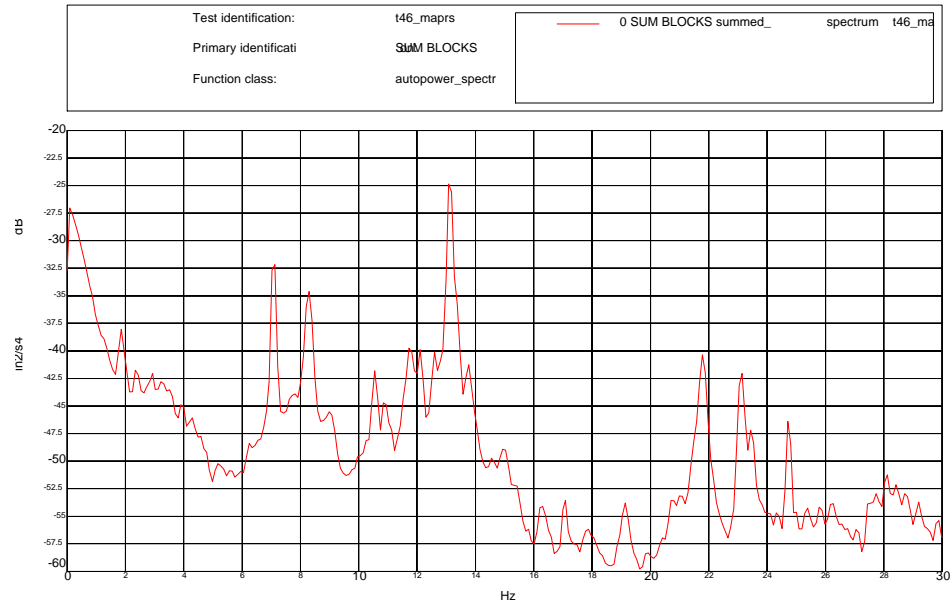


Figure 8.31.1  
Test #46 - Summed Auto Power of the Secondary

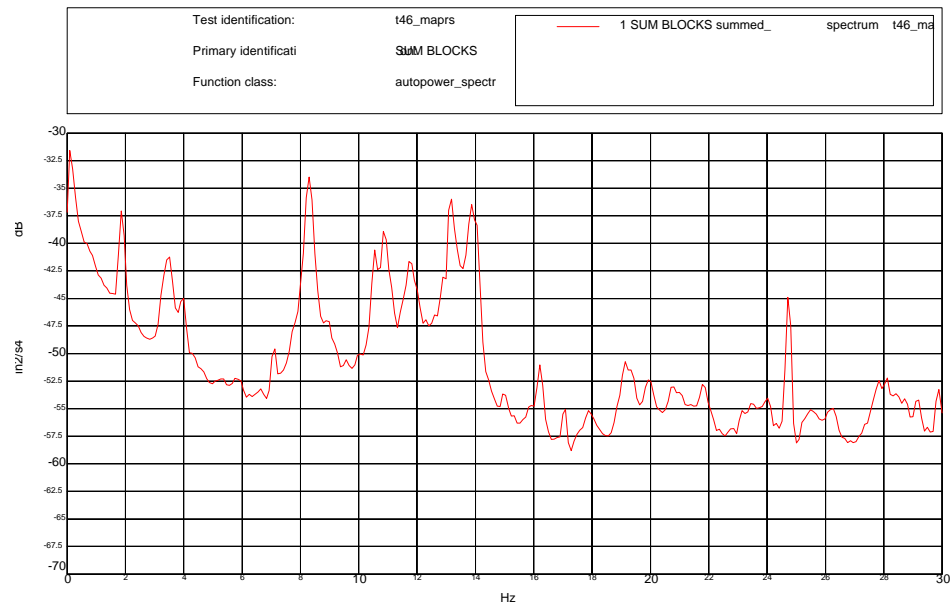


Figure 8.31.2  
Test #46 - Summed Auto Powers of the Primary





Table 8.31.1  
Test #46 - Peaks in the Auto Power Summation by Component

Secondary	Primary	Secondary	Primary	Secondary	Primary
1.855	1.855	14.941		25.342	
3.271		16.211	16.211	25.781	
	3.516	17.041	17.041	26.27	
	3.955	17.822		26.416	
4.004		19.092		26.562	
7.08	7.08	19.189	19.189	26.807	
8.301	8.301	19.336	19.336	27.1	
9.033			19.971	27.49	
10.596	10.596	20.752		27.637	
10.84	10.84	20.85		27.832	27.832
11.768	11.768	20.947			28.125
12.207		21.826	21.826	28.078	
12.598		23.096			28.418
12.891	12.891	23.438		28.516	
13.135	13.135	24.365			28.76
13.867	13.867	24.756	24.756	29.15	29.15
14.062	14.062	25			

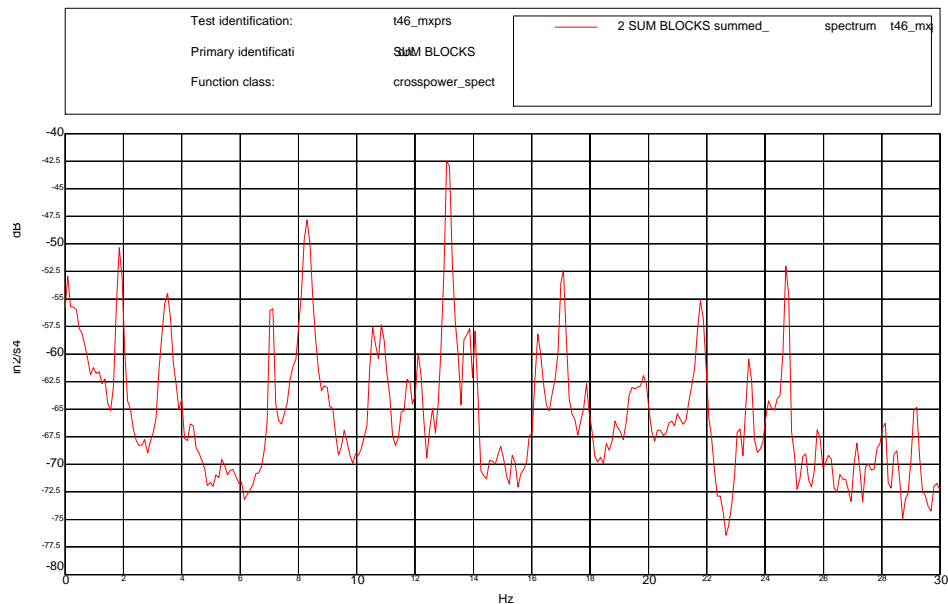


Figure 8.31.3  
Test #46 - Summed Cross Powers





Table 8.31.2  
Test #46 – Peaks in Cross Power

Frequency (Hz)	
1.855	16.211
3.516	17.09
7.129	17.871
8.301	19.336
10.547	19.824
10.84	21.777
11.816	23.438
12.109	24.707
13.086	25.781
13.867	28.125
14.062	29.199





8.32 Test #47 - (5z / 45° / 45° / 45° / Half / Open)  
(Reference Channel / Elevation / Zenith / Angle of Attack / Upwind Gate / Downwind Gate)

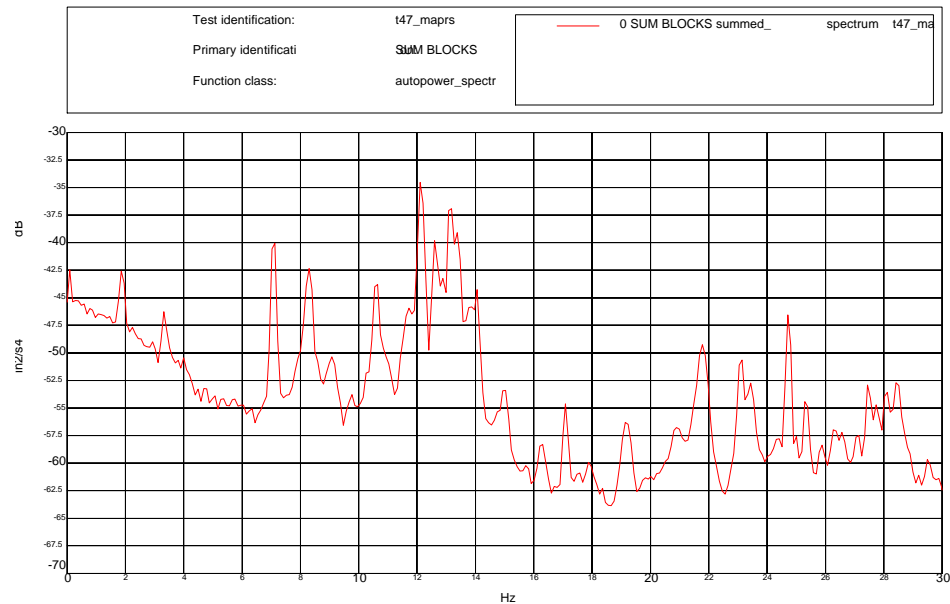


Figure 8.32.1  
Test #47 - Summed Auto Power of the Secondary

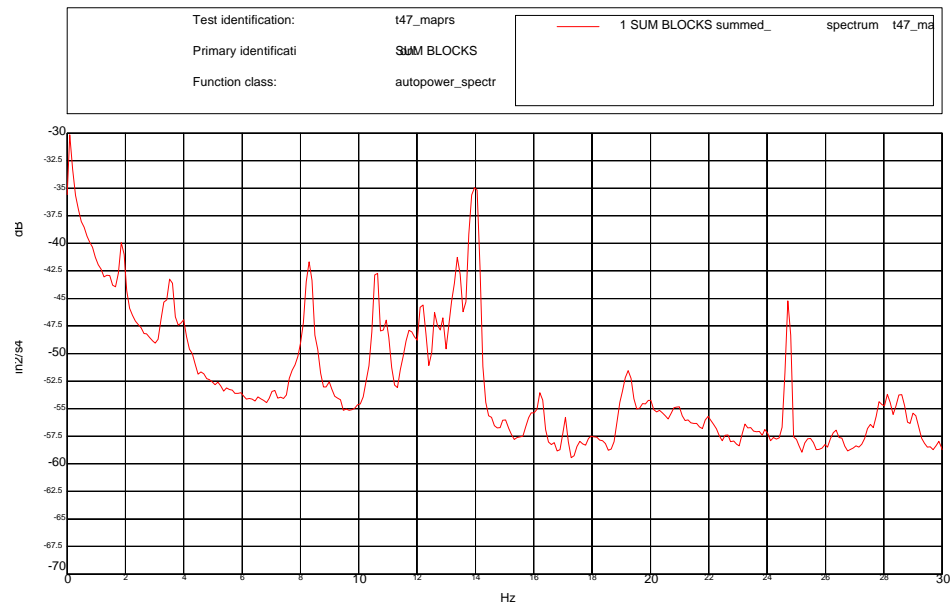


Figure 8.32.2  
Test #47 - Summed Auto Powers of the Primary





Table 8.32.1  
Test #47 - Peaks in the Auto Power Summation by Component

Secondary	Primary	Secondary	Primary	Secondary	Primary
1.904	1.904	12.598	12.598	23.096	
3.32	3.32		12.842	23.438	
	3.564	12.891		24.365	
	3.867	13.428		24.707	24.707
4.004	4.004	13.867	13.867	25	
7.08		14.014	14.014	25.342	
8.35	8.35	14.697		25.781	
8.894	8.984	14.98		26.66	
9.131			15.918	27.1	
9.326		16.26	16.26	27.49	
10.596	10.596	17.09	17.09	27.832	
10.84			18.125	28.076	
	10.938		18.516	28.467	
	11.719		18.994		28.613
	11.865	19.189	19.198	29.15	
	12.109		19.336		
12.207	12.207	20.898			

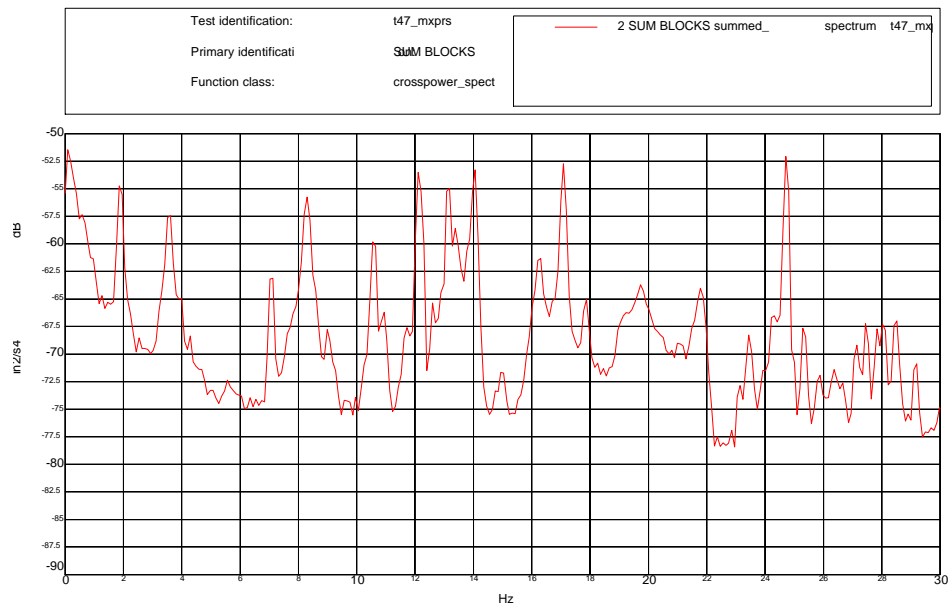


Figure 8.32.3  
Test #47 - Summed Cross Powers





Table 8.32.2  
Test #47 – Peaks in Cross Power

Frequency (Hz)	
1.855	17.09
3.613	17.871
7.129	19.727
8.301	23.438
8.984	24.707
10.547	25.293
10.937	27.148
12.109	27.441
13.184	27.832
13.379	28.027
14.062	28.516
16.309	29.199





8.33 Test #48 - (5z / 30° / 60° / 45° / Open / Half)  
(Reference Channel / Elevation / Zenith / Angle of Attack / Upwind Gate / Downwind Gate)

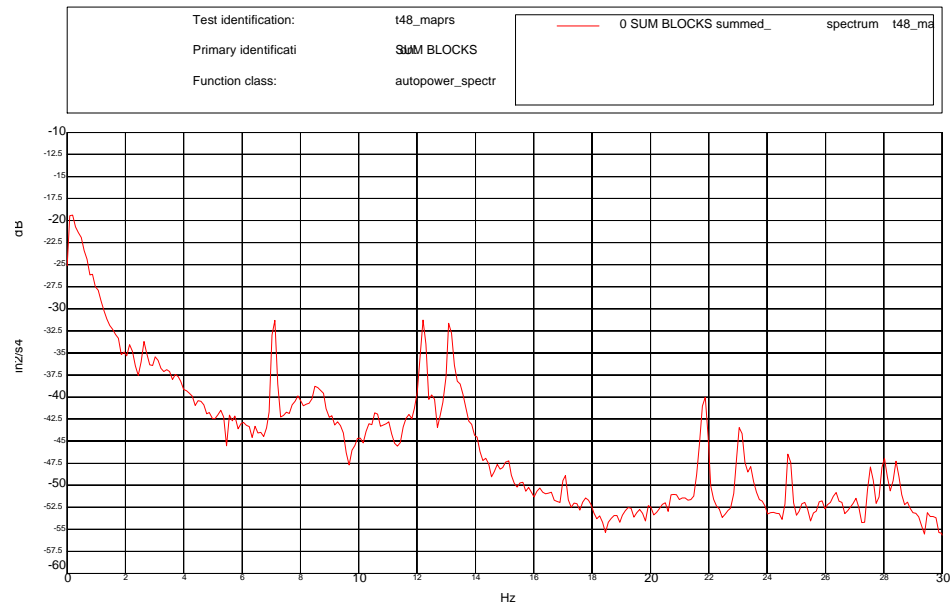


Figure 8.33.1  
Test #48 - Summed Auto Power of the Secondary

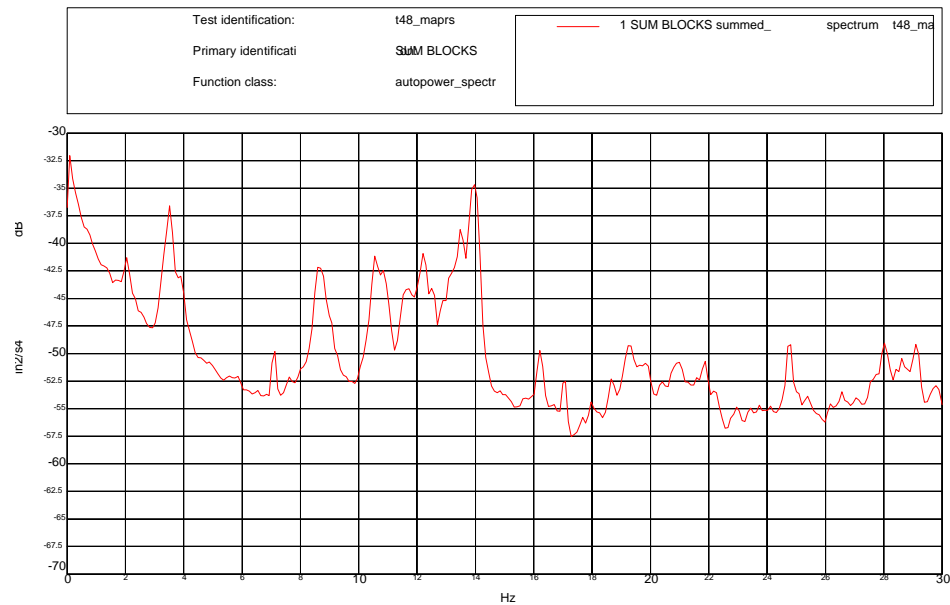


Figure 8.33.2  
Test #48 - Summed Auto Powers of the Primary





Table 8.33.1  
Test #48 - Peaks in the Auto Power Summation by Component

Secondary	Primary	Secondary	Primary	Secondary	Primary	Secondary	Primary
2.051	2.051	12.305			18.213	23.365	
3.32	3.32	12.549	12.549		18.701	24.756	24.756
	3.516	12.891	12.891	19.238		25.244	
	3.857	13.135	13.135		19.287	25.781	
3.906		13.477	13.477		19.58	26.465	
7.08	7.08	13.623			19.824	26.562	
	8.643	13.916	13.916		19.922	27.051	
	8.789	14.062	14.062	20.361	20.361	27.539	
9.277		15.039		20.85	20.85	27.93	
10.547	10.547	16.26	16.26	20.996	20.996		28.027
10.791		17.041	17.041	21.826		28.418	
	10.84		17.676		21.875		28.613
	11.523	17.725			22.217	29.053	
	11.67	17.969		23.046			29.15
	12.207		18.018	23.438			

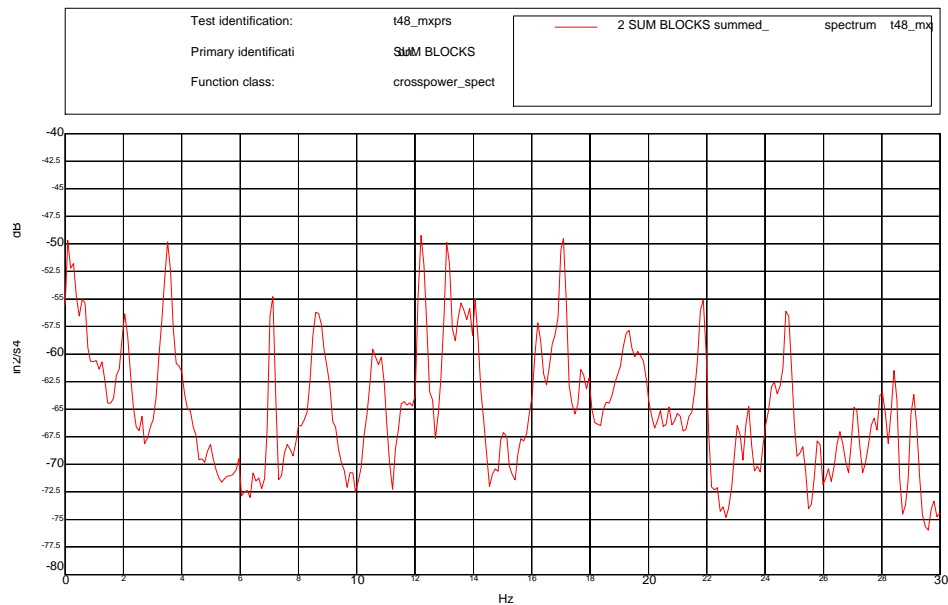


Figure 8.33.3  
Test #48 - Summed Cross Powers





Table 8.33.2  
Test #48 – Peaks in Cross Power

Frequency (Hz)	
2.051	17.09
3.516	19.336
7.129	21.875
8.594	23.047
10.547	23.438
10.84	24.316
12.207	24.707
13.086	26.562
13.574	27.051
13.867	28.027
14.062	28.418
15.039	29.102
16.211	





8.34 Test #49 - (5z / 30° / 60° / 90° / Closed / Open)  
(Reference Channel / Elevation / Zenith / Angle of Attack / Upwind Gate / Downwind Gate)

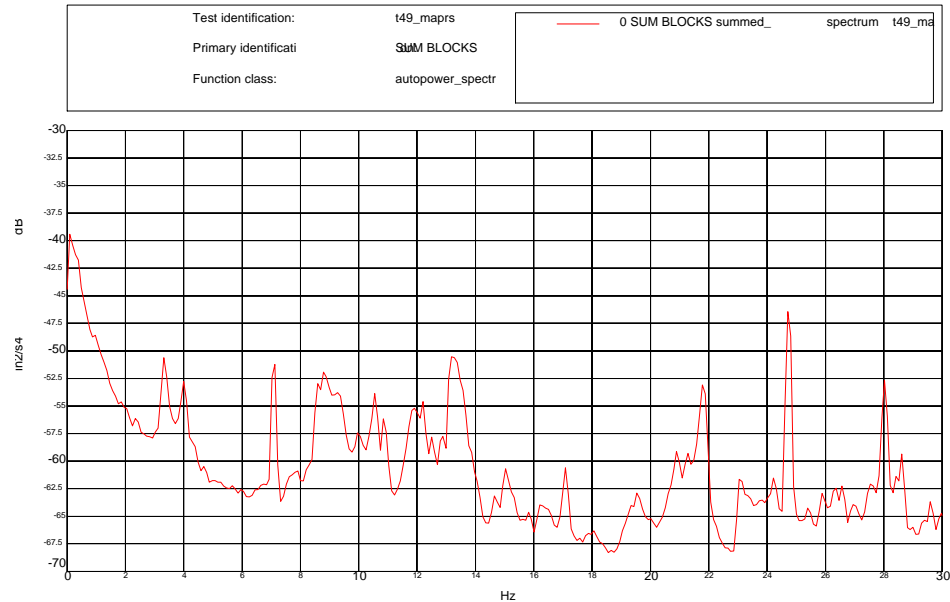


Figure 8.34.1  
Test #49 - Summed Auto Power of the Secondary

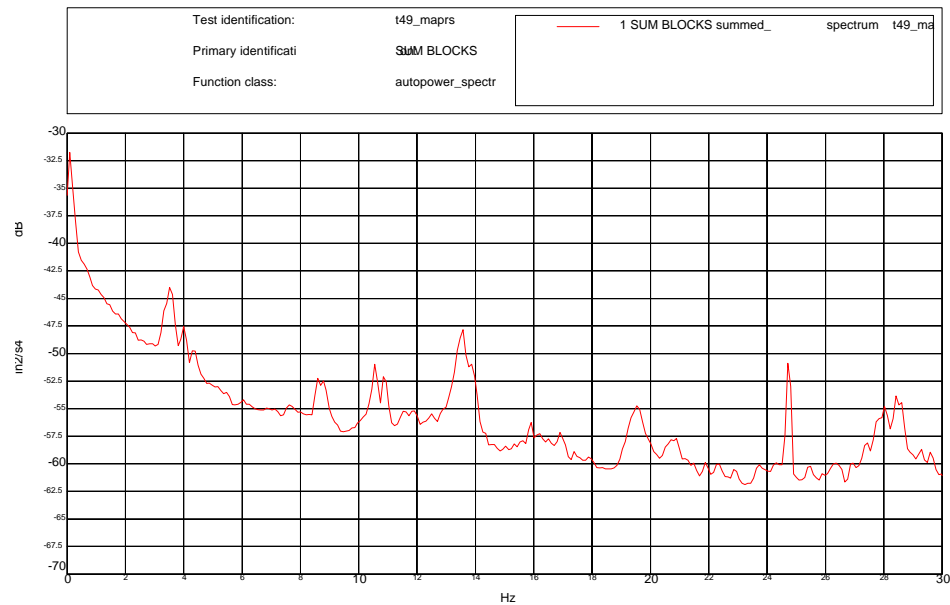


Figure 8.34.2  
Test #49 - Summed Auto Powers of the Primary





Table 8.34.1  
Test #49 - Peaks in the Auto Power Summation by Component

Secondary	Primary	Secondary	Primary	Secondary	Primary
1.953		10.596	10.596	24.414	
3.32		10.84	10.84	24.756	24.756
	3.369	12.305		25.244	
	3.516	12.549		25.781	
4.004	4.004		13.379	25.879	
	4.348	13.525	13.525	26.318	
7.08		13.916	13.916	26.611	
8.838		15.039		27.1	
	8.594	16.211			27.783
	8.789	17.09		28.027	28.027
9.082		19.385		28.418	28.418
9.229			19.513	28.613	28.613
9.326		20.898		29.053	
9.961		23.438			

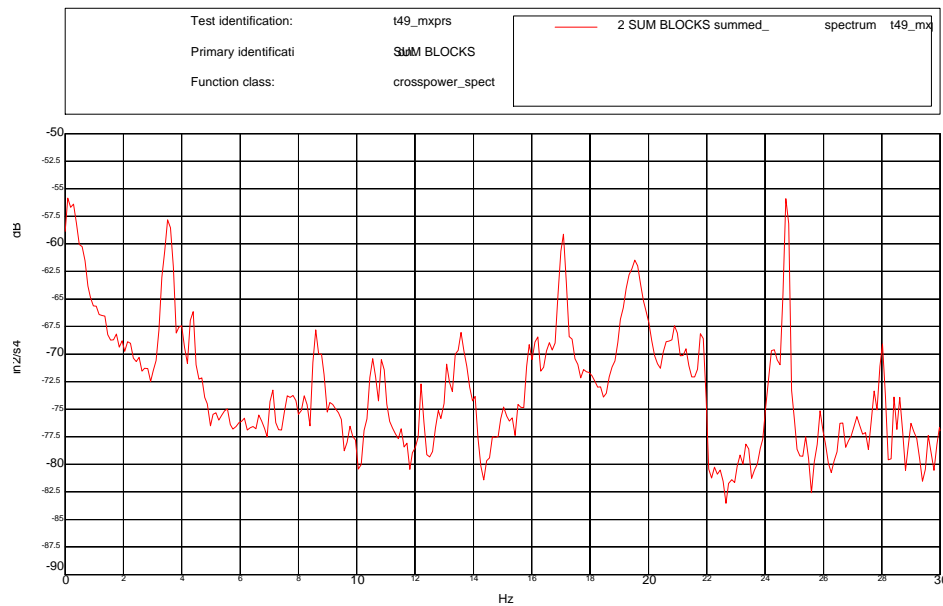


Figure 8.34.3  
Test #49 - Summed Cross Powers





Table 8.34.2  
Test #49 – Peaks in Cross Power

Frequency (Hz)	
1.758	19.531
3.516	20.898
4.395	21.777
8.594	24.316
10.547	24.707
10.84	25.879
12.207	26.66
13.086	27.148
13.574	27.734
15.039	28.027
15.918	28.418
16.211	28.613
17.09	29.004
17.773	





8.35 Test #50 - (5z / 30° / 60° / 135° / Half / Closed)  
(Reference Channel / Elevation / Zenith / Angle of Attack / Upwind Gate / Downwind Gate)

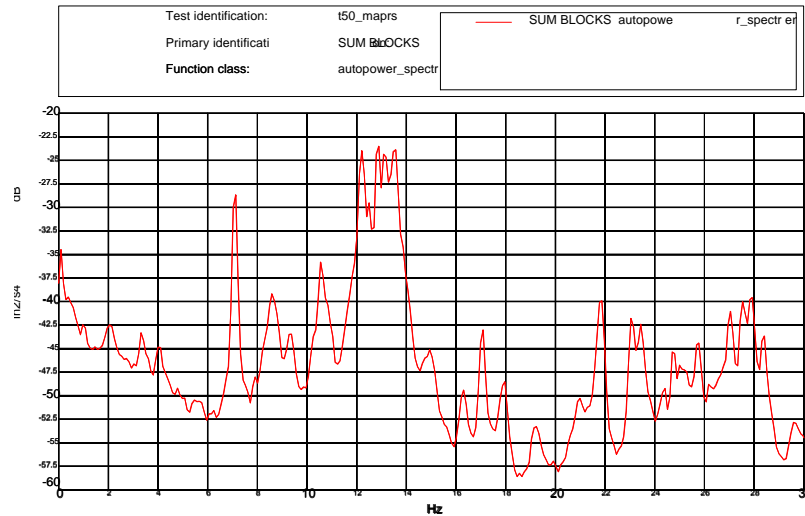


Figure 8.35.1  
Test #50 - Summed Auto Power of the Secondary

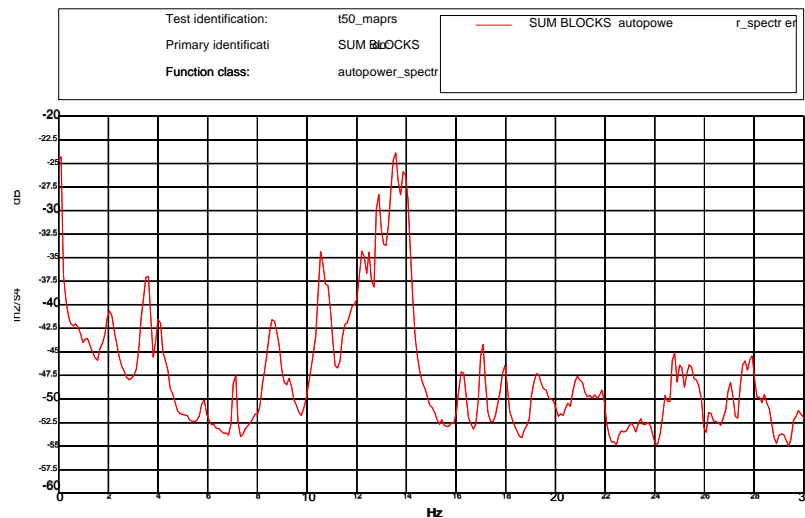


Figure 8.35.2  
Test #50 - Summed Auto Powers of the Primary





Table 8.35.1  
Test #50 - Peaks in the Auto Power Summation by Component

Secondary	Primary	Secondary	Primary	Secondary	Primary
	1.758	12.842	12.842	21.944	
2.002			13.037	21.826	
2.1	2.1	13.428	13.428	23.047	
	2.295	13.574	13.574	23.438	
3.32		13.867	13.867	24.414	24.414
	3.613		14.014		24.756
4.053	4.053	14.941		24.805	
	5.859		16.211	25.049	25.049
7.08	7.08	16.309	16.309	25.195	
	8.594	17.041	17.041		25.213
9.277	9.277	17.92			25.391
	10.547		17.969		25.488
10.595		19.092		25.732	25.732
10.791	10.791		19.141	27.002	27.002
	11.523	19.238		27.637	27.637
	11.865		19.287	27.881	27.881
	12.27	20.85	20.85	28.361	
12.305	12.305	20.947	20.947	29.102	
12.5	12.5		21.875		

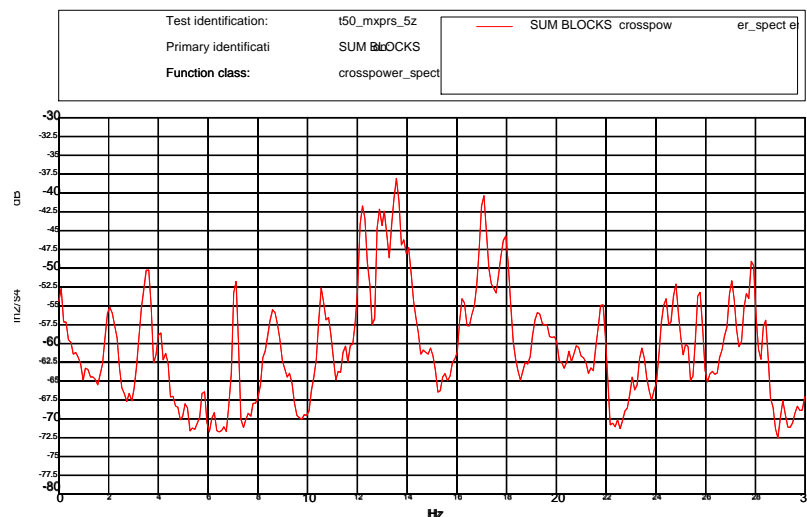


Figure 8.35.3  
Test #50 - Summed Cross Powers





Table 8.35.2  
Test #50 – Peaks in Cross Power

Frequency (Hz)	
2.051	17.09
3.613	17.969
4.102	19.238
4.297	20.801
5.859	21.875
7.129	23.438
8.594	24.414
10.547	24.805
12.207	25.195
12.891	25.781
13.086	27.051
13.574	27.637
13.867	27.832
14.062	28.418
16.211	29.102





8.36 Test #51 - (5z / 30° / 60° / 45° / Open / Open)  
(Reference Channel / Elevation / Zenith / Angle of Attack / Upwind Gate / Downwind Gate)

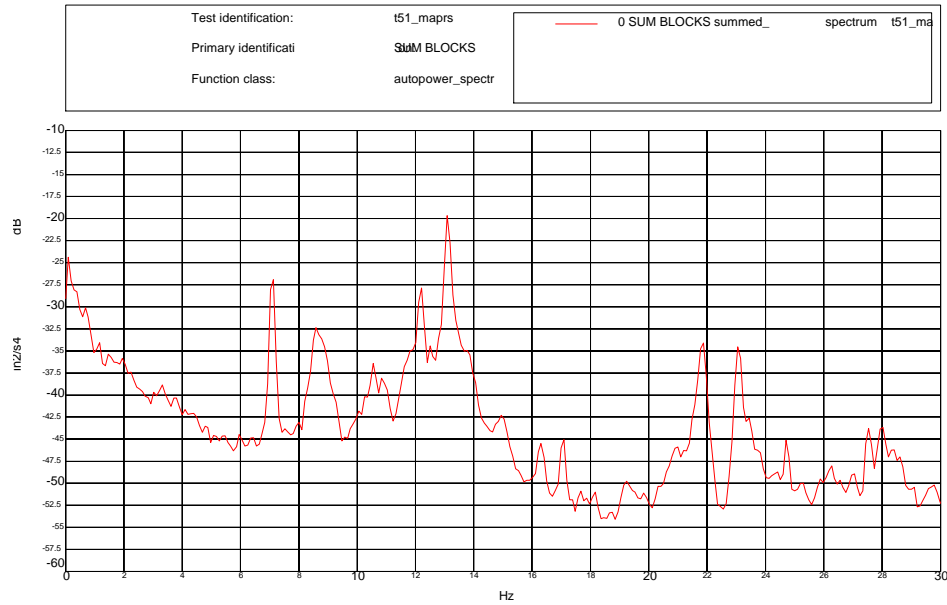


Figure 8.36.1  
Test #51 - Summed Auto Power of the Secondary

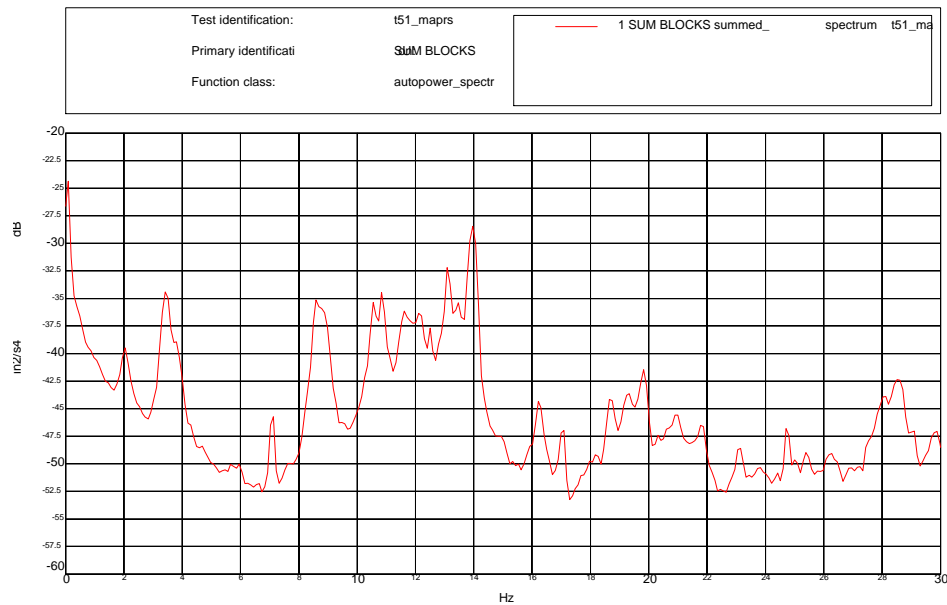


Figure 8.36.2  
Test #51 - Summed Auto Powers of the Primary





Table 8.36.1  
Test #51 - Peaks in the Auto Power Summation by Component

Secondary	Primary	Secondary	Primary	Secondary	Primary
	2.002	11.621		21.826	21.826
2.051			12.158	23.096	23.096
	2.295		12.5		23.438
	3.32	13.086	13.086	24.707	24.707
	3.376	13.428		25.049	
3.418		13.965		25.439	
3.809			14.893		27.49
7.08	7.08	16.26			27.979
8.594	8.594	17.041	17.041	28.076	
8.74	8.74	18.701		28.516	
8.93	8.936	19.336		28.613	
	10.303	19.824		29.053	
10.547	10.547	20.898	20.898		
10.84		20.996			

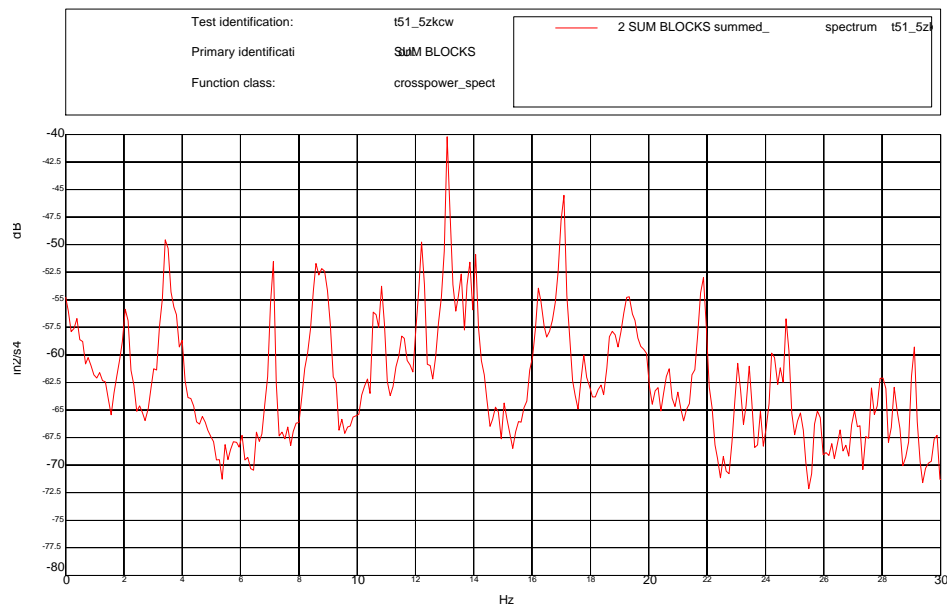


Figure 8.36.3  
Test #51 - Summed Cross Powers





Table 8.36.2  
Test #51 – Peaks in Cross Power

Frequency (Hz)	
2.051	17.09
3.418	17.773
4.004	18.75
7.129	19.336
8.594	20.703
8.789	21.875
10.547	23.047
10.84	23.438
11.523	24.219
12.207	24.512
13.086	24.707
13.574	27.637
13.867	28.027
14.062	28.418
16.211	29.102





8.37 Test #52 - (5z / 45° / 45° / 45° / Open / Open)  
(Reference Channel / Elevation / Zenith / Angle of Attack / Upwind Gate / Downwind Gate)

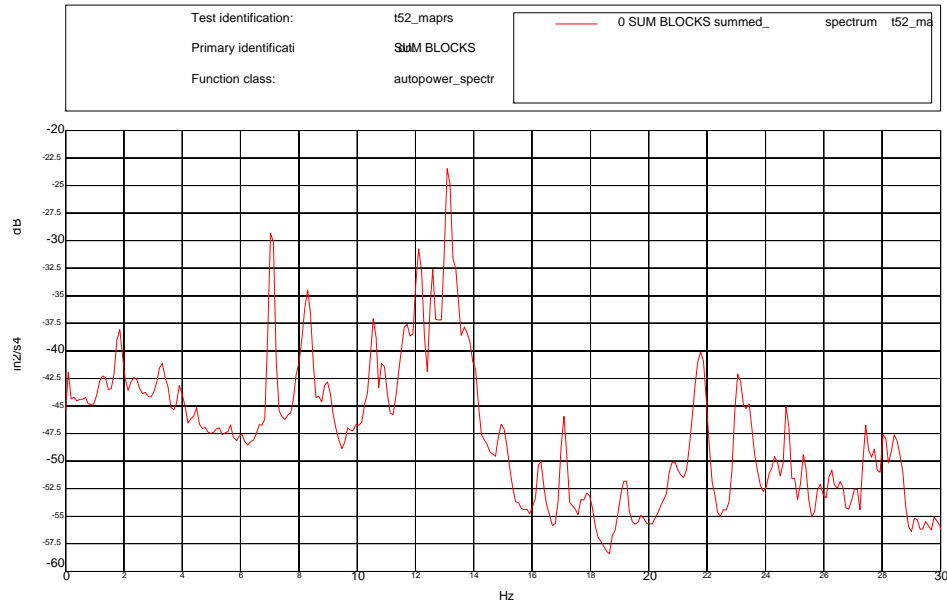


Figure 8.37.1  
Test #52 - Summed Auto Power of the Secondary

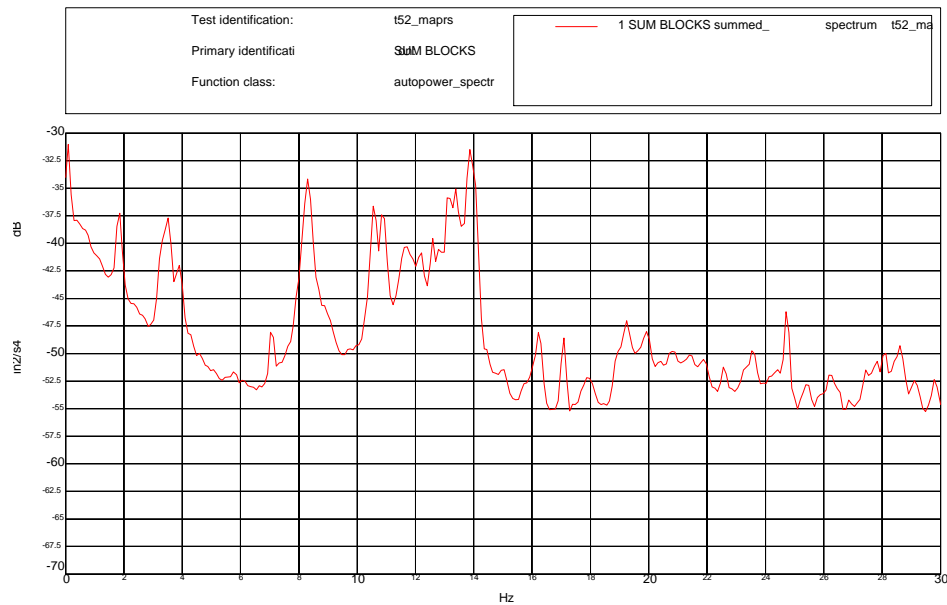


Figure 8.37.2  
Test #52 - Summed Auto Powers of the Primary





Table 8.37.1  
Test #52 - Peaks in the Auto Power Summation by Component

Secondary	Primary	Secondary	Primary	Secondary	Primary
1.855	1.855	14.941		25	
3.32		16.211	16.211	25.293	
	3.516	17.09	17.09		25.391
3.906	3.906	17.871			26.172
7.031	7.031	19.141	19.238	26.27	
8.3	8.301		19.922	26.66	
8.984			20.801	27.041	
10.547	10.547		21.387	27.441	27.441
10.84	10.84	21.777		27.734	
	11.719		21.875		27.832
12.207	12.207	23.047		28.027	
12.598	12.598	23.438			28.125
13.086	13.086		23.535	28.418	
13.379	13.379	24.316			28.613
13.867	13.867	24.707	24.707	29.102	29.102

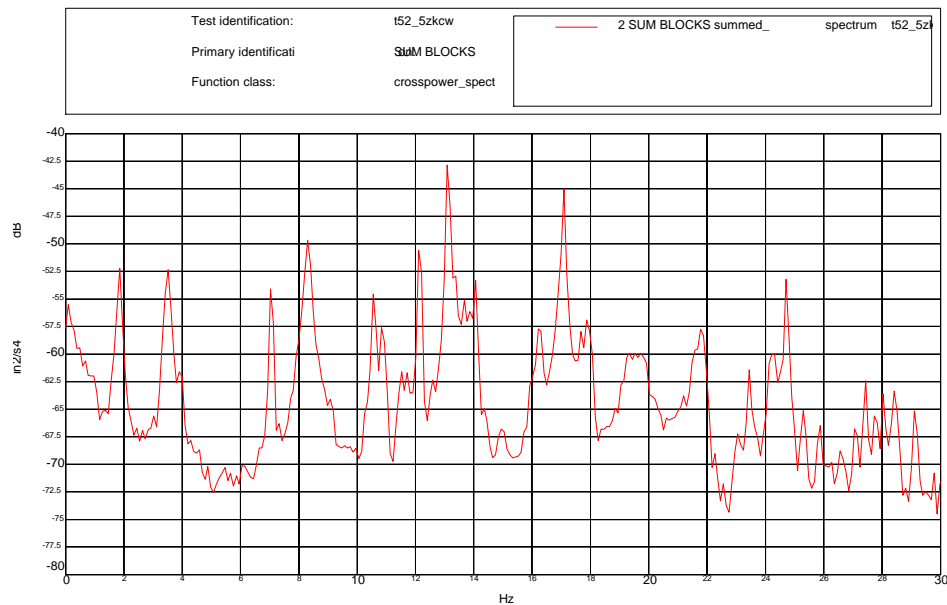


Figure 8.37.3  
Test #52 - Summed Cross Powers





Table 8.37.2  
Test #52 – Peaks in Cross Power

Frequency (Hz)	
1.855	17.09
3.516	17.676
3.906	17.871
7.031	19.336
8.301	19.531
10.547	19.727
10.84	21.777
11.523	23.438
11.719	24.316
12.109	24.707
13.086	27.441
13.379	28.027
13.672	28.418
14.062	29.102
16.211	





8.38 Test #53 - (5z / 60° / 30° / 45° / Open / Open)  
(Reference Channel / Elevation / Zenith / Angle of Attack / Upwind Gate / Downwind Gate)

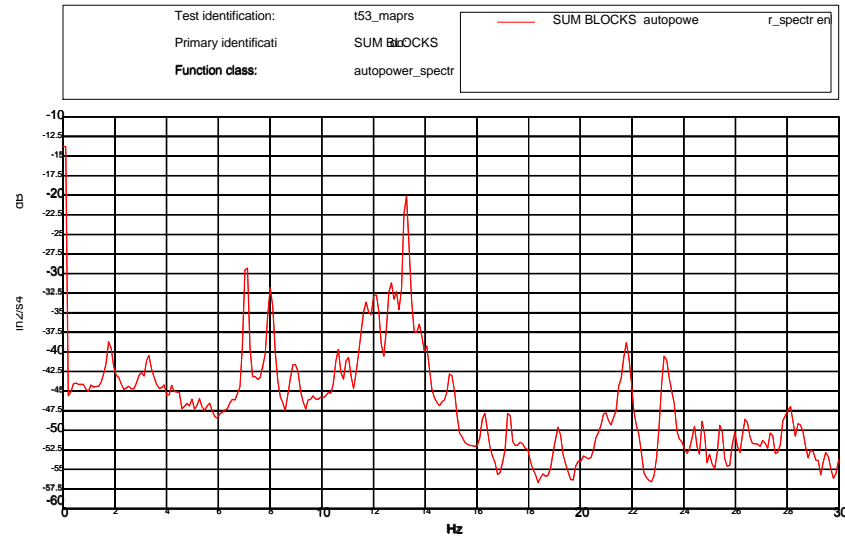


Figure 8.38.1  
Test #53 - Summed Auto Power of the Secondary

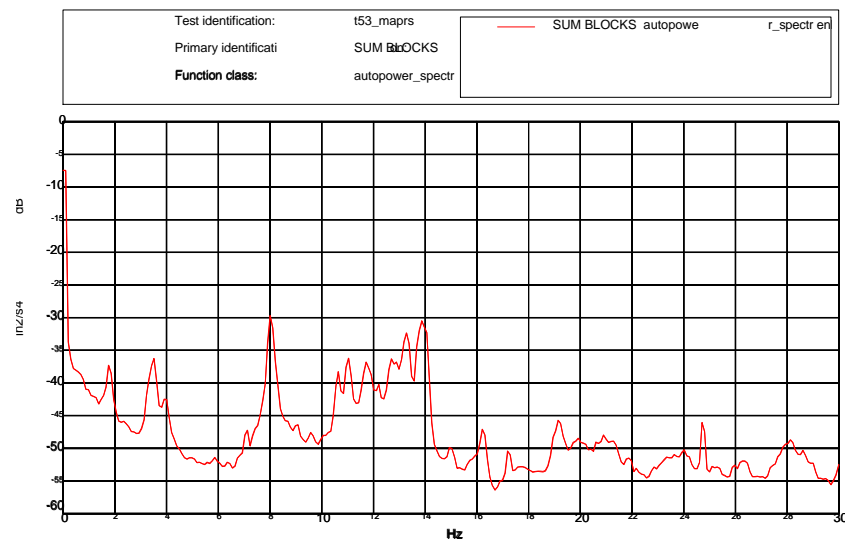


Figure 8.38.2  
Test #53 - Summed Auto Powers of the Primary





Table 8.38.1  
Test #53 - Peaks in the Auto Power Summation by Component

Secondary	Primary	Secondary	Primary	Secondary	Primary
1.807	1.807	13.232	13.232	20.947	
3.32			13.379	21.77	
	3.467	13.721	13.721	23.389	
3.955	3.955	13.867	13.867	23.584	
7.08	7.08	14.014	14.014	24.414	
8.057	8.057	14.99	14.99	24.756	24.756
8.836		16.26	16.26	25	
10.645	10.645	17.236	17.236	25.439	
10.986		17.968		26.416	
	11.035	19.141	19.141	27.051	
	11.768		19.922	27.148	
12.158	12.158		20.166	27.344	
	12.646		20.605	28.174	28.174
12.891	12.891		20.898	28.467	

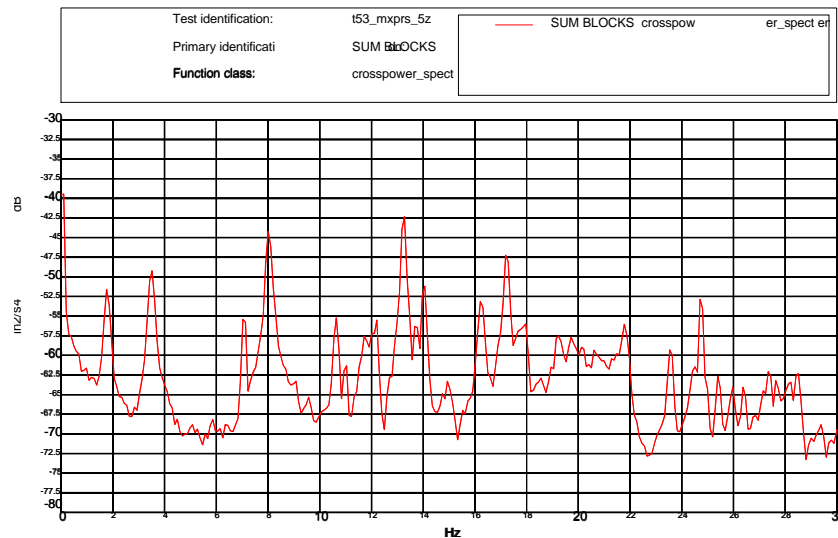


Figure 8.38.3  
Test #53 - Summed Cross Powers





Table 8.38.2  
Test #53 – Peaks in Cross Power

Frequency (Hz)	
1.758	19.727
3.516	20.117
7.031	20.605
8.008	21.777
10.644	23.535
11.035	24.512
11.719	24.707
12.207	25.391
13.281	25.977
13.672	26.367
14.062	27.344
16.211	27.637
17.188	28.223
17.969	28.516
19.238	





8.39 Test #54 - (5z / 75° / 15° / 45° / Open / Open)  
(Reference Channel / Elevation / Zenith / Angle of Attack / Upwind Gate / Downwind Gate)

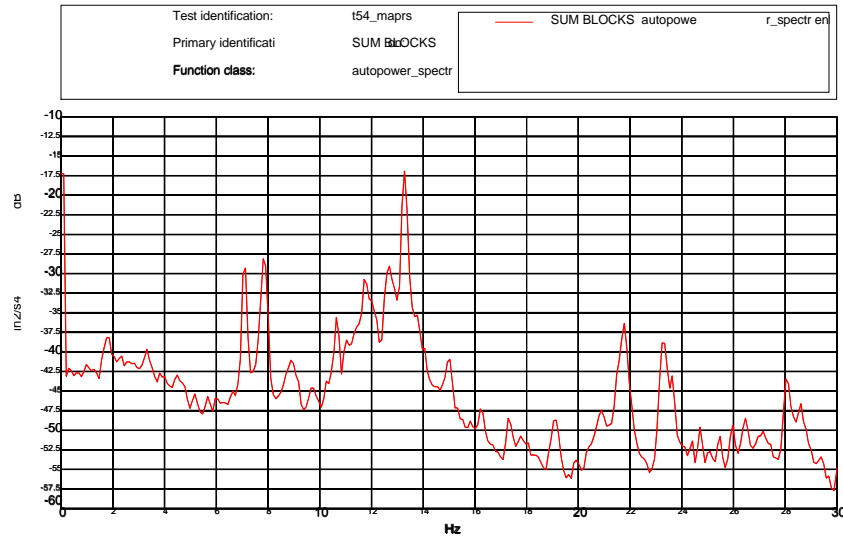


Figure 8.39.1  
Test #54 - Summed Auto Power of the Secondary

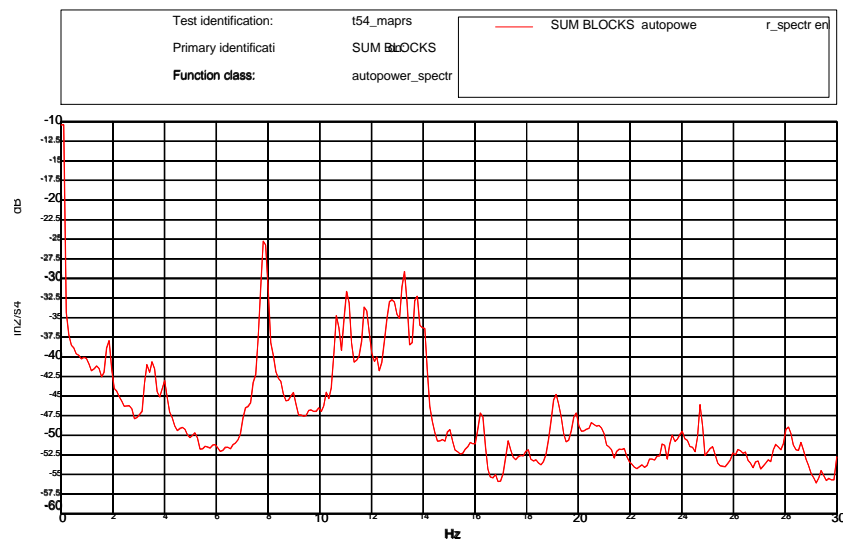


Figure 8.39.2  
Test #54 - Summed Auto Powers of the Primary





Table 8.39.1  
Test #54 - Peaks in the Auto Power Summation by Component

Secondary	Primary	Secondary	Primary	Secondary	Primary
1.807	1.807	13.281	13.281	24.365	
3.32	3.32	13.721	13.721	24.707	24.707
	3.546	14.014	14.014	25	
4.004	4.004	15.039	15.039	25.488	
7.08		16.26	16.26	25.928	
7.812	7.812	17.285	17.285	26.465	
8.936		17.773		27.148	
10.693	10.693	18.018		27.393	
11.084	11.084	19.141	19.141	27.588	
11.719	11.719		19.873	28.076	28.076
12.158	12.158	20.85		28.407	
	12.695	21.777		28.613	
	12.842	23.438		24.365	
12.891					
		23.633		24.707	24.707

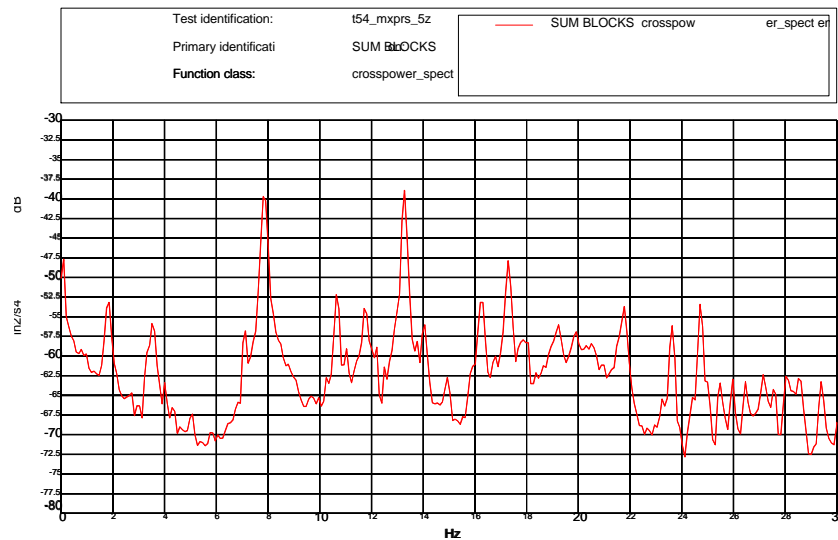


Figure 8.39.3  
Test #54 - Summed Cross Powers





Table 8.39.2  
Test #54 – Peaks in Cross Power

Frequency (Hz)	
1.855	19.922
3.516	21.777
7.129	23.633
7.812	24.707
10.644	25.488
11.035	25.977
11.719	26.465
12.207	27.148
13.281	27.539
14.062	28.027
16.309	28.516
17.285	29.395





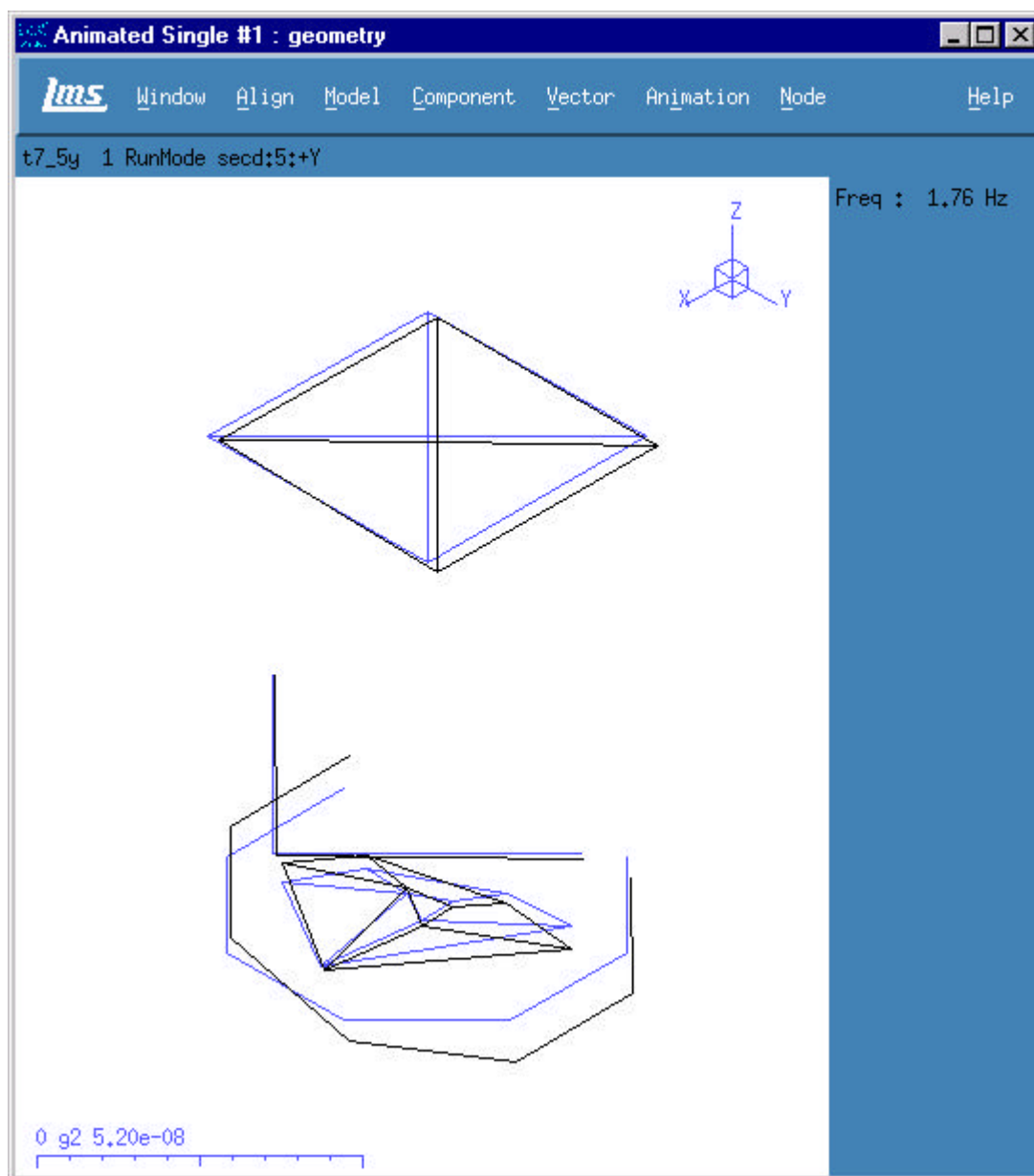
## 9.0 Reference

1. Gemini South 8m Optical Telescope Final Report, MACL Report # 05-08570-001, dated October 2000
2. Gemini South 8m Optical Telescope Test Setup Report, MACL Report # 05-08570-002, dated October 2000
3. Gemini South 8m Optical Telescope Data Cleansing Report, MACL Report # 05-08570-003, dated October 2000
4. Gemini South 8m Optical Telescope Modal Test Report, MACL Report # 05-08570-004, dated October 2000
5. Gemini South 8m Optical Telescope Operating Report, MACL Report # 05-08570-005, dated October 2000
6. Gemini South 8m Optical Telescope Correlation Report, MACL Report # 05-08570-006, dated October 2000
7. Gemini South 8m Optical Telescope DoE and Wind Data Report, MACL Report # 05-08570-007, dated October 2000
8. CD containing all pertinent test data and reports
9. Preliminary Data Assessment of Gemini South Optical Telescope Operating and Modal Data Report, dated June 2000
10. LMS Coda-X 3.4 Test and Analysis Software (TMON, FMON, Modal Analysis, Matrix Toolbox), Leuven Measurement Systems, Detroit Michigan
11. LMS Coda-X 3.5C Test and Analysis Software (TMON, FMON, Modal Analysis), Leuven Measurement Systems, Detroit Michigan
12. LMS Road Runner Data Acquisition System, Leuven Measurement Systems, Detroit Michigan
13. MEScpos VES Version 2.0, Vibrant Technologies, Jamestown, CA
14. Avitabile, P., "Overview of Modal Analysis using the Frequency Response Method", July 1997
15. Box, George E.P., Hunter, J. Stuart, and Hunter, William G., *Statistics for Experimenters: An Introduction to Design, Data Analysis, and Model Building*, Wiley, 1978.
16. Shina, Sammy G., *Concurrent Engineering and Design for Manufacture of Electronic Products*, Van Nostrand Reinhold, 1991.





## 10.0 Operating Mode Shape Plots – Test 7

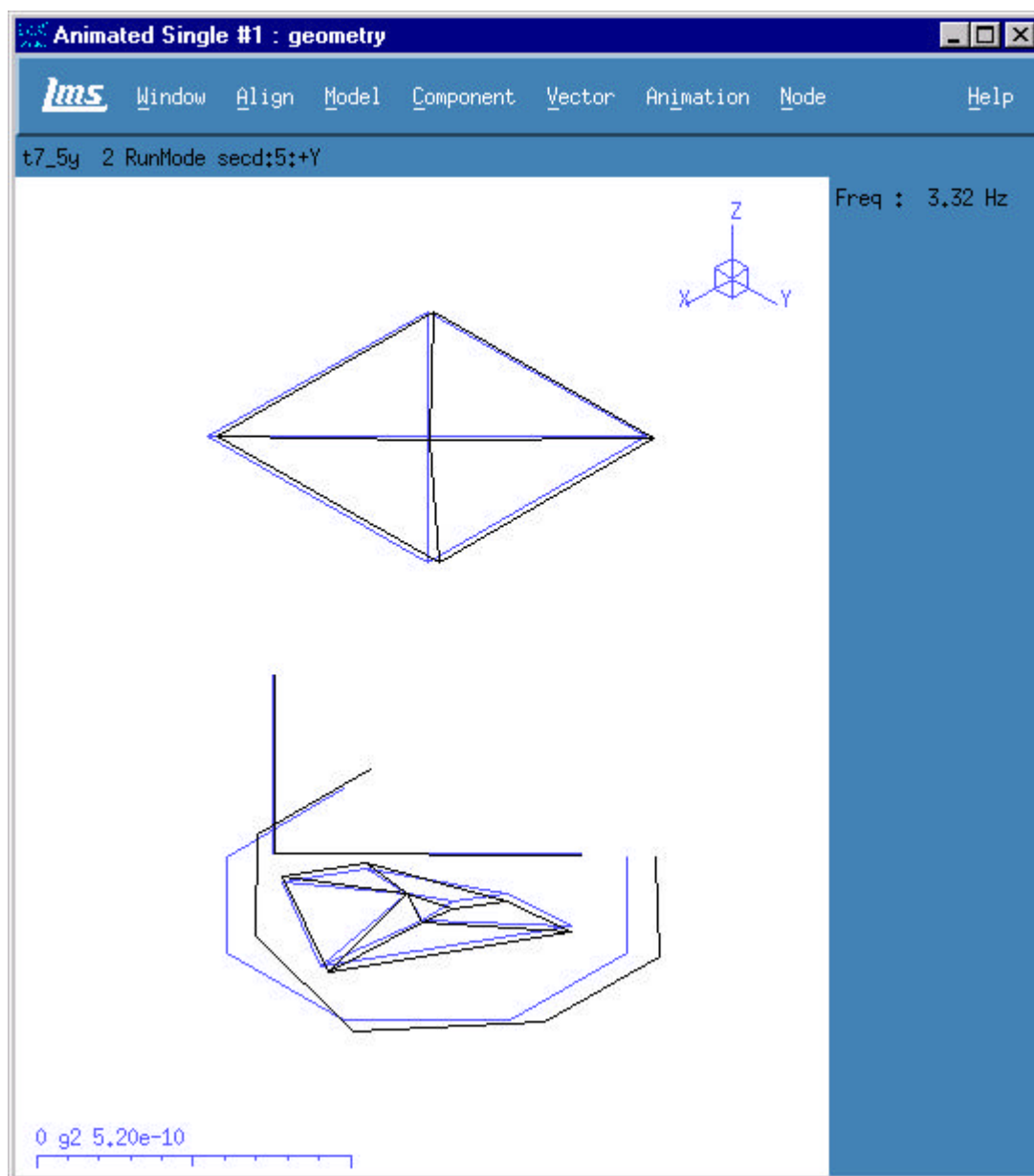


Test 7 – Operating Shape : 1.76Hz





## 10.0 Operating Mode Shape Plots – Test 7

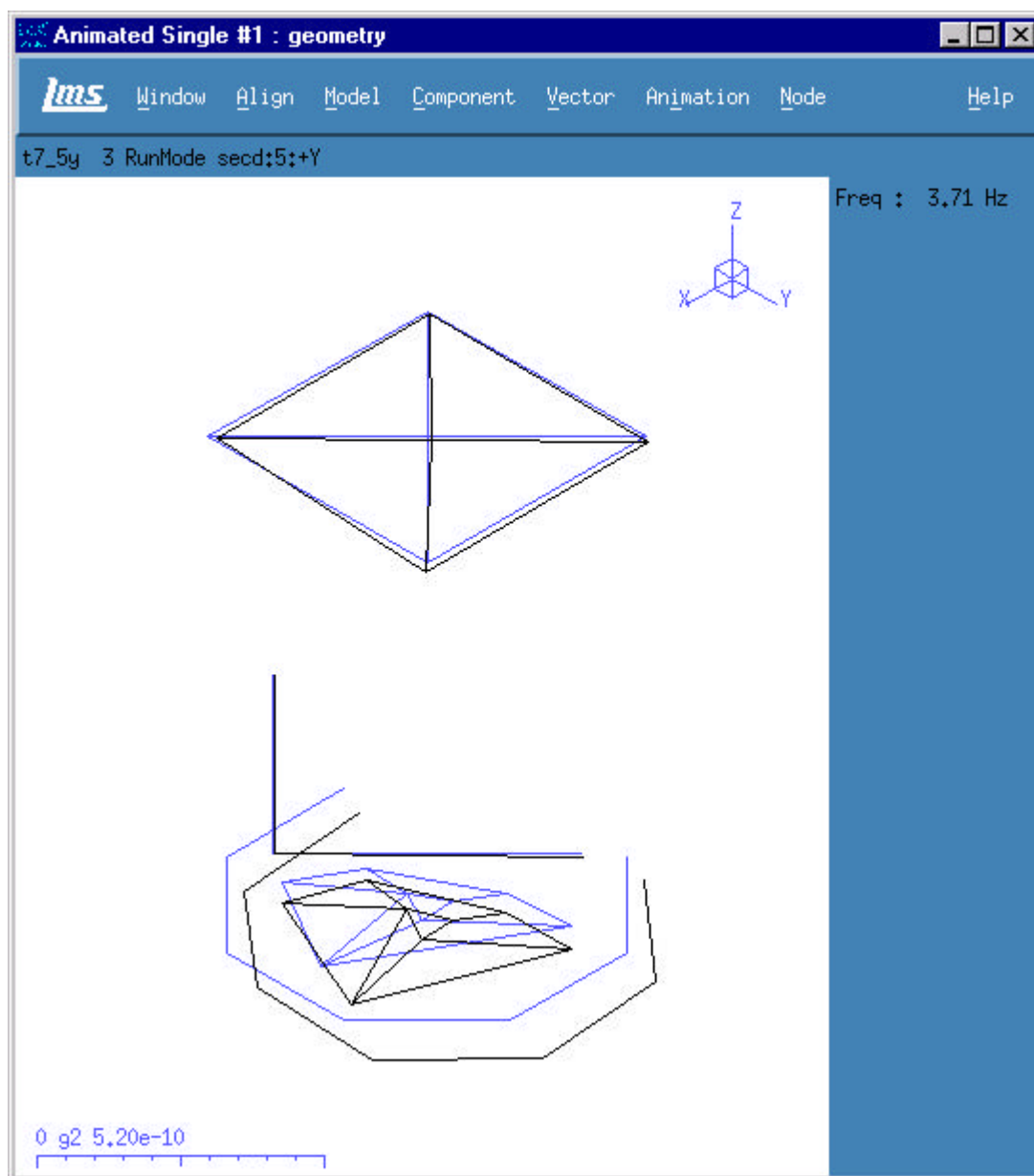


Test 7 – Operating Shape : 3.32Hz





## 10.0 Operating Mode Shape Plots – Test 7

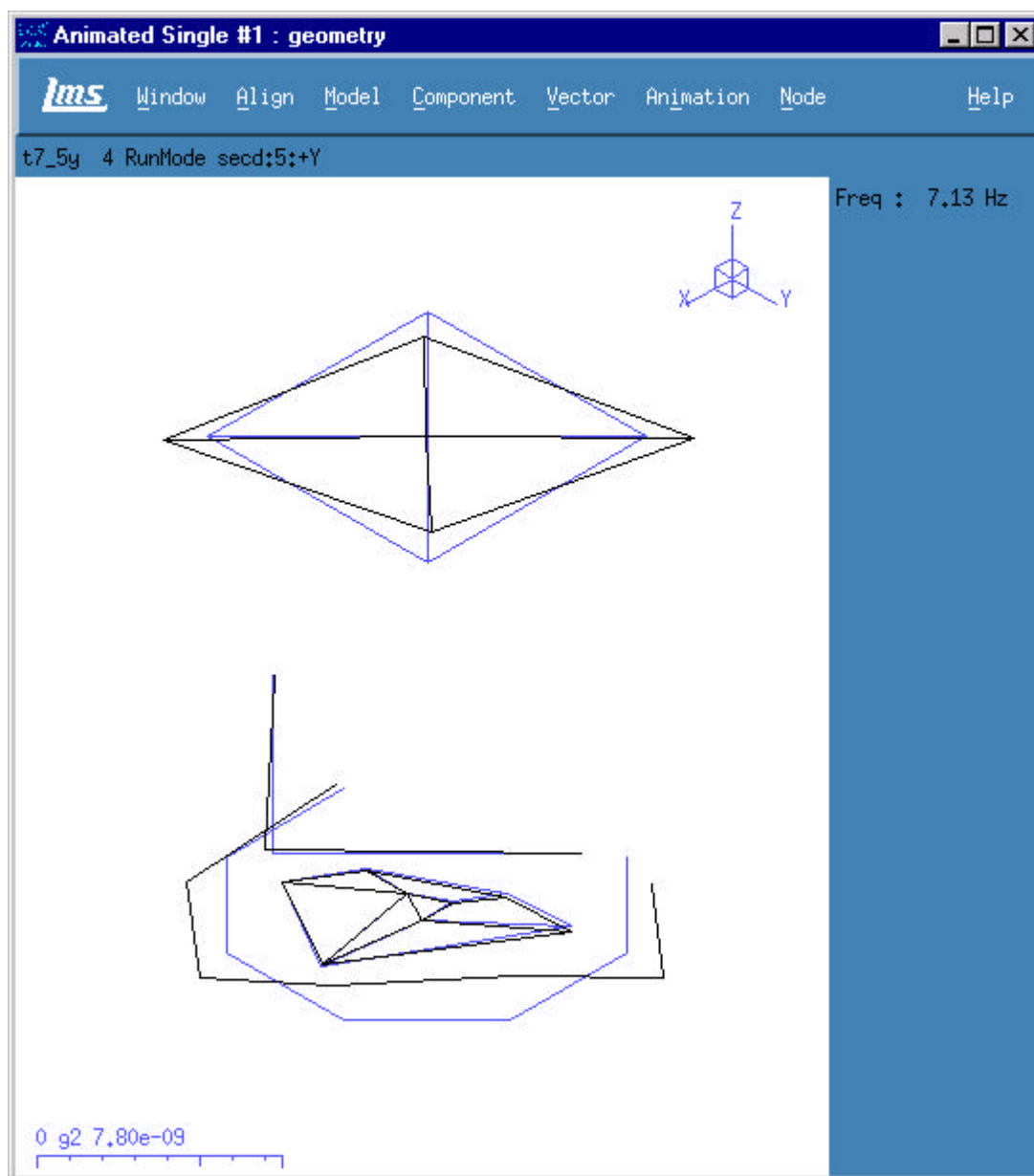


Test 7 – Operating Shape : 3.71Hz





## 10.0 Operating Mode Shape Plots – Test 7

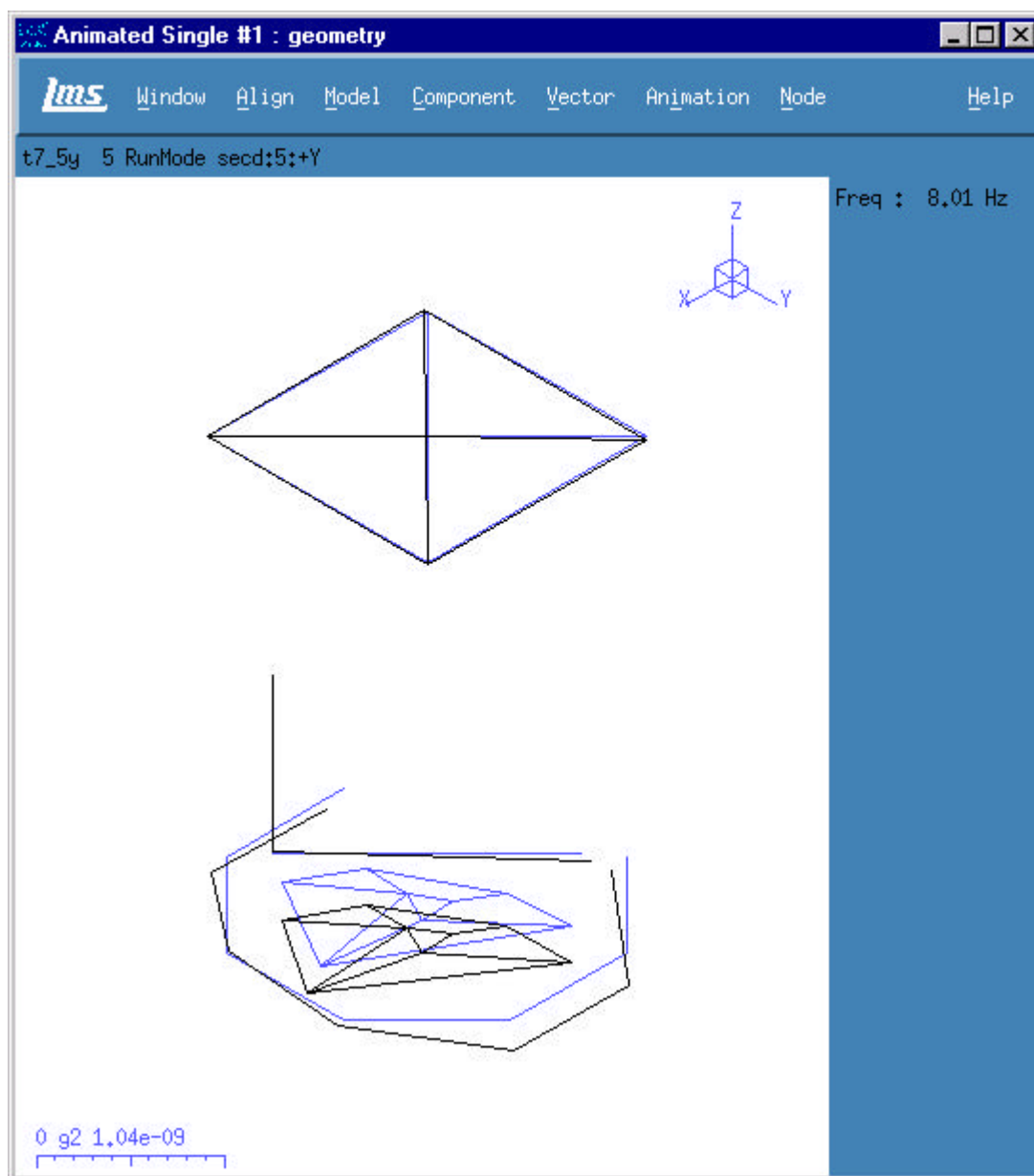


Test 7 – Operating Shape : 7.13Hz





## 10.0 Operating Mode Shape Plots – Test 7

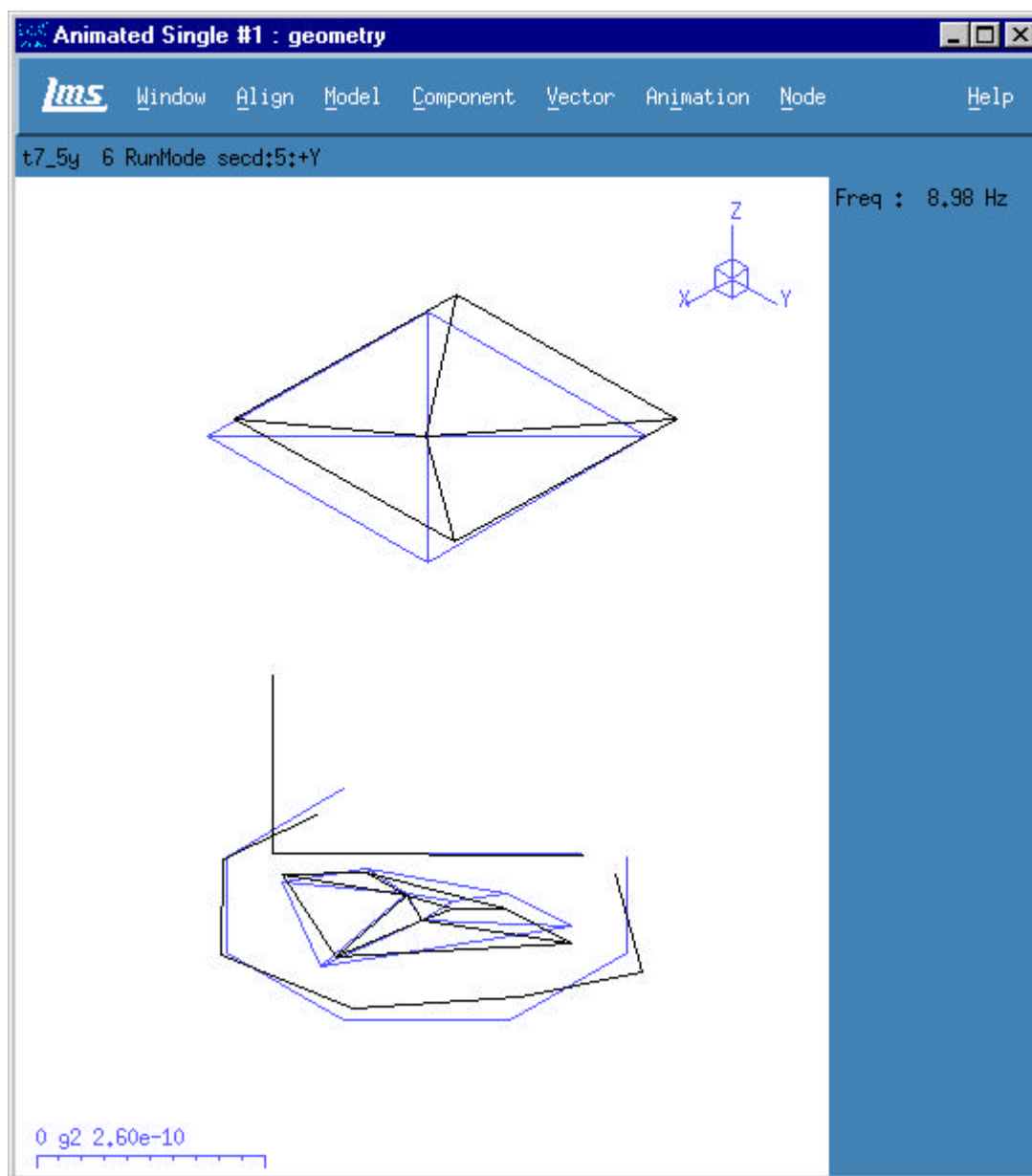


Test 7 – Operating Shape : 8.01Hz





## 10.0 Operating Mode Shape Plots – Test 7

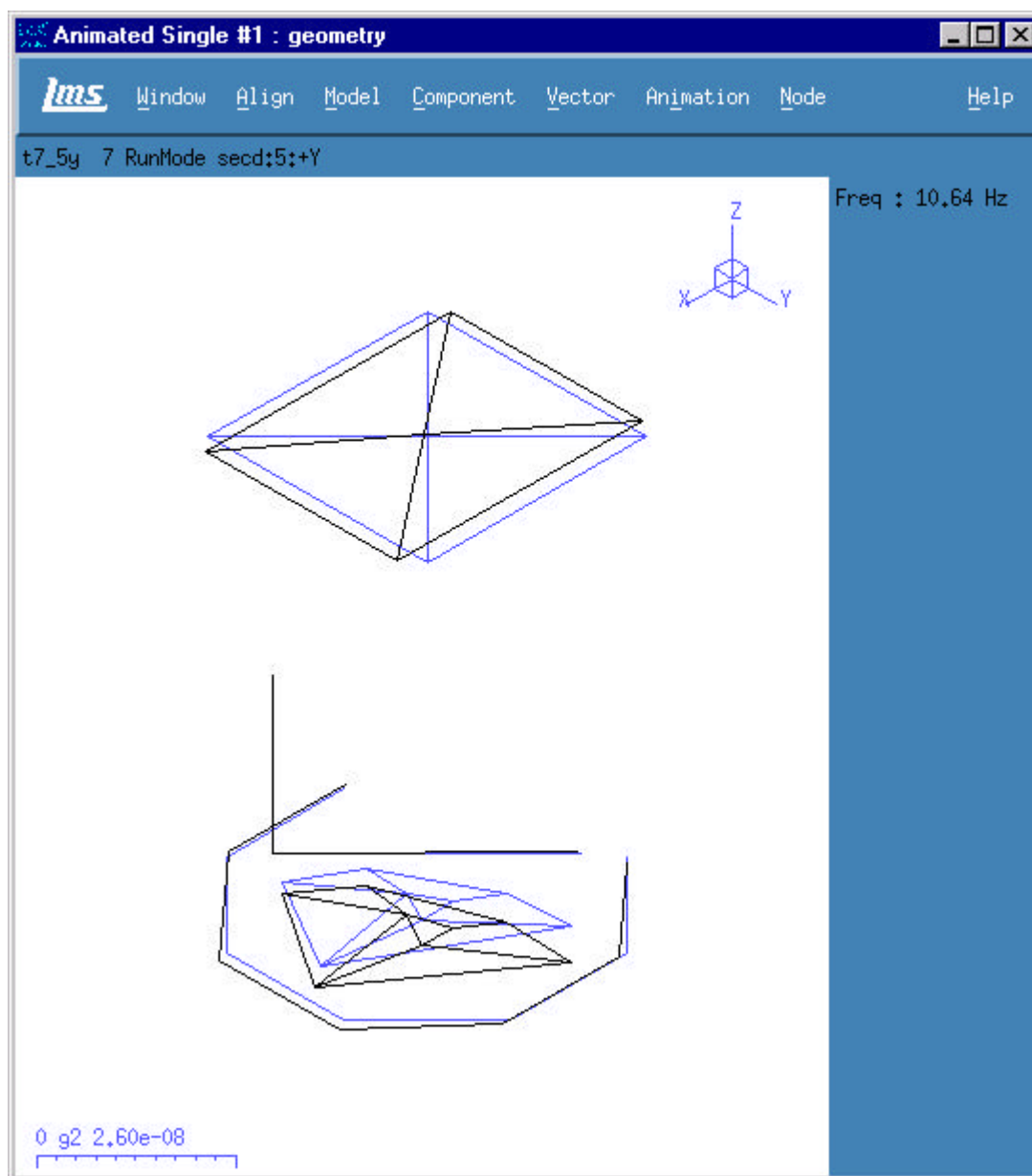


Test 7 – Operating Shape : 8.98Hz





## 10.0 Operating Mode Shape Plots – Test 7

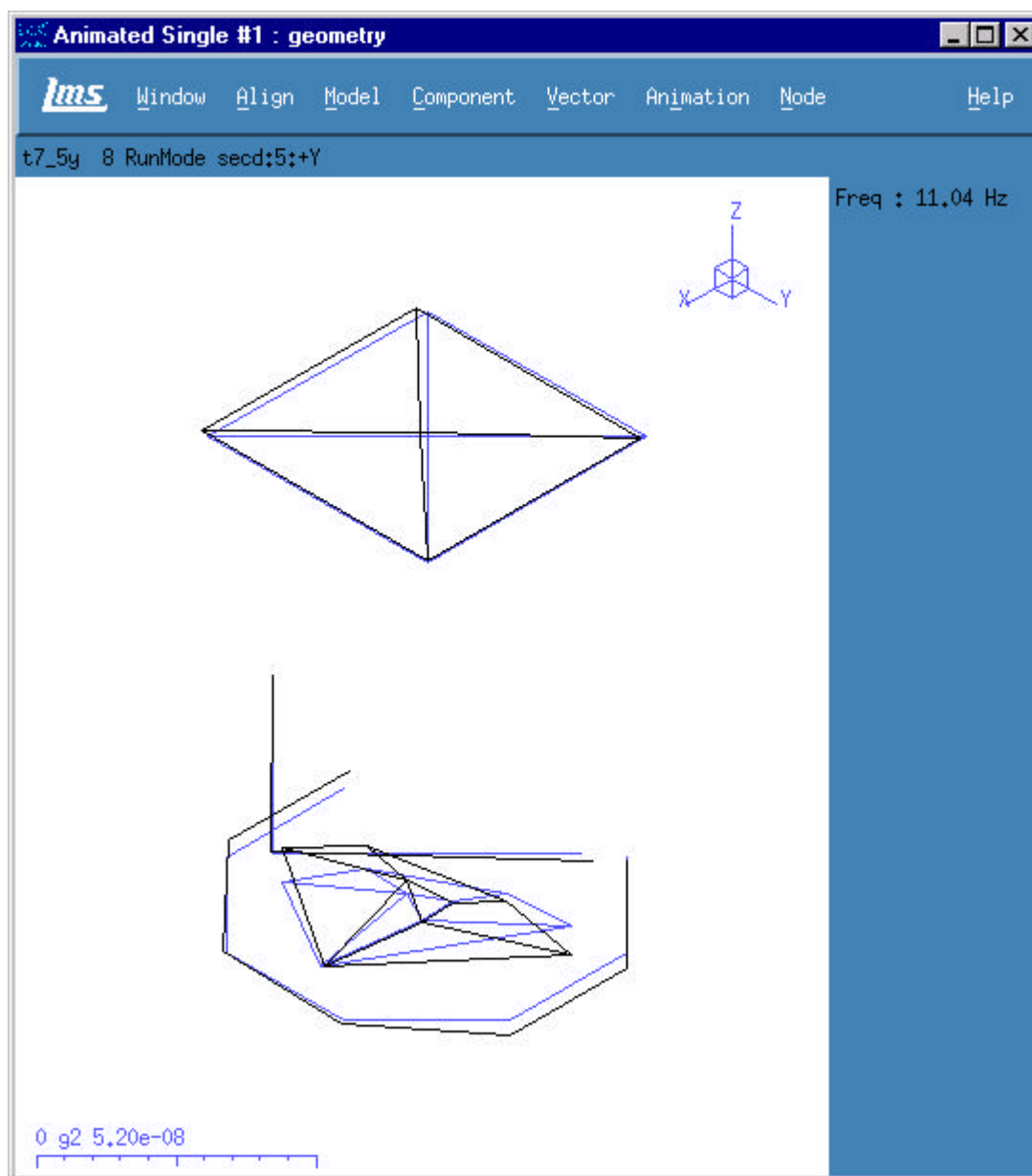


Test 7 – Operating Shape : 10.64Hz





## 10.0 Operating Mode Shape Plots – Test 7

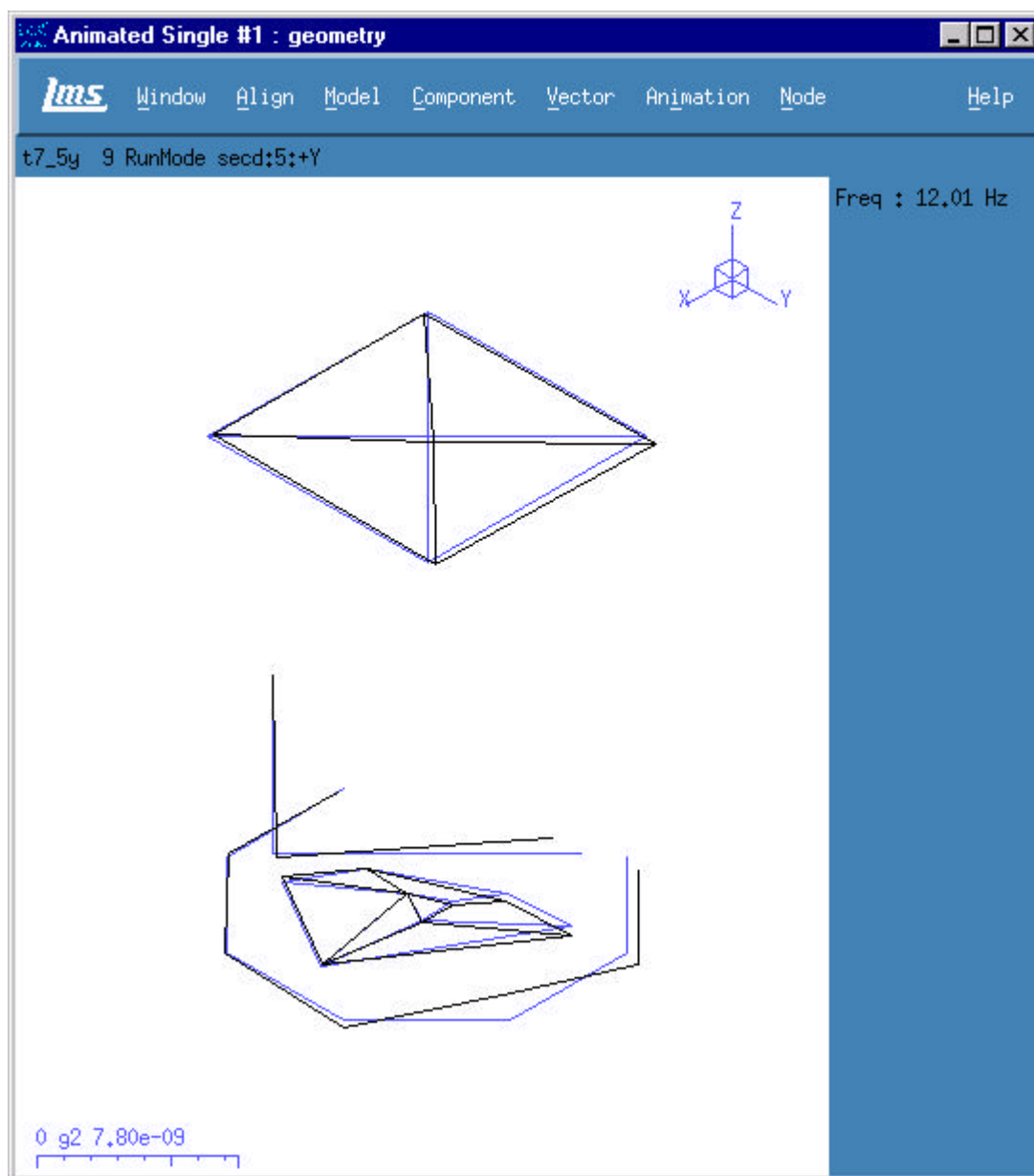


Test 7 – Operating Shape : 11.04Hz





## 10.0 Operating Mode Shape Plots – Test 7

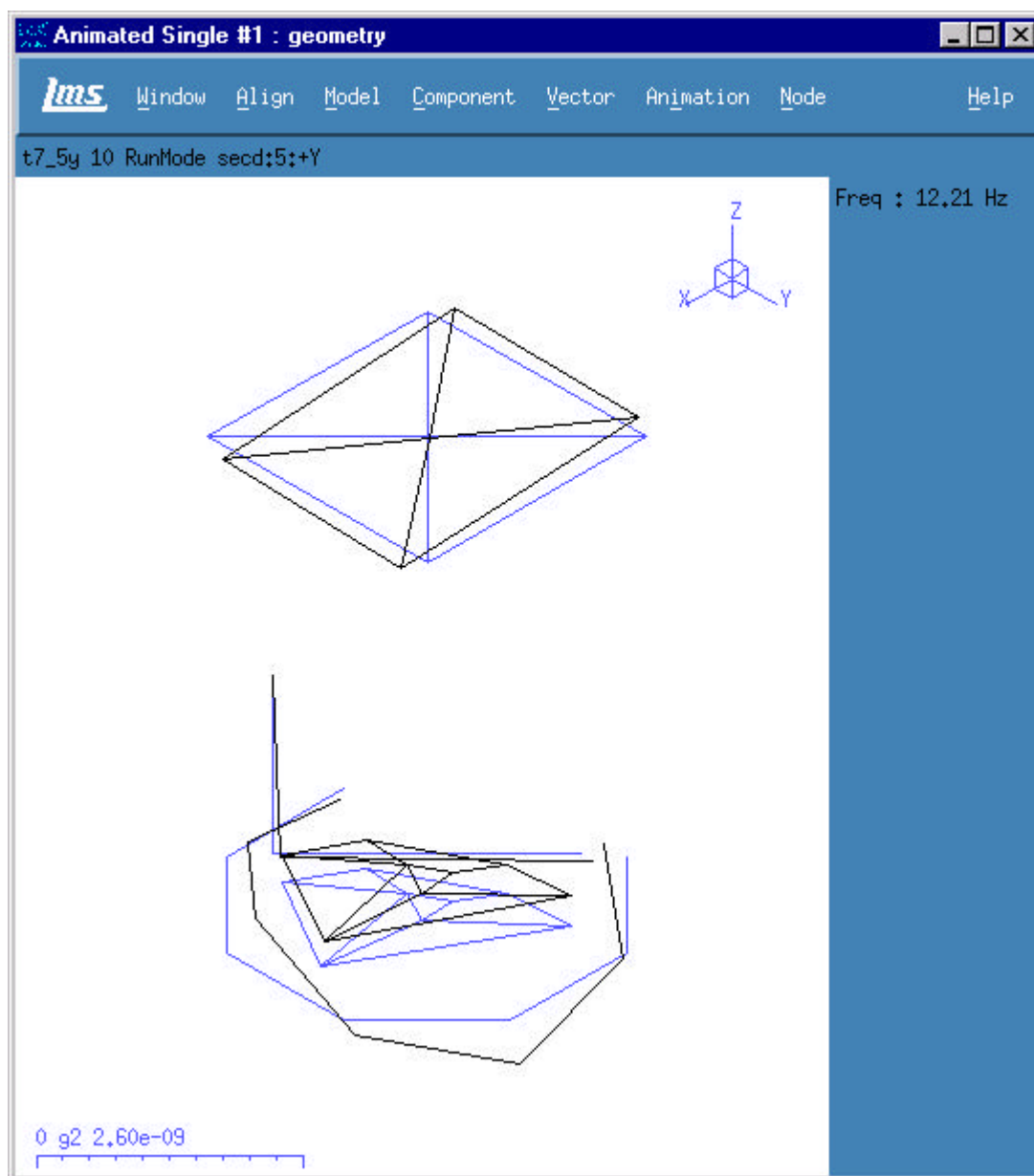


Test 7 – Operating Shape : 12.01Hz





## 10.0 Operating Mode Shape Plots – Test 7

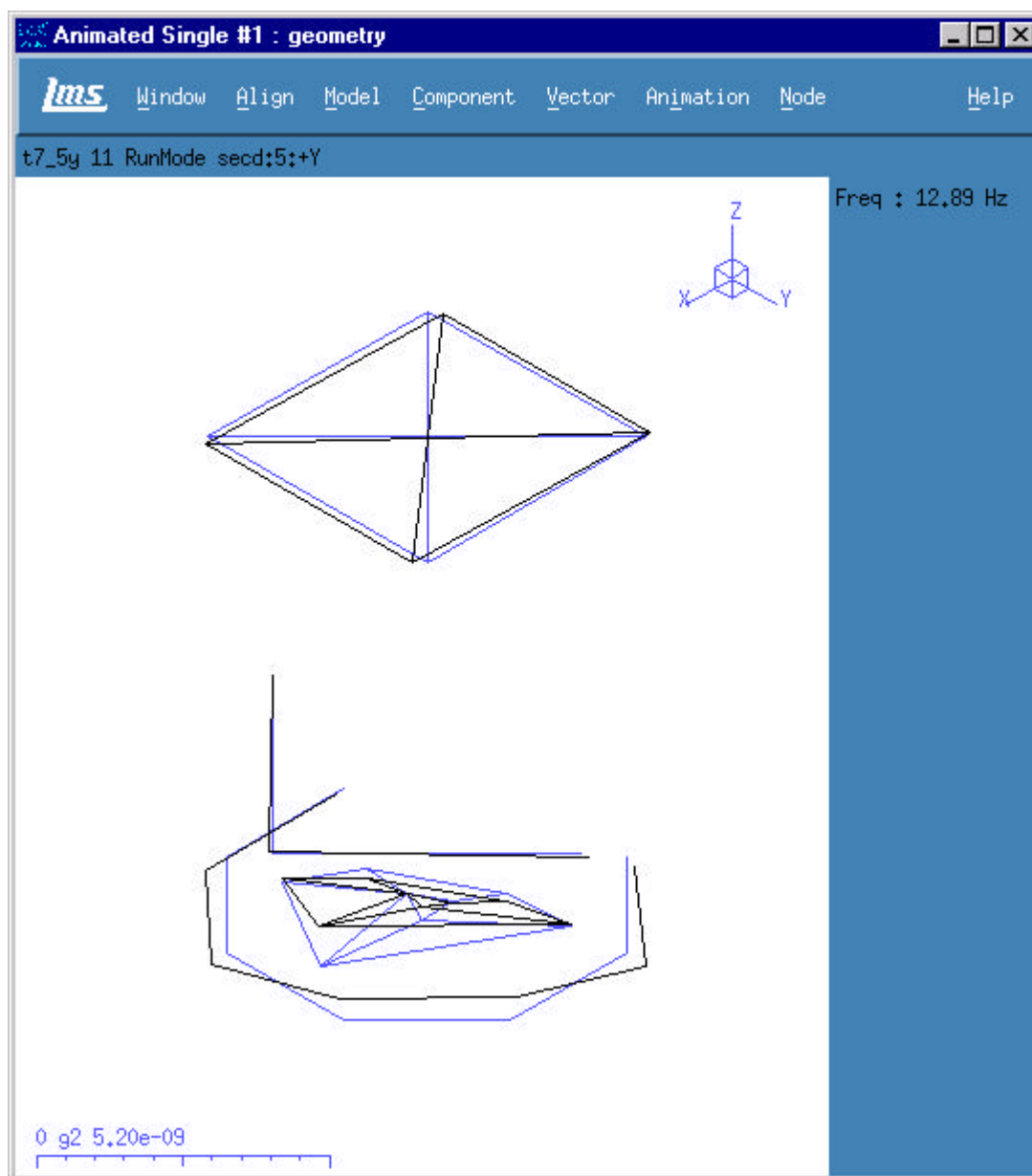


Test 7 – Operating Shape : 12.21Hz





## 10.0 Operating Mode Shape Plots – Test 7

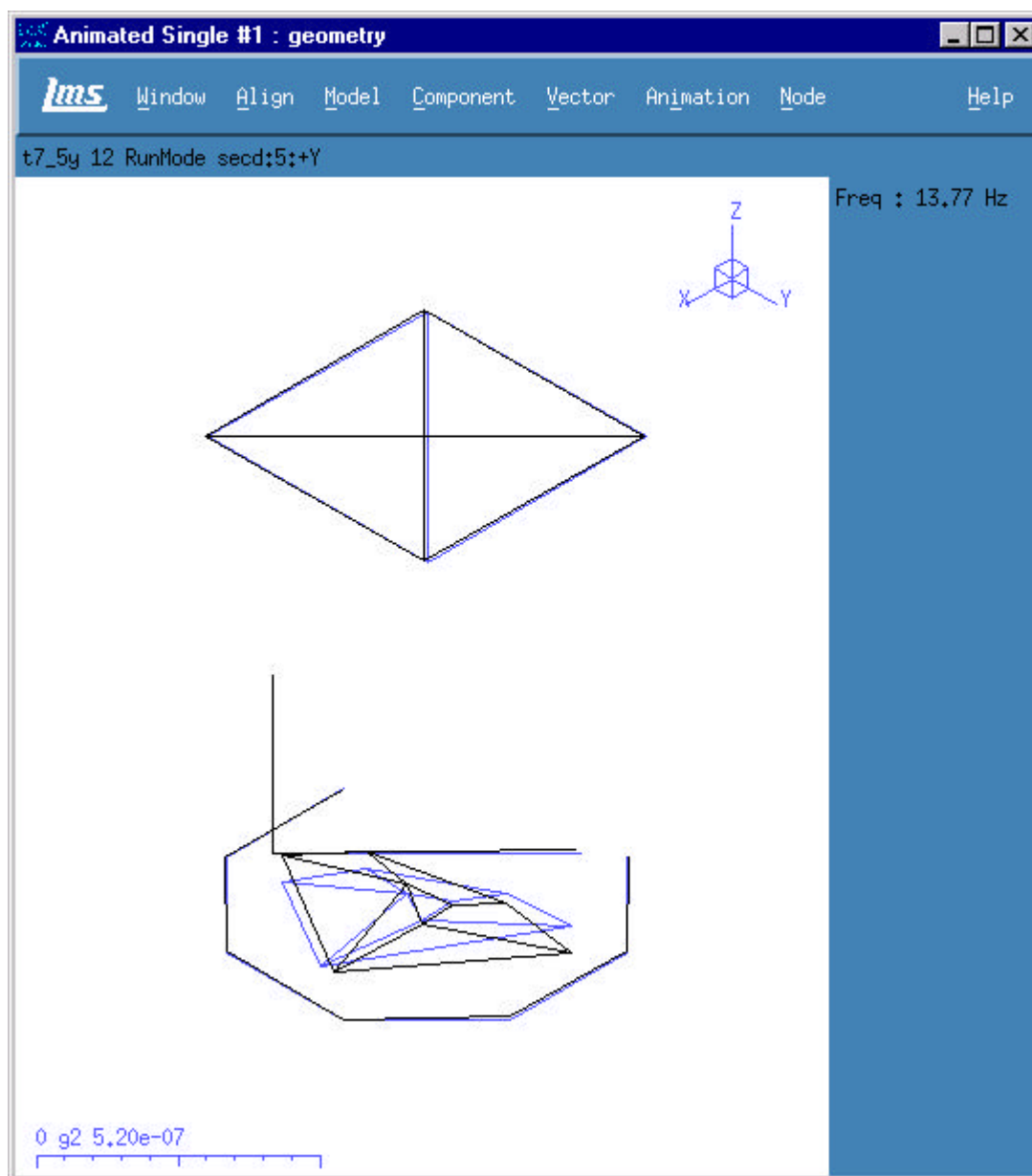


Test 7 – Operating Shape : 12.89Hz





## 10.0 Operating Mode Shape Plots – Test 7

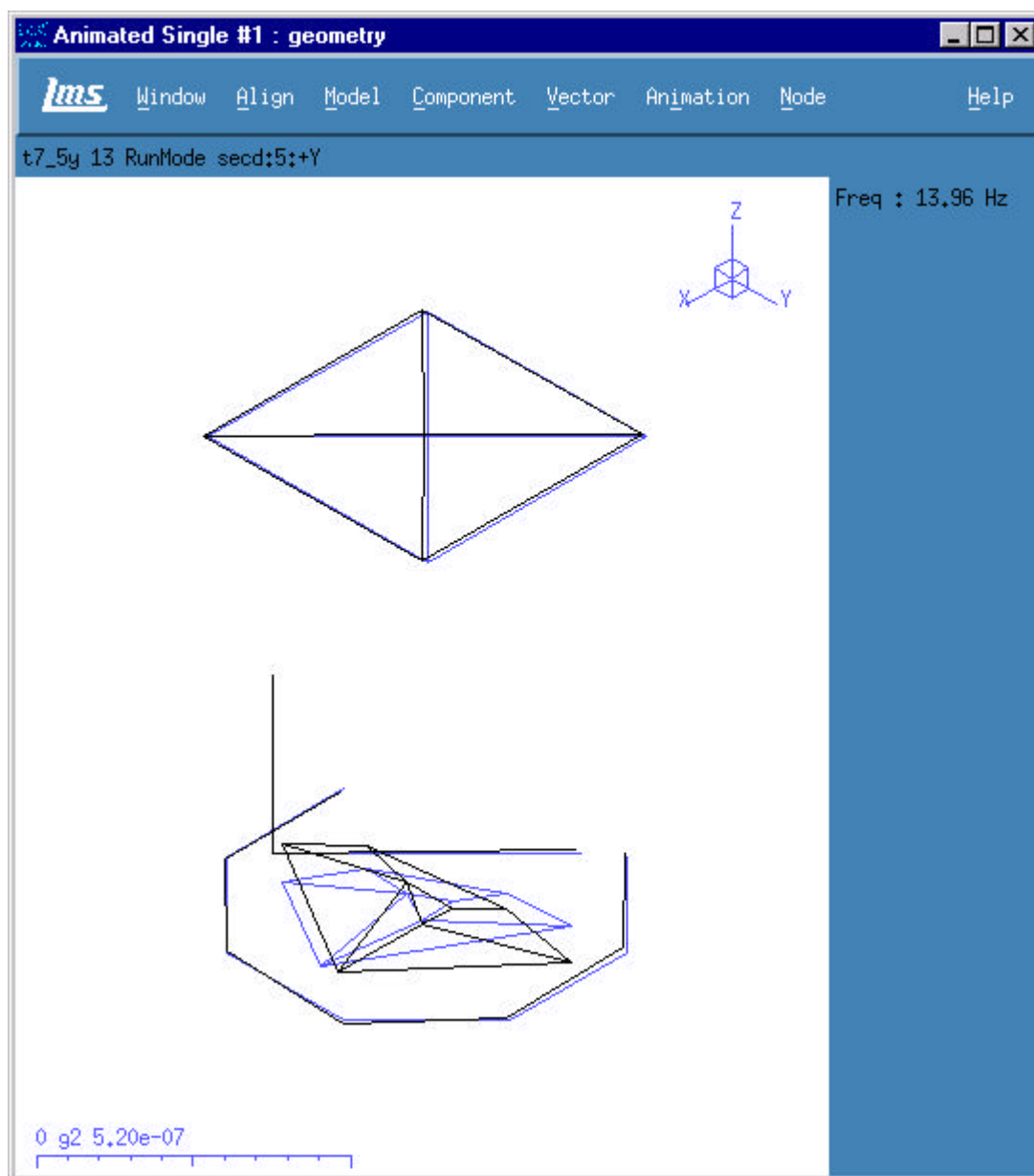


Test 7 – Operating Shape : 13.77Hz





## 10.0 Operating Mode Shape Plots – Test 7

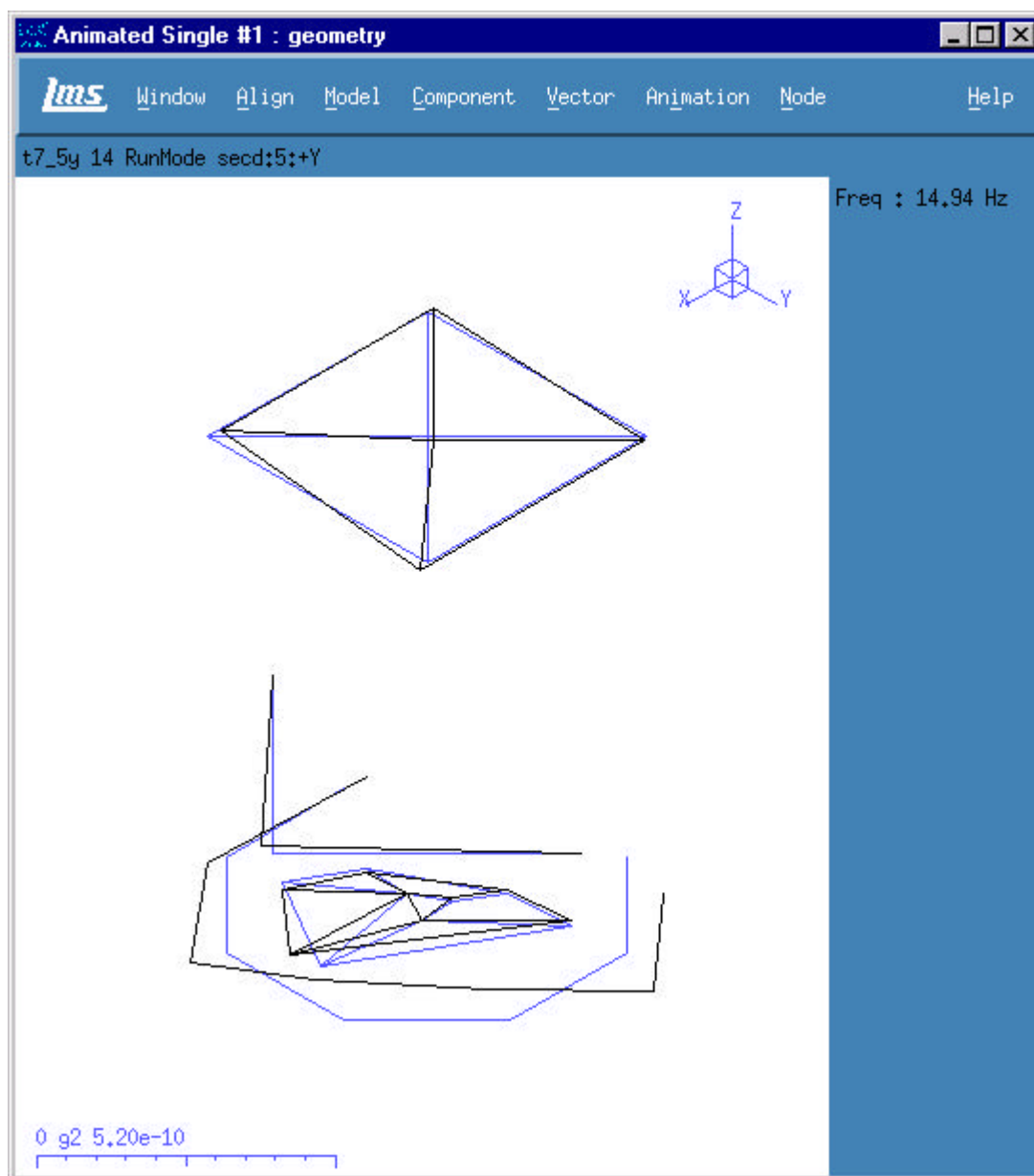


Test 7 – Operating Shape : 13.96Hz





## 10.0 Operating Mode Shape Plots – Test 7

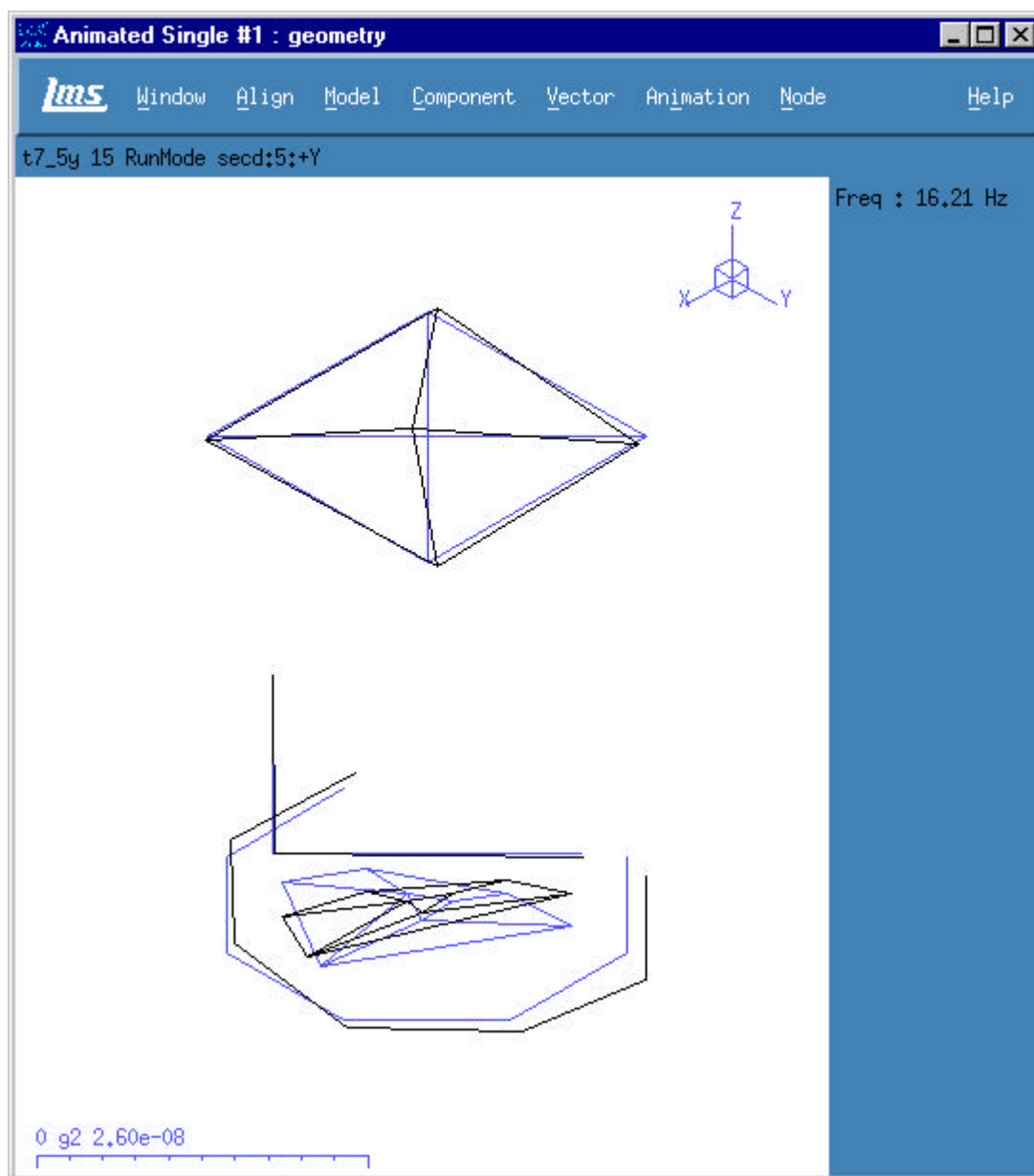


Test 7 – Operating Shape : 14.94Hz





## 10.0 Operating Mode Shape Plots – Test 7

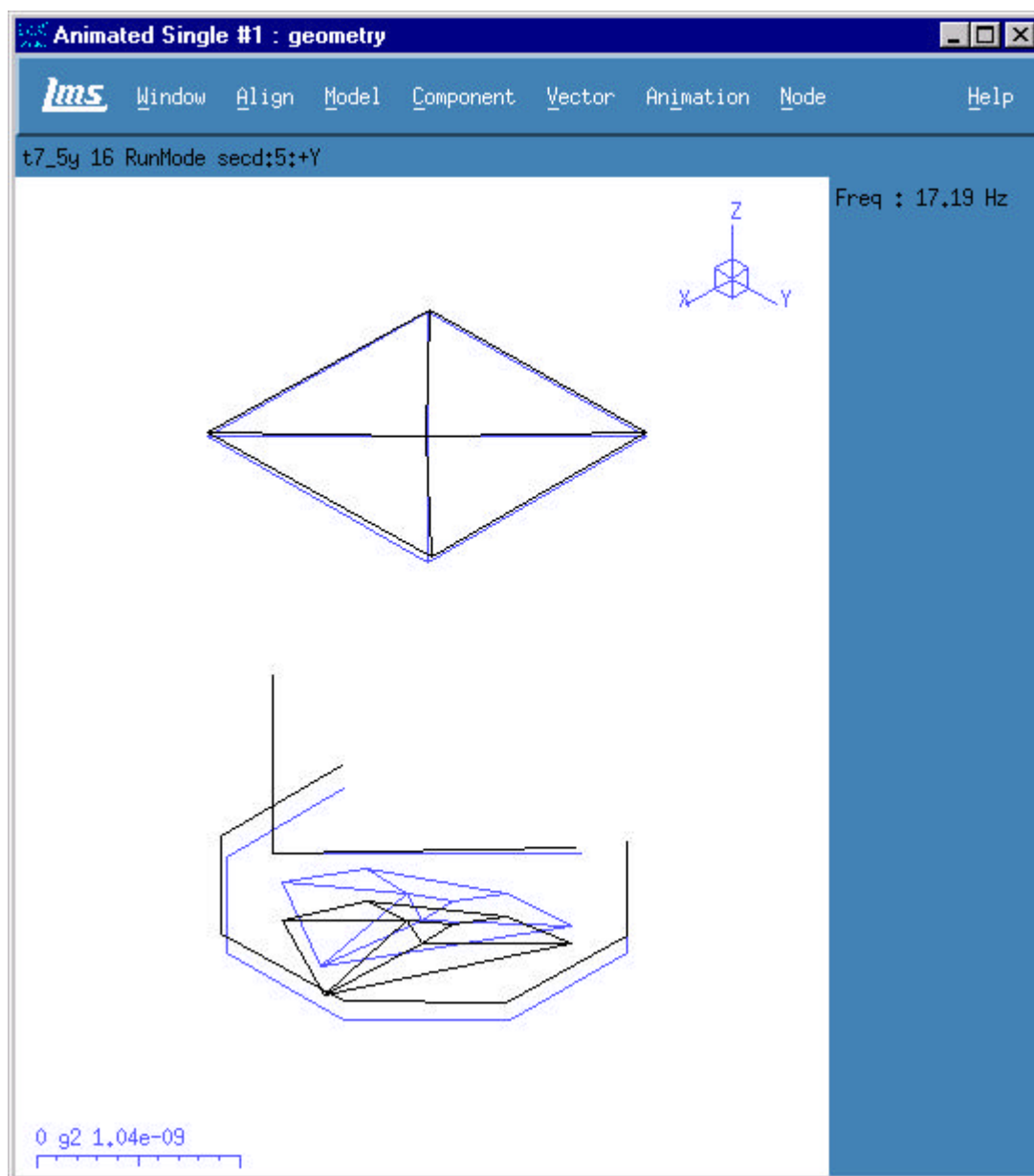


Test 7 – Operating Shape : 16.21Hz





## 10.0 Operating Mode Shape Plots – Test 7

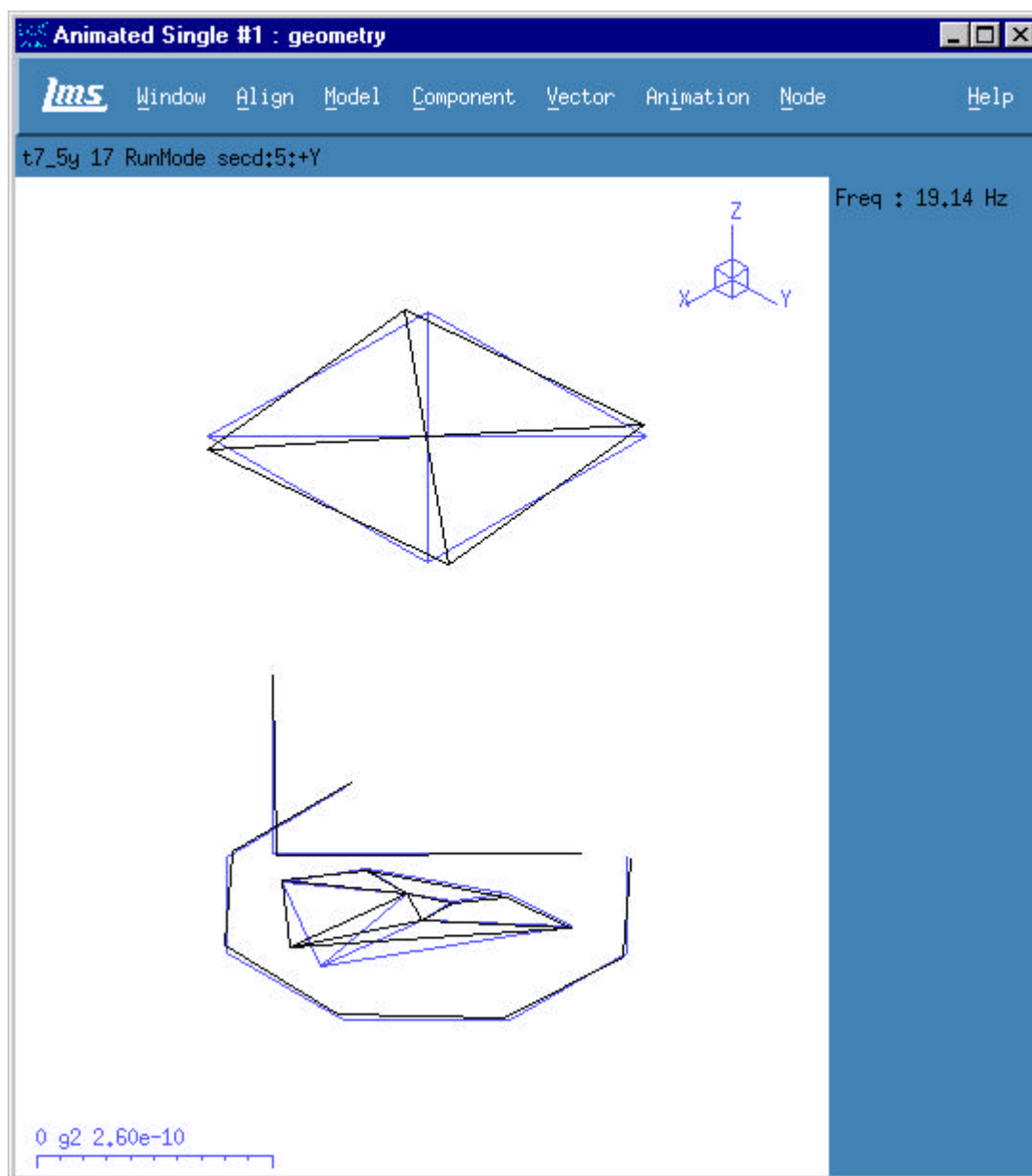


Test 7 – Operating Shape : 17.19Hz





## 10.0 Operating Mode Shape Plots – Test 7

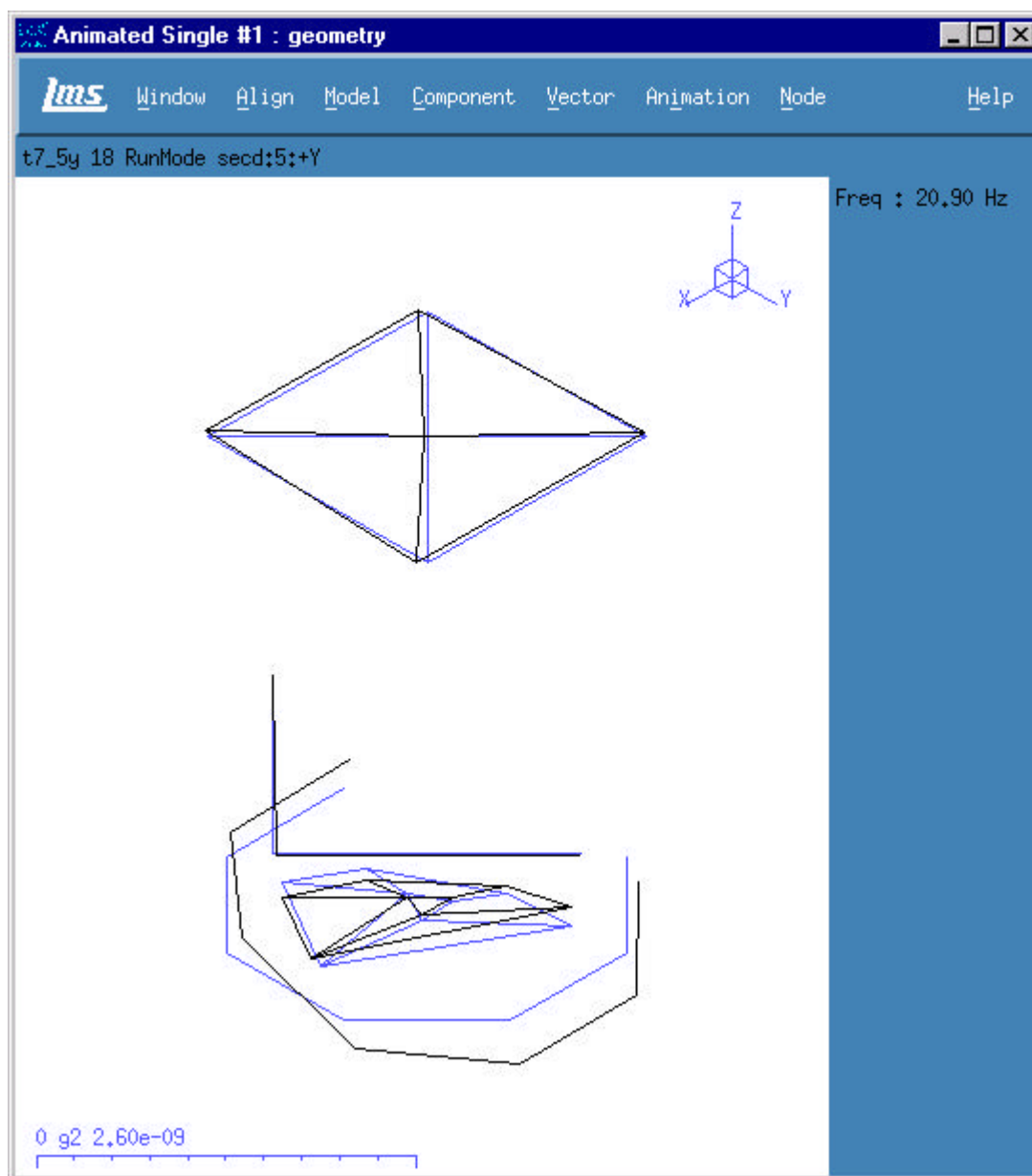


Test 7 – Operating Shape : 19.14Hz





## 10.0 Operating Mode Shape Plots – Test 7

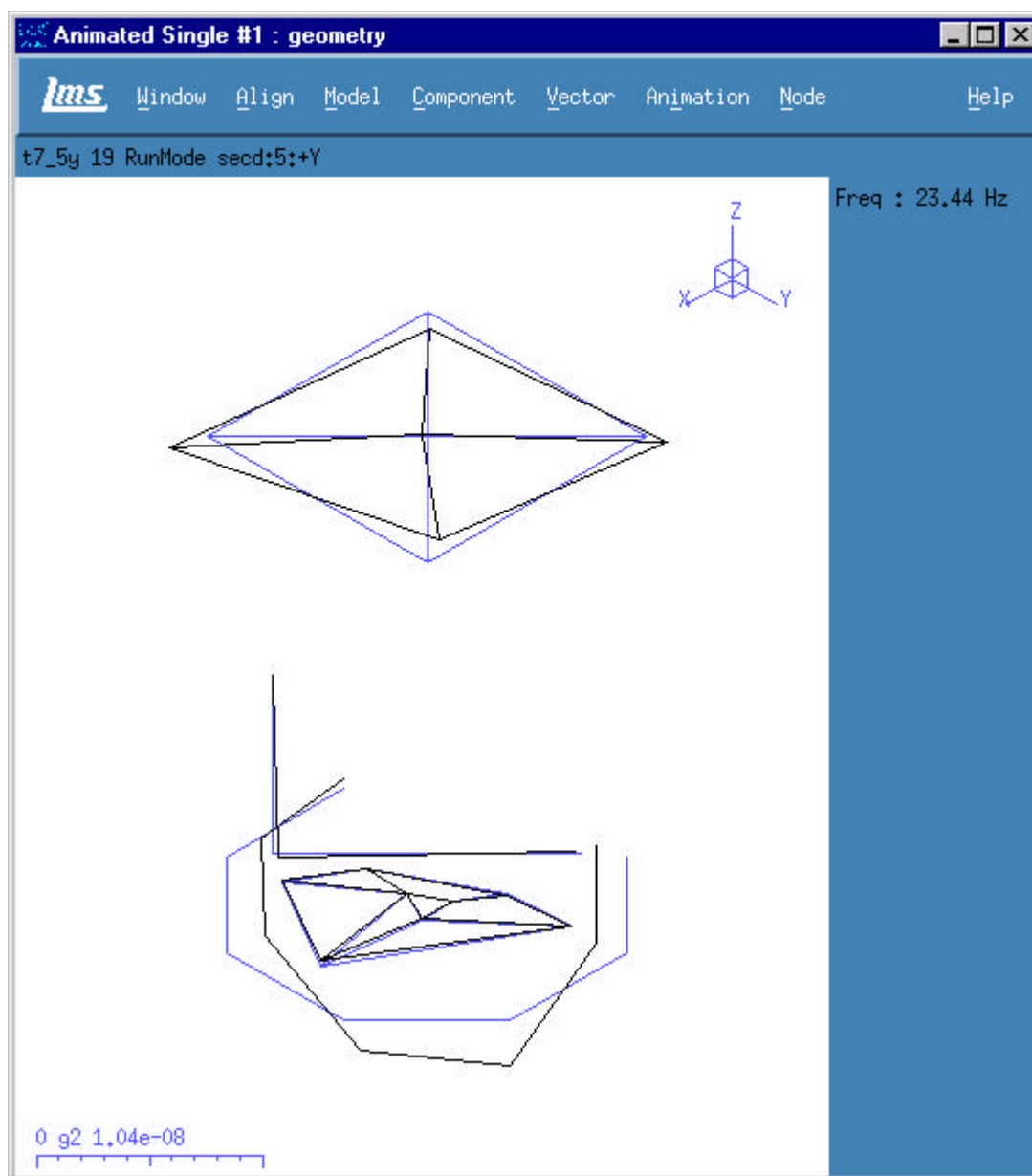


Test 7 – Operating Shape : 20.90Hz





## 10.0 Operating Mode Shape Plots – Test 7

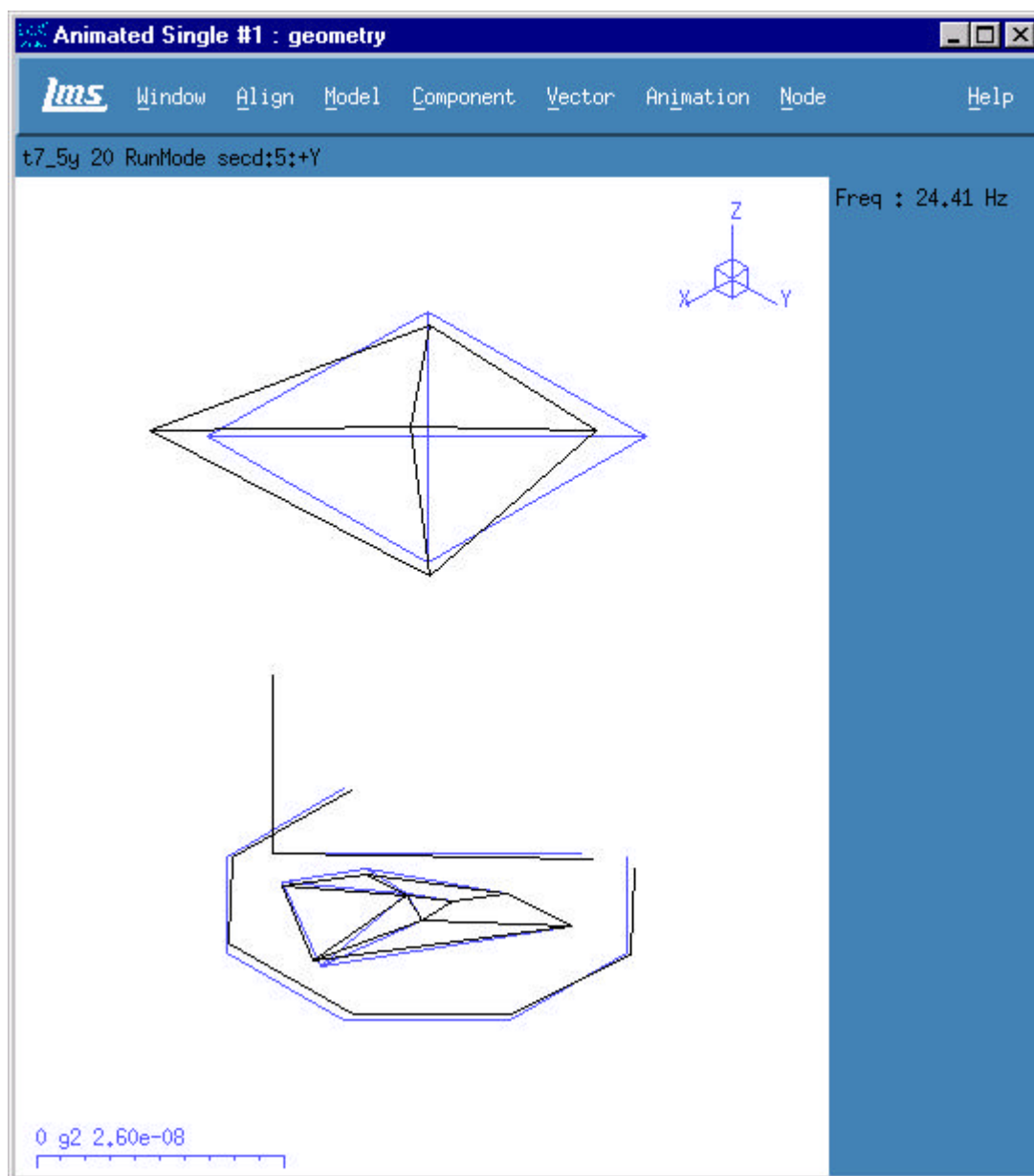


Test 7 – Operating Shape : 23.44Hz





## 10.0 Operating Mode Shape Plots – Test 7

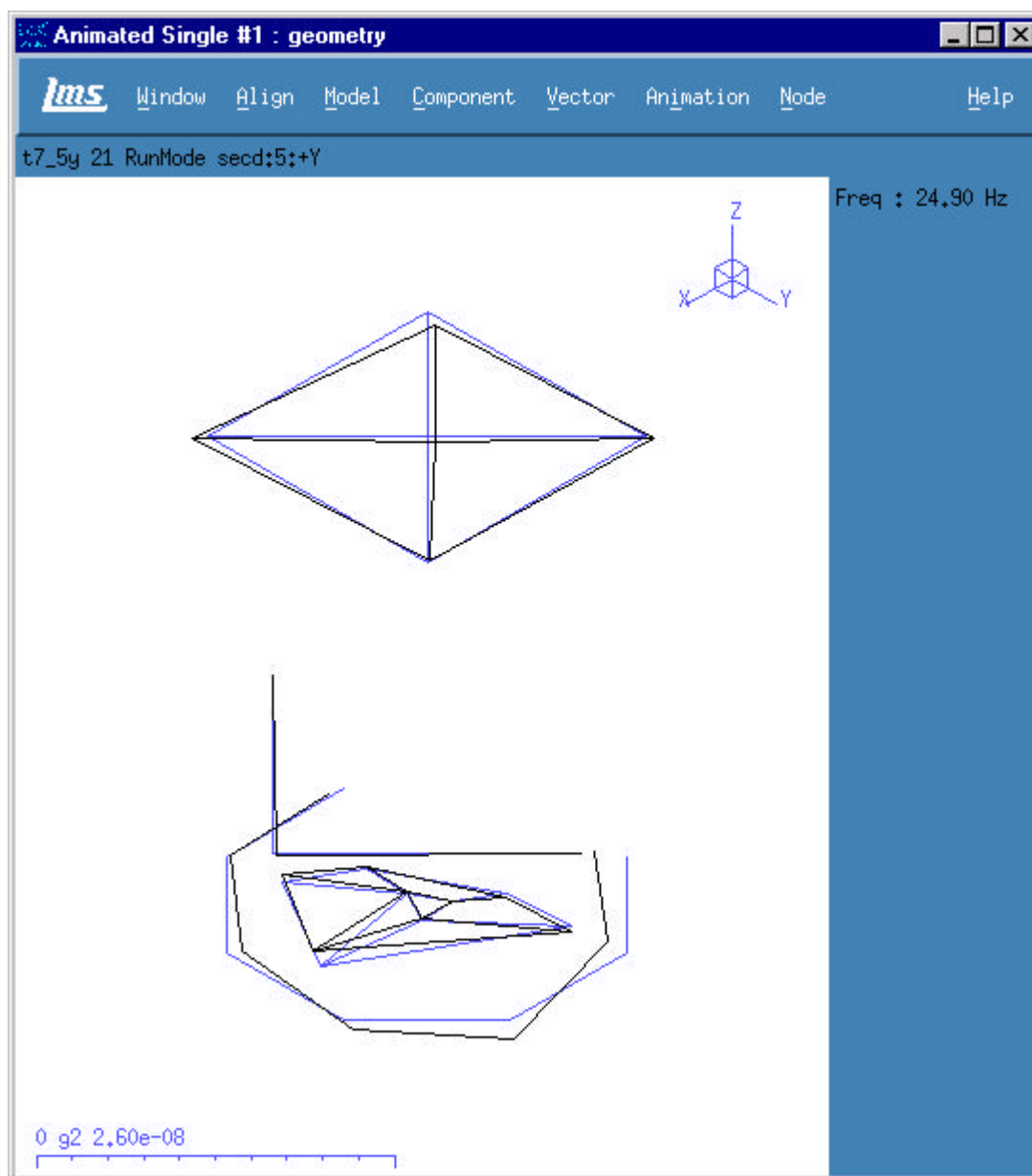


Test 7 – Operating Shape : 24.41Hz





## 10.0 Operating Mode Shape Plots – Test 7

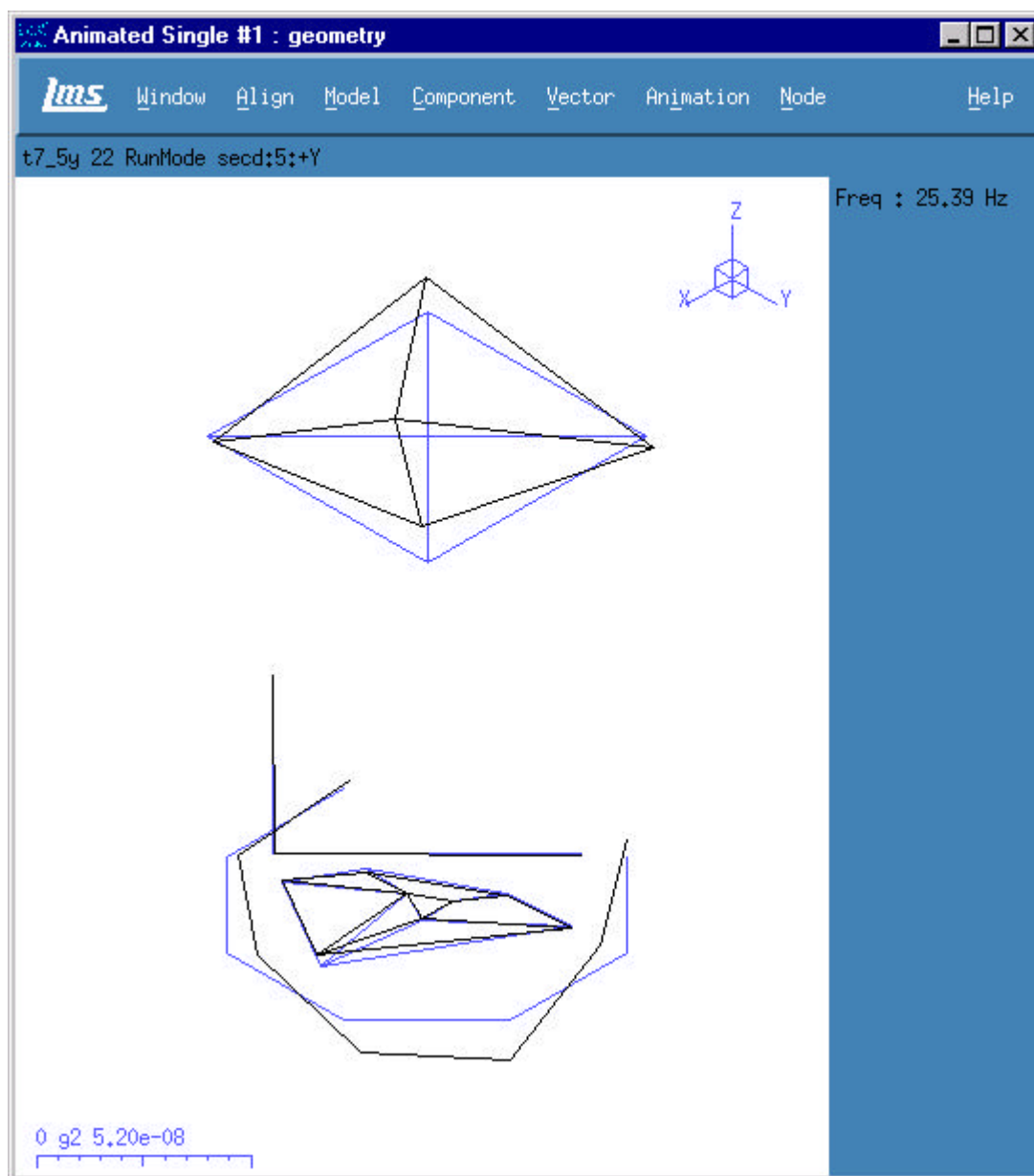


Test 7 – Operating Shape : 24.90Hz





## 10.0 Operating Mode Shape Plots – Test 7

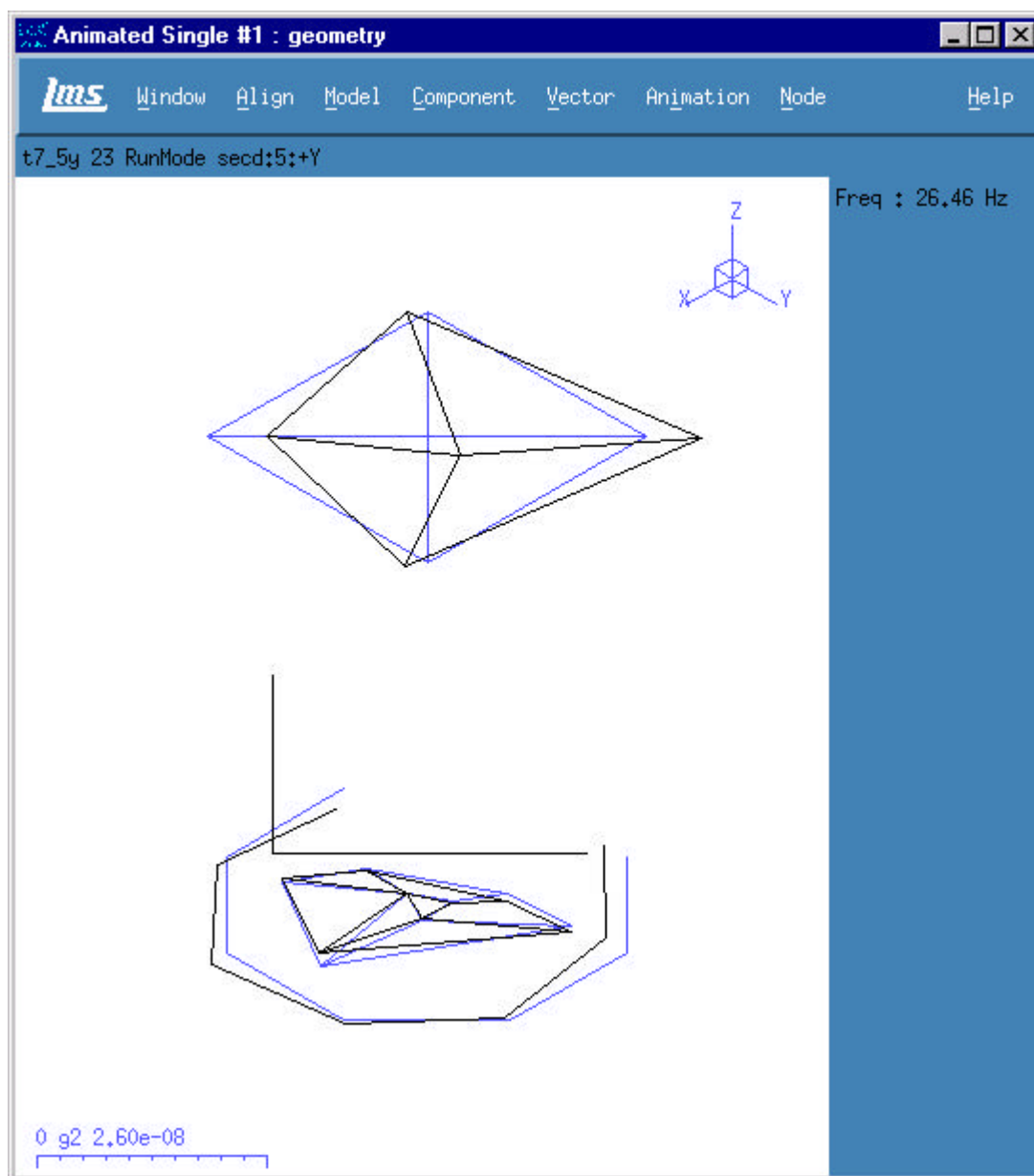


Test 7 – Operating Shape : 25.39Hz





## 10.0 Operating Mode Shape Plots – Test 7

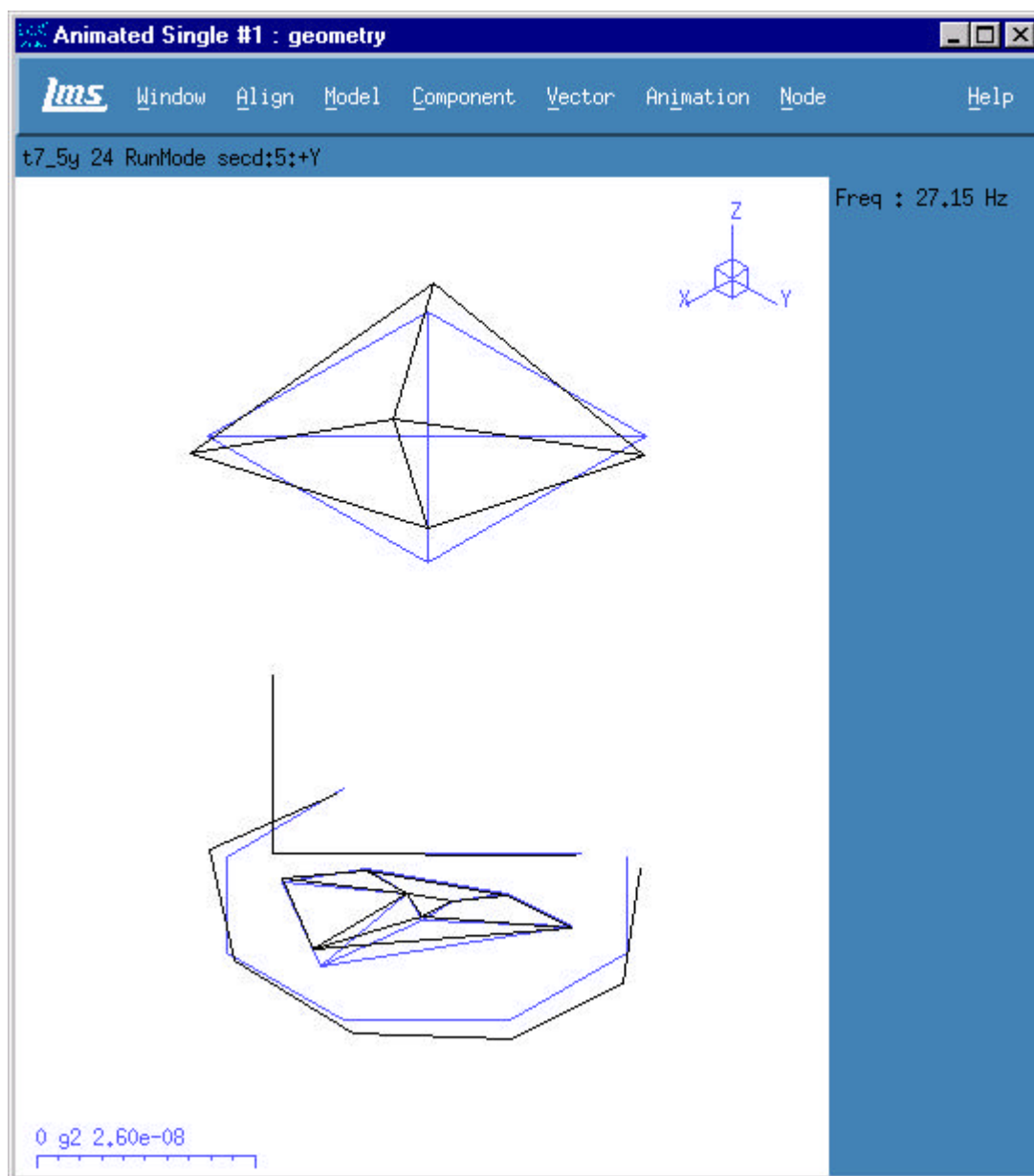


Test 7 – Operating Shape : 26.46Hz





## 10.0 Operating Mode Shape Plots – Test 7

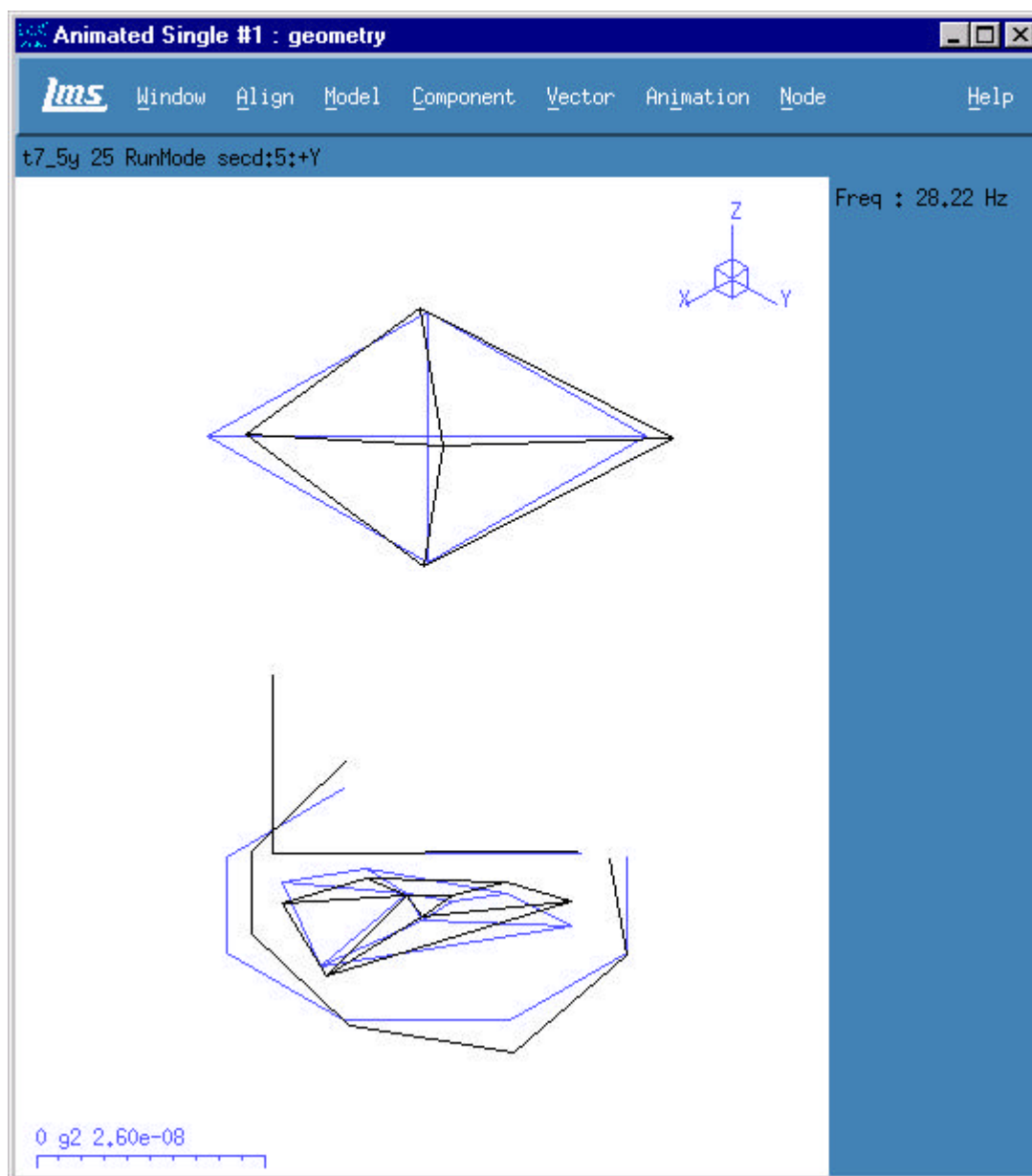


Test 7 – Operating Shape : 27.15Hz





## 10.0 Operating Mode Shape Plots – Test 7

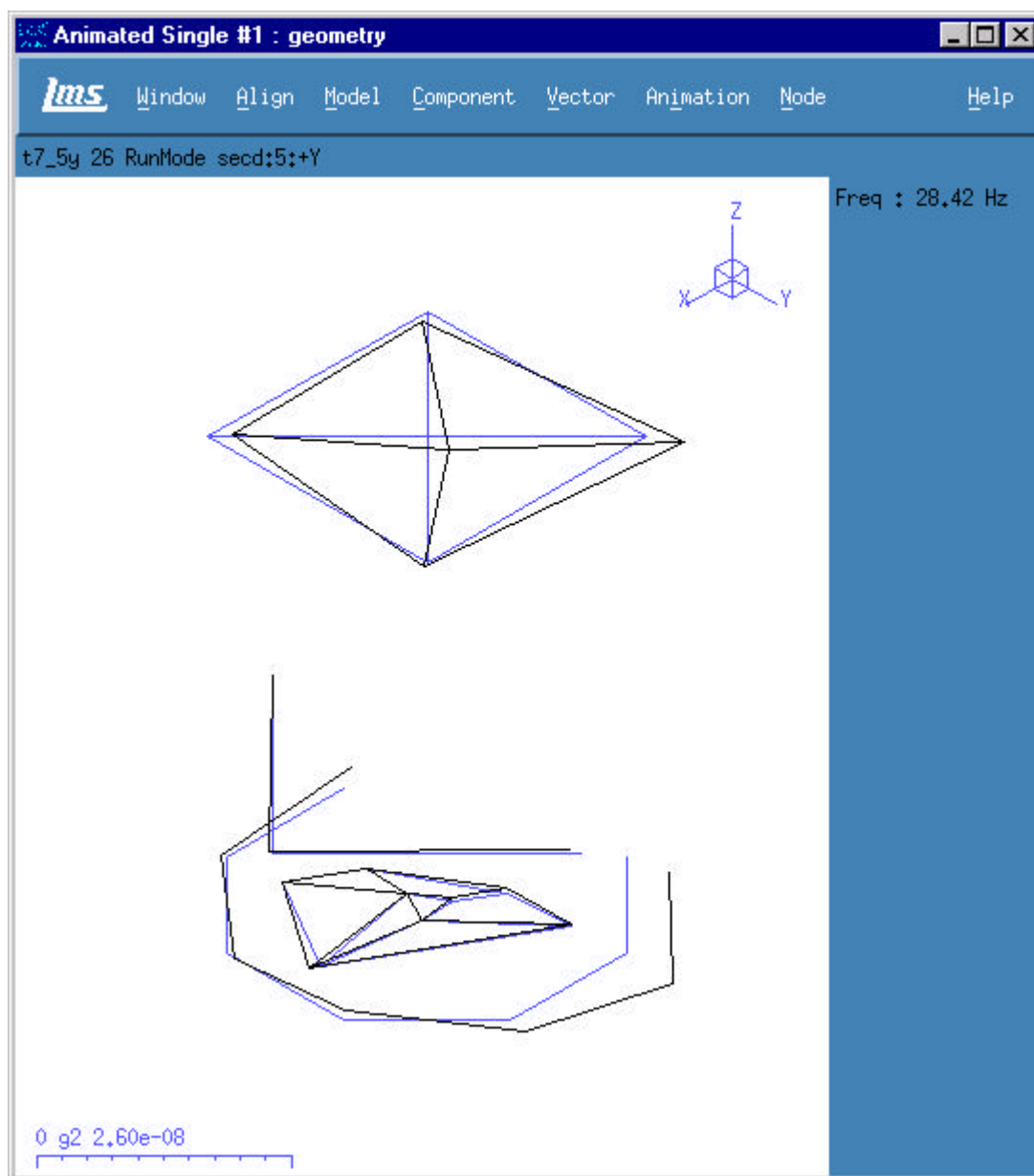


Test 7 – Operating Shape : 28.22Hz





## 10.0 Operating Mode Shape Plots – Test 7

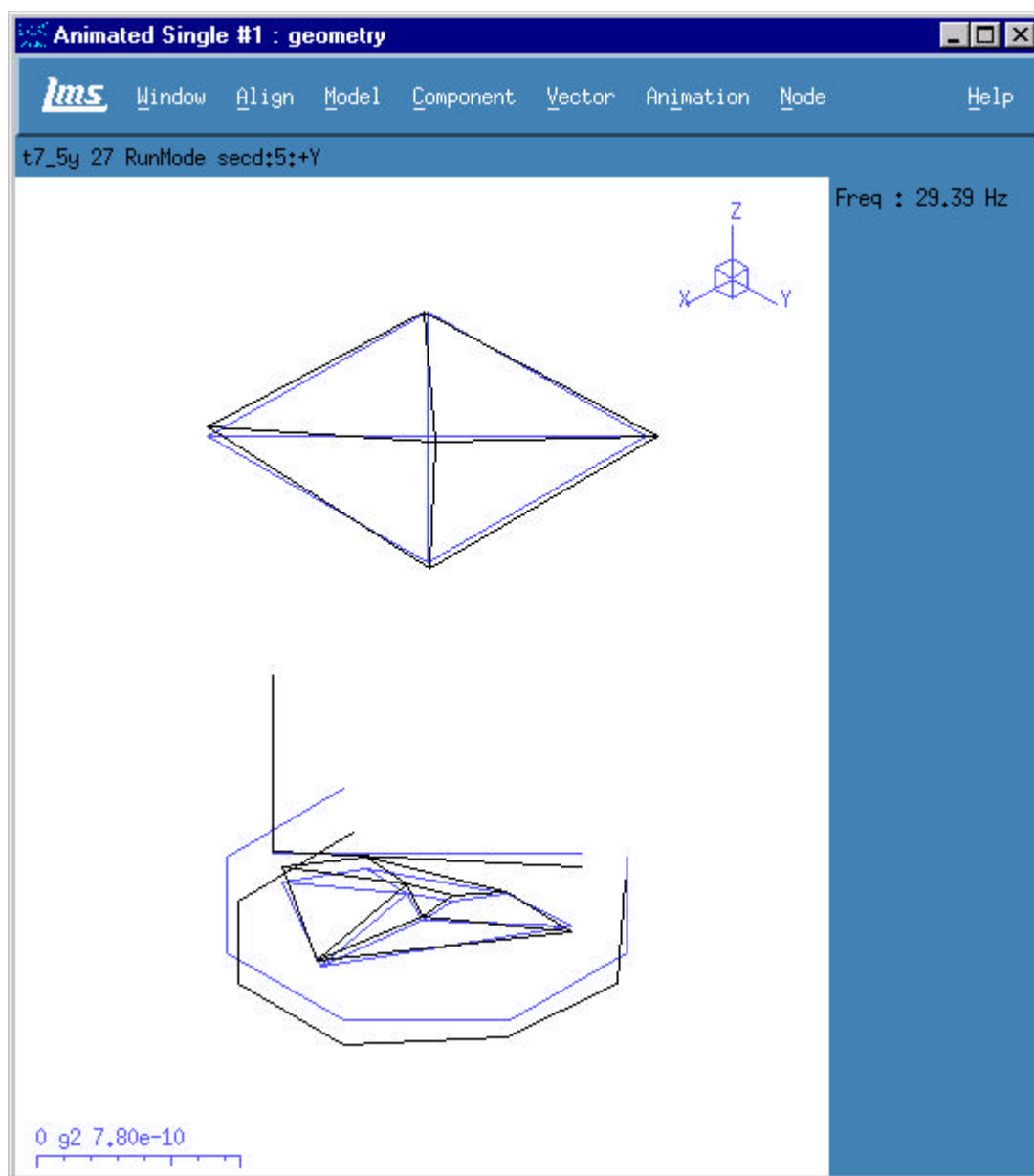


Test 7 – Operating Shape : 28.42Hz





## 10.0 Operating Mode Shape Plots – Test 7

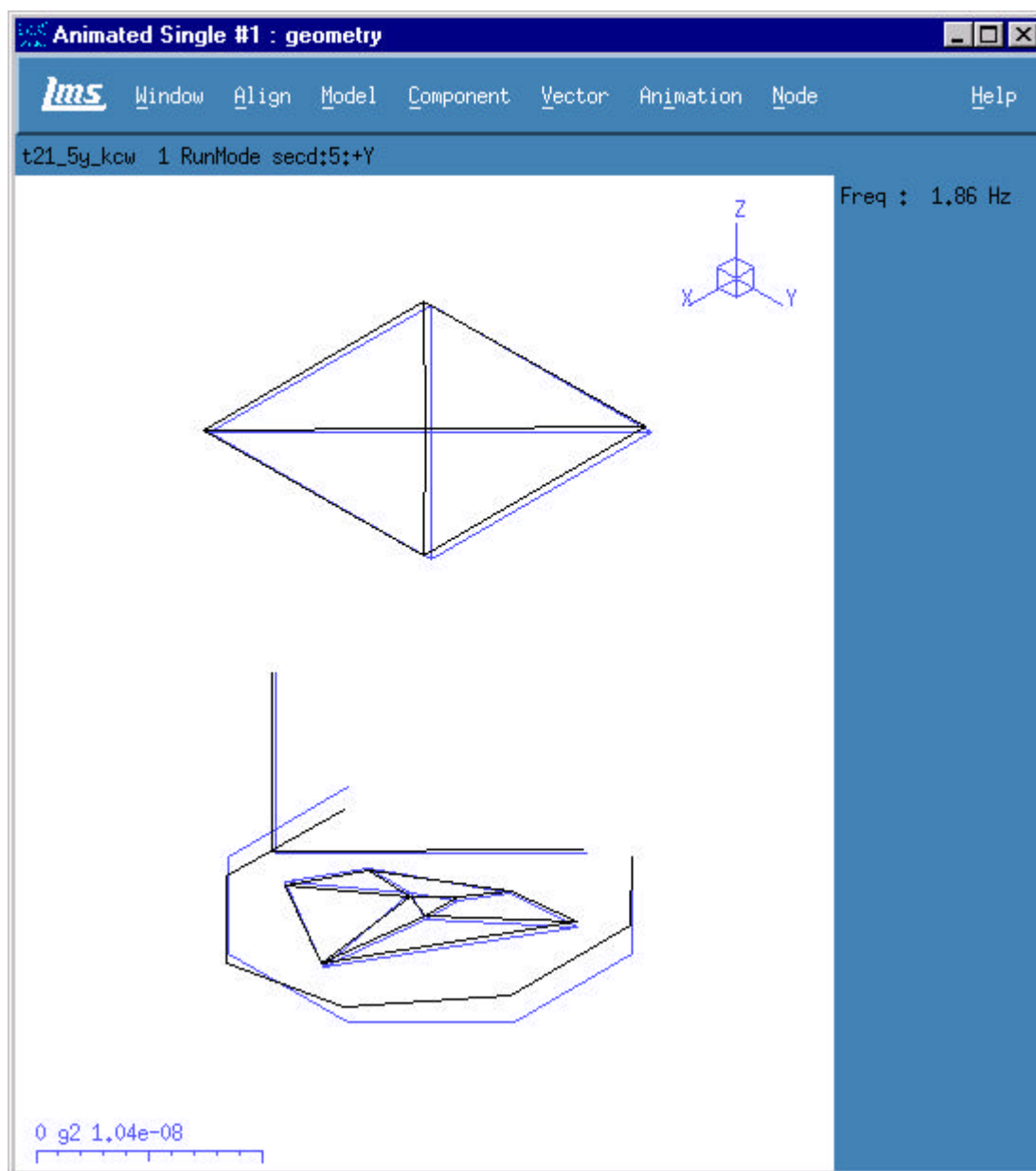


Test 7 – Operating Shape : 29.39Hz





## 10.0 Operating Mode Shape Plots – Test 21

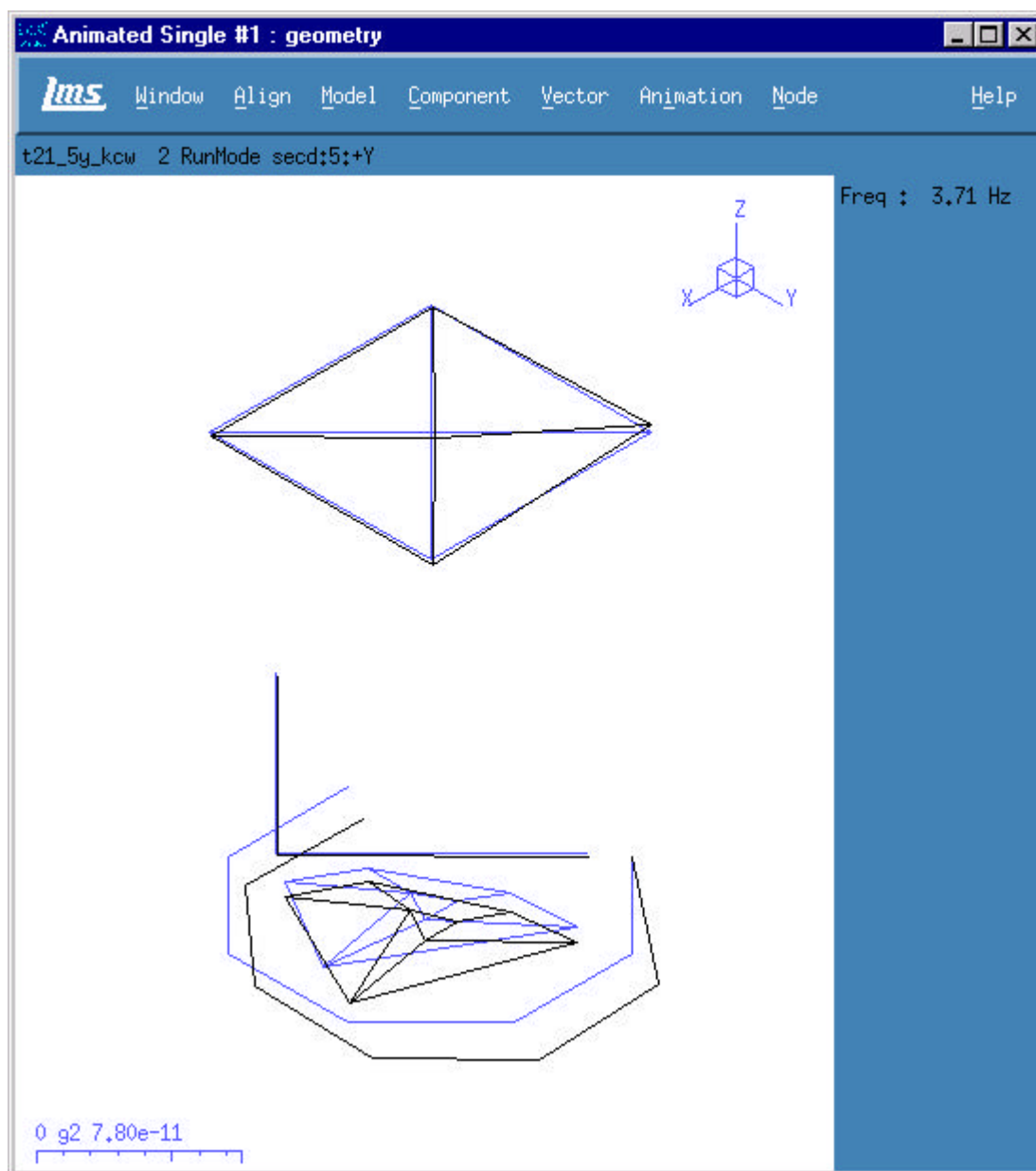


Test 21 – Operating Shape : 1.86Hz





## 10.0 Operating Mode Shape Plots – Test 21

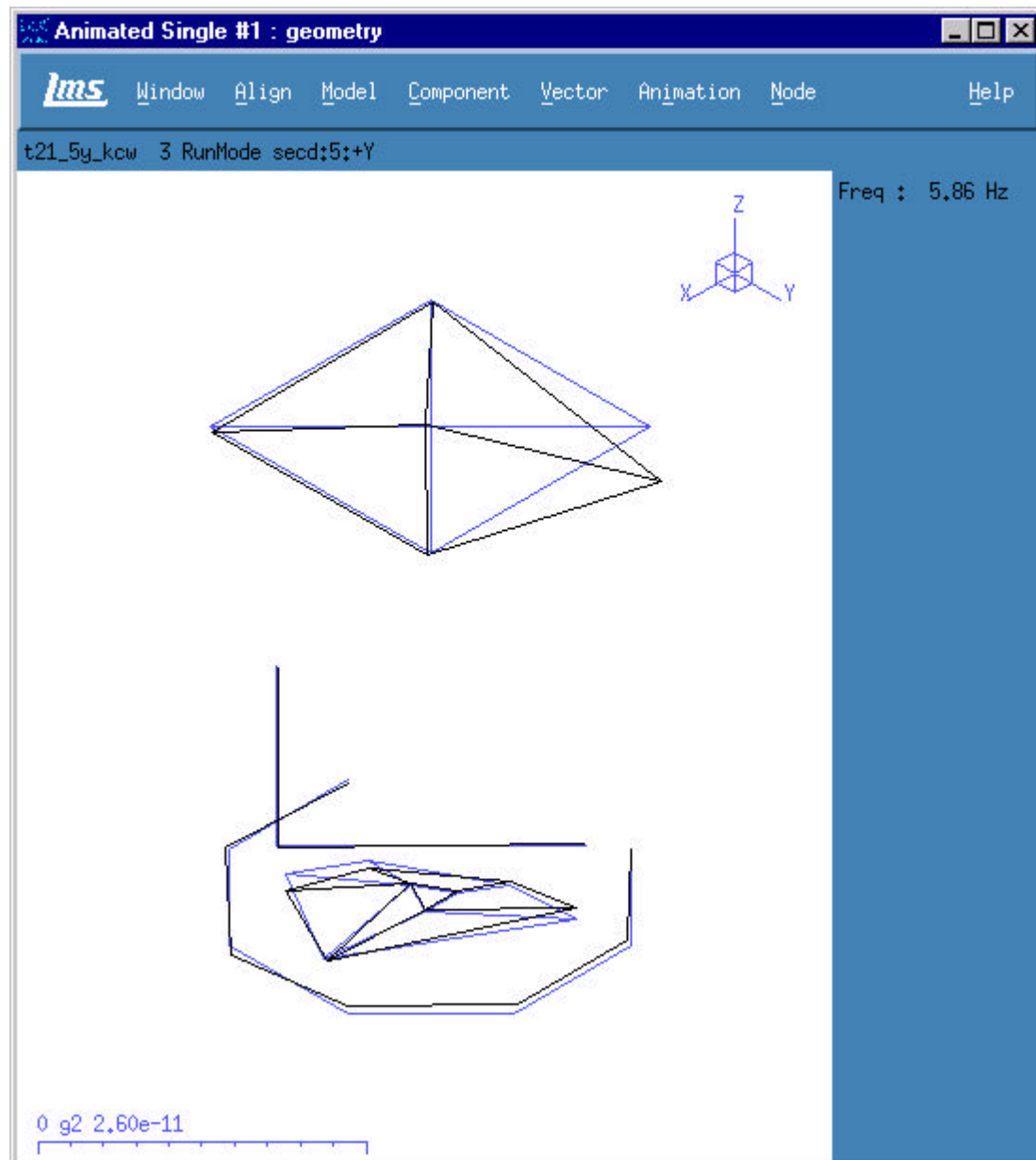


Test 21 – Operating Shape : 3.71Hz





## 10.0 Operating Mode Shape Plots – Test 21

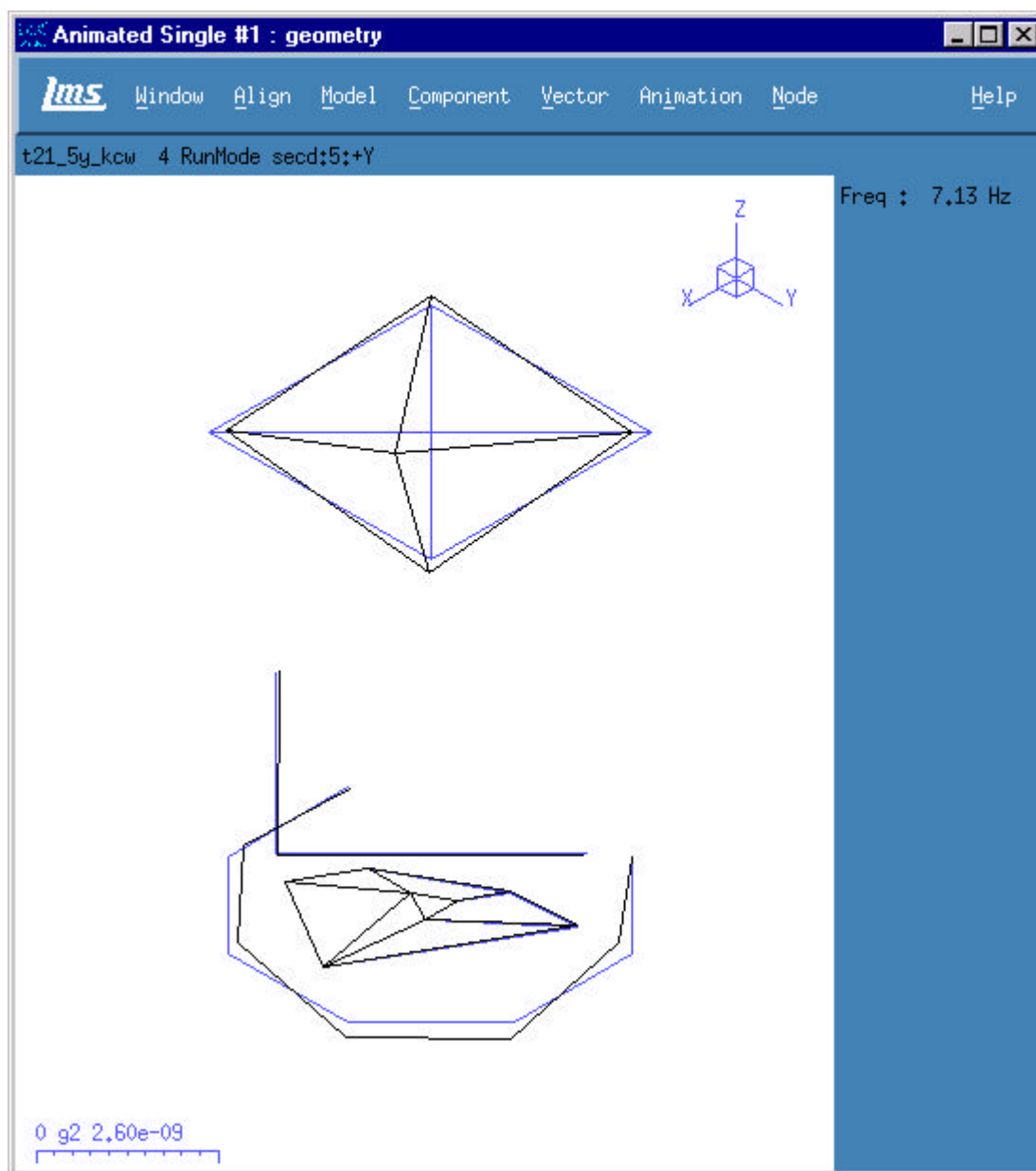


Test 21 – Operating Shape : 5.86Hz





## 10.0 Operating Mode Shape Plots – Test 21

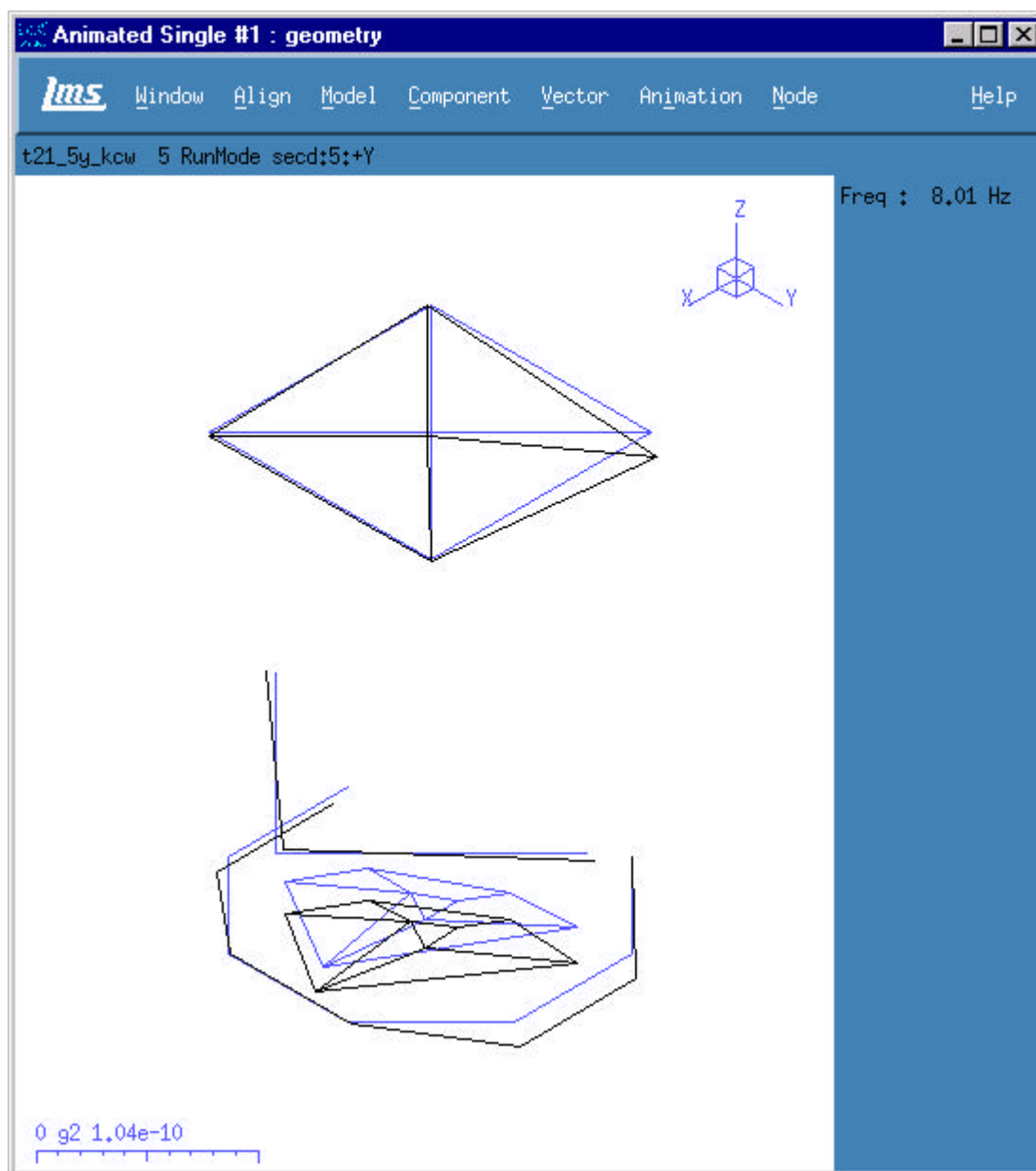


Test 21 – Operating Shape : 7.13Hz





## 10.0 Operating Mode Shape Plots – Test 21

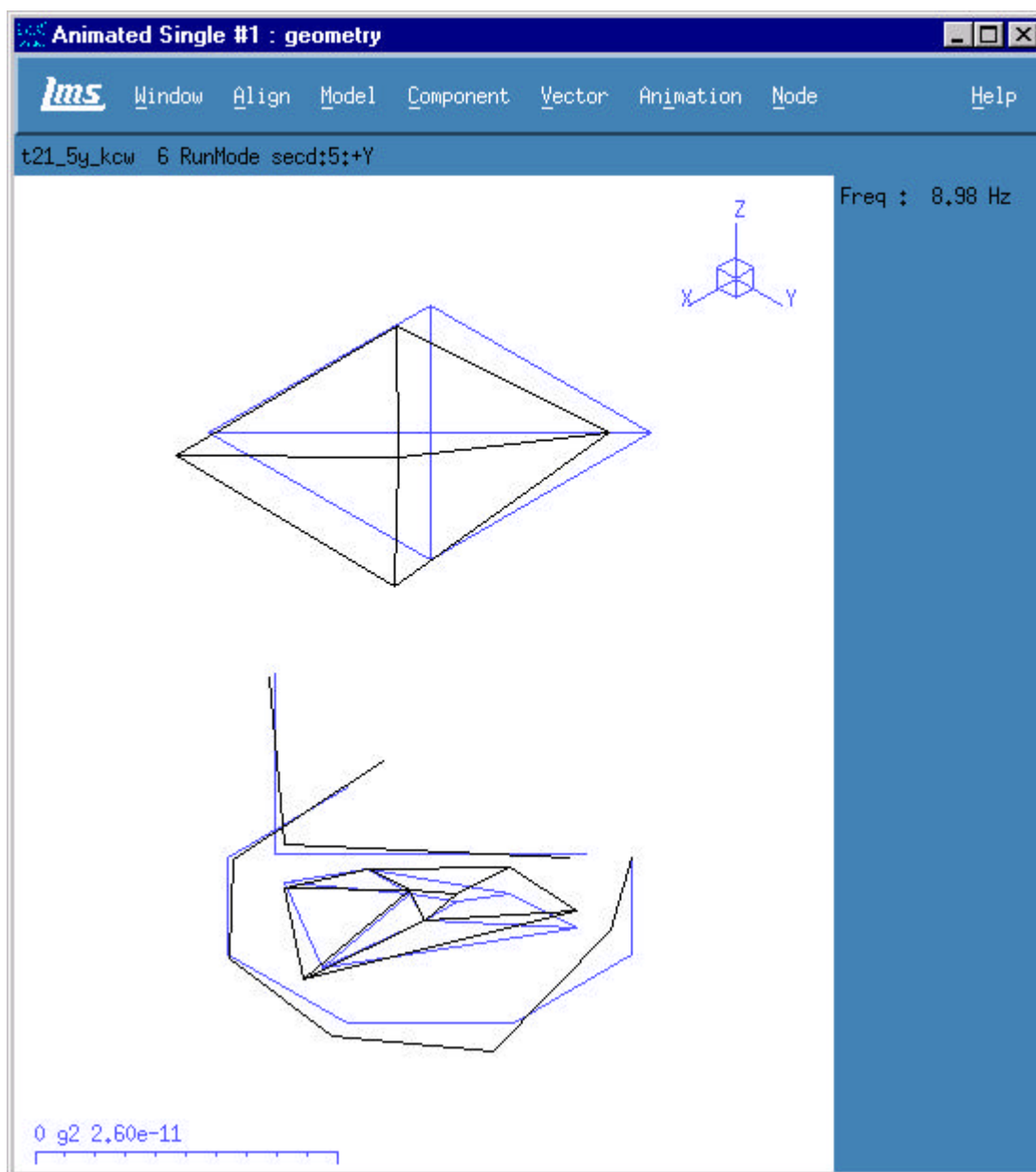


Test 21 – Operating Shape : 8.01Hz





## 10.0 Operating Mode Shape Plots – Test 21

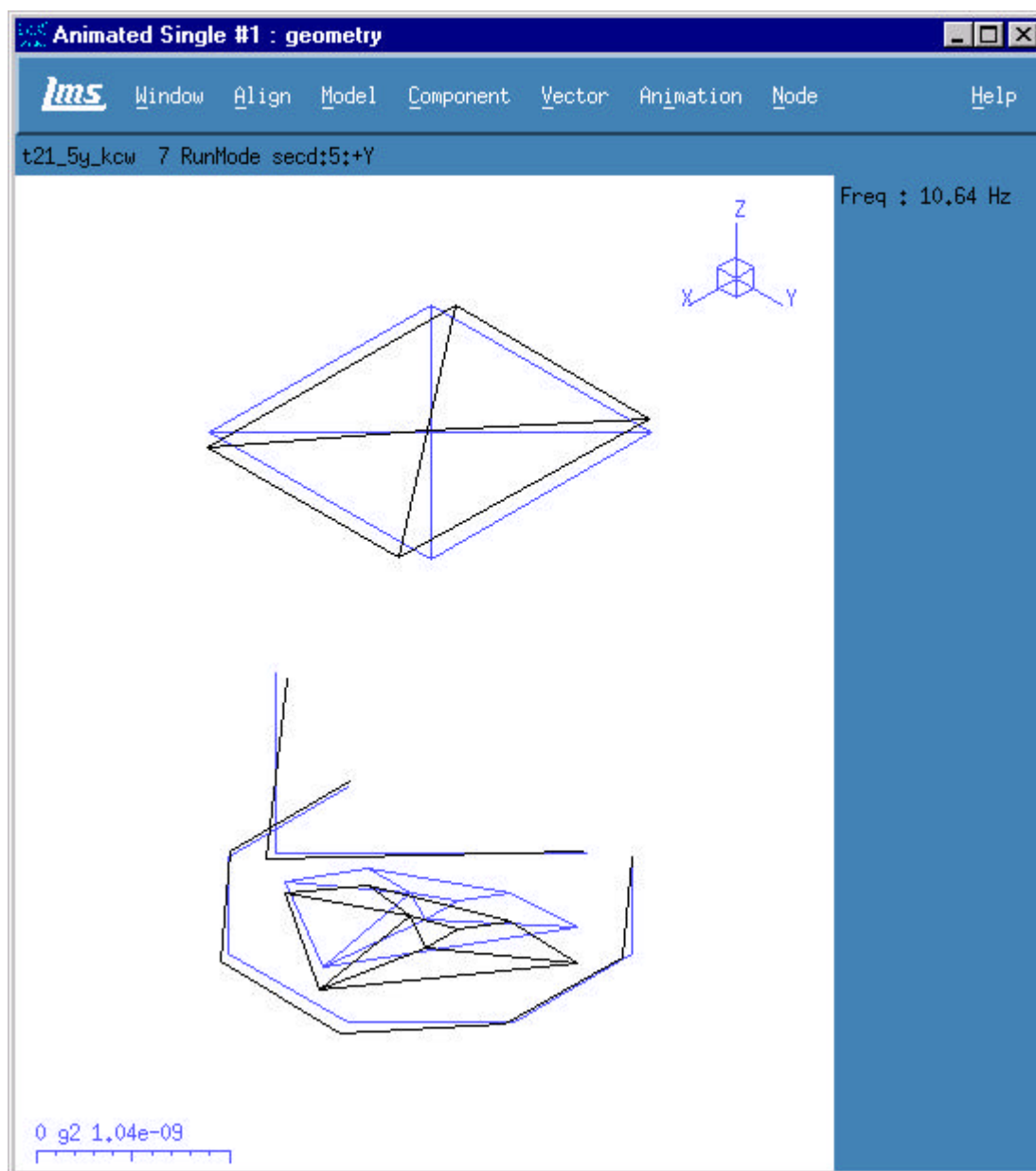


Test 21 – Operating Shape : 8.98Hz





## 10.0 Operating Mode Shape Plots – Test 21

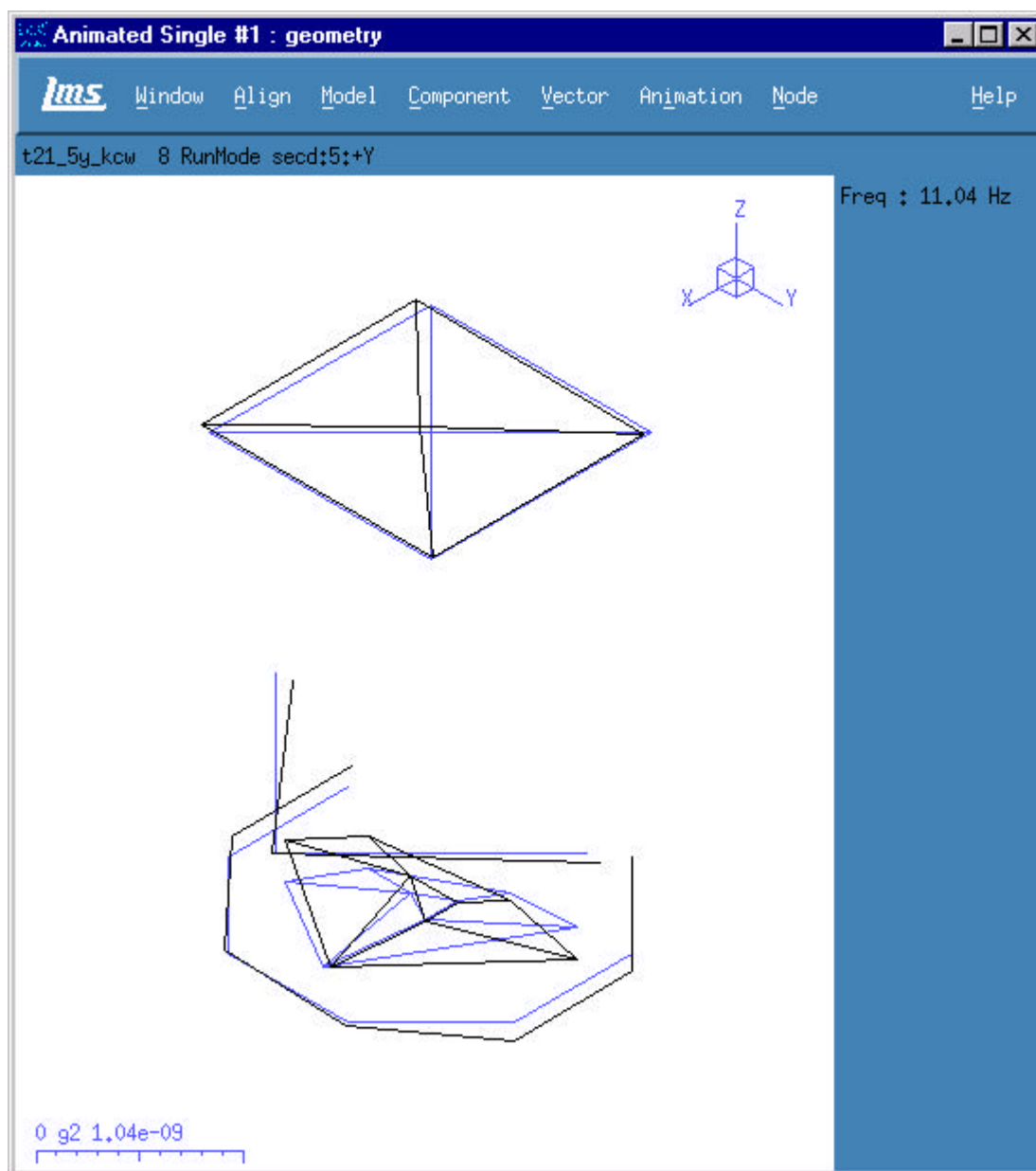


Test 21 – Operating Shape : 10.64Hz





## 10.0 Operating Mode Shape Plots – Test 21

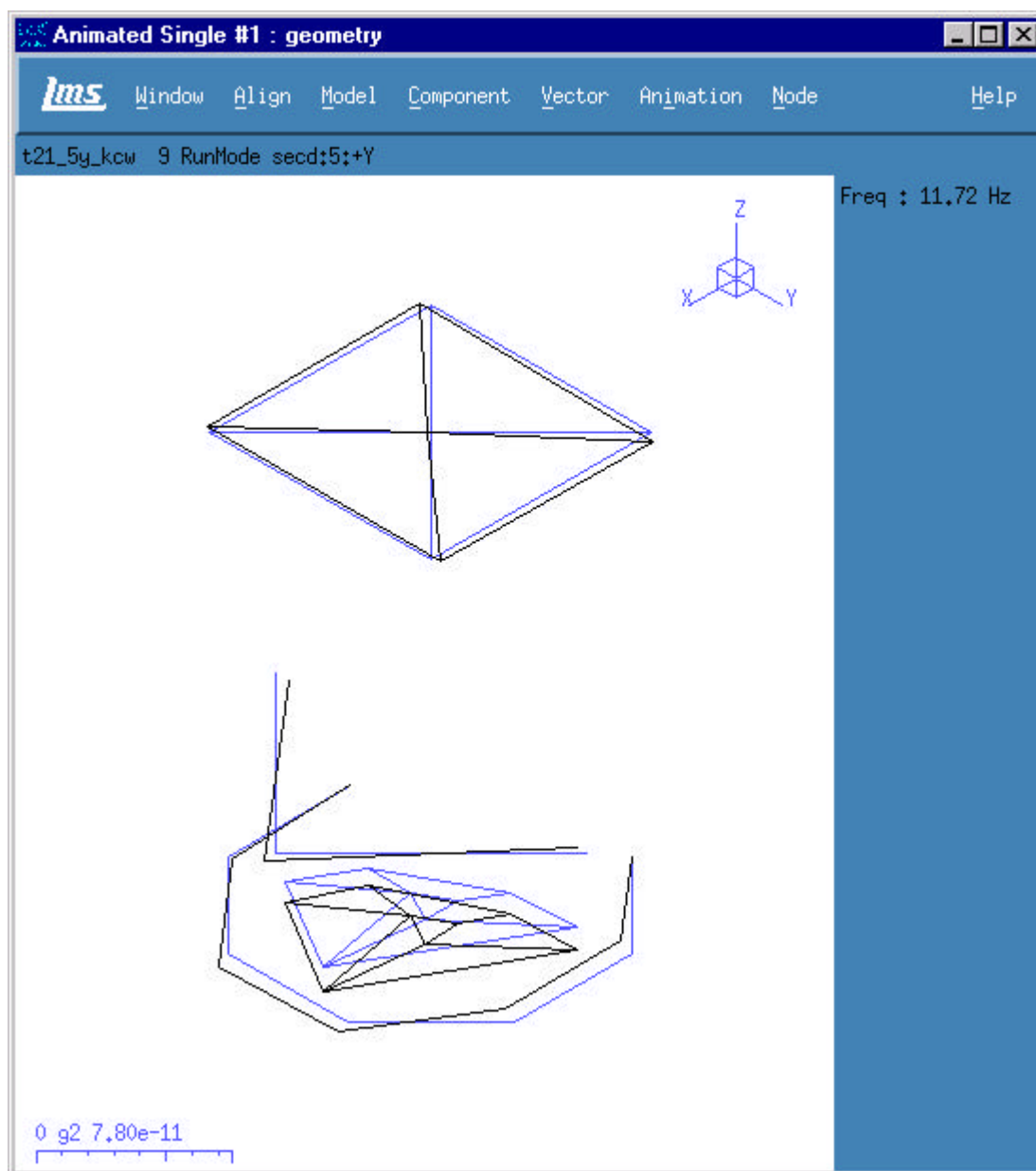


Test 21 – Operating Shape : 11.04Hz





## 10.0 Operating Mode Shape Plots – Test 21

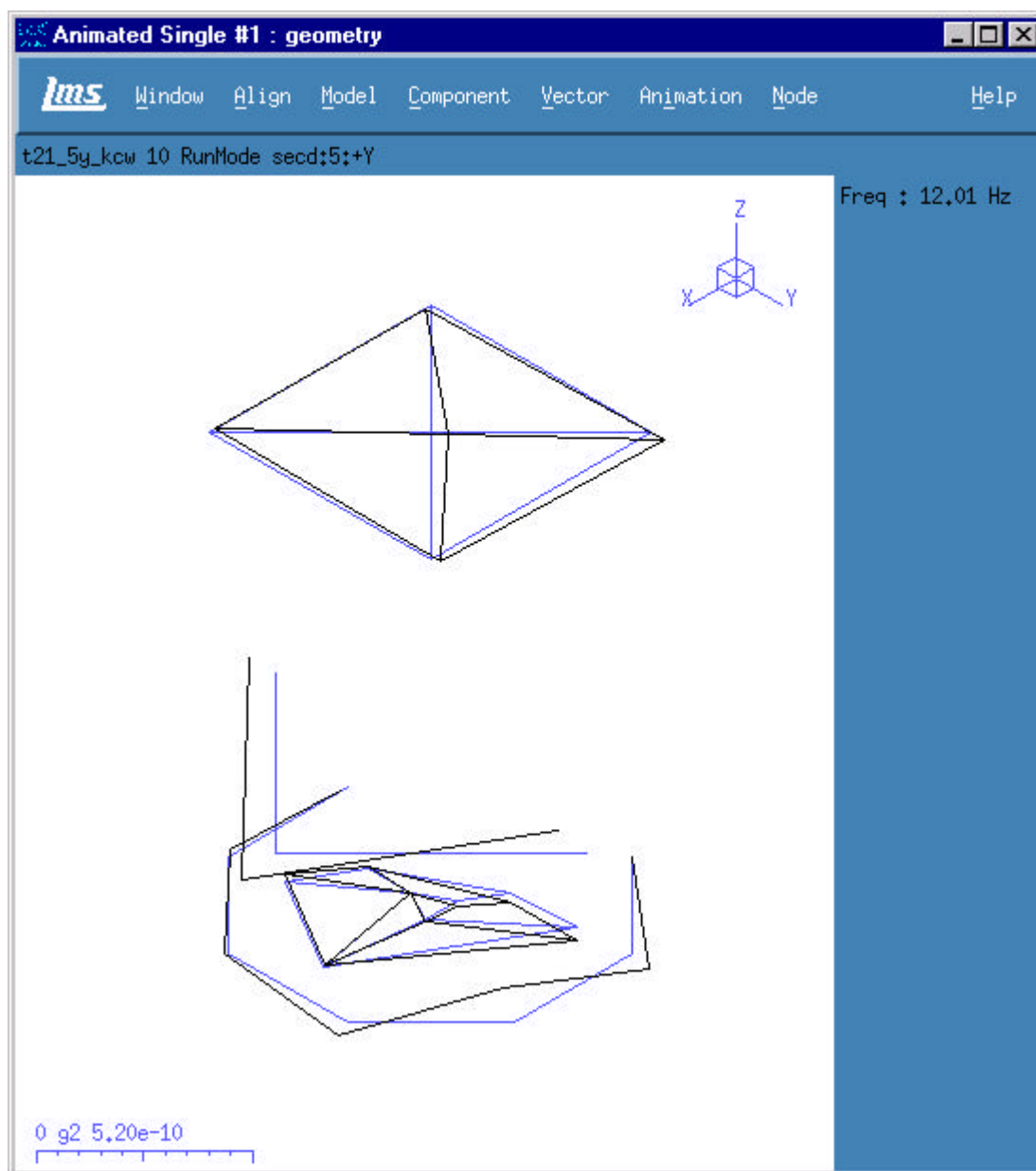


Test 21 – Operating Shape : 11.72Hz





## 10.0 Operating Mode Shape Plots – Test 21

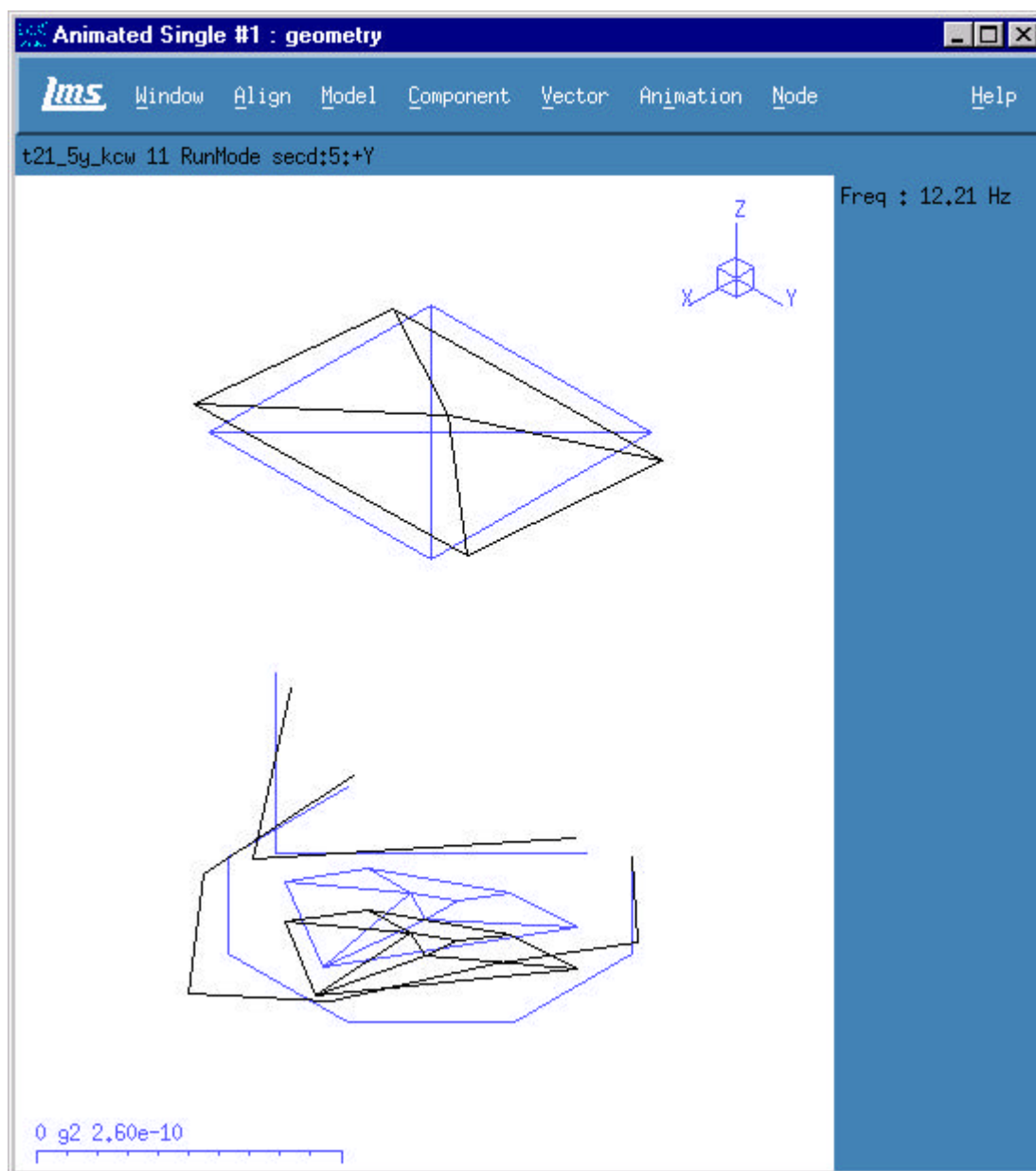


Test 21 – Operating Shape : 12.01Hz





## 10.0 Operating Mode Shape Plots – Test 21

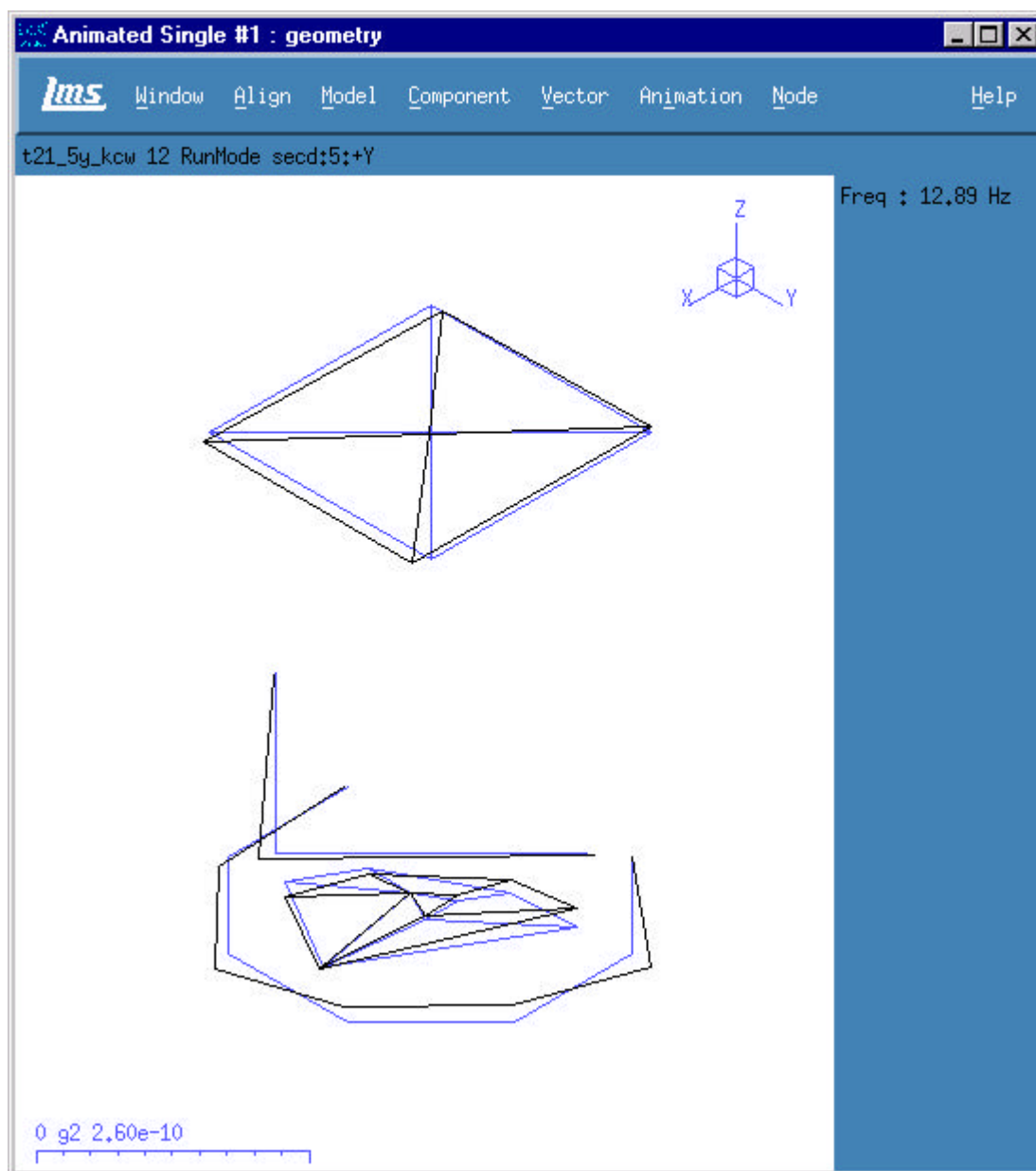


Test 21 – Operating Shape : 12.21Hz





## 10.0 Operating Mode Shape Plots – Test 21

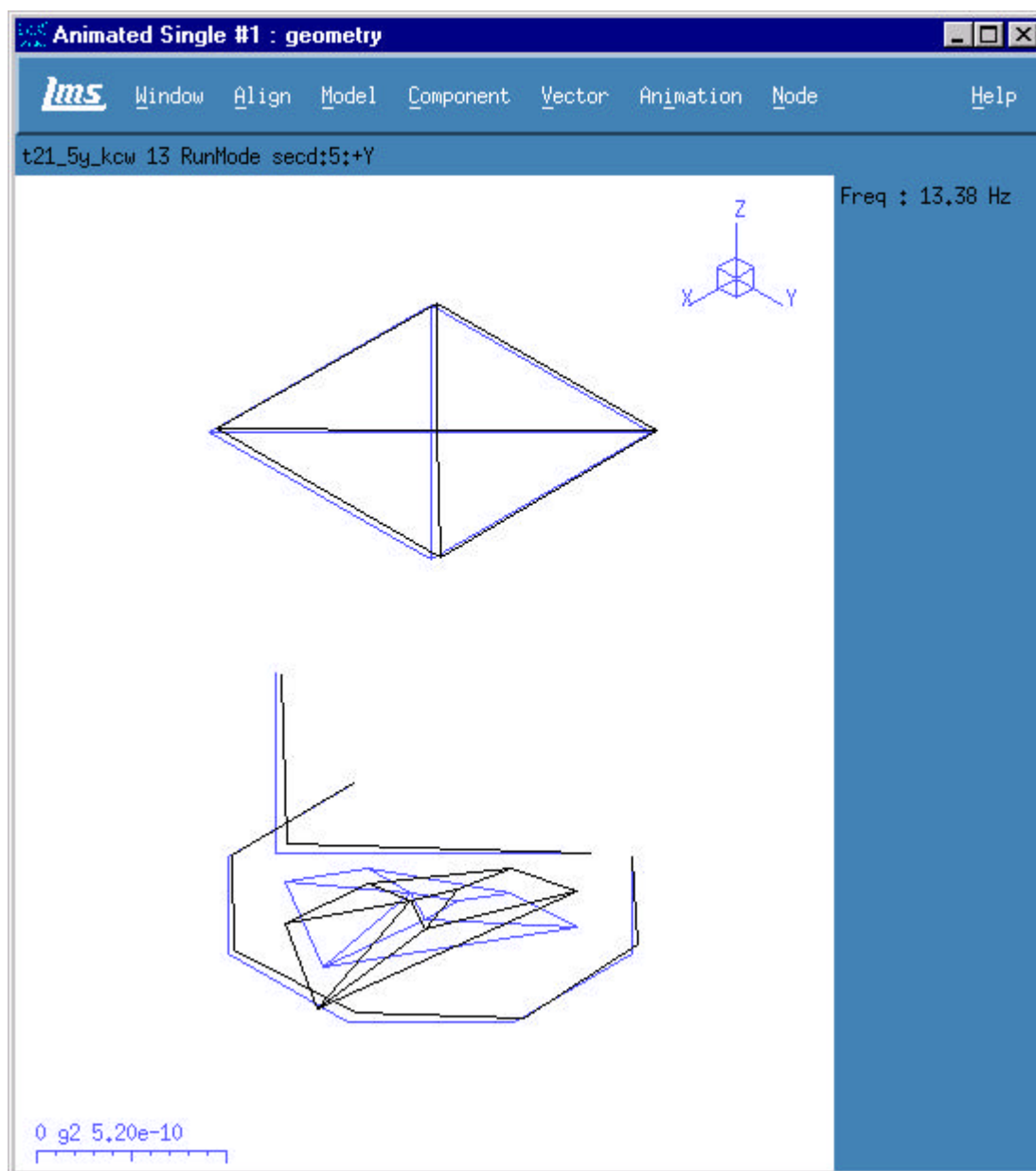


Test 21 – Operating Shape : 12.89Hz





## 10.0 Operating Mode Shape Plots – Test 21

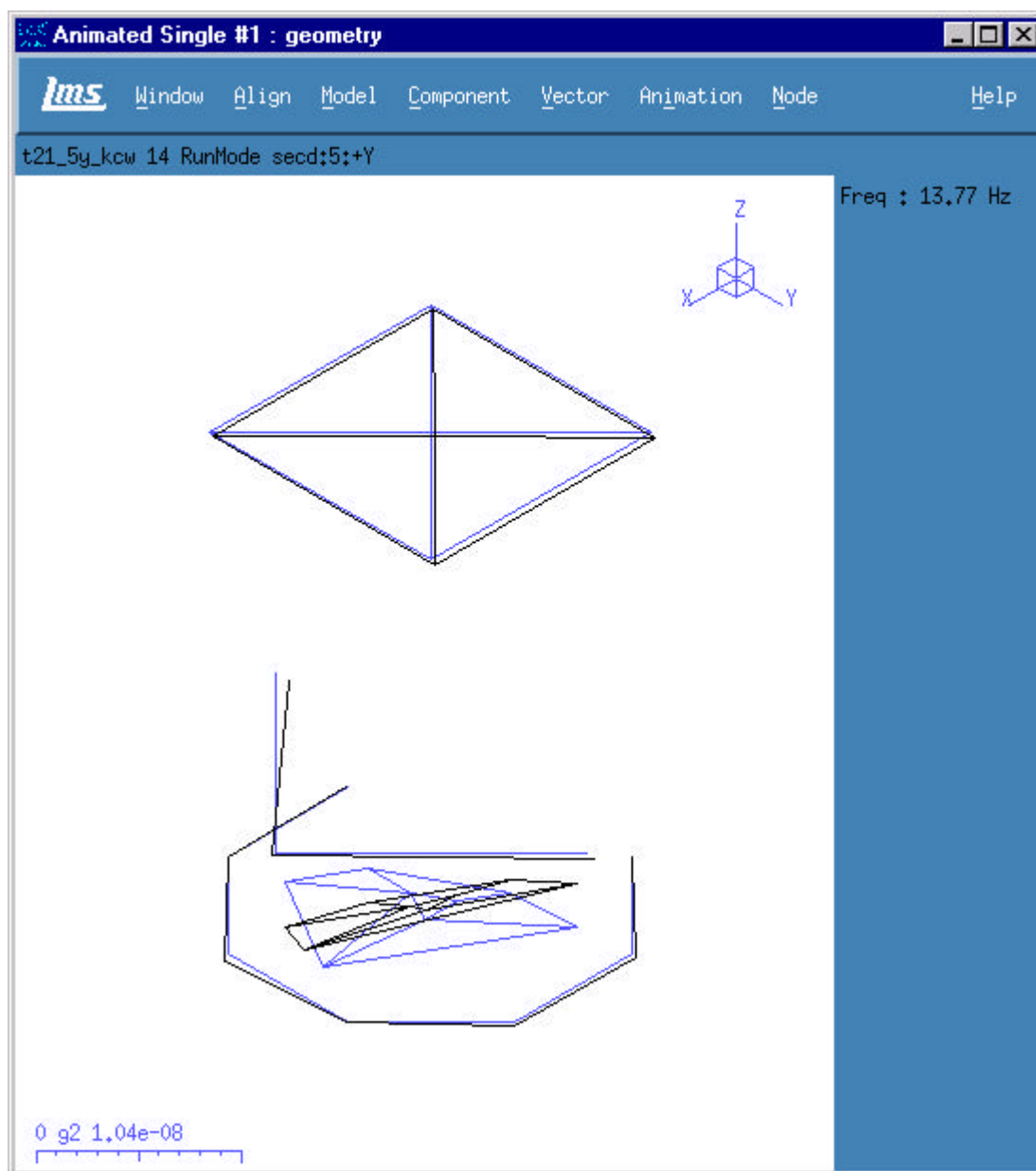


Test 21 – Operating Shape : 13.38Hz





## 10.0 Operating Mode Shape Plots – Test 21

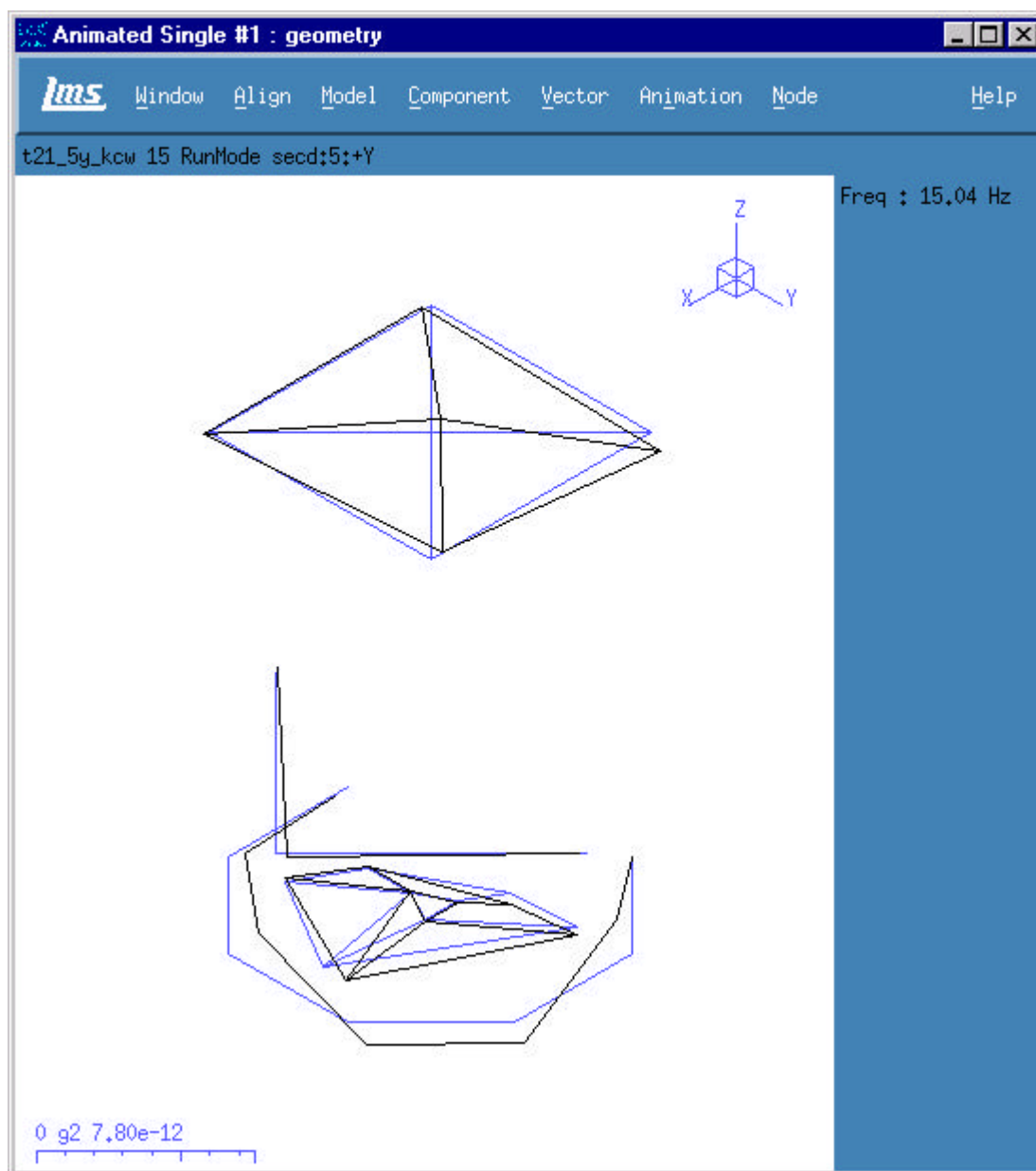


Test 21 – Operating Shape : 13.77Hz





## 10.0 Operating Mode Shape Plots – Test 21

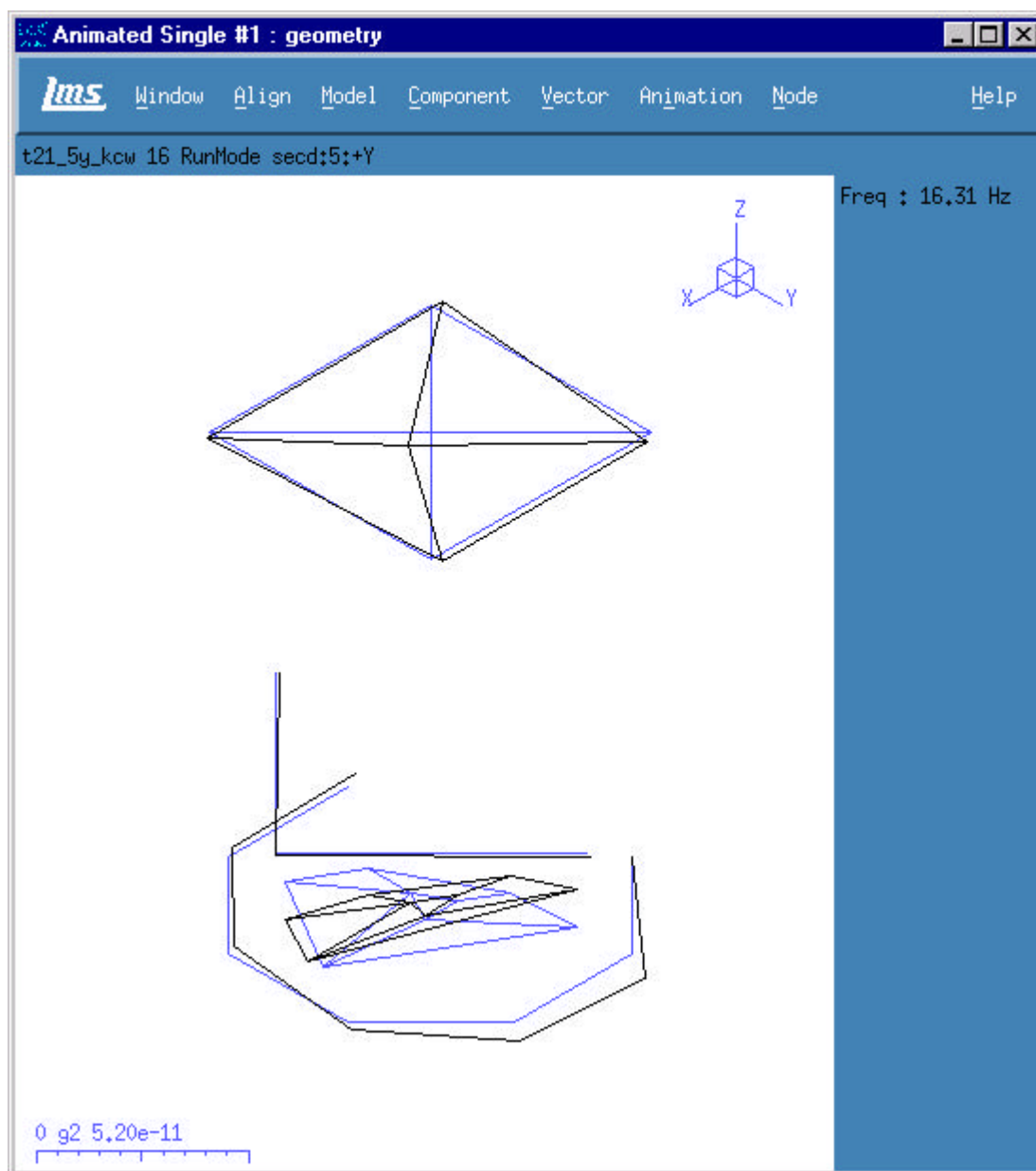


Test 21 – Operating Shape : 15.04Hz





## 10.0 Operating Mode Shape Plots – Test 21

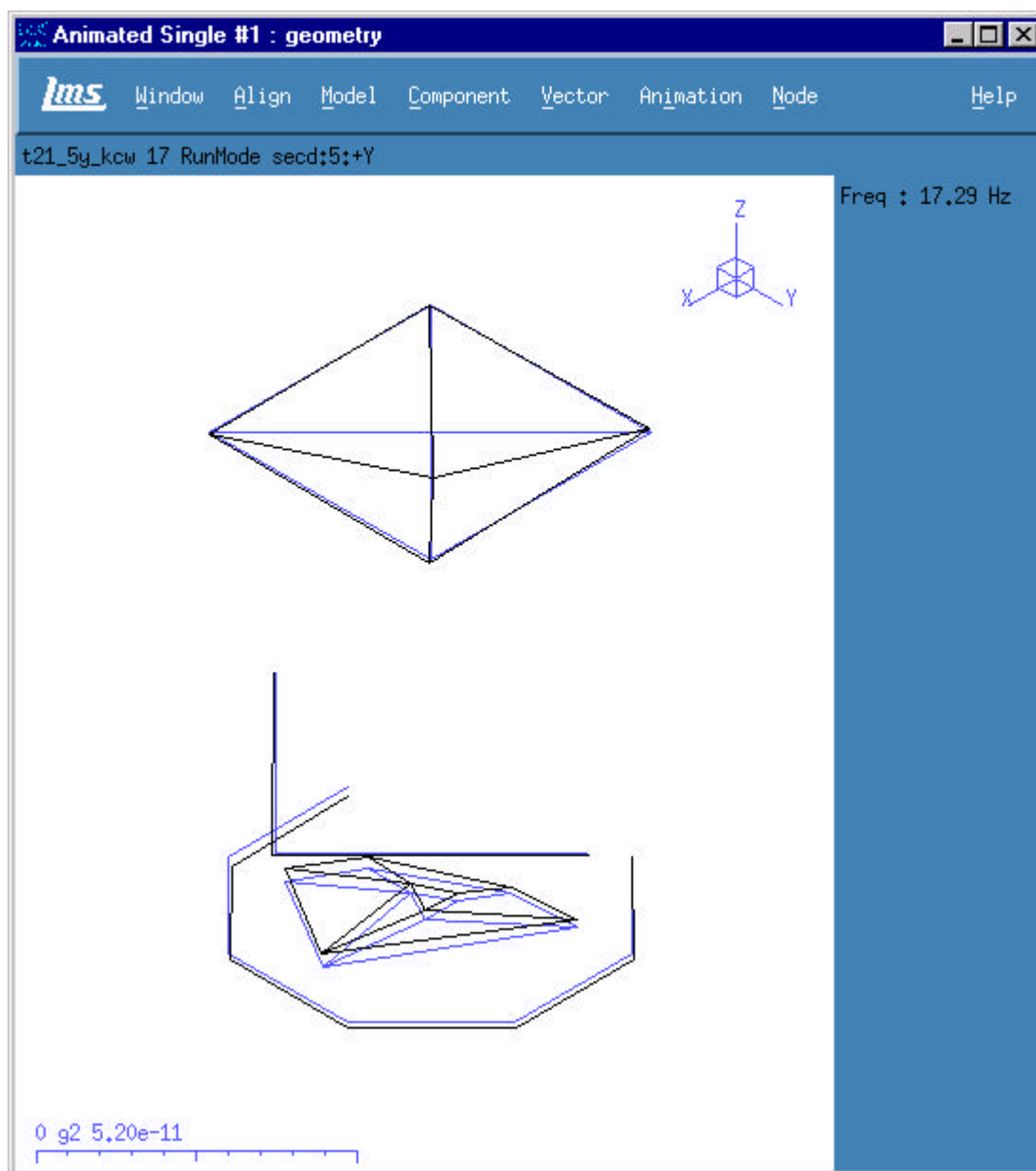


Test 21 – Operating Shape : 16.31Hz





## 10.0 Operating Mode Shape Plots – Test 21

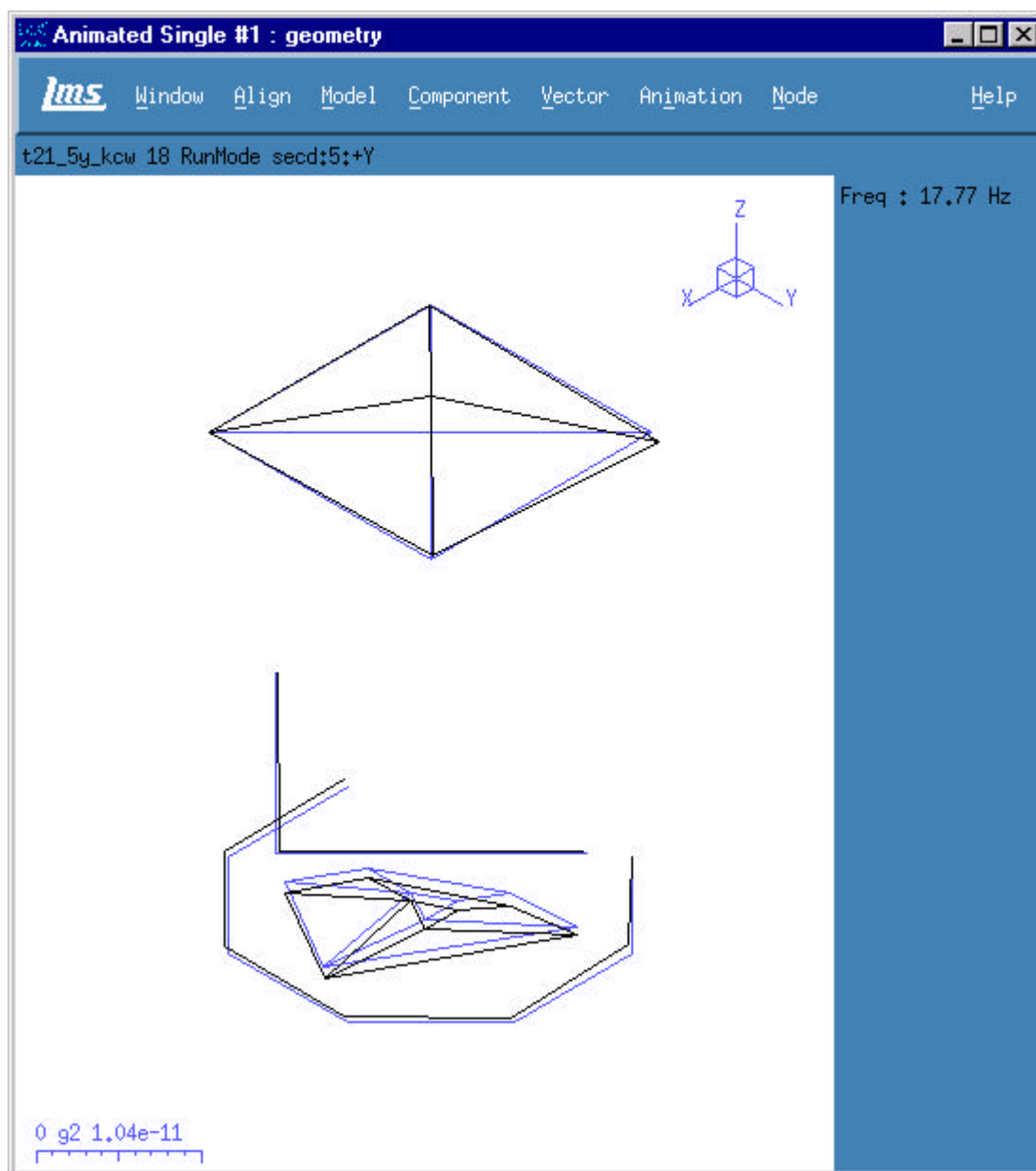


Test 21 – Operating Shape : 17.29Hz





## 10.0 Operating Mode Shape Plots – Test 21

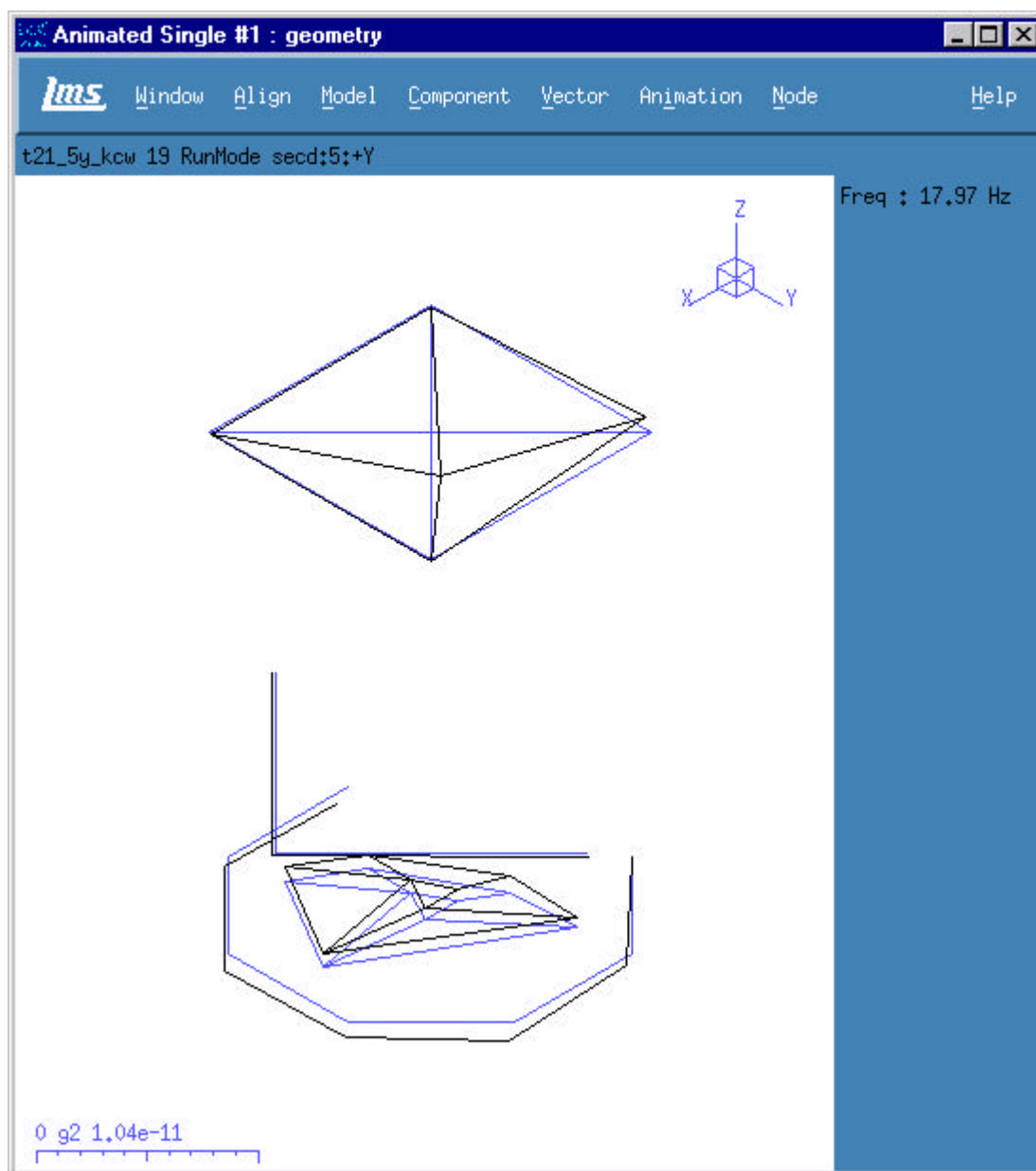


Test 21 – Operating Shape : 17.77Hz





## 10.0 Operating Mode Shape Plots – Test 21

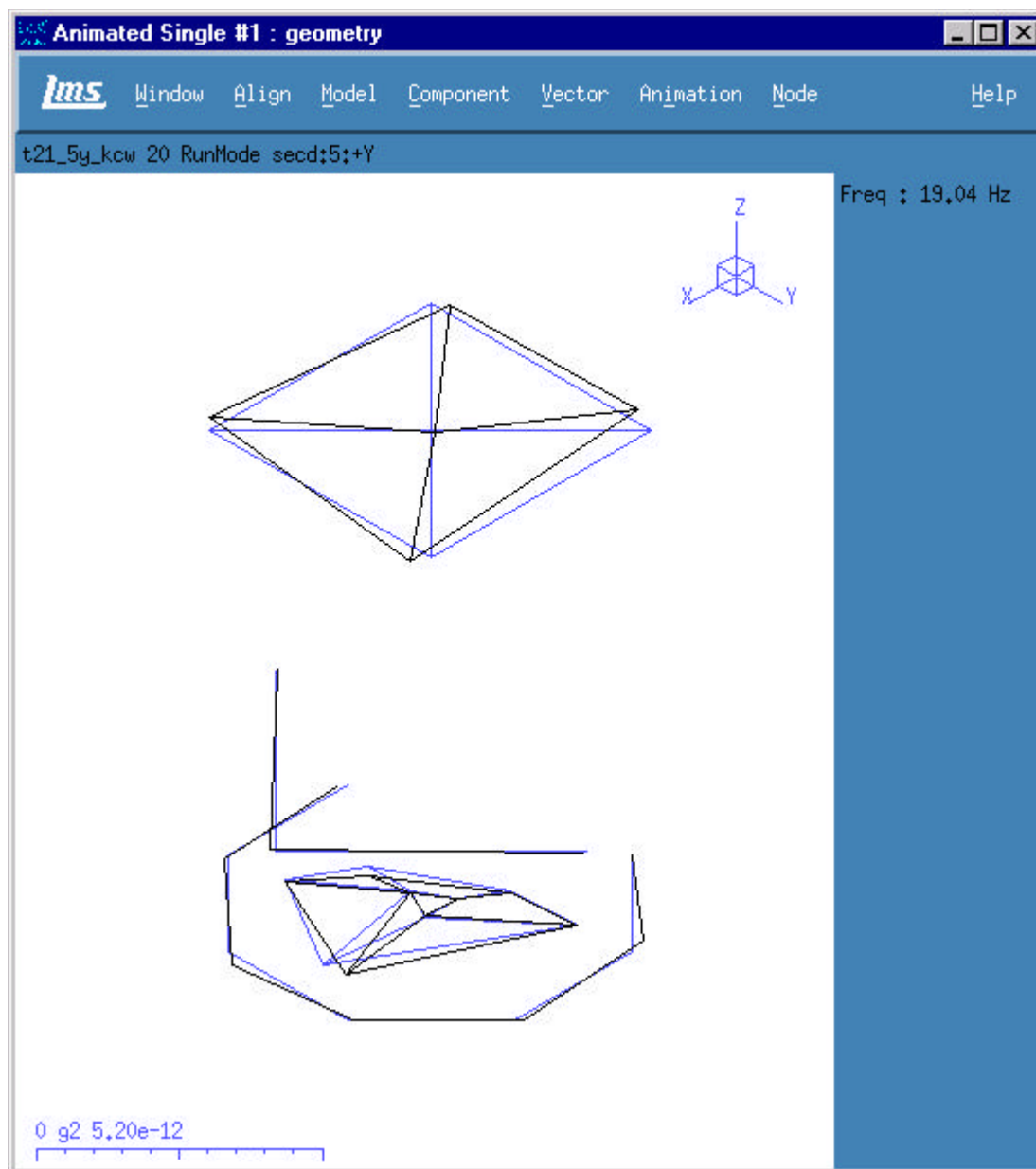


Test 21 – Operating Shape : 17.97Hz





## 10.0 Operating Mode Shape Plots – Test 21

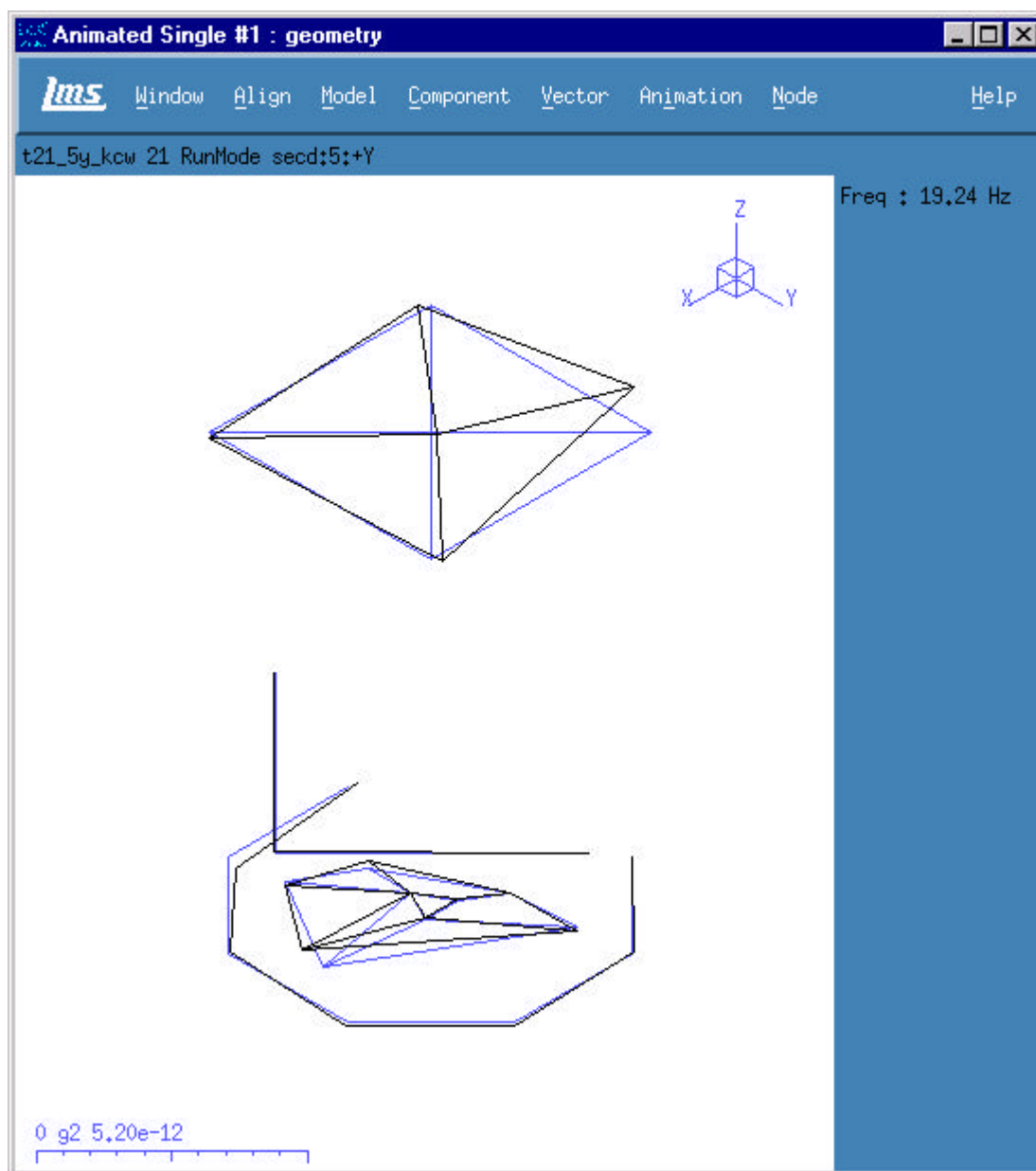


Test 21 – Operating Shape : 19.04Hz





## 10.0 Operating Mode Shape Plots – Test 21

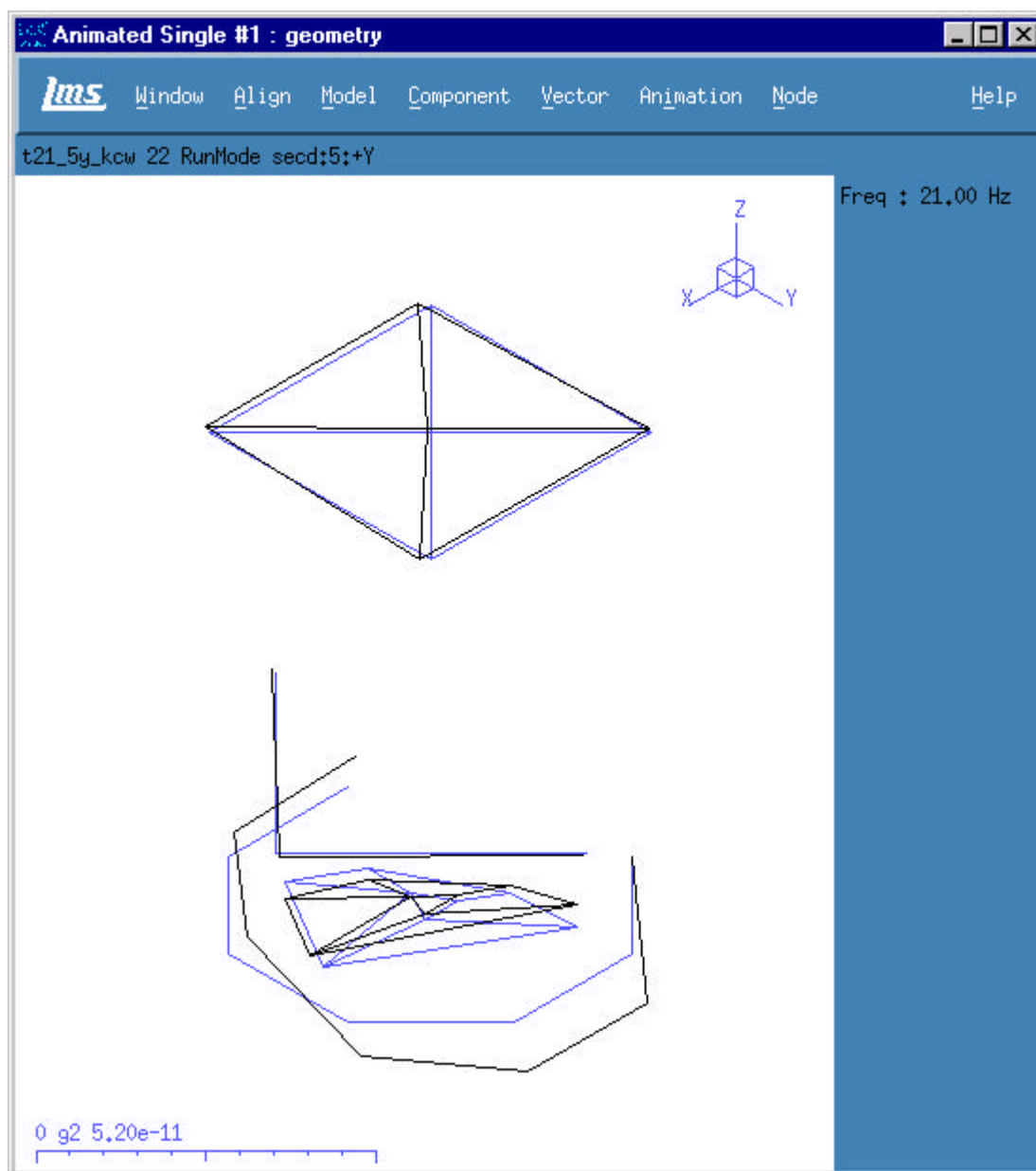


Test 21 – Operating Shape : 19.24Hz





## 10.0 Operating Mode Shape Plots – Test 21

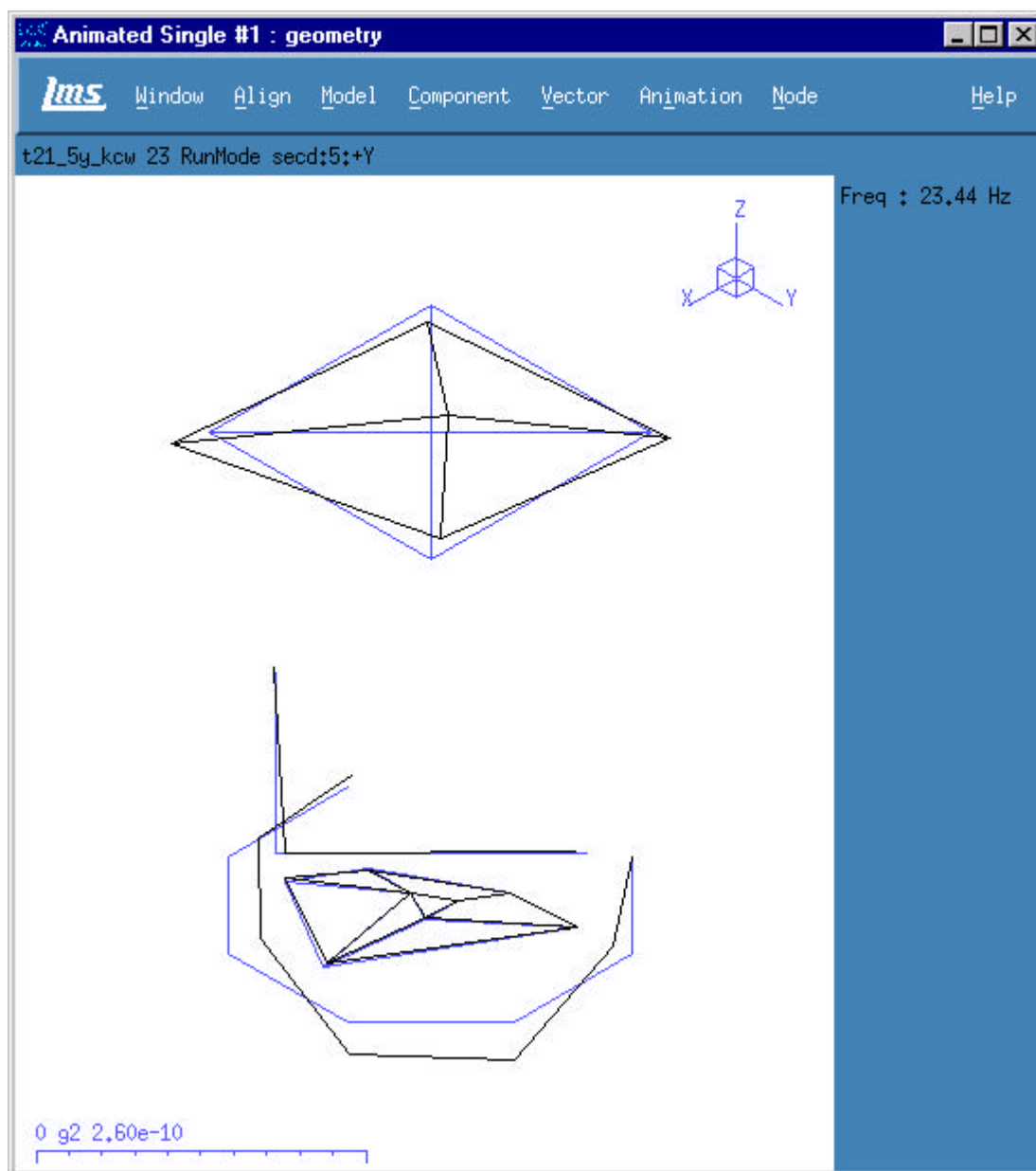


Test 21 – Operating Shape : 21.00Hz





## 10.0 Operating Mode Shape Plots – Test 21

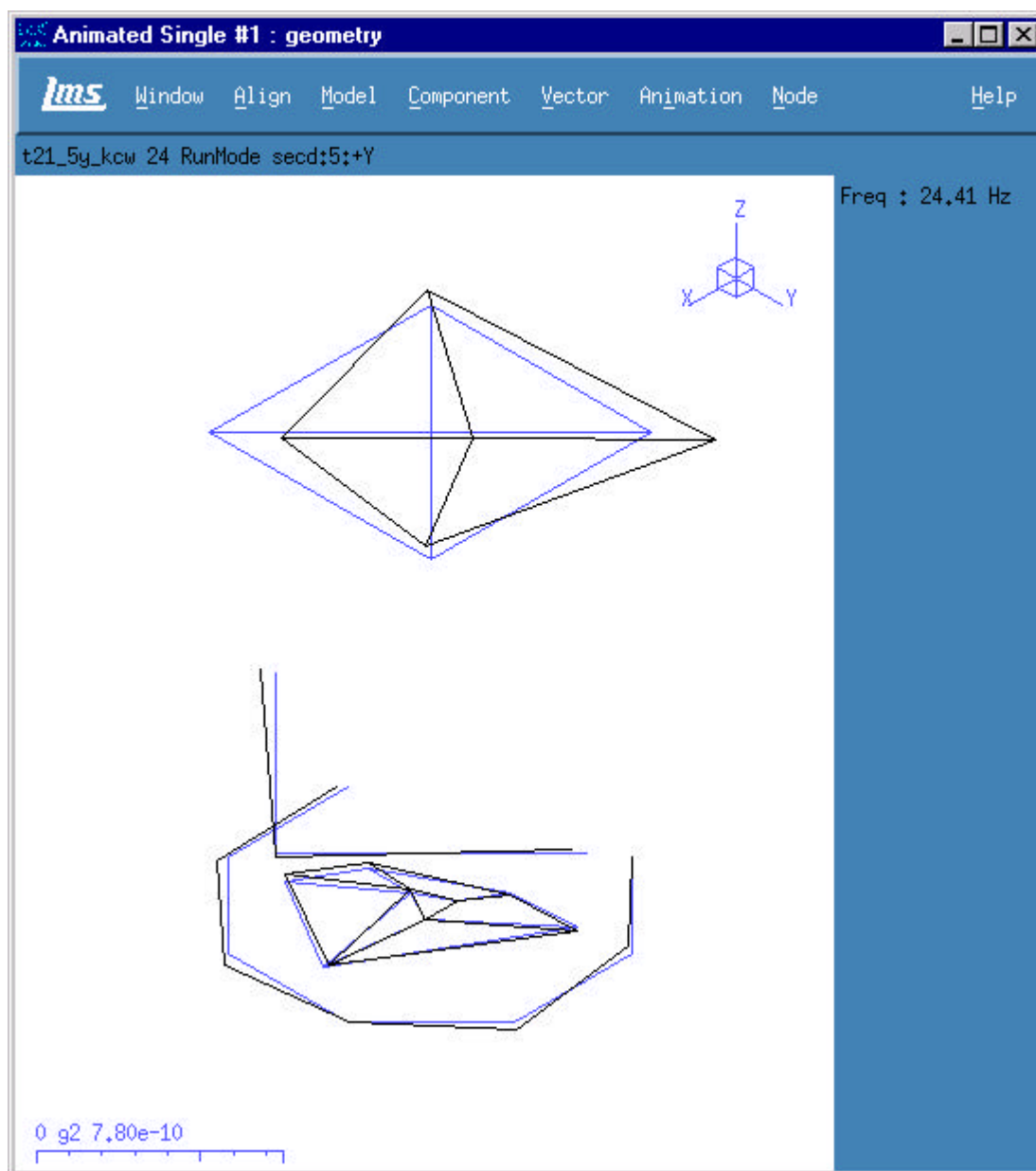


Test 21 – Operating Shape : 23.44Hz





## 10.0 Operating Mode Shape Plots – Test 21

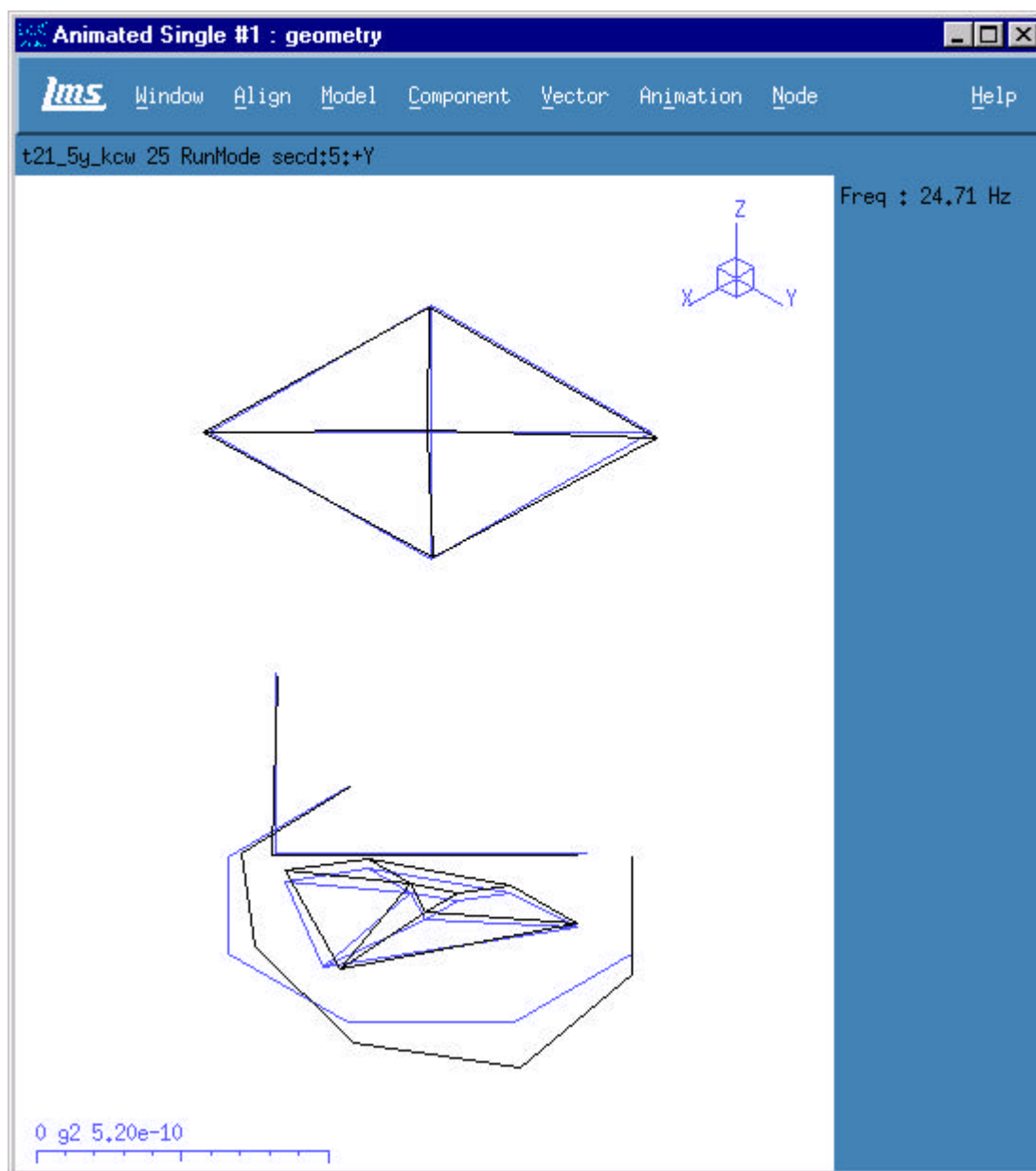


Test 21 – Operating Shape : 24.41Hz





## 10.0 Operating Mode Shape Plots – Test 21

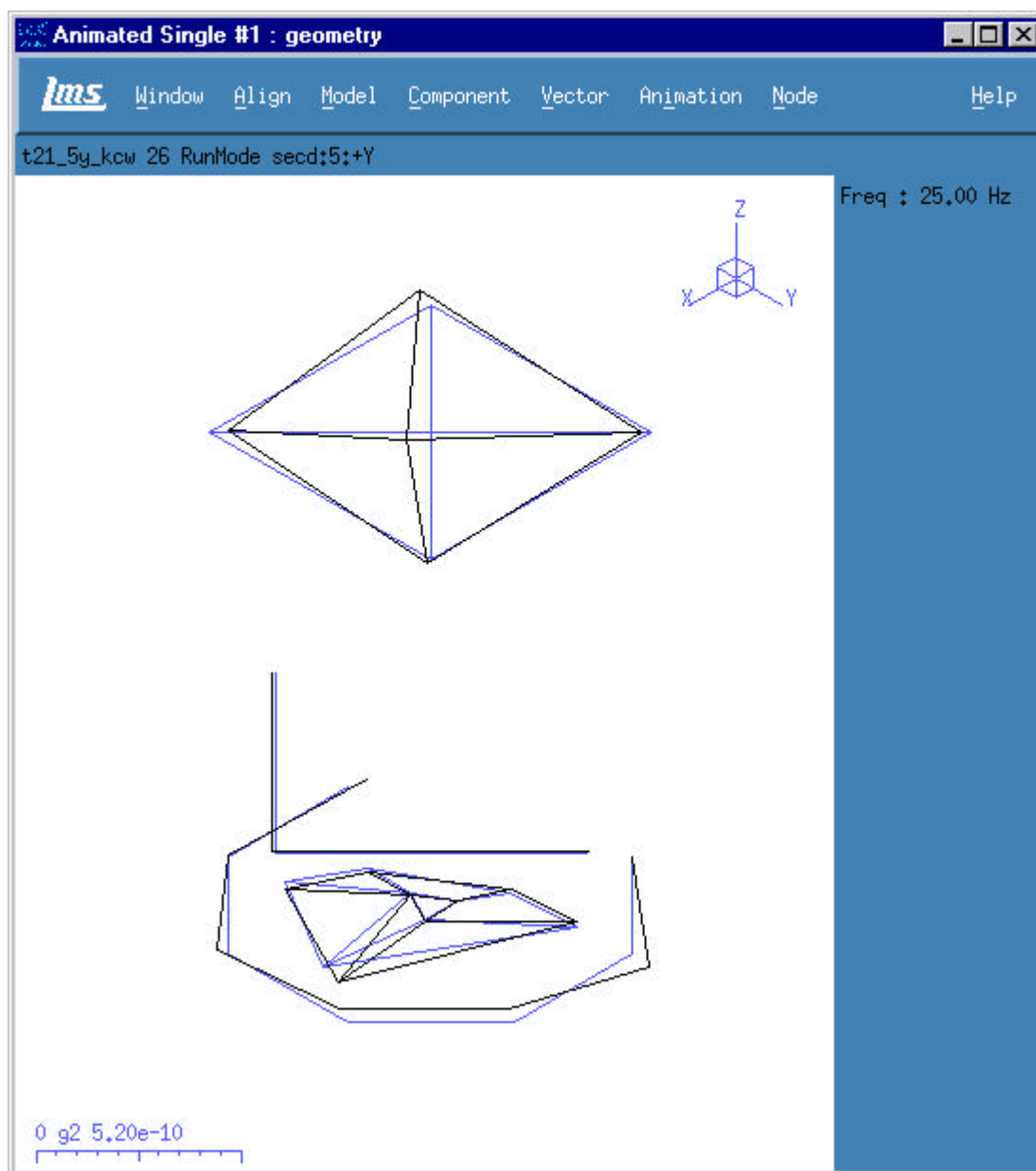


Test 21 – Operating Shape : 24.71Hz





## 10.0 Operating Mode Shape Plots – Test 21

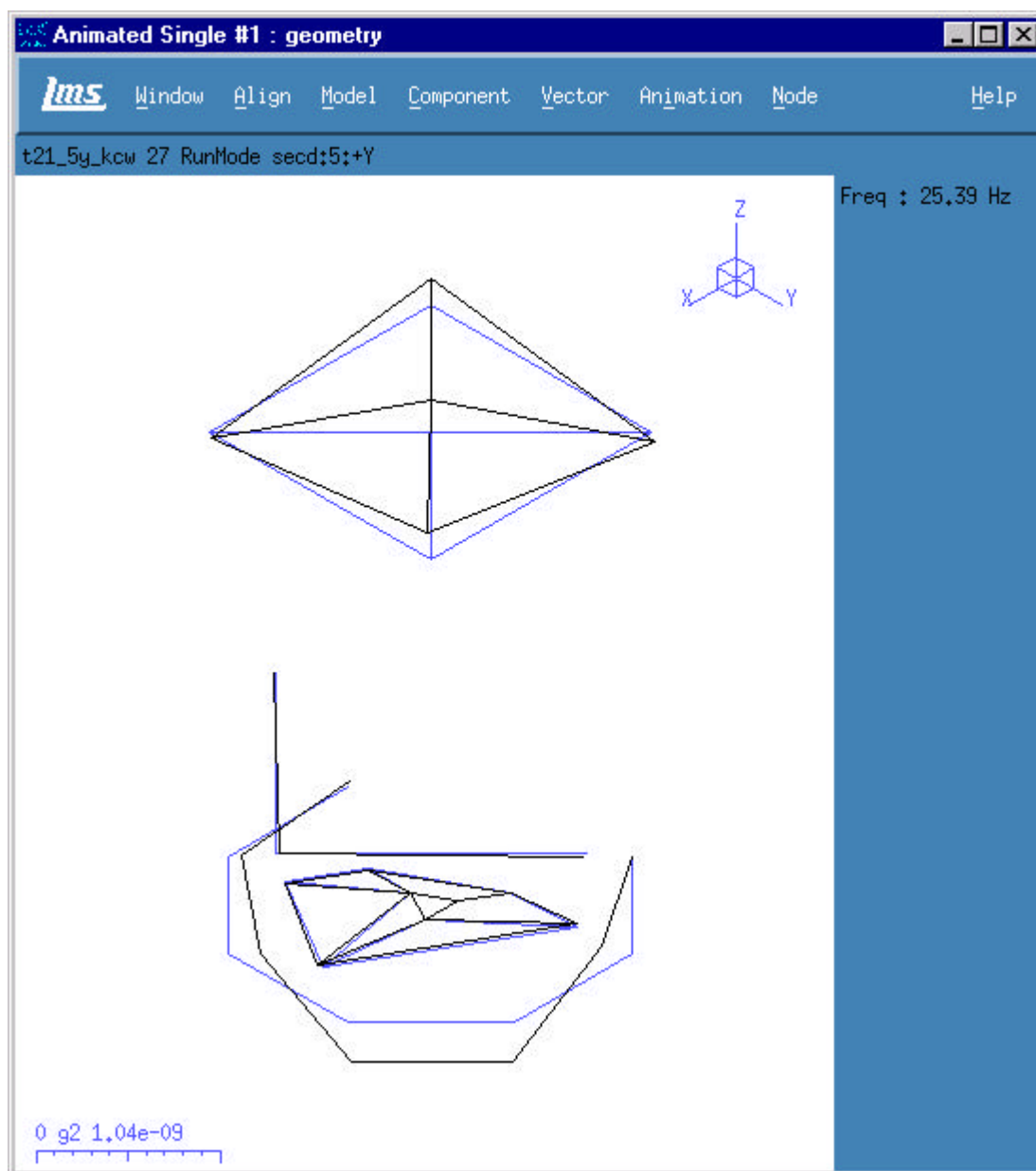


Test 21 – Operating Shape : 25.00Hz





## 10.0 Operating Mode Shape Plots – Test 21

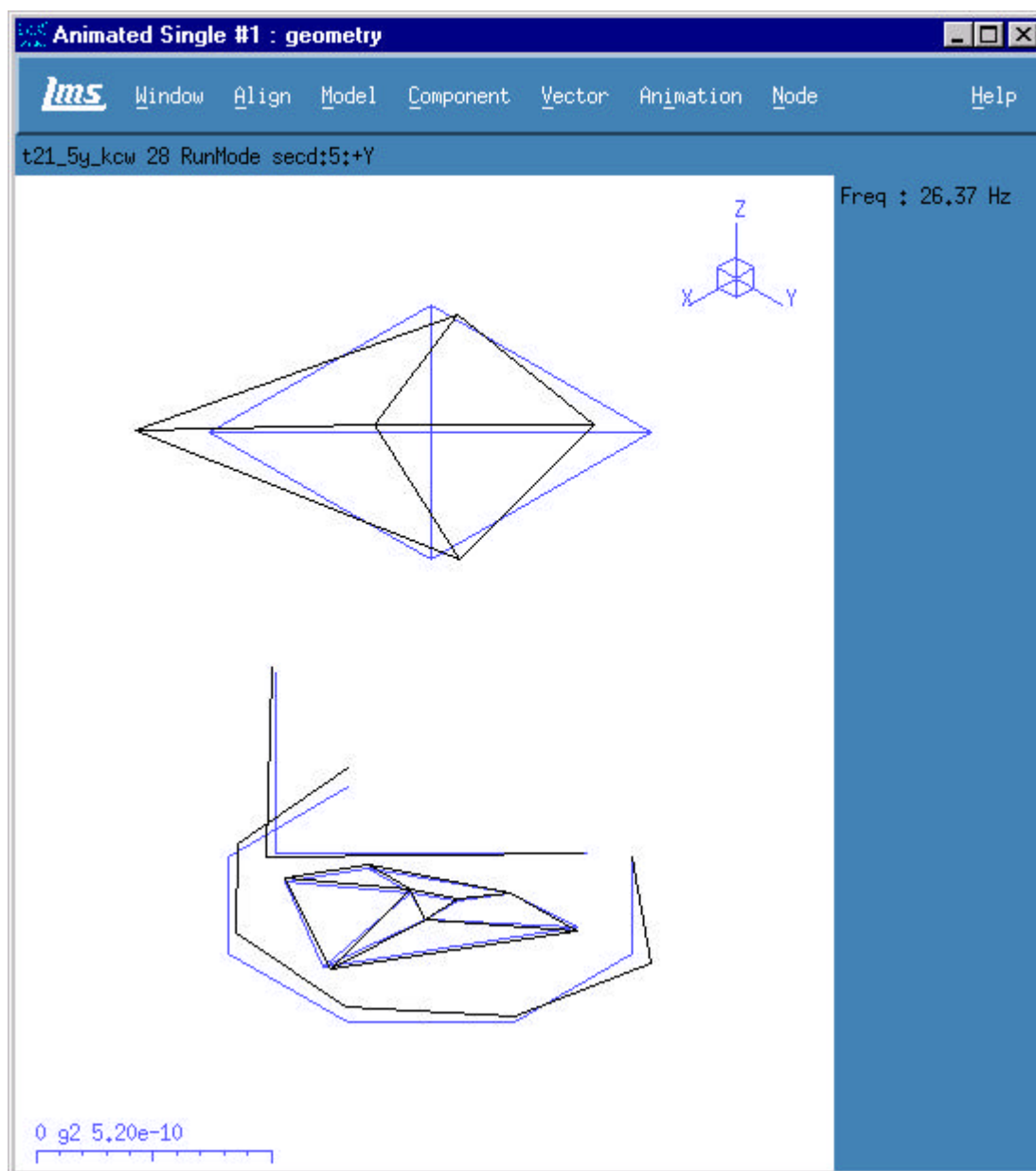


Test 21 – Operating Shape : 25.39Hz





## 10.0 Operating Mode Shape Plots – Test 21

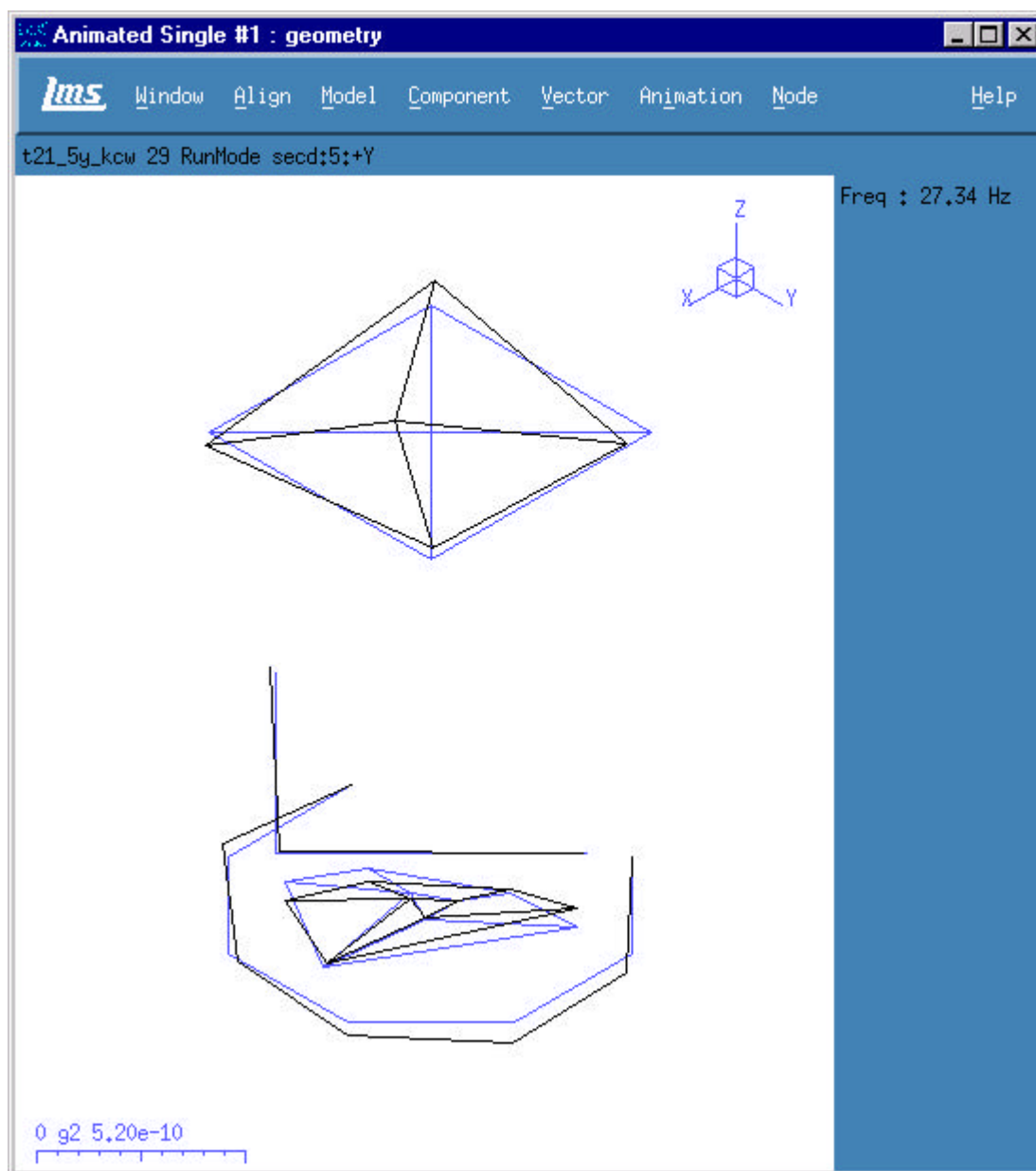


Test 21 – Operating Shape : 26.37Hz





## 10.0 Operating Mode Shape Plots – Test 21

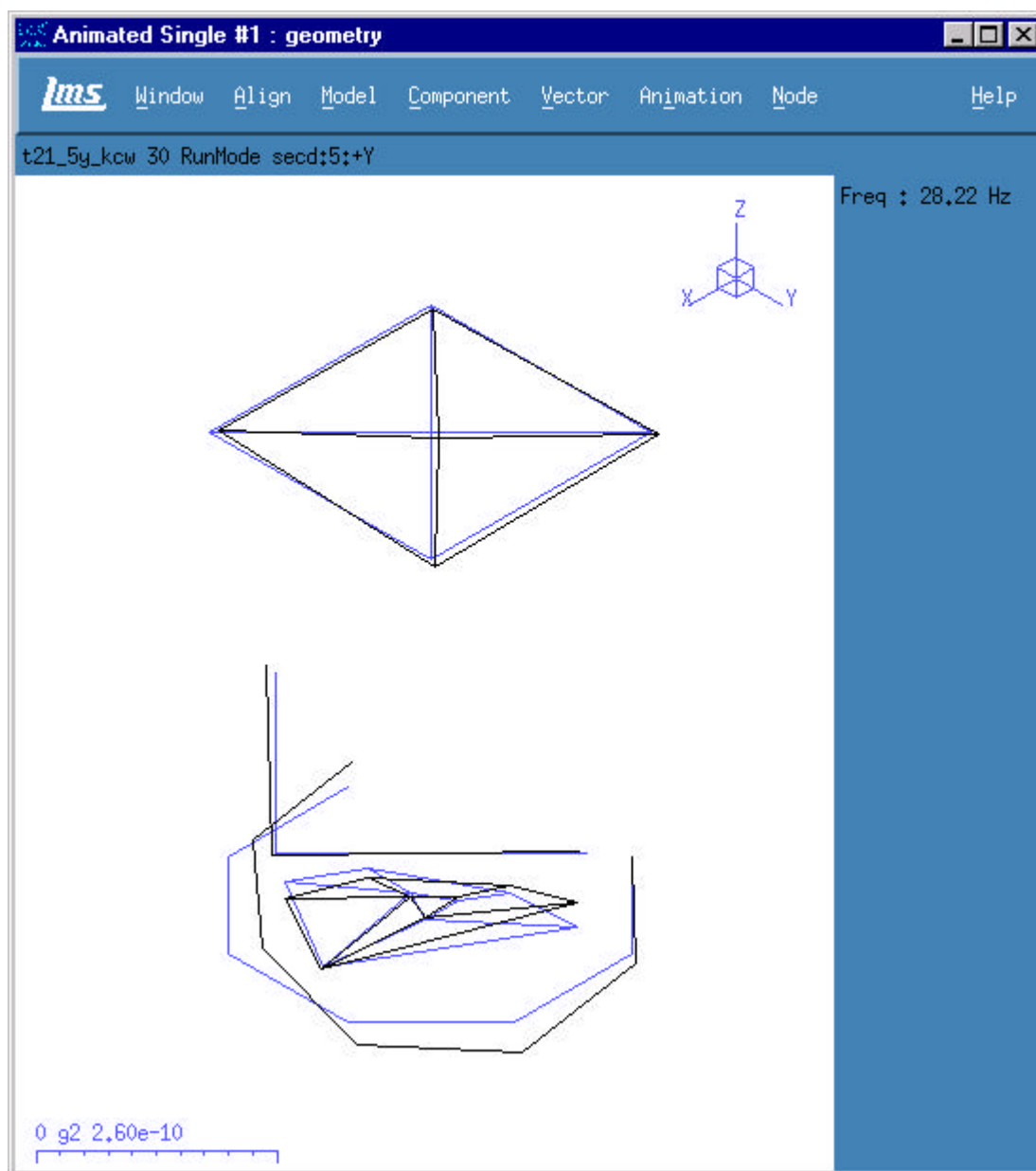


Test 21 – Operating Shape : 27.34Hz





## 10.0 Operating Mode Shape Plots – Test 21

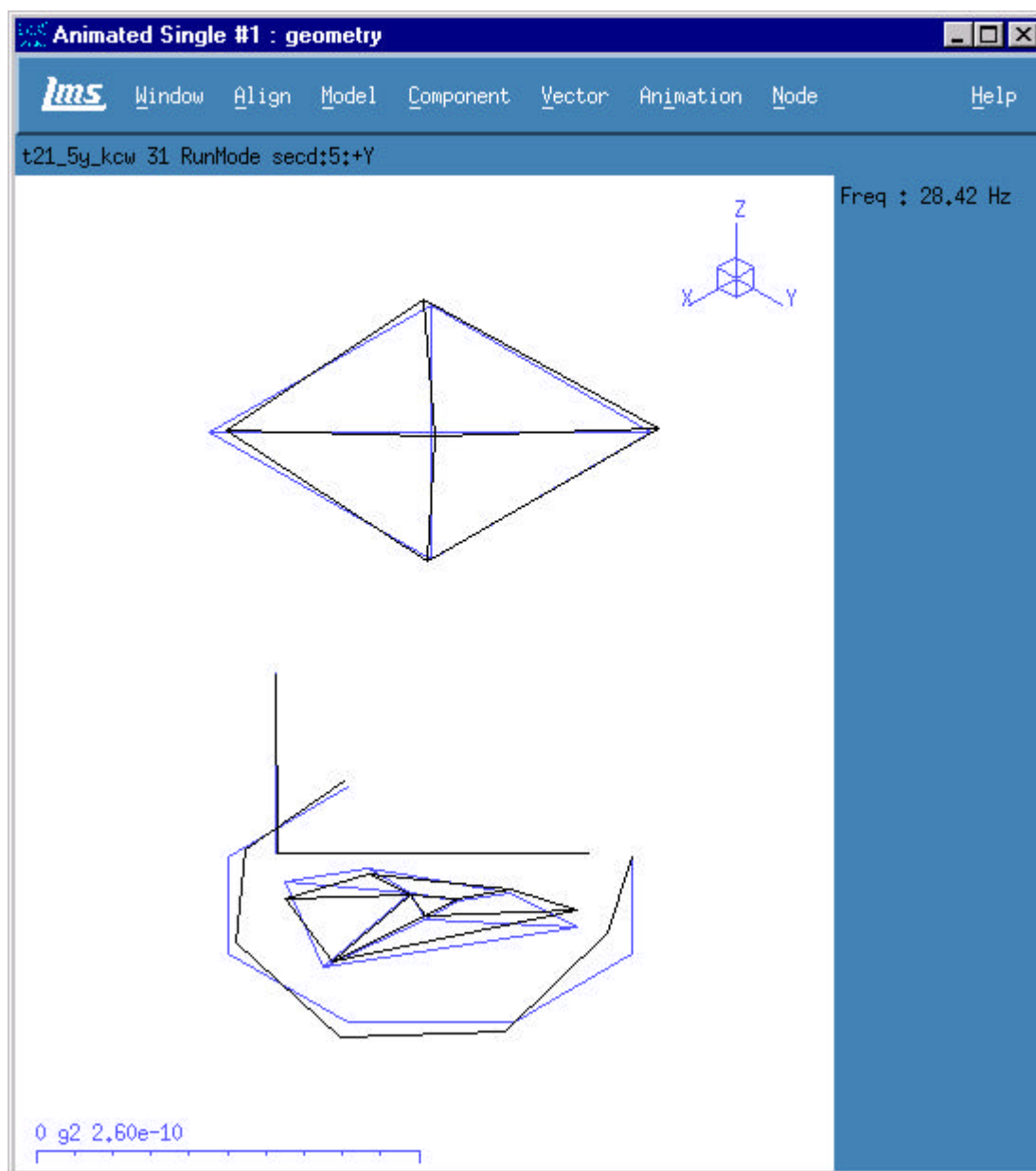


Test 21 – Operating Shape : 28.22Hz





## 10.0 Operating Mode Shape Plots – Test 21

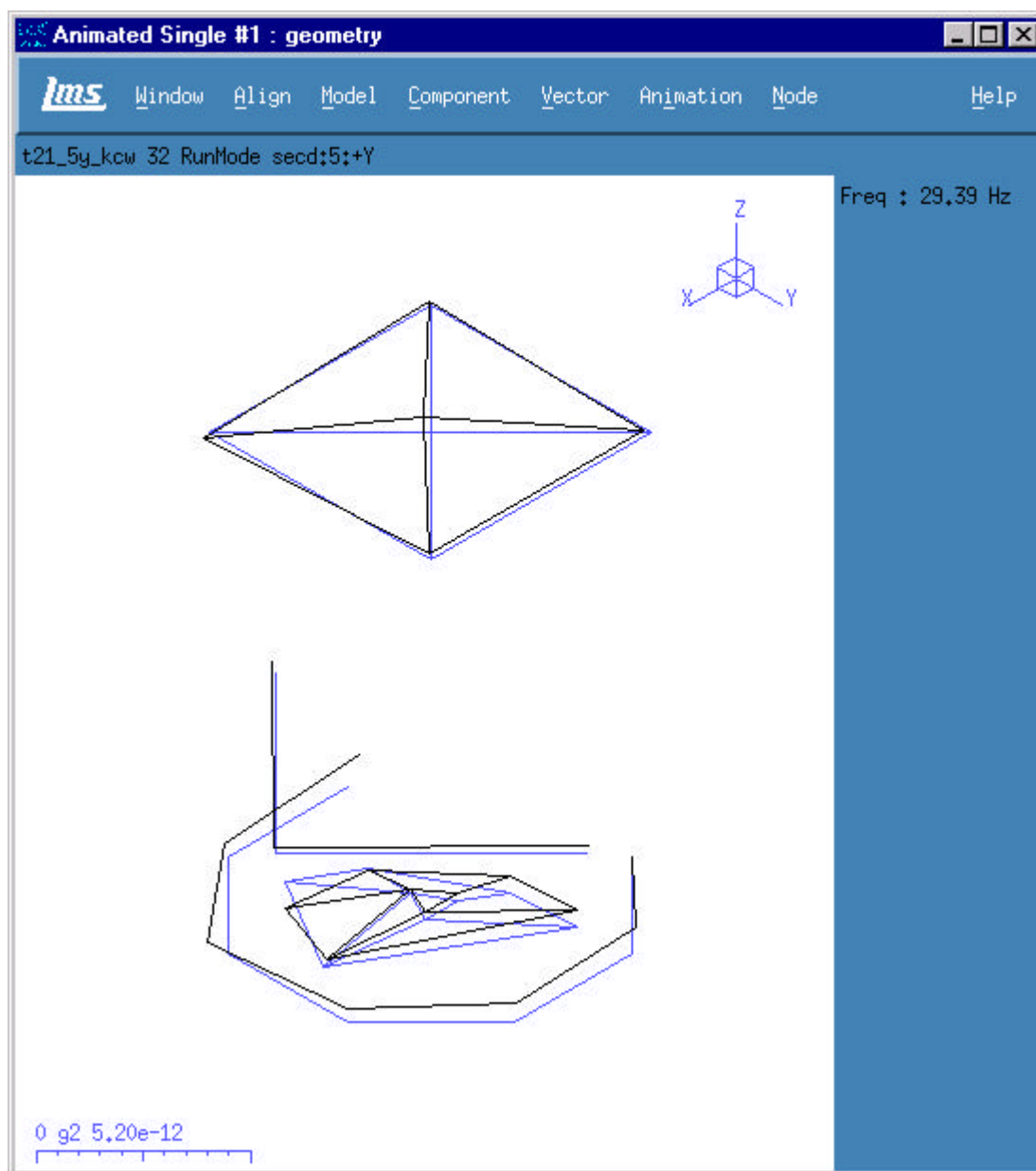


Test 21 – Operating Shape : 28.42Hz





## 10.0 Operating Mode Shape Plots – Test 21



Test 21 – Operating Shape : 29.39Hz







Modal Analysis and Controls Laboratory  
Mechanical Engineering Department  
University of Massachusetts at Lowell  
Lowell, Massachusetts

## **Gemini South 8m Optical Telescope**

### **Correlation Report**

**MACL Report # 05-08570-006**

October 2000

Approved By: \_\_\_\_\_

Date: \_\_\_\_\_





## **Intent of Report**

This report addresses aspects of the correlation analysis performed between the modal and operating results for the Gemini South 8m Optical Telescope in Cerro Pachon, Chile.



The experimental mode shapes are identified in the Modal Test Report [4]. The operating shapes are identified in the Operating Test Report [5].





## Table of Contents

- 1.0 Description of Analysis
  - 1.1 Correlation Requirement
  - 1.2 Test Identification Table
  - 1.3 Correlation Development
- 2.0 Summary of Correlation Analysis Results
- 3.0 Tables of MAC Values
- 4.0 References





## 1.0 Description of Analysis

The following sections detail the analysis data sets used for the correlation studies.

### 1.1 Correlation Requirement

Correlation analysis was performed between extracted modal parameters [4] and the operating test results [5] from the Gemini South 8m Optical Telescope tests.

### 1.2 Test Identification Table

The Table 2.1 below identifies the operating tests used for correlation to the experimental mode shapes.

Table 2.1 Operating Data used for Correlation

Test 03	Test 20	Test 37	Test 47
Test 07	Test 21	Test 38	Test 48
Test 09	Test 22	Test 39	Test 49
Test 11	Test 23	Test 40	Test 50
Test 12	Test 24	Test 41	Test 51
Test 13	Test 31	Test 42	Test 52
Test 14	Test 33	Test 43	Test 53
Test 16	Test 34	Test 44	Test 54
Test 17	Test 35	Test 45	
Test 19	Test 36	Test 46	

### 1.3 Correlation Development

All correlation was performed using LMS Cada-X Modal Analysis software [11].

The modeshapes [4] were checked for correlation to the operating deflection shapes [5] from various operating tests using the Modal Assurance Criterion (MAC). The MAC is a dot product of two vectors to determine the degree of similarity between the vector sets. Results are shown in Section 3.0.





## **2.0 Summary of Correlation Results**

A correlation of the experimental mode shapes to the operating deflection shapes was performed using a MAC (Modal Assurance Criterion) validation within LMS CADA-X [11]. The specific correlation analyses performed and corresponding MAC tables are presented in Section 3.0. The results of the MAC are summarized in Table 2.1. In general, the MACs show reasonably good correlation of the operating modes with the experimental modal analysis modes obtained from impact testing with the qualifications stated below.

For all correlation analyses performed, there are significant items which will generally degrade the degree of correlation obtained between the operating modes and the experimental mode shapes from impact testing. The three major items which effect these results are:

- A - The geometric configuration of the telescope for operating tests was different than that used for the experimental modal impact test
- B - The input excitation (wind) was not constant throughout the duration of the test and may not have produced a generally stationary excitation source for the tests
- C - The background noise during the tests contaminates the operating results obtained and is more significant with lower wind excitation tests

Several aspects of the extracted operating modes are discussed in the next sections relative to the three items mention above.





The operating modes were extracted using the frequency domain approach. As such, the time data collected was transformed to the frequency domain using the FFT algorithm to estimate frequency spectra. These spectra were then used to perform averaging and compute the necessary auto- and cross-spectra relative to the selected references on the telescope. The discussion of the generation of this data is contained in [5].

The estimation of operating mode shapes is heavily dependent on the accurate estimation of these spectra and that the operating excitation is constant and stationary during the entire range of tests performed. If this is not true then there will be differences in the computed response and operating modes of the system. This is anticipated (and expected) to be the case during testing performed on the telescope. The wind excitation was not constant during all testing performed. The vent gates were arranged into a variety of different configurations along with different telescope configurations. The vent gate positions had a direct effect on the wind conditions experienced by the telescope. But this is not the only source of difference.

The telescope was re-configured into many different geometric positions related to its pointing operations and relative to the angle of attack of the wind. The different geometric configurations will potentially produce slight variations of the modes of the telescope when compared to the parked, vertical upright configuration (which was the only configuration evaluated for the experimental modal tests). This implies that the MAC calculations will have some variation due to these geometric differences. While not evaluated or assessed as part of this study, the existing finite element model can be used to study the range of variation that can be expected when the telescope configuration is changed to determine the significance on the MAC values obtained.

The angle of attack has a significant effect on the resulting deformations of the telescope. This is due to the fact that the modes of the telescope are affected by the direction of the excitation force. This is strongly controlled by the modal participation factor (MPF) for each of the modes of the telescope. Certain modes of the telescope will be excited more





than other modes depending on the orientation of the telescope and its relationship to the angle of attack of the wind. The ratio of the MPFs do not remain constant as the telescope configuration changes along with changes in the wind direction. Thus, the modes respond differently for every configuration as well as due to the strength of the wind during each test. Since operating modal analysis does not attempt to measure this excitation force, there is no convenient mechanism to normalize these effects. (Note that during impact modal testing, the force is measured as part of the test and the frequency response spectra used for mode shape evaluation are normalized with respect to the excitation forces. In addition, coherence functions are also available for quality assessment of the estimated frequency response functions. This is not possible for operating modal testing approaches. It is also important to recall that the operating modes are the response measured due to the linear combination of all the modes that are excited by the excitation forces. The MPFs are a direct measure of the contribution of each mode to the particular operating mode at a particular frequency.) The operating modes extracted are, therefore, heavily dependent on the directional loading and geometric effects of the actual configuration used for all testing performed.

The wind excitation varied considerably during the conduct of the test. Each individual test was performed with different ambient wind conditions. In addition, the wind varied during the acquisition of data for each individual test. Since plant construction operations continued during almost all testing performed, the background noise of these plant operations cause a contamination of the data collected in two regards. During testing with minimal wind excitations, the ratio of desired signal to background noise was much more significant when compared to tests with maximum wind excitation. Thus, the measured spectra will have effects that vary as a result of the particular test evaluated but there is no signal processing mechanism to determine the amount of distortion that results. There were also effects of plant operations that clearly have an effect on the data collected. Some segments of data were so contaminated that use of the entire set of data was not possible. These obvious distortions of the data were not utilized in the evaluation





of the operating data. (The assessment of the data is discussed in [3].) However, all of the data sets have effects from these plant operations but it is not clear as to the magnitude of the distortion of the data that results from these effects. Thus, there are definite effects of this on the measured spectra. These have an effect of the extracted operating modes that is difficult to clearly identify.

Understanding the effects discussed above assists in the interpretation of the MAC values obtained for all the different configurations evaluated. From the MAC results obtained, several general trends can be observed from the data. (Of course, there are exceptions to these statements that are mainly attributed to the inability to clearly identify the effects of noise and MPFs for all the different cases and configurations studied.)

In general, the mode sets correlated best when the operating modes were obtained in a geometric configuration which is most similar to the configuration used for the experimental modal tests (vertical upright). The correlation tends to degrade gradually as the geometric configuration changes from the vertical upright configuration. The correlation also degrades gradually as the telescope pointing direction varies relative to the direction of the wind. Both of these trends are anticipated based on the discussion above.

Reviewing the summarized results in Table 2.1 and the MAC results in Section 3.0, the operating mode shapes appear to show reasonably good correlation to the experimental modal impact test results. In general, the modal frequencies that had the best correlation to the operating shapes were 1.86Hz, 7.08Hz and 7.74Hz. These are major primary modes of the telescope and are more easily excited than other modes of the structure. These modes are seen to correlate well to most of the different operating tests. In addition, the operating deflection shapes from Test 7 and Test 21 appear to have the best overall correlation to the experimental modal impact modes.

Test 7 configuration had the telescope pointed directly into the wind, 30 degrees from zenith, with the vent gates wide open. This is the closest geometric configuration to the





experimental modal impact tests performed and allows the maximum excitation of the modes of the telescope. This operating configuration is expected to produce optimum results from the acquired operating test data. Many of the operating modes of the telescope are very well correlated to the experimental modal impact modes for this condition.

Test 21 is the same geometric configuration as Test 7 except that the vent gates are closed. This particular test was of specific interest to the design engineers since a wind screen was included on the telescope dome; the wind screen was not used for any other test configurations evaluated during testing at Cerro Pachon. Since this was a critical test for design purposes, all plant operations were halted for the conduct of this test. This afforded maximum signal to noise ratio that is not available for any other operating test performed. Therefore, the operating modes from this particular test are considered to be of much better quality than those of other operating tests (even though the vents are closed providing maximum shelter to the telescope). Many of the operating modes of the telescope are very well correlated to the experimental modal impact modes for this condition.

Additional correlation studies, need to be performed with the use of the finite element model to confirm geometric issues discussed above. The finite element model can also be validated using the experimental modal impact results so that the model can be used with greater confidence for comparison to the different geometric configurations of the telescope operating mode shapes.





Table 2.1 Summary of Correlation

ID	Elevation	Zenith	AoA	Upwind Vent Gate	Downwind Vent Gate	correlated (>70%)	correlated (>80%)	correlated (>90%)
Test 03	60	30	0	Closed	Closed	5 to 6	3	1
Test 07	60	30	0	Open	Open	14 to 16	13 to 15	10 to 11
Test 09	60	30	45	Open	Closed	12 to 13	9	6
Test 11	30	60	45	Closed	Closed	6 to 7	6	4
Test 12	30	60	45	Open	Open	5 to 7	3	1
Test 13	30	60	0	Open	Closed	5 to 6	3	1
Test 14	30	60	0	Closed	Open	7	4	1
Test 16	30	60	90	Half	Half	5 to 6	3	1
Test 17	30	60	180	Open	Open	6	5	3
Test 19	45	45	90	Open	Closed	5	5	2
Test 20	45	45	0	Half	Open	6	4	2
Test 21	60	30	0	Closed	Closed	12 to 13	11	10
Test 22	60	30	0	Closed	Half	13	6	3
Test 23	60	30	90	Closed	Open	2	1	0
Test 24	60	30	180	Half	Closed	5 to 7	5 to 6	1
Test 31	60	30	0	Open	Open	11 to 15	10 to 14	8
Test 33	60	30	0	Closed	Open	16 to 18	13	8
Test 34	60	30	45	Closed	Closed	8 to 9	6	3
Test 35	60	30	45	Open	Open	10 to 11	8	5
Test 36	30	60	45	Open	Closed	8 to 11	6 to 7	3
Test 37	30	60	0	Closed	Open	6 to 9	6 to 7	3 to 4
Test 38	30	60	0	Closed	Closed	6 to 9	6 to 9	4
Test 39	30	60	0	Open	Open	4 to 6	5 to 6	3
Test 40	75	15	45	Closed	Closed	5 to 6	4	3
Test 41	75	15	90	Half	Half	8 to 11	8	5
Test 42	75	15	135	Open	Open	12 to 14	13	8
Test 43	45	45	135	Closed	Half	3	3	1
Test 44	45	45	90	Open	Closed	5 to 6	5	4
Test 45	45	45	90	Open	Half	10 to 13	8 to 11	5
Test 46	45	45	90	Open	Open	8 to 10	7 to 9	5 to 6
Test 47	45	45	45	Half	Open	10	8	4
Test 48	30	60	45	Open	Half	9 to 11	7 to 9	4
Test 49	30	60	90	Closed	Open	2 to 4	1	0
Test 50	30	60	135	Half	Closed	8 to 10	6 to 8	3
Test 51	30	60	45	Open	Open	8 to 11	6 to 9	5
Test 52	45	45	45	Open	Open	6	4	4
Test 53	60	30	45	Open	Open	12 to 15	9 to 11	8
Test 54	75	15	45	Open	Open	12 to 13	13	8





### 3.0 Tables of MAC Values

This section contains the correlation tables of the MACs between the operating deflection shapes of individual operating tests to the modeshapes.

#### 3.1 Test 3

Table 3.1 - MAC of ODS of Test 3 to modeshapes

freq Hz	1.82	3.24	4.13	7.08	7.74	8.88	10.69	11.05	11.63	12.07	12.84	13.26	13.67	13.79	13.94	14.95	16.32	17.56	19.06	20.85	23.28	23.49	23.62	24.23	24.58	24.77	25.41	26.51	27.12	28.1	28.22	28.31	28.44
1.86	95.8	3.2	0.2	0	0.8	0.1	1.1	41.3	1	0.6	1.3	0.8	9.4	0.5	4.8	0	1.8	0.3	0.5	35.2	3.6	0.7	29.6	1.1	1.9	0	1	0.4	1.4	3.8	1.6	1.9	12.8
3.61	1	1	0.8	0.2	31.7	1	20.9	0.7	15.8	13.1	3.4	3.3	0	0.7	0.4	0.1	2.3	0.4	6.9	3	2.9	0.4	0.2	1.6	1.9	2.6	0.8	1.6	0.7	2	0.1	0.5	2.1
4	0.6	2.7	0.1	0.2	32.6	0.8	21.3	1.3	15.1	14.8	3.1	4.9	0	1.6	0.5	0	0.9	0.1	6.5	2.9	2.6	0.7	0.1	1.6	0.5	0.9	1.3	2.7	0.6	2.1	0.3	0.5	2.7
8.01	0.1	0.3	0.6	0.1	93	3	41	1	32.4	19.4	2.5	10.8	0.1	0.5	0.8	0.7	0.5	2.1	1	0	0.1	0.1	0	0.6	1	1.2	0.4	1.1	0.2	0.7	0.5	0	0.2
10.64	2.5	0.1	0.8	0	45.2	1.6	88.9	0.2	52.6	22.3	5.9	8.8	1.2	1.7	0	0.8	0.7	3.7	0.4	1.3	0.6	0.5	1.3	0.9	0.8	3	0.1	0.3	0.4	0.8	0.1	0.1	0.8
11.13	33.8	2.8	5.2	0.2	0.9	0.2	0.4	71.5	4.3	1.4	2.5	6	59.6	1.3	56.5	1	7.4	0	12.9	0.4	1.9	0.3	2.1	0.9	1.1	3	2.7	1	1.1	0.5	0.2	0.2	1.4
13.48	7.6	3.5	3.4	0.3	0.6	1.3	1.9	41.4	4.2	1.8	1.7	10.5	85.8	7.5	76.9	0.1	38.8	2.2	2.6	12.3	1.7	0.7	0.4	1.2	6.2	3.2	0.9	2	1.2	1.7	0	0.6	2.5
14.94	0.5	3.2	4	19	2.6	0.5	3.8	1.1	4.2	19	37.1	6.3	0.4	21.5	0.1	71.6	0.3	7.5	2.3	0.4	1.4	47.5	0.1	12.3	15.6	13.5	2.5	16.4	1.5	26.1	40.8	47.3	30.5
16.21	7.1	15.8	0.1	0.2	2.9	2	2.3	5	2.9	2.1	0.4	3	25.8	5.5	29.2	0.9	45.4	18.3	4.2	37.2	0.3	0	19.8	0.1	3.6	0.5	7.4	3.1	10.7	0.5	0	0.8	6.6
17.19	0.5	16.5	0.3	0.6	3	0.6	9.6	2.4	15.8	9.9	4	4	1.1	0.9	3.1	0.5	2.6	19.1	0.5	1.6	0.4	0.4	0.5	1.5	6.3	3.6	0.4	1.1	0.9	1.2	0.8	0.9	0.3
19.04	2.7	3.4	3.6	0.3	2.5	0.9	2.7	3.5	7.7	3.5	0.9	10.5	1.4	0.6	4	0.6	0.2	13.5	25.8	3.7	3.8	0.4	2.9	2.9	1.1	6.5	7.2	1.6	5.3	2.2	0.1	1.1	2.1
20.9	27	0.9	0	0	0.5	0.2	1.9	3.7	3.7	2.5	0.3	1.1	5.8	0.4	9	0.6	19.9	2.5	0.2	75	4	0.4	28.9	0.3	3.7	3.9	8.6	3	10.9	5.6	1.7	4.8	11.4
23.34	0.4	0.5	3.1	4.5	0.1	0.5	2.8	0.2	8.2	6.4	12.3	3	0.6	16.1	1.1	32.7	2.6	1.4	0.3	2.7	2	36.2	0.8	12.3	23	4.7	3.5	7	9.4	26.9	19.3	20.8	11.8
23.63	8.6	4	8.3	0.7	0.8	0.5	1	0.2	3.3	4.7	3.4	2.5	1.3	1.9	1.2	2.4	6.1	3.2	1.7	16	2.7	5.9	22.5	17.3	37.3	8.8	2.8	2.9	4.6	1.5	0.5	0.9	8.3
24.32	0.4	0	9	1.7	2.4	1.9	3.3	0	11.5	7.2	1.8	0.4	0.1	1.4	0.2	1.3	0.1	0	0.7	1.4	5.3	5.7	1.6	12.4	18.3	7.8	0.5	0.3	1.3	4.2	1	3.5	2.7
24.8	0.2	5.1	3.2	1.8	3	1.3	4.6	0.1	11.2	16.3	11.4	7.6	0.1	2.8	0.6	11.3	0.2	2.6	0.3	2	1.5	11.6	1.6	2.9	3.3	8.8	1.9	4.2	1.5	3.4	17.5	6.9	7.8
25	3.3	3.7	5.5	2.6	5.4	3.4	1.2	3.5	2.3	0.8	7.7	16.3	0.3	4.1	1.3	2.4	6.2	4.1	0.1	5	1.9	4.5	4.2	6.5	17.7	1.9	11.9	2.5	18.3	14.1	5.9	2.5	1.3
25.29	1.1	4.1	2.1	7	1.7	0.9	1.1	2.2	2	0.3	6.5	10.7	0.3	10.3	1	13.5	11	5.7	0.2	5.2	1.1	16.7	2.3	2.8	16.2	7.3	30.9	1.7	32.5	32.2	8.1	18.5	7.6
25.59	1.8	14.9	0.1	3.9	1.2	13.2	1.8	0.1	2.9	5.2	1.6	11	0.9	9	1	7.6	6.3	16.2	0	6.5	10	6.6	7.2	3	28.7	24.5	3	6.3	5.2	9.2	2.5	6.3	3.5
26.46	1.8	20.4	0.5	1.8	0.5	4	0.5	1.8	1	3.5	8.8	9.8	1.2	0.8	0.2	5.2	1.4	14.4	0.6	3.9	18.8	7.1	5.9	13.9	1.8	1.7	8.8	61.1	0.3	0.7	7.8	3.4	2.3
26.76	2.1	3.5	4.1	2.5	0	7.7	1.2	2	3.8	6.2	6.2	2.6	0.6	0.2	3.2	6.9	1.6	4.6	0.1	6.7	9.4	16.6	16.6	7.9	8	9.1	3.2	1.7	6.2	6.9	6.9	8.1	11.2
27.15	1.6	4.1	1.9	7.1	0.8	0.4	0.8	5.4	2.2	8.1	4.7	6.6	1.9	7.2	4.6	9.8	8.5	1.6	0.8	4.7	1.3	15	11.6	3	0.5	1.8	28	6.3	46.7	15.9	17.6	13.7	7
28.42	11.2	14.1	1.6	13	1.4	2.4	1.9	3.5	2.2	11.8	29.5	10.6	3.4	8.1	4.1	16.4	2.5	4.1	0.7	8.6	1.9	16.7	4.5	8.2	1.3	5.7	2.6	9	4.8	24.7	31.2	32.1	49.4
28.61	8.6	14.3	1.4	14.3	0.3	7.8	3.3	4.4	3.5	14.4	39.6	16.4	2.8	5.3	2.7	28.7	2.3	2.3	0.5	3.1	3.8	17.6	3	7.1	3.4	0.9	2.6	10.4	0.7	7.7	36.6	29.2	53.8

#### 3.2 Test 7

Table 3.2 - MAC of ODS of Test 7 to modeshapes

freq Hz	1.82	3.24	4.13	7.08	7.74	8.88	10.69	11.05	11.63	12.07	12.84	13.26	13.67	13.79	13.94	14.95	16.32	17.56	19.06	20.85	23.28	23.49	23.62	24.23	24.58	24.77	25.41	26.51	27.12	28.1	28.22	28.31	28.44	
1.76	97.4	2.2	0.2	0	0.7	0.2	0.9	45.5	0.5	0.2	1.8	1.7	9.7	0.2	5.5	0.1	3.1	0.1	0.4	35.4	3	1.1	31.5	1.4	2.7	0.1	0.9	0	1.2	3.6	3.2	2	13.8	
3.32	17.2	67.3	5.5	0	1.7	3.6	1.1	5	1.9	1.2	1.4	2.7	5.1	2.4	0.4	0.2	12.7	46.8	0.5	6.4	7.7	1.6	6	0.1	0.9	3.2	3.9	5.3	0.4	13.6	1.1	0.3	6.5	
3.71	9	0.9	5.3	0.1	33.2	5.1	24.5	1	19.1	18	5.1	2.3	1.9	2.5	1.2	0.9	4.1	2.6	12.9	6.3	0.8	0.1	3.7	0	2.4	1.1	0.6	1.5	0.3	1.7	0.1	1	3.7	
7.13	0	0.1	3.9	98.5	0	1	0.1	0	0.1	11.7	24.2	0.3	0.2	17.3	0.9	33.8	0.2	0	0.3	0.1	1.7	11	0.1	4.5	5.5	3.5	0.5	8.4	5.4	44.6	53.5	60	35.2	
8.01	0.2	0.6	0.6	0.1	94.4	4	42.2	1.3	35.6	21	2.9	10.8	0	0.4	0.7	0.6	0.6	2.7	0.9	0	0.2	0.1	0	0.6	1.3	1.3	0.5	0.7	0.3	0.6	0.3	0	0.3	
8.98	0.4	2.7	13.7	1.7	1.6	69.4	1.3	1.5	2.5	0.8	2.3	4.9	2.7	2.9	2.5	0.2	2.5	3.1	4.2	0.1	5.4	2.4	0.1	9.5	2.1	0.1	1.5	2.2	1.9	2	1.2	1.2	0.3	
10.64	5.1	0.1	0.2	0.1	40.8	3.1	91.2	1.8	47.6	19.3	6.7	5.2	5.7	3.4	2	0.6	0.2	2.1	0.2	0.7	0.5	0.1	2.5	0	0.5	1.7	0.1	1	0.2	0.5	0.4	0	0.7	
11.04	45.6	1.7	0.3	0	1.1	0.6	3.2	92.7	3.4	1.9	2.2	10.1	52.3	2.9	48	0.2	7.1	0.4	1.2	2.6	1.6	0.5	4.1	1.7	0.7	1.8	7.4	2.6	3	0.4	1	0	1.7	
12.01	7.4	3.8	1.1	3.9	0.2	10.2	0.1	1.8	4.8	6.2	5	6.5	9.5	5.4	8.5	4.2	7.1	4.1	0.9	0.2	3.5	2.1	7.1	13.3	9.6	0.8	1.6	2	0.1	4.1	2	4.3	6.5	
12.21	0.3	0.1	5.6	29.9	13.1	1.5	10.3	1	41.1	68.5	8.2	2.7	0.3	27.2	0.2	26.3	0.1	1.8	0.7	0.2	0.9	23.6	0.8	7.2	3	0.3	1.1	7.3	2.9	21.8	28.3	27.8	18.1	
12.89	4.2	1.5	2.1	21.2	6.7	9.6	3.4	6.9	16.3	5.5	4	23.7	20	27.8	7.4	20	5.6	5	0.2	0.1	5.4	17.8	0.5	2.5	11	12.5	1	2.2	4.8	31	12	27.2	9.1	
13.77	11.1	2.9	0.3	0.2	0.2	0.8	0.3	56	0.9	1	2.9	10.6	96.3	7.8	91.9	0.4	43.2	1.6	3.9	10.5	1.3	0.2	0.8	0.9	4.8	5.4	1.7	1.8	1.1	1.1	0.5	0.5	1.4	
13.96	8.4	1.6	0.5	0.3	1	0.7	0	54.6	0.2	0.4	5.8	20.8	87.6	3.6	95.5	0.3	39.9	1.7	4.2	13.2	0.3	1.9	1.8	2.5	4.5	6.2	2.5	3.7	1.4	1.7	1.9	2.9	3.1	
14.94	0.1	1.7	14.2	31.7	0.4	0.1	0	0.6	0.4	7.4	26.3	1	2.4	43.5	3.1	89.2	0.7	1.3	5.1	0.1	2.2	51.9	0.2	13.7	21.1	11.3	1.3	10.5	3.7	43.1	38.6	52.1	37.1	
16.21	2.2	1.8	0.1	0.8	0.1	0.1	0	11.5	0.1	0.1	4.3	10.3	49.8	3.8	60.5	0.6	50	2.3	1.7	50	1.6	1.2	28.9	1.3	7.9	2.9	3.7	16.5	14.7	3.6	1.8	5.5	7.6	
17.19	0.5	1.2	0	0	0	12.6	1.5	30.9	4.2	46.4	35.9	1.5	14.2	1.1	0.2	3.8	0	4.5	6.5	0.4	1.3	5.9	0.6	2.6	0.4	0.7	8.2	2.4	1.1	1	1.3	1.2	0.1	0.3
19.14	0.2	0.1	13.3	0.2	0.1	0.1	0.1	0.5	0.4	1	2.4	0.9	3	1.4	4.4	2.7	0.3	1	95.8	0.5	0.8	1	0	0.2	0.9	2.4	0.6	0.4	0.3	1.6	0.5	0.3	0.3	
20.9	31.5	0.4	0.2	0.1	0.1	0	0	1.8	0.1	0.5	0.1	1.3	12.3	0.7	17.7	1.3	40.1	0	0.1	96.3	3.2	1	37.8	0.2	6.4	2.9	6.5	3.7	11.5	6	2.6	5	9.4	
23.44	2.1	0.5	2	9.1	0.3	0.2	0.1	0.5	0.2	9.6	21	0.1	0	18.2	0.8	59.9	3.2	1.2	0.2	3	3.8	89.4	2	20.1	11.3	12	5.1	8.6	3.9	31.2	40.3	44.3	24.5	
24.41	0.9	0.9	0.2	0.7	0.3	0.9	0.3	0.6	0.2	0.8	0.2	0.5	1.3	0.8	1.2	0.4	5.3	0.7	0.2	6.5	3.3	2.7	5.7	28.5	10	2.3	1.7	31.4	0.1	0.2	0.5	1.8	8.2	
24.9	0.5	1.9	2.8	21.3	0.2	1	0.2	0.3	1.2	9.9	23.7	1.3	0	23.1	0.4	57.2	0.5	0.7	0	3.1	1.7	57.4	6.7	15.4	23.3	11.6	1.4	25.4	11.3	35.5	48.7	49.2	36.4	
25.39	0	0.4	0.3	9.5	0.2	0.4	0	1.7	0.1	2.3	8.8	0.1	0	4	0.2	15.2	10.7	0.7	0.1	3.6	0.4	16.1	5.1	0.8	15.2	1.3	74.9	4.5	52.4	13.5	8.1	19.3	10.9	
26.46	0.6	7.9	0.1	1.8	0.7	3	0.4	2.6	0.3	1.2	6	5.6	1.1	0.5	0.4	3.1	0.6	4.6	0	4.1	5.5	7.1	14.3	26.9	1	0	6.9	82	10.3	0.5	4.6	1.8	2.5	
27.15	1.9	2.4	0.2	3.1	0.4	3.1	0.3	3.9	1.1	0.4	0.8	3.7	0.7	2.4	0.6	0.3	20	0.8	0.1	9.5	0.2	0.7	26.3	2.2	1.1	3.1	60.9	2	93.8	1.8	2.8	0.3	0.3	
28.22	9.1	13.4	0.3	10.8	1.7	0.8	0.3	5.6	0.3	4.6	3.3	15.2	8.1	5.2	16.9	12.5	4.9	3	0.1	17.4	0.8	8.8	11.1	0.7	6.6	6.3	0.3	6.7	5.3	26.1	5	8.9	11.4	
28.42	12.8	5.1	0.9	15.4	1	0.2	0.9	4.4	2.9	7.9	15.4	1.7	6.8	5.2	6.3	20.4	2.2	1.6	0.1	10	1.5	11.2	8.6	7.8	6.1	1.2	0.1	7.4	1	2.2	13.2	12.9	5.7	
29.39	2.6	0.1	0.3	0.8	7.4	0.7	0.1	1.6	0.8	0.5	0.6	0.9	2.1	0	3.4	1.3	0.7	0.5	0.4	0.7	4.3	0.5	0.7	2	5.4	0.9	0.4	1	1.3	1.5	1.1	0.3	1.4	





### 3.3 Test 9

Table 3.3 - MAC of ODS of Test 9 to modeshapes

freq Hz	1.82	3.24	4.13	7.08	7.74	8.88	10.69	11.05	11.63	12.07	12.84	13.26	13.67	13.79	13.94	14.95	16.32	17.56	19.06	20.85	23.28	23.49	23.62	24.23	24.58	24.77	25.41	26.51	27.12	28.1	28.22	28.31	28.44
1.66	94.6	2.7	0.2	0	0.6	0.5	0.8	44.1	0.4	0.2	1.9	1.5	8.3	0.2	4.5	0.3	2.8	0	0.4	33.9	3	1.2	25.4	1.1	2.8	0.1	0.7	0.1	1.2	3.1	3.3	1.7	10.4
2.93	0.8	19.7	1.2	0.1	19.6	4	13.3	5.1	8.3	7.2	3.8	7.4	2.8	1.8	6.2	0.6	3.1	12	3.3	1.7	0.7	0.5	0.1	2.6	2.6	0.1	1.5	2.3	0.1	5	0.8	0.5	0.6
3.61	2.8	3.9	1.1	0.2	32.9	0.3	22.3	0.3	17.5	14.5	2.5	4.4	0.5	1.5	0	0.2	2.3	2.9	7.4	3.6	3.9	0.6	0.8	0.7	1.2	2.5	0.7	2.7	0.6	2.3	0.3	0.5	3.6
4	3.6	2.8	3.8	0.2	31.6	1.1	22.9	0.1	16.6	18.1	2.8	4.2	0.9	3.8	0.3	0.4	1.4	0.1	9.3	3.7	2	1.2	0.9	1.8	0.1	0.4	1.5	2	0.6	1.4	0.3	0.2	2.9
4.3	1.4	0.8	21.2	0.2	20	7.8	16.8	0.2	9.7	5.3	7.6	1.7	0.6	2.6	1.8	3.1	8.6	5	7.2	2.5	2.3	1.7	0.4	1.9	6.3	8.1	0	2.1	1.1	0.4	0	0.1	0.1
4.79	5.9	0.4	1.6	0.3	31.8	3.7	25.7	4.5	17.9	14.6	2.8	4.7	1.6	3.6	1.7	0.8	8.7	3.4	7.7	5	2.5	0.4	2.3	1.3	1.1	1.8	0.5	1.9	0.7	2	0	1.5	3
5.86	2.6	2.5	32.8	1.4	25.8	4	7.5	0.3	6.7	1.4	4.2	1.1	3.1	3.1	5.6	2.1	4.8	2.3	0.9	3.5	5.3	4	0.1	3.1	9.2	5.7	0.4	0.8	0.9	3.5	2.4	0.7	0.2
7.13	0.1	0.3	3	98.6	0.1	9.1	0	0.1	0.2	10.8	13.4	0	0.3	11.5	0.3	4.8	0.3	0	0.1	0	1.6	0.8	0.3	5.6	1.4	1.2	4.9	0.8	11.2	34.7	50	47.2	34.5
8.01	0.3	0.6	0.7	0	95.3	4	38.7	1.4	31.1	17.1	2.6	11	0.1	0.4	0.5	0.4	0.6	2.8	0.9	0.1	0.2	0.1	0.2	0.7	1.2	1.4	0.4	0.6	0.3	0.6	0.1	0	0.2
9.19	0.1	3	6.5	5.5	17.9	72.9	11.1	0.4	12.1	3.6	4.2	6.6	0.1	6.2	0.1	3.5	0.5	1.3	3.3	0.1	6.3	0	0.8	6.6	0.6	0.8	3.6	7.1	4.2	1.2	1.6	1.6	0.6
10.05	2.1	0.9	2.8	0.8	48.9	0.6	66.6	4.4	57.1	36.1	3.4	11.5	2.8	2.9	2.6	0.4	2.5	3.9	0.1	0.2	1.2	0.7	1.4	3.2	2.2	5.7	0.6	2.5	0.1	1.1	2.5	0.1	0.5
10.64	4	0.2	0.4	0.1	38.6	2.5	92.4	1.3	52.6	22.4	6	5.4	2.7	2.5	0.6	0.6	0.2	1.6	0.6	0.6	0.8	0.1	0.8	0	0.7	1.7	0	1	0.2	0.5	0.5	0	0.4
11.72	3.3	0.6	0.8	0	35.7	3	50.4	16	83.7	59.8	2.2	13.3	3.4	0.9	5.7	0.3	2	3.5	1.2	0.4	0.6	0.5	0.6	1.5	1.6	7.1	1.9	0.2	1.6	0.5	0.6	0.1	0.4
12.21	0.1	0	3.4	22.2	13.1	1.2	12.3	1.2	47.2	78.5	4.9	4.1	0.1	20.3	0.7	16.6	0.6	1.9	0.5	0.2	0.4	16.6	0.7	5.3	1.2	0.2	0.4	4.2	2.8	18.3	26.5	24.2	16.7
13.28	2	0.1	0.8	0.2	1.7	0.2	0.7	7.3	1.6	1.4	3.1	4.3	9.6	11.4	13.6	0.2	4.1	0.4	1	0.5	1.4	0.5	0.9	0.7	0.3	2.2	1.4	0.5	0.6	3	1	0.4	0.1
13.96	6.9	1.6	1.1	0.3	0.8	0.2	0	45.6	0.2	0.4	4	20.5	86.1	2.9	95.7	0.8	34.3	1.3	4.3	13	0.4	2.5	1	1.5	3	4.7	1.6	3.7	1.3	1.9	2.1	3.2	2.6
15.04	0.5	3.3	13.9	6.5	0.5	1.1	0.7	1	1.6	8.7	19.5	1.5	7.8	23.7	11.7	76.5	2.7	1.3	4.6	4.6	1.2	45.4	0.1	9.5	16.7	11.9	3.3	8.7	2.2	33.7	25.7	36.2	15.1
16.21	4	2.7	0.2	0.1	0	0.1	0.3	7.5	0.8	1.3	1	3.9	45.1	2.9	50.3	1	49.6	0.7	1.2	51.8	1	1	23.6	0.2	6.2	0.7	2.5	12.1	11.3	3.4	1.4	5.8	4.2
17.29	0.2	2.2	0	0	4.2	1.1	10.9	0.9	15.7	11.9	0.7	4.4	0.4	0.4	1	0.1	0.3	4.2	0.2	0.4	2.7	0.3	0.6	0.5	0.6	2	0.6	0.2	0.1	0.3	0.3	0	0.1
17.88	0.4	6.6	0.2	0	3.7	1.7	9.8	0.7	14.6	10.5	0.3	3.3	0.3	0.9	0.7	0.5	0.3	4.7	0.2	0.3	3.7	0.4	0.5	1	2.5	1.5	0.5	0.3	0	0.5	0.2	0.4	0.3
19.04	0.5	7.7	5.1	0	1.2	0	5.1	0.3	9.9	4.1	1.3	0.9	1.6	2	3	0.7	2.1	4.5	32.7	3.7	2.8	0.2	0.4	1.6	0.9	1.1	1.2	0.7	0.4	2	0.4	0.1	2.2
19.53	1.2	2	0.2	0	4.4	0.6	16.7	1	28.1	23.2	0.6	6.2	1	1.2	0.1	0.6	0.6	2.6	1.1	6.9	7.4	1.4	1.7	0.2	2.6	2	4	0.2	6.3	0	2	0.6	0
19.92	0.5	1.7	0.2	0.2	2.5	0.7	13.7	1	22.9	16.6	0.1	7.2	0	0.1	1	0.7	1.4	4	2	0.3	6.6	0	0.8	0.9	4.4	3.9	3.7	0.1	3.4	1.3	0.1	0.7	0.3
20.9	20.4	0.6	0	0	0.3	0.3	3.8	1.7	7.8	7.9	0.2	0.7	8.6	1.3	10.6	0.5	21	1.4	0.3	66.4	6	0.6	24.6	0.4	6.2	2.8	6.8	2.5	11.5	3.6	2.5	4.3	7.7
21.78	0	1.1	0	0.5	0.1	0.2	1	0	1.4	1.4	0	2.2	0.8	3.3	0.4	1.5	0.9	0.5	0.5	3.2	7.4	0.6	0.1	0.9	7.5	0.1	1.8	0.5	2.6	1.3	0.1	1.8	2.4
23.63	28.9	0.8	0.8	0.7	0.1	0.7	0.2	1.6	0.8	1.2	0.3	0.3	0.4	0.2	0.4	0.5	9.4	0.9	0.3	32	3.3	0.2	88	1.6	0.2	2.3	6.8	8.6	16.4	6.1	2.3	4.9	6.5
24.41	2.8	1.2	0.9	1.7	1.2	1.5	0.4	0.6	1.5	1.1	1	1.8	1.3	2	0.7	4.3	3	0.4	0.2	4	2	6.6	8.9	24.3	14.3	0.6	2.6	18.4	0.7	1.7	0.4	7.2	19.3
24.8	0.4	5.2	1.2	5.2	0.6	5.2	5.3	2.4	13.4	3.7	3.1	17.2	0.5	7.2	4.1	16	0.4	4.8	0	0.5	1.8	12.5	1.4	9.7	21.4	10.8	0.9	0.1	3.8	23.8	4	16.3	3.6
25.39	0	0.3	0.1	0.5	0.1	2.2	0	1.3	0	0.8	7.4	0.2	0	3.8	0.2	22	12.3	0.5	0.2	3.7	0.5	18.9	3.4	0.2	19.9	2.1	76.3	8.4	54.2	7.5	3.2	11.3	4.4
25.88	1.5	2.1	2.9	21.9	0.7	5.5	0.3	0.1	0.1	8.9	28.2	3.4	3.1	11.3	3.3	33.3	6.4	1	0	9	3.9	33.3	1.9	15	0.2	15.1	7.1	13.1	14.1	16.9	48.7	34.8	20.5
26.46	0.8	6.5	0.7	2.4	0.5	5.3	0.5	4.3	0.7	2	6	3.7	2.8	0.5	1.9	2.9	0.8	7.1	0	1.5	10.3	4	11.4	25	0.5	1.1	5.9	80.1	2.9	0.5	3.5	1.3	2.3
27.15	1.2	1.2	0.3	17.4	0.2	6.5	0.8	2.4	2.6	0.6	0.5	1.6	0.5	2.5	0.5	0.1	16.5	0.6	0.1	7.2	0.6	0.7	17.7	2.9	0.8	1.8	59.9	0.2	92.5	5.9	9.2	5.1	2.5
27.34	0.8	0.9	1.5	23.8	0	1.7	0	1.2	0.9	4.3	13.5	0.3	1.2	13.3	1.9	30.8	7.5	0.1	0	5.1	1.6	22.8	17.5	11.6	9.1	7.4	15.7	12.4	39.5	32.4	34.8	50.4	32.1

### 3.4 Test 11

Table 3.4 - MAC of ODS of Test 11 to modeshapes

freq Hz	1.82	3.24	4.13	7.08	7.74	8.88	10.69	11.05	11.63	12.07	12.84	13.26	13.67	13.79	13.94	14.95	16.32	17.56	19.06	20.85	23.28	23.49	23.62	24.23	24.58	24.77	25.41	26.51	27.12	28.1	28.22	28.31	28.44	
1.86	95.7	2	0.2	0	1.5	0.3	1	43.1	1.2	1	1.6	0.9	9.2	0.4	5.1	0.1	2.7	0	0	31.9	3.6	1	25.8	1.2	2.1	0.1	1.2	0.2	1.5	2.9	1.9	1.4	11.9	
3.61	1.6	3.6	1.5	0.7	68.6	0.4	39.4	0.4	33	23.4	2.6	5.4	0.6	0.3	0.1	0.4	4.1	7.6	0.7	1.5	2.5	0.1	0.5	0.1	2.7	2.6	0.1	2	1.1	0.7	0.6	0.6	1.4	
4	1	10.6	4.2	0.4	61.4	8.5	38.3	0.5	27.4	21.8	9.2	12.2	1.4	3.8	0.4	0.3	0.1	2.3	3	0.9	2.6	0.4	0.4	1.1	1.3	1.3	1.9	3.8	0.1	2.7	2	0.5	2.6	
4.2	0.6	2.6	21.1	0	32.1	41.7	25.4	1.1	18.4	16.7	20.6	15.7	0.4	8.8	0.3	1.9	2.3	1.1	5.2	0.2	3.6	0.3	0.8	1.9	5	5.3	1.3	1.9	0.6	0.5	0.9	0.2	1.1	
7.03	0	0.6	6	98	0	7.3	0.1	0	0.2	10.9	15.3	0.2	0.4	9.3	0.3	3.9	0.3	0	0.2	0.1	1.7	1	0.4	6.2	1.6	0.6	4.6	0.8	10.6	33.7	49.3	45.8	32.9	
8.79	0.1	0.4	0.9	0.1	79.9	2.7	20.8	1	13.7	6.1	1.2	9.6	0	0	1	0.5	0.1	1.7	3	0	0.6	0.1	0.1	1.4	1.6	1.7	0.4	0.5	0.4	0.3	0	0.1	0.3	
10.55	13.4	0	0.8	0	21.7	1	59.9	17.5	28.6	9	2	0.7	10.4	3	6.3	1	0.4	0.7	1.9	1.3	0.2	0.2	1.3	0	0.7	0.7	0.9	1.3	0.6	0.3	0.2	0	0.4	
10.84	30.5	1.3	0	0	8	0.6	17.9	67.9	5.3	1.6	3.1	8.4	27.2	4.3	28.2	0.2	3.5	0.3	0.1	1.9	1	0.1	1.2	1.2	0.2	1.3	3.9	2.2	1.4	0.1	0.8	0.1	0.6	
12.21	15.2	0.8	2	1.2	6.9	13.1	2.7	20.3	5	6.4	12	41.2	24.7	1.9	32.4	0.9	9.9	7.8	3.4	0.1	8.2	7.5	2.1	3	4.1	6.2	2	2.3	2.1	1.7	6.3	2.6	0.1	
12.89	8	3.2	0.3	6	2.6	2.6	2.3	14.2	5.9	3.3	2.1	14.9	35.9	3.4	18	5.5	2.8	1.3	0	1	11.5	1.8	0.7	6.8	5.6	1.9	2.2	2.1	16.3	7.3	15.8	3.4		
13.09	3.9	1.4	2.9	1.2	1.3	0.5	2.1	14.6	3.1	3.1	0.7	1.6	20.2	11.1	19.6	2	6	0.5	3	0.8	1.2	1.5	0.5	0.6	0	0.8	1.2	0.6	0.3	3.8	1.6	1.8	0.5	
13.57	10.2	15.1	6.5	0.8	1.4	0.3	1	36.9	0.5	0.2	14.1	17.7	65	12	60.1	1.8	17.8	0.9	1.3	4.6	0.5	1.1	0	3.8	0.9	3.3	0.2	0.9	1.6	1.3	1.6	0.4	2.8	
13.96	8.3	1	2.7	0.5	1.1	0.8	0.1	46.8	0.6	0.9	3.4	22.5	82.5	1.9	93.9	1.8	32.7	2.1	5	10.4	0.2	4.2	1	1.5	2	5.2	1.9	4.3	1.2	3.6	3.4	5	1.5	
14.75	0.9	0.6	18.7	5.1	1.2	0.8	0	7.6	1.4	4.6	18.3	10.1	18.7	20	30.5	55.1	4.9	0.3	6.8	4.2	0.8	39.1	1.5	8.2	9.8	3	2.2	13.9	1	29.8	21.4	30.3	14.2	
14.94	0.6	3.9	16.8	4.2	0.5	1.3	0.2	4.1	1.4	5.2	18.5	5.2	14.6	24.8	20.9	67.9	3.8	1.9	6.2	3.9	0.8	39.4	1.2	7.4	11.6	4.2	2.2	12.1	0.8	26.9	18.6	29.8	14.2	
16.31	0.5	21.5	2.1	0.7	1.2	1	1.8	2.8	2	1.8	3.4	8.7	12.4	8	18.9	8.7	5.2	31.4	3.7	11.4	5.9	4.8	7	0.7	3.9	1.6	7.9	22.6	4	5.7	2	3.8	4.3	
17.05	0.1	0.7	0	0	5.9	0.9	15.1	1	21.2	17.9	1.3	8.4	0.2	0.9	0.7	0.1	1.4	9.5	0.1	0.1	3.9	0.5	0.9	0.1	0.6	3.4	1.3	1.1	0.3	0.9	0.6	0	0.1	
17.77	0.4	7.3	0.7	0	4.9	13.1	0.9	19.7	16.6	1	5.1	0.6	0.9	0.5	0.5	0.5	12.6	0.8	0.5	5.3	1	0.5	1.7	2.6	3.3	2.6	1.5	0.3	0.6	0	0.2	0.3		
19.63	2.3	2.3	0.6	0	2.7	1.2	12.7	0.5	17.5	17.6	0.4	3.6	1.9	0.7	1	0.4	0.3	3	8.3	8	3.4	0.1	0.8	2.6	6.1	4.7	3.5	0.4	3.7	0.3	1.2	1.4	0.8	
21	32	1	1	0	0	0.8	0.3	1.4	2.3	1.3	2	0.1	1.6	9.5	0.4	13.9	0.9	31.5	0.1	0.2	92.4	1.3	1.2	31.4	0	5.3	1.1	4.7	3	8.4	5.5	2.7	6.1	10.3
21.78	0.8	1.6	0.4	0.2	0.7	1	2.6	0	4.1	4	1	3.2	0.7	1.2	0.3	0.5	1.1	3.6	0.4	0.3	9.1	0.1	0.7	0.2	1.2	4	3.6	1.8	2.6	5	0.6	1	0.1	
23.44	13.7	0.6	2.7	0.2	0.3	0.7	0.1	1.2	1.2	0.9	9.5	0.3	0.4	5.9	0.7	34.1	1.7	0.2	0.5	13.3	0.8	43.8	38.4	14.3	9.9	13.4	0.2	18	4.9	7.6	7	21.4	27.5	
24.41	2	1.5	4.8	0.8	0.2	0.4	1.5	1.9	5.5	1.7	0.6	4.1	0.7	3.6	1.8	5.8	0.7	1.3	0.5	5.7	0.9	8	4.7	10.6	20.9	10.3	3.4	17.1	1.7	10.6	0.4	9.4	4.6	
24.8	0	7.2	4.1	12.7	0.5	8.9	2.2	0.4	3.3	1.7	1.3	12.3	0	10.9	2.3	10	0.5	9.2	0.3	5.3	7.5	1.9	3.2	29.7	9.4	5.8	21	18.9	0.6	30.5	8.4	21.9	13.7	
25.2	0.3	0.5	7.7	6.2	0	0.2	0.2	0.6	0	5.5	19.3	1.2	0.1	14.7	0.3	44.4	2.6	0.4	0.2	0.2	1.8	48	0.9	17.2	34.1	2.3	32	12.2	8.8	34.2	18.5	39.4	26.8	
25.78	0.2	3.8	1.9	1.5	0.3	3.5	0.2	1.1	1.6	4.7	19	1.9	0.7	6.7	1.6	39	5	2.9	0.2	0.8	48	43.2	0.1	7.7	7.6	7.3	41.1	9.8	42.5	22.7	38.1	41.4	23.3	
27.05	0.9	1.9	1	20.5	0.5	6	0.3	1.2	1	2.1	3.9	1.4	0.7	4	0.3	4.7	15.5	1.4	0.1	3.6	4.9	5	13	1.7	3.7	3.7	58.6	0.3	86.4	10.4	18.1	10.4	3.7	
27.64	1.1	2.8	5	11.2	0.2	0.4	0.1	1.4	0.8	3.3	8	3.6	5	9.8	10.1	24.3	8.1	0.4	0.3	11.3	5.9	23.3	12.9	11.6	18.6	1	7.1	6	3.1	58.6	12.2	46.2	19.8	
27.93	1.4	0.9	5.1	6.2	0.1	3	0.1	2.4	0.5	2.2	11.5	0.7	5.7	7.2	7.2	2.2	4.3	0	0.6	7.6	5.9	23.1	5.1	12.1	20.2	0.5	27.5	17.1	6.6	37.7	6.8	32.8	18.2	
28.42	3.1	12.2	3.4	11.5	0.1	1.5	1.7	0	3.8	11.2	26.3	11	0.9	6.2	0	22.7	1.5	4.9	0.1	2.5	1.9	19.2	6	2.4	3	0.7	3.3	28.5	2.5	14.9	3.6	17.2	29.3	
29.1	1.6	0.6	0.4	2.1	3	0.3	1.3	4.5	3.8	6	1.8	8.3	9.3	0.1	12.8	0.1	10	0.4	0.1	5.6	1.7	0.2	4.2	1.3	1.5	3.5	5	7.7	8.3	1.6	12.6	1.2	0.1	





### 3.5 Test 12

Table 3.5 - MAC of ODS of Test 12 to modes

freq Hz	1.82	3.24	4.13	7.08	7.74	8.88	10.69	11.05	11.63	12.07	12.84	13.26	13.67	13.79	13.94	14.95	16.32	17.56	19.06	20.85	23.28	23.49	23.62	24.23	24.58	24.77	25.41	26.51	27.12	28.1	28.22	28.31	28.44
1.76	89.5	3.7	0.2	0.1	1.8	0.1	0.6	38.4	0.3	0.3	1.3	0.3	8.8	0.3	4	0	1.8	0.4	0	31.8	3.8	0.3	27.8	1.9	2.7	0.2	0.8	0.9	0.9	3.2	0.7	1.9	13.8
3.71	1.4	1.3	0	0.5	68.6	2.3	36.8	0.2	26.8	21.1	3.6	5.1	0.2	0.5	0.2	0.7	1.2	0.8	1.4	1.3	0.9	0.5	0.1	0.3	2.1	0.5	0.4	1.4	0.5	0	0.7	0.6	1.5
7.13	0	0.2	5.3	97.2	0	7.6	0.1	0	0.1	11.3	14.5	0.1	0.3	9.3	0.3	3.8	0.4	0.1	0.3	0.1	1.9	0.9	0.5	5.7	1.6	0.8	4.7	0.8	10.9	32.8	47.5	44.4	32.2
8.89	0.3	0.5	1.2	0	76.3	3.8	22.3	0.8	16.5	7.4	1.4	10	0.1	0.2	1.5	0.9	0.2	1.8	3.4	0.1	0.5	0.7	0.1	0.7	1.3	1.9	0.6	0.5	0.6	0.5	0.2	0.1	0.1
10.55	3.8	2.9	0.6	0.5	29.6	2.5	59.6	3	20.5	5.6	3.9	1.8	3.3	0.9	1.2	1.1	0.6	0.3	2.9	0.3	0.2	0.2	0.7	1	1.4	0.2	0.3	2.2	0.2	0.3	1.9	0.8	0.4
12.21	14.8	3.6	1.7	1	8.1	13.8	2.5	21.7	4.6	5.2	15	39.9	17	1.2	23.7	0.5	10	8.9	2.1	0	8.8	4.4	0.9	3.1	4.5	4.2	1.4	1.4	1.5	0.6	4.6	1.1	0.4
13.09	4.3	3.1	3.2	1	0.4	0.6	1.3	13.1	3.7	1.5	1.8	0.3	38.8	8.9	34.5	1.2	8.7	0.4	2.9	1.3	0.6	0.3	3.3	1.8	1.6	0.4	0.6	0	0.1	2.2	0.2	0.9	1.7
13.77	9.9	1.4	5.3	1.9	0.7	0.8	0.5	42.9	1.6	3.3	1.1	16	75.9	4.2	79.4	6.2	31.3	1.5	6.5	7.2	0.8	3.5	0.4	0.1	2.3	6.9	0.6	2.2	0.1	8.4	4.3	3.4	1
13.96	8.7	1	4.2	0.6	1.8	0.8	0.1	49.3	0.9	1.3	3	24.9	73.6	1.2	88.7	2.7	31.4	2.5	5.7	9.8	0.3	4.8	1.5	1.8	1.4	5.8	1.7	4.6	0.9	5.6	3.7	5.6	1.3
16.21	1.2	3.2	1.7	0.6	0.4	0.9	0.4	9.1	1.3	0.6	3.9	7.6	34	4	42.3	1.4	32.7	2.5	1.6	29.9	2.4	2.8	16.1	2	7.2	3.3	2.1	10.8	6.6	5.5	4.9	9	5.6
17.09	0.2	0.3	0.3	0	6.5	1.1	13.4	1.2	17.2	15	1.3	6.5	0.1	0.4	0.7	0.1	1.7	3.4	0.1	0.2	2.3	0.6	1	0	1	1.3	0.7	0.7	0.2	0.3	1.1	0.1	0
17.88	0.8	4.2	2	1	6.3	1.5	8.6	2.1	10.6	9.5	2	3.6	0.7	0.1	1.9	0.2	0.5	0.5	1.1	1.1	1.7	1.6	0	1.4	1.6	0.1	0.3	0.5	0.6	1.4	2.9	0.9	0.3
19.24	1.9	5.4	0.6	0	2.7	1.7	10.7	2	18.9	14.1	0.5	5.7	0.4	0.2	0.3	0.9	0.4	2.7	13.4	6.1	7.3	0.7	2.5	0.1	3.9	0.8	2.2	0.1	5.2	0.2	2.3	1.4	0.4
21.88	0.5	0.7	0	0	0.1	0.2	3.4	0.3	5.3	4.5	0.3	1.3	0.1	1.7	0.2	0.2	0.7	1	0.1	1.2	3.8	0.1	0.7	0.3	3.5	0.9	1.5	0.4	2.8	1	1.1	0.7	0.2
23.44	23.2	1.1	3.2	0.2	0.5	1.3	0.1	3.1	0.1	0.7	5.4	0.1	0.3	0.7	1.1	13.7	5.6	0.7	0.6	23.6	0.2	16.7	48.4	6	3.4	10.8	0.9	13.9	5.3	4.8	1.8	11.7	16.9
24.32	2.1	0.1	2.2	1.3	1.3	0.1	1.7	1.4	5.8	4.1	2.4	1.9	0.5	2.3	1.8	6.8	1.1	0.6	0.4	3.6	0.5	6.9	1.5	10.7	7.4	12.7	1.3	19	0.3	13.8	4.7	10	2.2
24.8	0	9.8	1.1	8.9	0.4	9.3	2.7	0.6	3.7	2.2	2.9	14.4	0.1	6.6	2.3	5.3	0.8	10.7	0.3	7.4	5.8	12.3	6.5	25.2	4	6.5	5.9	32.2	1.5	20.4	3.9	12.3	7.5
25.1	0.2	1.6	7.2	9.4	0.1	0.9	0.4	0.8	0	8.5	20.2	1.8	0	15.6	0.3	47.7	1.4	1.6	0.3	0.9	2.3	53	3.4	20.3	28.8	4.3	15.3	15.3	4.1	34.1	24.4	42.1	28.5
25.68	0.1	1	1.2	19.2	0.2	7	0.2	1.4	1.6	1.2	4.5	0.8	0.5	5.5	1.3	15.4	6.5	2	0.1	0.1	5.7	16.1	1.9	6.1	8.8	5.4	53.2	1.9	66.1	17.4	22	24.2	11.8
27.64	0.5	5.2	4.4	12	0.3	0.2	0.2	1.7	0.6	3.1	7	6.4	4	10.8	10.2	22.4	5.6	1	0.4	7	4	22.2	7.6	11	17.6	1.5	8.3	4.7	1.4	63.4	11.4	40.8	17
28.42	3.3	5.3	2.1	11.1	0	0.3	1.6	0	4.6	10	20.5	6	0.9	7.4	0.5	21.4	1.1	2.1	0	4.1	2	13.9	7	4	5.2	2.2	1.2	22.6	1.7	13.7	24.8	15.2	29.1
29.1	1.4	0	0.4	5.3	2.8	0.7	1.1	4.9	4.1	7.2	2.2	6	8.5	0.2	11.4	1.6	11	1.2	0.1	5.8	0.9	1.7	4.4	1.3	1	4.8	2.5	4.8	5.3	5.5	14.3	2.6	2.1

### 3.6 Test 13

Table 3.6 - MAC of ODS of Test 13 to modes

freq Hz	1.82	3.24	4.13	7.08	7.74	8.88	10.69	11.05	11.63	12.07	12.84	13.26	13.67	13.79	13.94	14.95	16.32	17.56	19.06	20.85	23.28	23.49	23.62	24.23	24.58	24.77	25.41	26.51	27.12	28.1	28.22	28.31	28.44	
1.76	89.9	4.5	0.3	0.1	1.6	0.5	1.2	39.1	1.3	0.5	3.3	1.7	10.1	0.1	5.7	0	1.6	0.2	0.1	31.5	4.4	1	26.6	2.6	3	0.2	0.4	0	1.1	4.5	2.8	3	12.6	
3.71	0.3	0.9	1.6	0.4	62.5	1.6	37.1	1.4	31.6	19.6	3.5	6.7	0.2	0.6	0.5	0.5	3.9	6.1	0.7	1	2.8	0.5	0.1	1.1	2.2	2.6	0.1	1.7	0.1	1.8	1.2	1.5	0.8	
4	0.1	2.3	1.6	0.4	20.1	0.7	17.6	1.3	23	12.4	0.2	2.3	0.1	1.2	0.1	0.3	3.2	4.9	0.9	0.8	1.3	1.7	0.6	2.3	0.1	4	0.1	0.2	0.5	4.5	2.4	2.7	0.5	
4.2	0.1	5.9	2.4	1	6.6	12.2	10.6	1.3	13.3	8.4	2.7	2.8	0.1	5	0.3	2.7	4.7	8.6	2.1	0.1	0.6	1.2	0.7	1.2	1.6	2.9	0	0	3.3	2.5	2.3	3	0.6	
7.13	0	0.4	5.5	97.7	0	7.8	0.1	0	0.1	11.2	14.7	0.2	0.3	9.4	0.3	3.8	0.3	0	0.2	0.1	1.7	0.9	0.5	5.8	1.6	0.7	4.6	0.8	10.8	33.2	48.2	44.9	32.5	
8.79	0.1	1.1	0.6	0.1	78.5	3.9	23.4	0.4	15.8	7.9	1.8	11.4	0.1	0.4	1.4	0.8	0.1	1	2.6	0.1	0.5	0.3	0.1	1	1.4	1.7	0.4	0.7	0.4	0.6	0.5	0.1	0.1	
10.55	12.2	1.9	0.7	0.1	22	1.8	48.1	15	19.5	5.5	5.1	1	12.8	1.7	6.9	1.7	1.5	1	1.4	1.1	0.6	0.7	2.2	0.7	0.7	1.5	0.3	1.6	0.3	0.9	0.7	0.3	1.6	
10.84	22.9	4.6	0.4	0.2	5.6	0.1	19	53.2	6.5	0.3	1.4	6.6	26.5	2.9	25.1	0.6	6.5	2.9	0.1	1.2	3	0.2	2.3	0.3	0.2	1.9	2	1.1	0.7	1.6	0.2	0.8	2.5	
11.62	0.1	7.5	6.4	3.6	5.7	0.2	21	4.3	34.6	10.8	2.9	0.6	0.6	2.6	0.7	2.9	3.5	8.5	0.6	0.3	3.4	5.4	1	3.6	0.4	6.4	1.4	1.6	0.6	8.5	8.1	8.7	4	
12.3	0.7	0.1	10.4	33.8	6.6	2	6.4	1.2	16.8	39.1	12.6	3.9	0	24.2	0.7	22.7	0.2	1.2	1.4	0.3	2.3	24	0.8	11	4.1	0.8	0.5	4.9	5	31	35.6	36.4	23.9	
12.89	6.7	2.2	0.3	5.7	3.7	4.7	4	13	8.6	4.6	3.2	16.3	34.4	28.6	17.4	15.5	5.8	3.3	1.2	0.1	1	10.1	1.7	0.6	6.6	6.7	2.3	2.6	1.4	14.2	7	14.5	3.6	
13.09	2	0.2	3.3	1.4	3.6	3.7	2.5	5.7	6.5	2.1	0.5	10.9	26.1	16.4	18.3	0.3	4.4	1	2.9	0.5	0.3	1.3	3	1	1.6	1.2	1.2	0.1	0.4	7	0	2	1	
13.57	9.4	9.6	5.6	1.5	5.1	0.8	4	32.8	3	0.6	23.4	36.3	40.5	6.7	39.8	0.5	9.6	3.2	0.1	2.6	0	3.8	0.3	5.3	0.6	6.6	0.7	1.2	3.2	7.5	3.3	2.4	3.5	
14.06	8.3	0.8	3	1	2	1.1	0.1	48.4	0.5	1.2	7.9	27	70.5	2.7	85.2	3.1	28.8	2.4	4.8	9.9	0.1	6.3	1.6	4.1	3.4	4.9	2.7	6.1	1.3	4.6	5.4	6.7	4	
14.75	1	4	23.4	2.6	1.1	0.7	0.1	8.9	2.6	3.3	10.8	5.2	21.5	16.4	29.5	44.2	8.8	2.8	6.4	5.7	0.6	27.1	2.4	5.2	7.8	0.5	2.1	10.3	0.2	19.4	11.8	19.8	8.1	
15.04	0.6	2.1	18.7	4.1	1.2	0.6	0.1	5.4	0.7	2.1	12.9	8.8	14.9	25	24.6	60.8	3.6	0.2	8.1	5.3	2.5	37.8	1.1	6.9	9.4	6.3	1.1	10.3	0.7	32.7	18.7	30.7	11.4	
16.21	0.9	8.6	1.8	0.5	1	0.7	1	5.8	1.9	1.1	5	1.4	30.5	2.4	28.8	0.4	47.8	5	0.4	25.7	0	0.7	10.9	1.3	3.3	0.8	5	3.8	12.5	0.2	1.5	0	2.4	
16.99	0.1	2.2	0.3	0.1	5	0.5	14.5	1.5	22.3	15.4	0.2	4.5	0.3	0.5	0.6	0	0.8	9	0.2	0.3	4	0.1	1.1	0.6	1	4.2	1.1	0.2	0.2	1.4	0	0.5	0.3	
17.77	0.5	13.4	0.2	0.1	5.1	2.6	12.7	1.5	17.9	14.4	0.6	4.2	0.3	0.6	0.9	0.2	1.9	10.5	0.3	0.3	5.6	0.2	0.2	0.7	3.1	1.8	0.6	0.6	0.2	0.1	0.9	0.2	0	
19.73	0.4	5.8	2.6	0.2	3	2.1	9.8	0.2	12.8	14.2	2.3	6.5	0.6	0	0.6	1.3	1.6	0.2	4.5	1	2.8	1.6	1.9	0.3	2.5	1.3	1.4	0.5	3.1	0.9	4.2	0.5	0.4	
21.88	0.4	2.2	1	0.5	0.3	0.5	3.8	0.3	5.5	4.8	0.7	2.1	0.2	0.8	0.2	0.9	0.5	0.4	0.4	0.3	5.8	0.6	0.5	2	5	0.5	1.4	0.9	2.5	2.9	1.8	3	1	
23.44	9.2	0.6	0.8	0.1	1.1	0	0	1.1	0.1	3.4	7.6	1	0.1	12.6	1.9	39.1	7.5	0.6	0.1	11.3	3.4	54.3	13.3	6.7	6.3	8.8	8.2	2.2	6.7	17.6	11.7	18	4	
24.32	1.7	1	3.3	0.8	1.3	0	1.3	1.6	4.8	1.9	2.7	1.1	0.7	1.6	1.8	7	1	1.1	0.6	4.6	1.4	7.6	3.5	13.6	14.7	9.4	3	23.7	0.2	9.5	1.2	9	3.6	
24.8	0.4	13.8	18	10.5	0.4	5.5	1.6	1.5	2.2	6	5.3	8.4	0	1.9	0.7	4.9	0.4	24	0.5	5	8	15	37	28.8	7	3.3	5	28.9	1	15.4	5.7	11.3	8.1	
25.2	0.2	0.1	2.4	3.3	0.6	3.2	0.1	0.5	0.4	1.3	5.3	2.7	0.1	10	0.4	24.2	8.7	0.9	0	1	2	18	1.7	1.3	27.8	2.5	43.8	5	33	37.8	14.7	6.1	17.3	9.2
25.78	0.2	1.6	1.4	14.7	0.7	0.7	0.6	1.1	1.4	1.4	6.3	3	0.5	10.8	2.1	25	10.1	3.7	0.3	2	6.7	21.5	1.6	1.6	6.8	9.5	44	6	53.2	17.9	20.4	23	8.9	
27.05	0.2	0.9	3.3	35.1	0.4	7.2	0.3	1	1.2	2.5	4.4	1.1	0.2	7.7	0.3	7.6	8.6	1.2	0.1	1	9	5.2	5.4	6.2	6.6	44	48.9	1.5	73.2	22.9	28.8	24.9	11.4	
27.64	1.4	7.7	0.6	2.2	0.9	0.7	0.1	1.2	0.2	1	0.3	9.6	4.6	4.3	11.5	5.7	11	3.1	0.3	12.8	2.8	9.1	14.6	5.1	6.4	0.8	2.6	0.8	19.3	30.8	2	4.7	3.4	
27.93	0.9	2.3	0.9	4.3	0.5	2.6	0.2	2.9	0.7	2.2	2.5	6.2	6	6.1	13.2	20.7	9.7	0.1	0.2	8.4	2.1	17.7	4.4	1.4	13.9	3.6	27.7	9.1	30.7	27.6	5.2	16.3	0.3	
28.42	3.1	6	2.7	12.2	0.1	1.2	1.7	0.4	4	10.9	24.9	9.6	0.5	7.1	0.5	21.9	1.1	2.4	0.2	3.2	1.8	17.4	5.4	2.9	3.9	1.4	24	27.6	2	13.6	31.4	17.3	27.8	
29.1	0.9	0.3	0.1	4.6	2.5	0.6	1.4	4.8	4.2	7.7	4.3	8.1	8	0.6	11.1	0.3	11.3	1.1	0	6.9	2.3	1	4.7	0.3	0.5	6.4	2.9	6.3	6.8	1.2	15.7	3.6	1.9	





### 3.7 Test 14

Table 3.7 - MAC of ODS of Test 14 to modes

freq Hz	1.82	3.24	4.13	7.08	7.74	8.88	10.69	11.05	11.63	12.07	12.84	13.26	13.67	13.79	13.94	14.95	16.32	17.56	19.06	20.85	23.28	23.49	23.62	24.23	24.58	24.77	25.41	26.51	27.12	28.1	28.22	28.31	28.44
1.86	86.3	1.1	0.9	0.1	1.4	0.1	1.2	37.4	0.6	0.6	0.5	0.8	9	0.3	5	0.4	3.6	1.1	0.1	30.4	1.9	1.5	23.8	0.8	2	0.5	1.3	0.3	1.2	1.5	2.2	0.3	11
3.32	4.6	62.3	5.4	1.3	8.8	5.1	3.6	0.5	3.3	2.5	2.5	4.7	3.2	1.3	0.2	0.1	12.3	41.1	0.3	1.6	6.9	0.4	1.4	0.1	0.9	3.7	2.6	3.9	0.3	9.9	4.6	0.7	5.1
3.61	1.1	2.5	1	0	69.3	2	41.9	0.6	38	25.8	1.8	4.9	0.1	0.8	0.1	0.1	6.2	9.3	1.7	1.7	1.3	0.1	0.3	0.3	2.2	2.9	0	0.8	0.7	0.6	0.3	0.4	0.3
4.2	0.2	3.6	28	0	19.9	45.5	17.7	1.3	12.6	12.1	21.7	15.9	0.5	10.2	0.6	2.7	1.1	0.4	5.1	0	4.5	0.6	0.4	1.8	6	6.7	2	1.8	1.4	0.7	1.3	0.2	1.2
7.03	0	0.3	5.4	97.5	0	7.8	0.1	0	0.1	11.2	14.5	0.1	0.3	9.4	0.3	3.7	0.4	0	0.2	0.1	1.8	0.9	0.5	5.7	1.6	0.7	4.6	0.8	10.8	33	47.9	44.7	32.4
8.79	0.2	2.7	0.8	0	76	2.8	23.8	0.4	15.6	8	1.2	10	0	0.4	1.1	0.3	0.1	0.5	2.7	0	1.1	0	0.1	0.8	1.2	0.6	0.1	0.7	0.2	0.1	0.4	0.2	0.5
10.55	13.3	0	0.9	0	22.3	1.2	56.6	15.5	25.5	7.4	2.5	0.6	12.8	2.7	7.9	0.9	0.4	0.6	1.7	1.3	0.2	0.1	2.9	0.1	0.7	0.5	1	1.5	0.4	0.3	0.2	0.1	0.5
10.84	21.2	1.2	0.1	0	13.1	1.2	31.8	47.1	8.8	1.6	3.6	11.1	23.4	4.2	24.6	0.1	2.8	0.2	0.1	1.4	1.3	0.2	2.5	0.7	0.3	1.1	3.5	2.1	1.4	0.2	1.1	0.1	0.6
12.3	1.3	0	12.4	32.8	7.9	2.2	7.4	2.3	18.9	37.2	13.7	6.9	0.1	23.1	1.4	22.4	0.9	2.4	1.3	0.3	2.1	26.2	0.7	12.5	3.5	0.8	0.9	5.8	4.9	31.5	37.4	37.2	23.5
13.09	2.3	1	4.9	2.1	4.5	4.3	3.5	7.2	9.5	2.5	0.3	16.5	27.8	16.3	21.8	0.8	7.7	2.8	3.4	0.7	0.6	2.3	3.2	1.5	2.2	3.5	1.3	0	0.6	11.2	0.3	3.8	1.7
13.57	8.7	8.5	3.9	1.4	5.7	0.9	5	30	3.2	0.7	23.2	40	36.3	8.9	35.4	0.7	9	3.3	0.1	2.3	0	3.8	0.4	4.3	0.2	6.7	0.5	1.1	3.1	8.9	2.5	2.5	2.8
14.06	8.4	1.2	3	0.9	2	1.1	0.1	48.7	0.8	1.4	7.5	26.5	70.8	2.6	85.1	3.1	30.1	2.4	4.9	9.9	0.2	6	1.7	3.5	3.1	4.5	2.4	5.8	1.2	4.4	4.6	6.1	3.6
16.21	0.7	10.2	0.5	0.1	1.3	0.2	1	7	0.6	1.4	4.3	0.4	34.7	5	30	2	66.3	6.4	0.7	28.8	0.4	0.9	13.7	0.1	4.6	3.2	5.6	2.1	15.5	0.3	1.5	0.8	1.1
16.99	0.2	1	0	0.1	5.9	0.9	14.1	1.6	20.5	15.3	0.6	6.2	0.5	0.5	1.2	0	0.9	7.3	0.1	0.7	3.4	0.2	1.3	0.4	0.8	3.6	1.1	0.4	0.2	1	0.1	0.1	0.1
17.68	1	5.4	0.9	0.2	4.4	0.3	12.7	1.3	20.3	12.6	1.2	3.5	1.3	0.5	1.1	0.7	1.7	11.1	0.6	2.8	4.8	2	0.5	3.4	2.1	4.4	2.8	1	0.6	1.5	0.4	0.8	0.7
18.46	0.4	17.5	1.9	0.1	1.1	3.2	0.6	0.1	0.1	0.6	2.1	1.6	0.6	0	0.1	1.2	11.4	13.4	1.5	2.3	1.4	1.9	0.8	0.9	0.9	2.9	0.8	0.4	2	1.3	4.6	1.5	1
19.14	0.1	6	12.3	1.4	1.4	1.5	0.8	0.1	1.7	1.3	6.6	1.8	1.2	0.6	0.5	2.2	1	2.2	19.8	1.2	0.5	5.1	0.1	3.7	0.1	0.9	2	1.2	1.9	4.2	7.3	3.7	1.6
19.43	0.5	0.6	1.5	0.3	2.4	0.2	10.3	1.2	15.7	8.4	0.5	5.1	1.3	1.6	3	0.9	2.5	2.4	15.5	2.2	3.3	0.6	2.1	1.6	1.9	5.7	4.7	0.7	6	2.5	0.2	0.7	1.2
19.63	0.2	7.6	3.7	0.4	1.7	1.2	4.9	0.1	8.2	4.2	2.4	3.7	1.1	0.3	0.3	0.4	2.4	8.1	0.8	2	0.8	2.2	0.1	2.8	0.3	3.7	4.1	0.7	4.1	1.6	3.5	0.8	1.4
19.92	3.1	5.4	1.8	1.3	0.9	0.9	6.3	0.5	12.8	8.2	2.1	2	2.9	0	4.7	3	12.1	3.4	0.1	11.3	7.8	2.5	8	2.2	0.7	6.8	0.1	0	0.8	7.1	6.1	5.6	0.1
20.9	27	0.3	0.4	0.1	0	0.2	0.8	1.9	1.8	2	0.3	0.2	9.5	1	13.1	0.3	29.9	0.4	0.2	80.2	3	0.4	29.6	0.4	5.4	0.3	5.6	3.3	11.5	3	1.2	3.1	9.2
21.78	27	6.9	1.2	0.2	0.4	0.3	1.7	0.6	2.8	1.2	1.1	2.5	0.1	0.6	0.9	0.3	2.1	8.3	0	3.5	4	0.3	1.1	0.5	0.6	4	1.3	1.6	0.9	2.7	2.6	0.3	0.1
23.05	15.8	3.2	1.4	1.6	0.4	1.9	0.5	3.1	1.1	3.6	5.8	3.2	0	0.9	0.4	6.6	2.2	3.9	0.9	19.5	27.9	17.4	23.4	2.8	2.7	0.1	7.8	22.2	7.7	1.4	4.9	1	4
23.44	20.3	0.1	0.8	0.2	0.8	0.3	0	2.2	0	1.9	6.1	0.4	0.4	8.3	2.3	24	12.8	0.6	0.3	24.5	4.2	32	39.1	5.1	3	6.6	8.4	0.9	8.3	18.2	11	17.8	3.5
24.32	2	1.5	0.6	0.7	1.6	0	2.2	2.5	6.7	8.7	2.1	2.4	0.5	0	1.5	3.4	0.4	2.5	0.3	3.5	1.1	3.1	1.5	10.4	2.7	11.5	2.2	12.8	0.3	4.8	4	4	2.4
24.8	0.3	11.7	3.3	11.3	0.4	5.4	0.9	1.3	1	4.3	4.1	6.7	0	4.4	0.7	8.1	0.3	19.5	0.6	4.7	7.9	18.1	2.8	31.1	11.3	2.1	4.8	19.5	0.6	20.8	7.4	16.3	12
25.1	0.2	0.6	7.1	8.1	0.3	0.1	0.2	0.5	0.1	9.7	21.8	0.5	0.1	16.5	0.4	51.6	0	0.7	0.3	0.4	3	56.9	2.1	17.7	33	5.2	8.5	15.3	0	36.6	26.1	43.9	28.2
25.39	0.2	6.3	8.1	13.5	0.8	5.2	0.7	0.3	0.7	2.4	4.5	6.5	0.7	16.6	0.3	19.5	14.6	10.5	0.2	3.1	11.3	11.9	4.3	9.1	37.9	7.5	10.6	0.8	31.2	28.3	16.7	22	11.5
25.78	0.1	1.6	1	15	0.5	5.6	0.6	1.3	2.3	1.5	5.6	2.1	0.7	8.5	2.4	24.4	9.2	3.8	0.3	1.6	6	23.6	1.3	1.4	5.6	9.2	46.7	5.6	54.5	17	20.8	24.6	10.2
27.05	0.3	1.1	3	34.1	0.4	7.1	0.3	1	1.2	2.3	4	1.1	0.2	7.4	0.3	7.1	8.9	1.6	0.1	1	8.8	5.1	5.5	5.7	5.9	4.6	50.1	1.7	74.5	22.1	28.2	23.7	10.4
27.93	0.4	1.8	1.6	4.4	0.4	3	0.2	1.6	0.7	2.7	4.6	4.6	3.3	7.4	8.9	25.4	8.2	0.1	0.3	4.8	1.6	22.6	2.8	1.6	18.3	3.3	29.7	12.7	29	30.4	6	20.5	1.6
28.42	3.9	6.8	2.3	11	0.1	1.5	1.6	0.2	3.8	10.3	23.1	9.7	0.5	6.3	0.3	20.2	1.1	2.8	0.1	3.3	2	16.2	5.1	2.8	3	1.2	2.4	28.5	1.8	12.4	29.6	14.9	27.2
29.1	0.8	7.3	2.7	4.2	1.6	0.6	1	3.6	2.6	5.7	8	9	6.3	0.3	9.6	1.1	7.2	1.1	0	5.4	1.9	2.9	2.8	2.2	1.7	2.7	5.8	6.5	7.3	0.2	19.8	7.2	4.1

### 3.8 Test 16

Table 3.8 - MAC of ODS of Test 16 to modes

freq Hz	1.82	3.24	4.13	7.08	7.74	8.88	10.69	11.05	11.63	12.07	12.84	13.26	13.67	13.79	13.94	14.95	16.32	17.56	19.06	20.85	23.28	23.49	23.62	24.23	24.58	24.77	25.41	26.51	27.12	28.1	28.22	28.31	28.44
1.78	82.2	7.2	0.2	0.1	2.7	0.3	1.2	37.4	0.7	0.3	3	0.8	10.1	0.1	5.1	0	0.5	1.3	0.2	26.6	3.9	0.2	24	3.6	2.8	0.4	0.3	0.3	0.7	3.5	1.2	3.2	14.2
3.61	0.6	11.4	4.4	0.8	57.9	3.9	31.8	1.2	24.4	18.2	7.2	12.2	0.8	1.5	0.5	0.4	1.4	5.2	1.7	0.7	3.1	0.4	0.2	0.9	1.4	3.2	1.4	3.6	0	2.8	3.6	1.9	3.3
7.03	0.1	0.4	5.4	95.8	0.1	8.2	0	0	0.1	10.9	13.8	0.1	0.3	9.5	0.3	3.6	0.5	0.1	0.3	0.1	1.8	0.8	0.5	5.5	1.5	0.7	4.2	1	10.6	31.2	45.8	42.8	30.8
8.3	4	2.3	1.7	75.1	1.3	21.5	0.5	12.5	7.2	1.8	7.7	0.3	0.3	0.6	0.5	0	0.3	1.1	0.4	0.1	0.7	0.1	1.1	0.6	0.7	0	0.1	0.2	1	0.6	0.3	1.9	
8.79	0.3	0.9	0.8	0	78.5	4.4	22.4	0.7	15.6	7.5	1.8	11.1	0.1	0.3	1.5	0.9	0.2	1.2	3	0.1	0.6	0.4	0.2	0.9	1.2	1.7	0.5	0.6	0.6	0.5	0.3	0	0.1
10.55	12.4	0.4	1.2	0	22.1	1.8	51.1	15.3	25.6	9.2	2.1	0.5	11.8	1.7	7.5	0.7	0.5	0.4	2.7	1.1	0.1	0	2.3	0.1	0.9	0	1.6	1.7	0.5	0	0.8	0.3	0.3
10.84	31.5	1.9	0.6	0	8	0.8	13.3	70.5	1.8	0	6.4	13.3	32.3	2	34.4	0.1	4.7	0.6	1.4	2.1	0.9	0.4	2.3	1	0.5	1.5	4.9	1.1	2.9	0.1	0.8	0	1.1
11.52	9.8	1.6	0.7	0.1	20	2.5	17.4	27.5	27.3	16.7	2.3	13.6	10.8	0.8	15.1	1.4	0.9	1.4	1.2	0.2	0.4	2.8	0.1	7.8	4.2	8.2	2.6	0.5	1.6	0.2	1.8	0.5	0.6
12.3	0.3	1.1	10.8	33	8.1	0.7	5.1	0.6	16.3	53.2	13.6	3.1	4.2	20.2	4.9	22.9	1.9	0.8	2.7	0.4	1.5	25	0.8	11.4	3.6	1.7	0.8	6.4	4.1	33.1	41.5	40.1	26.5
13.09	3.5	2.6	4.1	1.4	0.6	1	12	10.4	2.6	1.3	2.8	1.5	34.6	11.2	28.8	1.9	8.6	0.3	3.1	1.1	0.9	0.9	3.6	2.3	0.3	0.7	0.4	0.1	3.2	1.3	2.1	2.2	
13.57	10.1	6.6	0.1	0.3	2.3	1	21	37.8	0.5	0.1	10.4	20.3	49.6	5.5	49.8	3.7	17.4	1.3	1	3.4	0.1	3.2	0.8	0.3	0	4	0.3	0.6	2.5	5.4	0.1	4.1	0.2
13.87	10.9	7.2	3.3	1.1	0.1	0.5	0.2	49.5	0.7	0.9	7.4	4.3	84	6.9	74.6	2.9	36.8	1.5	2.9	8.8	1.5	0.8	0.4	1.2	3.4	3.9	0.7	0.3	1.3	3	1.8	0.5	3
14.94	0.2	2.2	11.4	5.4	0.3	1.9	0	0.9	0	0.6	26.3	0.6	3.2	26.9	5.4	82.5	1.7	1.4	4.9	1.7	2.9	50.6	1.1	10.1	16.4	7.2	2.9	14.3	0.7	32.1	24.8	38.9	20.8
16.21	1.4	3	0.5	0.1	0.2	0.3	0.5	11.8	0.9	1.1	3.8	5.5	50.4	2.2	54.3	0	59	0.3	1	4.55	0.6	0	21.1	0.3	5.6	1.5	4	8.2	13.5	2.3	0.1	2.9	2.8
16.99	0.1	1.1	0.9	0.1	7.4	1.8	11.9	0.8	15.1	13.4	2.4	7.7	0.3	0.2	0.3	0.4	3.4	3.6	0.4	0.4	1.2	1.2	0.5	0.6	0.9	1.3	1.1	0.8	0.7	0.2	2.4	0.2	0.4
19.24	1	2.3	0.3	0	3.3	0.7	11.9	1.3	19.1	13	0.3	7.3	0.1	0.5	0.6	0.3	1.4	1.2	6.3	3.1	3.4	0.6	0.7	0.3	2.3	2.3	3.5	0.2	5.9	0.9	1.4	0.2	0
19.63	0.1	0.2	1	0.1	2.7	0.6	15.5	0.8	17.8	16.6	1.6	7.8	0.3	0	0.8	0.1	0.1	4.9	1.1	1.5	7.7	0.2	2.8	1.9	2.5	8.3	5.3	1.1	4.4	2.8	0.1	1.3	0.8
20.8	11.6	0.2	0.5	0	2.3	0.9	8.8	1.9	14.2	13.4	0.4	2.4	5.3	1.4	4.1	0.8	11.8	0.6	0.4	37.4	4.4	2	10.5	0.1	5.1	0.1	4.4	0.8	9.9	1	2.7	1.7	1.2
21.19	9.9	4.6	1.4	0.1	1.3	0	8.6	2.2	17.9	12.3	2.6	6.2	2.6	0.5	5.4	0.4	3.5	9.7	0.6	25.2	10.9	0.4	11.1	1.9	3.1	5.8	5.9	5.2	5.3	3.2	0.1	1.6	4.1
21.78	0.2	1.1	0.2	0.2	0.1	3.5	0.1	5.5	4.8	0.4	2.1	0	1.7	0.2	0.3	1	0.9	0	1.9	4.2	0.1	1.2	0.4	3.6	1.3	1.9	0.5	3.3	1.2	1.3	1.6	0.6	
23.05	5.9	10.1	0	1.9	0.5	3.1	1.7	1.8	2.3	7	7.9	4.8	0.1	2.3	0.2	11.3	0.4	12.6	0.5	3.9	43.8	21.2	4	2.9	3.7	7	8.2	10	1.7	5.6	7.4	5.7	2.9
23.44	33.4	0.2	1.3	0.3	1.3	0.6	0	3.3	0.1	0.5	0.6	0.8	0.4	1	1.2	0.3	18.9	0.7	0.3	39.7	1.2	1.9	63.6	0.7	1.2	0.1	6.3	3.5	14.8	5.9	3.4	3.6	4.3
24.22	5.6	0.6	3.5	0.7	2.3	1	3.6	2.8	10.4	1.3	2.5	2.3	0.8	1	1.1	1.9	0.3	0.8	0	1.7	0.6	5.5	2.9	0.3	0.5	2.3	0.4	5.7	1.2	0.9	6.7	1.7	1.3
24.51	0	0	0.6	0	2.1	0.6	3.8	4.1	11.3	9.9	0.2	5.1	3.6	0.2	5.6	0.6	3.6	1.8	0.1	2.1	1.5	1.2	4.8	0	0.7	7	5.7	2.1	6.7	0.8	0	0.4	3.2
24.8	0.7	5.5	1.4	0.3	5.3	1.6	3.1	1.9	9.9	10.7	1	2.3	1.8	0.7	2.4	0.2	0.6	4.4	0.2	2.5	0.4	1.8	3	7.1	2.8	0.2	0.2	9.8	0.4	1	1.4	1	1.7
25.88	4	2	4	7	0.6	0.7	0.4	1.6	6.8	9.7	0.9	4.2	9.5	5	13.3	6	2.1	0.1	19.6	4.2	11.3	9.4	13.2	16.4	8.8	0.1	14.1	4.3	3.3	11.6	6.8	15.6	
26.56	1.8	2.2	0.4	2.2	1.3	0.1	3.2	0.9	0.5	7.7	0.5	0.9	6.6	0.7	17.3	0.4	2.6	0.2	5.4	8.7	6.4	21.6	1.8	2.9	6.7	2.2	49.6	8	14.5	8.5	16.2	6.6	
27.05	0.3	1.4	0.4	2.4	46.2	0.4	6.8	0.2	0.3	0.9	3.4	5.5	0.1	0.5	6.1	0.5	2.8	7	1	0.1	1.4	6.5	2	4.6	7	2	5	38.6	1.1	61.6	21.4	35.2	26.7
27.93	3.6	0.1	4.1	8.1	0.8	0.6	0.1	6.1	0.5	2.7	9.3	5.7	12.6	2.9	13.7	4.2	5.8	1.3	0.3	15.8	2.8	5.6	5.4	1.4	3.8	1.5	12.3	1.7	5	7.8	3.8	5.1	20
28.42	3.1	4.1	4.4	12.5	0.2	1.1	2	1	3.7	10.4	19.8	10.7	0.7	2.4	0.5	14.3	0.8	0.6	0.6	0.1	3.5	12.4	2.3	12.8	7.5	1.5	2.7	35.2	1.9	5.9	22.8	21.8	14.7
29.1	0.4	0.9	1.9	3.5	2.8	0.5	1.6	3.7	4.4	7.7	4.9	10.1	5.8	0.6	9.1	0.6	8.5	0.9	0	7.1	3	1.1	5.5	0.3	1.1	5.4	2.4	6.6	4.2	0.4	15.7	3.3	1.6





### 3.9 Test 17

Table 3.9 - MAC of ODS of Test 17 to modeshapes

freq Hz	1.82	3.24	4.13	7.08	7.74	8.88	10.69	11.05	11.63	12.07	12.84	13.26	13.67	13.79	13.94	14.95	16.32	17.56	19.06	20.85	23.28	23.49	23.62	24.23	24.58	24.77	25.41	26.51	27.12	28.1	28.22	28.31	28.44
1.76	96.8	1.5	0.5	0	1.5	0	1.5	43.8	1	0.5	1.5	1.1	8.6	0.4	4.8	0.1	3.1	0.1	0.2	33.8	2.8	1.1	25.6	1	2.1	0	1	0.1	1.3	2.9	2.5	1.4	11
3.61	0.4	0.2	0.21	0.1	68.1	11.4	44.6	1.3	36.8	28.5	8.1	10.3	0.5	2.4	0.1	0.4	3.9	5.6	3.3	0.7	0.2	0.1	0.5	0.2	2.2	2.3	0.5	1.6	0.1	0.4	0.2	0.3	1.2
4.1	2.7	0.2	15.9	0.8	46.1	9.8	21.4	0	18.4	10	2.2	0	0.1	2	0.3	2	0.7	0.7	0	2	5.2	0.7	0	1.3	5.3	4.9	0.9	0.1	2.1	0.4	0.1	0.1	0.5
5.76	1.5	0.6	0.8	0.5	77.2	0.1	39.9	0.5	33.2	18.1	0.1	6	0.7	1	0.7	0.3	0.9	0.7	0.6	1.6	2.3	0.6	0.5	0.1	0.8	1.8	0.1	0.9	0.2	3.7	0.9	1.1	0
7.03	0	0.6	6.3	98	0	7	0.1	0	0.2	11.2	15.9	0.3	0.4	9.2	0.3	4.1	0.3	0	0.3	0.1	1.8	1.2	0.4	6.5	1.8	0.5	4.4	0.9	10.4	34	49.9	46.4	33.5
8.59	0.4	1.5	0.1	0	86.7	5.4	23.6	0.7	14.6	7.8	3	11.9	0.1	0.3	0.6	0.4	0	0.7	1.5	0	0.6	0	0.3	1.3	1.5	1.6	0.6	0.9	0.4	0.6	0.2	0	0.7
8.79	0.1	0.8	0.4	0	81.6	5	20.4	0.9	13.5	6.4	2	10.6	0.1	0.2	0.8	0.5	0.1	1.2	2.6	0	0.8	0.2	0.1	1.2	1.5	2	0.5	0.7	0.4	0.4	0.1	0	0.2
10.55	14	0	1.2	0	22.6	1.4	60.3	17.7	29.3	9.6	2.8	0.8	10.4	3.3	6.1	1	0.3	1	2.3	1.5	0.2	0.2	1.2	0	0.7	0.5	1	1.2	0.6	0.4	0.1	0	0.6
12.21	14.1	1.7	0.2	0.1	8.7	14.4	4.6	17.6	6.7	4.6	11	40.1	23.8	1.5	30.5	0.4	10	8.7	4.1	0.2	8.3	4.3	2.4	3.1	5.3	5.9	1.6	1.5	1.4	0.4	2.9	0.6	0.3
12.89	7.3	1.8	0.1	5.2	4.8	5.2	3.7	12.8	10.7	5.7	1.7	18.8	34.8	33.2	17.1	14.7	4.9	3.7	1.4	0.1	1.2	9.9	1.7	0.6	6.6	6.7	1.8	2	1.8	15.2	5.9	13.9	3
13.09	4.1	2.3	5.3	1.9	2.3	1.9	2.4	13.8	6.6	2.9	0.8	7.2	27.1	19.7	20.3	0.5	6.9	1.7	3.4	0.8	0.8	2	0.8	0.7	0.9	2.3	1	0.2	0.3	8	1	2.3	1.5
13.57	6.8	9.5	6	1.6	7.5	1.5	5.5	22.2	4.4	0.7	25.7	45.7	29.8	9.4	29.3	0.3	6.1	4.1	0.1	1.5	0	5.3	0.1	5.5	0.2	7.8	0.6	1.4	3.5	11.5	4	3	3.1
13.87	7.5	4.3	6	1.6	1.3	0.4	1.6	33.5	3.8	2.6	3.6	11.7	81.9	10	67	3	33	2.5	4.1	7.8	1.9	1	0.6	0.7	2.8	2.7	0.7	1.4	0.6	7.8	3.2	0.8	1.1
14.06	8.4	1.1	1.4	0.5	1.7	1	0.2	47	0.9	5.8	29.9	79.1	1	92.9	1	321	2.4	4.6	10.2	0.5	3.1	0.8	1.9	2.8	5.7	2.2	4.2	1.1	3	3.1	3.4	2.3	
16.21	0.6	8.8	3	0	1	0.2	3.3	6.9	5.5	4.6	1.4	0.9	50.1	3	41.5	1.4	78.6	7.3	1.3	38.7	0.1	0.6	11.9	0	3.6	1.6	9.6	1.1	22.2	0.2	1	22	0.7
17.09	0	0.7	0	0	5.8	0.8	14.5	0.9	20.6	16.1	0.5	5.9	0.2	0.5	0.7	0.1	1	6.5	0.2	0.1	3.6	0.2	0.9	0.2	1	2.7	0.7	0.3	0.2	0.9	0.2	0.2	0.1
17.87	0	3.2	1.5	0.2	0.9	0.6	6.2	1.2	9.7	7.9	0.1	3.6	1.5	0.2	3.2	0.2	3.8	5.8	0.2	1.5	0.5	0.8	2.6	0.2	2.7	1.3	0.3	1.6	0.1	1.1	0.5	0.3	0.2
18.85	0.5	0.8	0.1	0.1	3.4	0.8	17.8	0.6	29.7	23.1	0.2	6.6	1.3	0.7	0.1	0.1	0.5	2.4	0.8	4.1	5.3	0.2	0.9	1	4.4	4.8	4.1	0.1	5.4	0.8	0.8	1	0.4
19.04	0.7	0.2	0.5	0	3	0.6	16.5	0.9	26.8	22.1	0.3	6.5	1.2	0.4	0.1	0.1	1.1	2.3	1.9	3.7	4.7	0.4	0.6	0.7	4	4.3	4.2	0.1	4.9	0.4	1.5	0.6	0.2
19.34	0.3	0.4	0.4	0	3.2	0.4	17.6	1	29.3	23.2	0.3	7	0.4	0.2	0.3	0	0.4	2.3	1.4	1.2	6	0.5	0.7	0.7	3.2	4.9	4.3	0.3	4.4	0.9	1.1	0.3	0.1
19.73	0.7	0.5	0.2	0.1	2.6	0.4	15.7	1	26.3	20.9	0.3	7.8	0.6	0.5	0.1	0.1	0.8	2.2	0.2	2.3	5.4	0.3	0.4	0.6	3.4	5.7	5.1	0.2	5.2	1.1	1.2	0.6	0.3
20.61	0.4	0.1	0.5	0	3.2	0.6	16.5	0.8	27.2	21.5	1	9.6	1.2	0.4	1.1	0.4	0.7	3.9	1	4.7	9.3	0.2	3.4	0.7	4.2	7.3	6.8	0.7	6.4	1.6	1.4	1.3	0.5
20.8	2.7	0.1	0.4	0	2.6	0.4	14	1.2	24.3	19.7	0.9	7.7	2.7	0.5	1.7	0.3	3.7	3.1	0.8	14.7	10.9	0.5	5.6	0.9	5.4	6.3	9.1	0.8	9.2	1.3	1.8	1.9	1.6
21.87	0.4	0.2	0.1	0.2	0.3	0.3	2.9	0.1	5.3	3.8	0.3	0.4	1.1	3.5	0	0.4	1.3	2.1	1	0.7	2.2	0.2	0.2	0.9	7.6	1.4	2.8	0.1	2.9	2.5	0.2	0.8	0.3
23.44	12.1	1.2	1.8	0.6	0.8	0.1	0	0.6	0	4	11.9	0.1	0.1	10.3	1.7	41.6	12.1	1.7	0.1	17.2	6.6	60.7	30	13.3	5.8	6.2	8.4	3.5	7.1	26.9	22	30.6	8
24.22	4.2	0.7	0.3	0.2	2.4	0.3	2.9	2.1	7.2	11.2	3.9	1.6	0.4	0.9	0.8	8.1	0.1	2.3	0.2	1.5	1.9	6.3	0.6	8.3	0.1	21.1	1.4	13.8	0.2	5	6.3	4.7	1.1
24.41	3.6	5.8	0.9	1.7	0.9	0.6	0.9	2	2.6	5.6	3.5	2.4	0.2	0.6	1.2	7.6	1.4	7.4	0.7	7.3	0.5	10.6	1.6	1.6	8.7	6.5	4.4	10.9	0.2	11.2	4.5	8.3	0.7
24.8	0.1	12	4.7	11.6	0.5	4.5	0.9	0.8	1.3	3.2	3.9	4.1	0	3.8	0.9	7.4	0.2	19	0.6	4.1	8.4	17.6	1.8	32.4	12.1	1.6	2.9	18.1	0.5	21.8	7.3	16.9	13.3
25.78	0.3	3.3	2.7	20.7	0.3	5.1	0.5	1.2	2.6	1	8.2	1.1	0.4	9.3	1.8	26.9	10.2	5.6	0.2	1.9	9.1	25.9	1.5	4.9	7.6	9.1	46.7	3.9	55.6	23.6	31.3	32.6	13.3
27.05	0.2	1.3	2.2	32.6	0.3	7	0.2	0.6	1	1.9	3.4	0.7	0.3	6.4	0.1	6.5	10.6	2	0	1.4	8.3	5	5.9	4.3	5	5.7	54	2.1	77.6	18	27.1	21.1	8.9
27.64	0.7	6.7	2.3	0.9	0.7	1.1	0.2	0.8	0.1	1.8	0	10.3	2.1	5.2	7.8	8.6	8	2.8	0.5	9.4	3.5	14.4	12.1	5.2	10.2	2	22.5	1.4	14.8	38	0.7	6.7	0.6
27.93	0.2	0.9	1.6	5.7	0.6	4.1	0.2	2.3	0.7	2.3	4.4	4.7	4.2	7.4	9.3	23.9	12.7	0.2	0.3	6.5	2.4	22.1	4.9	1.4	15.2	5.1	29.3	10.9	33.9	29.6	6	18.4	2
28.32	6.4	7.9	1	7.7	0	0.7	1.5	0.9	3.8	7.2	11.6	3.4	3.7	5	1.7	15.9	2.5	4.8	0.1	4.2	3.2	13	3.8	2.9	1.6	1.2	1.2	27.2	1.3	8.2	19	9.1	28.3

### 3.10 Test 19

Table 3.10 - MAC of ODS of Test 19 to modeshapes

freq Hz	1.82	3.24	4.13	7.08	7.74	8.88	10.69	11.05	11.63	12.07	12.84	13.26	13.67	13.79	13.94	14.95	16.32	17.56	19.06	20.85	23.28	23.49	23.62	24.23	24.58	24.77	25.41	26.51	27.12	28.1	28.22	28.31	28.44		
1.86	90.6	4.6	0.1	0	1.9	0.1	1.1	40.9	0.3	0.2	1.8	0.8	10.2	0.1	5.3	0.1	1.5	0.9	0.3	30.8	2.9	0.3	25.8	2.3	2.7	0.1	0.7	0.2	0.9	2.4	0.9	1.8	14.4		
3.52	0.8	5.7	4.3	0.6	54.2	5.6	32.4	0.9	22.7	20	8.3	9.2	0.6	2.3	0.4	0.6	0.5	0.3	5.1	1.3	2.2	0.3	0.2	0.1	1.5	0.9	1.3	3.1	0.1	1.2	1.7	0.8	2.9		
4.39	3.3	4	0.5	0.6	57	1.3	30.8	0.4	22.8	18.8	4.4	6	0.2	0.2	0.2	1.1	1.1	0	2.1	3.2	2.9	0.4	0.5	0	2.8	0.9	0.7	2.8	0.6	0.9	1.1	1	3.3		
7.03	0	0	0.3	4.3	97.4	0	8.8	0.1	0	0.1	11.1	13.6	0.1	0.3	10	0.2	3.9	0.4	0	0.1	0.1	1.6	0.8	0.5	5.4	1.5	0.9	4.6	0.8	11	32.6	46.8	44.3	32	
8.3	0.3	1.6	0.1	0.1	84.8	5.6	30.4	0.6	21.3	12.7	3.5	12.6	0	0.4	0.8	1	0.1	0.7	1.6	0.1	0.4	0.4	0.1	1.6	1.6	1.6	0.5	1	0.4	0.4	1	0.2	0.5		
10.55	5.5	2.3	0.2	0.4	32.5	3.1	68.6	4.2	25.9	10.1	10.7	4	6	1.7	2.2	1.7	0.4	0.3	0.6	0.6	0.2	0.8	1.1	0.8	1	0.6	0	1.7	0.2	0.5	2.2	0.7	1.9		
10.94	34.9	2.5	0.5	0.1	5.1	0.4	7.8	81	6.2	1.4	1.8	10.7	39.6	0.9	38.9	0.1	7.6	2.2	1.5	2.1	2.4	0.3	1.7	1.2	0.3	3	4.9	2.4	2.1	0.5	0.4	0.1	1.1		
11.62	3	2	0.5	0	35.8	4.9	44.9	12.4	62.8	43.6	3.2	11.9	2	0.8	3.7	0.6	0.4	0.9	3.2	0.2	0.1	0.8	0.6	3.2	1.8	5.1	1.2	0.5	1.3	0	1.1	0.1	0.4		
12.21	0.3	0.3	6.5	25	12.5	0.7	7.6	0.6	27.	58.4	7.7	3.6	0.5	19.4	1.2	21.2	0.7	1.2	0.9	0.4	1.5	21.2	0.6	6.8	2	0.8	0.3	5.3	3.1	23.5	31.5	29.8	1.8		
13.09	4	2.8	1.1	0.4	0.4	1.1	0.6	11.8	0.9	0.7	2.9	0.9	35.1	14.2	28.4	1.1	8.4	0.1	1.7	1	0.8	0.1	3.2	1.3	0.3	0.3	0.5	0.2	0.2	1.1	0.3	0.6	1.5		
13.38	7.9	3.2	2.2	0.6	7.8	4.2	5	30.3	6.5	4.8	28.8	59.9	22	24	34.3	3.4	11.7	7	0.4	2.1	1.7	0.3	0.5	3	3.5	12.3	1.6	1.4	1.7	3	2.8	0.4	3.7		
13.67	9.5	12.9	3.3	0	0.9	0.1	1.8	35.5	0.6	0.5	1.1	3.7	69.5	18.8	48.8	1.8	30.5	4.8	2.4	4.4	0.8	1.2	0.5	0.2	4.4	2.5	1.6	1.4	1.6	1.5	1.4	1.8	0.2		
15.04	0.2	6.1	5.7	5.5	0.3	0.3	0.7	3.8	0.7	2.7	19.7	1.8	6.2	23.5	10.2	80.3	3	2.2	2.4	2.8	1.7	49.4	0.8	7.6	16.5	13.6	1.8	14.4	0.3	30.4	22.2	38.7	16.7		
16.21	1.8	2.3	0.8	0.2	0.1	0.2	0	11	0.1	0.1	1.8	4.1	46.5	3	49.8	0.1	67	2.8	1.1	44.5	1.4	0.2	22	0	4.7	4.5	2.6	5.4	12.8	3.1	1.1	3.2	1.6		
17.09	0.1	0.3	0.3	0	4.6	1	10.2	0.8	13.2	11.8	1.3	4.8	0.1	0.3	0.4	0.3	1.6	2.5	0.2	0.2	1.9	0.7	0.7	0.1	0.7	1.1	0.5	0.5	0.2	0.1	1.2	0.1	0.1		
17.77	0.3	2.4	0.5	0.1	4	1.3	10.8	1	14.9	13.3	0.9	4.2	0.1	0.1	0.9	0.1	0.6	0.3	0.2	0.5	1.9	0.5	1.7	0.3	1.2	0.8	0.2	0.3	0.1	0.3	1.2	0.1	0.3		
17.97	0.1	3.1	0.2	0.1	3.8	0.5	1.1	1.4	15.5	14.5	3.2	10.8	0.3	0.3	1.9	2.1	4.4	13.7	0	1.2	1.4	4.4	3.2	0.4	0.5	2	3	6.4	0.8	0.5	2.7	0.8	0.8		
19.14	2.5	0.9	0.6	0.1	6.4	1.8	14.9	2.2	17.8	18.4	4.4	10.4	1.3	1	0.6	0.4	0.3	5.3	5.1	4.5	3.3	1.7	0.3	0.4	0.8	4.5	5.8	0.2	4.8	0.1	2.5	0.6	0		
19.73	0.9	0.5	0.2	0	3.6	0.3	12.7	1.4	19.8	1.4	0.2	8.4	0.1	0.3	0.8	0	0.6	2.5	1.3	2	4.2	0.5	0.1	0.3	1.6	3.8	4.3	0.2	4.4	0.5	1	0.3	0.1		
20.8	11.9	0	0.3	0	1.6	0.6	5.6	1	8.2	7.8	0.7	3.5	6.2	0.7	8	0.5	13.3	1.7	0.5	41.2	4.9	0.5	19.5	0.2	2.2	5	5.8	1.6	8	4.4	3.1	3.5	6.2		
21.88	0.6	1	0.7	0.3	0.1	0.4	3.2	0.6	5.1	5.1	0.2	1.6	0.4	1.4	0	0.7	1.2	1.3	1.2	0.9	5.7	0.6	0.2	0.6	8.3	0.1	2.1	0.5	3.4	1.5	1.1	1.4	1.1		
23.44	31.3	0.7	0.9	0.4	0.3	0.5	0.1	4.1	1	0.3	1.1	0.2	0.6	0.4	1.3	4.7	13.5	0.3	0.5	31.8	2.7	3.4	64.2	3.2	1	5.5	3.3	5.9	11.3	5.4	2.5	8.7	8.4		
24.22	2.4	0.5	3.5	0.7	1.8	0.6	3.2	2.3	9.5	1.1	2.1	2	0.9	2.2	1.4	2.7	0.8	0.1	0	1.2	0.3	9.9	3	20.5	2.6	6.2	0.8	3.5	0.5	0.7	4	2.1	17.7		
24.41	1	2.4	4.7	2.1	1	0	2.1	4.6	5.5	11.4	5.8	4	2.3	2	3.8	10.9	2	1.9	0.1	3.7	7.2	13.7	1.7	11.1	5.8	6.7	1	6.4	0.1	7.9	10	7.3	9.4		
24.71	0.5	8.1	0.3	4.8	1.3	0.7	2.1	0.5	5.9	1.2	2.2	4.3	0.9	4.8	3.1	11.2	0.3	7.7	0	2.4	0.5	11	1.2	17.4	22.8	1.3	3.5	2.3	1.3	17.8	3.1	10.4	3.7		
25.29	0.2	0.3	3.4	5	0.1	1.5	0	0.3	0.3	3.1	12.2	1.2	0.1	12.7	0.2	35.7	5.1	0	0.1	0.8	0.4	32.8	0.7	5.7	42.2	1.3	40.8	9.6	26.8	25.7	13.6	30.8	16.5		
25.78	0.4	1	1.3	24.1	0.2	2.8	0.3	1.1	2.5	4	16.4	0.4	2.4	11.7	4.2	39.7	3.3	1	0.2	2.6	3.5	41.4	0.1	12.2	4.6	13	22.3	6.8	33.3	30.5	46.6	48.5	22.2		
27.15	1.2	1.8	0.5	18.4	0.7	7.1	0.4	1.3	1.1	0.9	0.8	1.4	1.4	3.6	1	0.5	18.1	1.1	0.1	5	2.4	0.9	14.5	3.4	0.8	3.4	0.8	3.4	57.7	0	88.9	6.8	11.9	5.3	1.7
27.44	1.4	4.8	1.8	12.2	0.6	0	0	1.5	0.5	3.5	8.4	1.2	7.6	8.1	7.1	28.4	16.6	1.8	0.1	11.1	1.4	22.7	19.6	9.3	14.9	2.4	4.8	10.1	21.8	25	14.8	45.6	27.2		
27.73	0.1	4.7	2	2.3	0.2	1.7	0	2.4	0.1	4.1	5	3.7	4.7	8.8	9.4	28.7	7.7	1.2	0.5	4.6	0.3	32.9	2.6	5.3	17.7	1.4	27.9	11	8.4	41.6	5.1	30.2	6		
28.03	0.9	1.4	4.1	1.9	0.6	0.1	0	3	0.4	6.8	11.2	5	5.8	1.6	9.8	30.3	4.9	0.6	0.2	6.6	2.1	23.6	2.8	4.1	17.3	6.6	0.8	13.2	6.2	57.6	21.8	34.2	10.3		
28.42	5.4	0.3	4.7	2.9	18.9	0.1	1	1.3	0.5	3.3	13.4	23.2	4	1	9.5	0.3	28.5	0.5	2.6	0.1	2.8	1.6	24.1	6.6	3.5	4.7	1.1	2.6	22.1	3.4	15.9	38.9	28.7	43.5	
29.1	2.6	0.3	0.3	1.2	2.8	1	1.1	4.6	3.7	3.4	0.9	7.7	6.2	1.8	8.8	1.5	6.9	1.8	0.2	2.5	3.4	0.3	1.8	0.9	1.5	8.9	1	2.6	1.9	2	8.2	2.4	1.4		





### 3.11 Test 20

Table 3.11 - MAC of ODS of Test 20 to modeshapes

freq Hz	1.82	3.24	4.13	7.08	7.74	8.88	10.69	11.05	11.63	12.07	12.84	13.26	13.67	13.70	13.94	14.95	16.32	17.56	19.06	20.85	23.28	23.49	23.62	24.23	24.58	24.77	25.41	26.51	27.12	28.1	28.22	28.31	28.44
1.76	90.5	4.3	0.1	0	1.5	0.2	0.7	41.2	0.2	0.2	1.9	0.9	10.3	0.1	5.5	0	1.7	0.7	0.3	30.9	3.1	0.2	25.7	2.5	2.9	0.1	0.6	0.2	0.8	2.4	0.9	1.7	14.1
3.61	1.8	1	2.3	0.5	57.6	4.4	31.1	0.3	23.6	22.7	6.1	7.7	0.3	1.5	0	0.2	2.4	1	4.2	1.8	1.6	0.2	0.5	0.2	1.5	0.4	0.8	2.1	0.3	0.6	0.8	1.1	3.3
7.03	0	0.3	4	97.6	0	9	0.1	0	0.1	11.2	13.5	0.1	0.3	10.2	0.2	4.1	0.4	0	0.1	0	1.5	0.8	0.5	5.4	1.5	1	4.7	0.8	11	32.8	46.9	44.5	32.4
8.3	0.4	1.6	0.3	0.1	84.2	5.4	30.4	0.6	20.9	11.6	3.1	11.9	0.1	0.3	0.8	1	0.1	0.6	1.9	0.1	0.4	0.3	0.1	1.3	1.5	1.6	0.6	0.9	0.4	0.4	0.8	0.2	0.4
10.55	7	2.1	0.4	0.5	29.9	2.8	65.3	5.7	24.5	9.1	9.2	3.2	7.8	1.9	3.4	1.4	0.6	0.3	0.4	0.5	0.2	0.5	1.3	0.8	0.9	0.7	0.2	1.6	0.1	0.6	2.1	0.6	1.9
10.94	31	1.4	0.3	0	6.2	0.2	15	72.1	7.3	1.3	1.5	10.2	35.6	1.9	35.2	0.3	7.1	2.5	0.8	1.6	2	0.4	1.9	0.8	0.3	3.1	4.8	2.6	1.7	0.5	0.6	0.1	1
12.21	0.4	0.4	8.9	29	9.7	0.6	6.9	0.9	27.3	53.2	9.3	2.4	0.2	24.2	0.4	22.1	0.2	0.4	1	0.4	2	21.8	0.5	10.5	3.1	0.8	0.4	4.8	3.7	28.1	33.4	32.6	21.5
12.6	8.3	4.8	15.2	5	5	7.1	4.9	18.4	13.3	3.5	6.7	17.5	36.6	4.3	31.3	1.7	12.8	4.9	7.9	0.2	0.9	3.6	3.2	3.2	0.4	5.5	3.3	1.8	1.2	12.7	6.6	6.2	5.7
12.89	4.1	3.2	0.6	4.5	5.6	9.3	6.5	9.4	9.2	5.9	12.9	28.7	23.8	18.1	12	15.1	7.5	5.4	0.6	0.2	0.8	6.9	1.2	0.4	7.7	10.6	4.3	4.7	0.8	7.1	5.6	9.4	2.8
13.09	2.3	1.8	2.6	1.2	4.1	4.1	3.3	8.2	7	2.2	1.5	18.8	28.3	17.9	21.8	0.2	9.2	2.9	2.1	1	1.1	0.9	2.7	1.1	1.3	5.1	1.9	0.6	0.6	9.6	0.3	2.1	1.1
13.48	11.8	2.6	0.8	0.8	3.9	2.5	2.4	44.2	2.4	1.8	20.3	37	42.6	1	52.6	1.2	21.5	6.1	0.7	3.5	1.7	0.7	0.7	2.3	3.1	8.7	1.3	1.1	1.6	1.1	1.9	0.1	3.6
13.67	9	10.9	3	0	0.9	0	1.9	35.9	1.2	0.8	0.6	6.3	69.4	17.7	50.5	1.6	30.8	5.3	2.7	5	1.2	1	0.6	0.2	5	3.5	1.8	1.8	1.3	1.7	1.6	1.5	0.3
14.05	7.3	3.5	2.8	0.1	0.8	0.3	0.1	45.4	1.2	0.5	2.7	16.3	68.2	1.9	75.1	0.8	35	5.1	3.7	10.4	1.1	1.8	1.8	0.8	2.2	5.7	1.4	2.9	0.8	2.8	1	2.4	1.1
16.21	1.1	9.3	1.1	0.2	0.5	0.3	0.4	7.9	0.3	1	4	1.2	38.2	5.3	36	2.3	68.4	5.2	1.5	31.3	0.3	1.3	14.3	0.2	5.3	3.3	7.4	4.5	16.5	0.7	0.8	0.7	1.6
17.09	0.2	0.1	0.2	0	5.3	1.2	11.2	1	14.3	12.6	1.6	5.8	0.2	0.2	0.6	0.3	1.6	4.1	0.2	0.3	1.8	0.8	0.7	0.1	0.6	1.4	0.7	0.5	0.2	0.1	1.2	0.1	0.1
17.77	0.4	1.7	0.4	0.1	5.2	1.1	12.3	0.9	16.3	13.5	0.8	5.2	0.1	0.6	0.4	0.2	0.9	1.4	0.1	0.6	3.2	0.7	0.5	0.3	2.3	0.9	0.6	0.4	0.3	0.3	1	0.1	0
21.78	3	1.9	0.5	0.5	0.2	0.2	3.8	0.7	5.5	4.6	0.3	3	0.3	0.7	0.3	1.4	1.9	2.6	0.5	3.8	5.7	0.9	1.8	1.2	5.6	0.6	0.9	2.5	1.6	2.3	0.5	1.4	1.6
23.05	10.5	2.6	1.6	1.5	0	3.7	0.5	1.9	0.9	8.2	9.3	1.3	0.1	6	0.6	26.1	3	2.2	0.6	14.9	36.4	44.3	9.6	6.6	3.7	7.1	8.1	10.7	6.4	13.9	16	13	4.5
23.44	25.5	0.7	1.2	0.3	0.1	0.1	3.2	0.9	0	2.3	0.2	0.7	0.4	1.4	9.3	11	0.3	0.8	28.3	0.8	9.9	61.7	4	1.8	8.2	2.3	8.9	9.1	5.2	2.2	12.4	13.1	
24.32	0.7	1.9	0.4	0.4	1.1	1.3	2.4	2.7	6.3	7.4	1.2	4.6	0.1	0.8	1.3	4.3	0.2	0.5	0.2	1.7	1.7	1.9	0.8	7.6	16.6	3.5	1.9	21.3	0.1	6.1	2	4	1.2
24.71	0.1	12.6	1.2	3.7	1.7	7.4	1.1	0.2	2.8	2	2.4	2.7	1.1	0.9	2	3.5	0.5	16.5	0	6.9	0.8	5.1	5.4	15	11.6	3.8	8.1	9	4.6	8.4	1.7	3.4	0.3
25	0.2	0.3	4.6	8.7	0.3	1.2	0	0.3	0.2	6.8	21.8	0.3	0.1	21.6	0.6	60.5	0.1	0.2	0.1	0.8	1	59.3	4.1	15.7	35.3	9.7	1.2	22.4	4.5	37.2	34.2	46.1	25.9
25.29	0.1	0.4	3.1	5.7	0	2.2	0	0.2	0.1	2.6	10.4	1.9	0.1	11.8	0.2	32.7	6.9	0.3	0.1	1.3	1	28.5	1.5	4.9	41.5	4.5	40	6.6	32.6	24	13.4	28.7	14.3
25.78	0.3	1.9	0.6	21.2	0.2	4.5	0.6	1.6	3.1	3.2	10.6	1.8	2.5	10.9	4.5	32.1	5.4	3.2	0.2	2.6	4.6	34.3	0.1	3.8	2.7	14.2	29.3	8.2	37	26.8	36.9	41.7	18.7
26.27	0.5	5.7	0.7	4.2	0.3	1.1	1.7	3.6	3.5	6.8	15.8	7.4	2.7	2.9	3.4	17.8	2.9	10.6	0	0.2	2.8	24.8	2.2	20.5	3.2	0.1	15.3	65.6	10.8	5.8	18.1	18.3	11.5
27.15	0.8	1.5	1.1	23.3	0.5	7.9	0.4	1.6	1.1	1.1	1.3	1.6	0.5	4.8	0.3	2.8	13.9	1.6	0	3.1	4.6	2.5	10.7	4.6	3	5	56.8	0.8	86.4	11.3	16.2	10.5	3.8
27.44	1.6	4.5	2.6	15.6	0.3	0.2	0.1	1.8	0.4	4.1	9.5	1	7.3	8	7.8	27.7	17.4	2	0	11.1	1.5	21.7	19.2	12.6	14.6	2	8	7.9	26	29.2	17.1	46.5	27.6
27.73	0	3.7	1.1	0	0.1	4	0.1	1.1	0.2	3	4.1	2.2	2.5	5.3	5.8	27.5	6.5	1.1	0.4	2.6	0.3	31.9	2	2.6	16.9	1.5	42.3	12.4	20	24	2	20.1	3.4
28.03	1.4	2.2	3.5	15.2	0.6	0.2	0	2.5	0.1	6.2	8.2	5.6	5	14.1	10.9	27.6	4.5	0.8	0.3	7.6	2.5	21.7	2.9	5.2	15.2	6.5	1.3	14.4	5.9	61.2	20.9	31.7	3
28.42	3.7	4.9	2.3	15.6	0	2	1.7	0.2	3.8	12.5	25	8.1	0.4	7.8	0.5	23.1	1.3	1.8	0.1	4	2	18.4	6	4.2	4	1.6	2.4	22.9	2.4	13.3	33.7	22.3	38.3
29.2	2.1	0.5	0.7	2.9	3.2	0.2	1.2	4	3.5	5.5	2.5	7.9	5.5	0.3	8.6	0	6.7	0.9	0.2	2.8	1.2	0.2	3.4	0.8	1.6	5.5	1.9	5.2	3.4	2	13.3	1.1	0.1

### 3.12 Test 21

Table 3.12 - MAC of ODS of Test 21 to modeshapes

freq Hz	1.82	3.24	4.13	7.06	7.74	8.88	10.69	11.05	11.63	12.07	12.84	13.26	13.67	13.79	13.94	14.95	16.32	17.56	19.06	20.85	23.28	23.49	23.62	24.23	24.58	24.77	25.41	26.51	27.12	28.1	28.22	28.31	28.44	
1.86	98.8	1.7	0.1	0.2	0.7	0.1	0.6	47.3	0.3	0.1	2.1	1.9	9.7	0.6	6.4	0.9	2.4	0.2	0.3	31.5	2.4	1.7	24.2	1	1	0	1.1	0.1	1.2	2.8	4.8	2	11.6	
3.71	1.9	0.1	9.6	0.1	34.4	6.1	27.4	1.1	17.8	16.5	4.9	4.8	0.5	6.1	0.4	3.2	5.4	5.1	10.5	3	0.6	0.3	0.6	0.2	1.7	2.5	0.4	0.6	0.1	0.9	0.4	0.4	1.2	
5.86	2.5	0.2	0.7	0.8	0.1	2.4	2.8	10	1.2	6.2	2.4	1.2	10.1	3	8.3	0.3	5.3	0.4	12.7	0.8	11.8	0.2	1.9	3.2	1.6	2.8	0.3	1.3	4.1	0.6	1	0.4	0.5	
7.13	0.1	0.2	4.3	99.2	0	7	0	0	0.3	9.4	13	0.1	0.2	11	0.2	3	0.3	0.1	0.1	0.7	2.2	0.3	1.2	5.4	0.8	0.6	4.8	1.1	9.9	34.7	48.1	47.2	34	
8.01	0.6	1.1	0.3	0.3	93.4	6.9	34.9	1.1	30.8	22.2	3.8	11.9	0.2	1	0.3	0.8	0.4	1.1	0.3	0	0.5	0.1	0.6	1.8	1.1	1.3	0.2	0.9	0.2	0.6	0.7	0.4	1.4	
8.98	0.5	1.4	18.3	9	0.9	68.2	0.6	0.7	0.9	0.9	2	2.7	0.9	2.9	0.8	3.7	0.6	0.5	6.2	0	3.2	0.1	0.6	11.2	1.4	1	6.7	6.1	8	2.9	4.9	3.6	3	
10.64	3.9	0.3	0.6	0	36.7	3.2	93.1	1.7	49	20.1	5.5	4.5	3.3	4.3	1.2	0.3	0.3	2.3	0.4	0.4	0.5	0	0.7	0.1	0.9	1.4	0.1	0.6	0.1	0.4	0.3	0.1	0.4	
11.04	44.5	1.7	0.2	0	2.5	0.5	3.8	92.2	4.4	2	3.2	8.9	41	3.3	39.4	0	5.8	0.5	1	2.3	1.6	0.4	0.9	2.9	1.1	2	6	2	2.1	0.2	1	0.1	1.3	
11.72	0.8	2	1.9	0.3	34	4.2	55.3	9.1	90.4	58.6	0.4	8.4	2.6	2.3	3.3	0.4	3.1	4.9	1.9	0.3	0.9	0.7	0.4	0.4	0.9	4.1	1.2	0.6	1.2	1.5	0.2	0.5	0.2	
12.01	4.2	0.4	0.5	2.8	0.8	8.6	0.1	2.4	4.4	5.5	2.6	13.9	9.6	17	11.7	1	3.8	2.5	1.2	0	7.8	1.7	5.3	14.3	4.8	1.6	1	2.5	0.1	1.5	0.6	1.5	5.8	
12.21	0.8	0.9	4.3	20	14.1	1.3	12.1	1	45.5	72.8	3.6	2.4	0	24.9	0.2	15.8	0.8	2.9	0.7	1.4	0.7	14.5	0.2	4.9	0.8	0.1	0.3	2.1	2.2	19.3	21.1	21.5	13.2	
12.89	2.2	0.5	0.2	5.3	8.4	17.3	11.1	4	10.8	10	44.7	46.1	10.4	11	5.6	1.9	5.1	9.2	0.3	0.1	1.7	7.7	1.4	2.8	10.3	10.1	5.2	9.1	0.3	3	13.9	11.2	6.6	
13.38	4.3	2.4	1.2	0.5	13.4	9.2	7.9	17.6	9	7.1	36.2	91.2	9.1	8.6	26.2	1.8	9.6	11.3	0.7	1.4	1.4	0.9	0.4	4.4	5.3	14.9	3.8	4.9	2.3	6.3	6.2	0	3.9	
13.71	10.5	2.8	0.1	0	0	0.5	0.4	47.6	0.4	0.4	2.9	6.8	97.2	11	87.2	0	38	0.8	3.2	10.1	1.3	1	0.5	0.8	5.3	3.1	1.8	1.6	1.5	0.6	0.4	1	1.6	
15.04	0.9	0.3	3.1	4.9	1.6	0.7	1	3.7	0.5	1.3	4.4	17.6	0.1	3.6	2.4	1.6	73.3	0.1	3.9	7.5	0.3	0.8	53.4	0.4	4.8	12.6	11.3	8.5	13	4	21.3	13.9	30.9	16
16.31	1.5	0.4	0.4	0.4	0.7	0.9	0.2	12.5	0.5	0.5	4.2	10.5	5.3	4.3	60.9	0.1	56.6	2.4	1.5	44.6	1	0.4	21.4	1	6.8	6.2	1.3	9.6	8.6	2.5	0.3	3.3	3	
17.29	0.1	2.4	0	0	4.5	0.7	11.1	1	20.4	17.8	0.6	6	0.4	0.3	1.3	0.2	0.6	5.2	0.4	0.4	4.4	0.3	2	0.2	0.5	3.2	0.6	0.5	0	0.6	0.6	0	0	
17.77	0.3	0.9	0.7	0.4	3.7	8.5	13	22.6	18.8	0	4.3	1.6	0.5	3	0.3	0.3	2.2	0.5	1.5	6.7	1.1	2.5	0.8	2.2	2	0.8	0.5	0.5	1.5	0.8	0.1	0		
17.97	0.2	10.5	0.1	0.1	2.8	0.4	5.3	1.6	14.1	14.8	1.6	7.8	0.1	1.1	1.4	1.1	6.7	24.1	0.8	0.5	1.3	1.8	2.6	0.4	2.8	4.3	1.7	2.8	0.2	1.7	1.7	0.4	0.3	
19.04	1.7	0.3	11.4	0	0.6	0.1	7.3	0.2	1.1	0.4	3.4	0.2	0.5	2.4	0.9	2.4	1.1	0.9	28.4	0	7.1	4	3.1	2.7	0	2.5	1.9	2.5	2.1	7.1	0.9	0.5	0.4	0
19.24	0.4	1.5	2.4	0.2	0.6	0.3	4.6	0.4	5.2	7	0.1	0.5	0.2	0.9	0.4	1	1.7	1.2	43.8	1.4	1.9	0	3.7	3.4	0.8	0.9	0.5	1.2	2.7	0.3	0.1	0.3	0	
21	28.3	0.4	0.1	0.5	0	0.2	0.2	1.7	0.7	2.3	0.2	1.1	12.5	1.2	16.9	3.6	36.5	0.1	0.4	96.3	2.8	2.2	30.9	0.2	6.6	5	6	1.5	9.7	6.3	5.1	6	7.4	
23.44	2.1	0.4	3.1	0.1	0.1	0.7	0	0.2	0.3	4.4	15.4	0.1	0	16.1	1.1	62.8	4.5	1.6	0.3	4.3	4.9	92.6	0.9	16.9	12.4	10.5	10.8	9.6	8.2	21.9	22.3	29.5	12.9	
24.41	0.4	1.2	0.1	2.4	0.2	0.4	0.9	0.6	0.4	0.2	0.1	1.5	0.4	1.1	0.3	2.8	0.1	0.1	3.6	3.1	1.6	2.3	42.7	4.8	3.4	3.7	43.6	0.2	1.2	3.8	2.6	14.6		
24.71	1.2	5.6	10.7	5.5	0.4	1.9	1.2	1.6	5.6	6.8	9.8	0	1.1	8.5	1.2	20.7	0.9	6.4	0.6	0.5	3.3	38.7	2.5	23.9	29.6	3.1	6.5	4.5	2.6	19.4	11.6	19.1	14.3	
25	0	0.6	4.5	2.3	0.1	0.2	0.5	0.4	1.5	2.9	18.3	0.4	0	22.3	0.5	59.8	0.1	0.4	0	0.2	3.6	62.6	2.4	17.2	25.5	9.3	0.7	18.5	3.4	30.8	30.1	37.7	19.4	
25.35	0.1	0.5	0.7	0.6	0.1	2.6	0.1	1.4	0.5	0.5	7.1	0.4	0	4.8	0.5	23.5	16	2.2	0.1	5.9	1	23.7	5.1	0.9	15.8	2	77.9	7.5	59.2	11.1	4.5	15.7	6.5	
26.37	0.1	3.5	0.8	3.8	0.8	2.8	0.7	2.8	1	3.6	10.8	5.7	1.6	0.6	1.7	7.7	1.6	8.6	0	0	10.1	13.1	3.7	33.6	1.2	0.3	4.5	86	0.9	2.1	8.5	7	10.3	
27.34	0.1	0.9	6.2	19.2	0.6	0.2	0	1.7	1.3	4.4	18.2	0.1	4.9	7.5	6.8	35.8	11.5	1.1	0	5.8	4.5	30.7	15	18.8	11.5	1.3	5.2	9.9	14.6	36.3	36	58.9	32.8	
28.22	4	6	1.9	13.8	0.4	0.4	0.2	7.3	0.4	6.3	4.5	10.2	10.4	14.3	18.9	26.2	6.8	2.4	0.1	17.5	2.5	16.9	6.3	0.8	13.5	7.9	0.8	6	3.7	48.4	16.4	23.7	4.9	
28.42	8.7	0.2	0.6	4.2	0.8	2.4	1.2	5.7	2.8	6	7.2	0.1	10.8	5.3	11	15.4	4.8	0.3	0	14	0.5	6.6	1.8	6.6	5.9	3.6	0	25.9	0.9	4.8	11.1	3.3	22.3	
29.39	4.6	1.3	0.5	1	16.7	3.6	2.9	7.2	0.7	1.9	1.5	0.1	12.7	2.1	12.6	2.4	7.9	0.7	0	13	3.2	1.5	0.9	1.9	2.9	3.4	0	1.2	2	2.2	2.9	1.2	3.3	





### 3.13 Test 22

Table 3.13 - MAC of ODS of Test 22 to modeshapes

freq Hz	1.82	3.24	4.13	7.06	7.74	8.88	10.69	11.05	11.63	12.07	12.84	13.26	13.67	13.79	13.94	14.95	16.32	17.56	19.06	20.85	23.28	23.49	23.62	24.23	24.58	24.77	25.41	26.51	27.12	28.1	28.22	28.31	28.44
1.86	91.2	4.5	0.1	0	1.1	0.1	0.4	41.5	0.1	0.1	1.7	0.9	10	0.2	5.3	0	1.6	0.8	0.4	31.4	3	0.3	26.3	2.3	2.6	0.1	0.7	0.2	0.9	2.6	1	1.9	14.6
3.52	5.5	3.3	10.4	0.8	26.7	5	19.9	1.2	12.3	13.4	8.7	5.2	1.8	3.9	0.9	1	3.8	2	11.9	4.6	2.1	0.2	3.1	0.2	3.1	2	1.1	3.8	1	0.5	1	1.4	5.5
3.71	2.4	0.7	4.3	0.4	29.4	3.4	16.4	0.8	10.9	15.1	5.6	4.6	0.6	2	0.5	0.1	7.2	5.2	11.8	3.8	0.8	0.6	0.8	0.2	1.8	0.5	0.5	1.9	0.5	0.6	0.4	1.7	4.1
7.13	0	0.3	2.8	98.2	0	8.7	0.1	0	0	11.2	13.6	0.1	0.2	10.9	0.1	4.6	0.3	0	0.1	1.5	0.7	0.6	4.9	1.3	1.2	4.7	0.8	11.1	33	47.3	44.9	32.4	
7.52	2.1	1	5.6	15.4	35.8	7.1	11.4	0	12.5	26.1	9.2	4.2	1	0.4	0.4	0.8	1.1	0.2	11.4	0.2	4.2	0.1	2.4	3.4	2	1	0.5	0.8	3.8	4	9.4	5.8	6.6
8.01	0.2	1.9	0.1	0.1	89.1	5.5	35.2	0.7	25.6	16.5	3.9	13.6	0.1	0.5	0.8	0.7	0.2	0.8	0.6	0	0.1	0.3	0.1	1.5	1.4	1.4	0.6	1.1	0.3	0.4	1	0.2	0.6
8.98	0	1.3	9.1	4.7	3.7	78.5	2	0.4	3.9	0.6	4.2	5.4	0.7	4	0.5	3.4	1.1	0.6	1.4	0	6.2	0.4	1.3	5.4	0.7	0.3	4.8	4.9	3	1.5	1.5	1.5	0.9
10.64	2.7	2.4	0.5	0.5	38.4	3.4	77.7	0.6	34.4	15.3	10.6	6.3	3.5	2	0.8	1.1	0.2	0.4	0.2	0.3	0.1	0.7	0.9	1	0.9	1	0.1	1.4	0.1	0.5	2.6	0.7	1.6
11.72	0.1	1.6	1.9	0.5	35.3	4.5	50.6	4.8	72.6	45.4	1.3	9.5	0.3	1.5	1	0.4	0.3	0.6	1.1	0.2	0.5	1.1	0.7	1.8	0.6	3.5	1.5	0.7	2.2	1.4	1	0.5	0.6
12.11	0.9	0.8	5	17.7	17.7	1.8	12.8	2.3	40.8	62.4	8.5	6.2	0	17.1	0.2	16	0.1	0.8	0.6	0.4	1.7	16.6	0.2	6.7	1.1	0.1	0.6	4.5	2.3	17	24.6	21.2	13.8
12.7	5.6	3.7	7.6	2.1	6.1	13.1	7.8	12.9	12.5	4.5	12.3	33	26	8.9	21.8	0.6	12.1	8.1	4.3	0.2	0.9	1.2	2.3	1.7	1.2	8.2	4.5	2.7	1.4	10.9	3.4	2.4	2.4
12.89	2.3	1.4	2	14.2	5	8.4	2.1	3.4	8.8	1.7	6.6	20	10.9	28	2.7	21.1	2.2	2.1	0.2	0.1	1.1	17.4	0.4	1.8	9.6	12.1	1.5	3.8	3.4	24.7	12.3	24	8.5
13.28	0.2	3.2	2.3	1	7.6	7.2	6.9	1.3	6.5	5.7	22.8	53.4	5.9	22	0.3	2.2	0.1	5.7	0.3	0	0.9	0.4	3	4.7	1.8	5.2	0.9	2.3	0.7	2.7	3.5	0.3	3.5
13.67	10	10.1	2.7	0.2	0.3	0.1	0.9	41.6	0.6	0.7	1	1.2	76.6	9.8	62.1	1.1	34.6	4.4	3	6.5	0.8	0.9	0.6	0.1	2.4	2.2	1.3	2	1.1	0.2	2.1	2	0.1
14.06	6.8	3.2	2.4	0.1	0.6	0.2	0.1	44.6	1	0.3	2.8	15.6	69.2	2.1	75.7	0.5	35.3	4.6	3.7	11.5	1.2	1.1	1.9	0.6	2.5	5.9	1.2	2.6	0.8	2.4	0.7	1.8	1.4
14.94	0	1.3	6.8	6.7	0.7	0.6	0.3	0.3	1.3	7.3	22.1	1.7	1.1	34.4	3.6	87.5	0.9	0.3	2.7	0.6	1.4	56.9	1.2	8.7	16.6	11.7	2.7	14.6	2	35.9	24.9	42	25.8
16.21	1.7	1.3	1.3	0.1	0.2	0.2	0.1	10.8	0.2	0	1.9	4.9	45.3	3.2	50	0.1	62.4	2.3	1.3	44.3	1.8	0.2	23	0	5.5	4.9	2	7.9	12.6	3.1	0.5	2.9	2.1
17.19	0.1	0.3	0.2	0	4.1	0.7	9.4	0.9	12.3	10.4	1	5	0.1	0.2	0.6	0.3	3	3	0.1	0.3	1.4	0.6	0.8	0	0.8	0.9	0.6	0.6	0.3	0.2	1	0.1	0.1
17.77	0.2	4.7	0.4	0.1	3.5	1.5	9.1	0.9	12.7	10	0.4	3.6	0.3	0.7	0.9	0.4	0.3	2.1	0.3	0.4	3	0.7	0.6	0.8	2.8	0.6	0.3	0.1	0	0.4	0.5	0.1	0.1
20.12	0.4	1.1	2.9	0.1	2.7	0.9	10.4	0.5	17.9	17.3	1.7	6.5	2.4	0.1	0.4	0.2	1.4	1.3	3.1	5.6	3.1	1.4	0.2	0.7	5.8	2	6.2	0.3	6.3	0	3.9	0.8	0.3
20.9	25.6	0	0.6	0.1	0.2	0.3	0.8	1.4	1.4	2.6	0.4	0	11.3	0.6	13.7	1	32.6	0	0.5	64.2	3.9	1.4	28.7	0.1	6.8	2	6.6	2.1	12.6	4.7	3.8	4.2	6.6
21.78	0.3	1.1	0.8	0.2	0.2	0.5	3.3	0.8	5.1	5.2	0.5	3.3	0.4	1.3	0.1	0.5	1.6	1.8	0.6	1.1	6.9	0.5	0.5	0.4	6.1	0.4	2.8	0.7	3.5	1.8	1.1	1.4	0.6
23.54	27	0.1	0.8	0.8	0.3	0.2	0	3.5	0.2	0.6	3.6	0.1	0.3	3.4	1	9.6	11.6	0.2	0.4	28.2	4.7	9.4	61.3	3.1	2.1	4.8	5.6	4.2	11	12.4	7.1	13.2	4.5
24.41	1.7	0.6	1.7	2.4	0.4	3.1	1	0.6	2.4	4.8	1.5	0.4	1.3	0.5	1.3	3.2	3.5	0.9	0.2	3.4	1.1	10.3	5	29.3	9.3	2.3	3.4	18.4	1	1.5	2.3	7.9	23.2
24.71	0.1	6.3	4.2	7.4	0.3	2	1	0.9	1.4	3	11.3	5.3	0.3	11.9	1.8	32.5	0.5	9	0.3	0.9	3.3	29.9	0.2	13	42.4	9.4	5.5	3.8	0.8	34.8	13.2	25.8	6.5
24.9	0.5	1.1	1.7	2.8	0.3	0.2	0.3	0.5	1.1	4.9	16.2	1.2	0.1	22.5	0.8	58.5	0.3	1.6	0.1	1.8	2.6	51.8	4.3	9.4	26.8	13.4	0.5	24.7	5.6	27.8	28.4	35.5	23.1
25.39	0	0.6	0.2	0.4	0.1	1.6	0.1	1	0.3	1	6.4	0.6	0	4.8	0.5	22.6	13.1	1.8	0.2	3.1	0.9	22.1	3.2	0.8	16.5	1.8	73.7	9.7	52.1	9.5	3.6	13.7	6
25.88	0.5	0.8	0.9	24.5	0.2	2	0.1	0.5	1.3	6.6	22.3	0.2	2.4	18.1	4.5	53	3.5	0.7	0.1	4.5	1.9	55.5	0.4	17	6	18.9	7.7	8.4	14.7	39.7	52.5	59.6	28.5
26.46	0.2	2.6	0.4	3.4	0.3	1.2	1	3.6	1.8	5	8.3	5.9	1.7	0.4	1.9	5.2	0.1	5.8	0	1.4	11.7	9.8	9.3	28.3	1.5	0.4	4.7	79.6	4.7	0.6	6.6	4.6	8
27.15	2.3	1.2	0.2	10.5	0.8	6.4	0.3	3.5	0.9	0.4	0.5	1.5	1.5	1.4	1.3	0.5	18.6	0.5	0.2	9.2	0.2	2.2	21.7	2.2	2.9	2.9	56.1	0.4	92.3	1.7	4.4	0.9	0.1
27.34	0.7	2	3.6	18.3	0.2	0.1	0.1	1.1	0.2	5.4	16.1	0.3	4.2	7.8	5.5	32.9	12.6	0.9	0	7.6	2.9	24.9	17.9	14.5	10	2.5	10.9	10.2	26.1	31.1	28.5	50.2	31.3
27.64	0.1	1.7	1.5	34.9	1.1	8.6	0.6	0	0.7	7.2	18.1	1.7	2.2	15.4	1.7	26.2	11.7	0.9	0.1	4	4.8	19.4	4	4.4	8	11.4	28.8	3.1	49.8	32.9	45.4	37.8	23.6
28.22	3.4	5.4	2.3	18.1	0.6	0.2	0.1	2.6	0.1	7.3	7.8	6.6	3.4	13.9	9.2	31.5	2.5	1.7	0.2	7.2	0.9	25.2	3.2	3.4	16.8	7.6	1.6	14.6	6.3	53.8	21.2	36.8	7.1

### 3.14 Test 23

Table 3.14 - MAC of ODS of Test 23 to modeshapes

freq Hz	1.82	3.24	4.13	7.08	7.74	8.88	10.69	11.05	11.63	12.07	12.84	13.26	13.67	13.79	13.94	14.95	16.32	17.56	19.06	20.85	23.28	23.49	23.62	24.23	24.58	24.77	25.41	26.51	27.12	28.1	28.22	28.31	28.44
1.95	56.4	2.6	1.5	0.4	1.7	0.2	1.6	28.5	2.4	0.8	0.3	0.6	5.2	2.3	3.3	0.3	3.2	0.7	0.2	22.4	2.3	0.2	20.9	1.8	2.1	1.3	1.2	0.9	1.9	1.2	0.6	1.2	11.8
3.61	1	5.7	7.5	0.4	31.6	3.3	20.7	0.6	13.3	15.8	6.6	6.9	0.6	4	0.2	0.5	0.9	1	11.3	2	1.5	0.6	0.4	0.4	0.8	0.8	1.7	2.9	0.2	1.3	1.2	0.9	3.8
8.01	0.3	0.5	0.3	0.1	88.4	5.1	33.4	0.6	24.1	15.5	3.4	11.3	0	0.4	0.8	0.8	0.6	2.1	0.4	0	0.1	0.3	0	1.3	1.6	0.9	0.5	0.7	0.1	0.3	0.7	0.4	0.5
10.64	4.3	3.5	0	0.3	36.6	4	68.8	1.4	35.3	17.7	7.3	5.1	4.1	1.1	1.1	1.3	0.3	0.3	0.3	0.2	0	0.3	1.2	0.7	0.6	0.5	0.1	1.7	0.1	0.5	2	0.5	1.4
11.43	5.7	0.9	1.3	0	21.9	4.6	24.9	24.4	60.5	41.7	0.8	14.1	9.6	0.7	12.9	0.9	2.8	1	5.5	0.1	0.4	1	1.7	2.6	1.3	3.9	2.1	1	1.8	0.9	1.2	0.1	0
13.28	0.8	2.2	4	0.2	17	13.3	14.4	4.7	15.2	13.2	28.7	77.7	0.9	19.1	6.2	1.5	1.9	6.9	0.7	0.3	3.7	0.3	0.8	2.1	5.2	10.2	2.7	4.4	2.5	7.4	3.4	1	2.6
15.04	0	2.9	5	3.5	5.5	2.3	8.3	1.1	10.3	16.4	22.2	4.4	0.2	19.3	0.8	72	1.8	3.3	3.2	0.4	2	41.9	0	5.9	15	15.2	5.1	16.9	0.2	15.1	19.8	29.2	17.5
17.29	0.1	3	0	0.1	3	0.8	6.1	0.9	9.4	6.9	0.5	2.9	0.8	0.1	1.8	0.5	0.5	2.9	0.1	0.2	1.3	0.7	1.1	0.5	0.4	0.1	0.2	0.3	0.4	0.3	0.2	0.1	
18.07	0.2	3.2	0.2	0.2	1.9	0.3	5	0.2	7	7	2	9.5	0.5	0.2	0.6	1.4	59.3	0.5	0.1	2	0.8	1.1	2.1	2.7	8.5	5.8	4.3	2.4	3.9	0.8	0.7	0.2	
19.34	0.3	1.2	1.3	0	5.6	0.4	14.9	0.7	20.9	16.4	1.9	11.4	1.2	0.1	0.3	0.2	3.7	11.4	4	2	5.9	1.2	0.2	0.3	2.2	4.8	6.5	1.1	4.9	0.7	1.2	0.1	0
20.21	0.5	1.9	1.1	0	3.4	0.5	12.3	0.4	18.2	14.5	1.6	10.4	0.6	0.4	0.2	0.5	1.4	6.1	1.2	0.8	0.7	0.1	4.4	2.7	4.2	0.7	4.4	0.4	1.7	0.4	0.4	0.3	
21	20.8	0.8	0.2	0.1	0.4	0.1	1.6	1.2	2.4	2.3	0.7	1.7	7.9	0.2	12	0.8	20.6	1.6	0.4	67	4.4	0.6	28.6	0.3	3.6	5.1	6.4	2.8	8.1	6.7	3	4.1	10.3
21.78	0.5	0.5	1.5	0.3	0.4	1	0.9	0	0.9	0.5	0.5	2	0.2	0.1	0.4	0.7	1.5	4.1	0.4	1.4	6.3	0.3	3.9	0	0.7	4.9	4.3	0	2.7	3	0.4	1.9	3
24.71	0.8	3.7	11.8	6.3	0.4	2.5	0.6	0.6	3.3	4.2	7.7	0.2	0.6	6.6	1.4	15.8	0.2	2.7	0.8	0.1	4.5	33.4	3.9	20.5	23.2	1.6	3.5	3.8	2	16.8	8.9	16.2	11.6
28.03	0.9	24.1	0.4	8.3	2.5	2.2	2.2	0.1	3.8	3.9	14.1	18.4	1.8	1.1	0.1	8.2	2.9	10.2	0.3	0.5	0.1	4.5	0	7.1	11.1	1.8	4.9	8.6	0.1	1.1	23.4	17	16
27.05	3.7	7.5	2.5	0.6	1.1	1.3	1.6	10.1	3.9	3.6	5.4	13.6	1.7	0.6	5.9	2.6	1.9	16.5	0.1	0.6	5.6	10	7.1	3	1.4	4.8	29.1	19.7	21.7	3.6	7.6	2.3	0.5
28.61	2.3	2.3	0.3	15.4	1.2	1	0.8	5.6	3.6	3.3	12.5	2.5	8.1	6	6.8	12.8	2.1	0.6	0.1	2.6	4.3	8	2.1	1.7	0.5	11.5	1.2	6.6	1.5	12.8	28	31.5	23.6
29.39	0.2	1.1	4.8	1.8	7.5	1.5	0.9	0.7	4.7	5.6	0	0	0.2	7.3	0.6	3.2	0.1	1.1	1.6	0.1	2	1.5	0.7	1.1	4	1.4	1.2	0.7	0.4	3.1	5.7	5.4	1.3





### 3.15 Test 24

Table 3.15 - MAC of ODS of Test 24 to modes

freq Hz	1.82	3.24	4.13	7.08	7.74	8.88	10.69	11.05	11.63	12.07	12.84	13.26	13.67	13.79	13.94	14.95	16.32	17.56	19.06	20.85	23.28	23.49	23.62	24.23	24.58	24.77	25.41	26.51	27.12	28.1	28.22	28.31	28.44
1.86	88.1	2.6	0.5	0.1	0.6	0.5	0.4	31.8	0.5	0.3	1.8	0.4	13.7	0.1	8.6	0.1	0.2	0.1	0.3	14.8	0.5	0.7	18	1	0.4	0.6	0.3	0.1	0.5	7.9	0	0.3	14.6
3.61	0.2	3.4	1.3	0.2	35.6	3.7	28.8	0.8	27	25	4.7	8.9	0.8	3.7	0.1	0.3	4.6	10.3	11	0.3	3.2	1.1	0	0.2	0	3.6	1.4	3	0.2	0.6	1.4	1.4	1.8
3.91	0	0.4	36.6	0	19.3	5.3	13.6	0.7	11.5	13.5	3.8	5.3	0.6	8.1	1.6	2.7	0.1	0.3	4.7	1.1	3.8	1.8	0.2	3.6	4.2	1.8	1.8	0.6	1.5	1	0.3	0.3	0.8
7.13	0.8	0.2	3.1	66.2	5	5	0.6	4.7	2.3	10.6	10	3.4	4.2	3.5	5.2	0.9	8.6	1.3	3	1.7	2.7	0.6	3.2	1.7	1.5	2.3	4.6	2	10.1	14.6	37	29.1	21.9
8.01	0.4	1.1	0.5	0.7	93.1	5.1	44.6	1.4	48	24.4	0.4	14.6	0.1	2.1	1.4	1.1	1.5	3.6	0.2	0.2	2.6	1.6	0	0	1.7	7.5	0.6	0.1	1.1	4.8	0.3	2.6	0.5
10.64	3.1	0.1	0.8	0.5	46.9	3	88.9	0.6	52.7	24.7	12.6	6	4.9	1.2	1.7	2.2	0.2	3.2	0	0.1	1	0.4	1.1	0.2	0.5	2.4	0.1	1.4	0.4	1.2	3.1	0.2	1.6
11.13	8.4	3.6	1.4	0.9	16.9	4.4	14.8	24.8	47.5	45.9	5	14.6	8.9	1.5	10.6	3.9	2.3	2.1	5.4	1.3	0.4	4.3	2.2	3.9	2.8	2.8	3.4	2.2	2.4	0.6	5.6	2.7	3
11.43	8.9	5.1	4.6	0.6	26.3	4	22.8	30.4	40.7	40.2	16.8	18.4	16	5.4	17.7	0.4	6.5	5.3	1.8	0.2	0.2	1.2	1.6	4.7	2.9	12.3	2	1.1	1.7	0.1	4.8	0.8	4.4
12.21	0.1	0.1	2.9	21.6	7.6	0.4	3.8	0.4	37.3	69.2	4.7	2	0.6	11.8	0.6	17.5	0.2	1.5	2	0.1	0.3	11.3	0.1	1.7	0.2	3.6	0	2.6	1	12.7	25.9	26.2	16.8
13.28	1.7	0.9	0.4	0.1	13.8	11	10.6	5.8	13.2	8.6	32.4	46.2	6	4.8	14.1	1.9	6.1	10.7	0.5	1.2	4	0.2	0.6	0.8	4.2	13.3	3.1	3.7	2.7	8.5	3.2	0.5	1.4
13.77	17.2	6.5	8	0.2	0.2	0.3	1.6	50.9	1.4	3.6	3.9	2.3	86.6	11.7	82.3	1.1	38.4	0.3	8.4	11.5	0.7	0.6	0.3	0.2	2.7	3.6	0.4	0.6	0.7	0.7	2.6	1.6	1.3
14.06	15.2	3.3	5	0	0.8	1.4	0.1	54.3	0.2	0.2	9.1	25.1	76.1	1.5	84	0.2	41.5	4.9	4.2	15.4	1.1	0.4	0.4	2.4	6.7	9.8	2.4	1.7	1.4	1.4	0.6	0.7	2.8
15.04	0.5	1.3	1.7	0.5	7.7	5.6	9.2	0.3	15.7	18.6	11.8	3.7	0.7	10.7	0.8	60.2	0.6	3.4	2.6	0.3	5.1	34.2	0.8	2.3	8.5	11.8	3.8	8.4	1.1	11	7.8	17.6	9.1
16.31	2.6	15.1	1	2.3	0.1	1.9	0.3	18.7	0.4	1.4	5	6.4	36.6	3.7	39	5	38.8	3.2	2.4	25.2	0.9	2.1	8.9	1	8.8	1.1	3.9	14.9	3.9	2.4	0.1	0.6	2
17.29	0.2	1	0.1	0.2	5.7	1.2	8.1	1.4	11.7	9	0.8	2.9	0.4	0.3	0.8	1	1.9	3.3	0.1	0.2	1.1	0.9	2	0.1	1.5	0.2	0.2	1	0.5	0.8	0.7	0.8	1
18.95	0.2	9	0.3	0.2	7.9	2.4	8.1	1.7	11.7	7	2	3.5	0.4	1.7	1.6	0.1	9.5	17.7	25.2	0.2	6.1	0.8	1.7	1.7	0.3	2.2	2.8	0.5	1.4	0.4	0.7	0.5	0.8
20.02	1.2	0.3	3.6	0	12.3	2.3	18.6	1.9	26.7	20.5	3	9.4	0.8	0.1	0.9	0.7	4.1	7.6	5.6	1.6	3.7	0.4	1.3	0.2	5.3	3	3.8	0.2	3.6	0.9	1.8	0.5	1.2
21.88	2.4	3.3	2.5	1.2	0.5	1.1	1	0.9	1.1	3.3	0.9	3	0.4	2.9	0.1	1.1	1.1	0	4.9	7.2	1.6	1.6	7.2	0.3	6.8	6.5	0.3	1.7	1.7	3.7	4.8	5.8	2.8
24.71	2.4	5.1	7.7	2.6	0	1.5	2.7	2.5	7.4	10.3	6	0.4	1.7	9	1.8	15.7	0.7	3.8	2.4	1	6.9	24.1	2.3	13.7	23.1	5.5	2.7	1.5	0.6	12.7	10	12.8	6.6
25.49	1.4	0.7	0.3	8.6	0.3	1.6	0.2	0.8	0.5	0	2.2	6.1	0.8	0.7	1.4	0.8	17.2	5	0.4	4.4	3.7	1.6	4.3	6.6	7	3.6	49.3	1.5	58.7	0.1	8.7	2.7	3.2
20.31	1.1	0.6	4.3	0.1	11.9	2	20.2	1	26.8	21.1	3.6	8.4	1.9	0.6	0.8	2.8	7	5.9	1.6	2.8	1	0.6	0.3	5	3.8	4.7	0.7	3.9	0.3	2.9	0.5	0.8	
26.46	0.1	0.2	5.5	2	0.5	5.6	0.2	1.4	0.8	0.8	0.7	4.5	0.1	3.9	0.4	4.6	0.1	1.1	0.1	1.1	13.1	1.2	5.4	33.2	7.4	23.3	0.9	38.4	0.1	5.6	2.6	6.6	5.5
27.44	7.6	1.8	0.6	3.5	2.3	0.2	0.9	15.2	0.9	1.4	8.9	2.5	23.9	7.6	20.2	6.9	32.1	0.5	0	16.4	0.6	8.5	14.4	1	1.8	4.7	15.4	9.5	32	7.5	15.2	12.7	6.6
28.03	0.1	11.4	1.6	4.2	3.4	0.3	4.9	0	6.7	2.5	4.4	17.3	0.2	4.6	1.6	3	1.3	4.7	1.1	1.5	5.2	0.6	4.5	0.3	17.4	11.9	10.7	0.9	3.4	31.2	7	6.3	3.8
28.61	3.9	1	1.1	2.6	3.9	4.5	1	18.5	0.8	1.3	8.4	15	26.8	3.4	28.4	1.1	20.9	0.9	1.6	9.2	0.2	2.3	1.8	1	2.3	0.2	1.9	4.1	1.9	2.1	11.8	8.8	17.6
29	1.2	0.5	7	3.7	1.1	3	1.6	0.8	6.2	12.4	12	5.1	1.2	4.7	0.6	5.7	0	2.3	0.4	0.4	6.6	6.9	2.5	5.1	2.2	4.3	0.4	0.4	0.2	3.1	11.7	5.8	7.9

### 3.16 Test 31

Table 3.16 - MAC of ODS of Test 33 to modes

freq Hz	1.82	3.24	4.13	7.08	7.74	8.88	10.69	11.05	11.63	12.07	12.84	13.26	13.67	13.79	13.94	14.95	16.32	17.56	19.06	20.85	23.28	23.49	23.62	24.23	24.58	24.77	25.41	26.51	27.12	28.1	28.22	28.31	28.44
1.76	95.7	3.2	0.8	0.1	0.5	0.3	0.7	40.9	0.6	0.4	3.3	1.2	16.4	0.3	11.5	0.2	0.8	0.2	0.2	13.7	0.2	0.4	13.4	0.4	0.9	1.4	0.3	0	0.8	7.4	0	0.5	15.6
3.61	1.6	1.5	2.7	0.2	35.9	3.2	29.4	0.8	28.9	27.5	5.4	8.7	0.8	4.2	0.2	0.4	1.4	1.5	9.6	1.1	2.7	1.8	0.3	0.7	0.5	2.7	0.7	3	0.6	1	2	1.5	2.7
7.13	0.1	0.8	2.2	99.3	0.6	9.4	0.3	0	0.7	11.8	6.4	0.2	0.1	6.2	0	0	1.3	0	0	0	1.4	1.9	1.1	1.3	0.6	0.6	9.2	1.7	12.3	27.5	50.9	43.1	26.2
8.01	0.1	0.5	1	1.3	96	4.5	44.1	2	45.1	19.8	0.4	13.7	0.3	2	1.2	1.1	1.2	4.6	0.6	0.2	2.2	1.7	0.2	0.1	1.9	7.3	0.8	0.1	1.4	6.2	0.6	3.2	0.4
10.64	3.1	0.2	0.5	0.3	44	2.6	94.8	0.9	52.2	21.5	10.3	5.7	3.3	3.2	1	1.8	0.2	2.4	0.2	0.3	0.9	0.5	0.5	0	0.6	2	0	1.4	0.4	1.2	2.6	0.1	1.1
12.21	0.1	0.2	3.5	22.1	11.9	0.6	11.2	0.8	52.5	78.1	4.1	3	0	21.7	0.2	1.7	0.4	1.5	0.4	0.3	0.1	12.7	0.6	3.7	1.2	0.3	0.3	2.8	2.7	19.3	29.9	27.4	17.7
12.89	2.8	0.5	3.4	8.8	13.9	7.7	2.2	3.7	8.5	4.2	12.2	26.5	8.8	21.7	2.5	17.8	4.2	6.5	0.5	0.1	2.4	11.7	0.7	0.4	6.9	13.7	2.3	3.3	2	25.1	10.9	21.3	4.2
13.28	0.4	1.1	0.4	0.5	0.4	0.6	1.5	1.3	2.5	2.1	0.5	6.7	4.3	19.5	2.2	1	0.9	1.4	0.4	0.2	2.6	0.2	0.7	0.4	0	0.3	0.2	0.1	0	1.3	0.3	0.5	0.4
13.40	18.7	6.2	1.5	0.1	0.3	0.1	0.4	51.2	1.5	2.5	8.4	9.6	86.9	3.3	86.6	7.9	34.4	0.5	3.2	11	1	0.6	0.7	0.9	2.9	6.2	0.3	1	2.1	0.8	0.1	0.6	2.6
13.67	15.4	3.8	0.4	0	0.3	0.9	1	50.3	0.6	0.6	1.5	7.3	95	14.8	84.2	0.3	43	1.3	3.8	12.4	1.8	1.6	0.7	0.5	6.1	2.7	2.2	1.6	1.6	1.3	1.5	2.1	1.2
14.06	12.1	1.9	1	0.2	0.8	0.7	0	54.1	0.2	0.3	6.5	22.4	85	3.5	95.4	0.4	41.2	2.1	4.6	19.1	0.6	2.7	0.9	2.1	4.8	6.6	1.4	3.4	1.5	1.7	2.6	3.5	3.8
14.94	4.3	2	9.7	0.1	0.2	4.2	1.2	16.4	4.7	7.3	18.8	4.5	22.1	24.1	19.5	56.5	7.7	8	5.6	2.7	2	41.1	0.8	7	13	2.9	4.9	7.3	2.9	7.9	7.8	17	13
16.21	1.4	2.6	0.2	0.4	0.4	1.9	0.5	21.8	0.3	0.7	3.5	6.5	53.8	5.9	57.4	0.4	62.2	0.2	2.1	40.1	0	1.1	15.3	0.5	3.9	1.3	4.3	11.6	10.9	3	1.7	3.8	2.1
17.19	0.3	0.5	0.1	0	8.8	1.8	12.6	1.2	17.2	13.1	1.5	5	0.2	0.4	0.9	0.4	1.2	4.6	0	0.4	1.4	0.4	1	0.1	0.9	1.4	0.3	0.5	0	0.5	0.5	0	0.1
17.77	0.3	0.2	0.2	0.3	7.4	1.1	13.3	0.6	18.8	13.9	0.8	4.5	0.3	0.9	0.8	0.3	1.9	3.4	0.4	0.8	1.5	0.3	1.4	0.2	2.4	0.6	0	0.5	0	1	0.9	0.1	0.5
19.04	2	0.7	8.4	0.4	0.6	0.2	0.7	1.2	0.2	2.4	3.4	0.7	4.2	0.6	4.2	1.3	0.9	0.4	86.9	0.4	1.6	0.5	1.2	0.3	4	4.7	0.5	0.4	0	0.4	1.4	0.1	0.2
21.78	0.4	3.7	1.9	0.7	3.3	0.8	2	0.2	2.6	3.5	0.4	0.8	0.4	6.9	0.8	0.8	1	1.4	3.6	5.7	2	0.4	1.9	5	2	2.9	1	3	4.5	0.7	7.2	5.9	
23.63	1.3	0.8	0.6	3.1	0.5	2.8	0.2	0.1	0.4	0.4	1.2	0.1	0.9	0.5	1	9.4	4.6	0.1	1.6	14.3	1.6	10.2	80.3	3.5	0.1	7.2	1.9	13	6.3	4.6	0.4	4.8	8.4
24.51	1.5	0.4	0.9	2.8	0.2	3.3	0.4	4.1	1	3.3	1.4	1	0.5	2	0.3	4.2	1.8	1	0.4	1.1	2.4	7.5	3.1	52.5	4.7	7.2	0.5	29.5	0.2	0.3	3.1	7.9	36.2
25	0.1	0.6	1.5	0.3	2.2	1	0.4	0.1	3.4	10	13.9	0.6	0	14.2	0.1	58.9	0.5	0.3	0.1	2.7	0.9	5	6.4	21.4	11.6	0.2	20.8	3.7	18.6	26.7	30.1	15.1	
25.49	0.1	1	0.2	3.6	0.2	5.3	0.3	1.8	0.9	1	3	0.2	0	0.6	0.1	11.5	10.6	0.3	0.3	1.8	1.7	11.7	5.6	0.2	17.8	0.8	81	2.8	72.9	3	5.8	7.5	1.1
25.88	0.2	0.8	2	22.1	2.5	6.5	0.6	0.1	2.3	1.1	17.2	0.4	1	11.4	1.8	41.2	2.5	0.1	0.5	1.6	1.8	42.5	0.4	6.9	6.7	17.2	11.8	5.8	24.2	26.3	53.1	49.9	17.4
26.46	0.2	4.8	0.1	1.4	0.1	7.5	0.8	2.1	1.7	2.6	7.3	3.8	1.3	0.2	1.1	7.2	0.4	3.2	0	3.5	8.1	7.5	13.6	30.6	1.2	0	4.7	90.2	5.9	0.2	4.9	1.8	3.4
27.15	0.4	0.9	0	12.9	0.9	6.5	0.9	0.8	1.7	0.5	1.9	1.5	0.2	1.7	0.1	2.5	13.1	0.5	0.1	2.1	3.3	5.3	13.5	1.8	1.6	1.6	74.5	0.6	94.1	1.8	10.8	4	0.2
27.73	0.9	1.5	2.7	33.5	1.4	7.3	2	0	4.5	12.7	16.5	2.1	0.7	9.2	1.2	28.3	1.2	0.4	0.1	0.7	4.5	22.6	0.6	2	8.3	6.5	18.6	6	29.3	41.4	56.2	61.8	26.3
28.22	3	5.3	0.3	9	2.6	0.2	0.1	5.5	0.6	3.9	0.8	13.3	6.4	10.3	1.5	19.2	7.1	0.2	0.1	14.2	0.9	9.7	3.9	2.2	9	4.8	0.6	6.2	26	51.3	7.8	22.5	5.9
29.39	0.1	0.9	1.8	3.1	2.1	1	1.5	0.4	2.2	3.5	0.6	0.6	0.7	1.4	0.9	0.2	1.3	2.3	0.3	0.4	3.7	0.3	1.5	0.7	6.1	0.4	0.2	0.2	1.5	0.1	3.5	0.3	0.5





### 3.17 Test 33

Table 3.17 - MAC of ODS of Test 34 to modes

freq Hz	1.82	3.24	4.13	7.08	7.74	8.88	10.69	11.05	11.63	12.07	12.84	13.26	13.67	13.79	13.94	14.95	16.32	17.56	19.06	20.85	23.28	23.49	23.62	24.23	24.58	24.77	25.41	26.51	27.12	28.1	28.22	28.31	28.44
1.76	96.9	3.1	0.7	0	0.9	0.7	0.9	40	0.8	0.6	3.3	1.4	15.8	0.3	11.4	0.2	1.4	0.3	0.4	14.9	0.1	0.3	14.7	0.4	0.9	1.1	0.3	0	0.7	7.2	0	0.6	15.4
3.52	0.6	0.1	2.5	0.2	38.1	5.4	31.1	0.5	30.5	28.4	5.4	7.4	1	3.6	0.3	0.2	1.9	2.9	12.5	0.3	1.8	0.7	0.2	0.4	0.5	2.8	0.5	2.9	0.3	0.6	1.3	1.6	2.2
7.13	0.1	0.8	2.2	99.3	0.5	9.5	0.4	0	0.8	11.8	6.3	0.2	0.1	6.3	0	0	1.3	0	0	1.4	1.9	1.2	1.3	0.6	0.6	9.1	1.9	1.2	27.5	50.3	42.8	26.1	
8.01	0.2	0.8	0.4	0.4	96.1	3.6	45.3	2.1	45.8	22.2	0.7	14.1	0.1	1.9	0.9	1.2	0.8	4.1	0.6	0.2	2	1.7	0.2	0.1	1.9	7.3	0.5	0.1	1.1	4.6	0.2	2.3	0.3
9.08	1.2	4.2	8.4	6.7	3.3	84	1.7	0.3	2.1	0.3	6.6	6	2.2	4	2.1	4.8	3.9	0.9	2.7	2.8	9	0.1	5	8.5	0.1	0.6	5.9	9.9	2.8	3.1	5.7	4.4	1.3
10.64	2.9	0.2	0.5	0.4	43.9	2.7	94.7	0.7	52.8	22.1	10.3	6	3.2	2.9	0.9	1.8	0.2	2.6	0.2	0.3	0.9	0.5	0.6	0	0.7	2.1	0	1.5	0.4	1.2	2.8	0.1	1.1
11.04	35.1	2.2	0.2	0.2	4.8	0.4	10.5	84.7	10	4.9	1.7	9.4	46.6	3.9	47.8	1.2	12.9	0.4	1.2	0.3	0.9	0.6	0.1	3.7	2.1	3.7	6	3.4	0.8	0.9	2	1.3	0.5
11.23	11.7	2.2	1	0	35.3	2.4	51.7	48.9	46.5	20.9	7.4	17.1	18.9	1	24.5	0.6	8.7	2.5	2	0.8	2	1.6	1.2	3.6	2.1	7.2	5.2	2.4	1.3	1.3	1.2	0.6	0.7
11.72	0.3	0.8	2	0.6	51	2.5	62	3.3	94.2	66.1	3.9	9.6	0	3.9	0.6	4	0.7	3.2	0.4	0.6	1.1	2.2	0.7	1.5	0.5	4.2	1.6	1.7	1.5	2.1	3.5	1	2.4
12.21	0.1	0.1	3.4	21.4	12.4	0.7	11.1	0.9	52.1	76.4	4.3	3.6	0.2	22.1	0.3	17.1	0.7	1.8	0.4	0.3	0.3	13	0.6	3.6	1.4	0.3	0.4	2.9	2.8	18.9	28.9	26.5	16.9
12.99	0.4	1.9	4.5	8.7	3.5	10.8	14.7	0.8	6.2	9	65.7	32	5.1	5.8	1.4	26.7	3.4	12.5	1.9	0	1.4	11.1	2.7	3.5	5.3	10.5	3.5	9.2	0.1	2	24.8	16.8	11.7
13.26	1.9	1.1	0.3	0.7	0.8	0.2	0.4	7	0.6	0.8	1.4	1.5	11.7	16.2	10.6	1.9	4.1	0.3	0.6	1.2	3.2	0.1	0.4	0	0.7	0.9	0.4	0.1	0.1	2.1	0	0.8	0.6
14.06	1.2	18	1.1	0.3	0.8	0.8	0	53.6	0.4	0.5	6	22.8	84.8	2.9	95.3	0.9	41.3	2.1	4.6	19.2	0.7	3.3	1.1	2.2	4.6	6.5	1.5	3.7	1.4	2	3	4.1	3.5
14.75	0.1	1.4	10.8	1.3	0	1.4	4.4	3.5	10.4	14.9	22	2.7	2.8	21	2.6	77.3	1	4.8	2.6	1.3	1.1	49.3	2.1	7.8	14.4	4.4	3.5	9.8	1.3	11.5	17.4	24.3	16.9
15.04	0.4	3.2	6.8	0.9	0.1	2.7	5	0.1	15.6	21.7	17.4	3.6	2.2	15.6	1.7	73.6	4.1	2.1	3.3	0.6	0.6	43.6	1.7	5.2	6.3	2.9	2	11	1	10.1	20	23.3	15.8
16.31	1.1	2	2.3	0.3	0.5	1	0.7	17.5	0.4	0.8	2.9	7.2	45.4	4.3	50.8	1.6	55.9	0.2	3.8	43.1	0.2	1.2	14.1	0.5	7.7	1.9	3.3	12	8	4.3	1.7	3.2	3.7
17.19	0.2	0.5	0.1	0	8.8	1.8	12.9	1.2	17.6	13.5	1.6	5.4	0.3	0.4	1.1	0.4	1.1	4.5	0	0.7	1.5	0.5	1.3	0.1	0.9	1.3	0.2	0.7	0	0.5	0.7	0	
17.77	0.5	4.4	0.3	0.2	7.6	1.6	11.1	0.9	16.2	11.8	0.8	2.6	0.2	0.1	0.9	0	1.1	0.8	0.3	0.5	2.1	0.2	1	0.8	2.7	0.7	0.2	0	0	0.6	0.4	0.2	0.1
19.14	0.9	0.5	10.6	0.1	0.8	0.1	0.5	1.4	1.5	0.2	2	1.3	3.7	1	5.4	0.9	2.2	0.1	86.5	1.9	2	1.7	0	0.1	4.3	8.1	0.2	0.5	0.5	1.9	1.6	1.2	0.1
19.73	0.5	0.5	0.4	0.3	20.5	2.3	25.7	1.5	36.5	23.3	0.7	7.1	0.1	0.5	0.4	0.1	0.8	4.3	2	0.6	5.6	0.6	0.3	0.7	1.2	4.2	4.1	0.1	5	2.3	0.2	1.1	0.3
20.9	12.1	0.3	0.9	0	0.3	0.4	1	0.3	1.2	1.9	0.2	2.2	12.8	1.2	17.9	0.4	29.3	0.1	1.2	93.9	0.4	0.4	20.1	0.5	3.6	2	5.4	4.2	4.9	12.2	0.9	4.2	10.3
21.78	1.1	1	5.5	0.9	2.1	0.5	2.1	0.2	2.7	2.7	2.3	2.3	0.5	2.3	0.2	4.1	1.2	1.5	1.4	0.7	7.8	0.8	0.8	0.1	3	1.5	1.3	0.6	1.4	5	0.9	4.6	2.5
23.63	15.1	0.6	0.3	1.4	0.1	2.3	0.4	0.1	0.5	1.1	0.1	0.2	1	0.5	0.7	0.9	6.8	0.2	0.8	18	1.5	1.3	87.3	1.2	0	2.3	5.1	11.2	12.3	7.4	0.2	1.7	4.6
24.51	1.8	0.3	0.7	3.1	0.3	2.8	0.4	3.9	1	2.7	0.7	1	0.8	1.7	0.5	2.6	2.3	0.6	0.7	2	1.7	3.9	3.3	41.5	6.6	3.3	1.1	30.6	0.3	0.3	1.5	6.3	33.7
24.8	0.9	6.1	2.6	1.7	4	11.2	5.6	0.9	6.4	2.5	4.2	26.5	0.2	12.4	2.3	6.3	2	6.7	0.2	4.1	6.4	5.9	0.8	6.4	28.3	5	1.4	2.8	1.8	21.7	1.2	7.8	0
25	0	0.4	1.7	0.4	2.3	0.8	0.4	0.1	3.3	10	13.4	0.5	0.1	14.6	0.1	58	0.5	0.2	0.2	2.5	1.3	59.7	4.7	7.2	22.6	12	0.2	19.3	4.4	19.8	27.9	30.7	15.1
25.49	0.1	0.8	0.2	3.3	0.1	5.4	0.2	1.7	0.8	0.7	2.7	0.4	0.1	1.1	0.2	12.1	9.8	0.2	0.2	2.9	1.3	10.8	5	0.5	20.3	0.3	78.1	4.3	67.6	4.5	3.1	6.8	1
25.88	0.1	1.2	1.5	26.2	2.8	8.1	0.6	0.6	2.6	8.8	11.2	0	1.4	8.5	2.5	36.4	1.9	0	0.4	0.5	2.1	36.6	0.3	5.4	16.5	20	3	34.2	23.7	54	50.9	17.2	
26.46	0.1	3.5	0.1	4.6	0.1	7.4	0.7	2.3	1.3	3.1	6.1	4.2	1.1	0.3	1.1	4.4	0.5	2.8	0.1	2.8	8.5	9.1	11.7	32.3	1.2	0.7	7.2	78.9	5.6	2.3	5	5	10.9
27.25	0.7	0.9	0.3	11.1	1.2	4.4	0.6	0.7	0.9	0	0.3	1.3	0.7	2.2	0.7	0.4	15.6	0.4	0.1	4.1	2.5	0.9	18.9	3	0.6	2	68.6	0.3	92.8	3.5	11.9	3.9	1.3
27.44	0.5	1.8	4.6	20.7	2.1	0.5	0.1	0.6	0.5	9.2	10.6	0.3	2.4	7.7	1.9	29.5	9	0.2	0.1	4.4	3.2	19.9	10.2	6.8	5.5	7.5	10.2	6.8	20.2	33.1	45.6	62.5	31.8
27.83	0.7	0.9	2.5	35.6	1.1	6	1.8	2	4.3	14.1	12.7	0.3	4.3	12.2	5.4	26.9	5.1	0.1	0	2	4.7	20.7	2.6	2.1	7.5	8.2	17.6	2.5	31.1	41.2	53.1	58.4	23.5
28.32	5.5	3.9	0.3	8.2	2	0.4	0.2	5.2	0.6	4.4	0.1	10.3	5.7	6.3	13.8	15.4	5.4	0.1	0.4	13.6	0.5	7.4	3.4	5.4	6.2	5	0	12.4	5.5	51.6	12.2	21.2	2.7

### 3.18 Test 34

Table 3.18 - MAC of ODS of Test 34 to modes

freq Hz	1.82	3.24	4.13	7.08	7.74	8.88	10.69	11.05	11.63	12.07	12.84	13.26	13.67	13.79	13.94	14.95	16.32	17.56	19.06	20.85	23.28	23.49	23.62	24.23	24.58	24.77	25.41	26.51	27.12	28.1	28.22	28.31	28.44
1.88	82.6	1.6	0	0.5	0.9	0.6	0.4	43.9	0.2	0.1	2.4	2.7	19.7	0.3	17.7	0.9	1.7	1.8	0.8	7.7	0.2	0.7	6.1	0.8	0.1	0.3	0.2	2.3	2.3	3	1.2	0.8	9.4
3.52	0.4	0.5	0.4	0	35.7	1.8	25.9	0.3	24.5	20.6	2.4	4.8	0.8	2.4	0.1	0.2	1.5	4.3	8.1	0.1	2.7	0.8	0.2	1.9	1.5	5.3	0.1	1	0.1	0.5	0.2	0.3	0.8
4	0.5	0.6	10.4	0.3	26.9	6.7	21.9	0.3	18	21.2	6.9	9	1.8	7.9	0.6	1.2	0.9	1.9	13	0.3	1.2	1.1	0	0.7	1.2	1	1.4	2.2	0.7	1.4	1.6	0.8	1.5
7.13	0.1	2.3	0.1	80	0.9	15.3	0.6	0.2	0.7	8.5	2.9	0	0	7.7	0.1	0.4	1.3	0.1	0	0.4	1.4	1.3	0.4	0.8	0.3	0.3	5.7	1.2	8.9	19.8	37.2	31.2	17.8
8.01	0.2	0.5	0.8	1.1	94.6	3.9	43.1	2.3	43.7	19.8	0.4	14.3	0.2	2.1	1.3	1.4	1.4	4.7	0.5	0.4	1.6	1.6	0.1	0.1	2.5	8.5	0.8	0.1	1.3	5.7	0.5	3.2	0.6
9.08	0.4	7.4	11.8	7.1	2.8	71	1.9	1	1.3	0	2.3	3	1.6	6.8	0.7	2.4	0.8	0.1	1.4	0.7	5.7	0.4	2.1	10.1	0.6	0.5	3.9	7	1.9	3.4	6.8	3.7	1.8
9.67	1.7	11.2	14.7	4.8	11.2	14.3	27.5	0.6	28.9	26.4	6	2.4	7.3	1.5	4.9	0.6	6.1	14.2	1.6	2.6	4.3	5.6	2.1	12.6	3.7	3.3	0.9	5.4	0.8	0.2	11.7	2.4	0.8
10.64	3.4	0	0.4	0.3	43.9	2.6	93.2	1.5	51.2	22.1	9.7	5.4	4.1	3.1	1.5	1.4	0.2	3.2	0.1	0.1	0.8	0.3	0.5	0	0.6	1.8	0	1.3	0.4	1.1	2.3	0.1	1





### 3.19 Test 35

Table 3.19 - MAC of ODS of Test 35 to modeshapes

freq Hz	1.82	3.24	4.13	7.08	7.74	8.88	10.69	11.05	11.63	12.07	12.84	13.26	13.67	13.79	13.94	14.95	16.32	17.56	19.06	20.85	23.28	23.49	23.62	24.23	24.58	24.77	25.41	26.51	27.12	28.1	28.22	28.31	28.44	
1.86	92.4	3.7	1.1	0.2	0.3	0.3	0.4	37.5	0.7	0.8	2.8	1.1	14.5	0.6	10.2	1.1	1	0.5	0.2	16	0.3	0.3	14.1	0.6	1.7	0.9	0.5	0.2	0.4	5.7	0.2	0.5	19.1	
3.61	0.9	0.8	3.2	0.4	32.3	0.7	25.7	0.5	26.1	22	2.4	5.3	0.5	2	0.2	0.8	1.6	1.4	5.6	1.3	4.4	0.8	0	1.9	2.3	5.1	0.2	3.1	0.6	1.3	1.8	2.7	3.9	
7.13	0.1	0.8	2	98.7	1.7	9.8	0.1	0	0.2	10.5	6.3	0.1	0.1	6.4	0	0	1.4	0.1	0	0	1.4	1.5	1.2	1.3	0.4	0.7	9.2	1.8	12.6	27.9	50.5	43.8	26.3	
8.01	0.2	0.9	0.7	0.7	96.5	4.2	44.9	2.1	45.6	21.1	0.5	13.6	0.1	2	1	1.1	0.9	4	0.5	0.2	1.8	1.7	0.2	0	1.9	7.1	0.7	0.1	1.3	5.1	0.3	2.8	0.3	
10.64	3.7	0.3	0.4	0.4	45.2	2.4	92.8	1.4	53.5	23.4	9.7	5.5	3.5	2.4	1.1	1.9	0.1	2.4	0.3	0.2	0.8	0.5	0.7	0	0.6	1.9	0.1	1.5	0.5	1.2	2.5	0.1	1.1	
11.82	1.3	1.1	1	1	0.6	50.4	3.1	55.7	6.1	92.9	71.8	4.6	10.4	0.7	3.1	1.4	4.5	0.6	3.5	0.7	0.3	0.8	2	1.2	1.7	1.3	6.2	1.6	1.7	1.1	0.7	3.7	0.6	
12.21	0.5	0.2	4.6	21.7	7.9	0.5	5.7	0.2	38.6	72.4	3.9	3	0.2	14.9	0.6	18.3	0.6	1.7	1.5	0.3	1.4	15.6	0.7	1.5	0.7	1.3	0.3	4.2	2.7	18.7	32.5	29.2	14.4	
13.28	2.7	0	0.4	0.2	5.8	1.2	1.3	12.1	2	1	12.6	15.6	11.2	6.8	20.4	0.4	9.9	3.1	0.9	2.8	1.4	0.7	0.9	1.6	1.9	7	1.9	1.2	0.9	7.7	2.5	0.8	0.7	
14.06	11.9	2	1.1	0.3	1.5	0.9	0.2	54	1	0.7	6.8	26	82.4	2.7	95	0.7	41.3	2.7	4.3	18	0.7	3.2	1	2.2	4.1	7.1	1.7	3.9	1.3	2.4	3.2	3.7	3.4	
16.31	0.6	1.2	2.1	0.8	0.9	0.7	0.9	16.6	1	1.4	1.6	7.2	44.2	3.5	50.5	6.1	41.1	2.7	3.2	36.9	0.4	3.9	15.2	0.9	4.1	1.5	0.7	18.6	5.1	4.8	2.9	5.9	2.2	
17.19	0.2	0.8	0.1	0	8.6	1.7	12	1.3	16.2	11.7	1.2	5.1	0.4	0.4	1.3	0.1	1.1	3.3	0.1	0.6	1.2	0.2	1	0.3	1.1	1.1	0.2	0.5	0	0.8	0.4	0.1	0.1	
17.77	0.5	0	0.3	0.3	4.4	1.5	8.5	0.5	12.5	9.4	1.2	3.6	0	0.3	0.6	0.1	1.7	4.7	0.2	1	1.4	0.4	2.7	0.1	1	1.5	0	0.5	0.1	0.7	0.8	0.2	0.2	
19.63	3.8	2.8	0.7	0.2	14.7	1.5	25	1.3	34.9	29	2.7	5.7	2.2	0.8	1.1	0.7	0.5	5	0.7	1	2.8	0.4	0.5	1.1	2.9	5.2	2.2	0	2.5	0.2	1.3	0.8	0.5	
19.92	1.7	2.2	1.2	0	16.8	2.8	25.6	1.5	34.7	25.8	2.7	10.1	0.1	0.2	0.4	0.4	1.6	4.1	0.7	0.5	2.7	0.1	0.7	0.8	1.6	8	2.9	0.2	2.5	1.5	1.5	1.4	0.2	
21.78	1.3	0.7	2.3	0.4	3.2	1.1	3.4	0.1	4	2	2	1	4.5	0.4	3.7	1	0.9	2.6	0.8	8.3	1.9	0.8	0.7	4.8	0.7	1.3	0.8	1.7	3.7	0.6	3.8	2.7	3.4	
23.63	15.4	0.4	0.5	1.7	0.5	2.5	1.1	0	1.5	1.9	0	0.4	0.6	0.2	0.5	0.7	6.1	0.5	0.6	17.8	1.8	0.7	84.7	1.4	0.1	3.6	6.4	10.2	12.5	8.2	0.5	3.1	4.6	
24.51	1.9	0.3	1.4	5.9	0.2	1.9	0.8	5.8	2.6	6.8	3.4	2.4	1	2.3	0.8	5.9	3.1	2.1	0.7	1	2.2	11.3	3.9	45.9	8.6	4.5	0.9	21.2	0.7	1.4	6.3	11.5	41.6	
24.71	3.1	6.7	6.6	1.1	0.7	2.8	1.4	0	2	0.4	0.9	7.1	0.4	9	0.5	6.1	0.2	4.1	1.2	4	9.6	8	0.1	8.8	22.2	0.2	1.4	0.7	1.5	12.2	1.8	6.2	0.7	
25.49	0	1.6	0.4	2.6	0.6	3.8	0.1	1.2	0.5	0.4	1.2	2.5	0	2.6	0.5	11.4	10.8	0.2	0.2	4.5	0.9	11.5	5.4	0.4	21	0.8	71.7	2.8	63.6	6.7	2.9	6.8	0.6	
25.88	3.4	3.3	0.2	1	0.5	4.5	0.9	1.6	2.7	2.7	4.1	11	4.7	4.3	9.6	4	5.9	3.9	1.3	29.6	1.3	3.3	13.8	3	2.5	5.7	5.6	18.1	3.1	16.5	4.8	18.8	19	
26.56	0	1.9	0	4.2	0.9	10.1	1.1	2	2.3	1.6	1.6	3.7	6.2	2	2	2.8	0.3	0.6	3.5	0	3	13.1	3.9	12.9	30.9	0.5	3	2.6	79.3	1.9	4.6	1.3	2.4	9.4
27.25	0.4	1.2	1	13.2	1.3	7.7	1.3	0.4	2.4	0.7	2.3	1.3	0.7	2.4	0.7	3.4	1.7	1.5	0.3	4.4	3.3	6.3	12.8	0.1	3.5	2.1	69.8	0.1	88.9	2.1	10.1	5.4	1.2	
27.54	1	1.4	2.2	9.5	2.3	0.2	0.2	1.9	0.5	7	8.1	0.8	4.9	9.5	3.1	30.4	14.4	0.6	0	7.7	1.9	21.5	13	2.9	6	14.4	12.3	12.6	31.1	19.5	35	45.2	20.3	
28.22	4.8	0.9	0.5	11.2	0.5	0.4	2.2	12.3	3.5	10.9	3.7	2.3	16.3	5.2	20.8	15.2	9.1	0.1	0.2	13.8	0.5	5.9	4.8	1.8	2.5	2.4	0.4	10.2	3.8	27.1	18	15	9.2	
28.61	23.6	5.2	0.5	13	0.1	1.1	0.2	13.1	0.5	1.6	6.4	2.8	16.1	2	15.8	4	7.4	0.7	0.9	3.3	1.6	1.1	0.4	15.4	3.1	0.8	0	15.4	2.1	1.9	3.5	9.3	59.3	
29.39	1.1	0	0.8	0.2	2	0.1	1	1	2.2	1.5	0.4	0.8	0.8	0.5	1.5	0	0.6	1.7	1	0.6	1.9	0.6	0.6	0.5	1.7	1.3	0.9	0	0.7	1.3	0.3	1.3	1	

### 3.20 Test 36

Table 3.20 - MAC of ODS of Test 36 to modeshapes

freq Hz	1.82	3.24	4.13	7.08	7.74	8.88	10.69	11.05	11.63	12.07	12.84	13.26	13.67	13.79	13.94	14.95	16.32	17.56	19.06	20.85	23.28	23.40	23.62	24.23	24.58	24.77	25.41	26.51	27.12	28.1	28.22	28.31	28.44
1.86	95.8	3.9	0.5	0.1	1.8	0.7	2	39.3	2.3	1.8	2.8	0.7	16.7	0.4	11.4	0.4	0.7	0.2	0.2	13.5	0.2	0.2	14.3	0.5	0.7	1.2	0.3	0	0.7	7.5	0.1	0.7	16.6
3.61	0.1	1.9	1.5	0.1	74.5	2.3	50.4	1.6	51.4	32.6	2.6	11.3	1	2.8	0.4	0	1.2	3	2.2	0	1.6	0.1	0.3	0.1	0.2	3.5	0.5	1.8	0.1	2.6	1	0.1	0.8
4	0.1	1.8	1.5	0.1	67.8	8.9	47.5	3.8	48.5	33.5	9.5	17.9	0.5	4	1.3	0.6	2	2.4	2.8	0.4	0.8	0.3	0.2	0	0.6	4.3	0.9	3.8	0.1	1.9	2.3	0.5	1.6
7.13	0.1	0.9	3.8	98.3	0.6	9.2	0.3	0	0.6	11.5	6.9	0.2	0.2	5.1	0.1	0.1	1.3	0.1	0.1	0	1.5	1.9	1.2	1.6	0.8	0.6	8.7	1.9	11.6	26.4	50.3	41.8	25.3
8.79	0.3	1.8	0.6	1.5	84.9	3.4	29.8	2.1	30.3	10.6	0	11.7	0	1.9	1.7	3.5	0.5	2.5	2.1	0.1	2.3	3.8	0.3	0.1	3	9.1	0.6	0.1	1.8	7	1.7	6.6	1.4
10.55	11.6	0.3	1.5	0.1	31.5	2	63.8	15.7	34.6	13.1	6	1.4	10.6	1.8	6.8	2.7	1	1.1	2.5	0.4	0.7	0.4	0.8	0.2	0.9	1.1	0.9	1.5	0.9	1.3	1.4	0.3	1.2
10.84	28.3	2.4	0.3	0	12.4	0.1	17.5	80.2	4.6	0.1	6.4	13	33.1	3.3	38.7	0.4	11.1	1.1	1.1	0.2	1.6	0.2	0.3	2.8	1.6	4.7	5.9	1.7	1.3	0.4	0.7	0.7	1.1
11.82	13	2.8	0.9	0.1	30	1.3	23.9	39.1	39.9	26	4.3	12.7	18.3	2.7	22.3	1.5	6.4	2.4	10.7	1.1	1.3	1.3	2.1	6.8	10.3	14.7	2	0.1	0.6	0.2	0.6	0	2.6
12.21	9.2	2.2	0.4	0.8	10.2	14	4	16.7	3.5	1.7	13.6	50.9	29.5	3.9	42.2	0.2	22.2	13.9	4.7	3.7	4.4	3.6	0.6	2.8	10	13.5	2.3	2	0.9	3.9	1.1	2.8	0.2
12.6	9.3	4.1	11	5.5	7.2	3.4	5.3	16.1	10.9	3.9	13.6	18.1	36.7	8	28.9	1.4	12.3	5.7	8.7	0.6	1	1.6	7.8	3.3	1.7	2.7	3	1.8	0.6	10.7	9.9	5.1	5.4
13.09	6	3.4	2	0.8	0.9	0.6	1.4	18.7	3.5	2.7	0.4	0.4	26.8	17.4	24.7	2.5	8.8	0.5	2.5	2.8	1	0.5	0.3	0	0.7	1.1	0.7	0.3	0	2.9	0.6	1.1	0.6
13.48	17.8	4.4	2.1	0.2	4.9	1.4	1.8	53.5	2.3	1	17.9	36.9	64.1	1.2	76.6	1.1	30.1	5.5	2.1	9.3	0.5	2	0.1	3.7	4.3	11.3	2.1	2.1	1.6	1.8	1.4	0.8	3.3
13.87	14.8	4.8	4.2	0.4	0.8	0.9	0.4	48.4	1.7	1.8	1.1	15.3	87.9	7	85	2.7	41.9	2	5.4	12.6	2.4	0.6	0.7	0.2	4.9	6.2	1.1	1.2	0.7	5.8	1.4	0.5	0.9
14.06	13.1	2	3.5	0.2	2.6	1.6	0.5	54.4	1.9	1	6.7	29.3	79	1.4	93.4	1.2	42	4	5.2	15.8	0.9	4	1	1.8	4.2	7.9	2	4	1	3.9	3.4	4.3	2.1
16.21	1.6	1.4	0.8	0.2	0.7	1.1	1.6	23.2	2	2.6	2.5	8	58.7	4.3	60.9	0.6	73	1.9	1.8	40.9	0	1	12.3	0.1	4.7	1.3	2.8	7.5	11	3.7	4.2	6	2.5
17.09	0.3	0.3	0.2	0.1	0.2	12.3	2.2	17.5	1.1	23.4	17.6	1.9	6	0.3	0.2	0.9	0.6	1.6	5.1	0.1	0.7	1.3	0.4	1.5	0.1	1	2	0.3	0.7	0	0.5	1.1	0.1
19.43	0.3	0.4	7	0.1	12.9	1.5	21.6	0.5	31.8	23.3	3	5.3	2.4	0.1	0.7	1.2	1.9	15.9	16.8	4	4.1	1.3	0.3	0.6	4	3.1	5	0.6	4.4	0.2	0.8	0.5	0.5
20.8	8.1	2	0.2	0.2	6.3	2.7	11.8	1.1	15.9	1.6	0.3	5.7	11.5	1.3	13.7	1.2	25.8	1.4	0.4	62.1	0.1	0.6	10.6	1.2	1	0.4	2.3	2.2	1.3	7.5	3	3.9	5.3
21.78	0.4	0.8	0.1	0.3	4	0.3	3.6	0.1	3.9	2.4	1.2	1.5	0.6	4	0.1	1.6	0.3	0.5	0.1	0.6	5.7	0.6	1	0.4	3.1	2.7	0.9	0.5	1	3.9	0.7	4.4	0.1
23.05	2.1	8.7	0.1	0.7	0.9	9	3.1	0.1	5.6	9.2	5.3	4.1	0.6	1.8	0.3	9.5	0.8	6.6	0.8	1.6	48	21.5	3.8	1.8	0.9	5.2	3.6	10.6	0.4	9.1	4.4	5.8	2.2
23.44	18	0.9	0.9	2.1	0.2	1.7	0.2	0.5	0.1	0.2	1.7	0.9	0.1	0.9	0.1	6.2	11.3	0.4	0.4	29.1	0.4	5	71.7	3.7	5.7	3.1	2.1	12.6	8.6	6	0.3	1.5	6.5
24.22	3	0.1	4.3	2.2	0	1.7	6.2	2.7	13.1	17.9	8.8	1.7	2.3	7.2	2.3	16.5	2.1	2	2	2.4	12	20.3	4.2	2.6	1.8	0.5	0.2	14.2	1.6	11.4	13.4	15.6	4.1
24.71	2.9	1.2	4.6	3.3	0	0.6	5	9.8	11.7	14.7	8.2	5.1	3.8	5.3	5.1	6.2	2.5	3.1	0.6	0.7	0.5	9.1	1.2	11.8	10.7	16.6	3.5	1.4	1.8	6.8	8.8	11.5	12.1
25.29	0	1.2	2.9	1.3	0.9	2.1	80.2	1.7	1.2	4.9	9	1	0.5	6.5	0.1	36.7	3.3	0	0.3	0.6	0.6	37.5	0.8	2.9	32.3	1	43.3	6.5	27.9	21.8	82	30.5	14.5
25.78	0.2	2	2.4	31.8	0.8	4.4	0.6	1.6	0.8	5.8	7.3	1.6	3.4	7.3	3.9	2.9	12.4	0	2.3	10.9	4.7	2	12.2	11.6	6.4	1.8	27.7	6	39.4	10.9	37.4	16.8	16.2
27.15	1.5	0.4	0.1	21.3	1.6	10.9	0.7	1	0.9	0.3	0.4	3.5	2.1	7.2	2.5	0.1	15.9	1.9	0	2.6	8.2	1.2	8.2	0.4	2.3	6.4	54.2	2.3	71.3	9.6	15	9.2	1.3
28.03	7.1	1.5	0.8	3.6	0.1	1.1	0.2	10.2	0.1	0.2	5.3	2.8	8.2	1.2	10.5	1.5	3.1	1.2	0.2	21.7	0.8	1.6	5.9	6.9	4	4.7	12.4	1.1	11.4	2.2	2.4	12.9	4.8
28.52	3.8	3	1.8	0.4	0.1	2.4	2.3	5.2	6.4	9.9	17.2	16.8	6.5	0	10.5	11	8.5	3.6	0.4	5.6	3.3	14.1	7.7	1.6	1.1	1.9	1.6	43.4	3.3	3.1	21.3	5.6	2.4
29.1	0	1.3	2.1	9.9	0.7	0.3	3.1	1.8	6.2	10.8	8.3	10.8	5.5	0.6	9	1.2	14.9	2.1	0.1	15.9	1.1	2.1	6.3	0.1	0.6	5.9	5.6	7	10.5	2.7	30.6	6.7	3.0





### 3.21 Test 37

Table 3.21 - MAC of ODS of Test 37 to modes

freq Hz	1.82	3.24	4.13	7.08	7.74	8.88	10.69	11.05	11.63	12.07	12.84	13.26	13.67	13.79	13.94	14.95	16.32	17.56	19.06	20.85	23.28	23.48	23.62	24.23	24.58	24.77	25.41	26.51	27.12	28.1	28.22	28.31	28.44
1.86	94.6	2.9	0.7	0.1	1.3	0.4	1.3	39.3	1.8	1.3	3.5	1.2	16.9	0.2	11.9	0.5	1.4	0.5	0.3	14	0.2	0.3	13.6	0.6	0.9	1	0.2	0.1	0.8	6.7	0	0.3	16
3.61	0.1	1.9	2	0.2	70.9	0.8	46.9	2	47.6	29.9	2.2	11	0.4	1.9	0.5	0.1	1.2	3.3	1.7	0.3	2.7	0.1	0.1	0.2	0.4	3.5	0.5	2.2	0	2.3	1.4	0.3	1.1
4	0	8.2	12.6	0.1	45	27.4	30.5	1	30.6	22.8	13.6	15.9	0.9	8.7	0.6	0.4	0.4	0.5	3.2	0	0.6	0	0.5	0	1.2	2.9	1.5	3.4	1	5.2	1	0.6	1.1
7.13	0.1	0.9	4.1	98.2	0.9	9.3	0.2	0	0.5	11	7.1	0.2	0.2	4.9	0.1	0.1	1.1	0	0.1	0	1.5	1.7	1.2	1.7	0.8	0.6	8.5	2.1	11.4	26.8	50.7	41.9	24.9
8.59	0.3	0.3	1.5	1.8	87.2	4.8	31.6	1.4	31.4	11.4	0.2	12	0.1	1.9	1	1.8	0.7	4.2	1.5	0.1	2.4	2.7	0.3	0	2.9	8.4	0.8	0	1.7	6.8	1.7	5.3	0.7
9.77	1.2	10.3	0.9	0.9	31.1	5.7	37.9	1.2	37.1	22.3	2.9	6.8	3.7	1.2	0.8	1.4	5	15.6	2.5	0.1	2.6	1.2	2.3	6.5	5.5	11.6	0	3.2	1.2	2.2	4.6	0.6	0.8
10.55	11.9	0.1	1	0.1	26.3	1.6	62.7	17.5	31.7	10.5	4.4	1.1	13.3	3.8	8.6	2.2	1.8	1.1	1.4	0.2	0.3	0.4	0.5	0.4	1.5	2	0.8	1.8	0.5	1.6	1.9	0.2	1
10.84	22.8	2.1	0.1	0.1	11.8	0.7	29.7	59.1	10.8	2.6	3.2	9.7	27.2	7.1	29.9	2.2	8.9	1.1	0	0	0.6	0.5	0.1	1.9	0.9	4.9	3.8	3.5	0.4	1.3	1.6	0.6	0.7
12.3	1.4	0	7.2	19.3	15.3	5.8	13.9	3.7	29.3	37.1	11.2	19.7	3.6	20	7.7	10.9	4.7	7	1.3	0.8	1.1	16.4	0.8	3.9	0.6	2.6	1.5	3	4.6	22.5	26.9	25.9	12
12.8	15.9	7.7	12.3	6	2.2	2.1	4.1	20.6	6.4	3	15.1	5.5	50	9.2	36.8	3.7	11.4	3.2	10	0.4	0.4	2.2	6.6	2.1	1.1	0.4	1.7	1.9	0.3	7.5	10.5	6.6	8.8
13.09	5.9	2.6	3.2	0.9	1.4	0.4	1.2	19.8	3.5	2.8	0.4	0.3	30.5	16.6	28	2.5	10.7	0.2	3.5	3.6	1.5	0.7	0.4	0.1	0.9	1.3	0.8	0.1	0	3.4	1.1	1.5	0.5
13.46	18	4.6	1.7	0.1	5.5	2.3	1.1	52.3	2.6	1.5	18.1	44.9	59.5	0	74.5	2	30	6.6	2	8.4	0.9	1.1	0.2	3.6	5.2	13.7	2.4	2.1	1.4	2.6	1.1	0.5	3
13.87	15.3	3.8	3.5	0.2	0.6	1.1	0.3	51.3	1.6	1.7	1	18.4	89.8	4	91.5	2.2	43.8	2.3	5.8	13.7	1.9	0.5	0.9	0.2	4.9	7.3	1.4	1.8	0.7	4.4	1.9	1.3	0.3
14.06	13	2.2	3.6	0.2	2.4	1.9	0.3	53	1.9	1.2	7.3	31.4	77.5	1.3	92.4	1.3	41.4	4.3	5.7	15.6	0.9	4.1	1	1.9	4	8.1	1.7	3.9	0.9	4.1	3.2	4.3	2.5
16.21	2.2	7.9	2.8	0.5	1.8	0.3	2.4	14.6	1.8	1.5	4.7	2.6	31.5	9.7	31.8	4.2	47.5	3.6	1.4	20.6	0.4	0.5	6	0.8	8.4	2.2	5.4	3.6	10.4	2.3	2.3	0.9	4.4
17.09	1	0.1	0	0.4	10.3	1.6	16.2	1.1	21.5	17.9	3.5	7.5	0.1	0.6	0.8	1.6	1.1	5.9	0.1	1.7	1.7	0.9	2.1	0.1	0.4	3.3	0.2	1.8	0.1	0.1	2.9	0.5	0.3
19.14	1.3	1.6	0.9	0.1	18.2	2.3	25.4	0.3	34.2	26.2	1.1	6.3	1.8	0.2	0.6	0.2	4.4	9.8	8.2	1.2	5.2	0.1	0.7	1.1	2.5	5	2.2	0.1	2.1	0.7	0.4	0.6	0.4
19.43	0.2	3.9	2.3	0.2	14.1	5.1	24.5	1.1	34.8	26	1.4	7.2	0.4	1.5	0.1	0.1	0	0.2	0.8	1	3.7	0.7	0.6	0.2	6.4	0.5	2	0.2	5.1	1.1	0.5	0.2	0
20.9	6.2	0.4	1.7	0	6.4	1	9	0.5	12.2	7.9	0.9	5.5	11.2	3.5	16	0	21.8	1	3.2	55.6	1.9	0	17.3	0.6	1.3	8.2	5.9	2.8	4.1	8.9	0.2	4.2	13
21.78	0.5	0.6	0.5	0.3	4.5	0.1	3.7	0.3	4.6	4.1	3.7	2.7	1.1	1.6	0	1.1	0.6	2.6	0.5	0.2	7	0.5	0.5	0.1	0.8	5.7	2.1	1.6	1.6	6.9	1.2	3.6	0.4
23.44	13.9	0.1	1.2	0.1	2	1.8	0.3	0.2	0.4	1.6	0.5	1.5	0.3	6.7	0.7	12.3	14.4	0.4	0.2	22.8	1.5	25.2	56.6	0.6	2.4	1.2	8.2	4.2	14.3	15.9	1.5	4	0.6
24.32	2.7	1.3	0.1	1.2	0.2	3.8	4.7	1.8	6.2	10.2	7.9	3.3	0.9	2.5	1.4	10.6	2.1	2.6	1.5	5.4	1.3	9.3	3.4	20.3	10.8	18.4	5.1	7.5	2.9	1.2	9.1	6.8	24
24.8	2	2.3	5.3	0.5	0.3	6.6	3.5	2.3	5.5	3	1.5	6.5	2.3	3.6	4.6	1.4	2.5	2.4	0.7	4.2	4.8	2.8	1.5	10	8.6	7.7	0.4	10.2	0.4	2.9	0.2	2.2	2.5
25.29	0.1	1.5	3.9	1.7	0.7	1.6	0.2	1.4	0.7	3.1	6.3	1.8	0.4	8.4	0.1	29.5	2.9	0.2	0.4	0.7	1.5	26.9	0.9	3.8	40	0.7	38.6	3.9	23.8	23.7	5.5	25.3	11.5
25.78	0.2	2.4	2.8	25.1	3.4	8.2	0.1	0.7	1	3.6	6.9	0.3	0.4	6.1	1	23.3	3.7	1.8	0.4	0.1	6.9	24.9	2.3	5.2	6.2	5.7	42.9	2	52.9	17	44.6	40	16
26.37	0.6	6.1	1.7	3.3	0.5	3.9	2.9	3	4.7	8.3	15.6	10.6	3.6	0.1	3.7	10.8	4	11.1	0.4	0.6	12	18.3	1.9	36.3	3.3	3.5	6.2	66.8	0.2	2.4	12.1	11.8	14.8
27.15	1.8	0.8	1.1	23.1	1.3	6.4	0.7	0.3	1.2	1.3	1.9	0.5	1.1	4.1	0.6	3.2	14.9	0.5	0	1.7	5.7	4.5	10.3	1.4	5.2	3.5	64	0.6	89.9	8.2	25.6	14.6	2.5
27.64	1.1	5.2	3.5	5.4	3.6	1.4	0.1	2.7	0.1	4.4	1.5	5.3	3.7	8.8	6.7	24.9	7.7	0.4	0.2	8.3	4.7	21.6	4.9	3.4	13.2	0.7	11	5	3.4	56.2	8.5	41.9	9.3
28.03	0.1	0.7	0.7	1.2	0.2	3.3	0.1	23.3	0.2	0.4	2.6	7.4	23.8	0.7	29.6	2.3	15.5	1	0.2	20.8	1	3.2	4.9	4.9	3.8	7	26.4	2.7	25.2	7	0.8	5.8	7.7
28.52	3.5	5.8	1.7	15.7	0.2	2.3	4.4	0.7	9.9	18.6	25.3	11.4	0.3	7.6	0.8	19.5	2.7	1.4	0.1	8.3	1.8	15.3	9	3.9	2.4	2.2	2.3	17.2	2	13.3	40.3	26.3	46.2
29.1	0.7	0.6	1.4	5.9	0.6	0.4	2	5.9	3.5	6.1	5	10.4	12	0.3	15.7	0	20.6	1.8	0	17.8	0.9	0.4	6.2	0.2	0.6	5.7	8.7	7.8	15.9	1.8	23.2	3.5	0.4

### 3.22 Test 38

Table 3.22 - MAC of ODS of Test 38 to modes

freq Hz	1.82	3.24	4.13	7.08	7.74	8.88	10.69	11.05	11.63	12.07	12.84	13.26	13.67	13.79	13.94	14.95	16.32	17.56	19.06	20.85	23.28	23.49	23.62	24.23	24.58	24.77	25.41	26.51	27.12	28.1	28.22	28.31	28.44	
1.86	95.7	2.9	0.6	0.1	1.5	0.6	1.4	39.5	1.6	1.1	3.2	0.9	16.4	0.3	11.3	0.2	0.9	0.3	0.2	13.6	0.2	0.4	14.1	0.5	0.6	1.1	0.3	0	0.8	7.6	0	0.5	15.6	
3.52	0.6	0.5	0.2	0	72.7	7.7	49.1	0.4	48.8	34.8	4.9	12.4	1.4	5.2	0.1	0.2	1	3.5	3.2	0.1	0.9	0.2	0	0.1	0.1	1.3	0.4	1.4	0.3	2.3	0.5	0.2	1.2	
3.91	0.1	3.5	15.7	0.3	25.4	45.2	20.6	1.5	19.5	17.4	25.3	18.5	0.9	8.6	1.2	2.7	5.6	6.7	5	0.3	1	0.9	1	0.9	4.1	5.5	3.3	3.6	0.9	1	0.8	0.3	0.6	
7.13	0.1	1	4.2	98.3	0.6	9	0.4	0	0.7	11.9	7	0.2	0.3	5.1	0.1	0.1	1.2	0	0.1	0	1.4	1.7	1.2	1.7	0.8	0.6	8.6	1.9	11.5	26.7	50.9	42.2	25.6	
8.5	0.1	0.7	0.7	1.2	86.1	4.8	30.5	1.7	31	12.3	0.1	13	0.1	2	1.6	3.5	0.8	3.5	1.3	0	3.5	4	0.6	0	1.5	8.5	0.8	0.2	1.7	6.9	1.3	5.4	0.9	
8.69	0.5	0.5	0.6	1.3	85.4	3.3	35.2	0.6	32.1	11.2	0.4	10.6	0.6	2.3	0.4	3	0.3	3.2	1.6	0.1	2.3	4.2	0.2	0.1	2.1	9.4	0.9	0.1	2.8	8.2	1.5	6.1	0.7	
10.55	12.7	0.1	1	0.1	25.7	1.8	60.7	19.2	30.6	10.1	3.9	0.5	14.1	3.4	9.6	2.2	1.9	0.7	1.4	0.2	0.3	0.3	0.4	0.5	1.2	1.5	0.9	1.8	0.7	1.2	1.5	0.4	0.8	
12.3	0.6	0	8.2	20.8	15.9	4	15.3	2.1	38.7	46.7	11.2	14	1.1	20.4	2.8	13.4	2.4	5.6	0.9	0.4	0.8	16	1	5	0.8	1.1	1.5	3.4	4.8	23.2	29	26.6	15.3	
12.89	9	3.4	0.4	1.6	7	7	4.4	16.2	8.7	5.5	4.5	23.8	35.8	25.8	19.7	8.8	10.5	7.2	1	0.5	1.4	3.6	2.4	0	4.6	6.8	3.1	2.3	0.8	11.6	2.5	6.1	0.3	
13.67	11.6	7.4	4.3	1.1	8	1.1	5.3	32.1	2.8	0.4	29.6	47.6	33.9	5.2	41.6	2.1	13.3	8.5	0.4	4.5	0.1	3	0.1	4.5	1.7	10.9	0.3	1.1	1.8	8.9	3	2	3.6	
13.87	15.8	4.1	2	0.3	0.5	0.8	0.5	1	1.9	2.2	0.7	14.8	90.9	7.5	8.6	2.1	42.6	2	4.3	12.6	2	0.2	1	0.1	4.6	5.4	1.6	2	0.8	4.1	2.1	0.9	0.3	
14.06	14.6	2.6	1.3	0.1	1.4	1.9	1.1	56.3	1	0.8	7.1	27.5	84	1.5	94.9	0.7	43.1	3.7	4.7	15.6	1	3.2	0.9	2	4.8	7.7	2.1	3.7	1	2.3	2.8	3.5	2.4	
16.21	3.2	2.4	0.1	0.3	2	0.8	2.3	24.6	2	2.1	5.6	5.6	58.3	7.8	60	0.4	67.2	0.3	1.8	31.3	0.2	0.1	11	0.4	2.9	2.4	3.6	6.4	10.1	2.4	0.5	2.4	0.7	
17.09	0.2	0.5	0.1	0	13.2	1.9	18.7	1	24.6	18.7	2.4	6.8	0.3	0.7	0.5	0.7	1.5	6.8	0.1	0.4	2	0.7	0.8	0.1	0.8	2.2	0.5	0.5	0.1	0.4	1.1	0	0.1	
17.77	0.7	4.6	0.4	0	0.2	12.3	3.7	1.8	1	24.7	19.6	2.9	7.5	0.1	0.6	0.4	0.6	0.1	9.7	0.5	0.6	2.7	0.7	1.1	0.3	1.4	3.2	0.8	0.4	0.2	0.2	1.2	0.3	0.1
19.14	2.1	4	4.6	0	10.7	2.5	14.7	0.1	16.4	1.8	2.4	4.3	1	3.3	1.2	0.3	3.3	5.8	13.6	1	2.2	0.5	1.1	0.4	4.9	4.4	0.7	1	1.3	0.9	0.6	0.2	0.2	
19.94	3.5	2.5	5.7	0.2	3.7	1.2	0.4	15.8	4.1	6.1	2.8	12.5	26.6	11.3	37	57.2	8.9	0.5	1.9	8.6	0.2	35	2.7	1.3	3	7.1	0.3	10.6	0.4	17.7	8	17.8	3.4	
19.34	1.2	2	0.6	0.1	18	3	25.9	0.3	40.1	27.6	1.1	9	0.5	2.7	0.1	0.8	0.7	2.9	7.3	0.8	3.9	0.5	0.4	0.5	0.4	4.9	1.1	0.1	2.4	1	0.8	0.1	0.9	
19.53	2	4.9	0.7	0	16.6	2.2	24.3	0.6	30.7	22	1.1	6.7	0.5	1.2	0.2	0.8	0.5	1.8	1.1	0.9	2.3	0	0.1	0.4	3.2	4.6	1.9	0.1	4.1	0.8	1	1.7	0.2	
20.9	3.7	0.2	0.7	0.3	7	0.5	11.1	0	16.2	11.1	0.2	1.6	6.5	8.9	7.1	0.5	9.8	1.1	1.7	30	0.7	0.5	11	0.4	0	6.2	3.8	1.6	2.8	2.8	1.1	3.5	12.5	
21.78	1.4	0.2	0.7	0.4	6.3	0.1	5.9	0.2	6	3.4	2.4	2.1	1.4	1.2	0	2.5	0.8	1.7	0.2	0.8	6.9	1.3	0.1	0.8	2.7	3.2	2.2	0	3	7.5	0.2	4.9	1.2	
23.44	14.2	0.7	1.7	1.7	1	0.8	0	0	0.2	1.4	0.7	1.3	0.5	3.8	1.1	8.7	15.5	1.8	0.8	23.2	5.2	19.3	58.1	2.6	1.1	1.6	5.9	2.1	11.2	16.1	1.6	5.3	0.3	
24.41	0.5	5	0.6	1	0	0.1	1.4	1.1	1.8	3.2	1.4	3.7	0.4	1.7	0.9	1.9	0.7	4.6	1.6	3	2	2.6	0.8	15.2	13.1	7	4	17.3	1.1	2.4	3.3	2.1	4	
24.8	0.2	7.1	1.6	3.7	10.5	2.1	0.5	2.7	2.5	3.4	7.6	0.2	2	1.2	0.4	0.3	12.6	0.9	5.8	7.1	5.4	3.2	21.5	8.1	1.3	3.4	32.5	1.8	5.5	1	2.3	2.8		
25.78	0.5	2.1	2.1	20.2	3.3	9.7	0.9	1.1	3.2	3.4	5.8	1.6	0.7	6.8	2	25	5.2	2.7	0.5	0.6	6.9	26.9	1.3	2.2	5.1	6.9	43.9	2	53.5	18	31.9	35.6	11.6	
26.27	0.3	2.4	2.1	22.4	2.8	4.3	1.8	3	3.9	5	8.7	6.2	2.3	4.5	3.7	10.3	2.7	3.3	0	3.2	0.7	9.5	11.3	0.8	7.3	0.2	43.5	24.3	56.7	14.4	40.5	26.9	5.9	
27.05	1.1	0.6	1.4	30.5	1.5	8.6	0.7	0.9	1.3	2.1	2.2	1.3	0.6	5.1	0.5	4.2	8.5	0.9	0	0.5	9	5.3	6.2	3.1	5.5	3.2	60.3	1.8	80.5	14.6	33.5	24.2	6.4	
27.73	1	3	0.9	3.4	1.2	0.1	0	4.1	0.4	2.8	0.2	10.4	6.9	6.7	14.2	10.2	17.7	0.9	0.2	19.6	4.7	10.7	1.5	7.5	7.4	2	14.2	0.6	11.6	52.3	5.1	15.3	4.3	
28.03	1.8	0.5	1.9	17.5	1.8	0.8	0.7	5.2	2	4.5	2.8	5.3	7.6	11.9	11.7	18.1	9.4	0.3	0	9.8	3.8	11.1	3.7	1.4	8.5	5.7	7.9	6.6	23.3	45.2	16.3	29.8	3.4	
28.52	1.6	6.6	3	15.3	0.3	2.6	2.8	2.1	6.9	14.5	27.7	11.5	1.3	7	2.3	19.8	4.1	1.3	0.2	8.3	2	14.8	8.1	3.9	3.4	3	2	19.8	1	12.2	40.7	27	4.1	
29.1	0.1	1	0.9	8.8	0.4	0.3	3.5	2.1	7.1	11.3	8	10.6	6.3	0.9	10	1.7	15.7	1.7	0.1	16.8	1.5	1.6	7.4	0.1	0.1	7.7	5.7	11.3	12.2	2.2	29.7	6.4	2	





### 3.23 Test 39

Table 3.23 - MAC of ODS of Test 39 to modes

Freq Hz	1.82	3.24	4.13	7.08	7.74	8.88	10.69	11.05	11.63	12.07	12.84	13.26	13.67	13.79	13.94	14.95	16.32	17.56	19.06	20.85	23.28	23.49	23.62	24.23	24.58	24.77	25.41	26.51	27.12	28.1	28.22	28.31	28.44
1.86	95.4	3.5	0.7	0.1	1.3	0.3	1.2	41.1	1.3	0.9	2.7	0.9	17.5	0.4	12	0.2	0.6	0.3	0.2	12.9	0.3	0.5	13.6	0.4	0.5	1.3	0.4	0.1	0.8	7.8	0	0.5	15
3.52	0.1	1.9	0.4	0	73.5	7.2	50.5	1.5	50.3	36.1	5.5	13.6	0.6	3.9	0.4	0.1	1.5	2.7	2.4	0.3	0.7	0.1	0	0.1	0	1.9	0.3	1.7	0.2	2.1	1.1	0.3	1.1
4	0.4	3.7	16.4	0.3	38.4	30	25.8	1	29.9	21.5	18.4	19.6	1.3	8.9	0.9	1	1.4	1.8	4.2	0	1.1	0.5	0.9	0.7	2	6.8	1.6	3	2.1	3.3	1.4	0.1	1.6
7.13	0.1	1	4	98.4	0.6	9.5	0.4	0	0.7	11.7	6.9	0.2	0.3	5.1	0.1	0.1	1.1	0	0.1	0	1.4	1.8	1.2	1.7	0.8	0.6	8.6	2	11.3	26.7	50.7	42.1	25.7
8.59	0.2	0.3	0.5	1.2	89.8	3.1	33.6	0.8	32.9	12.7	0.1	11.3	0.5	2	0.6	2.5	0.7	3.7	1.1	0.1	3.2	3.4	0.2	0	2.6	8.6	0.7	0	2	7.2	1.3	5.3	1
8.79	0.1	0.7	1.4	1.6	84.6	4	30.8	0.9	29.2	10	0	11.7	0.2	2.1	0.9	2.7	0.7	3.3	2.2	0.3	2.4	4	0.3	0	3.6	10.5	0.6	0	2.1	7.1	2.2	6.8	1.4
10.55	9	0.1	0.8	0.1	29.3	1.9	68.5	12.8	33.5	10.9	4.6	1.2	10.2	3.5	6.2	2.2	1.4	1	1.4	0.2	0.3	0.4	0.5	0.3	1	1.9	0.6	1.7	0.5	1.3	1.6	0.2	0.8
10.84	18.5	1.7	0	0	17	0.8	40.6	52.5	15.3	2.9	4.3	10.6	23.2	6.4	26	1.1	8.7	1.4	0.1	0.1	0.9	0.2	0.1	1.5	1	4.6	3.3	2.9	0.3	1.1	1.2	0.3	0.5
12.81	8.5	1.5	1.8	1.3	11.2	9	5.3	15	11.7	8.6	15	38.3	27.5	1.9	36.5	1.7	18.3	10.4	2.8	3.7	6.2	6.8	0.4	4	6.9	8.7	1.7	2.8	1.5	1.8	4.9	3	1.7
12.8	14.1	6.7	13.7	7.5	5	3.4	2.9	19.3	10.8	6.2	9	9.2	45.2	5	35.8	4.1	12.5	3.8	10.1	0.3	0.4	3.6	6.4	2.2	1.3	1.5	2.1	1.9	0.7	11.6	12.1	9	8.4
13.09	2.8	1.9	3.4	1	7.4	4.2	2.8	10.6	7	2.5	3.4	16	19.6	18.6	15.1	0.1	8.2	4.7	2.5	1.7	0.7	1	1.2	0.5	2.1	5.1	1.9	0.6	0.7	12.3	0.6	1.6	0.1
13.67	16.1	7.5	1.5	0.6	5.5	0.8	3.3	44.8	1.2	0	23.4	34.1	57.4	4.5	62.9	1.7	22.8	5	1.2	6.9	0.1	3.2	0	3.6	1.5	9.4	0.5	1.3	1.8	5.2	1.3	2.5	2.9
14.06	13.3	2.4	1.4	0.2	1.5	1.8	0.2	55.7	1.3	1.1	6.8	28.3	83.1	1.2	94.6	1	42.9	3.8	4.8	15.7	1	3.5	1	2.1	4.7	7.6	2.1	4	1	2.5	3.3	3.8	2.4
15.04	2.4	7.2	9.6	0	5.1	0.9	0	12.4	1.2	3.1	2.9	11.6	19	15.7	28.9	67.5	7.5	0.1	2.9	6.2	1	41.7	0.9	1.7	5.1	10.7	0.4	5.5	0.2	21.6	6	21.1	5.6
16.21	1.7	6.1	1	0.8	1	2.7	1.3	19.1	1.2	0.7	5.5	2.9	47.5	9.5	45.7	2	71	1.6	2.1	26.8	0.2	1	11	0	3.2	1.2	6.3	4	12.9	1.4	1.1	3.2	2.3
17.09	0.2	0.8	0	0	12.8	2.3	17.7	1.1	23.5	18	2.5	7.7	0.3	0.9	0.8	0.5	1	8.1	0.1	0.5	2	0.6	1	0.1	0.7	2.5	0.5	0.7	0.1	0.5	0.9	0	0.1
17.77	0.6	7.7	1	0.5	13.6	1.8	19	1	23.3	18.3	2.8	5.4	0.4	0.3	0.7	0	0.4	13	0.3	0.7	3.5	0.5	0.4	1.1	1.9	3.9	1.5	0.8	0.2	0	0.9	0	0.1
19.43	0.6	3	0.4	0	17.1	2.1	24.7	1.2	35.2	26.5	2.2	8.7	0.8	1.5	1	0.1	1.3	2.6	0.4	0.7	4.5	0.6	1	0.5	2.2	5.1	3.2	0.2	4.6	1.3	0.8	0.9	0.2
19.92	1	2.5	0.9	0.1	12.4	1.4	20.7	1	26.9	23.4	1.8	6.1	1.5	1.6	1.9	0.1	0.9	1.4	3.4	0.9	1.1	0.5	0.9	0.3	2.3	9.5	1.8	0.2	1.8	0.8	2.6	1	0.4
24.41	0.4	3.9	1.1	1	0	0	1.5	1.6	2.4	4.5	2.2	3.1	0.7	2.3	1.5	0.4	0.9	3.2	1.7	4	3.5	1.2	1.1	19.8	8	10.9	2.2	14.1	0.7	0.8	4.8	1.3	6.9
24.8	0	9.2	1.5	5.2	0.4	9.6	1.9	0.8	2.5	3.5	4.1	7.7	0	1.4	0.6	2	0	17	1.1	5.4	7.7	10.9	2.9	27.3	8.8	0.9	4.2	33.6	1.7	8.9	2.8	5.5	5.3
25.29	0.2	0.7	3.6	3.6	0.9	2.8	0	0.8	0.4	2.2	4.2	2.6	0.4	8.5	0.2	26.2	6.4	0.3	0.2	1.3	2.7	24	2.6	4	39.9	0.8	38.4	1.3	34.4	21.5	7.7	25.3	10.7
25.78	0.4	2.9	1.8	21.3	2.9	10.6	1	1.9	3.1	2.4	4	1.8	1.3	4.8	2.5	17.3	4.8	3.4	0.6	0.4	7.3	19	1.3	1	3.3	6.8	51.6	2.8	58.1	13.5	30	29.6	8.7
27.05	1.1	0.6	1.5	30.1	1.4	8.2	0.6	0.8	1.2	2.1	1.9	1.1	0.5	4.9	0.5	4.3	8.6	0.9	0	0.5	8.8	5.2	6.6	3.1	5.7	3.3	60.3	1.8	81	14.2	33.4	23.5	5.9
27.84	0.2	4.6	1.7	3.5	2.2	0.9	0.1	5.5	0	2.5	0.7	7.7	8.1	4.4	14.9	16.4	18.2	0.5	0.1	15.3	3.9	13.4	11.7	4.9	8.5	0.5	18.7	2.4	14.3	46.5	6.6	27.3	7
27.93	0.4	1.5	0.7	2.1	1.2	3.5	0.4	3.1	1.6	3.6	1.9	5.1	3.9	5.2	9.8	23.4	10.6	0	0.2	8.7	1.1	18.9	4.2	5.8	15.2	2.5	25.8	12.8	25.4	34.4	3.6	22.2	0.4
28.52	1.7	6.9	3	15.3	0.2	2.4	3.2	2.2	7.8	15.8	28.8	11.8	1.3	7.3	2.4	21.4	3.9	1.4	0.2	8.9	2	15.7	7.9	3.9	4	3.4	1.8	19.3	1.7	12.6	42.1	28	41.3
29.1	0.9	0.4	0.4	3.4	0.9	0.1	1.5	5.5	3.6	5.7	3.7	10.2	11.7	0	14.9	0.2	17.8	1.4	0.1	15.9	1.3	0.4	6.1	1.3	1.3	4.5	7.3	10.8	12.9	2.2	18.5	1.9	0

### 3.24 Test 40

Table 3.24 - MAC of ODS of Test 40 to modes

Freq Hz	1.82	3.24	4.13	7.08	7.74	8.88	10.69	11.05	11.63	12.07	12.84	13.26	13.67	13.79	13.94	14.95	16.32	17.56	19.06	20.85	23.28	23.49	23.62	24.23	24.58	24.77	25.41	26.51	27.12	28.1	28.22	28.31	28.44	
1.95	85.1	3.8	0.5	0.2	0.9	0.3	0.2	45.4	0.2	0.2	4.2	3.2	22.9	0.1	18.6	0.9	3.8	1.6	0.6	9.6	0.1	0.3	10.2	0.8	1.7	1.4	0.3	0.2	0.9	3.6	0	0.1	14.1	
3.61	1.3	0.1	0.9	0.2	9.2	1.8	10.2	1.4	9.1	12.2	2	2.2	1.9	2.3	1.4	0.6	2.4	1.5	15.2	0.5	3.2	1.8	0.1	2.3	2.7	5.1	0.5	1.5	0.8	0.2	0.6	1.7	1.5	
3.91	1.6	7.1	39.5	0.7	3.7	0.8	2.2	6.8	1.4	1.9	1.2	6	8.9	3.8	10.5	2	11.1	4.2	1.1	3.1	5.3	2.1	0.4	5.4	3.1	4	0.3	0.3	1.2	1.2	1.9	0.6	0.1	
4.2	2.2	1.4	67.2	0.2	1.6	5.5	2	3.1	0.5	4.9	10.6	3.1	1	10.7	2	6.8	2.1	1.2	11.1	0.2	1.3	2.2	0.3	4.2	4.4	2.6	2.7	0.6	0.9	0	2.2	0.3	0.2	
7.81	0.2	1.6	0.1	0.7	96.5	6.4	47.7	2.1	48	24.8	1.5	16.2	0.2	3.1	0.7	1	0.8	3.5	0.1	0.2	1.2	0.9	0.1	0	1.7	6.3	0.6	0.2	1.1	4.7	0.1	1.7	0.1	
7.13	5.2	8	0.1	15.5	2.9	1.6	1.8	3.8	1.4	0.8	0.5	0	7.5	4.7	5.6	5.6	6.6	5	0.3	0.6	1.8	6.1	2.7	0.3	3.5	1.8	1.9	7.5	1.9	3.7	2.3	3.6	2.8	
9.57	1	15.9	19.9	3	11.6	14.9	28.2	0.1	29.4	28.1	10.6	6.9	2.6	4.1	1.3	0.6	3.8	14.4	2.9	0.4	4.5	5.7	2.1	9.4	4	4.2	1.5	8.6	0.6	0	10.2	1.5	2.9	
10.64	2.1	0.4	0.5	0.5	46.8	2.6	97.7	0.1	57.1	26.4	12.3	7.7	2.1	2.3	0.3	1.9	0.2	3.1	0.1	0.2	1	0.5	0.6	0	0.3	2.4	0.1	1.7	0.4	1	3.4	0.3	1.4	
11.82	1.3	1.5	1.7	0.6	46.1	2.1	55.6	0.5	92.7	75	2	5.9	1.7	3.4	0.4	4.4	0.7	1.9	0.1	0.8	0.8	2	0.3	0.3	0.1	2.1	0.6	1.4	1.1	1.1	4.1	1.2	2.4	
13.28	2.5	2.4	1.2	0.7	2.2	0.5	0.3	8	0.8	1	12.9	5.9	8.3	12.9	11.1	3.3	6.4	0.6	0.3	2.1	2.3	0.1	0.1	0.6	3	3.4	0.6	0.8	0.7	1.2	1.3	0.6	3.6	
11.13	14.2	3.8	1.2	0.8	17.7	1.7	13.8	52.6	27	19.8	4.8	15.3	26.9	0.4	32.8	2.8	10.4	0.2	1.3	2	0.6	4	0.9	5.9	3.2	5.2	4.6	3.9	1.8	2	4.4	3.7	1.3	
12.21	3.6	2.6	1	11.1	9.2	3.3	9.7	3.9	38	50.1	6.1	11.4	2.7	10.4	4.7	11.9	2	7.6	0.1	2.3	0.3	8.1	4.5	2.9	2.5	1.1	1.3	7.3	2.6	6	22.6	13.5	9.3	
12.7	5.9	4.1	10.4	2.6	4.1	6.1	5.2	7.5	12.4	8.6	13.7	27.8	6.4	5.4	12.1	3.4	5.1	16.6	2.7	1.8	1.6	10.5	4	3.8	3.3	8.9	6	6.6	3.8	11.6	10.4	11.2	7.3	
12.89	3.7	2.4	0.6	0	47	23.4	6.4	4.2	7.3	5.7	44	51.4	1.3	19.2	2.7	4.8	3.1	10.2	0.1	0.3	0.4	0.7	0	1.6	7.8	8.9	3.4	2.9	2.4	3.8	3.9	0	3.1	
15.92	4.9	8.1	20.6	0.2	17	11.8	1.6	6.3	4.8	5.9	5.7	5	3.7	9.7	6.7	7.7	4.7	6.1	18.5	2.4	0.3	0.2	1.1	0.8	1.6	0.3	0.3	3.1	1	1.6	0.3	2.4	0.7	3.3
16.31	0	36.1	0.9	3.7	4.5	0.8	4	2	5.9	5.3	4	3.6	8.4	4.1	4.4	5.8	20.5	39.3	0.5	2.7	8.5	8.1	0.5	3.8	0.9	3.4	8.8	14.4	6.2	0.3	0.4	0.6	0.5	
17.29	0	4.4	0.1	0.1	5.2	2.3	9.4	1	13.1	10.3	2.2	4.1	0.6	0.8	1.3	2	1.2	1.4	0.1	0.7	1.3	1.3	1.7	0.3	1.4	0.3	0.1	1	0.3	0.7	0.8	0.8	1.6	
17.87	0.4	10.8	11.6	0.4	0.4	1.8	0.4	0.9	0.3	1.7	10.9	13.7	0.2	5.6	0.4	1.1	12	31.2	0.2	0.1	0.7	2.3	0	4.2	2.3	5	0.6	1.4	0	1.1	1.8	1	0.9	
18.07	0.2	34.4	9.1	0	3.7	1.4	1.8	0.5	1.4	1.5	3.4	7.4	0.7	1.8	0.5	0.7	19.5	57.6	0.3	0.3	3.9	0.2	0.3	0.3	1.9	10.1	2.2	0.6	0.1	1.2	0.1	1	1	
20.12	1.3	3.6	0.9	0.1	10.7	4.8	17.4	3.2	23.8	16.5	2.4	10.3	1	0.4	2.2	1.2	5.7	6.3	0.8	2.8	1.4	0.1	0.3	0.2	4.7	4.8	1.4	0.1	1.8	0.6	0.7	0.9	0.5	
20.41	4.4	0.7	2.6	0	14.5	3.3	22.9	1.5	32.8	21.8	2.3	9	0.1	1.6	1	0.7	3.4	5.2	1.4	4.2	1.9	0.1	2	0.6	1.9	5.3	1.1	0.2	1.9	1.4	0.3	0.6	1.4	
20.9	9.7	0.9	2.5	0.2	3.9	1.4	6.9	0.1	11.1	5.9	0.6	8	4.2	2.6	9.6	0.6	14	4.8	2.2	54.9	1.5	0.4	16.8	0.7	1.3	7.7	4.3	3.9	1.7	10.2	0.3	4.6	14.4	
21.19	3.2	4.6	4	1	5.1	2	16.2	0.2	27.5	22.7	2.9	10.2	0	6.6	0.8	2.8	0.9	4.1	0.5	6.6	0.6	4.2	5.5	0.2	1.9	1.6	0.5	3.8	0.2	1.3	3.5	2.4	8.3	
21.58	2.3	5.3	4.3	2.3	0.6	0.9	7.7	0.1	14.4	15.8	0.1	1.5	0.5	3.4	0	6.5	0.2	0.7	1.6	1.4	0.5	7.4	2.5	0.5	2.4	2.7	0.1	2.1	0.7	4.3	4.3	8.7	7.8	
22.46	0.1	4.7	0.8	0.1	3.5	1	10.4	0.8	17.3	12	3	10.5	1.2	4.1	0	0.1	1.5	5.3	0.6	0.4	4.2	2.3	1.3	0.1	3.5	5.1	2.1	0.8	2.2	1.9	1.3	0.4	2.3	
23.24	0.1	1.3	3.4	0.8	3.9	1	11.1	1	19.3	13.8	2.7	8.7	1.3	1.9	0.7	1.4	2.2	8.3	0.3	0.4	5.3	3.8	2.2	12	0.1	9.8	1.9	1.3	0.6	0.4	2.8	0.3	2.7	
23.54	5.1	0.6	1.9	2.9	4.2	0.1	11.4	2	18.2	13.1	2.3	7.9	0.1	1	1.5	0.3	3.8	5.9	0.2	5.4	2.9	1.1	8.4	0.2	1.8	8.9	2.1	0.5	2.6	1.5	1.9	0.3	0.3	
23.93	0.1	0.1	2.2	0.5	6.3	0.9	15.2	2.8	24	17.3	3.8	9.2	0.1	1.7	1.4	1.1	6.2	0	0.4	5.8	1.9	2.1	1.8	0.3	13	4	1.7	2.2	0.7	2.7	0.2	1.6		
24.71	3.2	5.9	2.9	1.2	0	2.8	3.7	1.2	8.3	9.4	2	0.3	0.4	7.7	1.9	0.9	7.5	0.2	1.8	0.3	2.4	2.5	8	0.4	5.2	18.9	4.9	2	0.9	1	7.3	4.8	6.5	2.5
25.49	1	1.7	0.1	5.2	3.8	2.7	1.3	3.2	1.8	0.6	2.2	5.3	0.1	0.5	0.6	1.1	12.6	6.6	0.8	3.4	3.1	2.1	3.6	1.7	4.8	3	61.3	2.9	61.2	0.4	0.6	1.9	1.5	
27.15	0.2	2.4	0.6	9.4	0.9	0.6	1.1	1.5	0.3	0.4	0.1	0.4	1.5	3.5	0.1	1	0.3	11.4	2.8	0.6	5.1	3.3	0.1	16.5	0.6	1.6	1.4	64.2	1.1	78.1	4.3	12.7	4.4	4.3
28.12	1.5	8.3	0.3	13.6	1.1	13.1	5.7	4.1	9.4	13.5	12.4	13.2	3.8	2.7	0.2	0.9	0.7	0.2	0.8	5.4	0	0.3	2.1	4.5	9.2	1	22.1	3	10.2	5.1	40.3	12.9	20	
28.52	14.4	0.6	1.5	10.8	2.1	1	0.3	2.5	0.9	2	3.9	0.3	1.7	9.8	1.7	6.6	0.7	1	0.8	3.2	3.1	4.6	0.4	14.8	0.1	5.4	1.9	18.7	1.8	18	8.6	18.8	38.9	





### 3.25 Test 41

Table 3.25 - MAC of ODS of Test 41 to modeshapes

freq Hz	1.82	3.24	4.13	7.08	7.74	8.88	10.69	11.05	11.63	12.07	12.84	13.26	13.67	13.79	13.94	14.95	16.32	17.56	19.06	20.85	23.28	23.49	23.62	24.23	24.58	24.77	25.41	26.51	27.12	28.1	28.22	28.31	28.44
1.95	94	1.1	0.7	0	0.3	1	0.3	41.5	0.6	0.4	4.1	2.9	16.7	0.2	14.1	0.2	1.8	1	0.3	11.4	0.2	0.9	12.3	0.4	0.6	1.2	0.4	0.4	0.7	5	0.2	0.3	13.3
3.52	0.4	1.3	2.6	0.3	10.3	1.6	11.3	0.3	10.1	12.4	3.8	3.3	0.5	1.9	0.1	0.7	0.5	0.2	15.8	0.5	3.1	1.4	0.1	1.7	2.2	5.2	0.3	2.2	0.6	0.1	1	1.8	2.6
7.13	0	0.2	1.2	85.7	15.9	10	3.2	0.2	2.7	2.2	5.3	0.5	0.1	6.2	0.1	0.3	1.1	0.8	0	0	1.1	0.9	1	1	0.1	1.3	8.8	1.9	12.7	29.7	43.2	40.8	22.6
7.81	0.2	0.8	0.7	0.6	98.3	4.7	48.5	2.2	49.1	24.3	0.9	14.2	0.1	2.2	0.9	0.9	1.1	4.6	0.1	0.2	1.4	1.3	0.1	0	1.3	6.3	0.7	0.2	1.1	4.7	0.2	2	0.1
10.64	2.1	0.4	0.5	0.5	48.5	2.5	97.8	0.1	58.5	27.2	11.1	7.4	2.1	2.4	0.3	1.7	0.2	2.9	0.1	0.2	1.2	0.5	0.5	0	0.3	2.2	0.1	1.5	0.5	1.1	3.1	0.2	1.3
11.04	38.4	5.3	0.6	0.1	6	0.6	2.8	94.7	4	1.1	7	13.6	51.4	1.4	54.3	0.4	15.8	0.7	2	1.1	0.5	0.4	0.4	5.5	5	7.9	5.7	1.1	0.7	0.2	0.1	0.4	2.8
11.82	0.2	0.6	1.4	0.7	51.8	2.9	57.9	4	96.5	74.4	4.4	12.5	0.2	2.6	1.2	5.2	1.6	4.6	0.8	0.9	1.9	2.7	0.8	1	1.2	4.7	1.4	2.5	0.9	1.1	4.7	1.2	3.1
12.21	2.3	2.2	1.4	20.8	8.3	0.2	6.5	0.4	44.6	70.6	3.3	1.8	2	8.6	1.9	18	0.6	2.3	2.1	0.2	1	12.4	1.3	2.6	0.7	0.9	0.6	5.6	2.3	10	30.2	21.6	12
13.28	2	0.1	0.4	0.4	5.4	1.7	2.3	8.4	4	2.2	10.3	20	7.8	12.1	15.5	0.2	8.4	4.2	1	2.3	0.7	0.9	1.4	1.8	1.6	6.6	1.8	1.4	0.6	7.2	2.3	1.1	0.9
13.67	14.2	2.8	2.3	0.1	1	0.3	1.5	41.6	2.5	2	3.3	2.5	75.4	9.8	68	2.4	25.3	0.2	2.6	9.9	2.3	0.5	1.7	1.2	1.5	2.3	1	2.5	2.1	1.1	1	2	0.4
8.98	1	4.9	2.6	0.8	21.4	48.4	13.7	2.4	15.4	9.1	16.3	12	2.1	5.4	2.5	8.6	4.2	0.2	0.1	6.6	2.7	4.1	7.5	4.7	1.8	1.1	6.4	16.1	1.6	2.8	0.4	2.8	2.4
13.96	13.6	5.4	0.9	0.2	2	0.8	0.7	56.6	0.4	0.2	10.3	21.4	80.7	3.4	89.6	0.8	38.3	1	3	16.6	1	0.3	0.3	2.1	5.1	8.7	2.3	1.4	1.2	1.7	0.5	0.3	3.5
15.04	1.9	5.6	9.9	0	1	1.1	0.7	5	2.4	6.3	6.9	3.6	2.2	19.2	5.4	69.4	1.9	4.6	2.1	1.7	1.3	36.5	0.7	1.6	10.5	10.7	2.6	3.2	0.8	13	4.1	14	7.2
16.31	0.9	2.4	1.6	0.1	0.3	2.1	0.4	19.1	0.2	0.4	3.1	9.1	56	3.4	59.7	0.3	73.2	1.1	3.1	40.7	0.1	0.5	15.7	0.6	3.6	2.2	3.9	9.7	11.5	3.5	1.1	3	2.6
17.29	0.4	0.8	0.5	0.1	6.1	2.3	10	1.3	14.3	10.2	1.8	5.2	0.3	0.5	1.1	0.2	1	5.9	0.1	0	1	0.9	0.9	0.2	0.9	0.9	0.2	0.5	0.2	0.4	0.3	0.6	0.8
19.92	3.3	6	1	0.3	14.5	2.6	20.8	0.8	29.9	19.8	0.8	3	0.2	1.1	0.5	0.4	3	4.3	2.3	5.3	2.8	1.6	0.6	1.4	3.8	0.2	1.4	0.5	1.9	2	0.2	1.5	0
20.8	5.2	3.2	0.6	0	13.1	2.5	21.8	0.6	29.8	23.9	1.7	6.4	3.3	1.5	2.3	0.2	5.8	4.8	1.4	20.9	1.9	0.5	2	1.1	3.3	2.4	3.3	0.3	3.1	0.7	1	0.5	1.8
21.88	0.4	2	0.2	1.6	0.1	0.2	2.3	0.1	4.9	8	0.6	6.5	0	14.1	0.1	5.9	0.1	0.8	0.6	1.4	5.2	4.9	0.6	0.1	3.4	1.9	0.2	3.5	0.9	3	4.1	7.2	4.3
23.63	19.8	1.5	1	1.1	0.1	2.1	0.5	0.9	0.7	1.7	0.7	0.5	3.1	1.1	1.8	0.8	3	1.2	1	15.2	3.4	3.2	73.5	1	2	1.7	6.6	7.7	11.7	13.8	1	4.5	1.6
24.71	2.9	4.8	3.3	1.7	0.1	1.9	4.5	1.7	10.5	13.4	4.2	0.4	0.4	7.6	0.8	9.1	0.3	2.2	0.3	1.5	2.7	9.5	0.8	5.1	16.7	8.7	1.9	1.5	1.1	7.8	7.6	8.5	3.5
25.49	0.3	2.5	1	7.6	1	1.6	0	1.2	0	0.6	0.3	4.2	0.4	1.9	1	2.5	10.5	0.1	1	6.2	1.5	1.5	6.6	1.7	20	1	73.5	0.6	55.6	4.8	11.1	0.7	2.1
25.98	6.1	0.3	4.5	3.7	1.7	0.9	1	0.7	2.3	4.1	1.5	2.4	1.6	3.2	2.4	12	4.9	0.9	0.9	23.1	1.6	12	13.1	4.5	7.5	2.5	4	14.3	6.8	9.9	11.3	18.9	17.4
26.46	0.1	3.3	0.5	3	2.2	3.8	1.1	1.3	1.4	0.3	1.3	4.1	1	2.7	1.8	0.7	0.5	4.7	0	3	18.3	1.3	10	27.2	0.9	5.4	2.8	64.9	0.1	7.3	0.4	5.5	14.1
27.25	2.4	1.4	2.2	15.3	0.7	1.6	0	1.3	0.2	1.3	1.8	0	5.1	5	5.3	1	20.1	0.4	0.1	6.3	2.9	1	15.5	0.3	6.8	1	50.5	1.7	71.1	3.5	13.9	5.7	1.5
28.12	10.2	18.2	0.2	10.6	3.8	3.6	5.3	4.8	6.9	11.1	10.3	16.2	5.9	1.5	1	9.3	0.6	0.8	0.3	4.9	2.2	6.6	4.4	2.8	7.1	6.2	15.5	1.4	10.6	7	31.9	19.4	13.7
28.52	15.2	4.2	4	17.4	0	0.5	0.9	4.9	1.7	4.9	12.8	4.6	3.3	3.7	5	2.2	2.4	0.4	0.6	7.7	2.9	2.7	0.3	23	0.5	1.7	0.1	28	24	13.8	18.9	20.8	57.1
29.39	0.9	0.2	0	1.3	1.5	0.1	3.5	0.3	7.6	9.2	2	1	0.2	2.4	0.4	3.3	0.5	0.6	0.7	2	1.6	3.2	1.9	0.3	1.6	3.8	0.1	0.5	0.6	0.1	4.4	0.6	1.5

### 3.26 Test 42

Table 3.26 - MAC of ODS of Test 42 to modeshapes

freq Hz	1.82	3.24	4.13	7.08	7.74	8.88	10.69	11.05	11.63	12.07	12.84	13.26	13.67	13.79	13.94	14.95	16.32	17.56	19.06	20.85	23.28	23.49	23.62	24.23	24.58	24.77	25.41	26.51	27.12	28.1	28.22	28.31	28.44
1.86	96.9	3	0.7	0.1	0.3	0.4	0.3	43	0.4	0.3	3.6	2.1	18.2	0.3	14	0.3	1.8	0.6	0.2	12.9	0.2	0.4	13.6	0.3	0.8	1.6	0.4	0.1	0.6	6.2	0	0.5	15.5
3.32	0.2	64.1	1.6	0.1	3.2	3.3	2.7	0.3	2.6	2.7	0.3	2	0.3	1.2	0.5	0.2	15.8	52.9	1.6	0.1	2.1	0.9	0.1	1.3	7.3	8.7	2.5	0.9	0.4	7.2	1.9	0.5	0.8
3.61	1.8	0.5	3.8	0.7	11.4	1.5	13.2	1.4	12.7	15.7	3.8	2.7	1.6	1.8	1.1	0.4	1.1	0.4	17.3	0.8	3	1.6	0.1	1	2.3	4.4	0.5	2.7	0.8	0.5	2.3	3.3	3.6
7.13	0.2	0.6	1.2	96.4	5.1	9.4	0.5	0	0.3	8.7	5.8	0	0	6.9	0	0.1	1.4	0.3	0	0.1	1.5	1.6	1.2	1	0.3	1	9.6	1.8	12.7	27.4	48.6	44	26.2
7.91	0.2	0.8	0.5	0.6	98.3	4.7	48.8	2.2	49.5	24.7	0.9	14.5	0.1	2.4	0.9	0.9	1.1	4.4	0.1	0.2	1.5	1.2	0.2	0	1.3	6.3	0.8	0.2	1.1	4.8	0.2	2.1	0.1
8.99	0.8	4.2	0.7	5.2	22.8	85.5	16.6	0.5	17.5	7.4	12.9	12.5	0.4	5.1	0.8	3.9	1.3	0.2	0.2	0.9	5.7	0.5	5.2	3.6	0.7	3	8.1	9.9	4	2.8	1.9	2.4	0.7
10.64	1.9	0.3	0.4	0.5	47.7	2.4	98.4	0.1	57	25.6	11.1	7.1	2	2.7	0.3	1.5	0.3	3	0	0.3	1.1	0.5	0.5	0	0.4	2.4	0.1	1.4	0.5	1	3	0.2	1.1
11.82	0.8	0.6	1.4	0.7	50.9	3	59	1.6	97.9	76.9	3.8	9.2	0.4	3.5	0	4.5	0.4	3.6	0.2	0.6	1.6	2	0.7	0.7	0.2	3.7	1.2	1.9	1.1	1.3	4.5	1	2.8
12.21	0.2	0.1	2.3	17.2	18.6	0.8	17.8	0.6	66.5	88.4	4.8	5	0.1	16.2	0.3	15.5	0.7	2.4	0.6	0.3	0.1	11.2	0.7	2.8	0.6	0.6	0.3	3.3	1.7	13.3	26	21.2	14.6
13.28	2.3	0.1	0.1	0.3	3.7	0.8	1.1	8.9	2.1	1.1	6.6	8.4	9.8	11.2	15.7	0.5	7.5	1.6	0.9	2	1.3	0.5	0.9	0.9	1.1	4.6	1.4	0.6	0.6	5.8	1.2	0.9	0.2
14.06	12.6	2.2	0.8	0.1	1	0.8	0	55.5	0.5	0.4	5.4	23	86.9	2.6	97.4	0.4	43.3	2	4.6	18.7	0.9	1.9	0.9	1.7	4.7	7.4	1.5	3.1	1.2	1.9	2.2	2.8	2.6
15.04	0.3	2	10.1	1	0.2	1.7	4.1	0.2	10.5	17.8	14.6	0.6	0.2	22.7	1	92.8	0.2	2.3	2.1	0.3	1.4	54.9	1	4.2	13.5	11.8	2	8.2	1	20.6	16.2	32.2	18.7
16.21	1.2	1.4	0.3	0.9	0.7	0.8	1	20.6	0.9	1.4	3.4	10.2	46.8	2.8	55.1	1.7	46.4	2.4	1.8	40.4	0.8	2.5	14.8	1.2	4.1	2.6	1	18.3	5.8	4.8	2	4.1	1.5
17.29	0.1	0.3	0.1	0	6.7	1.5	10.3	1	14.5	10.9	1.1	4.1	0.3	0.3	0.9	0.4	1.6	4	0.1	0.4	1.2	0.6	1.1	0.1	1	0.7	0.2	0.6	0	0.5	0.4	0	0.1
17.97	0.2	3	0.2	0.4	7.5	1.9	12.3	2.5	17.8	1.4	6	13.4	1.3	0.6	3.4	2.6	37	28.1	0.1	2.7	1.3	4.1	3.4	0.5	1.1	4.7	1.4	4.8	0	0.6	1	0.1	0.2
19.14	4.4	10.6	5.9	0.1	7.9	1.2	10.4	4.6	15.9	7.5	1.6	0.7	3.1	1.8	4.3	1.2	2.4	5.2	22.1	5	0.6	0.4	0.1	1.4	2.3	0.9	0.6	0.3	0.6	2.1	0.3	0.8	1
20.02	3	4.6	0.3	0	14.8	3.1	22	0.5	29.5	20.3	1.2	7.9	0.1	0.3	0.4	0.3	3.7	5.5	1	2.6	4.2	0.1	1	0.8	3.6	2.3	1	0.1	2.1	2.4	0.1	1.5	0.1
20.7	3.3	1.7	1.2	1.1	14.3	3.5	26	1	38.8	30.1	1.7	10.1	4	1.5	4.3	0.9	9.8	5.4	2.2	20.7	2.8	2	1.5	0.4	2.9	1.2	1.8	0.1	1.8	2	1.1	0.4	0.9
21.78	0.6	1.1	1.8	0.5	2	0.6	2.7	0.5	4.4	5.3	1.6	3.7	2.1	6.4	1.8	3.8	0.8	0.2	3.6	1.9	11.4	2.6	0.9	0.7	3.8	0.1	1.1	1.3	1.3	2.3	0.8	4.3	3.5
23.63	16.5	0.4	1	2.1	0.1	2.6	0.3	0	0.3	0.7	0.2	0	1.7	0.6	0.9	0.2	6.3	0.1	1.1	17	2.8	0.6	82.1	0.8	0.9	2.9	4.9	10.7	11	10.5	0.5	2.3	2.2
24.41	0.6	1.6	1.2	2.4	0.1	4.6	0.7	3.4	1.6	3.1	2.7	2.2	1	0.3	0.7	3.8	4.8	3	0.8	4.9	1.5	5.6	3.9	39.7	12.1	1.1	5.5	2.6	2.2	0.1	4.7	8.5	23.6
24.71	3.2	7.2	3.1	0.8	0.1	2.5	1.9	0.6	5.3	7.3	2.5	0.3	0.1	7.6	0.3	11.9	0	4.1	0.2	2.7	3.9	12.2	0.2	5.1	25.9	7.7	3.6	1.8	0.8	10.7	6	8.5	1.6
25.46	0.1	1.3	0	6.1	0.2	5.8	0	1.5	0.2	0	0.8	0.8	0	0.1	0.4	6.7	12.9	0.7	0.5	4.9	2.6	6.8	6.1	1.5	11.8	0.9	85.8	2.6	74.8	1.4	7	2.8	0.2
26.46	0.1	1.4	0.4	4.5	0.3	6.9	0.4	2.9	0.7	1.2	3.1	3.3	1.1	0.6	1.6	0.7	0.3	3.3	0.1	2.9	14.8	3	10.1	37.9	0.4	1.2	3.8	86.3	2.2	1.7	1.4	1.3	11
27.25	1.4	0.3	0.5	17.3	1.2	5.4	1.4	1.3	2.6	1.7	2.6	0.8	1.4	2.3	1	2.5	14.2	0.3	0.3	3.6	2.6	6.4	14.8	0.2	3.4	2	64.9	0.6	94.8	3.8	18.7	10.6	2.1
27.64	0.7	0.8	1.6	24.7	1.7	8.7	2.6	0.6	5.5	11.5	15.5	3.6	1.6	10.6	2.4	25.3	2.8	0.5	0.2	0.4	3.3	26.1	0.9	2.6	6.7	4.2	29.3	5.3	41.6	35.6	42.5	49.2	20.3
28.32	6.3	3.7	0.5	11.4	2.1	0.5	0.2	3.1	0.7	5.1	0.6	8.3	3.3	6.4	9.8	15.4	3.7	0.2	0.6	11	0.5	8	3.2	5.4	7.4	5.3	0.2	13.5	5.2	5.75	1.7	26	1
29.39	2	1	1.5	1.5	2.1	0.5	2.5	3.1	5.1	6.2	5.5	4.1	1.9	2.2	3.9	2.9	2.1	0.6	0.8	2	2	2.1	2.5	0	0.5	4.5	0.4	1.7	0.1	0.8	4.7	1.4	1.7





### 3.27 Test 43

Table 3.27 - MAC of ODS of Test 43 to modeshapes

freq Hz	1.82	3.24	4.13	7.08	7.74	8.88	10.69	11.05	11.63	12.07	12.84	13.26	13.67	13.79	13.94	14.95	16.32	17.56	19.06	20.85	23.28	23.49	23.62	24.23	24.58	24.77	25.41	26.51	27.12	28.1	28.22	28.31	28.44
3.32	0.2	66.8	3.7	0.4	4.4	4.6	3.2	0	3.3	2.2	0.2	1.4	1.4	0.8	0	0.2	18.7	59.2	0.3	0	3.5	0.6	0	1	6.1	7.4	3	1.1	0.1	5.1	2.9	0.2	1.4
3.61	0.4	14.1	2	0.4	50	0.9	36.1	0.4	36.6	26.2	2.3	11.1	2.4	3.9	0.2	0.2	4.4	11.7	4.1	0	2.6	0.4	0.1	0	0.7	3.3	1.3	2.3	0.1	4.1	2.1	0.2	1.8
4.1	0.4	0.8	51.2	0.1	1.2	29.9	0.6	0.9	0.1	2.5	21.8	6.2	1.1	8	2	5.2	1.6	2.1	4.8	0.1	3.3	2	1.2	3.6	6.3	5.5	3.5	1.4	1.4	0.2	1.1	0.1	0.3
7.13	0.5	5.2	4.6	94.8	0.3	10	0.8	0.4	1.4	13.2	7.7	0.4	0.5	6	0.1	0.2	0.5	0.3	0.1	0.2	1.1	1.3	1	2	0.7	0.9	8.2	1.2	10.9	24.6	53.9	43.2	28.1
8.3	0.1	0.1	0.8	1.4	86	9.9	37.5	2.2	38.8	16.7	1.9	19.3	1.3	3.2	2.3	0.6	2.2	4.8	1	0.6	2.7	1.4	0.4	0.1	4	12.9	1.4	0.8	1.5	6.9	0.3	2.6	0.3
9.08	1	2.9	17.9	4.6	0.7	64.9	0.2	1	0.3	0.2	3.4	3.7	5.4	1.9	4.5	4.2	4.3	0	2.6	4.2	8.5	0.3	5.6	8.7	0.7	0.8	6.3	8	1.6	1.1	6.2	2.5	0.3
10.16	0.2	11.9	4.2	1.5	17.6	4.7	30	0	31.1	20.7	19.2	19.5	1.4	4.2	0.1	3.1	3.8	25.2	1	0.7	2.9	0.7	0.5	5	2.4	4.1	0.2	0	0.1	0.9	7.1	0.9	1.6
10.45	9	3.6	2.9	1.2	27.4	3.4	59.2	7.3	46	24.1	15.7	6.8	7	1.6	3.8	7.7	2.2	3.8	2.3	0.2	1.1	1.4	0.7	0.3	0.5	0.2	0.5	1.3	0.1	1.4	6.7	1	5.4
10.94	35.9	4.3	0.4	0	4	0.1	4	88.7	2.7	0.6	6	10.5	43.4	0.4	44.7	0.7	9.9	0.4	1	0.1	0.1	0.2	0.2	4.6	1.3	4.7	4.3	2.1	1	0.1	0.5	1.3	1.2
11.43	7.6	3.9	4	1.2	3.1	0.3	1.4	25.8	5.3	2.5	3.3	4.2	16.1	4.8	18.9	1.4	3.5	2.3	17.1	2.3	2.1	0.1	2.4	5.7	10.7	11.6	0.1	0.4	0.8	0.2	2	1	5.8
12.21	3.7	3.3	7.4	12.9	0.5	3.8	2.7	2.9	13.9	28.5	3.8	2.1	7.8	14.2	6.1	4.2	3.2	2.1	1.2	0.5	1	2.5	1.5	1.2	3.4	1.5	1.4	1.5	0.8	7.9	16	15.5	16.5
12.6	13.9	5.2	9.6	4.5	9.4	2.5	9.3	22.9	22	10.9	1.2	6.6	43.7	3.1	36.9	1.8	17	3.2	7	1.1	1	0.8	3.6	0.9	1.3	3.1	2	0.9	0.3	7.8	5.4	2.4	2.3
13.48	2.1	0.8	9.2	0.1	13.5	10.5	7.2	9.7	9.8	3.3	25.9	75.7	6.9	13.6	20.8	0.4	13.4	15.2	3.9	3.5	2.4	1.3	0.7	1.7	7	20.1	0.9	2.4	1	13.8	1.5	1.2	1.9
13.77	6	1.9	10.8	0.5	9.9	4.3	4.2	25.7	7	1.6	7	42.2	26.5	4.2	47	3.9	18.8	4.6	7.6	6.4	2.2	8.4	1.5	0.5	1.4	12	0.3	3.1	1.1	18.1	3.3	8.9	0.4
13.96	11.9	0.8	10.8	0.1	7.2	1.7	4.2	31.8	4.8	1.1	12.8	3.9	51.3	14.1	38.5	0.2	15.5	3.7	0.2	4.3	0.4	6	0.1	1.2	0.4	1.8	3.2	0.5	3.9	2.8	0.4	0.6	
14.16	4.1	1.4	9.6	0.3	8.9	5.4	5.1	23	10.9	3.6	12.5	61.3	24.3	4.6	44.3	0.1	16.8	5.7	7.8	7.7	2.2	1.1	1.1	1.6	10.6	19.9	0.9	2	0.2	10.1	1.5	0.4	2.7
15.04	0.2	2.6	8.6	0.2	1.9	4.2	1.7	0.1	4.1	7.4	20.3	7.5	0.7	4.1	0.3	61.1	2.5	6.6	4	2.4	2.2	28	3	3.9	21.8	7.9	1	12.8	0.2	2.6	10.9	15.7	14.7
16.21	0.5	3.1	3.5	3.9	3.5	1.4	3	2.6	3.9	2.4	6.7	11.7	1.3	4.7	1.3	2.8	12.6	53.1	0.3	1.3	3.9	6	1.5	4	0.1	9.8	7.3	12.5	4.9	1.4	0.1	1.6	0.2
17.09	10.6	1.8	8.5	0.2	12.3	0.1	9	8	11.2	8.8	6.9	3.2	7.5	1.2	5.2	11.7	1.6	13.5	0	1.3	4	1.9	1.6	0.2	6.1	5.3	2	1.2	0.6	1.1	1.5	0.3	1
18.16	2.2	2.4	14.6	2	1.6	4.2	3	1	5	2.4	0.8	0.3	0.3	5	1	3.1	3	16.1	0	4.8	1.5	0.5	1.1	0.1	7.1	7.4	0.3	3.8	1.2	0.5	2.2	2.5	2.4
20.9	9	5.3	6.2	1.9	2.1	0.4	3.2	0.8	6.1	4.5	3	7.5	4.2	0.4	7.8	0.4	12.5	4	0.5	51.7	1.8	2.3	16.4	4.1	0.7	2.2	7.3	7.6	4.7	7.9	5.1	3.9	17.3
23.44	1.9	0.1	3.5	6.2	2.3	3.8	0.4	0.3	0.6	0.9	3.7	0.6	0.6	8.3	1.1	31.7	3.8	0.3	1.3	3.5	10.6	40.5	12.4	10.6	18.8	5.8	5.9	5.2	5.7	2.6	1.6	2.8	5
24.71	0.9	1.2	7.2	0.6	0.6	3.4	5	2.2	8.8	6.9	4.2	7.3	0.8	7.5	2.2	2.6	0.3	0.7	1.7	0.8	4.1	2.8	1.7	10.3	22	16.9	1.4	2.2	2	4.4	3.1	3	3.4
25.39	3.6	0.5	4.4	2.5	7.4	0.5	5.6	6.7	7.1	4	3.6	18	5.9	7.5	10.1	10.3	21.8	6.3	0.8	6.9	3.9	1	6.2	4.8	39.6	25.4	12.2	0.2	20.5	4.1	4	3.6	1.4
25.88	1.1	0.4	4.1	9.4	9	4.7	4.4	5.3	8.4	2.1	0.9	9.6	11.1	0.7	20.4	6.2	11.8	2.6	1.2	26.2	1.9	10.3	6	2.3	7.5	9.7	4.1	3.4	3.8	28.1	17.4	23.9	4.5
26.27	0	4.3	0.3	1.6	2	2.6	2.8	7.6	6	5.8	5.9	12.6	10.7	0.4	17.1	4.6	12.2	14.9	0.4	13.8	13.8	12.9	8.6	26.5	5.9	8.3	1.1	52.8	1.5	1.6	6.3	5.3	8
27.25	4.3	2.7	0	25.9	3.5	6.3	1.2	7.9	1.5	3.7	4.9	0.3	12.2	14.1	10.4	6	19.3	1.9	0.6	4.5	2.5	10.4	4.2	3.7	0.4	2.5	13.1	4.6	27.8	20.5	31.7	31.5	17.7
28.03	2.5	8	0.3	1.1	2.5	0.4	2.6	6.7	2.7	4	10.1	8.4	11.8	3.2	9.5	2.1	6	0.5	0.5	7.9	1.3	4.7	4	0.8	13.7	0.2	0.3	3.9	0.9	1.2	9.7	4.3	5.5
29.2	5.6	0.9	0.8	10.2	1	1.2	0.7	11.2	1.9	4.5	10.8	4.3	12.8	11.3	16.2	7.3	15.2	1.5	1.2	8.3	2.2	3.8	4.4	0.2	0.2	4.9	2.5	3.8	2.8	0.7	12.9	10.4	19.9

### 3.28 Test 44

Table 3.28 - MAC of ODS of Test 44 to modeshapes

freq Hz	1.92	3.24	4.13	7.08	7.74	8.88	10.69	11.05	11.63	12.07	12.84	13.26	13.67	13.79	13.94	14.95	16.32	17.56	19.06	20.85	23.28	23.49	23.62	24.23	24.58	24.77	25.41	26.51	27.12	28.1	28.22	28.31	28.44
1.96	95.2	3.3	0.6	0.1	0.9	0.5	0.8	42.9	0.7	0.5	3.4	1.5	18.5	0.4	13.7	0.3	1.4	0.6	0.3	13	0.2	0.4	13.2	0.4	0.9	1.3	0.4	0	0.7	6.5	0	0.4	14.9
3.42	0.1	2.5	0.5	0.1	62	4.9	44.4	1.5	44.5	33.1	5.2	10.8	0.6	3.2	0.2	0.1	0.7	1.1	5	0.1	1	0.2	0.1	0.3	0.2	2.5	0.2	2.2	0.1	1.6	1.5	0.6	1.5
7.13	0.1	1.1	3.4	98.6	0.6	9.8	0.4	0	0.7	11.9	6.5	0.2	0.2	5.6	0.1	0	1	0	0.1	0	1.4	1.7	1.2	1.5	0.6	0.6	9.1	1.9	11.8	26.9	51.1	42.4	25.9
8.3	0.3	0.9	0.6	1.3	92.9	4.9	38.9	1.9	38.9	16.3	0.4	13.7	0.1	2.2	1	1.5	0.7	3.7	1.1	0.2	2.4	2.1	0.1	0	2.9	8.4	0.7	0.1	1.6	5.9	0.8	4	0.6
10.64	6.2	0	0.4	0.3	33.9	2	83.9	5.7	38.3	13.3	10.3	2.9	7.6	2.9	3.8	1.8	0.4	1.8	0.3	0.1	0.7	0.3	0.6	0.1	0.5	1	0.2	1.1	0.5	1	2.1	0.1	1.1
12.11	5.1	3.1	0.1	0.5	14.1	8.8	6.9	8.8	6	2.2	4.5	26.5	28.5	0.1	35.9	0.1	18.8	8.5	3.6	4.9	7.8	3	1.2	5.4	4.3	4	0.8	1.8	0.7	0.2	0.3	1	0.9
13.09	6.5	3.9	1.3	0.4	0.4	0.3	0.8	20.9	1.5	1.3	1.1	0.2	28.2	18.6	26.1	1.5	9	0.9	2	3.3	1.2	0	0.1	0.1	0.6	0.9	0.6	0.1	0.2	1.1	0	0.3	0.4
13.48	14.3	4.2	2.3	0.2	9.6	4.5	4.1	42.2	6.1	3.4	28.9	63.2	38.8	1.1	57.8	2.9	22.6	10.8	1.5	6.2	1.1	0.9	0.2	4.6	6.1	18.3	2.5	2.1	1.5	4.6	2.4	0.2	4.4
13.67	16.2	6.3	1.5	0	0.6	0.5	1.7	45.5	0.9	1	1.1	4.1	91.6	17.8	73.5	1.7	37.6	1.3	3.8	8.8	1.9	2.3	1	0.1	5.2	0.9	2.1	1.7	1.4	2	2.4	3.5	0.5
16.21	2.1	9.4	1	1.3	1.7	1.4	2.3	21.3	2.5	3.1	4.6	4.1	51.2	6.7	50.8	2.4	56.7	3	2.8	25.9	0.7	0.7	8.5	0.3	4.4	1.2	8.8	5.6	11.8	3	0.9	3.3	1.1
17.09	0.1	1.4	0.2	0	10.2	1.6	14.2	1.1	18.7	14.6	1.8	5.2	0.4	0.8	0.8	0.7	1	4.2	0.1	0.6	1.6	0.7	1.2	0.1	0.6	1.3	0.2	0.7	0	0.4	1.1	0	0.1
17.97	0.7	0.4	3.5	0.3	9.6	1.7	16.6	2	24.4	18.1	2.8	6.3	1.3	0.6	2.6	7.3	3.2	7.8	0.3	4.1	0.7	4.2	3.4	0.2	0.1	2.7	0.7	6.3	0	0.2	2	0.7	0.3





### 3.29 Test 45

Table 3.29 - MAC of ODS of Test 45 to modeshapes

freq Hz	1.82	3.24	4.13	7.08	7.74	8.88	10.69	11.05	11.63	12.07	12.84	13.26	13.67	13.70	13.94	14.95	16.32	17.56	19.06	20.85	23.28	23.49	23.62	24.23	24.58	24.77	25.41	26.51	27.12	28.1	28.22	28.31	28.44
1.86	95.8	2.5	0.7	0.1	0.9	0.7	1	40.5	1.1	0.8	3.3	1.4	16.6	0.3	12.2	0.3	1.5	0.6	0.3	13.9	0.1	0.4	13.9	0.4	0.8	1.1	0.3	0	0.7	6.9	0	0.5	15.5
3.52	0.2	0.3	1.3	0.1	60	4.1	42.9	1.5	43.2	30.6	5.3	11.4	0.9	2.8	0.4	0.3	1.9	3.7	5.3	0.2	1.9	0.2	0.2	0.3	0.4	4.5	0.5	2.7	0	1.4	1.3	0.5	1.4
4	2.2	2.1	46.5	1.1	14.8	17.6	14.8	1	18.7	10.9	26.2	7.1	0.5	1.5	0.1	6.3	1.3	1.7	4.7	0.3	3	2.2	1.4	3.6	6.8	7	1.6	3.5	0.3	1.2	4.8	3.1	4.5
7.13	0.1	0.9	3.2	98.5	1.1	10.3	0.2	0	0.4	10.7	6.1	0.1	0.2	5.7	0.1	0	1.1	0.1	0.1	0	1.4	1.8	1.3	1.5	0.7	0.6	9.2	2.1	11.9	27.4	50	42.1	24.9
8.3	0.2	0.9	0.7	1.1	93.1	4.5	39.4	1.9	39.8	16.7	0.3	13.4	0.1	2.1	1.2	1.6	0.8	3.8	1.1	0.2	2.2	2.2	0.2	0	2.6	8.2	0.7	0	1.5	5.9	0.8	3.9	0.6
10.55	6.9	0.4	0.6	0.3	38.3	2.4	82.7	5.5	46.4	19.6	8.7	3.2	6.4	1.7	3	2.9	0.3	1.4	0.8	0.3	0.7	0.6	0.8	0.1	0.8	1.4	0.2	1.8	0.6	1.1	2.6	0.1	1.4
10.84	36	3.1	0.7	0.1	7	0.1	8.8	89	1.9	0.1	5.5	11.5	38.2	3.3	41.9	1	11.2	1.1	1.1	0.2	0.9	0.2	0.1	3.9	1.9	5.1	6.2	1.9	1.3	0.3	0.6	0.7	1.4
12.11	4	1.1	1.8	0.8	2	9.6	0.3	2.9	1	3.7	12.1	26.6	18.2	3.3	23.4	0.5	11.6	7.9	1.6	4.3	7.5	3.5	1.5	7.3	4.7	5.3	2.1	2	1	0.6	0.2	1.5	0.8
13.09	5.1	2.3	0.9	0.5	0	2.1	2.5	15.7	4.2	3.8	3.3	5	23.7	26.9	19.5	2.8	5.5	2.2	1.3	2.4	1.3	0.1	0.2	0.1	0.1	0.2	0.2	0.3	0.2	0.7	0.5	0.3	0.9
13.57	15.9	2.8	0.1	1.3	4.2	0.5	1.8	54.4	0.8	0.2	13.8	38	68.1	0.4	85.4	1.3	35.7	5	2.3	12.1	1.6	1.2	0.8	2.8	5	11.6	1.1	2.5	1.3	2.7	3	0.9	2.4
13.87	18.1	6.1	0.9	0.3	0	0.6	0.2	55	0.8	1.7	4.6	6.7	95.4	6.9	89.1	2.9	42.2	0.7	3.4	11.8	1.3	0.2	0.5	0.6	3.2	4.7	1.5	1.3	1.2	1.3	1.1	1.1	1.3
14.06	14.6	2.7	1.8	0.2	1.7	1.6	0.3	57.1	1.1	0.6	9.1	25.3	82.5	3.8	93.2	0.4	41.4	3.1	4.4	15	0.8	3.3	0.6	2.4	4.7	7.3	1.9	3.2	1.2	1.5	2.6	3.3	3.9
14.94	0.4	6	7	0.5	5.2	6.4	1.3	2.9	2.2	6.5	10.8	0.8	2.3	22.8	5.7	68.4	0.6	4.6	2.8	3.3	2.7	44.6	0.3	2.7	6.1	8.1	0.9	4.3	0.6	18.7	5.8	20.6	10.1
16.21	2	11.1	1.2	0.6	0.2	1.9	0.3	21.2	0.3	1	1.7	5.1	57.1	4.6	56	0.1	82.3	5.6	2	33.8	0.1	0	11.9	0	4.2	1.6	5	3.6	13.3	2.9	1.3	3.8	0.8
17.09	0.3	1.3	0.2	0	8.4	2.7	12.9	0.7	17.2	13.9	2.6	5.2	0	0.4	0.3	1	1.3	5.3	0.1	0.4	1.3	0.6	0.9	0.1	0.9	1.8	0.3	0.4	0.1	0.2	0.9	0.2	0
17.48	2.3	5.5	1.7	0.8	1.4	0.2	1.9	6.3	2.2	3.4	5.8	6.7	7.7	0.8	7.4	1.2	2.2	8.5	0.3	5.9	0.6	2.2	3.1	2.3	2	0.9	1.4	2.9	2.2	0.1	2	0.6	3.4
17.87	0.1	20.9	0.4	0.5	1.2	0.8	0.7	1.6	0.5	0.8	5.5	7.5	1	0.1	2.4	0.9	20.5	59.8	1.6	2.4	1.8	0.6	1	3.1	3.8	8	1.5	3.3	0.2	1.3	0.4	0.7	1.2
19.34	0.9	2.2	2.8	0.2	15.5	1.8	24.9	1	36.6	26.9	3.2	4.8	0.6	0.4	0.1	0.8	0.9	4.2	14.5	1.5	3.7	1.4	0.2	0.7	5.4	1.9	2.8	0.5	3.7	0.2	1.2	0	0
19.63	1.6	1.8	0.8	0.1	15.1	1.5	25.5	0.2	37.1	27.8	2.1	7.1	1.5	0.8	0.2	0.4	1.4	7.6	1.8	2.3	3.7	0.6	0.3	1.3	2.4	4.5	2.8	0	3.1	0.2	1	0.5	0.2
21.78	1.6	0.3	0.7	0.4	3.7	0.7	4.1	0	4.4	3.7	1.5	1.5	1.2	3.3	0.2	2.1	1.2	1.5	0.9	0.9	7	0.8	0.4	0.7	4.8	1	1	0.3	1.9	4.4	0.3	3.1	0.7
23.14	1.7	8.2	0.4	2.1	0.4	6.9	1.8	0	2.9	8	4.2	1.7	1.7	2.7	0.7	11.5	1.5	6.7	2.8	1.7	55.9	24.8	3.6	2	0.9	1.4	4.1	9.5	0.4	14.7	5.9	10.2	3.4
23.44	17.8	0.5	0.7	1.2	0	2	1.1	0.2	1.7	2.9	0.5	0.2	0.5	1.1	0.4	0.1	10.1	0.9	0.7	21.8	0.1	1.4	72.3	1.1	0.1	2.6	5.7	4.3	10.6	10.4	1.4	2.4	3.1
24.71	1	1.6	6.6	0.4	0.8	3.1	6.1	2.7	10.4	8	4.6	8.4	0.9	7	2.5	2	0.5	1.1	1.3	1.2	4	1.9	1.3	9.1	17.9	16.4	1.7	3.3	2	4.1	2.9	2.6	3
27.15	1.1	0.1	0.8	35.9	3.1	7.6	0.8	0.3	1	2.2	3	0.4	1.1	10.8	1.1	2.8	11.1	0.6	0.1	1.6	7	1.5	7.5	2.6	2.7	4.9	50.5	0.1	75.1	20.7	38.8	28.2	9.3
28.12	6.9	5	0.8	2.4	2	0.5	0.3	7.3	1	3.4	0.2	9.9	7.2	4	15	10.6	7.3	0.2	0.2	16.7	1.3	7.8	3	6.3	2.8	2.1	0.1	10.5	3.4	38.3	5.6	11.3	6.9
29.2	0.9	0.1	1	7.8	0	0.2	3.6	5.4	6.3	10	8	13.9	9.7	0.2	14.9	0.7	19.3	3.5	0.1	13.3	1.9	1.8	4.5	0.5	1	6.3	2.4	5.7	6.8	4.2	25.4	3.9	1.5

### 3.30 Test 46

Table 3.30 - MAC of ODS of Test 46 to modeshapes

freq Hz	1.82	3.24	4.13	7.08	7.74	8.88	10.69	11.05	11.63	12.07	12.84	13.26	13.67	13.79	13.94	14.95	16.32	17.56	19.06	20.85	23.28	23.49	23.62	24.23	24.58	24.77	25.41	26.51	27.12	28.1	28.22	28.31	28.44
1.86	96.7	3.3	0.6	0.1	1	0.5	1.1	42.2	1.2	0.9	3.6	1.6	18.8	0.3	14	0.2	1.9	0.4	0.2	12.4	0.1	0.4	13.1	0.4	0.7	1.2	0.3	0	0.8	6.2	0	0.4	15.3
3.52	0.4	1.6	0.3	0.2	61.5	3.4	44.4	1.7	44.9	32.3	3.8	11	0.7	3.1	0.3	0	0.7	1	4.5	0.1	1.6	0.2	0.2	0.5	0.2	2.6	0.2	2.1	0	1.8	1.3	0.4	1.4
7.13	0.1	1	3.3	98.5	0.7	10.1	0.3	0	0.6	11.5	6.3	0.1	0.2	5.5	0.1	0	1.2	0.1	0.1	0	1.4	1.9	1.3	1.5	0.6	0.6	9.1	2	11.8	26.6	50.5	42.1	25.4
8.3	0.2	0.9	0.8	1.2	93.3	4.8	39.8	2	40.3	16.9	0.3	13.8	0.1	2.2	1.3	1.6	1	4.1	1.1	0.2	2.3	2.2	0.2	0	2.5	8.2	0.7	0	1.5	6.3	0.8	4	0.6
10.55	9.2	0.1	1	0.2	36.4	3.1	77.8	9.7	45.1	19.6	7.5	2.1	9.2	2.4	5.4	2.6	0.7	1.5	0.6	0.2	0.5	0.4	0.5	0.4	0.9	0.7	0.3	1.5	0.5	1.3	2	0	1.6
10.84	34.2	2.9	0.4	0	10.6	0	12.5	87.9	4.1	0.2	5.9	13	37	2.4	42	0.6	11.1	1.5	1	0.1	1	0.3	0.2	4.7	1.9	6.1	6	2.2	1.2	0.3	0.5	0.6	1.3
11.82	2	1.7	0.7	0.7	45.1	2.9	50.1	12.9	81.6	60.4	4.8	13.1	3	3.1	5.2	4.7	1.8	2.8	3.4	0.4	0.7	2.3	1.9	3	3.3	8.1	1.8	2	0.8	0.6	3.2	0.7	3.6
12.11	4.2	0.9	3.5	1.1	1.2	6.8	0	7.8	1.6	3.2	7.5	18.9	10.9	1.2	15.7	1.2	8.8	6.6	0.8	2.4	6.4	1.7	1.3	9.5	5.7	6.4	1.8	1.6	0.6	0.3	0.1	0.7	4
13.09	5	2.6	1	0.5	0	2	2.1	16.1	3.5	3.2	4.1	6.2	24.5	26.8	19.7	2.8	5.7	2.3	1.4	2.5	1.5	0.1	0.2	0.2	0.1	0.3	0.2	0.2	0.3	0.5	0.6	0.3	0.9
13.87	17.6	5.6	0.5	0.3	0.1	0.8	0.2	53.8	1	1.7	2.7	8.8	95.3	6.7	90	2.2	43.5	1.1	3.8	11.9	1.7	0.3	0.6	0.4	3.7	4.7	1.4	1.6	0.9	1.6	1.4	1.1	1.1
14.06	14.9	2.8	1.2	0.1	1.2	1.2	0.1	57	0.5	0.3	6.7	20.9	87.4	3.8	96	0.4	42.7	2.5	4.8	16	0.7	2.8	0.7	1.9	4.3	6.5	1.8	3.1	1.3	1.4	2.1	3.3	2.6
16.21	2.2	1.4	1.4	0.2	0.6	1.5	0	27.7	0	0.4	3.7	10.8	60.7	3.4	66.7	0.7	69.1	1.5	3.1	42.5	0.4	1.2	15.2	0.3	4	3.1	3	9.6	9.7	5.6	2	5.7	1.5
17.09	0	0.5	0	0.1	10.6	1.7	15.2	1	20.9	16.1	1.9	6.1	0.6	0.6	1.1	0.8	1.9	4.8	0	0.6	1.8	0.6	1.2	0	0.8	1.2	0.2	0.8	0	0.7	1.2	0	0.2
17.87	0.3	30.2	1.7	0	3.2	2.3	2.6	1.1	2.6	3	4.9	8.8	1.7	1.1	0.9	1.6	13.7	67.3	0.7	1	1.5	0.2	0.5	4.3	3.3	9.8	1.5	1.7	0.4	1.7	0.1	0.8	0.2
19.34	0.9	2.6	5.4	0.2	11	0.8	17.1	2.4	26.7	14.6	0.1	4.7	1.5	3.5	3.4	1.8	3	3.5	27.8	1.2	3.1	0.9	0.7	0.6	0.3	1.7	0.9	0.1	1.5	0.5	0.1	0	0.5
19.63	0.9	1.7	0.8	0	21.6	1.7	31.1	1.6	42.6	30.5	3.1	10.1	0.4	0.6	0.3	1.6	6.1	0.3	1.3	3.3	1.2	0.4	1.3	1.1	6.5	3.9	0.3	3.4	0.6	1.8	0.1	0.2	0.2
21.78	1.4	0.3	0.9	0.3	4.7	0.3	4.2	0	4.7	3.6	1.3	1.5	0.5	5.8	0	2.5	0.4	1.4	0.7	0.1	7.5	0.8	0.6	0.2	4.2	1.4	1.1	0.3	2.2	5.6	0.4	4.4	0.8
23.44	17.1	1.3	0.8	2.7	0.2	2	1.3	0.1	1.9	2.2	0.3	0.4	0.5	0.8	0.5	2.1	9.1	0.4	0.8	22	0.5	0.7	73.4	2	0.9	3.9	3.8	7.7	9.4	7.2	0.6	2.3	5.1
24.71	1.2	1.3	6.9	0.6	1.1	3.5	6.4	0.7	10.8	8.2	4.6	8.2	1.2	7.2	2.7	2.6	0.7	0.9	1.3	1.2	3.7	2.7	1.2	9.8	19.5	16.1	1.4	2.6	2	5	2.9	3.2	3.4
25.78	0.7	6.8	5.8	14.6	3.3	2.1	0.4	2.1	0.9	2.5	7	4.9	2.4	7.8	1.5	0.8	8.2	6	1.3	11.2	0.4	2.5	10.4	8	1.1	2.5	24.1	7.3	24.1	10.6	20.6	13.1	13.8
28.12	10.2	7.4	0.3	0.2	1.1	0.4	0	13.7	0	0.6	3.4	11.8	14.1	0.6	2.3	4.4	11.9	0.4	0.5	21.8	0.8	2.8	3.9	7.8	2.4	1.2	0.2	11.5	2.9	27.8	3.8	4.7	17.7
29.2	0.7	0.1	1.2	7.6	0.6	0.4	3.4	3.5	6.2	10.3	4.4	10.4	9.5	0.1	12.1	13	16.7	2.7	0	1.7	1.2	1.5	3.4	1	1.4	4.5	3.5	2.5	6	5.2	22.2	2.4	1.4





### 3.31 Test 47

Table 3.31 - MAC of ODS of Test 47 to modeshapes

freq Hz	1.82	3.24	4.13	7.08	7.74	8.88	10.89	11.05	11.63	12.07	12.84	13.26	13.67	13.79	13.94	14.95	16.32	17.56	19.06	20.85	23.28	23.49	23.62	24.23	24.58	24.77	25.41	26.51	27.12	28.1	28.22	28.31	28.44
1.86	95.6	1.6	0	0.1	0.5	3.5	0.5	39	0.5	0.2	3.8	1.4	14.6	0.5	11.3	0.3	1.7	0.8	0.3	13	0.1	1.1	13.2	0.5	0.3	0.8	0.2	0.4	1.3	8.1	0.4	1.2	17.5
3.61	0.2	1	2.3	0.1	69.7	7.1	47	2.2	46.2	31.5	3.6	13.5	0.2	4.4	0.3	2.1	1.2	4.7	5.5	0.1	0.9	0.8	0.3	0.2	0.6	5.2	0.9	0.9	0.4	2.8	0.1	0.2	0.1
7.13	0.1	0	4.2	98.3	1.9	9.9	0	0.1	0.1	7.9	4.1	0	0.2	5.8	0.2	1.1	1	0.4	0	0.6	2	4.1	2.5	1.1	2.2	0.4	9.9	5.2	11	28.3	48.6	44.7	24.8
8.3	0.4	1.9	1	1.1	93.1	6.4	40.2	2.3	41.5	18.6	0.7	15.4	0	2.8	1.4	1.2	0.7	2.9	1.3	0.3	1.8	1.6	0.3	0	3	8.2	0.4	0.2	1.2	5.9	0.4	3.1	0.1
8.90	0.5	3.1	7.6	4.8	53.9	49.5	26.5	3.5	27.7	9.6	5	15	2	3.6	4.3	2.7	2.8	1.8	3.2	2	7.9	0.8	2.8	2.1	2.9	6.2	5.2	6.6	2.7	4.5	3.1	4.2	0.5
10.55	7.5	0.1	1.7	0.1	35	3.2	81	7.8	41	15.7	7.3	2	7.7	3.7	4.6	2.2	0.6	1.8	0.7	0.2	0.3	0.2	0.3	0.5	1.5	0.8	0.5	1.3	0.5	1	1.9	0.1	1.5
10.94	35.7	3.7	0.1	0	10.6	0.1	12.5	88.3	7.7	1.3	4.3	12.9	42.1	2.7	46.1	0.8	13.2	1.4	1.1	0.4	0.9	0.4	0.3	4.9	3.9	7.9	5.8	2.8	0.9	0.6	0.9	0.8	1.3
12.11	3.9	2.2	0.3	0.3	14.4	12	7.8	7.4	7.5	5.7	10.9	35.5	25	1.9	33.3	0.9	21.6	12.5	3.1	7.8	6.7	5.3	0.8	5.8	6.3	4.3	1.5	4.8	0.8	1	1.5	1.7	0.2
13.18	4.4	1.7	0.8	0.3	0.3	4.2	3.2	13.9	4.6	4.2	7.7	11.8	22.8	35.1	17.3	3.1	4	5.5	1.2	3	1.6	0.1	0.1	0.3	0	0.6	0	0.2	0.6	0.4	0.7	0.2	1.3
13.38	8.8	2.8	2.6	0.3	14.4	7.1	6.9	25.3	8.7	6.2	43.7	78	17.8	7.2	33.4	3.1	17.6	21.2	0.2	4.8	1.7	1.7	0.2	4.8	4.5	18.2	2.6	3.6	2.3	8.3	5.4	0.3	5.6
14.06	16	4.6	1.4	0.1	1.5	2	0.1	57.2	1.1	0.7	6.8	27.3	86	1.9	96	0.5	45.5	3.7	4.9	16.7	1.2	2.7	0.8	2	5.9	9	2	3.3	0.9	2.3	2.5	3.2	2.7
16.31	2.4	6.6	0.2	0.3	0.6	2.5	0.4	21.6	0.2	0.2	4.7	9.6	57.7	5.2	59.8	1	84.7	7	1.6	33.2	0.3	1.4	12.3	1.3	4.5	5.9	3.1	5.7	12.4	1.8	1.4	3.9	1.8
17.09	0.5	0.2	0	0.1	10.7	1.4	15.4	0.5	21.5	17.3	3	6	0.1	0.7	0.2	1.5	2	6.9	0.1	0.6	1.7	1	1.6	0.1	0.5	1.6	0.4	1	0.1	0.5	1.7	0	0.2
17.87	0.6	23.2	4	1.1	4	0.2	5.7	0.3	7.4	10.7	11.3	9.8	3	1.1	1.9	4.6	13	67	1.3	0.5	2.3	7.2	0.7	5.8	5.4	7.5	2	2.8	0.3	3.3	4.1	5.6	3.1
19.73	1.9	0.3	1	0.7	21.8	0.8	32.6	0.5	48	39.2	4.4	8.3	1.8	0.7	0.1	2.9	0.4	4	3.7	0.2	6.6	2.5	1.2	0.2	2	5.3	3.8	1.3	3.4	0.2	5	1.1	0.4
23.44	11.5	1.1	0.7	8.7	0.5	9.3	1.4	0.3	2.1	2.9	0.5	1	0	2.7	0	2.5	10.5	1.7	1.4	15.3	0	2.9	74.2	3.1	0.1	3.5	1.7	6.1	6.5	6.4	2.6	2.5	2.8
24.71	0.9	2.1	4.3	0.2	3.2	2	9.7	3.2	15.7	11.1	4.8	11.1	1.4	4.9	3.3	2.2	1.4	2.5	1.7	2.5	4.5	2.7	1	6.9	20.1	20.6	4	3.7	4.4	5.1	2.3	1.9	2.2
25.29	0.5	4.3	3	1.7	0.9	3.6	0.1	1.4	0.4	1.2	2.9	3	0.2	5.1	0.4	23.9	7	0.6	0	5.7	0.6	26	5.2	0.5	29.6	1.3	59.4	1.5	49.1	19.7	3.2	19.1	3.7
27.15	2	1.2	1.2	25.6	2.6	11.6	1.4	0.2	2.1	0.4	1.5	1.4	0.3	4.4	0.1	2.9	11.5	0.6	0.1	0.8	7.8	3.1	7.3	3.1	4.7	2.8	64.1	2.4	86.9	9.5	25.8	13.7	1.3
27.44	4.1	12.8	1.5	5.6	3.2	1.2	0.1	3.4	0.1	2.9	1.3	1.9	9.8	5.5	7.4	19.9	20.9	2.8	0	6.9	3.8	12.9	15.5	2.6	4.2	3.2	12.3	5.7	27.9	17.3	13.7	34.3	13.5
27.83	4	8.6	0.7	0.7	1.7	3.6	0.4	20	0.2	1.1	0.2	5	22.2	0	26.2	14.1	22.8	0.7	0.3	11.3	0.5	12.8	5.2	1.5	10.6	4	34.5	3.9	25.1	11.9	0.9	17.2	1.4
28.03	2.9	0.8	2.9	1.4	0.1	1.8	1.2	18.6	1.3	1	4	6.7	17.7	4.7	20	5.5	12.8	2.7	0.1	20.8	0.4	0.9	5.7	11.2	4.3	12	6.9	6.9	3.8	6.6	0	1.3	29.6
28.52	1.3	0.3	0.9	6.2	0	5.9	2.8	0.5	6.7	12.5	19	12.2	1.4	2.3	28	13.5	8.8	5	0.4	3.5	1.5	11	7.3	3.8	2.1	5.2	0.8	29.4	1.3	3.6	23.1	10.3	20.9
29.2	0.6	0.3	1.7	7.8	0.2	0.4	2.6	3.9	4.5	7.1	8.6	13.1	8.4	1.1	13.5	0.4	22.1	5.1	0.3	15.6	3.2	0.5	5.1	0	1.3	7.7	2.6	5.8	7	1.2	26.1	3.6	2

### 3.32 Test 48

Table 3.32 - MAC of ODS of Test 48 to modeshapes

freq Hz	1.82	3.24	4.13	7.08	7.74	8.88	10.69	11.05	11.63	12.07	12.84	13.26	13.67	13.79	13.94	14.95	16.32	17.56	19.06	20.85	23.28	23.49	23.62	24.23	24.58	24.77	25.41	26.51	27.12	28.1	28.22	28.31	28.44
2.05	94	3.3	0.4	0.2	3.5	1	4	36.3	4.7	3.5	2.6	0.5	16.4	0.2	10.9	0.5	0.4	0.1	0.2	12.9	0.1	0.3	14.8	0.4	0.6	0.7	0.3	0.2	0.5	6.8	0.2	0.4	15.9
3.52	0.1	0.6	1.1	0.1	75.8	2.5	50.4	2.3	52.3	33.7	3	11.9	0.7	2.4	0.5	0	1.8	4.5	2.1	0.1	1.5	0	0.2	0.1	0.5	4.3	0.7	2	0.1	1.9	1	0.1	0.5
7.13	0.1	0.9	4.1	98.3	0.6	9.2	0.3	0	0.6	11.6	6.9	0.2	0.2	5.1	0.1	0.1	1.2	0	0.1	0	1.5	1.9	1.3	1.6	0.8	0.6	8.8	1.9	11.6	26.4	50.5	41.7	24.8
8.59	0.3	1.4	0.9	1.8	87.8	5.2	31.1	1.8	31.4	11.4	0.1	13.1	0.1	2.5	1.5	2.9	0.9	3.5	1.5	0.3	2.2	3.5	0.2	0	2.8	9	0.7	0	1.9	7.1	1.8	6.1	1.1
10.55	11	0.4	0.9	0.1	28.7	1.9	65	14.1	33.8	11.8	4.2	0.6	10.9	1.7	6.9	2.8	1.5	0.4	1.9	0.4	0.6	0.4	0.6	0.6	1.5	1.5	0.8	1.9	0.6	1.1	1.7	0.1	1
10.84	24.1	2.5	0.1	0.1	15.6	0.3	26.6	67.5	6.3	0.1	5.9	12.9	27.3	4.8	32.4	1.4	9.8	1.7	0.2	0.1	1.4	0.2	0	1.8	1.1	5.6	4.9	2	1	1	0.8	0.6	0.9
12.11	9.1	1.8	0.6	0.2	10.8	11.4	4.6	16.4	5.7	3.1	13.7	44.1	30.4	1.2	41.5	0.1	20.7	11.9	3.6	4.2	6.1	4.2	0.6	3.5	8.3	11	2.1	2.3	1	1.2	1.5	1.4	0.2
13.09	6.3	3.5	2.7	0.8	0.4	0.3	1.1	20.1	2.8	2.1	3.1	1.3	27.1	1.6	25.3	2.5	8.7	0.4	2.1	3.3	1.4	0.1	0.1	0.4	0.8	1.5	0.5	0.1	0.1	1.4	0.4	0.6	1
13.57	9.3	11.1	6.6	0.6	8.7	1.7	6.2	24.3	3.6	1.5	37.7	53.6	27.3	7.5	29.5	4	9.1	8.7	0.2	3.2	0.3	1.4	0.2	5.2	2.2	1.2	0.7	1.3	2	7.7	3.8	0.8	3.3
13.87	15.2	3.9	3.7	0.2	0.7	0.9	0.4	50.8	1.9	1.9	0.9	16.7	90	4.9	89.4	2.4	42.8	1.9	5.8	13.3	2	0.4	0.8	0.2	4.8	6.4	1.2	1.7	0.7	4.2	1.6	1	0.4
14.06	14.5	2.3	1.8	0.2	1.7	2.1	0.3	55.8	1.7	1.3	7.2	29.8	81.5	1.1	93.8	0.9	42.5	4.3	4.8	14.9	1	3.7	1	2.1	4.5	7.7	2.1	4.2	0.9	2.6	3.4	3.9	2.5
15.04	2.4	6.5	8.4	0.5	3.1	2.6	0.4	3.7	3.2	6.3	12.3	3.2	7	14.9	11.1	73.7	2.4	1.5	2.8	0.7	0.3	48.7	3	4.6	8.5	4.2	1.8	11.5	1.2	18.7	12.3	25.8	15.6
16.21	2.3	6.9	0.8	0	0.6	1.3	2.1	21.3	3	3.8	1.3	6.4	60.8	4.3	60.7	2.1	81.8	5.7	1.3	35.6	0.3	0.9	10.1	0	2.3	2.4	3.4	3.1	11.2	3.8	1.6	3.4	0.4
17.09	0.3	1.1	0.1	0	11.6	2.6	16.3	0.6	21.8	17.1	1.8	5.6	0.3	0.6	0.4	0.6	1.7	5.3	0.1	0.6	1.7	0.5	1.1	0.1	1	1.6	0.2	0.5	0	0.4	0.9	0.1	0
19.34	0.3	0.2	3.9	0.1	14.2	1.7	23.2	0.7	33	24.4	2.6	6	1.7	0.2	0.4	0.1	2.1	8.2	11.9	1.8	3.2	1.1	0.5	0.6	5	2.3	4.1	0.7	4.3	0.4	0.9	0.3	0.6
21.87	2.3	1.6	0.9	0.1	3	0.6	4.1	0.1	4.7	3.6	1.2	0.4	0.3	6.1	0.2	0.8	0.1	0.5	0.4	0.1	4.1	0.2	0.6	0.1	5.4	0.2	0.3	0.2	1.5	2.1	0.3	1.5	0
23.05	1.1	6.9	0.2	1	2.1	7.3	3.8	0.2	6.1	8.1	6.1	5.1	0.6	1.8	0.6	9.3	1.5	7.1	0.5	0.3	51.1	16.9	3.3	3.1	5.8	11.3	4.1	8.7	0.1	8.2	5	5.2	2
23.44	18.5	1.1	2.6	2.6	0.3	1.6	0.1	0.2	0	0.2	1.2	0.9	0.2	0.5	0	4.4	11.1	12.6	26.7	0.9	4.2	70.1	2.3	4.2	2.8	1.9	11.7	8	7.4	0.1	1.1	4.9	
24.32	3.7	0.4	1.1	0.4	1.3	1.8	0.6	0.1	1	5	3.6	0.5	0.1	0.6	1.1	10	1.2	0.2	0.7	4.1	1.7	12	0	14.4	3	20.4	0.5	20.9	1.3	10.3	8.6	9.8	4.7
24.71	2.4	2.6	5.6	1.6	0.1	3.1	5.1	8.4	10.5	10.9	7.3	6.4	4.3	6.1	6.1	3.3	2.8	1.4	1.2	1.3	1.1	5.9	1.3	10.1	11.5	17.3	1.9	0.3	1.1	4.1	5	6.6	9.1
26.56	0.4	3.4	0	4	0.3	5.6	0	2.9	0	0	2.7	0.5	2.2	2.4	1.7	7.6	0.4	2.9	0.3	4.1	5	2	25.9	9.3	0	3.3	6.2	59.9	12.2	4.1	1	3.1	3.6
27.05	0.9	0.2	1.2	31.4	1.3	10.2	0.7	0.1	1	1.4	1.6	0.7	0.2	4.3	0	1.5	10.5	0.4	0.1	1.2	7.7	2	8.2	4.3	4.6	1.7	61.3	0.6	82.7	11.1	31	17.2	5
28.03	10.6	0.3	0.5	1.7	0.7	1.8	0	6.2	0.1	0.5	0.7	3.6	5.2	0.4	3.4	3.2	0.5	0.2	24.5	1.3	4	5.5	8.7	5.6	12.3	15.5	2.3	23.6	21.4	7	18	20.8	
28.42	3.4	8.1	1.6	4	0.2	2.5	3.7	2	9	12.8	18.8	8.3	2.3	4.6	0.5	20.1	0.8	1.7	0	3.6	2.8	12.6	9.7	2.3	2.3	3.2	1.8	37.2	2.1	5.1	23.2	8.7	22.1
29.1	0.5	0.9	1.4	7.1	0.3	0.1	3.5	6	6.6	10.6	5.8	11.2	11.9	0.4	16.1	0.6	19.8	1.5	0	18.7	1.3	1.6	6.2	0.1	0.6	4.9	5.5	7.7	11.1	2.6	25.3	4.6	1.3





### 3.33 Test 49

Table 3.33 - MAC of ODS of Test 49 to modes

Freq Hz	1.82	3.24	4.13	7.08	7.74	8.88	10.69	11.05	11.63	12.07	12.84	13.26	13.67	13.70	13.94	14.95	16.32	17.56	19.06	20.85	23.28	23.49	23.62	24.23	24.58	24.77	25.41	26.51	27.12	28.1	28.22	28.31	28.44
1.76	0.5	0.3	0.7	0.1	18.8	0.1	13.5	1.7	15.1	8.5	1.1	1.8	1.7	4.4	3.2	0.6	2.6	1.1	0.1	0.8	0.6	0.4	1.2	1.2	1.2	2.8	0.9	0.5	0.2	1.4	0.8	0.4	0.2
3.52	0	1.7	0.7	0.1	73.5	4.9	50.1	3.2	51.1	35.1	5.3	16.4	0.4	3.3	0.8	0.1	1.4	2.7	2.4	0.2	0.9	0.1	0.1	0	0.2	3.3	0.8	2.7	0.1	2.5	1.8	0.3	1.2
4.39	0.3	0.7	1.7	0.1	74.8	1.4	47.4	1.7	49	30.1	2.1	6.5	0.3	1.2	0.1	0.4	0.3	1.5	1.3	0	1.5	0.1	0.2	0.2	0.4	2.2	0.2	1.2	0	1.1	0.5	0.1	0.4
8.59	0.1	0.1	3.7	1.2	85.3	3.8	32.1	3.2	32.2	12.4	0.2	14.9	1.2	1.4	4	0.6	4.4	6.1	1.2	1.9	2	1.8	0.6	0	3.5	9.4	1	0.5	1	6.8	0.6	3.2	0.5
10.55	13.2	0.4	4.5	0.3	28.6	1.4	57.6	14.4	32.2	13.2	4.3	0.3	9.6	1	7	4.1	0.1	3.2	2.1	1.4	0.5	0.1	0.2	0.9	1.4	0.2	1.7	2.2	1	0.6	2.3	1	0.9
10.84	29	3.6	0.5	0.4	8.7	0.2	12	72.8	1.2	0.3	9.2	13.1	31.2	4	35.1	4.1	11.6	2.1	0.2	0.4	0.7	0.3	0	2.2	1.2	9.4	5.2	0.9	0.7	0.8	0.3	0.2	2.9
12.21	6.8	4	0.9	0.4	2.7	2	4.3	6.2	5.4	6.7	4.2	22.9	15.1	1.3	23.6	1.7	7.3	10.6	2.5	4.6	6.2	4.3	2.6	1	2.5	3.4	1.8	5.1	0.6	3.5	4.1	2.5	2.2
13.09	5	0.7	2	0.1	7	6	8.1	13.2	7.8	9.8	17.3	18.9	12.2	13.2	17.4	1.4	3.9	3.3	2.8	2	2.1	0.7	0.3	0.5	0.9	10.8	1	2.9	0.4	2.4	1.4	0.7	3.3
13.57	2.3	2.3	24.8	0.1	3.3	8.8	0.6	9	2.9	0.5	17.3	47.2	13.4	5.8	26.2	0.9	17.2	12.3	7.1	4.2	2.4	3.7	1	0.9	3.6	12	1	2.7	1	15	1.4	2.6	0.8
15.04	0.1	10.3	24.8	0.1	2.2	1.4	2.3	0	2.8	0.5	4.7	5.3	2	1.3	0.5	23.6	6.1	9.6	3.3	1.6	0.1	9.1	0.1	0.1	9.7	7.3	0	2.6	1.1	1	0.8	4.5	4.7
15.92	0	14.9	16.7	0.1	11.4	4.4	11.6	1.9	19.5	11.3	20.1	34.6	2.7	7.2	5.7	5.1	18.9	39.9	2.2	3.8	5	4.6	1	2.4	7.2	10.9	3.3	6.1	2.2	3.9	3.3	0.7	2.3
16.21	0.1	0.8	6	0.2	8.5	4.1	12.2	8.5	18.4	12.5	8.6	21.9	23.1	0.2	26.3	2	46.6	14.4	3.8	23.2	2.1	0.7	4.9	0.3	9.5	4.6	1.3	5.7	5.4	1.3	3.5	1.9	4.6
17.09	0.4	0.9	3	0.3	8.9	0.9	15.4	1.6	22	17.4	2.3	4.4	0.1	0.2	0.6	1.5	3	5.9	0.1	0.2	0.4	1.4	1.7	0.2	0.3	1.4	0.3	1.3	0.1	0.1	2	0.4	0.8
17.77	0.1	3	2.3	0.8	6.9	4.6	12.9	2.1	19.5	16.1	11.9	20	1.4	5.6	1.9	0.2	9.5	19.5	1.9	0.4	5.4	4.5	0.3	0.8	1.4	1.4	4.8	2.3	5.6	2.7	4.4	2.3	1.4
19.53	0.5	0.7	0.2	0	14.5	2.2	24.7	0.6	34.5	27.6	1.6	8	0.9	1.2	0.1	0	1.1	4.5	0.3	1.2	2.2	0.5	0.3	0.3	2.5	5.3	2.3	0.1	2.7	0.6	1.4	0.7	0.1
20.9	0.5	0.7	3	0	12.1	2.1	18.5	0.6	24.8	18.9	2.6	7.2	4.2	2.3	3.1	0.3	3.4	3.9	1.5	18.9	4.1	0.5	3.8	0.4	2.6	5.3	8.8	1.5	7.4	3	0.3	3.1	6
21.78	1.8	1.5	1.9	0.2	3.2	0.9	4.6	2.1	7.1	5.2	7.1	2.7	0.1	2.1	0.9	0.1	0.2	1.1	0.3	0.4	1.1	0.4	0.6	0.5	3	1.3	0.9	1.2	1.5	3.5	2.5	0.2	1.4
24.32	1	2.9	9.8	1.3	2.9	0.5	2.3	1.1	2.2	4.7	1	0.3	0.7	3.1	1.2	6.4	0.7	1.1	0.5	2.8	3	3.9	0.5	13.6	14.5	24.5	0.2	17.3	3.3	3.5	4.8	5.9	0.4
24.71	2.9	2.5	4	3.4	0.1	0.9	5.4	10.9	12	14.8	8.9	5.9	4.4	5.6	5.7	4.9	2.9	5.6	0.6	0.1	0.6	8.9	1.6	15.3	11.4	18.7	4.6	2.5	2.5	6.8	7.4	9.6	11.9
25.88	0.5	2.6	0.6	3.2	1.7	3.5	0.6	4.1	1.6	0.1	0.5	4.6	10.4	0	16.6	3	11.1	1.7	3.9	20.7	2	7.2	6.2	0.7	8.9	9.9	0.5	4.2	0.6	10.8	9.5	11.6	3.3
26.66	0.2	2.3	4.7	8.4	0.9	8.5	0.7	5.5	0.8	1.5	2.5	2.4	4	0.2	4.3	0.7	3.7	1.6	0.3	3.1	2.1	3.1	16.3	4.2	1.7	0.4	6.2	21.6	9.1	6.9	3.8	10.5	14.9
27.15	1.1	1.5	0.5	15.5	0.3	2.6	0.1	6.1	0.1	3.1	1.4	1.3	10.9	8.2	10.9	3.2	18.5	0.9	0.2	10.8	3.5	2.4	9	2	0.8	2.4	24.5	7.6	40.3	6	12.6	7.6	5.9
27.73	7.2	8.8	0	3.9	0.6	2.5	2.8	15.8	4	6.6	20.2	10.8	24.3	4.6	25	10.1	17.1	2	0.4	9	2.4	8.2	5.2	5.9	8.7	1.1	6.3	9.8	7	2.7	6.3	6.3	10.5
28.03	8.6	11.3	0.8	1.5	1	0.8	0	3	0.2	0.7	0.3	9	3.1	13.2	1.9	4.8	0.2	2.8	0.5	4.2	3.9	7.2	0.3	4.7	7.2	0.4	2.5	2.7	1.1	34.1	0.1	7.8	1
28.42	24.5	1.8	1.7	1.5	1.2	1.1	0.8	36.6	1.5	2.2	2.4	7.9	32.9	12.1	33.6	7.3	16.9	1.3	2.4	2	2.2	1.2	4.2	2.3	1.4	3.4	3.5	2.8	0.2	1.6	0.4	0.9	6.5
28.61	10.4	0.8	2.4	0	0.3	2.3	2.4	20.8	5	3.7	0.1	4.5	24.7	4.6	20.5	1.1	7.8	0.4	1.2	1.8	3.1	0.9	1.8	2.7	3.4	7.2	2.3	2	0.9	0.6	3.3	1.1	1.1
29	15.7	1.1	0.4	6.5	0.6	1.4	2.9	20.1	4.3	7.7	7.1	1.8	15.7	7.2	15.8	4.1	2.9	0.5	1.1	0.9	0	2.4	3	0	2.8	0.3	6.7	0	3	2.6	6.2	3.7	15.8

### 3.34 Test 50

Table 3.34 - MAC of ODS of Test 50 to modes

freq Hz	1.82	3.24	4.13	7.08	7.74	8.88	10.69	11.05	11.63	12.07	12.84	13.26	13.67	13.79	13.94	14.95	16.32	17.56	19.06	20.85	23.28	23.49	23.62	24.23	24.58	24.77	25.41	26.51	27.12	28.1	28.22	28.31	28.44
2.05	94.6	2.8	0.5	0.1	1.8	0.7	2.1	39.7	2.5	1.8	2.9	0.7	17.4	0.4	12	0.4	0.7	0.3	0.3	12.8	0.1	0.2	14	0.5	0.6	1	0.2	0.1	0.7	7	0.1	0.5	16
3.61	0	3.7	2	0.1	72.5	4.9	49.7	2.4	51	33.6	5.2	15.4	0.7	3.6	0.6	0.1	1	2.3	2.3	0.1	1	0.1	0.2	0	0.5	3.6	0.8	2.7	0.2	3.1	1.8	0.1	1.2
4.1	0.4	0.5	30.9	0.3	5	38	1.9	0.1	3	0.4	21.7	6.1	0	4.6	0.2	3.9	0.9	1.5	1.3	0.2	4.2	1.3	1	2.2	6.8	6.1	3.8	1.6	1.9	0.4	0.3	0.3	0.4
4.3	1.6	2.2	10.1	0.7	48.2	6.7	29.1	0.1	32.3	18.4	2.8	0.6	1.2	0.3	0	2.5	0.2	0.1	0.1	0.5	3.7	0.3	0.1	0.7	2.9	1.9	0.5	0.7	0.4	1.5	0.9	0.3	0.4
5.86	0.6	4.7	12	3.4	46.4	11.5	23.4	0.6	27	9.6	11.1	0.7	0.8	0.1	1.1	3.5	0.9	2.3	0.2	0.2	2.6	1.7	0.5	0.8	0.8	0	0.4	0.6	0.1	5.9	2.6	2	1.1
7.13	0.1	0.9	4.1	98.4	0.6	9	0.3	0	0.7	11.6	6.9	0.3	0.2	5	0	0.1	1.3	0	0.1	0	1.5	1.9	1.3	1.6	0.9	0.6	8.7	1.9	11.7	26.3	50.5	41.7	24.8
8.59	0.2	1	1	1.1	88.8	4.1	31	1.3	31	11.6	0.1	12.6	0.1	2.2	1.2	3.1	0.8	3.3	1.3	0.2	2.2	4	0.3	0	2.4	8.8	0.6	0	1.7	7.1	1.4	5.5	0.8
10.55	12	0.2	0.9	0.1	27.2	2	64.7	16.4	31	10	4.5	0.7	12.5	3.3	8.1	2.4	1.7	0.6	1.4	0.3	0.4	0.4	0.5	0.5	1.1	1.4	0.8	2	0.6	1.4	1.6	0.1	1.1
12.21	5.3	1	2.2	3	15.2	10.1	8.6	9.9	17.1	15.5	12.6	37.3	19.1	4.6	27.8	2.4	14.8	11.2	2.5	3.3	5.5	8.8	0.7	2.4	4.4	6.7	1.9	3.1	2.1	4.4	7.6	6.5	1.5
12.89	12.3	3.9	0.7	2	5.5	3.1	1.5	19.7	4.6	2.6	0.6	14.6	43	28.1	24.1	8.2	9.9	4.8	1.5	0.5	1.1	4.2	2.5	0.1	3.5	3.3	1.7	1.2	1.3	12.5	2.2	7.5	0.4
13.09	5.7	2.5	3.6	0.9	3	1.4	1.2	18.2	4	2.2	0.3	6.1	29.4	19	25.9	0.4	11.5	1.9	3.6	2.6	0.6	0.6	0.9	0.2	1.7	2.7	1.5	0.4	0.1	6.9	0.9	1	0.2
13.57	8.2	10.6	9.7	0.8	8.5	1.5	5.7	18	4.3	1.4	32.2	39.6	27.5	11.1	18.6	2.5	4.2	9.2	0.2	1.7	0.4	3	0.3	5	0.6	7.1	0.2	0.5	3	11.5	3.4	1.8	2.9
13.87	15.3	4	3.6	0.3	0.8	1	0.5	49.6	1.9	1.8	0.3	17.9	88.8	5.6	87.8	1.9	42.3	2.5	5.8	12.3	2	0.5	1.1	0.1	4.8	6.4	1.4	2	0.6	4.7	2.3	1.1	0.2
14.06	14.9	2.5	1.5	0.1	1.6	1.8	0.2	56.9	1.2	0.7	7.2	27.5	83.3	1.8	94.9	0.5	42.5	3.7	4.9	15	1	3.1	0.9	2.1	4.7	8	2	3.6	1	2.2	2.6	3.2	2.4
16.21	2.3	1.5	1	0.1	2.6	1.2	22	2	3	1.3	6.6	10.3	54.3	4.7	59.1	0	70.1	1.8	2	3.71	0.8	0.8	13.6	0.5	3.2	3.2	3.2	8.9	10.2	4	1.1	4.4	2.5
17.09	0.3	1.1	0.2	0	11.6	2.3	16.2	0.8	21.2	16.6	1.8	5.5	0.1	0.6	0.4	0.4	1	4.3	0.1	0.3	1.8	0.4	0.9	0.2	1	2.1	0.3	0.4	0.1	0.5	0.8	0.1	0
17.97	0.2	0.2	0	0.9	11.1	2.6	18.6	0.8	28.4	20	5.1	13.5	0.5	1.2	2.6	2.5	3.4	20.1	0	1.8	0.8	4.3	3.2	0.5	1	4.1	2.5	7.1	0.6	1.4	1.5	0	0.1
19.24	0.4	2.9	5	0.1	12.2	1.7	21.4	0.3	29.9	26.2	3	5.2	2	0.4	0.5	0.3	1	7.2	14.2	2	2.3	1.2	0.5	0.6	5.5	3.7	0.7	3.7	0.3	1.4	0.2	0.1	0
20.8	5.1	2.1	0.6	0	10.7	2.8	18.3	0.6	23.4	22	0.6	6.7	5.7	2.8	5.8	0.4	13.3	1.3	0.7	31.4	0.6	0.2	3.6	1.4	0.7	2.9	0.5	1	0.3	2.4	2.5	0.8	1
21.88	1.6	1.6	0.4	0	2.5	0.5	3.3	0.1	4	2.8	0.5	0.6	0.1	7.8	0.2	0.3	0.3	0.9	0.8	0.4	2.9	0	0.9	0	6.7	0.4	0.1	0.2	1.2	2.2	0.1	1.4	0.3
23.44	19.9	0.3	2	1.2	0.3	28.4	0	0	0.3	1.2	0.2	0.5	0.2	1.7	0.5	0.3	14.9	0.5	0.1	31.9	1.4	24	81.9	1.4	0.3	0.2	5.6	6.6	13.1	1.4	0.8	3.2	3.4
24.41	0.8	4.5	0.5	1	0.1	0.6	0.4	0.6	2.2	1.8	2.2	2.2	1.9	3.1	2.3	2.9	2.7	2.5	8.7	3.5	3.4	1.9	15.1	9.4	13.5	3.9	12.9	1.9	3	5.1	4.3	2.2	
24.8	0.1	7.3	1.9	5.5	0.8	10.9	2.5	1.3	3.2	3.4	3.9	10.8	0	2.7	0.7	1.3	0.4	15.6	1	5.1	6.8	7.7	3.8	20.3	6.4	3.5	2.9	33.7	2	9.4	2.6	6.2	5.4
25.2	0.2	0.6	2.6	2.2	0.7	6.1	0.3	1	1.6	3.1	7.6	0.6	0.2	6.4	0.2	32.5	6.8	0.5	0.1	1	1.2	29.4	1.1	0.9	34.5	0.8	55.9	8.1	39.2	15.2	5.5	2.2	8.7
25.78	0.7	2.3	0.7	17.4	24	11.8	1.2	1.8	3.6	1.7	3	1.7	1.1	2.9	2.3	16.7	6.2	3.5	0.8	0.7	6.7	20.4	1.3	0.3	2.3	7.4	55.8	3.9	59.7	7.5	18.3	20.6	5.6
27.05	0.9	0.5	1.3	29.8	1.4	10	1	0.8	2	2.5	3.4	1.5	0.4	5.2	0.3	7	7.3	0.8	0	0.3	8.9	8.6	4.9	2.8	5.9	3.8	59.8	3.1	78.2	14	32.9	25.5	7.1
27.64	0.8	5.6	0.2	0.1	0.8	0	0.1	2.6	0.1	0.8	1	10.1	5.2	4.6	10.5	7.9	19.1	1.5	0.2	18.2	2.8	31.1	19.8	3.1	7.9	3.1	28.4	3.9	32.5	27.5	1.4	3.5	0.3
27.83	0	2	0	9.5	0.6	6.3	0.3	2.2	1	1.1	0.6	3.1	2.9	1.6	6.9	18.1	14.3	0.1	0.2	5.5	1	18	5.3	5.1	12.9	3.7	49.4	8.6	48.3	7.8	6.2	9.1	2.5
28.42	3.4	5.5	0.7	5.3	0.2	2.3	3.3	0.7	8	11.2	14.6	8.4	0.6	3.7	0	14.8	1.2	1.9	0.1	4.1	3.6	11.8	9.1	3.2	1.1	2.7	2.3	36.4	2.8	5.8	19.9	8	24.8
29.1	1.3	1.8	2.3	4.3	0.4	0.1	3	1.3	5	6.4	5.3	8	2.9	1.2	6.5	0.7	10.6	0.9	0.1	9.8	2.5	0.3	5.2	1.9	2.4	6.1	5.2	9.4	9.2	0.6	15.7	2.9	0.8





### 3.35 Test 51

Table 3.35 - MAC of ODS of Test 51 to modeshapes

Freq Hz	1.82	3.24	4.13	7.08	7.74	8.88	10.69	11.05	11.63	12.07	12.84	13.26	13.67	13.79	13.94	14.95	16.32	17.56	19.06	20.85	23.28	23.49	23.62	24.23	24.58	24.77	25.41	26.51	27.12	28.1	28.22	28.31	28.44
2.05	95.2	1.4	0.1	0	1.4	2.7	1.5	40.7	1.8	1	3.1	0.8	17.4	0.7	13	0.4	1	0.5	0.3	9	0.1	1.6	11.2	0.4	0.6	1	0.3	0.6	1.5	6.9	0.5	0.7	15.6
3.42	0.9	0.4	1.6	0.2	78.1	4.7	49.7	3.7	51.2	32.3	2	13.8	0.5	3.8	0.6	1.3	2.7	7.5	2	0.8	1.1	0.7	0.4	0	1.6	6.3	0.8	0.8	0.3	0.1	0.1	0.3	0
4	0.4	9.9	4.9	0.2	73.7	12	46.3	2.8	48.5	27.8	5.6	13.6	0.2	5.8	0.7	0.5	0.2	0.3	2	0.3	0.6	1.2	0.5	0.3	0.6	3.2	0.4	1.3	0.7	5.5	0.3	1.5	0.1
7.13	0.1	0	5.5	98.6	0.8	8.3	0.1	0	0.2	9.5	5.1	0.1	0.1	4.8	0.1	1.4	1.6	0.5	0.1	0.4	2.1	4.4	2.4	1.2	2.3	0.7	9.4	4.5	11	26.5	50.2	43.9	24.5
8.59	0.5	2.2	1	1.3	90.3	5.5	33.2	2.1	34.6	14.3	0.3	14.2	0.1	2.6	1.4	2.1	0.5	2.1	1.4	0.4	1.8	2.5	0.4	0	2.7	8.2	0.4	0.1	1.4	6.7	0.8	4.4	0.2
8.79	0.5	2.4	1.3	1.6	86.9	6.4	31.3	2.5	32.9	12.8	0.4	14.1	0	2.4	1.9	2.2	0.5	2.2	2.2	0.3	1.6	2.7	0.5	0.1	2.8	8.9	0.6	0.3	1.5	6.3	1.1	5.1	0.4
10.55	9.3	0.1	3.1	0	33.7	3.4	68.8	12.1	33.3	11.3	5.9	1.3	8	2.4	5.3	2.6	0.7	1.1	2.8	0.5	0.5	0.3	0.6	0.6	1.3	1	1.1	1.3	1	0.9	1	0.4	1.3
10.84	30.5	3.1	1.4	0.1	14.6	0.4	18.9	79.5	5.4	0.5	7.2	14.3	31.7	3.7	37.7	1.1	10.9	1.7	1.3	0.2	1.8	0.1	0.2	2.9	1.7	5.7	6	1.6	1.5	0.5	0.8	0.7	1.6
11.52	13.8	3.2	3.9	0	26.8	1.7	20.4	32.8	35.8	25.4	2.3	8.1	16.1	6.1	18	4.1	5.5	2.7	14.9	0.8	1.3	2	2.4	5.8	10.1	11.8	1.3	0.1	0.3	0.2	0.2	0.2	3.9
12.21	7.4	2.5	0.5	0.3	12.4	10	5	15.4	6	2.9	15.3	45.1	29.6	2.8	41.2	0.9	25.1	14.5	4.9	7.6	4.9	6	0.1	4.2	8.5	9	2	3.9	1.2	3.2	2.9	3.2	0.7
13.09	6.3	2	1.7	0.3	0.9	0.8	0.8	22.3	2.2	1.6	0.9	0	29	21.7	28.7	1.8	10	0.4	2.5	5	1.2	0.1	0.3	0.4	1.6	2.1	1	0.4	0.1	2.2	0.1	0.5	0.6
13.57	13.2	7.2	2.8	0.5	8.1	1.7	4.1	33.3	1.4	0	33.8	47.1	37.4	6.4	45.4	2.2	17.6	11	0.3	5.7	0.3	4.5	0.1	3.8	1.4	11.1	0.7	1.8	2.3	10.4	2.9	3.7	3.1
13.87	16.1	3.8	2.3	0.1	0.4	0.7	0.4	52.5	1.3	1.3	1.2	13.8	92.5	8.1	87.8	1.4	43.2	1	5	15.5	1.9	0	0.8	0.3	7.2	6.4	1.6	1.6	1	3.5	1.4	0.6	0.8
14.06	16.1	4.4	1.4	0.1	1.7	2.1	0.2	57.5	1.3	0.9	7.2	27.5	85.7	1.9	95.8	0.4	45.2	3.9	4.9	16	1.2	2.8	0.7	2	5.8	9.1	2.1	3.1	0.9	2.2	2.5	3.2	2.6
16.21	3	7.6	0.8	0.8	2.2	2.2	3.7	21.4	4.4	6.7	0.7	3.4	62.4	7	59.1	0.6	77.7	3.1	2.3	36.5	0.4	0.6	9.9	0	2.7	0.7	4.3	2.5	11	3.1	3.2	7.1	0.7
17.09	0.4	0.6	0.1	0.1	14.1	2.1	18.8	1.6	26.1	19.8	3.4	8.1	0.4	0.5	1.4	1.4	0.9	6	0.2	1.3	2.3	0.9	1.8	0.1	0.3	2.2	0.5	1.3	0.1	0.9	1.9	0	0.1
17.77	0.1	7.6	2.2	0.4	0.5	0.3	1	1.5	1.1	2	4.5	2	1.7	1.3	2.5	1.2	9	21.2	0.3	0.8	0.4	4.2	0.6	3.6	4	3	0.9	1.4	0.8	3.8	2	4.5	2.5
18.75	15.2	2.2	1.6	0.2	13.6	0.5	15.3	43.4	28	18.9	2.6	19.9	40.5	1.2	44.6	2.1	20.1	5	6.8	1.4	6.2	4	1.2	1.3	4.6	4.2	4.2	2.7	0.8	0.6	2.9	0.6	0.7
19.34	2.8	0.1	1.6	0.9	21.1	1.3	32.9	1.2	47.6	41	8.4	12.9	0.9	1.1	0.1	2.9	2.1	10.5	5.8	0.4	5.8	3.2	1.9	0.4	1.2	7.6	4	2.3	3.1	0.4	6.1	0.8	1.2
21.87	4.4	0.4	0.4	0.4	4.6	0.4	6.4	0.2	8.2	8.6	4.1	1.3	1.4	10.2	0.3	0.5	0.1	1.2	0.2	1	8.8	0.5	1.8	0.4	0.9	1.7	0.7	1.8	0.9	2	3.9	0.5	0.8
24.71	2.1	2.1	3.1	2	2.8	0.5	9.8	11.2	17.3	16.3	7.5	9	5.9	4.2	9.3	2.9	6.3	7.7	1.1	3.2	0.2	3.1	1.6	8.5	21.9	34.4	5.3	2.4	2.4	1.4	4.9	2.5	4.5
29.1	1.5	0.4	2	5.6	0.6	1.2	1.5	8.4	2.8	5.3	4.2	10.6	16.6	0.8	19.7	0.1	26.9	3.2	0	20.2	2	0.1	4.4	0.5	1.2	6	5.9	6.9	11.7	1.9	24.1	3.5	0.3
23.05	1.6	8.2	0.2	1.7	0.9	6.8	2.9	0.2	5.1	8.6	6.4	4.4	0.7	1.5	0.5	13.7	1.1	7.8	1.1	0.9	53.9	25.1	4.7	2.2	2.9	6.3	4.9	11.9	0.2	12.9	6.7	8.6	2.9
23.44	16.7	0.6	0.1	3.5	0.2	8.7	0	0.1	0.1	0.9	0.6	1	0.8	2.3	1.2	1.7	15.8	1	1.1	26.8	1.2	4.3	87.2	1.6	2.9	3.6	5.4	3.5	11	15.2	2.9	6.6	3
24.22	4.3	4.8	0.3	0.9	0.1	0.2	5.3	2.3	9.8	11.9	3.6	0.3	3.6	7.4	2.5	12.4	3.8	7.2	1	0.5	1	14.2	6.6	1.6	4.4	2.4	0.1	12.9	3.5	7.7	6.5	5.5	5.6
24.51	0.1	0.6	0.6	1.9	1.4	2.1	3.8	10.6	7.7	6.9	7.2	11.4	10.8	2.5	16.5	1.4	19.9	8.4	1.7	22.3	1.5	0.6	9	0.7	23.4	30.2	9.7	2.2	4.4	3.2	1.6	0.8	8.7
27.64	4.1	12.8	0.8	0.9	1.8	0.3	0.8	8.2	0.2	0.8	1.8	6.8	11.9	1.2	14.4	6.8	19.1	0.4	0.2	11.7	3.3	7.7	11.4	0.4	13.6	0.9	28.1	2.3	20.8	23	0.4	12.6	2.2
28.03	2.9	0.9	1.4	3.1	0.2	2.1	0.9	18.4	0.9	2.1	1.2	4.2	18.4	0.1	21.6	3.5	10.4	0.8	0.1	26.5	1.7	1.6	6.9	9.4	2.6	15.4	8	3.5	10.7	17.6	7.9	22.2	26.7
28.42	6.9	0.3	1.3	0.2	0.1	3.9	2.9	8.7	6.3	8.9	7.6	8.5	11.8	0.3	11.4	9.8	8.2	1.8	0.4	2	1.5	7.4	4.7	4.7	0.3	4.4	2.1	47.9	6.3	0.1	16.8	2.4	7
20.7	6.4	3.2	0.4	0	17.8	4.8	22.1	3.5	32	19.4	1.2	16.3	9	0.3	16.9	0.3	23.9	3.7	3.5	50	2.3	0.8	11.7	0.2	2.7	8.7	0.8	1.9	0.1	9.7	0.3	2	7.3

### 3.36 Test 52

Table 3.36 - MAC of ODS of Test 52 to modeshapes

Freq Hz	1.82	3.24	4.13	7.08	7.74	8.88	10.69	11.05	11.63	12.07	12.84	13.26	13.67	13.79	13.94	14.95	16.32	17.56	19.06	20.85	23.28	23.49	23.62	24.23	24.58	24.77	25.41	26.51	27.12	28.1	28.22	28.31	28.44	
1.86	95.9	3.1	0.8	0.1	1	0.4	1.1	41.3	1.4	1	3.6	1.8	18.3	0.2	13.5	0.3	1.5	0.5	0.2	12.5	0.2	0.5	13.6	0.4	0.8	1.1	0.3	0.1	0.7	6.1	0	0.3	14.3	
3.52	0.2	1.1	0.5	0.2	63.9	3.5	44.8	1.8	45.7	33.1	4.5	12.3	0.4	3.1	0.3	0	1.4	2.4	4.7	0.4	2	0.2	0.1	0.3	0.1	3.1	0.5	2.5	0.1	2.3	1.4	0.5	1.5	
3.91	1.7	4	18.5	0	39.2	21.6	30	5.3	27.3	26.1	16.4	20.1	0.4	9.6	0.7	2.2	3.3	4	6.5	0.1	0.4	0.5	0.1	0.3	1.5	2.3	2.6	0.8	1.2	1.4	0.4	0.4		
7.03	0.1	0.9	3.4	98.4	1.1	10	0.2	0	0.4	10.9	6.2	0.1	0.2	5.6	0.1	0	1.2	0	0.1	0	1.4	1.7	1.2	1.6	0.7	0.5	9.1	1.9	1.2	27.7	50.7	42.6	25.1	
8.3	0.4	1.1	0.9	1.1	92.7	4.7	39	2	39.2	16.3	0.3	13.3	0	2	1.2	1.5	0.9	3.8	1.2	0.3	2.2	2.3	0.2	0	2.6	8	0.7	0	1.5	5.7	0.8	4	0.6	
10.55	8	0.1	0.8	0.2	34.8	2.4	79.4	8.4	41.6	16	8	2.2	8.6	2.3	4.8	2.2	0.6	1.5	0.7	0.2	0.5	0.3	0.5	0.2	0.9	0.8	0.3	1.2	0.6	1.1	1.9	0.1	1	
10.84	34	2.6	0.7	0	9.1	0.2	11.1	89	3.2	0.1	6.4	13.1	38.1	2.4	42.9	0.5	10.9	1.2	0.8	0	1	0.5	0.3	4.4	1.5	5.2	6.7	2.3	1.6	0.3	0.8	1.1	0.9	
11.52	9.1	1.6	0.9	0.4	36.8	1	32.5	30.1	55.2	38.8	3.9	11.1	11.2	3.6	14.3	2	3	3.2	7.2	0.4	0.8	2	2.1	6	6	11.5	2.1	0.3	0.8	0.3	1.1	0.1	2.6	
11.72	2.6	1.4	0.7	1.4	42.9	1.3	47.6	11.9	79.5	64.4	5.4	9.1	2.8	4.3	3.3	4.4	0.5	3	1.7	0.2	0.4	2.8	2.3	4.6	3	7.6	1.3	1.6	0.8	0.9	5.2	1.4	4.6	
12.11	4.3	1.9	0.3	1.5	9.6	14.9	4.6	4.8	2.9	2.3	8	33.7	18.4	2.6	25.7	0.1	14.8	11.7	2.2	2.9	7.9	3	1.5	5.5	6.9	6.6	1.4	2.1	0.6	1	0.3	1.5	1.6	
13.09	5.7	2.5	1	0.4	0	1.5	2	18.3	3.4	3.2	3.3	3.6	26.2	24.3	22.4	3	6.6	1.7	1.4	2.8	1.3	0.1	0.2	0.2	0.2	0.5	0.2	0.2	0.3	0.6	0	0.3	0.9	
13.67	9.7	4.1	4.2	0.5	10.8	5.3	5.2	31.9	6.7	4.2	39.5	69.3	24.6	3	40.9	3.8	17.7	14.1	0.5	5.2	1.4	1.4	0.3	5.4	5.9	18.6	2.6	2.7	1.9	5.5	4.3	0.1	4.9	
13.96	15.9	6.8	1.2	0	1.9	0.8	2.3	40.5	1.1	0.5	2.3	5.2	86.3	17.5	63.1	1.2	32.1	1.2	3.4	7	2.7	1.9	0.9	0.2	5.4	0.8	1.9	0.8	1.9	4.5	1.1	2.8	0.4	
14.06	13.9	2	1.8	0.2	1.6	0.2	55.3	1.6	1.3	6.4	28.9	82.1	1.4	94.5	1.1	42.5	3.9	4.9	15.9	1.1	3.5	1	2	4.7	7.3	2.1	4.3	0.9	2.7	3.6	3.8	2.4	0.1	
16.21	2.1	0.5	0.6	0.2	0.5	1	0.4	25.2	0.3	0.9	3.1	8.4	59.6	5	64.5	0.5	67.5	1.3	2	42.9	0.2	0.8	14.6	0.2	4.1	3.1	2.3	9.9	9.8	4.4	2.2	4.6	1.2	
17.09	0.4	0.9	0.1	0	9.4	2.5	13.9	1.2	18.5	14.7	2.5	6.3	0.1	0.6	0.7	0.7	0.9	5.7	0.1	0.4	1.4	0.6	1	0.1	0.9	1.8	0.3	0.5	0	0.3	1	0	0	
17.68	0.3	3.1	0.2	0.3	8.2	1.6	11.2	0.7	14.8	10.6	1.3	3.7	0.7	0.6	1	0.1	0.2	5.1	0.4	0.6	2.2	0.5	0.5	1.5	2.1	1.7	0.6	0.4	0.1	1.1	0.3	0.3	0.2	
17.87	1.3	25	0.9	0.3	0.7	2.1	3.3	0.2	5.9	3.5	1.1	2.3	0.1	0.4	0.8	0.7	12.5	38.6	0.1	3.1	0.5	1.1	2.9	3.5	6	3.8	1.2	4.1	0	1.2	0.4	0	0.3	
17.09	0.4	0.9	0.1	0	9.4	2.5	13.9	1.2	18.5	14.7	2.5	6.3	0.1	0.6	0.7	0.7	0.9	5.7	0.1	0.4	1.4	0.6	1	0.1	0.9	1.8	0.3	0.5	0	0.3	1	0	0	
19.34	1.5	2.4	4.6	0.2	14.6	2.8	24.6	0.8	34.9	27.9	4.3	7.3	1.3	0.1	0.3	1.3	1.9	6.9	10.7	3.2	3.3	1	0.2	0.8	3.2	4	3.2	0	2.9	0	1.8	0.5	0.5	
19.53	0.7	0.7	0.23	0	14.8	2.3	24.5	0.4	33.8	26.9	3.9	8	2.2	0.4	0.5	0.6	0.8	8.2	3.1	0.2	3.5	0.8	0.4	0.9	2.6	6	4.6	0.4	4.1	0.4	1.3	0.1	0.4	
19.73	1.2	1.1	2.1	0	14.5	1.6	25.3	0.7	36.4	27.5	2.1	7.4	1.1	0.8	0.1	0.6	0.3	4.9	1.5	0.4	2.6	1	0.9	0.1	3.6	3.4	3.1	0.4	3.5	0.6	1.4	0.5	0	
21.78	0.2	0.2	0.7	0.4	3.8	0.7	3.5	0.1	3.7	2.8	1.2	0.7	2.4	0.2	0.7	1.8	1.6	0.9	0.8	1.4	5.1	0.8	0	0.7	5.2	0.6	1	0.2	2.3	4.4	0.2	3.8	1.2	
23.44	14.2	0.9	0.4	3.9	0.5	2.4	0.7	0	0.6	0.5	1.6	0.1	0.5	0	0.9	10.6	6.7	0.2	1.2	20.2	0.5	8.5	68	3.3	2.3	9.4	1.9	9.2	6	7.3	1.3	6.6	7.4	
24.32	1.9	0.7	0.6	0.7	0.7	3.3	0.2	4.3	0.9	0.7	0.4	1.7	1.8	1.8	4	0.3	3.2	0	1.9	3.9	7.6	0.9	1.1	44.3	2.1	12.2	1.6	37.3	0.3	2	0.3	0.1	21.3	
24.71	1.5	2.7	4.1	1	0.3	5	5.5	4.2	11.1	10.2	4.1	5.5	1.3	6.6	3.3	4.6	1.5	0.4	0.2	1.7	0.5	5.8	0.5	9.4	18.2	9.1	2.2	1.6	1.9	6	5.2	6.8	4	
27.44	2.4	3.4	1.8	9.2	3.2	0.8	0.4	20.3	0.5	7.5	5.3	0.3	7.1	6.3	5.6	3.1	13.5	0.5	0	6.4	2.5	22.4	13.9	2.7	7.2	5.3	7.3	10.6	23.1	23.7	25.9	48.3	23.7	
28.03	10	3.5	0.5	0.6	0.9	0.2	0.4	1.3	0.8	3.4	0.6	5.1	9.5	9.2	2.2	16.2	9.6	6.8	1	0.2	22.8	1.6	4.6	6.2	7.5	2.6	8	1.5	10.6	4.8	24.5	5.9	5.4	14.7
28.42	2.8	5.6	1.5	7.6	0.4	4.3	5.9	0.2	12.7	19.7	26.8	1.4	0.5	5.2	0.1	21.9	1.4	1.9	0.1	5	2.7	16.3	11.2	1.2	1.2	2	2.6	32.5	2.4	9.1	34.2	17.9	27.8	
29.1	1.4	1.4	1.7	5.4	0.4	0.6	2.6	4.3	3.9	5.9	5.8	11	8.8	0.5	13.2	0.4	19.4	2	0	13.3	1.7	0.2	3.2	0.5	2	5.7	4.9	4.7	8.7	1	19.4	2.7	0	





### 3.37 Test 53

Table 3.37 - MAC of ODS of Test 53 to modeshapes

freq Hz	1.82	3.24	4.13	7.08	7.74	8.88	10.69	11.05	11.63	12.07	12.84	13.26	13.67	13.79	13.94	14.95	16.32	17.56	19.06	20.85	23.28	23.49	23.62	24.23	24.58	24.77	25.41	26.51	27.12	28.1	28.22	28.31	28.44	
1.76	94.9	2.5	0.8	0.1	0.6	0.4	0.4	39.5	0.5	0.4	3.1	1.4	15	0.3	10.9	0.2	1.7	0.7	0.2	15.5	0.2	0.5	0.5	14.5	0.4	0.9	1	0.3	0.1	0.7	7.2	0	0.4	15.2
3.52	0.4	0.2	0.2	0.2	0.4	0.4	2	31.7	1	31.3	25.7	3.5	7.3	0.5	2.2	0.1	0.1	2.3	3.7	8.7	0.6	3.3	0.5	0.1	1	0.9	4.7	0.3	2.4	0.2	0.7	1.1	1.3	2
7.03	0.1	0.8	2.2	98.9	0.9	10.1	0.2	0	0.5	11.4	5.9	0.1	0.1	6.2	0	0	1.2	0.1	0	0	1.5	1.9	1.3	1.4	0.6	0.7	9.2	1.9	12.1	27.2	50	42.9	25.7	
8.01	0.2	0.9	0.7	0.8	96.6	4.5	44.9	2.2	45.8	21.1	0.6	13.8	0.1	2.1	1	1	0.9	4.1	0.5	0.2	1.7	1.6	0.2	0	1.9	7.1	0.8	0.1	1.3	5.2	0.4	2.8	0.3	
10.64	1.3	0.3	0.3	0.3	46.7	2.5	96.1	0.2	54.2	22.8	11.1	7.5	1.2	2.3	0.1	1.9	0.2	2.6	0.3	0.3	1.1	0.7	0.7	0.1	0.8	2.6	0.2	1.7	0.5	1.2	2.6	0.1	1.2	
11.04	36	3.1	0.6	0	10.9	0.3	7.4	95	5.9	1.4	5.8	14.7	44.3	1.7	49	0.5	13.6	1.6	1.6	0.3	1	0.5	0.4	5.4	3.2	7.5	7.1	1.6	1.6	0.3	0.6	0.8	1.5	
11.72	0.8	0.8	0.6	0.8	52	2.3	56.5	5.1	93.5	72.9	3.4	9.3	0.3	3.9	0.9	4.2	0.4	3.5	0.5	0.3	1	2.2	1.2	1.7	0.8	5	1.2	1.6	1	1	3.9	0.9	3.1	
12.21	0.1	0.2	2	20.7	13.2	0.6	11.1	0.9	55	84.5	3.2	3.2	0	20.5	0.3	16.4	0.6	1.7	0.4	0.4	0.3	12.3	1	2.5	0.8	0.5	0.1	2.9	2.1	16.4	28.4	25.8	16.4	
13.28	3.1	0.3	0.2	0.1	4.7	0.8	0.8	13	1.5	0.6	9	8.6	14	7.8	21	0.4	9.9	1.7	1.3	2.7	1.8	0.6	0.7	1	1.6	5.2	1.6	1	0.7	5.9	1.6	0.7	0.3	
13.67	17.4	5.4	1.2	0	0.1	0.5	0.4	52.9	0.5	0.7	1.9	5.4	98	8.5	86.6	0.4	41.9	0.9	4.2	11.1	1.7	0.6	0.7	0.3	4.3	2.6	1.4	1.7	1.4	0.7	1.6	1.9	0.6	
14.06	13.3	2.5	1.2	0.1	1.1	1.3	0.1	55.6	0.9	0.7	6.2	25.3	85.6	2.2	96.3	0.6	43.3	2.6	4.9	17.5	1	2.5	0.9	1.8	4.9	7.3	1.7	3.4	1	1.9	2.4	2.9	2.8	
16.21	1	1.6	0.7	0.2	0.4	1.3	0.9	21.1	1.1	1.8	1.5	7.1	54.8	3.5	59	1.5	62.6	0.2	2.9	44	0.1	1.3	15.3	0.2	4	0.9	2.7	12.2	9.4	5.1	2.9	5.4	1.9	
17.19	0.6	0.6	0.1	0.1	8.3	1.8	12.5	0.9	16.8	12.7	1.3	4.6	0.1	0.3	0.6	0.6	1.8	3.5	0.1	0.6	1	0.4	1.1	0.2	1.5	1.1	0.2	0.6	0	0.6	0.9	0.4	0.1	
17.97	0.1	2.4	1.8	1.4	3.4	4.7	6.8	1.1	9.7	6.5	0.9	5	1	1.9	2.1	1.1	1.2	1.8	0.4	0.6	0.1	2.8	1.1	0.9	2.1	0	0.5	0.5	1.1	5.3	0.9	5.7	3.3	
19.24	2.2	16.9	2.5	0	8.8	1.8	12.9	0.9	18.1	11.9	0.2	1.4	0.6	2.3	1.4	1.1	3.6	9.6	18.9	2.3	2.5	0.3	0.2	1.6	1.5	0.1	0.8	0.4	0.6	1.4	0.4	0.3	1	
19.73	1.5	2.9	0.8	0	11.3	0.8	20.2	0.9	28.6	22.8	0.6	2.6	2.3	0.7	2	0.2	0.9	2.8	0.7	1.1	4	0.4	1.1	0.5	3.8	2.9	2.1	0.4	3.1	1.1	0.3	1.2	0.1	
20.12	0.9	2.4	1	0	13.6	3	21	1.3	28.1	20.7	2.1	8	0.1	0.3	0.2	0.3	1	5.5	1.5	0.5	2.9	0	0.4	1	4	6.1	3.4	0.4	3.4	1.8	0.2	1.5	1.1	
20.61	0.3	0.7	1.7	0	14.3	2.1	21.5	0.7	29.9	23.1	3.5	8	2.7	0.9	2.7	0.3	2	6.3	1.5	12.3	4	0.5	4.1	0.7	4.4	5.9	5.1	1.6	5.5	2.9	0.5	1.4	1.5	
21.78	0.4	0.5	1.1	0.8	2.5	0.5	2.7	0.2	3.1	4	0.9	2.3	1.3	5.5	0.7	4.3	1.2	0.7	1.2	1.9	6.9	2.7	0.1	0.5	5.3	0.5	0.9	0.8	1.8	4.8	1.1	6.5	2.7	
23.54	16.8	0.4	1.1	2.1	0	2.2	0.7	0.2	1	1.8	1	0.1	1.7	1.8	0.7	1.6	5	0.4	1.2	15.2	2.2	2.9	72.7	1	3.4	4.2	5	6.1	9.7	14.1	1.6	4.3	1.2	
24.51	1	0.5	1.6	5.4	0.2	1.1	1.3	11	4.2	7.2	4.8	5.8	3.9	3.4	5.8	4.3	9.9	4	1.5	6.4	2.4	7.9	5.6	33.2	16.6	9.1	1.4	11.7	1	0.9	4.8	10.9	41.1	
24.71	2.2	5.7	6.7	2.2	0.1	3	1.2	0.9	3.8	5.3	3.7	0.5	0.6	8.6	1.2	18.8	0.2	3.2	1.2	2.6	4.7	26.2	0.7	12.9	27.4	1.2	3	1.2	0.6	17.4	9.7	15	4.3	
25.39	0.2	2.2	0.7	2.7	0.4	3.7	0.1	1.6	0.6	0.5	2.3	1.1	0	1.3	0.5	14.4	10.8	1	0.3	3.8	1.1	15.8	4.2	0.2	22	0.3	76.8	3.9	60.9	6	3.1	9	1.9	
25.98	1.6	0.7	1.3	0.7	0.7	0.2	0.2	3.2	0.8	0.9	5	2.5	9.7	2.6	12.4	0.6	9.6	1.7	1.5	29.4	3.2	0.9	10.2	10.1	5.5	7	1.1	11.4	1.4	0.7	1.4	2	5.6	
26.37	0.5	4.4	1.8	2.9	1.2	4.6	1.1	2.9	1.9	2.7	5.6	6.4	1.4	1.3	1.3	0.8	0.1	8	0.1	2.1	18.1	5.7	9.5	44.8	2.8	5.7	3.3	78.4	1.2	1.1	2.3	0.6	6	
27.34	0.6	1.6	2.7	14	1.8	0.2	0.2	0.7	0.7	7.8	8	0	3	7.2	3.2	28.8	10.7	0.2	0.1	5.9	3.2	16.6	14.8	4.7	3.2	7	21	9.5	38.4	25.6	39.4	46	23	
27.84	3.1	2.5	1.9	27.4	0.5	9	1.6	2.4	3.7	10.4	15.1	4.5	6.7	15.7	5.5	17.4	6.6	0.4	0	1.4	3.9	11.9	2.5	4.3	4.8	2.9	17.8	1	29.4	35.3	42.9	44.1	29.5	
28.22	2.8	1.9	0.7	13.8	1.1	0.4	1.6	8.4	3.1	12.2	2.9	4.1	10.6	6.5	16.5	23.4	5.8	0.3	0	10.2	1.4	10.8	2.4	2.6	6	6.4	0.5	13.7	5.6	46.9	25.3	30.4	1.2	
28.52	12.8	0.1	1.1	15.8	0.1	1.2	0.9	9.5	1.9	2	2.6	0.6	10.5	8.9	9.6	4	2.5	0.3	0.3	3	3	1.9	0.7	15.2	1.8	0	0.6	17.9	0.9	9.9	3.9	16.7	63	

### 3.38 Test 54

Table 3.38 - MAC of ODS of Test 54 to modeshapes

freq Hz	1.82	3.24	4.13	7.08	7.74	8.88	10.69	11.05	11.63	12.07	12.84	13.26	13.67	13.79	13.94	14.95	16.32	17.56	19.06	20.85	23.28	23.49	23.62	24.23	24.58	24.77	25.41	26.51	27.12	28.1	28.22	28.31	28.44
1.86	96.8	2.8	0.7	0.1	0.4	0.4	0.3	40.7	0.4	0.4	3.1	1.6	15.7	0.2	11.4	0.3	1.2	0.6	0.3	14.5	0.1	0.3	14.5	0.4	0.9	1.5	0.3	0	0.6	7	0	0.5	15.3
3.52	0.6	2.1	1.2	0.6	12.2	0.9	13.7	1.6	14.1	16.2	2.7	3.9	0.8	1.3	0.5	0.1	3.1	2.9	15.2	1.1	4.6	1.4	0.1	1	1.7	4.5	0.6	3.4	1	0.2	2.1	3.3	2.8
7.13	0.1	0.9	1.5	97.9	3	9.2	0.3	0	0.3	10.2	6.6	0.2	0.1	6.3	0	0.1	1.6	0.1	0	0	1.5	1.7	1.2	1.3	0.4	1.1	8.8	1.8	12.4	26.8	49.6	43.5	26.1
7.81	0.2	0.8	0.6	0.6	98.3	4.6	48.3	2.1	49	24.1	0.8	14.1	0.1	2.2	0.8	0.9	1	4.4	0.1	0.2	1.4	1.3	0.1	0	1.4	6.3	0.7	0.2	1.1	4.8	0.2	2.1	0.1
10.64	1.2	0.4	0.5	0.5	49.6	2.5	98.6	0.2	59.1	27.2	11.4	7.9	1.2	2.1	0.1	1.6	0.3	3.1	0.1	0.3	1.1	0.6	0.5	0	0.5	2.7	0.3	1.5	0.5	1	3	0.2	1.1
11.04	40.5	3.4	0.2	0	5.1	0.2	1.9	98.7	2.3	0.5	4.4	11.9	49.8	1.7	52.3	0.4	13.5	1.2	1.5	0.1	0.7	0.6	0.3	5.6	2.5	6	7.2	2.3	1.7	0.2	0.8	1.1	1.2
11.72	1.3	0.6	1.1	0.7	50.6	3.1	56.9	1.9	96.9	77.1	4	8.5	0.8	3.3	0.1	5.2	0.1	3.6	0.1	0.4	1	2.4	0.8	0.9	0.4	3.9	1.2	2	1.1	1	4.4	1	2.9
12.21	0.5	0.6	1.7	16.5	19.1	0.2	17.8	0.8	68.2	92	2.2	2.9	0.9	12.1	1.2	12.7	0.7	0.9	0.5	0.5	0.2	8.8	0.8	2.2	0.4	1	0.1	2.5	1.2	9.8	25.7	20.5	13.2
13.28	2.3	0	0.2	0.2	7	1.9	2.1	10.5	3.3	1.6	14.8	19.8	8.9	7	18	0.2	9.2	3.9	0.8	2.5	1.1	0.7	1	1.8	2.1	8.1	2	1.4	0.9	8.5	2.6	0.7	0.8
14.06	12.3	2.5	0.9	0	0.9	1.1	0.1	54.2	0.5	0.4	5.8	24.5	86.7	3	97.3	0.2	43.8	2.1	4.9	18.6	1	1.5	0.8	1.6	5.4	7.7	1.6	3.1	0.9	2	1.7	1.7	2.8
16.31	1.7	0.3	1.1	0.2	0.9	1.3	0.2	23.1	0	0.2	1.8	9.7	55.5	5	62.7	3.1	60.4	2.5	3.2	36.1	0.3	3.4	14.7	0.3	2.7	2.8	0.9	12.3	6.8	4.9	3.3	6.3	1.5
17.29	0.2	0.4	0.6	0	8	1.7	13	1	18.9	14.3	2.1	5.8	0.4	0.5	1.1	0.8	1.6	4.6	0.2	1	0.9	0.9	1.6	0.1	0.7	0.9	0.1	0.8	0	0.7	1.1	0.1	0.2
19.24	2.9	13.3	2.9	0	6.1	1.5	12	0.6	16	14.1	0	1.2	1.5	3.9	1.6	1.5	3.1	7.7	19.6	3.1	0.8	0	1.2	0.9	1.5	0.5	1.1	0.5	0.1	1.7	0.7	0	3.9
19.92	3.7	4.7	1.8	0.1	8.4	0.5	14.1	0.8	21.1	12.4	2.5	0.7	1.3	1.6	2	0.4	3.5	1.9	3.6	10.5	2.1	0.5	1.2	2.3	1.9	0.2	2.5	0.4	1	1	0.7	0.7	0.4
21.78	1.1	0.8	1.4	0.5	1.7	0.8	2.2	0.3	3.3	3.6	1	2.5	0.9	4.7	0.5	4.8	0.9	0.5	3	0.6	10.1	3.1	0.8	1.1	5.1	0.1	0.8	0.8	1.2	4.6	0.3	4.4	2.9
23.63	14.7	0.1	1.2	1.3	0	23	0.4	0	0.6	1.4	0.1	0.1	1.4	1.1	0.7	0.1	6.8	0.4	0.9	17.2	2.5	1.9	83.5	0.3	0.8	2.5	6.3	9.3	13.2	9.7	0.6	1.7	2.3
24.71	3.4	5.2	4.5	1.3	0	2.5	2.9	1.5	7.1	7.9	3.2	0.1	0.6	6.9	1.3	10.7	0.3	2.3	0.5	2.3	4	14.4	0.6	6.9	3.9	3.7	2.6	1.8	0.9	8.7	6.7	7.5	1.9
25.49	0	1.6	0	8.3	0.1	5.6	0	1.8	0.1	0.2	0.7	21	0.4	0.2	0.7	3.7	13.8	0.1	0.9	9.1	1.7	3.3	8.8	1.5	19.7	0.7	85.7	0.7	74.9	1.3	11.9	2.1	1.3
25.98	2.6	0.6	0.7	2.8	0.4	0	1	3.1	2.4	3.2	5.2	7.7	7.4	1	11.8	2.3	1.3	1.5	1.7	32.1	1.7	2	13.5	2.9	15.8	6.7	4.2	16.9	7.9	3	7.5	8	13.5
26.46	0.1	1.2	0.5	3.3	0.6	7.6	1	1.8	1.4	1.7	4.9	5.6	1	0.9	2	0.7	1.5	3.5	0.1	4.4	16.2	3.5	10.9	36.1	0.5	1.5	32	86.9	1.8	2.8	0.9	0.9	8.3
27.15	0	0.1	0.4	9.1	1.2	3.9	0.8	1	1.1	0.1	0.4	1.1	0.2	2	0.2	0.5	14.4	1	0.5	6.2	1.1	2.1	19.9	0.2	1.7	1.9	65.3	1.7	88.1	0.4	8.2	1.9	0.2
27.54	0.6	1.4	2.8	19.1	1.8	5.6	2.3	1.6	5.2	9.4	14.9	3.5	1.3	5.2	2.9	24.6	1.3	0.4	0.2	1	3.5	22.8	1.1	3.2	10.8	1.7	3.5	4.5	4.2	29.2	39.3	43.9	18
28.03	7.2	14.6	2	9.7	2.3	3	3.1	3.8	3.9	6.1	7.5	14.7	3.4	1.3	0.2	9.3	1.5	0.1	0.4	6.1	1.3	6.4	3.7	2.1	10.7	5.3	21.8	0.8	12.8	7.5	30.3	26.2	13.6
28.52	23.7	1.3	1.5	18.7	0.1	0.2	1	3	2.6	6.5	10.6	1.2	2.9	8.4	0.9	7.1	0.1	0.1	1.4	7	3	4.8	2.1	29.5	1.5	2.2	0.5	20.3	1.1	20.2	13.1	21.3	67.5
29.39	0.7	0.7	1.1	1.3	0.4	0.8	5.1	0.9	9.3	10.9	4.7	3.4	0.4	1.7	1.1	2.6	1.3	0.7	0.4	2.2	1.5	4.1	2.4	0.1	1.3	1.9	0.2	1.7	0.7	0.2	5.7	1.5	2.3





#### **4.0    References**

1. Gemini South 8m Optical Telescope Final Report, MACL Report # 05-08570-001, dated October 2000
2. Gemini South 8m Optical Telescope Test Setup Report, MACL Report # 05-08570-002, dated October 2000
3. Gemini South 8m Optical Telescope Data Cleansing Report, MACL Report # 05-08570-003, dated October 2000
4. Gemini South 8m Optical Telescope Modal Test Report, MACL Report # 05-08570-004, dated October 2000
5. Gemini South 8m Optical Telescope Operating Report, MACL Report # 05-08570-005, dated October 2000
6. Gemini South 8m Optical Telescope Correlation Report, MACL Report # 05-08570-006, dated October 2000
7. Gemini South 8m Optical Telescope DoE and Wind Data Report, MACL Report # 05-08570-007, dated October 2000
8. CD containing all pertinent test data and reports
9. Preliminary Data Assessment of Gemini South Optical Telescope Operating and Modal Data Report, dated June 2000
10. LMS Coda-X 3.4 Test and Analysis Software (TMON, FMON, Modal Analysis, Matrix Toolbox), Leuven Measurement Systems, Detroit Michigan
11. LMS Coda-X 3.5C Test and Analysis Software (TMON, FMON, Modal Analysis), Leuven Measurement Systems, Detroit Michigan
12. LMS Road Runner Data Acquisition System, Leuven Measurement Systems, Detroit Michigan
13. MESpoe VES Version 2.0, Vibrant Technologies, Jamestown, CA
14. Avitabile, P., "Overview of Modal Analysis using the Frequency Response Method", July 1997
15. Box, George E.P., Hunter, J. Stuart, and Hunter, William G., *Statistics for Experimenters: An Introduction to Design, Data Analysis, and Model Building*, Wiley, 1978.
16. Shina, Sammy G., *Concurrent Engineering and Design for Manufacture of Electronic Products*, Van Nostrand Reinhold, 1991.



Modal Analysis and Controls Laboratory  
University of Massachusetts at Lowell  
Lowell, Massachusetts

**Gemini South 8m Optical Telescope**  
**DoE and Wind Pressure Report**  
**MACL Report # 05-08570-007**

October 2000

Approved By: \_\_\_\_\_

Date: \_\_\_\_\_





## **Intent of Report**

This report addresses aspects of the wind data and statistical analyses performed for the Gemini South 8m Optical Telescope in Cerro Pachon, Chile.







## Table of Contents

- 1.0 Administrative Data
  - 1.1 Purpose of Analysis
  - 1.2 Drawing
  - 1.3 Test Log
  - 1.4 Dates of Tests
  - 1.5 Analysis Performed By
- 2.0 Test Description
  - 2.1 L8 Array (1)
  - 2.2 L9 Array (1)
  - 2.3 L8 Array (2)
  - 2.4 L9 Array (2)
  - 2.5 Elevation Sweep
  - 2.6 Lower Wind Screen
- 3.0 Summary of Test Results
  - 3.1 Metric #1: Wind Pressure RMS
  - 3.2 Metric #2: Accelerometer RMS
  - 3.3 Wind Pressure Data
- 4.0 Test Schematic and Geometry
- 5.0 References





## **1.0 Administrative Data**

### **1.1 Purpose of Analysis**

The purpose of the DoE analysis is to determine which of the experimental factors are statistically significant in the wind loading and structural response of the Gemini 8m telescope. Additionally, the analysis provides the relative importance of the factors and reveals the effects of changing the configuration of the telescope. This not only yields guidance for determining worst case conditions from this set of experiments, but also provides the information necessary to design future experiments.

Additional analysis on the wind data has been performed to show a typical power spectrum of the wind velocity in the dome. This information is necessary in modeling the response of the telescope to wind loads. Additionally, the coherence between different wind-related measurements has been calculated in order to reveal any relationships in their response. Such relationships could be important in providing practical, real-time monitoring of the wind loading conditions on the telescope during operation.

### **1.2 Drawing**

Drawings and schematics of test configuration are available in Section 5.0 of this report.

### **1.3 Test Log**

A logbook containing documentation of equipment used, transducer information, and test details for all tests conducted, is on file at the Modal Analysis and Controls Laboratory. Individual test notes are located with their respective test data in the appendix.





1.4 Dates of Tests

May 8-12, 2000

1.5 Analysis Performed By

David Smith

Johann Teutsch





## **2.0 Test Description**

The test configurations were selected according to standard Design of Experiments (DoE) practice in order to reduce the number of tests. This was necessary because it was impractical to cover the parameter space fully, given the time available and the variability of the wind conditions.

To illustrate the difficulty in fully covering the parameter space, consider varying the azimuth angle from 0 (looking into the wind) to 180 (looking out of the wind) in 45 degree increments. This results in a total of five values. Varying the elevation angle to 30, 45, 60, and 75 degrees provides four distinct values. Finally, there are three positions of interest (open, half, and closed) for each of the vent gates. Covering the full combinations of this parameter space would result in  $5 \times 4 \times 3 \times 3 = 180$  tests. Unfortunately, it would be impossible to obtain this many tests with anything resembling constant wind conditions. Further, it is worth noting that in the entire testing run less than 50 operating tests were performed, so even this coarse sampling would not have been achievable.

Since it was impossible to provide full coverage of the parameter space, a statistical approach was implemented using standard design of experiments (DoE) approaches [15]. In this way, better resolution in each of the parameters was obtained with fewer tests. The tests obtained using this approach were grouped into two L8 arrays (which could be combined into a single L16) and two L9 arrays. While more detail for each of these tests is given below, the L8's provided information on two levels for each experimental factor, but also yielded information on the interactions between the factors. The L9's provided information only on varying one effect at a time, but yielded information at three levels for each experimental factor.





As detailed below, the combined tests covered five levels in AoA, four in EI, and three each in the UVG and DVG position. Since the experiments were chosen as outlined above, they provide statistically optimal coverage of the full parameter space that would have required 180 tests to cover fully.

## 2.1 L8 Array (1)

The first L8 array [15], consisted of 8 tests and covered azimuth angle of attack (AoA) of 0 and 45 degrees, elevation angle (EI) of 30 and 60 degrees, Upwind Vent Gate (UVG) open and closed, and Downwind Vent Gate (DVG) open and closed. At 0 (and later, 180) degrees AoA, the definition of "Upwind" was ambiguous, so the vent gate to the right of the telescope pointing direction was chosen to be the UVG. When combined with the L8 array listed in 2.3, this test constituted a full-factorial (fully covered parameter space) L16 array spanning two values in each of the four parameters. The experiments were chosen to provide optimal "blocking." That is, the two L8's were chosen in such a way that systematic differences have the minimum effect on the combined L16 array. As a result, if the mean wind were to be different on the two major testing days (which would be expected), it would have no impact on the analysis. The combined L16 experiment is particularly important because it provides information on the interactions between the parameters. This is, if there is a synergistic effect of changing two of the parameters simultaneously, this will be detected by the analysis of the L16 array.





## 2.2 L9 Array (1)

In order to obtain information at more levels for each factor, we also conducted experiments according to an L9 array. The levels for the first L9 were:

AoA: 0, 90, and 180 degrees

El: 30, 45, and 60 degrees

UVG: open, half, and closed

DVG: open, half, and closed.

It is important to note that this test makes full use of the efficiency of the statistical approach, and as a result can not be used to determine the interactions between two parameters. However, it provides more detailed information on the average effects of varying an individual parameter.

## 2.3 L8 Array (2)

The second L8 was similar to the one described in Section 2.1, and it covered the same levels. However, the configurations were chosen so that they filled out the optimal L16.





## 2.4 L9 Array (2)

The second L9 was performed to expand the range of coverage in the parameter space. The levels for this set of tests were:

AoA: 45, 90, 135 degrees

El: 30, 45, 75 degrees

UVG: open, half, closed

DVG: open, half, closed.

Taken with the first L9, this experiment provides coverage of the entire parameter space. However, as with the first L9, the coverage is in the main effects only and does not reveal any interactions between factors.

## 2.5 Elevation Sweep

At the request of Dr. Myung Cho, we conducted a sweep in Elevation only. For this set of tests, the conditions were:

AoA: 45 degrees

El: 30, 45, 60, 75 degrees

UVG and DVG open.

## 2.6 Lower Wind Screen

A single test was made (at the request of Mike Sheehan) with the lower wind screen raised. The test configuration was

AoA: 0 degrees

El: 60 degrees

UVG and DVG closed





### **3.0 Summary of Results**

In order to analyze test results using DoE, it is necessary to define a metric for each test. In this analysis, we have used two different metrics. The first is the RSS (root sum squared) of the RMS values of the individual pressure readings on the primary mirror. This metric, therefore, represents the wind pressure variability on the mirror. It has the advantage of being largely independent of sources other than the wind, but does not represent the actual deformation of the primary. The second metric was the combined RMS of the accelerometers on the primary reflector. This metric directly represents the structural motion, but is also sensitive to effects that are not wind-induced. This section contains the results of the DoE analysis for each metric.

#### **3.1 Metric #1: Wind Pressure RMS**

Three major cases were considered. The first is an examination of the combined L8 tests, which construct a full L16. The next two are L9 tests, which provide information on the main effects at more locations in the parameter space.

##### **3.1.1 L16 Analysis**

Because of the choice of test configurations, the resulting L16 array has optimal ‘blocking.’ That is, if there is a systematic error in an uncontrolled parameter (i.e., the wind) it will not affect the analysis, though variations in the amount of noise introduced by the uncontrolled parameter could still affect the data. The cost of using this ‘blocking’ approach for the L16 is the loss of any information about the four-way interaction. That is, if there is a synergistic effect that can only be seen by simultaneously varying all four parameters (AoA, EI, UVG, and DVG), the blocked L16 will miss the effect. However, it is physically very unlikely that there are any significant four-way interactions (Box , 1978). Indeed, since it is unlikely that there are





any significant three-way interactions, the values produced for those can be used as an error estimate on the experiment. Such an error estimate is essential in determining which effects are actually statistically significant.

The levels used in the L16 were:

Factor	Level 1	Level 2
AoA	0	45
EI	60	30
UVG	Closed	Open
DVG	Closed	Open

The L16 results are shown in Table 3.1 below. The statistically significant effects are shown in bold face type.

Table 3.1 L16 Results

Identifier	Estimate (Pa)	Level 1	Level 2	Ratio
Average	7.51			
<b>A (AoA)</b>	<b>4.46</b>	<b>5.28</b>	<b>9.74</b>	<b>1.85</b>
B (Elevation)	1.06	6.98	8.04	1.15
AB	0.54	7.24	7.78	1.08
<b>C (UVG)</b>	<b>11.76</b>	<b>1.63</b>	<b>13.39</b>	<b>8.23</b>
<b>AC</b>	<b>5.93</b>	<b>4.54</b>	<b>10.47</b>	<b>2.30</b>
BC	0.53	7.24	7.77	1.07
ABC	1.38	6.82	8.20	1.2
<b>D (DVG)</b>	<b>5.06</b>	<b>4.98</b>	<b>10.04</b>	<b>2.02</b>
AD	-0.02	7.52	7.50	1.00
BD	0.96	7.03	7.99	1.14
ABD	2.70	6.16	8.86	1.44
<b>CD</b>	<b>3.62</b>	<b>5.70</b>	<b>9.32</b>	<b>1.63</b>
ACD	1.27	6.87	8.14	1.18
BCD	0.17	7.42	7.59	1.02
Noise	3.28			





The noise estimate is constructed from the root sum squared (rss) of the three-way interactions. It is worth noting that the ‘ABD’ interaction (that is, the effect of simultaneously varying AoA, El, and DVG) is the largest of these. However, eliminating it from the error estimate does not change which other effects are above the statistical noise. The significant effects revealed by the L16 are (in order of importance according to this metric):

- 1) Position of the Upwind Vent Gate (UVG)
- 2) Interaction of changing the AoA and the UVG simultaneously
- 3) Position of the Downwind Vent Gate (DVG)
- 4) AoA
- 5) Interaction between the UVG and DVG

It is a bit surprising that the elevation angle (El) is not statistically significant in the rms wind pressure variation on the primary mirror. This suggests that future studies of surface pressure variations can skip (or at least reduce resolution) in this factor.

### 3.1.2 First L9 Test

The first L9 test covered the following levels:

Factor	Level 1	Level 2	Level 3
AoA	0	90	180
El	30	45	60
UVG	Closed	Half	Open
DVG	Closed	Half	Open





The analysis of the resulting L9 matrix is summarized in Table 3.2 below.

Table 3.2 First L9 Results (Pa)

Identifier	Level 1	Level 2	Level 3
Average	7.53		
A (AoA)	6.98	13.38	2.22
B (Elevation)	8.56	10.05	3.98
C (UVG)	1.43	10.98	10.17
D (DVG)	6.76	10.70	5.13
Noise	Not Avail.		

The results do not have the benefit of an error estimate, because there are not multiple repetitions of each test. However, the most dramatic change occurs between a closed and even partially open UVG condition. The DVG position is not as strongly important, but reaches a significant maximum at the ‘Half’ position. The AoA results indicate that the pressure variation is significantly higher in a crosswind than in either the direct front or rear wind loading. This is to be expected, as the enclosure geometry provides some protection in the latter configurations. Finally, there is an unexpected trend in the EI that there is little variation between 30 and 45 degrees, but substantially lower excitation at 60 degrees. It is unclear from examination of the test matrix whether this is real or just a selection effect based upon the particular tests that include this elevation angle. Specifically, the tests that correspond to this elevation angle either have direct front/back loading, or have the UVG in the ‘Closed’ position. This issue is revisited in the Elevation Sweep test (Section 3.1.4).





### 3.1.3 Second L9 Test

The second L9 tests was conducted using the following parameter levels:

Factor	Level 1	Level 2	Level 3
AoA	45	90	135
EI	30	45	75
UVG	Closed	Half	Open
DVG	Closed	Half	Open

The analysis is summarized in Table 3.3 below.

Table 3.3 Second L9 Results (Pa)

Identifier	Level 1	Level 2	Level 3
Average	5.09		
A (AoA)	8.00	4.81	2.45
B (Elevation)	4.68	5.58	5.01
C (UVG)	0.75	7.07	7.45
D (DVG)	2.47	7.29	5.51
Noise	Not Avail.		





As before, the most striking effect is even a partial opening of the UVG, and the DVG provides its greatest contribution when in the half-open position. Additionally, there is a trend evident in AoA, though this time the maximum occurs at 45 degrees rather than at 90. However, there is still no significant variation due to elevation. Combined with the other L9 results and the L16 matrix, the conclusion can be drawn that the elevation is not a dominant factor for wind pressure variation on the primary reflector. The worst case configuration predicted by the experiments (for this metric) is given in Table 3.4. However, the results suggest that most of the disturbance is achieved once the UVG is half-open, and there is no statistically significant benefit from opening the downwind vent gate. Further, there is no strong elevation angle dependence in the data.

Table 3.4 Predicted Worst Case Configuration

<b>AoA</b>	<b>EI</b>	<b>UVG</b>	<b>DVG</b>
45	45	Open	Half

#### 3.1.4 Elevation Sweep Test

In order to obtain additional data about the elevation dependence of the pressure RMS, an elevation sweep test was performed. For this experiment, four consecutive tests at varying elevations were conducted. Though the full analysis of the previous experiments was not yet available, initial analyses suggested that setting AoA to 45 degrees and both UVG and DVG to full open would provide the strongest excitation. The more complete analysis summarized above suggests that the excitation may have been slightly stronger with the DVG set to the ‘Half’ position, but also indicates





that the effect would not have been statistically significant. The results from the test are summarized in Table 3.5 below.

Table 3.5 Elevation Sweep Results (Pa)

<b>Elevation</b>	<b>RMS</b>
Average	16.90
30	20.09
45	12.27
60	17.89
75	17.37
Noise	Not Avail.

These results suggest that there is a minimum in the response at El=45 degrees, which is not consistent with the other tests. In the absence of additional data in either case, it can be noted that there does not appear to be a strong dependence in Elevation, but that there may be a low point in the response between 45 and 60 degrees. If better understanding of the elevation effect is needed, additional experiments must be performed.

### 3.2 Metric #2: Accelerometer RMS

Since the conclusions from the analysis of the experiments depend upon the metric, the analysis was repeated using the RMS of the accelerometers on the primary reflector. As shown below, the accelerometer RMS on the primary is high enough in the quiescent state that the additional dynamic variation induced by the wind appears to be only marginally significant. It is possible, however, that this metric is dominated by high frequency components, and that future studies may wish to filter the data or choose the amplitude of a particular mode as the metric. As in the previous section, three cases were considered: the L16 and two L9 arrays.





### 3.2.1 L16 Analysis

The levels used in the L16 were identical to the other case, and the results are shown in Table 3.6 below. As before, the statistically significant effects are shown in bold face type.

Table 3.6 L16 Results

Identifier	Estimate (in/s <sup>2</sup> )	Level 1	Level 2	Ratio
Average	0.66			
A (AoA)	-0.12	0.72	0.6	0.84
B (Elevation)	-0.03	0.67	0.64	0.96
AB	-0.08	0.70	0.62	0.89
<b>C (UVG)</b>	<b>0.19</b>	<b>0.56</b>	<b>0.75</b>	<b>1.34</b>
AC	0.03	0.64	0.67	1.05
BC	-0.10	0.71	0.61	0.86
ABC	0.09	0.61	0.71	1.16
<b>D (DVG)</b>	<b>0.21</b>	<b>0.55</b>	<b>0.76</b>	<b>1.38</b>
AD	-0.08	0.70	0.62	0.88
BD	0.00	0.66	0.66	1.00
ABD	0.12	0.60	0.72	1.21
CD	0.01	0.65	0.67	1.02
ACD	-0.01	0.66	0.65	0.98
BCD	0.06	0.63	0.69	1.10
Noise	0.17			

As before, the noise estimate is constructed from the root sum squared (rss) of the three-way interactions. Also, note that the ‘ABD’ interaction (that is, the effect of simultaneously varying AoA, El, and DVG) is the largest of these. However, eliminating it from the error estimate does not change which other effects are above the statistical noise (though in this case, it brings the AoA effect to a possibly significant factor). Thus, the only significant effects revealed by the L16 are:





- 1) Position of the Downwind Vent Gate (DVG)
- 2) Position of the Upwind Vent Gate (UVG)

These are both, however, only marginally significant. Given the more dramatic results from the wind pressure measurements, this is surprising. However, it appears that the acceleration measurements are more sensitive to other external disturbances. These external disturbances include the movement of personnel in the dome, as well as the operation of machinery (pumps, fans, etc.). Avoiding such effects may require filtering of the data before calculating the RMS. Alternatively, the analysis could be repeated for the amplitude of specific deformation modes of the structure.

### 3.2.2 First L9 Test

Qualitatively, the first L9 test shows the same marginal effects as the L16. However, for completeness, the results are given in Table 3.7 below.

Table 3.7 First L9 Results (in/s<sup>2</sup>)

Identifier	Level 1	Level 2	Level 3
Average	0.73		
A (AoA)	1.01	0.85	0.31
B (Elevation)	0.69	0.62	0.87
C (UVG)	0.90	0.63	0.65
D (DVG)	0.61	0.59	0.99
Noise	Not Avail.		

The results do not have the benefit of an error estimate, because there are not multiple repetitions of each test. However, the most surprising result is that the results predict that a peak RMS in the primary would occur with an AoA of 0 degrees, an Elevation of 60 degrees, a closed UVG and an open DVG. While it is possible that the excitation of the nodding mode of the





telescope could account for the higher response to frontal wind loading, the vent gate results are puzzling. Based on the analysis from the L16, it can be surmised that there is likely to be some additional structural excitation.

### 3.2.3 Second L9 Test

The second L9 test results are similar to the first. It was conducted using the same parameter levels as for the wind pressure analysis, and the results are shown in Table 3.8 below.

Table 3.8 Second L9 Results (in/s<sup>2</sup>)

Identifier	Level 1	Level 2	Level 3
Average	0.28		
A (AoA)	0.23	0.21	0.40
B (Elevation)	0.37	0.21	0.27
C (UVG)	0.19	0.37	0.29
D (DVG)	0.34	0.22	0.27
Noise	Not Avail.		

As with the first L9, the results are nothing like the wind pressure results, and the levels are (in most cases) similar to the levels taken in maximally quiet conditions (closed dome and shutter). Future studies will either need to use a different metric in the analysis, or take special precautions to reduce ambient disturbances if the wind effects are to be specifically isolated.





### 3.3 Wind Pressure Data

This section discusses the coherence of wind pressure to accelerometer and wind speed data.

#### 3.3.1 Coherence with Accelerometers

Since it is impossible to put wind pressure sensors on the primary after the real mirror is installed, it is useful to know if the pressure sensors correlate with one another or with any of the accelerometers on the primary. If such a correlation exists, then it may be possible to make an equivalent measurement with other sensors.

To investigate this, two different sets of calculations were performed. In the first, the coherence was calculated between the pressure transducers 008, 009, 010, 011, and 014, and several accelerometers on the primary mirror (numbers 43, 48, 47, 41, and 44). Since some of the points are located in close proximity to each other, this provides the maximum likelihood of significant pressure-acceleration coherence. In the second case, the coherence between different pressure transducers was computed to determine the spatial coherence of the wind pressure on the primary structure.

As illustrated by a typical result (Figure 3.1), there is no coherence between the acceleration of the primary mirror and an individual pressure transducer. Figure 3.2 shows a similar lack of coherence between different pressure transducers. To understand how poor this coherence is, consider that Figure 3.3 has a comparable coherence, but was generated by two random (white noise) traces of the sample length and sample time as the real data.





Thus, statistically there is no coherence between different pressure locations, and they can be treated as independent random inputs. The exception to this is the closest-spaced pressure locations, which are 1.4m apart (Figure 4.3). These points do show significantly higher coherence at low frequency, below 2 Hz, although they still do not exhibit a strong correlation as seen in Figure 3.2 below.

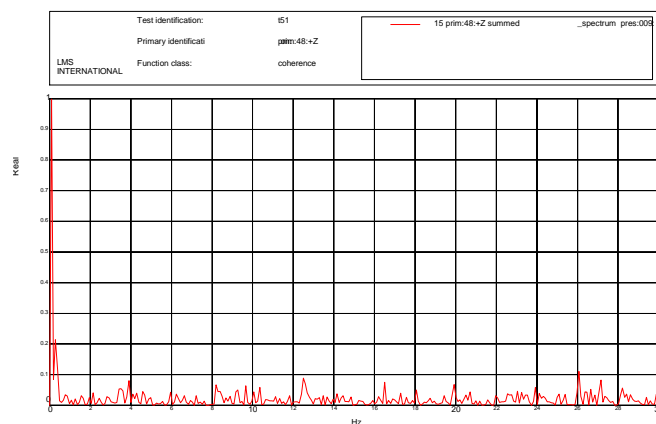


Figure 3.1 Coherence between the acceleration of the primary mirror, 48, and an individual pressure transducer 009



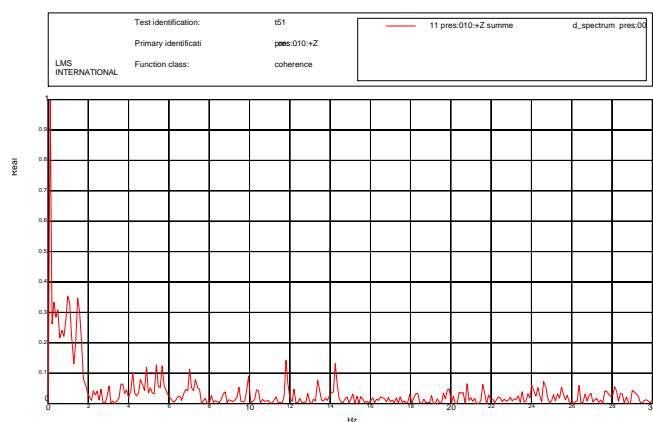


Figure 3.2 Coherence between pressure transducer 009 to pressure transducer 010

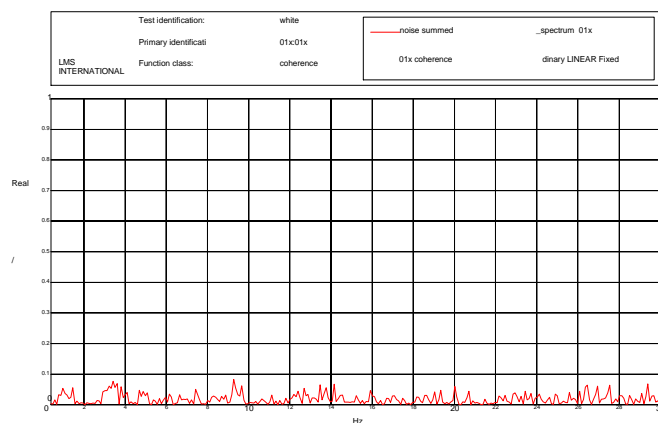


Figure 3.3 Comparability coherence generated by two random signals (white noise)





### 3.3.2 Coherence with Wind Speed

The motivation for seeking correlation between wind speed and surface wind pressure is identical to that of seeking correlation between wind pressures and accelerometer readings. Specifically, if such a correlation exists, then an estimate of the primary mirror surface loading conditions could be predicted from a more practical set of measurements. Calculating the coherence between the sensors revealed, as in the previous case, no significant coherence between either the wind speed measurements and the surface pressures (A typical result is shown in Figure 3.4) or even between two different wind speed measurements (e.g., Figure 3.5). Additionally, there are no peaks visible in the power spectrum (e.g., Figure 3.6) above the noise for the test. This suggests that on-site wind measurements are of limited utility in determining the instantaneous wind speed at other locations on the structure.

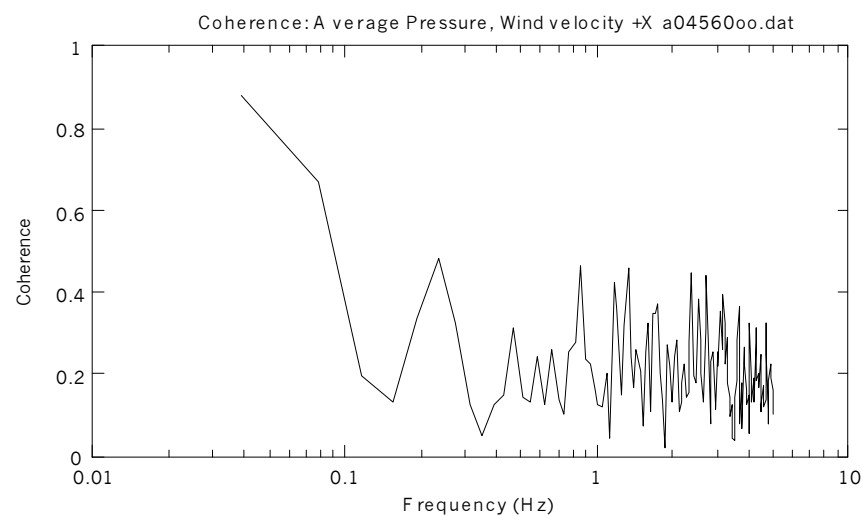


Figure 3.4 Typical coherence between wind speed and surface pressure



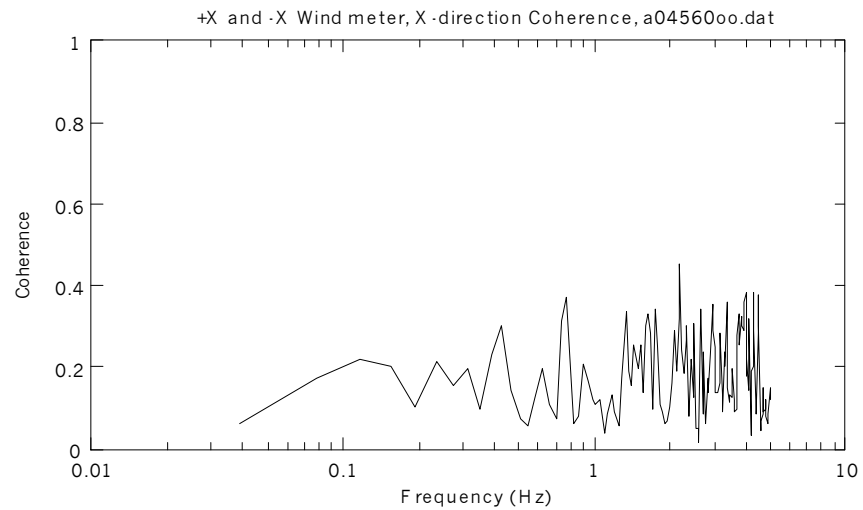


Figure 3.5 Typical coherence between two different wind speed measurements

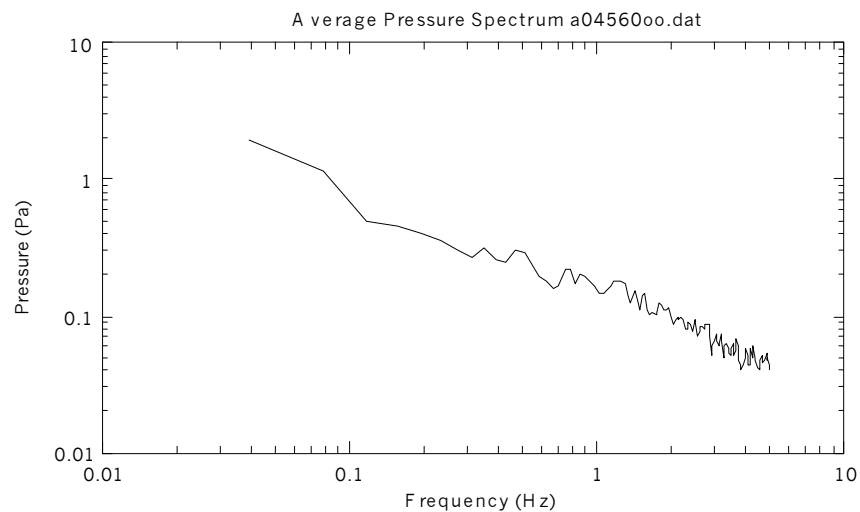


Figure 3.6 Typical power spectrum





#### 4.0 Test Schematic and Geometry

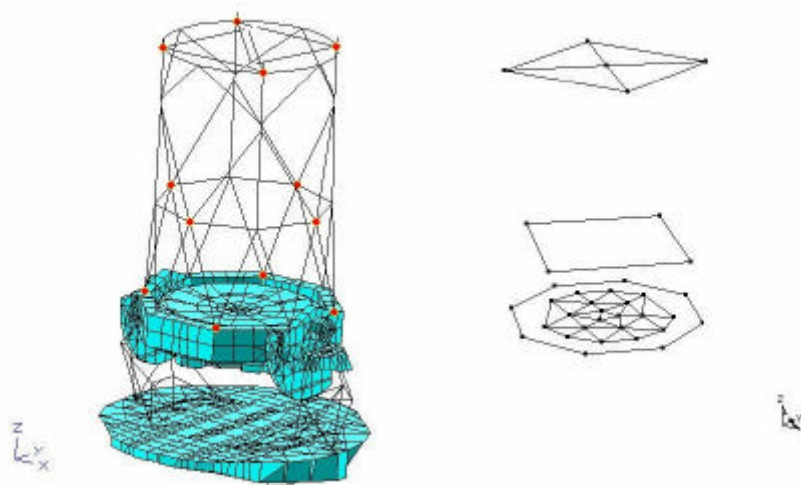


Figure 4.1 General Test Schematic

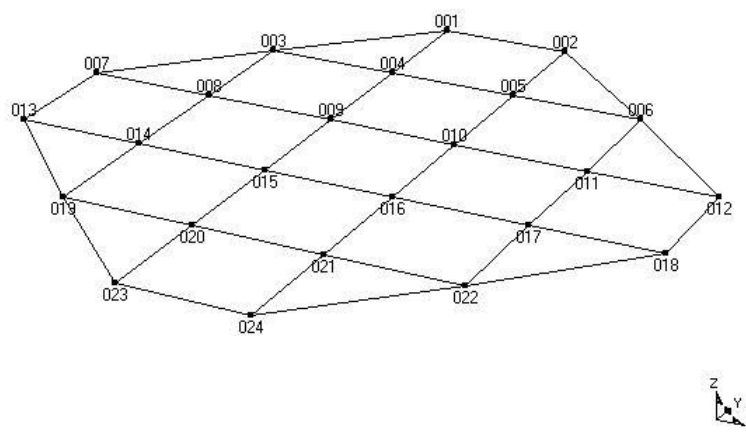


Figure 4.2 Pressure Transducer Location Numbering



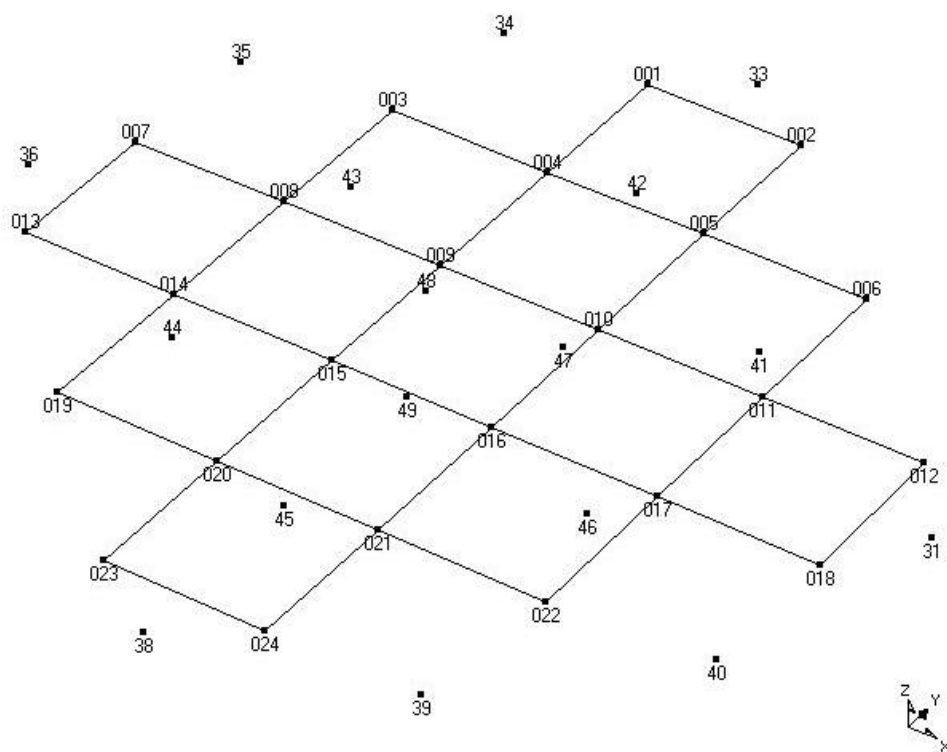


Figure 4.3 Pressure Transducer and Accelerometer Location Numbering





## 5.0 References

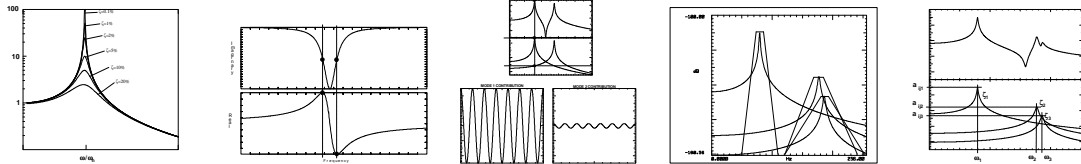
1. Gemini South 8m Optical Telescope Test Report, MACL Report # 05-08570-001, dated October 2000
2. Gemini South 8m Optical Telescope Test Setup Report, MACL Report # 05-08570-002, dated October 2000
3. Gemini South 8m Optical Telescope Data Cleansing Report, MACL Report # 05-08570-003, dated October 2000
4. Gemini South 8m Optical Telescope Modal Test Report, MACL Report # 05-08570-004, dated October 2000
5. Gemini South 8m Optical Telescope Operating Report, MACL Report # 05-08570-005, dated October 2000
6. Gemini South 8m Optical Telescope Correlation Report, MACL Report # 05-08570-006, dated October 2000
7. Gemini South 8m Optical Telescope DoE and Wind Data Report, MACL Report # 05-08570-007, dated October 2000
8. CD containing all pertinent test data and reports
9. Preliminary Data Assessment of Gemini South Optical Telescope Operating and Modal Data Report, dated June 2000
10. LMS Coda-X 3.4 Test and Analysis Software (TMON, FMON, Modal Analysis, Matrix Toolbox), Leuven Measurement Systems, Detroit Michigan
11. LMS Coda-X 3.5C Test and Analysis Software (TMON, FMON, Modal Analysis), Leuven Measurement Systems, Detroit Michigan
12. LMS Road Runner Data Acquisition System, Leuven Measurement Systems, Detroit Michigan
13. MEScope VES Version 2.0, Vibrant Technologies, Jamestown, CA
14. Avitabile, P., "Overview of Modal Analysis using the Frequency Response Method", July 1997
15. Box, George E.P., Hunter, J. Stuart, and Hunter, William G., *Statistics for Experimenters: An Introduction to Design, Data Analysis, and Model Building*, Wiley, 1978.
16. Shina, Sammy G., *Concurrent Engineering and Design for Manufacture of Electronic Products*, Van Nostrand Reinhold, 1991.



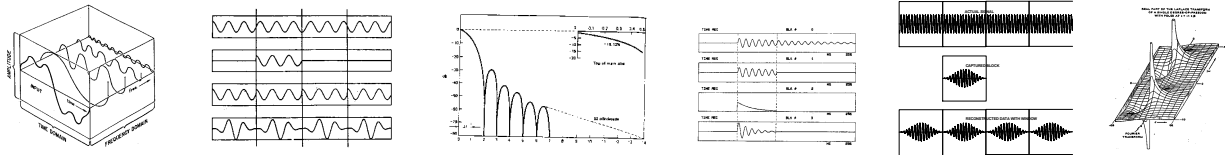


## OVERVIEW OF EXPERIMENTAL MODAL ANALYSIS USING THE FREQUENCY RESPONSE METHOD

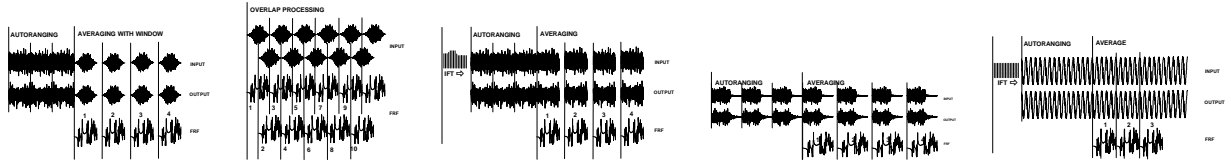
### PART 1 - REVIEW OF MODAL THEORY



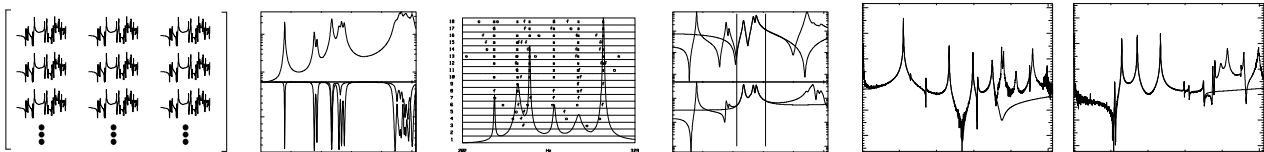
### PART 2 - DIGITAL SIGNAL PROCESSING CONSIDERATIONS



### PART 3 - EXCITATION TECHNIQUES



### PART 4 - MODAL PARAMETER ESTIMATION TECHNIQUES



Peter Avitabile  
Dynamic Decisions, Inc  
64 Woodward Road  
Merrimack, NH 03054  
603-424-1852

**DRAFT DOCUMENT**

© Copyright July 1995 - Reprinted with Permission



# OVERVIEW OF EXPERIMENTAL MODAL ANALYSIS USING THE FREQUENCY RESPONSE METHOD

Peter Avitabile  
Dynamic Decisions, Inc.  
Merrimack, NH 03054

## *DRAFT DOCUMENT*

© Copyright July 1995 Reprinted with Permission

Experimental modal analysis has become a common tool for solving structural dynamic problems. This series of articles is intended to overview some of the common techniques for developing an experimental modal model using the Frequency Response Method. While this document is written in a summarizing format, all the pertinent information is provided. Eventually, this document will be expanded in future revisions with more explanation in all areas. The material is broken down into four main areas.

- Part 1 covers the basic theory of single degree of freedom and multiple degree of freedom systems to identify some common terminology for modal testing and analysis. Equations are developed in the time, Laplace and frequency domains to show the interrelationship that exists between the analytical and experimental techniques.
- Part 2 reviews basic digital signal processing techniques and concepts as they pertain to modal testing. Digital signal processing concerning sampling, aliasing, leakage and windows are discussed. Frequency Response Functions are developed for different estimators. Errors associated with all aspects of digital signal processing relative to the development of the Frequency response Function are discussed.
- Part 3 reviews some of the more common of the excitation techniques for developing measured functions. Impact and shaker excitation excitation techniques are reviewed. Single input/single output as well as multiple input/multiple output techniques are described.
- Part 4 covers modal parameter estimation techniques and modal model validation tools currently available. Estimation using local and global, time and frequency based techniques are described. Approaches to validating the model are discussed.

Appendix A - Review of Linear Algebra and Matrix Notation

Appendix B1 - Example - Eigenvalue Problem for Two DOF System

Appendix B2 - Example - Pole, Residue, Transfer Matrix, FRF Problem for Two DOF System

Appendix B3 - Example - Pole, Residue, Transfer Matrix, FRF Problem for Three DOF System

Appendix C - Review of Some Basic Mathematical and Important Relations

Displacement, Velocity and Acceleration Relationships

Review of Complex Numbers

Conversion Factors



# **OVERVIEW OF EXPERIMENTAL MODAL ANALYSIS USING THE FREQUENCY RESPONSE METHOD**

## **PART 1 - REVIEW OF MODAL THEORY**

### **INTRODUCTION**

Today, several techniques exist to assist in the development of a model for dynamic applications. Finite element models and experimental modal models are two such techniques.

For many years, finite element modeling (FEM) has been used for the characterization of dynamic systems. The FEM process has been very successful in the early stages of the development of prototypes and allows for the optimization of specific design parameters. Thus, before hardware is manufactured, the majority of the design characteristics can be included and tuned to some degree. These dynamic finite element models are generally developed to study the response of structures due to design specification or measured input forces. The analytical model can be modified easily to achieve the appropriate or desired response prior to actually committing to actual hardware. Once a design has been identified, prototypes are fabricated for testing purposes to verify that the desired characteristics have been obtained. Depending on the severity of the dynamic application, many times the finite element model may need to be verified based on actual test data and adjustments made to the finite element model.

Experimental modal analysis (EMA) techniques have become very popular over the past decade due to the affordability of modal test systems and the ease of use of their associated software packages. The experimental modal test performed will provide the measured frequency, damping and modal vector information for the structure. Experimental modal testing has been under a large growth development for the past 20 years. A number of significant developments have taken place over the past decade which have greatly enhanced the overall data acquisition and data reduction process. The main item of significant importance during this period has been the development of multiple input / multiple output data acquisition and data reduction schemes. This has allowed for better test data from which to acquire parameters and has also allowed for more accurate modal models to be developed. In addition, a number of computational tools have been added to aid and assist the test engineer to better decipher and interpret measured frequency response data.



The purpose of this section is to review the basics of modal analysis. The first part contains some basic definition information pertaining to single degree of freedom systems followed by modal theory for multiple degree of freedom systems. Only the pertinent theory is reviewed and developed where necessary. The reader is referred to any good vibration text book for further theoretical development. Additional information on all types of issues related to modal analysis can be obtained from the Proceedings of the International Modal Analysis Conferences (IMAC) that have been held over the last 15 years.

Some of the more important aspects of modal analysis theory and experimental modal testing are noted below.

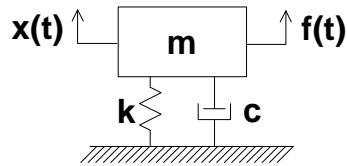


## BASIC MODAL ANALYSIS THEORY

A review of the pertinent equations for single and multiple degree of freedom systems for the development of the theory of experimental modal analysis are contained herein. More detailed theory can be found in the references.

### Single Degree of Freedom System Equation

Equations of motion are generated with the assumption that the mass of the system is modeled as a lumped mass, the spring stiffness is proportional to displacement on a linear basis and the dashpot is proportional to velocity on a linear basis. (The equations will be described first from a classical approach and then from the Laplace domain approach.)



With these assumptions, a force balance can be performed to derive the second order differential equation with constant coefficients for the equation of motion as

$$m \frac{d^2 x}{dt^2} + c \frac{dx}{dt} + k x = f(t) \quad \text{or} \quad m \ddot{x} + c \dot{x} + k x = f(t)$$

Assuming a solution of an exponential form for the homogeneous solution, then we can write

$$(ms^2 + cs + k) X e^{st} = 0$$

Since the exponential term cannot be zero and if  $x=0$  then a trivial solution exists, only the term in parentheses can be zero. The *characteristic equation* can then be written as

$$ms^2 + cs + k = 0$$

The *roots* or *poles* of this characteristic equation are given by

$$p_{1,2} = -\frac{c}{2m} \pm \sqrt{\left(\frac{c}{2m}\right)^2 - \frac{k}{m}}$$



Now this equation can be evaluated for three distinct cases. One solution exists for systems with damping less than that of critical damping, one solution exists for systems with damping equal to critical damping and one solution exists for systems with damping greater than that of critical damping. While the other solutions are important, only the case with damping less than that of critical is considered since this is an important solution for the structural dynamic engineer.

The roots can be expressed (for the case of damping less than critical) simply as

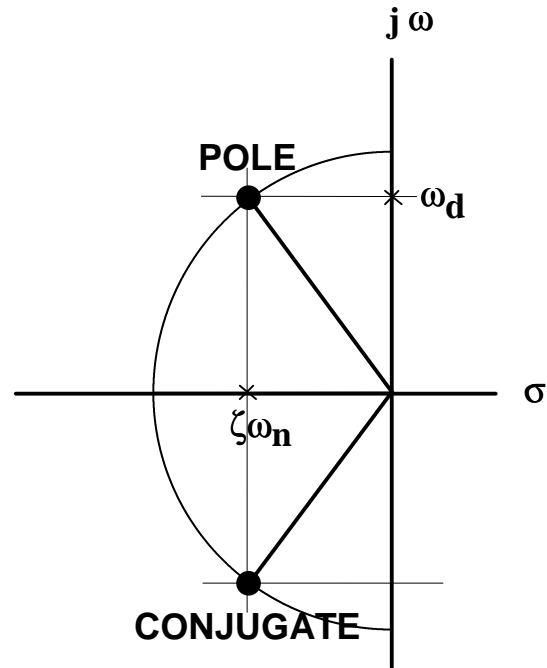
$$p_{1,2} = -\zeta\omega_n \pm \sqrt{(\zeta\omega_n)^2 - \omega_n^2} = -\sigma \pm j\omega_d$$

where

$\sigma = \zeta\omega_n$	<i>damping factor</i>
$\omega_n = \sqrt{\frac{k}{m}}$	<i>natural frequency</i>
$\zeta = \frac{c}{c_c}$	<i>percent of critical damping</i>
$c_c = 2 m \omega_n$	<i>critical damping</i>
$\omega_d = \omega_n \sqrt{1-\zeta^2}$	<i>damped natural frequency</i>

These definitions are typically used by most structural dynamic and vibration engineers. Several items need to be noted here. First, the damped natural frequency is approximately equal to the natural frequency for small values of damping (less than 10%). Second, the natural frequency of the system increases/decreases as the stiffness increases/decreases. Third, the natural frequency increases/decreases and the mass decreases/increases. Notice that the natural frequency is independent of the damping in the system - only the damped natural frequency changes as the damping changes. It is also important to notice that the roots of this equation are expressed as a complex number with real and imaginary parts to describe the pole. These roots occur in complex conjugate pairs with the real part of the root associated with the damping of the pole and the imaginary part of the root associated with the frequency of the pole.





## S-PLANE NOMENCLATURE

Another descriptive plot is the famous S-plane plot which is a plot of the location of the root in terms of its real (damping) and imaginary (frequency) parts. As the damping increases, the pole moves to the left of the  $j\omega$  axis and the value of the damped natural frequency decreases. As the damping increases, the pole maps out a circular path in the S-plane. As the damping approaches critical damping, the root and its conjugate approach the  $\sigma$  axis. The length of the vector from the origin to the pole (radius of a circle) is the natural frequency.

## Single Degree of Freedom System Response due to Harmonic Excitation

An important case to consider is the forced response due to harmonic excitation. Without laboring through all the mathematics to develop this equation, the response of a single degree of freedom system due to a harmonic input can be written in terms of displacement and phase as

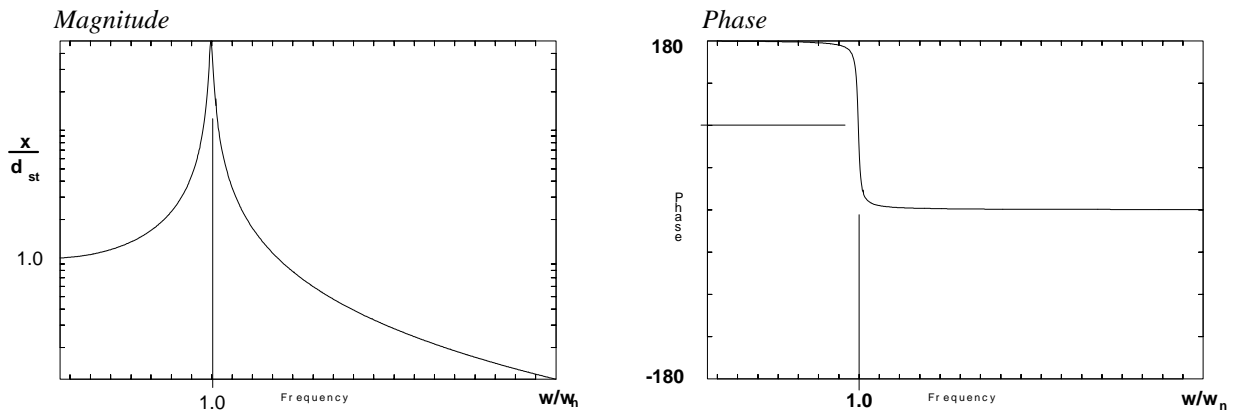
$$x = \frac{F_0}{\sqrt{(k - m\omega^2)^2 + (c\omega)^2}} \quad \phi = \tan^{-1}\left(\frac{c\omega}{k - m\omega^2}\right)$$

Using the definitions made above for a single degree of freedom system and letting  $\beta$  be the ratio of driving frequency of the excitation to the natural frequency of the single degree of freedom system, the response can be written in normalized form as



$$\frac{x}{\delta_{st}} = \frac{1}{\sqrt{(1-\beta^2)^2 + (2\zeta\beta)^2}} \quad \phi = \tan^{-1}\left(\frac{2\zeta\beta}{1-\beta^2}\right)$$

In this form, the function can be plotted in dimensionless form in terms of the dynamic displacement relative to the static displacement with the driving frequency represented in terms of a percentage of the natural frequency of the single degree of freedom system. The *dynamic magnification* and *phase* for the single degree of freedom system is then



From these equations, it can be seen that for a lightly damped system, the peak amplitude occurs at the damped natural frequency (which is approximately the natural frequency) and that there is a lag of 90 deg between the force and response at resonance.

### Damping Estimation for Single Degree of Freedom System

Many times the damping of the system may need to be measured. The damping can be computed by several different techniques. Two popular techniques are the half power method and the log decrement method.

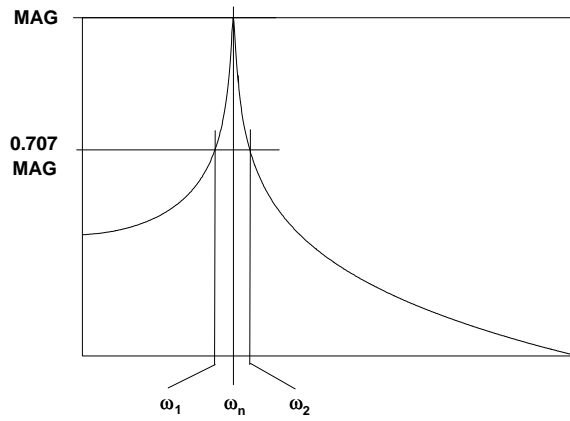
In the half power method, the damping is related to the frequency divided by the difference of the frequencies obtained at the 'half power' points. This is often referred to as the 'Q' of the system or the amplification factor. For instance, a system with a damping of 1% of critical damping has a Q of 50. In the log decrement method, a decay in amplitude in one or several cycles of the system is used to determine the damping.

It must be noted that the damping is the only mechanism to minimize the response at resonance since the inertial forces are counterbalanced (equal and opposite) to the elastic forces in the system.



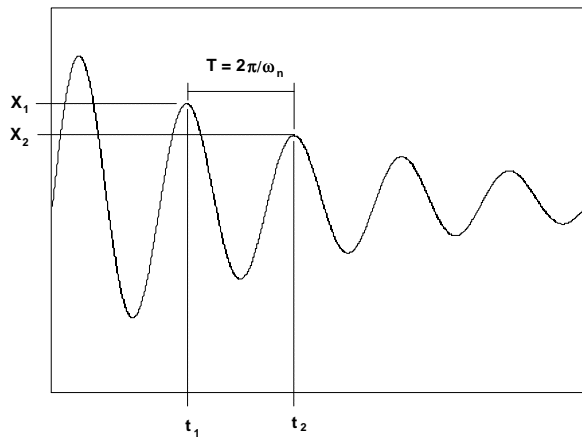
Half Power Method

$$Q = \frac{1}{2\zeta} = \frac{\omega_n}{\omega_2 - \omega_1}$$



Log Decrement Method

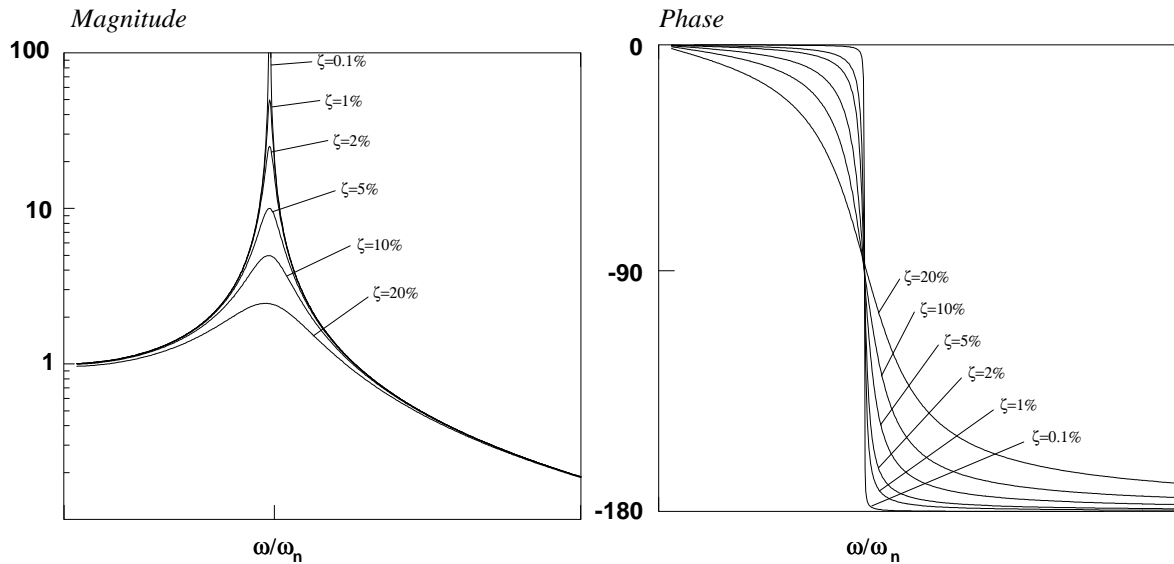
$$\delta = \ln \frac{x_1}{x_2} \approx 2\pi\zeta$$





## Response Assessment with Varying Damping

As the damping is varied for the single degree of freedom system a set of magnitudes and phases can be plotted for comparison



From these plots, it can be seen that as the damping is increased, the response of the system decreases. In fact at resonance, the inertial forces of the system are counterbalance by the elastic forces in the system. This implies that the only mechanism to counterbalance the applied force is the damping in the system. Notice that as the damping increases, the response amplitude changes more gradually over a wider frequency range. Also notice that the phase lag occurs more gradually over a wider frequency range.

*(need an elaborate Walk Thru S-Plane here)*



## Laplace Domain for Single Degree of Freedom System

Now let's write the equations of motion for the single degree of freedom system using a Laplace domain approach. Starting from the equation of motion

$$m \ddot{x} + c \dot{x} + k x = f(t)$$

The Laplace transform for acceleration, velocity, displacement and force is

$$\mathcal{L}(\ddot{x}) = s^2 x(s) - s x_0 - \dot{x}_0$$

$$\mathcal{L}(x) = x(s)$$

$$\mathcal{L}(\dot{x}) = s x(s) - x_0$$

$$\mathcal{L}(f(t)) = f(s)$$

where the 0 subscript denotes initial conditions.

Taking a Laplace transform, substituting and rearranging terms, the equation of motion becomes

$$(ms^2 + cs + k) x(s) = f(s) + (ms + c)x_0 + m\dot{x}_0$$

Assuming initial conditions (velocity and displacement) are zero, this equation can be written as

$$(ms^2 + cs + k) x(s) = f(s)$$

If we let  $b(s) = (ms^2 + cs + k)$  then the more commonly written form of the system equation is obtained

$$b(s) x(s) = f(s)$$

Solving for the displacement variable gives

$$x(s) = b^{-1}(s) f(s)$$

This can be written as

$$x(s) = h(s) f(s)$$

where  $h(s)$ , the *system transfer function* is given by



$$h(s) = \frac{1}{ms^2 + cs + k}$$

From the system equation, if we solve the homogeneous solution (ie,  $f(s)=0$ ), then  $b(s)x(s) = 0$  and since  $x(s) = 0$  is a trivial solution then  $b(s)=0$  is the only possible solution. Again the solution to this equation for a system with less than critical damping results in

$$p_{1,2} = -\zeta\omega_n \pm \sqrt{(\zeta\omega_n)^2 - \omega_n^2} = -\sigma \pm j\omega_d$$

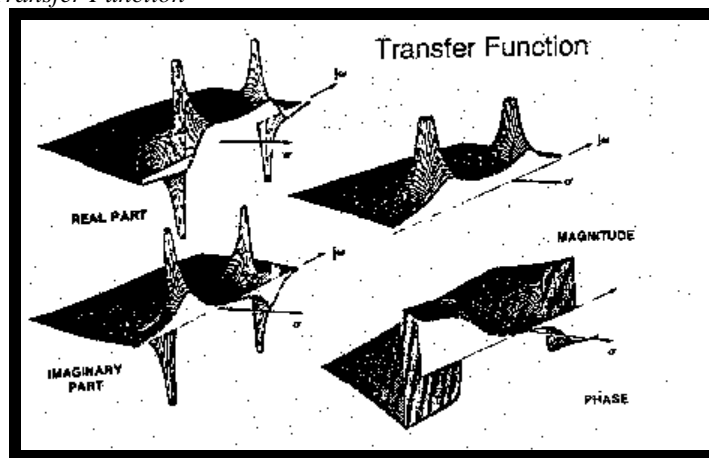
For the undamped case evaluated, the roots of the characteristic equation are complex valued.



## System Transfer Function

The system transfer function is a complex valued function. Since the system transfer function is a function of two variables, then a plot of this function produces a surface plot, with  $\sigma$  and  $j\omega$  axis, above the s-plane. Typically this plot can be viewed in several different forms - magnitude portion, phase portion, imaginary portion or real portion of the transfer function surface as shown below. If the system transfer function is evaluated at the root or pole, then the function is undefined..

*System Transfer Function*





## Different Forms of the Transfer Function

This system transfer function can be expressed in several common forms. One form is as presented earlier where the expression is left in *polynomial form*. Another form is the factored form of the polynomial which is referred to as the *pole-zero form* where the poles are seen in the denominator and the zeros are seen in the numerator in factored form. The most popular form is the *partial fraction expansion form* where the expression is clearly seen to contain the contribution from the pole and its complex conjugate. If a dirac delta pulse is applied to the system and an inverse Laplace transform is made, then the impulse response (commonly referred to as the *complex exponential form*) is obtained. It is very important to note that in each of the equations the same information is displayed in different forms. There is no difference in any of these representations of the single degree of freedom system.

Polynomial Form	$h(s) = \frac{1}{ms^2 + cs + k}$
Pole-Zero Form	$h(s) = \frac{1/m}{(s - p_1)(s - p_1^*)}$
Partial Fraction Form	$h(s) = \frac{a_1}{(s - p_1)} + \frac{a_1^*}{(s - p_1^*)}$
Complex Exponential form	$h(t) = \frac{1}{m\omega_d} e^{-\zeta\omega t} \sin \omega_d t$



## Residue of the Single Degree of Freedom System

As stated earlier, the system transfer function is not defined when it is evaluated at one of the roots of the system. In order to evaluate this function at one of its roots, then a mathematical tool called the residue theorem is used. The resulting value referred to as the residue of the single degree of freedom system is obtained when the system transfer function is evaluated at one of its roots using the residue theorem and is shown to be

$$a_1 = h(s)(s - p_1) \Big|_{s \rightarrow p_1} = \frac{1}{2j\omega_d}$$

In a similar fashion, the complex conjugate pole residue is shown to be

$$a_1^* = -\frac{1}{2j\omega_d}$$

In some of the literature, residues are often times referred to using 'r'. In regards to the notation presented herein

$$r_1 = 2j a_1 \quad \text{and} \quad r_1^* = 2j a_1^*$$

It is very important to note that the system transfer function (as well as the frequency response function in the next section) can be obtained from just two parameters - the *pole* and the *residue*. From these two parameters, we can construct the frequency response function over *all frequencies* as well as the transfer function surface for all values of  $\sigma$  and  $j\omega$ .

## Frequency Response Function for a Single Degree of Freedom System

The frequency response function is the transfer function evaluated along  $s=j\omega$  and is

$$h(j\omega) = h(s) \Big|_{s=j\omega} = \frac{a_1}{(j\omega - p_1)} + \frac{a_1^*}{(j\omega - p_1^*)}$$

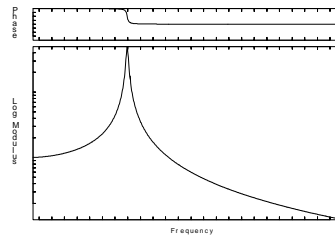
The frequency response function is nothing more than a slice taken out of the system transfer function surface. It is very important to remember that the system transfer function is a complex valued function as well as the frequency response function. A review of some pertinent complex notation is contained in the Appendix for reference.



Some common forms of the frequency response function are the Bode plot (magnitude and phase), the coincident and quadrature plot (real and imaginary) and the Nyquist or Argand plot (real vs. imaginary).

### Bode Diagram

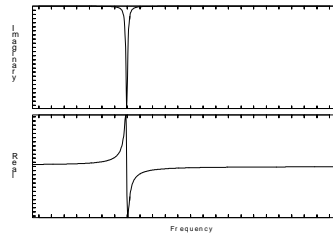
The most common form of the frequency response plot is the Bode plot which displays the magnitude and phase together in one plot. Notice that the magnitude is a peak at resonance and that the phase angle is 90 degrees; there is a loss of a total of 180 degrees as you cross over the resonant frequency.



*Bode Plot*

### Coincident-Quadrature Diagram

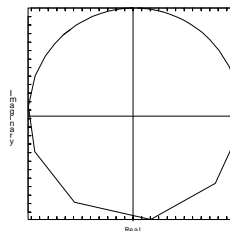
Another very common form is to convert the magnitude and phase into the real (coincident) and imaginary (quadrature) parts and is often referred to as the Co-Quad plot. Notice that the real part of the frequency response function is zero and the imaginary is a peak at resonance.



*Coincident-Quadrature Plot*

### Nyquist

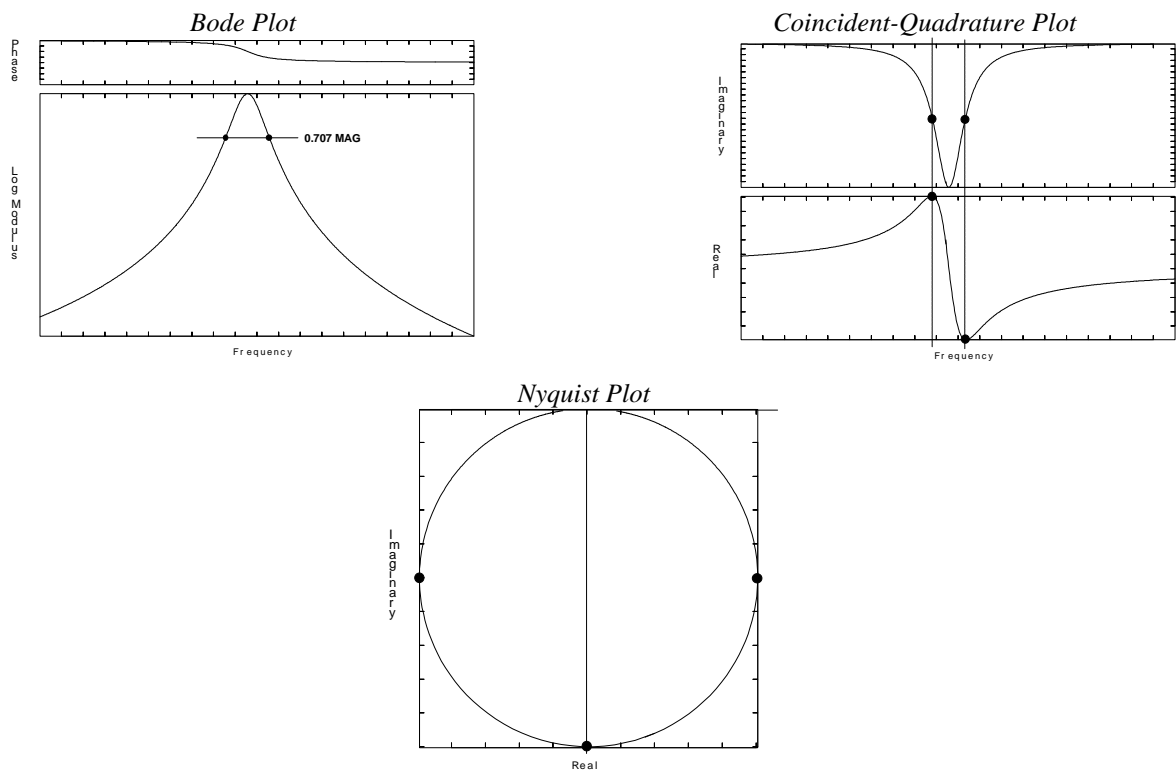
Yet another popular form is a plot of the real vs. the imaginary part of the frequency response function which is called the Nyquist or Argand plot. Notice that the shape looks like a circle when we plot the data in this fashion.



*Nyquist Plot*



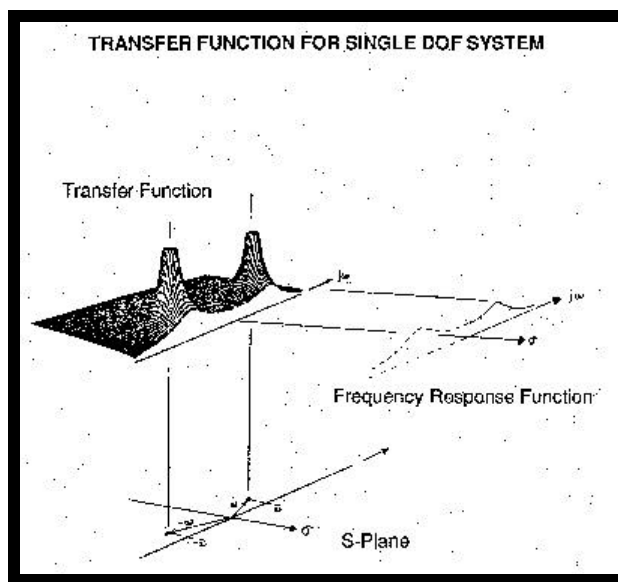
Now if we take a closer look around the resonant frequency of the system, there are several things to note. Let's look at the half power points of the Bode plot which occur at 0.707 of the peak amplitude. If we take a look at the imaginary part of the frequency response function, the half power points occur at half of the peak amplitude of the imaginary part. This amplitude in the imaginary occurs at the peaks in the real part of the frequency response function which is exactly the same amplitude of the half power of the imaginary part. Viewing these same points on the Nyquist plot, the peak of the imaginary part is directly opposite 0,0 with no real part value. The half power points occur at points that are 90 deg away from the peak in the imaginary part.





## Transfer Function/Frequency Response Function/S-Plane for a Single Degree of Freedom System

The slice of the *system transfer function* ( $s=j\omega$ ) can be projected away from the surface and is commonly called the *frequency response function*. If we project the location of the poles down onto the system transfer function, the *s-plane* can be viewed. This is shown in the figure below.



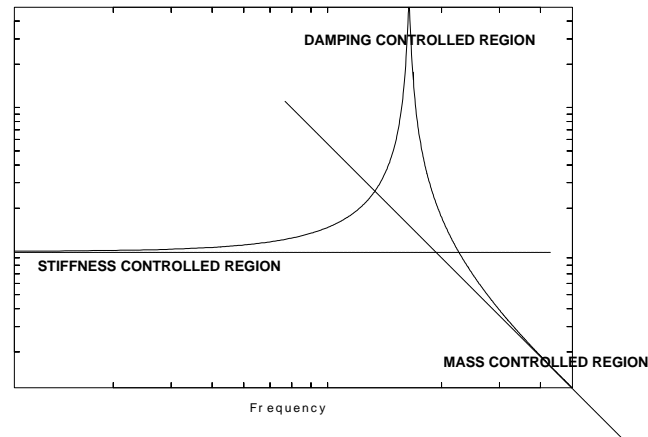
This figure is included to show the inter-relationship between the system transfer function, the frequency response function and the s-plane. Half of the frequency response function is shown in dotted lines since we typically only look at the positive part of the frequency axis but the conjugate does exist.

## Frequency Response Function Regions for a Single Degree of Freedom System

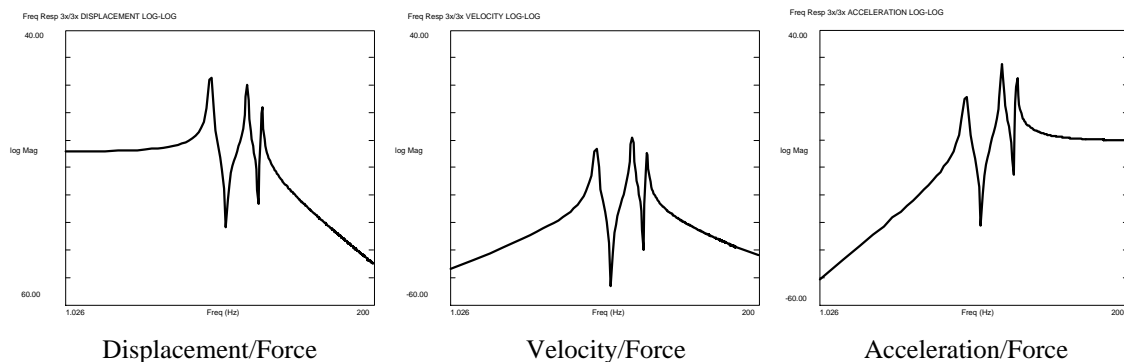
The frequency response function is made up of different regions. At frequencies much less than that of resonance, the response of the system is dominated by the stiffness of the system. At frequencies much greater than that of resonance, the response of the system is dominated by the mass inertia of the system. At frequencies close to resonance, the response of the system is controlled by the amount of damping in the system; at resonance, the inertial forces are counterbalanced by the elastic forces of the system such that the only way to counterbalance the



applied forces to the system is through the damping forces in the system. Typically, regions of the frequency response function will be described in terms of the stiffness controlled portion of the frequency response which is less than that of the resonant frequency, the damping controlled portion of the frequency response which is in the region of the resonant frequency and the mass controlled portion of the frequency response which is greater than that of the resonant frequency.



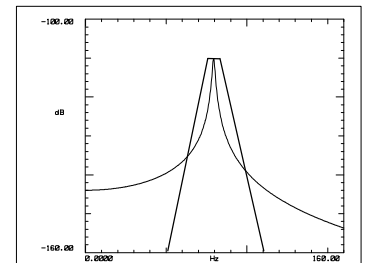
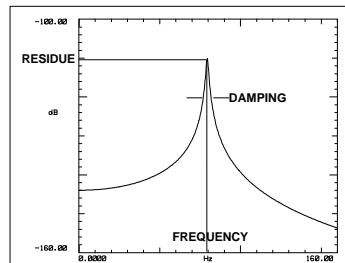
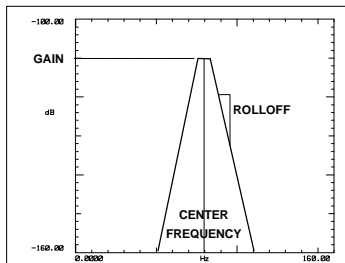
Up until this point, we have only discussed the frequency response function in terms of the displacement relative to the input force which is referred to as the dynamic compliance. We could also measure the frequency response function in terms of the velocity relative to the force which is referred to as the mobility. And we could also measure the frequency response function in terms of the acceleration relative to the force which is referred to as the inertance. In addition, the inverse of these relations can also be measured for displacement, velocity and acceleration and are referred to as the dynamic stiffness, impedance and dynamic mass, respectively.





## Analog Filter Analogy for a Single Degree of Freedom System

A direct analogy can be made between the single degree of freedom system and an analog bandpass filter. Both amplify and attenuate signals on a frequency basis. The analog filter is described in terms of its center frequency, rolloff and gain - this is analogous to the single degree of freedom natural frequency, damping and residue respectively.



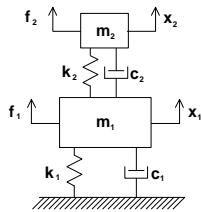
So now I can see that my single degree of freedom system is nothing more than a bandpass filter which knows how to amplify and attenuate input signals on a frequency basis. This is exactly what I would expect since I only describe the character of the system through the poles and residues.



## Multiple Degree of Freedom System Equations

Next a multiple degree of freedom system is considered. As was assumed for the single degree of freedom system, the equation of motion can be written as shown below with the following assumptions. The mass is modeled as a lumped mass. The spring stiffness is proportional to displacement on a linear basis. The dashpot is proportional to velocity on a linear basis. In addition, it is important to note that the system is linear and time invariant. The system can be described by a second order differential equation with constant coefficients.

First, let's consider a simple two degree of freedom system. Again a force balance can be performed for each of the two masses of the system resulting in two equations and two unknowns. For details on developing these equations, refer to any vibration textbook.



$$\begin{aligned} m_1 \ddot{x}_1 + (c_1 + c_2) \dot{x}_1 - c_2 \dot{x}_2 + (k_1 + k_2) x_1 - k_2 x_2 &= f_1(t) \\ m_2 \ddot{x}_2 - c_2 \dot{x}_1 + c_2 \dot{x}_2 - k_2 x_1 + k_2 x_2 &= f_2(t) \end{aligned}$$

Notice that the first equation has terms that involve the displacement and velocity of mass two as well as the terms involving displacement, velocity and acceleration of mass one. Likewise the second equation involves terms of mass one and mass two. In other words, these equations have terms that are inter-related or coupled.

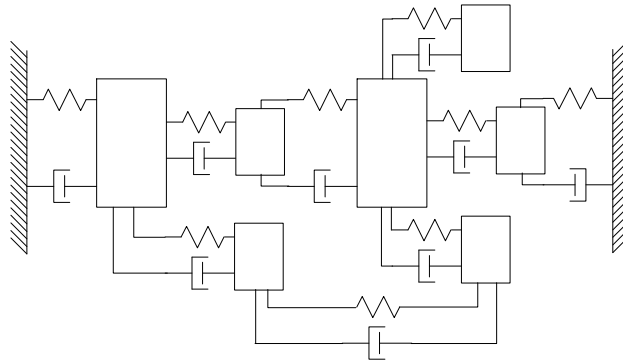
For simplicity, these equations can also be cast in matrix form for the 2 dof system as a matrix of masses times a vector of accelerations, plus a matrix of dashpots times a vector of velocities, plus a matrix of stiffnesses times a vector of displacements which is equal to a vector of applied forces.

$$\begin{aligned} &\begin{bmatrix} m_1 & 0 \\ 0 & m_2 \end{bmatrix} \begin{Bmatrix} \ddot{x}_1 \\ \ddot{x}_2 \end{Bmatrix} \\ &+ \begin{bmatrix} (c_1 + c_2) & -c_2 \\ -c_2 & c_2 \end{bmatrix} \begin{Bmatrix} \dot{x}_1 \\ \dot{x}_2 \end{Bmatrix} \\ &+ \begin{bmatrix} (k_1 + k_2) & -k_2 \\ -k_2 & k_2 \end{bmatrix} \begin{Bmatrix} x_1 \\ x_2 \end{Bmatrix} = \begin{Bmatrix} f_1(t) \\ f_2(t) \end{Bmatrix} \end{aligned}$$



Notice that the damping and stiffness matrices have off-diagonal terms which are the terms that describe the coupling between mass one and mass two. The size of these matrices is directly related to the number of degrees of freedom used to describe the multiple degree of freedom system. Therefore, these matrices are all square and it is important to note that they are all symmetric.

While these equations are useful to look at for the 2 dof system, the more general case of multiple dof system will be addressed hereafter. A brief review of matrix and vector operations is contained in the Appendix.



The equation of motion for a multiple degree of freedom system can be written in matrix form as

$$[M]\{\ddot{x}\} + [C]\{\dot{x}\} + [K]\{x\} = \{F(t)\}$$

where  $[M]$  is the mass matrix (n,n),  $[C]$  is the damping matrix (n,n),  $[K]$  is the stiffness matrix (n,n),  $\{F\}$  is the forcing vector (n,1) and  $\{x\}$  is the vector (n,1) of displacements, velocities and accelerations as noted. These equations are coupled as before. It would be very convenient if these matrices could somehow be cast in an uncoupled form for easier processing - the eigensolution helps to achieve this simpler solution.

The eigensolution is obtained using only the mass and stiffness matrices with an assumption that the damping matrix is zero or proportional to either the mass and/or stiffness matrix.

$$[[K] - \lambda [M]]\{x\} = 0$$



The eigensolution provides a set of eigenpairs - frequencies (*eigenvalues*) and mode shapes (*eigenvectors*). Many different numerical schemes exist to determine the eigenvalues. In any event, for each eigenvalue, there is a corresponding eigen-vector which satisfies the equation above. For convenience, the *modal matrix* is constructed by arranging the eigenvalues in diagonal form and the eigenvectors in column fashion.

$$\begin{bmatrix} \backslash & & \\ & \Omega^2 & \\ & & \backslash \end{bmatrix} = \begin{bmatrix} \omega_1^2 & & \\ & \omega_2^2 & \\ & & \backslash \end{bmatrix} \text{ and } [U] = [\{u_1\} \quad \{u_2\} \quad \dots]$$

What we would like to do is find some new coordinate system wherein the equations describing the system can be written in simpler form where the coupling is eliminated. The modal transformation equation helps to do this. Now this modal matrix [U] will be used to uncouple the physical set of equations. The modal transformation which transforms *physical space* to *modal space* is shown below.

$$\{x\} = [U] \{p\} = [\{u_1\} \quad \{u_2\} \quad \dots] \begin{Bmatrix} p_1 \\ p_2 \\ \vdots \end{Bmatrix}$$

The modal matrix can be as large as (n,n) but in general will only be of size (n,m). While there are 'n' possible modal vectors that can be obtained, generally only 'm' modes are extracted since this is all that is typically necessary to solve most structural dynamic problems. If we now substitute this modal transformation expression into the equation of motion and premultiply the equation by the transpose of the projection operator to put the equations into normal form, this gives

$$[U]^T [M] [U] \{\ddot{p}\} + [U]^T [C] [U] \{\dot{p}\} + [U]^T [K] [U] \{p\} = [U]^T \{F\}$$

Due to the orthogonality condition, this transformation *uncouples* the highly coupled set of equations in physical space into a set of uncoupled single dof systems in modal space as

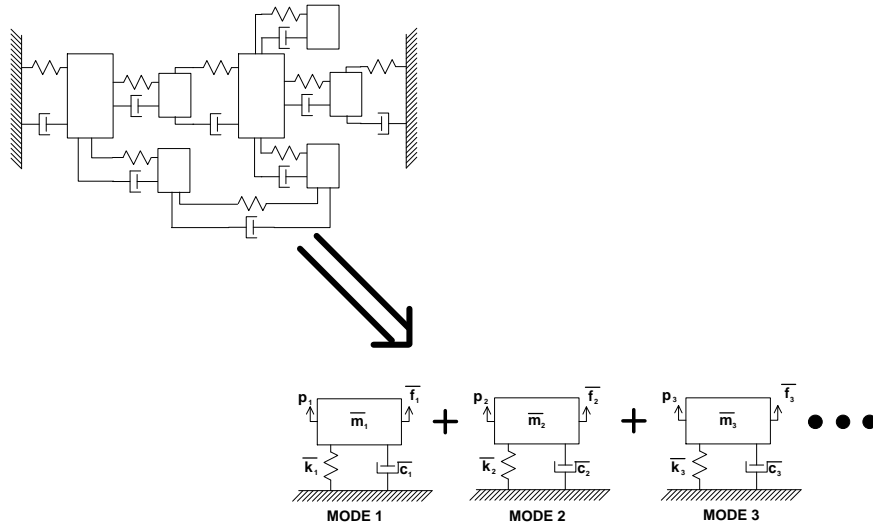
$$\begin{bmatrix} \overline{m}_1 & & \\ & \overline{m}_2 & \\ & & \backslash \end{bmatrix} \begin{Bmatrix} \ddot{p}_1 \\ \ddot{p}_2 \\ \vdots \end{Bmatrix} + \begin{bmatrix} \overline{c}_1 & & \\ & \overline{c}_2 & \\ & & \backslash \end{bmatrix} \begin{Bmatrix} \dot{p}_1 \\ \dot{p}_2 \\ \vdots \end{Bmatrix} + \begin{bmatrix} \overline{k}_1 & & \\ & \overline{k}_2 & \\ & & \backslash \end{bmatrix} \begin{Bmatrix} p_1 \\ p_2 \\ \vdots \end{Bmatrix} = \begin{Bmatrix} \{u_1\}^T \{F\} \\ \{u_2\}^T \{F\} \\ \vdots \end{Bmatrix}$$



where diagonal matrices of modal mass ( $\bar{m}$ ), modal damping ( $\bar{c}$ ) and modal stiffness ( $\bar{k}$ ) (with assumed proportional damping in the model). It is very important to note that the size of these matrices is ( $m, m$ ) and not ( $n, n$ ). This can also be written as

$$\begin{bmatrix} \bar{M} \\ \bar{C} \\ \bar{K} \end{bmatrix} \begin{Bmatrix} \ddot{p} \\ \dot{p} \\ p \end{Bmatrix} = [U]^T \{F\}$$

These diagonal equations drastically reduce the complication of the problem especially if the necessary number of *modal dofs* needed to characterize the problem are much less than the number of *physical dofs* (ie,  $m \ll n$ ). In essence, the complicated set of coupled dofs has been reduced to a more simplistic problem of a system that is described by a set of single degree of freedom systems that are related to the multiple degree of freedom system through the modal transformation equation.



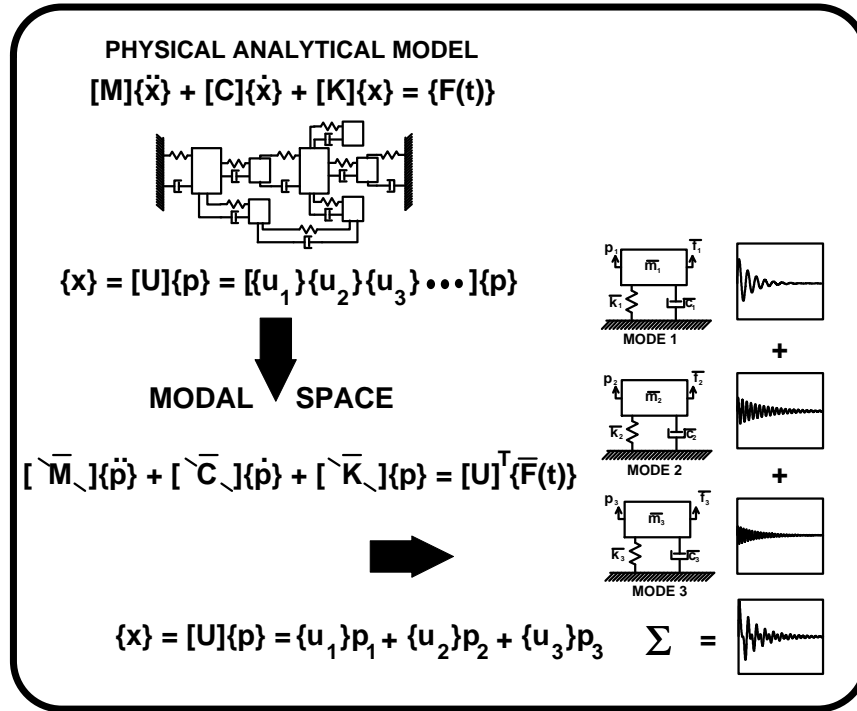
Before we proceed, it is very important to note that the modal vectors are orthogonal and linearly independent set of vectors. The orthogonality condition is

$$\begin{aligned} \{u_i\}^T [M] \{u_j\} &= \begin{cases} \bar{m}_{ii} & \text{when } i = j \\ 0 & \text{when } i \neq j \end{cases} & \{u_i\}^T [K] \{u_j\} &= \begin{cases} \bar{k}_{ii} & \text{when } i = j \\ 0 & \text{when } i \neq j \end{cases} \end{aligned}$$

In modal space, each mode describes the contribution to the physical response for that particular mode. Since the modes are linearly independent to each other and orthogonal with respect to the system mass and stiffness matrices,



the contribution to the physical space system can be made up from the linear combinations of each individual mode uncoupled from every other mode. This is illustrated in the figure below.



### Laplace Domain for Multiple Degree of Freedom System

Similar to the Laplace evaluation done for the single degree of freedom system, we will perform the same transformation for the multiple degree of freedom system. The original equation of motion in physical space can be transformed into the Laplace domain using the Laplace transform and is shown below

$$\begin{aligned} & \left[ [M] s^2 + [C] s + [K] \right] \{x(s)\} = \{F(s)\} \\ & + \left[ [M] s + C \right] \{x_0\} + [M] \{\dot{x}_0\} \end{aligned}$$

where  $s$  is the Laplace variable. The main advantage of this formulation is that the equation has the characteristic equation, the applied force and the initial conditions all in one equation. If we assume that the initial conditions are zero, then



$$[[M]s^2 + [C]s + [K]]\{X(s)\} = \{F(s)\}$$

The homogeneous equation can be written as

$$[[M]s^2 + [C]s + [K]]\{x(s)\} = 0 \Rightarrow [B(s)]\{x(s)\} = 0$$

where  $[B(s)]$  is referred to as the *System Matrix*. Note that since the mass, damping and stiffness matrices are square symmetric, then the system matrix  $[B(s)]$  is also square symmetric.

The solution of the homogeneous equation yields  $2n$  solutions where  $n$  is the number of equations. If the damping is less than critical damping then the solution to this equation contains roots which are referred to as the *poles* of the system and occur in complex conjugate pairs given by

$$\det[[M]s^2 + [C]s + [K]] = 0 \Rightarrow p_k = -\sigma_k \pm j\omega_{dk}$$

This complex valued function has a portion of the pole (real part) which is the percent of critical damping,  $\zeta$ , times the undamped natural frequency of the system,  $\omega_n$ , and a portion of the pole (imaginary part) which is the damped natural frequency,  $\omega_d$ . Notice that the poles occur in complex conjugate pairs.

Returning to the system equation and rearranging terms to obtain a ratio of response to input gives

$$[B(s)]\{x(s)\} = \{F(s)\} \Rightarrow [B(s)]^{-1} = \frac{\{x(s)\}}{\{F(s)\}}$$

The inverse of the system matrix  $[B(s)]$  gives the *System Transfer Matrix*

$$[B(s)]^{-1} = [H(s)] = \frac{\text{Adj}[B(s)]}{\det[B(s)]} = \frac{[A(s)]}{\det[B(s)]}$$

which is the adjoint of the system matrix divided by the determinant of the system matrix.

If we expand this out, then we would see the following



$$\begin{bmatrix} h_{11}(s) & h_{12}(s) & h_{13}(s) & \cdots \\ h_{21}(s) & h_{22}(s) & h_{23}(s) & \cdots \\ h_{31}(s) & h_{32}(s) & h_{33}(s) & \cdots \\ \vdots & \vdots & \vdots & \ddots \end{bmatrix} = \frac{\begin{bmatrix} a_{11}(s) & a_{12}(s) & a_{13}(s) & \cdots \\ a_{21}(s) & a_{22}(s) & a_{23}(s) & \cdots \\ a_{31}(s) & a_{32}(s) & a_{33}(s) & \cdots \\ \vdots & \vdots & \vdots & \ddots \end{bmatrix}}{\det[B(s)]}$$

The system transfer function is a complex valued surface. The numerator of this equation is  $[A(s)]$  which is referred to as the *Residue Matrix*; the denominator of this equation is the  $\det[B(s)]$  which is a scalar quantity and is called the *characteristic equation*. The denominator yields the poles of the system and it is interesting to note that the poles are constant and do not depend on which term of the residue matrix is evaluated.

Now in order to evaluate some interesting items in the system transfer matrix, let's write

$$[B(s)][B(s)]^{-1} = [I]$$

and substitute the system transfer function into the equation. Rearranging terms,

$$[B(s)][A(s)] = \det[B(s)][I]$$

When the system transfer function is evaluated at a pole of the system, the solution can be written as

$$[B(p_k)][A(p_k)] = 0$$

which can be broken up into column format as

$$[B(p_k)][\{a_1(p_k)\} \quad \{a_2(p_k)\} \quad \cdots] = [\{0\} \quad \{0\} \quad \cdots]$$

which implies that



$$\begin{aligned}
[B(p_k)] \{a_1(p_k)\} &= \{0\} \\
[B(p_k)] \{a_2(p_k)\} &= \{0\} \\
[B(p_k)] \{a_3(p_k)\} &= \{0\} \\
&\vdots
\end{aligned}$$

Notice that every column of this equation is a solution to this equation. Also due to symmetry, every row of this matrix is also a solution to this equation. Therefore, every row and column is a solution to this equation when the system transfer function is evaluated at a pole of the system. This means that in order to evaluate the modal vector, any one of the rows or columns may be used to estimate the system vector characteristics.

As was done for the single degree of freedom system, the system transfer function can be written in *partial fraction form* as

$$[H(s)] = \sum_{k=1}^m \frac{[A_k]}{(s - p_k)} + \frac{[A_k^*]}{(s - p_k^*)}$$

or in *pole-zero form* (or in polynomial form by expanding out the factors) as

$$[H(s)] = \prod_{k=1}^m \left[ \frac{(s - z_k)(s - z_k^*)}{(s - p_k)(s - p_k^*)} \right]$$

or by taking the inverse Laplace transform, the *impulse response function* in the time domain is given by

$$[h(t)] = \left[ \sum_{k=1}^m \frac{1}{m_k \omega_{dk}} e^{-\sigma_k t} \sin \omega_{dk} t \right]$$

Now if we were to look at a particular term of the matrix, then we could write the system transfer function in *partial fraction form* as

$$h_{ij}(s) = \sum_{k=1}^m \frac{a_{ijk}(s)}{(s - p_k)} + \frac{a_{ijk}^*(s)}{(s - p_k^*)}$$

or in *polynomial form* as



$$h_{ij}(s) = \frac{a_{ij}(s)}{\det[B(s)]} = \frac{s^{2n-1} + b_1 s^{2n-2} + b_2 s^{2n-3} + \dots}{s^{2n} + a_1 s^{2n-1} + a_2 s^{2n-2} + \dots}$$

or as the *impulse response* as

$$h_{ij}(t) = \sum_{k=1}^m \frac{1}{m_k \omega_{dk}} e^{-\sigma_k t} \sin \omega_{dk} t$$

## Frequency Response Function

The *Frequency Response Function* (FRF) is the *System Transfer Function* evaluated at  $s=j\omega$ . If we let  $s = j\omega$  (which effectively takes a slice out of the transfer function surface), then the *Frequency Response Function* (FRF) is given by

$$[H(s)]_{s=j\omega} = [H(j\omega)] = \sum_{k=1}^m \frac{[A_k]}{(j\omega - p_k)} + \frac{[A_k^*]}{(j\omega - p_k^*)}$$

Again we must realize that an individual '*ij*' term is given by

$$h_{ij}(s)_{s=j\omega} = h(j\omega) = \sum_{k=1}^m \frac{a_{ijk}}{(j\omega - p_k)} + \frac{a_{ijk}^*}{(j\omega - p_k^*)}$$

Notice that the frequency response function is made up of a collection of single degree of freedom systems summed up over all of the modes of the systems. The frequency response function is the same one shown previously for the single degree of freedom system but now there is a contribution to the total frequency response function due to each mode.

Now we have already seen that the solution to the system equation can be obtained using any row or any column of  $B(s)$  and that when the system transfer function is evaluated at a pole of the system then we get a corresponding shape vector. Now let's look at this a little further using some advanced techniques. Using singular valued



decomposition techniques, when  $[H(s)]$  is evaluated at a pole, it can be shown that  $[H(s)]$  is singular and of rank = 1 and can be decomposed as

$$[H(s)]_{s=p_k} = \{u_k\} \frac{q_k}{s - p_k} \{u_k\}^T$$

Considering all of the modes of the system, we can write

$$[H(s)] = \sum_{k=1}^m \frac{q_k \{u_k\} \{u_k\}^T}{(s - p_k)} + \frac{q_k \{u_k^*\} \{u_k^*\}^T}{(s - p_k^*)}$$

Notice that from this we can write a relationship between the residue matrix and the mode shapes of the system as

$$[A(s)]_k = q_k \{u_k\} \{u_k\}^T$$

where  $q$  is a scaling constant that will be discussed shortly.

Looking at the adjoint matrix and expanding out some of the terms of this equation for the  $k$ th mode of the system we get

$$\begin{bmatrix} a_{11k} & a_{12k} & a_{13k} & \cdots \\ a_{21k} & a_{22k} & a_{23k} & \cdots \\ a_{31k} & a_{32k} & a_{33k} & \cdots \\ \vdots & \vdots & \vdots & \ddots \end{bmatrix} = q_k \begin{bmatrix} u_{1k} u_{1k} & u_{1k} u_{2k} & u_{1k} u_{3k} & \cdots \\ u_{2k} u_{1k} & u_{2k} u_{2k} & u_{2k} u_{3k} & \cdots \\ u_{3k} u_{1k} & u_{3k} u_{2k} & u_{3k} u_{3k} & \cdots \\ \vdots & \vdots & \vdots & \ddots \end{bmatrix}$$

It is very important to note that the residues are directly related to the system mode shapes. For illustration purposes we can expand out some of these terms. Let's regroup some of these terms in the form of vectors in each column.

$$\left[ \begin{bmatrix} a_{11k} \\ a_{21k} \\ a_{31k} \\ \vdots \end{bmatrix} \begin{bmatrix} a_{12k} \\ a_{22k} \\ a_{32k} \\ \vdots \end{bmatrix} \begin{bmatrix} a_{13k} \\ a_{23k} \\ a_{33k} \\ \vdots \end{bmatrix} \cdots \right] = \left[ q_k u_{1k} \begin{bmatrix} u_{1k} \\ u_{2k} \\ u_{3k} \\ \vdots \end{bmatrix} \quad q_k u_{2k} \begin{bmatrix} u_{1k} \\ u_{2k} \\ u_{3k} \\ \vdots \end{bmatrix} \quad q_k u_{3k} \begin{bmatrix} u_{1k} \\ u_{2k} \\ u_{3k} \\ \vdots \end{bmatrix} \right]$$



So we can see the first column of this matrix contains an estimate of the kth mode of the system scaled by  $q_k$  and  $u_{1k}$

$$\begin{Bmatrix} a_{11k} \\ a_{21k} \\ a_{31k} \\ \vdots \end{Bmatrix} = q_k u_{1k} \begin{Bmatrix} u_{1k} \\ u_{2k} \\ u_{3k} \\ \vdots \end{Bmatrix}$$

And the second column of this matrix contains an estimate of the kth mode of the system scaled by  $q_k$  and  $u_{2k}$

$$\begin{Bmatrix} a_{12k} \\ a_{22k} \\ a_{32k} \\ \vdots \end{Bmatrix} = q_k u_{2k} \begin{Bmatrix} u_{1k} \\ u_{2k} \\ u_{3k} \\ \vdots \end{Bmatrix}$$

And the third column of this matrix contains an estimate of the kth mode of the system scaled by  $q_k$  and  $u_{3k}$

$$\begin{Bmatrix} a_{13k} \\ a_{23k} \\ a_{33k} \\ \vdots \end{Bmatrix} = q_k u_{3k} \begin{Bmatrix} u_{1k} \\ u_{2k} \\ u_{3k} \\ \vdots \end{Bmatrix}$$

Now let's regroup some of these terms in the form of vectors in each row.

$$\begin{bmatrix} \{a_{11k} & a_{12k} & a_{13k} & \cdots\} \\ \{a_{21k} & a_{22k} & a_{23k} & \cdots\} \\ \{a_{31k} & a_{32k} & a_{33k} & \cdots\} \\ \vdots \end{bmatrix} = \begin{bmatrix} q_k u_{1k} \{u_{1k} & u_{2k} & u_{3k} & \cdots\} \\ q_k u_{2k} \{u_{1k} & u_{2k} & u_{3k} & \cdots\} \\ q_k u_{3k} \{u_{1k} & u_{2k} & u_{3k} & \cdots\} \\ \vdots \end{bmatrix}$$

So we can see the first row of this matrix contains an estimate of the kth mode of the system scaled by  $q_k$  and  $u_{1k}$

$$\{a_{11k} \quad a_{12k} \quad a_{13k} \quad \cdots\} = q_k u_{1k} \{u_{1k} \quad u_{2k} \quad u_{3k} \quad \cdots\}$$



And the second row of this matrix contains an estimate of the kth mode of the system scaled by  $q_k$  and  $u_{2k}$

$$\{a_{21k} \quad a_{22k} \quad a_{23k} \quad \dots\} = q_k u_{2k} \{u_{1k} \quad u_{2k} \quad u_{3k} \quad \dots\}$$

And the third row of this matrix contains an estimate of the kth mode of the system scaled by  $q_k$  and  $u_{3k}$

$$\{a_{31k} \quad a_{32k} \quad a_{33k} \quad \dots\} = q_k u_{3k} \{u_{1k} \quad u_{2k} \quad u_{3k} \quad \dots\}$$

For unit modal mass scaling, the scaling constant can be shown to be (will add more on scaling later!!!)

$$q_k = \frac{1}{2j\omega_k}$$

From the above equations, it can be seen that the frequency response function can be obtained from the eigenvalues and eigenvectors of the system. If this frequency response function could be measured, then the parameters of interest (frequency, damping and mode shape) can be extracted from measured data.

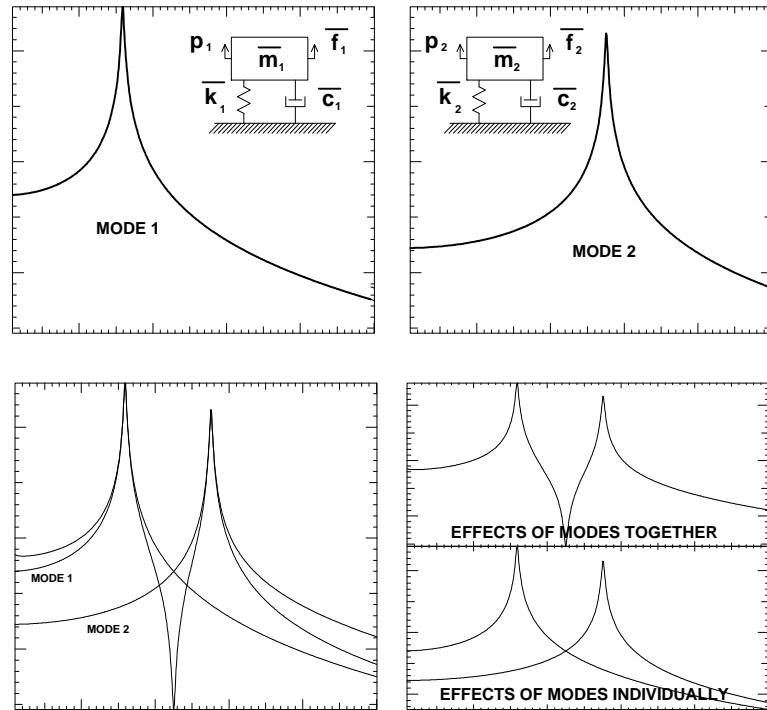


## Point to Point Frequency Response Function

The point to point frequency response function will be evaluated next. Let's consider the response at point  $i$  due to a input at point  $j$  in the system. Evaluating the system transfer function at  $s=j\omega$  for a particular  $ij$  (input-output) location, we get

$$h(s)_{ij} \Big|_{s=j\omega} = h_{ij}(j\omega) = \sum_{k=1}^m \frac{a_{ijk}}{(j\omega - p_k)} + \frac{a_{ijk}^*}{(j\omega - p_k^*)}$$

It is very important to note that this is the same as written earlier for the single degree of freedom system except that now the effects of all the modes are summed together. This is shown in the figure below (considering only two modes of the system).



In addition, if we recall that  $a_{ijk} = u_{ik} u_{jk}$  then we can see that the point to point frequency response function is

$$h(s)_{ij} \Big|_{s=j\omega} = h_{ij}(j\omega) = \sum_{k=1}^m \frac{q_k u_{ik} u_{ij}}{(j\omega - p_k)} + \frac{q_k^* u_{ik}^* u_{jk}^*}{(j\omega - p_k^*)}$$

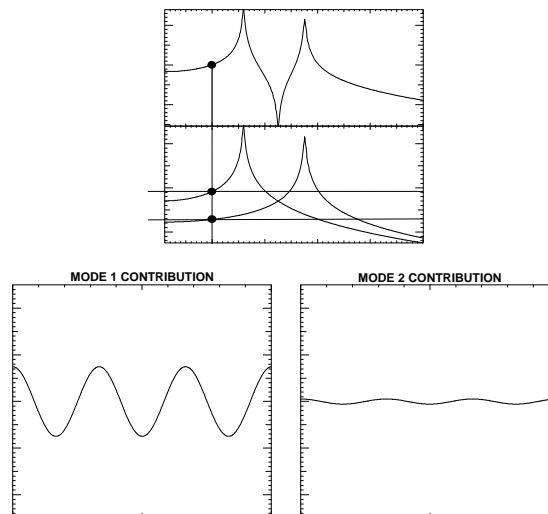


From this equation we could say that the point to point frequency response function is made up a set of single degree of freedom oscillators and that the amplitude of each of these oscillators is controlled by the filtering effect of the input excitation location (based on the value of the mode shape at the 'j' dof) and the filtering effect of the output response location (based on the value of the mode shape at the 'i' dof).

## Response of Multiple Degree of Freedom System due to Harmonic Excitations

Previously we had evaluated the single degree of freedom system due to sinusoidal excitations. Now let's look at the same sinusoidal excitation for the multiple degree of freedom system. The response of the multiple degree of freedom system due to a sinusoidal excitation is the sum of the response of each of the single degree of freedom systems that make up the multiple degree of freedom system. In order to illustrate the effects of contribution due to each of the modes, several different excitation frequencies for a simple 2 dof system are shown.

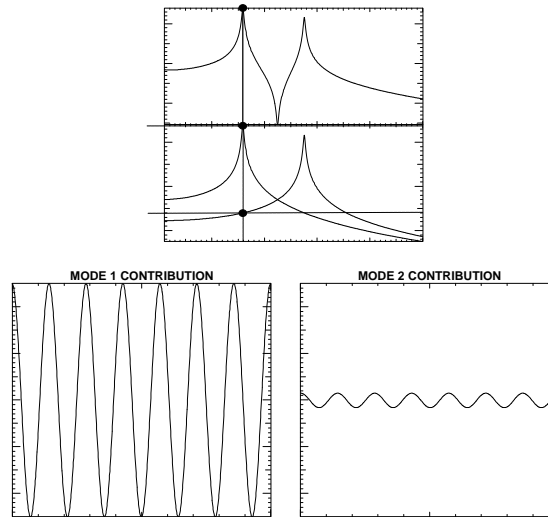
First let's consider a sinusoidal input where the excitation frequency is lower than both of the natural frequencies for the two modes of the system. The response is mainly made up of the response of the first mode which is larger than the response from the second mode. The upper plot shows the contribution of each of the frequency response functions for each mode to the total frequency response function. The lower portion of this plot shows the corresponding time domain response due to mode 1 in the left plot and mode 2 in the right plot.



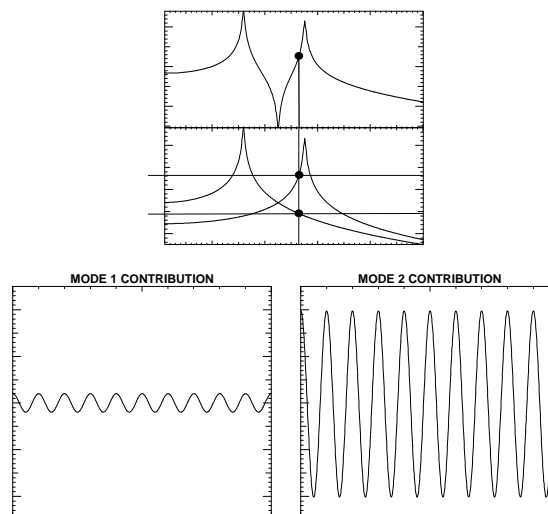
In the second plot, the excitation frequency is close to the natural frequency of the first mode and the majority of the response is due to the first mode although there is a small contribution due to the second mode. Again the upper plot



shows the contribution of each of the frequency response functions for each mode to the total frequency response function. The lower portion of this plot shows the corresponding time domain response due to mode 1 in the left plot and mode 2 in the right plot.



In the third plot, the excitation frequency is between that of the two modes but is fairly close to the natural frequency of the second mode. The majority of the response is due to the second mode of the system while there is some response from the first mode. Again the upper plot shows the contribution of each of the frequency response functions for each mode to the total frequency response function. The lower portion of this plot shows the corresponding time domain response due to mode 1 in the left plot and mode 2 in the right plot.

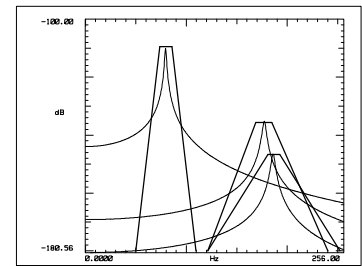
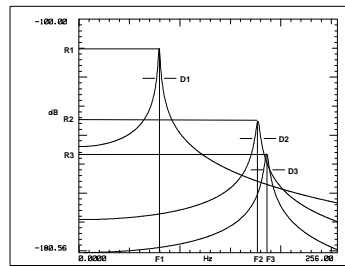
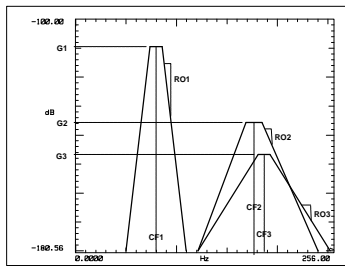




From these plots, it becomes much more apparent of the advantage that is gained through the modal transformation of the system. It is much easier to understand the response of the system if the response can be broken down into the modes which contribute to the response.

### Analog Filter Analogy for a Multiple Degree of Freedom System

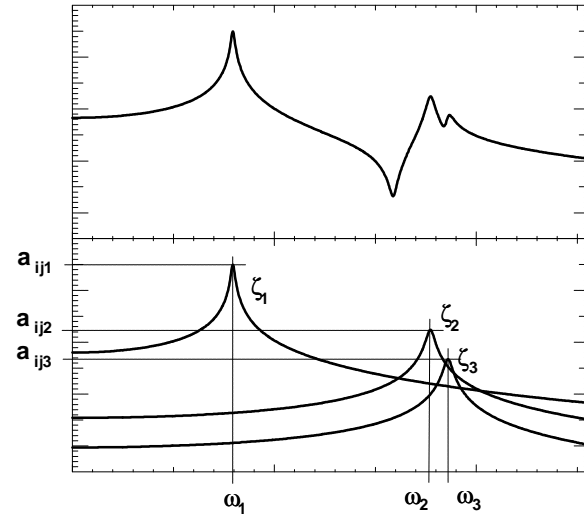
Again as was done with the single degree of freedom system, a direct analogy can be made between the multiple degree of freedom system and a set of analog filters. Both amplify and attenuate signals on a frequency basis. The analog filters are described in terms of their center frequency, rolloff and gain - this is analogous to the multiple degree of freedom natural frequencies, damping and residues respectively. So we can see that the frequency response function between two points on a structure is nothing more than a very elaborate set of bandpass filters that know how to amplify and attenuate signals on a frequency basis.





For example, the frequency response function can be expanded for three modes as shown below. The frequency response equation presents the parameters that effect this set of bandpass filters; for each mode of the system, the pole describes the filter (center frequency) and rolloff (damping) and the residue identifies the gain of the filter.

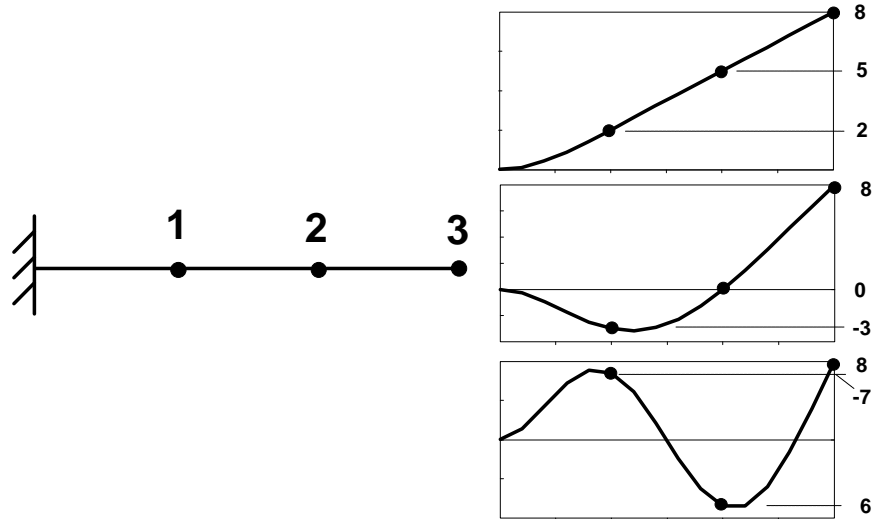
$$h_{ij}(j\omega) = \frac{a_{ij1}}{(j\omega - p_1)} + \frac{a_{ij1}^*}{(j\omega - p_1^*)} + \frac{a_{ij2}}{(j\omega - p_2)} + \frac{a_{ij2}^*}{(j\omega - p_2^*)} + \frac{a_{ij3}}{(j\omega - p_3)} + \frac{a_{ij3}^*}{(j\omega - p_3^*)}$$



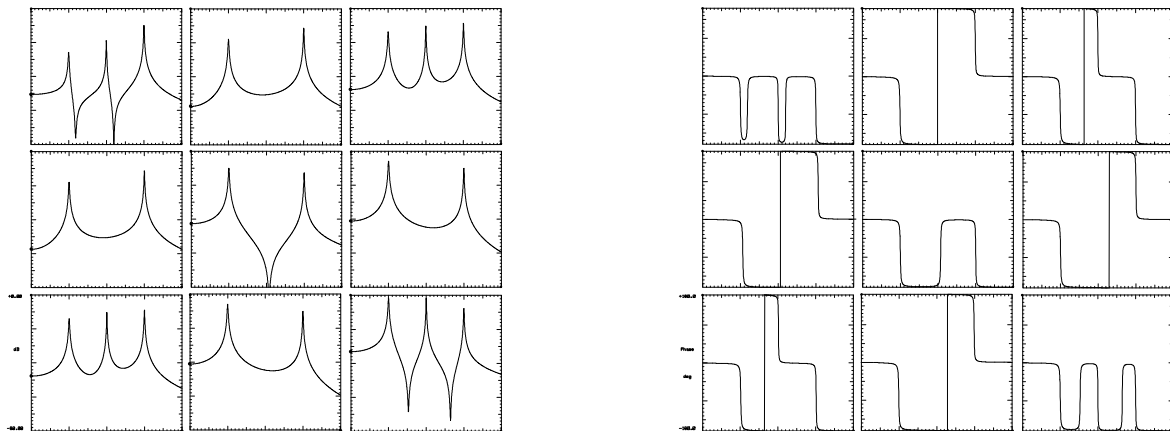


## Cantilever Beam Model with Three Measured DOF

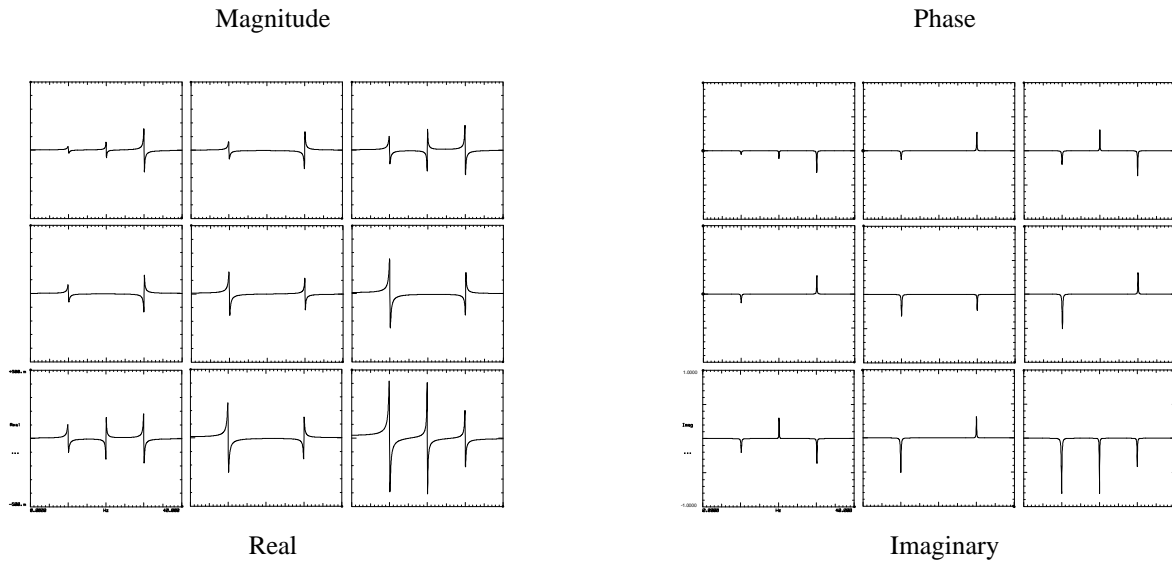
As an example, a cantilever beam is used to develop the frequency response matrix for three measurement points for the first three modes of the beam (the values for the mode shape for each of the modes is shown).



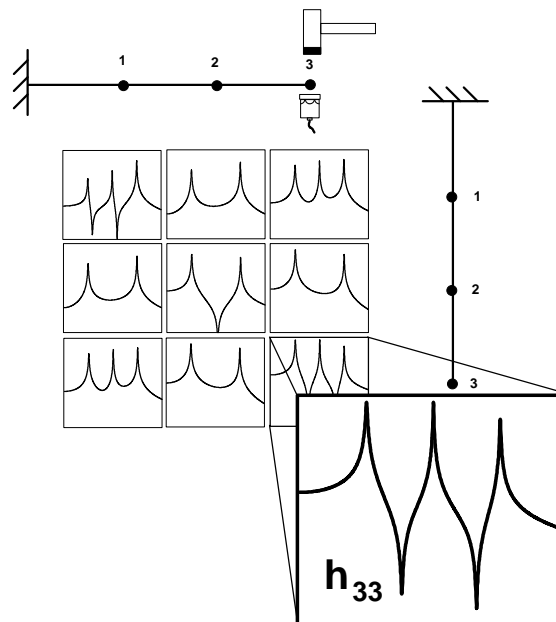
If I would like to measure three locations along the length of the beam, then we know that we could make 9 total frequency response function measurements for this beam; there would be a total of three possible input forcing locations and three possible output locations to measure the response of the system. Below we have shown the 3x3 frequency response function matrix that would result. Notice that there are 4 sets of frequency response function matrices - magnitude, phase, real and imaginary. This shows us all the measurements that could possibly be made on this beam with three measurement locations. Now let's take a look at measuring each individual location by first considering an impact test situation and then a shaker test situation.







Now let's describe the measurements that could possibly be made for this beam and let's describe a typical set of measurements that could be acquired. Let's assume that a force is applied at the tip of the beam at point 3; this is called the reference location. If we were to measure the response of the beam also at point 3, then we would measure  $h_{33}$  the tip driving point FRF for the beam. The driving point measurement is a special measurement where the input force and response of the system are measured at the same location.

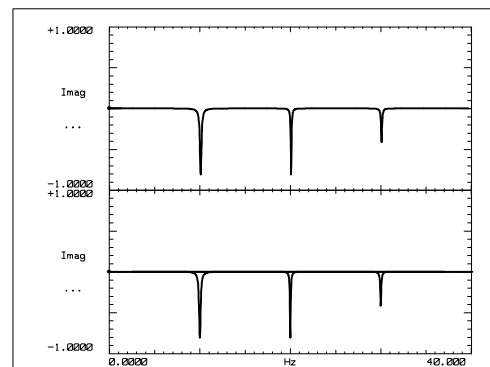
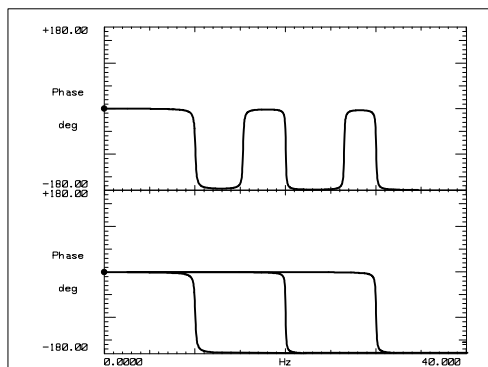
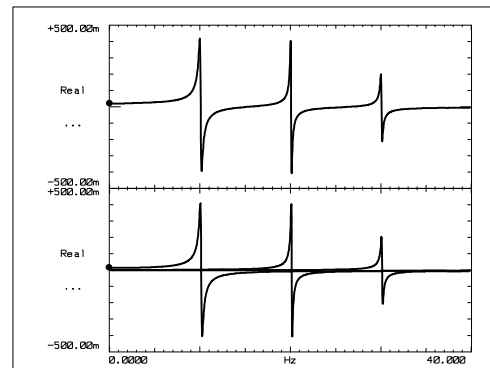
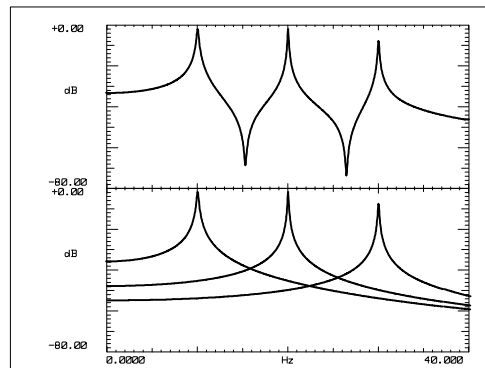


For a driving point measurement several items can be noted:



- all resonances are separated by antiresonances as seen in the magnitude plot
- the phase loses 180° of phase as we pass over a resonance and gain 180° of phase as we pass over an antiresonance
- the peaks in the imaginary part of the FRF must all point in the same direction

The drive point measurement at the tip of the beam can be viewed as a summation of all the modes or as the contribution due to each mode. As seen in the four plots below, the upper plot contains the summation due to all the modes and the lower plot shows the contribution due to each mode. For the first three modes of the beam, the FRF is made up of the sum of each of the single degree of freedom oscillators describing each mode of the beam. For reference, recall that the frequency response function equation can be written as either residues or mode shapes.

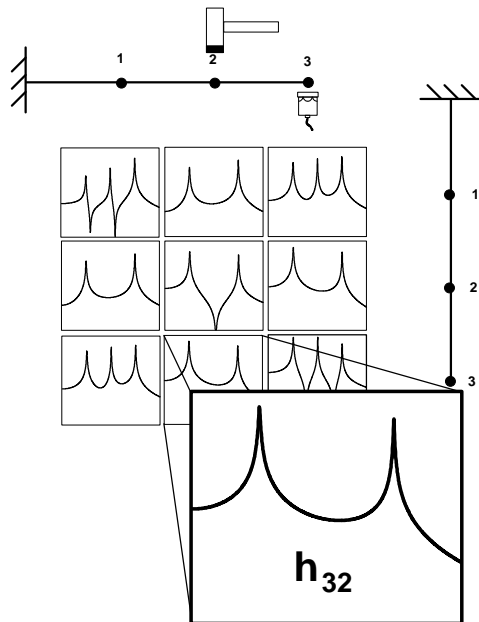




$$h_{ij}(j\omega) = \frac{a_{ij1}}{(j\omega - p_1)} + \frac{a_{ij1}^*}{(j\omega - p_1^*)} \\ + \frac{a_{ij2}}{(j\omega - p_2)} + \frac{a_{ij2}^*}{(j\omega - p_2^*)} \\ + \frac{a_{ij3}}{(j\omega - p_3)} + \frac{a_{ij3}^*}{(j\omega - p_3^*)}$$

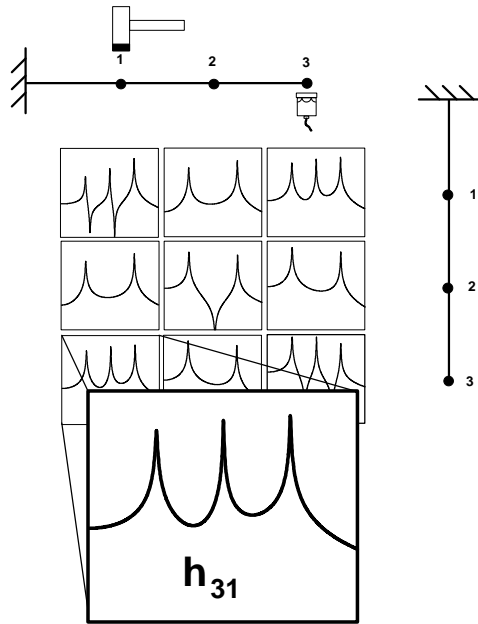
$$h_{ij}(j\omega) = \frac{q_1 u_{i1} u_{j1}}{(j\omega - p_1)} + \frac{q_1 u_{i1} u_{j1}^*}{(j\omega - p_1^*)} \\ + \frac{q_2 u_{i2} u_{j2}}{(j\omega - p_2)} + \frac{q_2 u_{i2} u_{j2}^*}{(j\omega - p_2^*)} \\ + \frac{q_3 u_{i3} u_{j3}}{(j\omega - p_3)} + \frac{q_3 u_{i3} u_{j3}^*}{(j\omega - p_3^*)}$$

Now let's excite the beam at point 2 and measure the response at point 3. This would correspond to  $h_{32}$ .



Now let's excite the beam at point 1 and measure the response at point 3. This would correspond to  $h_{31}$ .

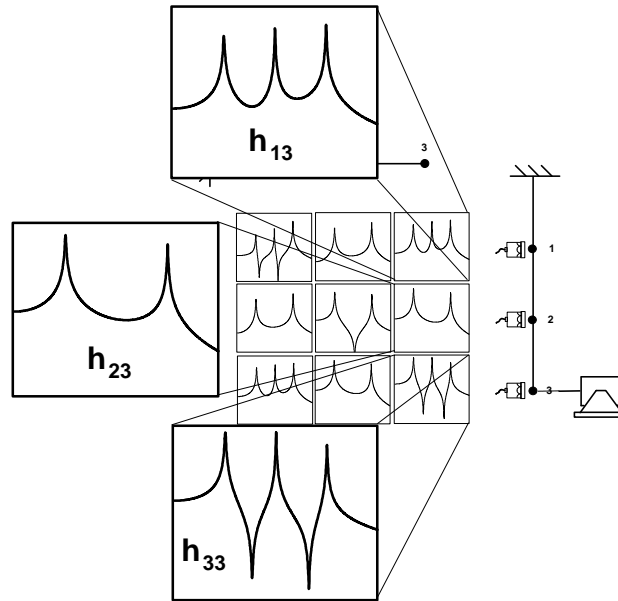




Due to the manner in which these measurements were acquired, one row of the FRF matrix, namely the last row, was acquired. Note that the response location was the same for all three measurements which implies that this is the reference location and determines which row of the FRF matrix was acquired. (If the reference accelerometer was located at point number 1 and all the points were excited with this reference location, then the first row of the FRF matrix would be acquired.) This is a typical test setup configuration used for impact testing. Typically in impact testing the response transducer is stationary and the system is excited with an impact hammer at all the measurement locations. Thus for this type of test a row of the FRF matrix is acquired.

Now if the input force was stationary (as in shaker excitation), then columns of the FRF matrix would be acquired; the column extracted would depend on where the input excitation were placed. A typical measurement of a column of the FRF matrix is shown below for 3 measurement locations.





Now let's recall that the residue matrix for this beam can be written for the 'kth' mode as

$$\begin{bmatrix} a_{11k} & a_{12k} & a_{13k} & \cdots \\ a_{21k} & a_{22k} & a_{23k} & \cdots \\ a_{31k} & a_{32k} & a_{33k} & \cdots \\ \vdots & \vdots & \vdots & \ddots \end{bmatrix} = q_k \begin{bmatrix} u_{1k} u_{1k} & u_{1k} u_{2k} & u_{1k} u_{3k} & \cdots \\ u_{2k} u_{1k} & u_{2k} u_{2k} & u_{2k} u_{3k} & \cdots \\ u_{3k} u_{1k} & u_{3k} u_{2k} & u_{3k} u_{3k} & \cdots \\ \vdots & \vdots & \vdots & \ddots \end{bmatrix}$$

Now if we realize that the scaling constant  $q$  and value of the mode shape at the tip of the beam are just constants, then we would see that for the first mode this equation becomes

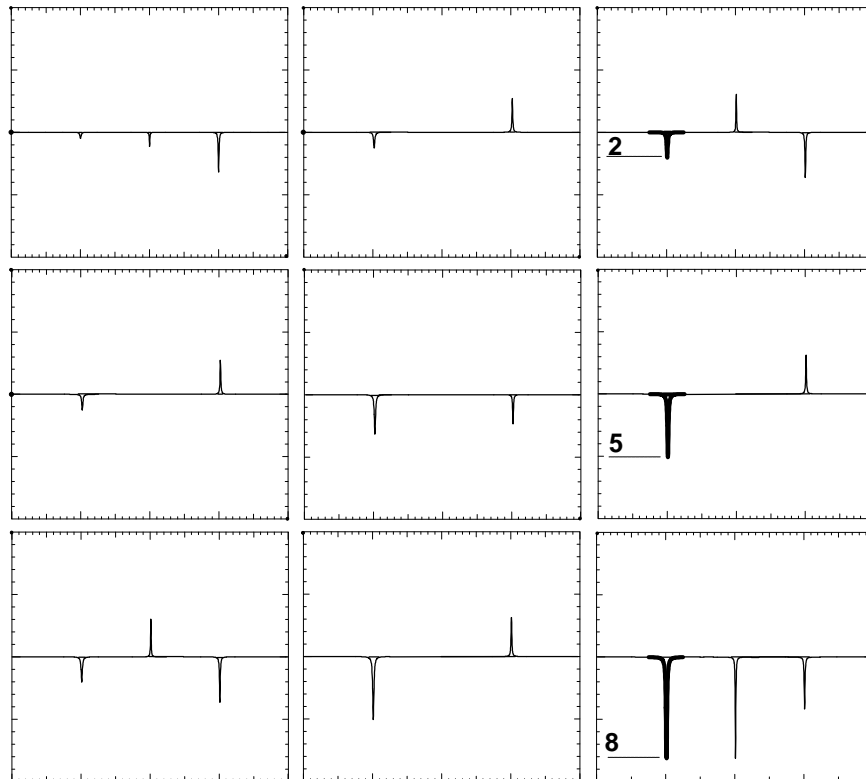
$$\begin{Bmatrix} a_{13k} \\ a_{23k} \\ a_{33k} \end{Bmatrix} = q_k u_{3k} \begin{Bmatrix} u_{1k} \\ u_{2k} \\ u_{3k} \end{Bmatrix}$$

Now if I look at the first mode of the system with dof 3 as a reference, then I can see that

$$\begin{Bmatrix} a_{131} \\ a_{231} \\ a_{331} \end{Bmatrix} = q_1 u_{31} \begin{Bmatrix} u_{11} \\ u_{21} \\ u_{31} \end{Bmatrix} \qquad \begin{Bmatrix} a_{131} \\ a_{231} \\ a_{331} \end{Bmatrix} = q_1(8) \begin{Bmatrix} 2 \\ 5 \\ 8 \end{Bmatrix}$$

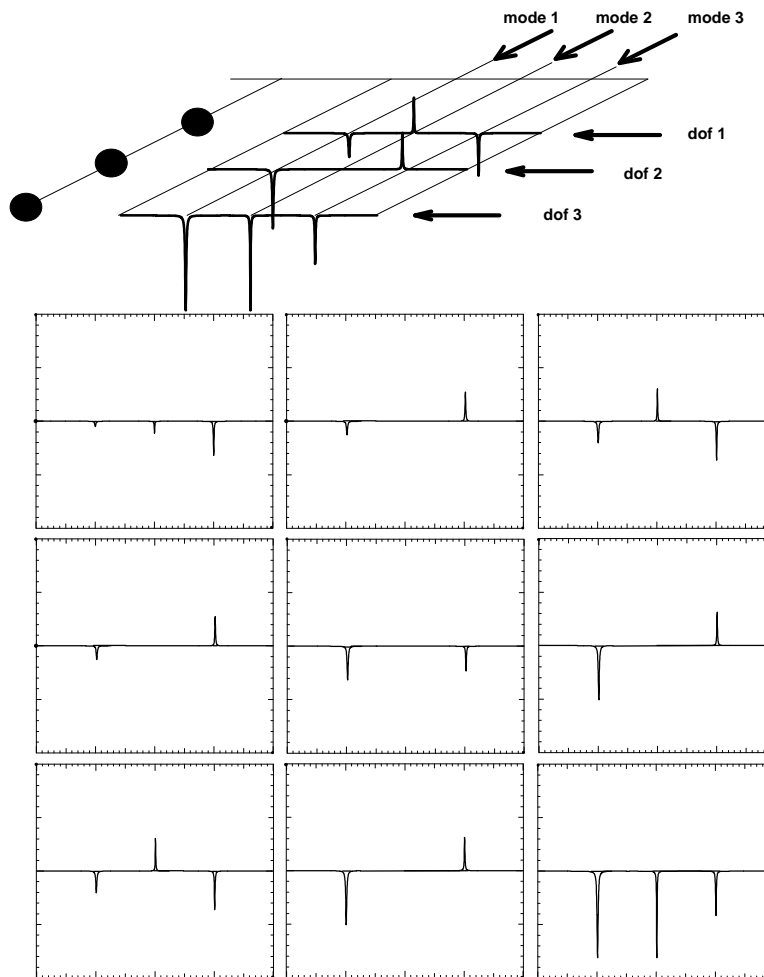


Now if I look at the third column of the FRF matrix for the first mode, I can see that the amplitude of the FRF is directly related to the mode shape. You can actually look at these plots and read the amplitudes! (This could also be done for mode 2 and 3 as well).





So the 3x3 matrix of measurements describes all the possible measurements. Any one of the rows or columns can be used to extract information pertaining to the frequency and mode shape for the beam. The cantilever beam is shown with a waterfall plot of the imaginary part of the frequency response plot using the tip of the beam as a reference. The mode shape can be clearly seen from the measurements.

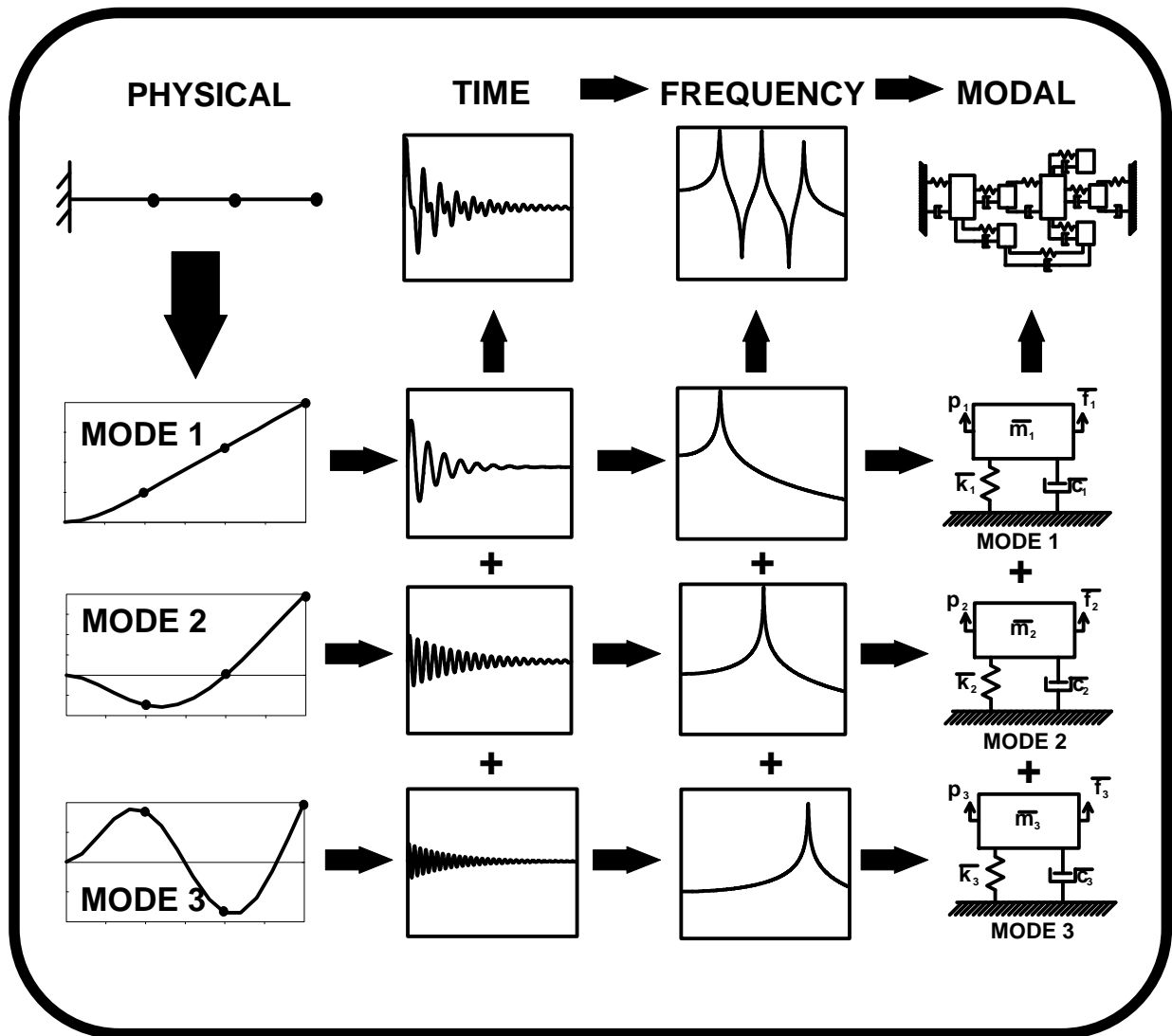




## SUMMARY OF TIME / FREQUENCY / MODAL DOMAINS

As a further illustration of the response of the system, the following figure overviews the whole time-frequency-modal relationship. The system can be described as a physical system or in terms of an analytical representation of that system. If we consider the response of the system due to some excitation such as an impact, then we see that we can measure the response in either the time domain or the frequency domain. If we look at the time domain response at the tip of the beam, we see that the total response is made up of the sum of a set of damped exponentially decaying sine waves due to mode 1, mode 2 and mode 3. In the frequency domain, we see that the total frequency response function is nothing more than the sum of all the single degree of freedom modal oscillators that are activated by the input excitation. We can also see that we can easily convert the response of each single degree of freedom system from the time to frequency domain and from the frequency to time domain. We can also notice that the physical model can be described in terms of its modes for mode 1, mode 2 and mode 3. If we were to make an analytical model of the system, we could decompose the coupled model in physical space into a set of single degree of freedom modal oscillators in modal space. Notice how all the time-frequency-modal information is all interrelated.





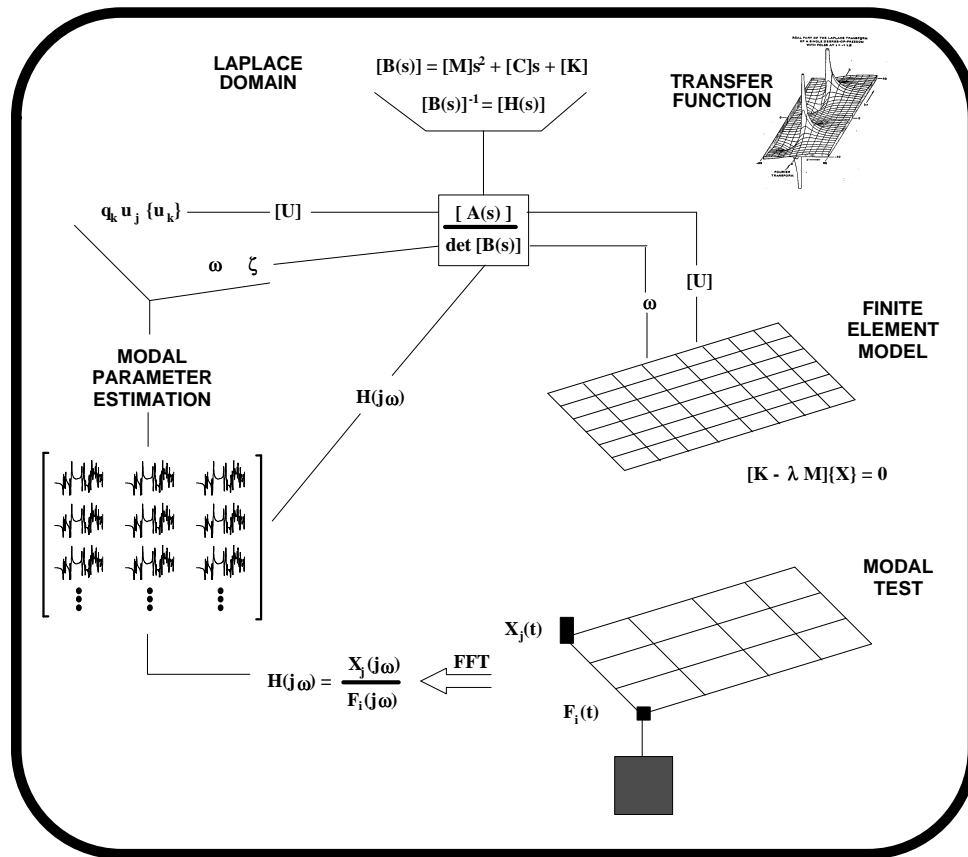


## SUMMARY

The schematic below summarizes the whole experimental modal analysis process. Let's describe some of the pieces of this schematic to re-emphasize some of the material already covered.

The finite element model is generated based on assumptions of the mass and stiffness distributions in the system. The large number of highly coupled equations are decomposed using an eigensolution technique to extract the system frequencies and mode shapes. I can also cast these same equations in the Laplace domain and formulate the system transfer function. The key to modal analysis lies in the fact that the system transfer function is the adjoint of the system matrix divided by the determinant of the system matrix which is directly related to the residues (mode shapes) and the poles (frequencies). So that the Laplace domain is nothing more than another form of the system representing the same thing as the finite element model. Now we know that we can synthesize a frequency response functions for any input-output location and in fact could generate the whole frequency response matrix. Since we know that the frequency response function is made up from the poles and residues (frequencies and mode shapes), then it seems reasonable that we should be able to extract this information backout from the frequency response function - this is referred to as Modal Parameter Estimation commonly called curvefitting. Now rather than developing frequency response functions from assumptions of the mass, damping and stiffness distributions in the Laplace domain, let's consider measuring input-output characteristics. If we measure the input force used to excite the system and measure the response of the system due to the time input excitation, then this time data can be transformed to the frequency domain and basically a ratio of output to input can be used to compute the frequency response function. Once this frequency response function and a series of frequency response functions are acquired, then we can extract the parameters of interest from the data. This sounds very simple but there are a few significant items that need to be understood and addressed. These are digital signal processing techniques, excitation considerations, and modal parameter estimation techniques all of which are discussed in the following sections.





## OVERVIEW OF ANALYTICAL AND EXPERIMENTAL MODAL ANALYSIS



## **OVERVIEW OF EXPERIMENTAL MODAL ANALYSIS USING THE FREQUENCY RESPONSE METHOD**

### **PART 2 - DIGITAL SIGNAL PROCESSING CONSIDERATIONS**

#### **INTRODUCTION**

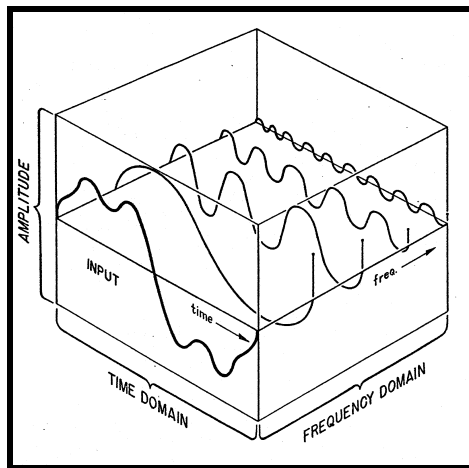
Upon reviewing the modal theory, it is evident that from the mass, damping and stiffness matrices, the system transfer relationships can be determined and that the point to point frequency response function has embedded in it the parameters of interest, namely the frequency, damping and residue or mode shape for all of the modes of the system. If the frequency response function could be measured, then mathematical procedures can be employed to extract this information from measured functions. In order to obtain these frequency response functions from an experimental standpoint, several issues relating to digital signal processing must be addressed.



## Digital Signal Processing Concepts

### Time and Frequency Domain

Many times time domain signals are very difficult to understand. By transforming from the time domain to the frequency domain, many times a complicated signal can be more easily understood. For instance, in the figure below, the summation of four sine waves at different amplitudes and phases can be extremely difficult to interpret in the time domain. However, in the frequency domain, it is much clearer as to which frequencies have which amplitudes and phases. A Fourier series is an example of a transformation that allows a complex time representation to be characterized as a series of sine waves at different frequencies with amplitude and phase.



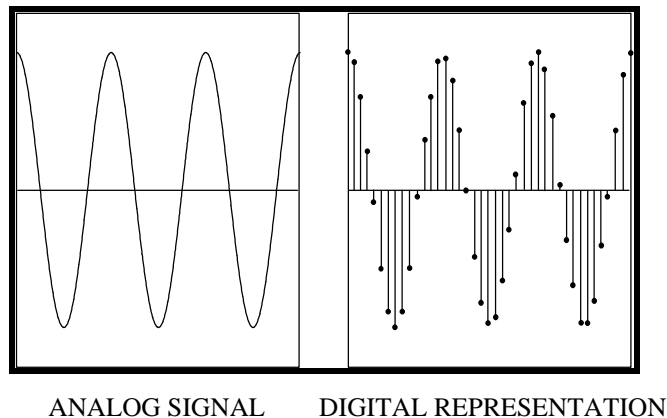
The advent of the digital computer brought the ability to digitally acquire data and then perform Fourier transforms of time data to represent it in an equivalent form in the frequency or Fourier domain. Until the introduction of the *Fast Fourier Transform* (FFT) algorithm by Cooley and Tukey, the analysis of time domain signals were limited to very special critical needs. With the efficient FFT algorithm, it became possible to analyze time signals on a routine basis. However, the digitization and capturing of time domain signals presents some new considerations that must be carefully handled, otherwise distortion of the time signals will result thereby producing erroneous results.



## Digitization of Time Signals

With analog sampling devices, only the performance of the analog instrumentation was of concern. With the use of digital signal processing (DSP) techniques, additional consideration must be given to the analog to digital conversion (ADC) process. The analog signal must be digitized and several additional items become important in order to minimize distortion of the original signal. These are *quantization*, *sampling*, *aliasing* and *leakage*.

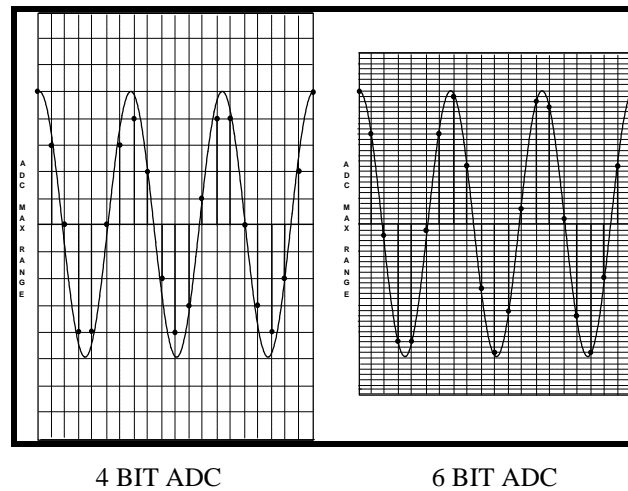
Two important parameters of digital signal processing used in converting an analog signal into a digital signal are *sampling* and *quantization*. Sampling refers to the timing at which the analog signal is sampled to form a digital signal. If a signal is not sampled at a fast enough sample rate, then higher frequency signals can alias themselves into the frequency analysis band as lower frequencies which will distort the analysis being performed. In order to prevent aliasing, most signal analyzers offer anti-aliasing filters to prevent this from occurring. Quantization refers to the accuracy by which the amplitude of an analog signal is digitized. If sufficient resolution is not available then the signal will be distorted.





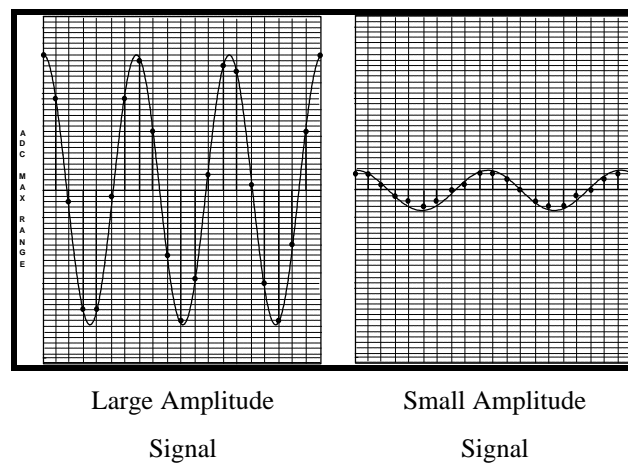
## Quantization

Depending on the number of bits in the analog to digital converter (ADC), digitization of the analog signal may cause some distortion of the actual signal. Shown below is a comparison of a 4 bit and 6 bit ADC used to measure the same sine wave to show the differences that may result in the amplitude of the signal measured.



## ADC Underload

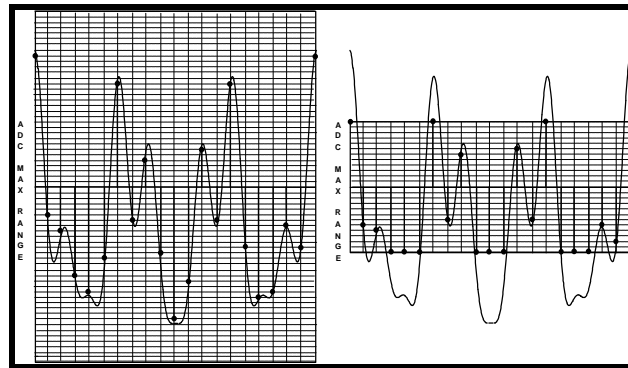
Optimization of the ADC through autoranging minimizes some of the problem but the signals with low amplitude generally still suffer from quantization error since the ADC level is set based on the largest signal amplitude and is not necessarily optimized for all of the components of the signal.





## ADC Overload

Overload of the ADC can occur if the ADC levels are not properly set. This can cause a severe distortion of the measured signal due to clipping of the measured signal.



Proper Range Setting

Overload Situation

In both the case of underload and overload, the distortion of the signal is seen in the incorrect amplitude in the frequency domain as well as the presence of other frequency components that result from the distortion of the amplitude in the time domain. The distortion is most pronounced in the severe overload clipping situation but can also be observed in the underload situation as well.



## Sampling Theory

In order to extract valid frequency information, digitization of the analog signal must occur at a certain rate.

Shannon's Sampling Theorem states

$$f_s > 2 f_{\max}$$

That is, the sampling rate must be at least twice the desired frequency to be measured. For a time record of T seconds from Rayleigh's criteria, the lowest frequency component measurable is

$$\Delta f = 1 / T$$

With these two properties above, the sampling parameters can be summarized as

$$f_{\max} = 1 / 2 \Delta t \quad \text{or} \quad \Delta t = 1 / 2 f_{\max}$$

With respect to the number of sample increments per period N

$$T = N \Delta t$$

$$BW = N \Delta f / 2$$

where

- $\Delta t$  - sample interval; time resolution
- N - # of data points
- T - sample record length
- $f_{\max}$  - highest desired frequency - BW
- $f_s$  - sampling frequency
- $\Delta f$  - frequency resolution

For example, if we choose  $\Delta f = 5 \text{ Hz}$  and  $N = 1024$ , then

$$T = 1 / \Delta f = 1 / 5 \text{ Hz} = 0.2 \text{ sec}$$

$$f_s = N \Delta f = (1024) (5 \text{ Hz}) = 5120 \text{ Hz}$$

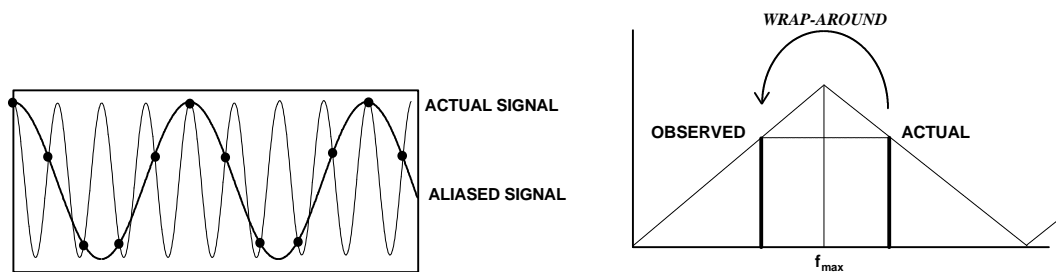
$$f_{\max} = f_s / 2 = (5120 \text{ Hz}) / 2 = 2560 \text{ Hz}$$



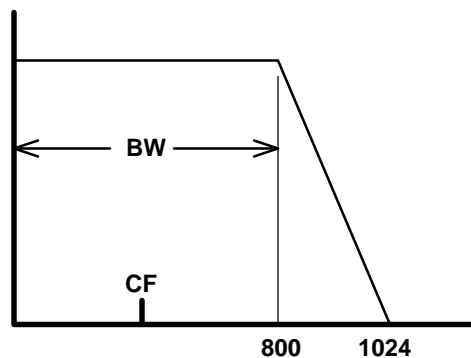
## Aliasing

*Aliasing* occurs when sampling occurs at less than twice the desired frequency. If frequency components larger than one half the sampling frequency occur in the analog time history, then both amplitude and frequency errors will result.

*Aliasing* is sometimes referred to as wrap around error because the undesired high frequency components *fold* or *wrap around* into the desired lower frequency range.



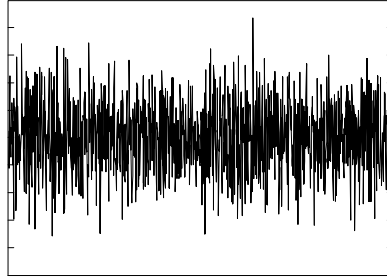
Most good FFT analyzers have anti-aliasing filters which protect against aliasing. These filters typically have a roll off rate and are not ideal. Usually only 80% of the anti-aliasing filter range is used to provide additional protection against aliasing. This is why most FFT analyzers only provide spectral resolution of 400, 800, 1600, etc. lines of resolution. Some analyzers allow the use of all of the available spectral lines of resolution of 512, 1024, 2048, etc., but the user must be cautioned that the last 20% of the frequency block may not have sufficient alias protection and should be used with care.





### What is the Fourier Transform Anyway ?

An arbitrary signal may be very difficult to interpret. For instance, the random time signal below has certain characteristics, but they are very difficult to determine from the time representation of the signal.



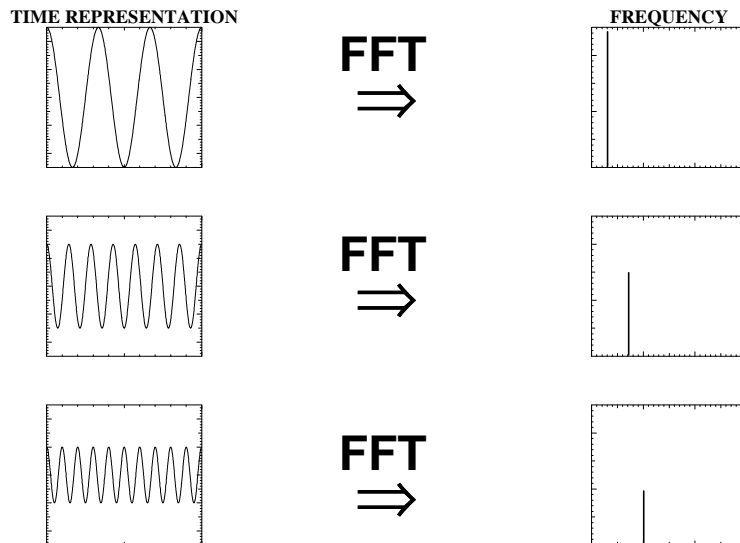
Any signal can always be broken up into a series of sine waves with different amplitudes and different frequencies. This is what **FOURIER** said and is the basis of the famous Fourier Series. By breaking up the complicated signal into its parts, certain characteristics can be seen much more clearly. For instance, we will be able to determine

- frequency content of the signal
- particular frequencies that are more predominant
- amplitude on a frequency basis

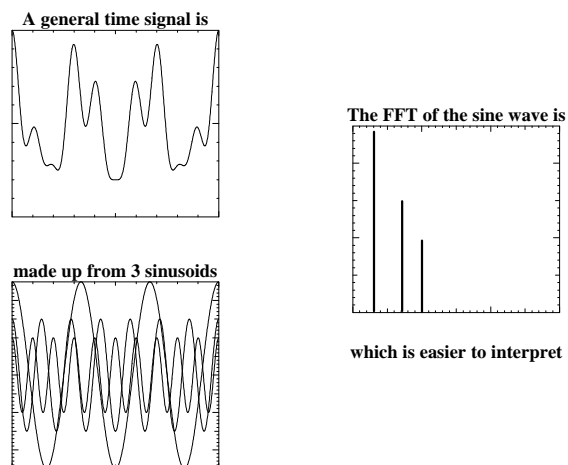
The **F**ast **F**ourier **T**ransform (**FFT**) is the Fourier Series written in discretized form with some extra restrictions.



Consider some simple sine waves at different frequencies



Considering the summation of the three sine waves above, the information is more clearly understood in the frequency domain than in the time domain as seen below.





## Fourier Transform

The discrete Fourier transform algorithm is the basis for the formulation of the frequency signal representation in most FFT analyzers available today. Since this transform is written as a continuous integral for all time, there must be some consideration given to the fact that sampled time data is recorded only for short time periods. Provided that the signal contains an integer number of sinusoids used to represent the time signal in the frequency domain or provided that the signal is totally observed in one sample record, then there is no distortion of the signal in the transformation process. If this is not true, then significant distortion of the signal may result. This distortion is referred to as *leakage* and is by far the most serious of the signal processing errors that can occur. Leakage can be minimized through the use of special excitations techniques or through the use of time weighting function referred to as *windows*.

## Fourier Transform

The transformation from time to frequency and back is given by

Forward Transform

$$S_x(f) = \int_{-\infty}^{+\infty} x(t) e^{-j2\pi ft} dt$$

Inverse Transform

$$x(t) = \int_{-\infty}^{+\infty} S_x(f) e^{j2\pi ft} df$$

## Discrete Fourier Transform

Although the actual time signal is continuous, the signal is discretized and the transformation at discrete points is

$$S_x(m\Delta f) = \int_{-\infty}^{+\infty} x(t) e^{-j2\pi m\Delta f t} dt$$

This integral is evaluated as

$$S_x(m\Delta f) \approx \Delta t \sum_{n=-\infty}^{+\infty} x(n\Delta t) e^{-j2\pi m\Delta f n\Delta t}$$

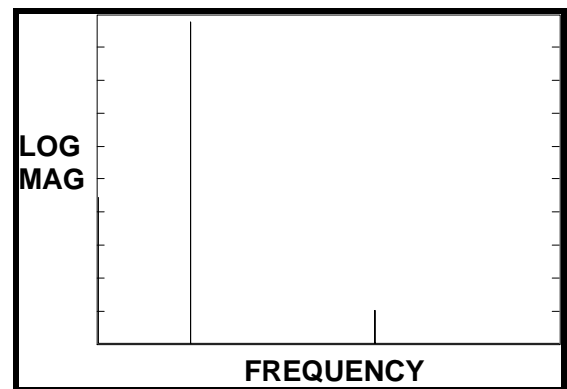
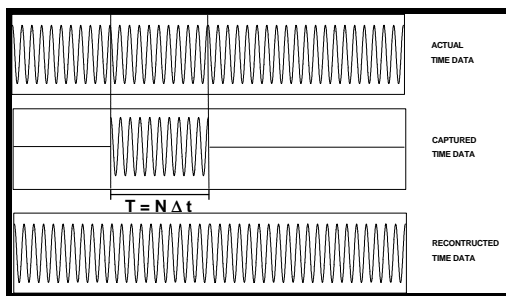
However, if only a finite sample is available (which is generally the case), then the transformation becomes

$$S_x(m\Delta f) \approx \Delta t \sum_{n=0}^{N-1} x(n\Delta t) e^{-j2\pi m\Delta f n\Delta t}$$



## FFT - Periodic Signal

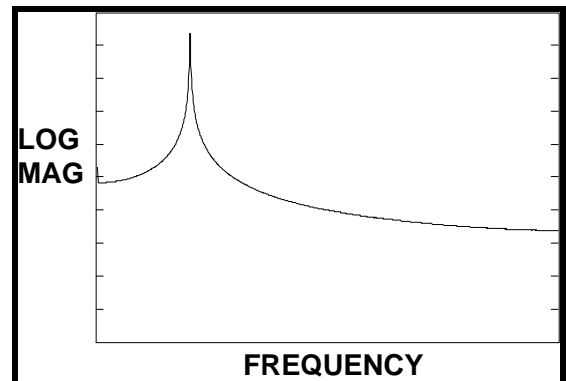
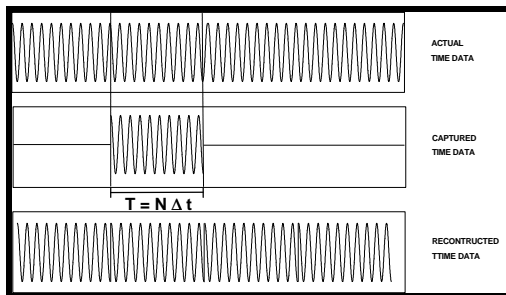
When the transformation is made from the time to the frequency domain, the mathematical representation of the Fourier series is exact provided that we know the signal from minus infinity to plus infinity. However, because we only take a sample that is  $T$  seconds long, we do not have the entire signal. Provided that the measured signal is periodic in the sample interval, then the FFT of the sampled signal produces the correct frequency representation of the observed signal. Below the actual time signal is shown along with the  $T$  sample of data. If an integer number of cycles of the signal is obtained, then the original signal can be recreated from the sample as shown in the lower time trace. The FFT of this signal correctly results in one spectral line in the time domain.





## FFT - Non Periodic Signal

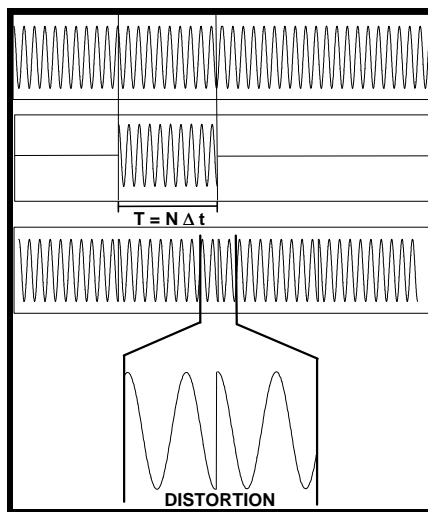
When the transformation is made from the time to the frequency domain, the mathematical representation of the Fourier series is exact provided that we know the signal from minus infinity to plus infinity. However, because we only take a sample that is  $T$  seconds long, we do not have the entire signal. If the signal is not periodic in the sample interval (does not contain  $N$  integer cycles of the signal), then errors will result in the FFT process. Below the actual time signal is shown along with the  $T$  sample of data. If we try to recreate the signal we notice a discontinuity in the lower time trace indicating that we do not have an integer number of cycles of the sine wave captured in  $T$  sample of data. If we take an FFT of this  $T$  sample of data, we do not get a single spectral line as expected due to this distortion of the time signal due to our sampling process.





## Leakage

When the measured signal is not periodic in the sample interval, incorrect estimates of the amplitude and frequency occur. This error is referred to as *leakage*. Basically, the actual energy distribution is smeared across the frequency spectrum and energy *leaks* from a particular  $\Delta f$  into adjacent  $\Delta f$ s. The time signal appears to be distorted from one time sample to the next.



Leakage is probably the most common and most serious digital signal processing error. Unlike aliasing, the effects of leakage can not be eliminated. Leakage effects can only be reduced. These effects can be reduced by

- averaging techniques
- increased frequency resolution
- use of periodic/special excitation
- use of window functions



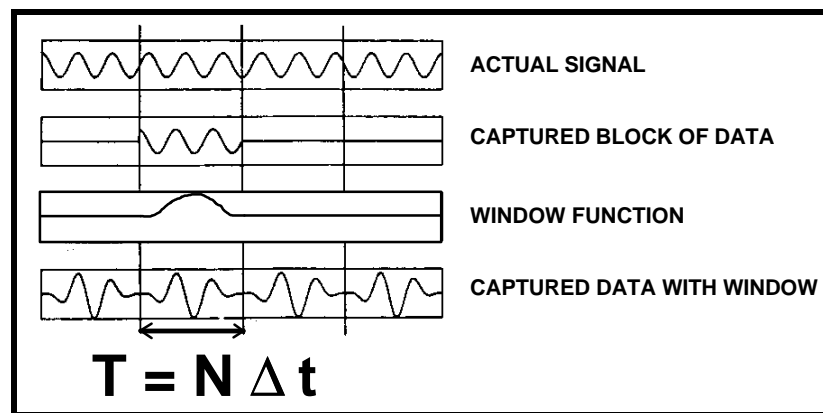
## Minimization of Leakage

A window is a weighting function that is applied to the measured signal. The function of the window is to make the measured signal appear to look more periodic in the sample interval thereby reducing the effects of leakage. There are many different windows that could potentially be used and too many to exist to list and described herein.

Several common window types used for experimental modal analysis are

- Rectangular
- Hanning
- Flat Top
- Force
- Exponential

The intended process of a general window function is shown in the four frames below.



For the most part for experimental modal applications, a hanning window is used for random signals, a flattop is used for calibration, a rectangular window is used when the signals are guaranteed to satisfy periodicity and force/exponential windows are used for impact testing.



## Windows and Leakage

Window functions typically employed for experimental modal analysis testing are Hanning, Flattop, Rectangular, Force and Exponential windows. A rectangular window (or uniform window or boxcar window) is used only when the signal is known to contain an integer number of sinusoids making up the time signal or when the captured time signal is totally observed within one sample interval of the analyzer; this is basically uniform weighting of the data. A Hanning window is normally applied for random excitations where the contents of the signal measured are completely unknown. The Hanning window offers reasonably good frequency resolution while the amplitude accuracy of the measured signal can contain as much as 16% error. The Flattop window is normally employed on signals that are sinusoidal in nature and offers measured signal amplitude accuracy to within 0.1% but lacks significant frequency resolution; generally this is a good window for calibration purposes. The Force and Exponential windows are typically employed in impulsive excitation testing; the exponential window is applied to the response of the system in an attempt to weight the time response to enforce the need to observe the entire transient within one sample interval of the analyzer.

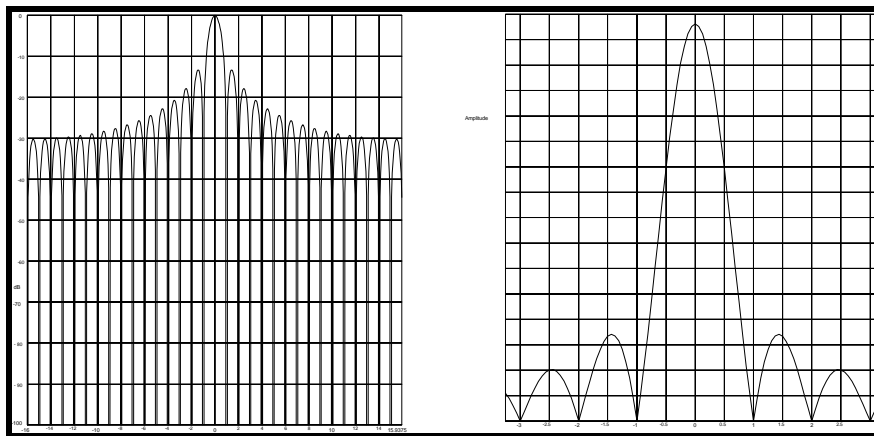
Windows, while a necessary requirement in order to minimize the signal processing error of leakage, distort the measured time data to some degree. The distortion will always appear as a loss in accuracy in the measured peak amplitude in the frequency domain and will always present the measured frequency data with a larger appearance of damping in the system.

The rectangular, Hanning and Flat Top will be described next followed by an example to show the effects of the window. Basically all windows are evaluated based on the width of the main lobe (which controls the amplitude accuracy) and the roll off of each of the side lobes (which controls frequency discernability). For each of the windows described next, the frequency representation of the window is shown in Log Mag with  $\pm 15\Delta f$  on either side of the main lobe and also in Magnitude with  $\pm 3\Delta f$  on either side of the main lobe



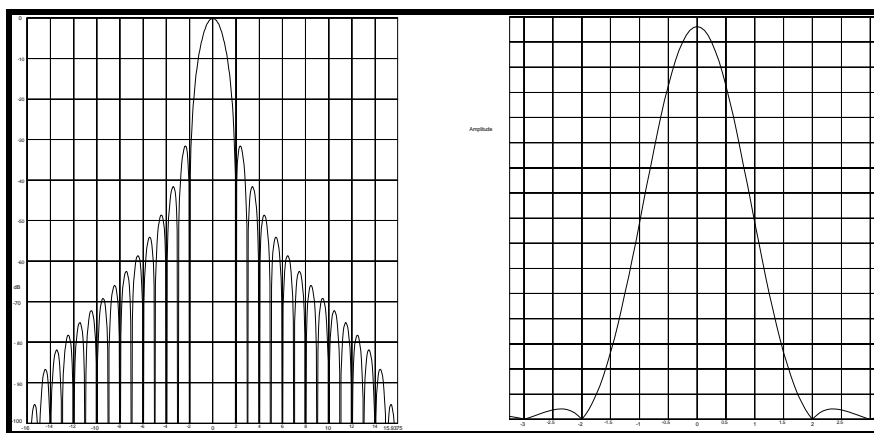
## Rectangular Window

The time window shape for a rectangular window is a unity gain for the entire  $T$  seconds of data to acquire the signal. The rectangular window is also referred to as a box car, uniform window or no window. The rectangular window function is shown below. The main lobe is narrow, but the side lobes are very large and roll off quite slowly. The main lobe is quite rounded and can introduce large measurement errors. The rectangular window can have amplitude errors as large as 36%.



## Hanning Window

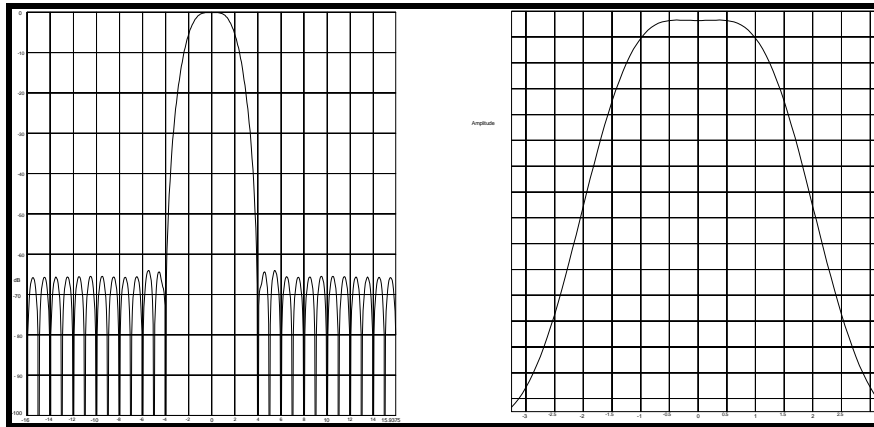
The time representation of the hanning window is a half cosine curve. The hanning window function is shown below. The first few side lobes are rather large, but a 60 dB/octave roll-off rate is helpful. This window is most useful for searching operations where good frequency resolution is needed, but amplitude accuracy is not important; the hanning window will attenuate the signal by as much as 1.5 dB (16%).





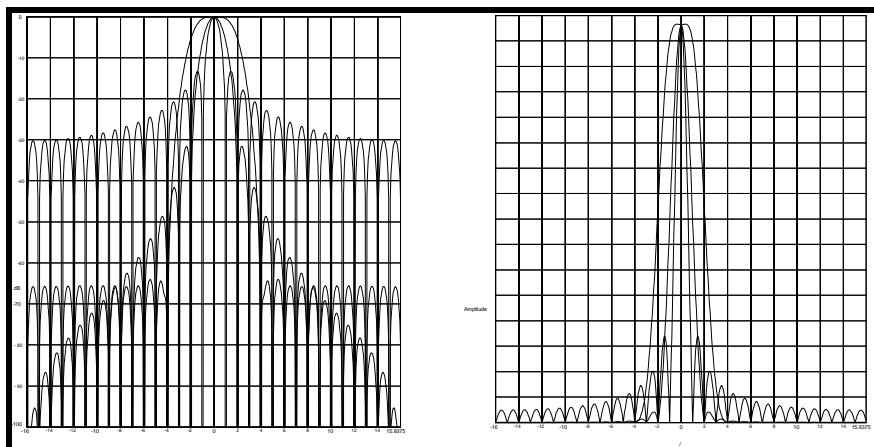
## Flat Top Window

The time representation of the Flat Top or P301 window is a series of 4 sine waves with the following coefficients ... The flat top window function is shown below. The main lobe is very flat and spreads over several frequency bins. While this window suffers from frequency resolution, the amplitude can be measured very accurately with less than 0.1% error.



## Comparison of Rectangular, Hanning and Flat-Top Window

An overlay plot is shown for the comparison of the Rectangular, Hanning and Flat-Top windows are shown below. Notice how the rectangular window has very little rolloff of the side lobes when compared to the Hanning and Flat-Top windows.



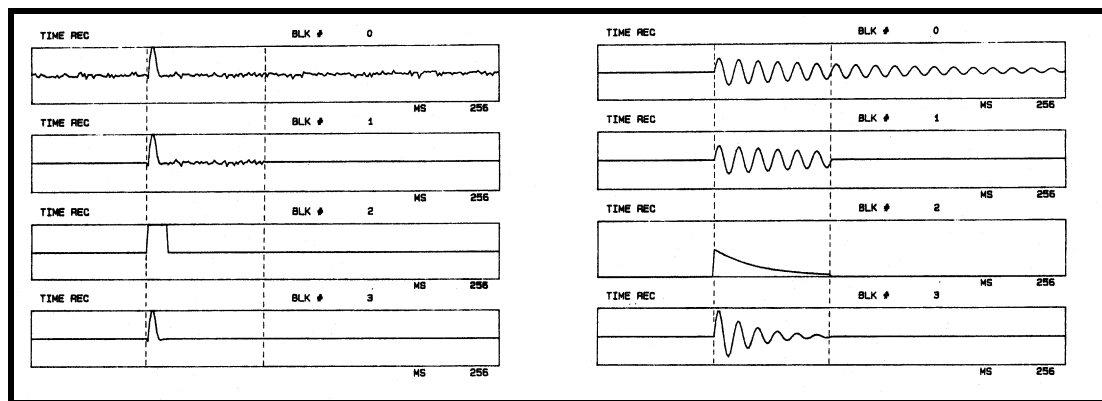


## Force Window

In many applications, measurements are acquired through impact tests. When acquiring data in this fashion, noise may be present on the input channel and the use of a hanning or flat top window is not appropriate for this type of signal. The force window is a unit amplitude window over a specified portion of the sample interval and zero over the balance of the sample interval. The force window is an effective mechanism for reducing noise on the input channel for an impulsive type of excitation.

## Exponential Window

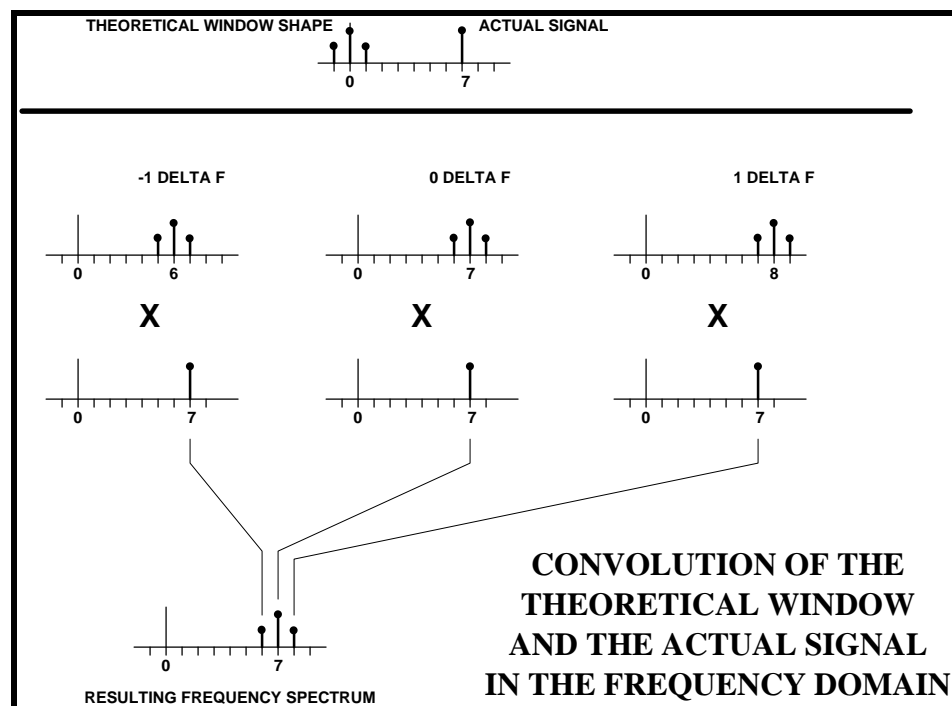
In many applications where impact excitation is used, the response of the system is the summation of damped sine waves. As in the case of the excitation force, a hanning or flat top window is not appropriate for this type of signal. An exponential window can be used to force the response of the system to be periodic within the sample interval. There are instances when the time sample is long enough to allow the system to naturally decay within the sample interval. In this case there is no reason to apply any window. A signal that has this characteristic is referred to a *self-windowing* function.





## Convolution of the Window in the Frequency Domain

While windows are applied in the time domain by multiplying the actual captured time signal by the window time shape, the effects of the window can be more clearly seen in the frequency domain. In the frequency domain, the window line shape is actually convolved with the actual signal in the frequency domain. These effects are shown simply in the figure below where a 3 spectral line window shape is shown with a single discrete sine wave.





### **Example of a Periodic Sine Wave with Rectangular/Hanning/Flat Top Windows**

As an example of the effects of windows, a signal which is known to be periodic in the sample window of the analyzer is evaluated with a rectangular, Hanning and Flat Top windows. A sine wave with 1 volt amplitude at 16 Hz is used.

First let's evaluate a rectangular window. The actual time signal, captured time signal and reconstruction of the time signal from the sample data is shown. The FFT analyzer is used to compute the spectrum of the input and is shown in both Mag and LogMag over the frequency range from 0 to 32 Hz. Notice that the peak amplitude of the sine wave in the frequency spectrum is 1 volt which was the actual input. Notice that only one spectral line is seen.

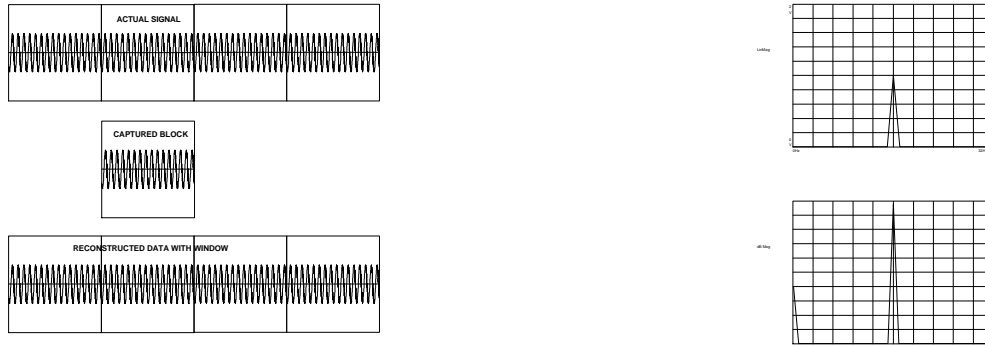
Now let's use the Hanning window. The actual time signal, captured time signal and reconstruction of the time signal from the sample data is shown. The FFT analyzer is used to compute the spectrum of the input and is shown in both Mag and LogMag over the frequency range from 0 to 32 Hz. Notice that while the amplitude of the peak of the sine wave is 1 volt, there are two side lobes at 0.5 volt each. This is the effect of the Hanning window. But since the signal was actually periodic in the sample interval, no window was actually needed and the signal is actually distorted due to the window.

Let's finally use the Flat Top window. The actual time signal, captured time signal and reconstruction of the time signal from the sample data is shown. The FFT analyzer is used to compute the spectrum of the input and is shown in both Mag and LogMag over the frequency range from 0 to 32 Hz. Notice that there are more sidelobes for this case as expected.

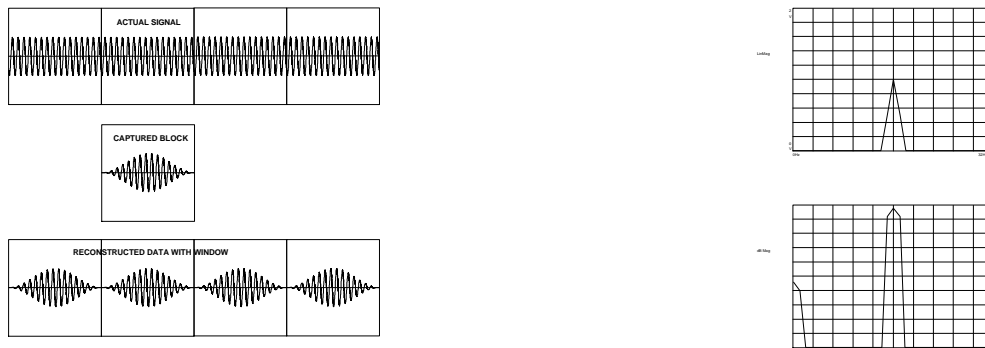


## Example of a Periodic Sine Wave with Rectangular/Hanning/Flattop Windows

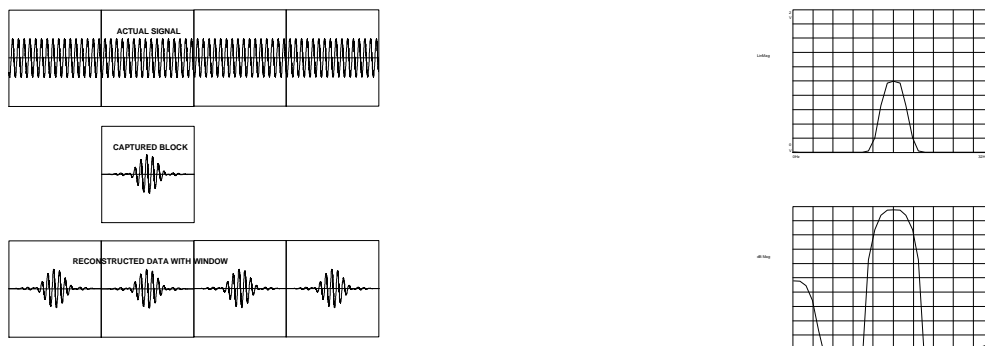
### Rectangular Window with Periodic Signal



### Hanning Window with Periodic Signal



### Flattop Window with Periodic Signal





### **Example of a Non-Periodic Sine Wave with Rectangular/Hanning/Flat Top Windows**

As a further example of the effects of windows, let's now consider a signal which is not periodic within the sample interval of the analyzer and look at the effects of using rectangular, Hanning and Flat Top windows. A sine wave with 1 volt amplitude at 16 Hz is used.

First let's evaluate a rectangular window. The actual time signal, captured time signal and reconstruction of the time signal from the sample data is shown. Right away we notice that the time signal contains a discontinuity across one record to the next in the reconstructed data. The FFT analyzer is used to compute the spectrum of the input and is shown in both Mag and LogMag over the frequency range from 0 to 32 Hz. The magnitude of the spectrum is approximately 0.64 volt which means that the amplitude is in error by approximately 36% as expected. Notice the extreme amount of leakage in the LogMag plot.

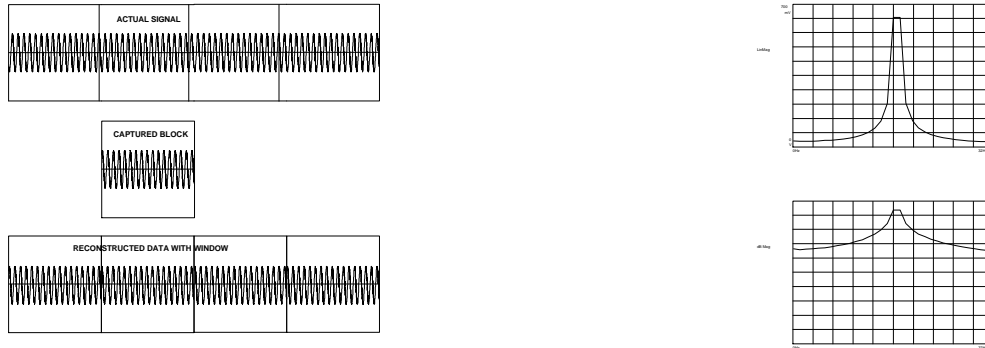
Now let's use the Hanning window. The actual time signal, captured time signal and reconstruction of the time signal from the sample data is shown. The FFT analyzer is used to compute the spectrum of the input and is shown in both Mag and LogMag over the frequency range from 0 to 32 Hz. The magnitude of the spectrum is approximately 0.85 volt which means that the amplitude is in error by approximately 15% as expected. Notice the LogMag plot shows a significant reduction in the total leakage when compared to the results with the rectangular window.

Let's finally use the Flat Top window. The actual time signal, captured time signal and reconstruction of the time signal from the sample data is shown. The FFT analyzer is used to compute the spectrum of the input and is shown in both Mag and LogMag over the frequency range from 0 to 32 Hz. The magnitude of the spectrum is approximately 0.998 volt which means that the amplitude is in error by approximately 0.1% as expected. Notice the LogMag plot shows a significant reduction in the total leakage when compared to the results with the rectangular window.

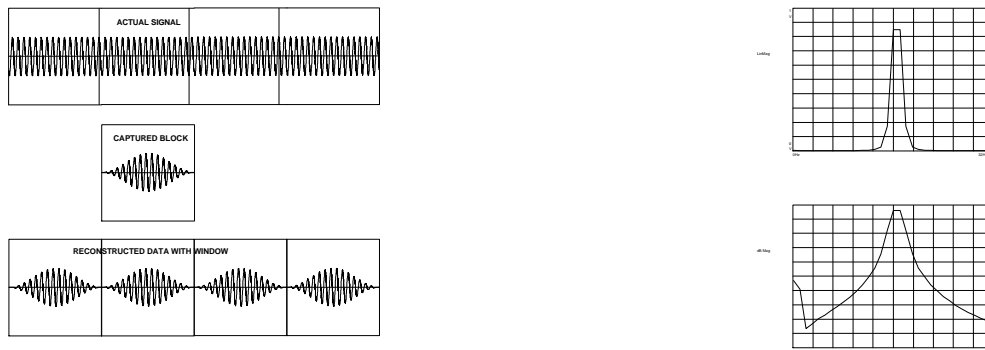


## Example of a Non-Periodic Sine Wave with Rectangular/Hanning/Flattop Windows

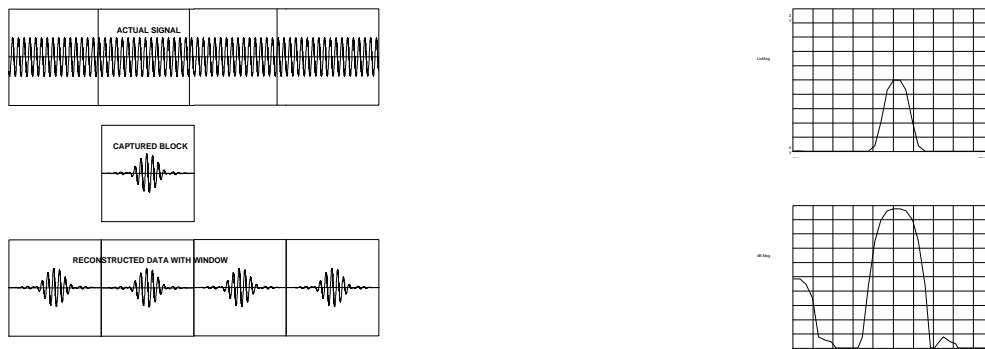
### Rectangular Window with Non-Periodic Signal



### Hanning Window with Non-Periodic Signal



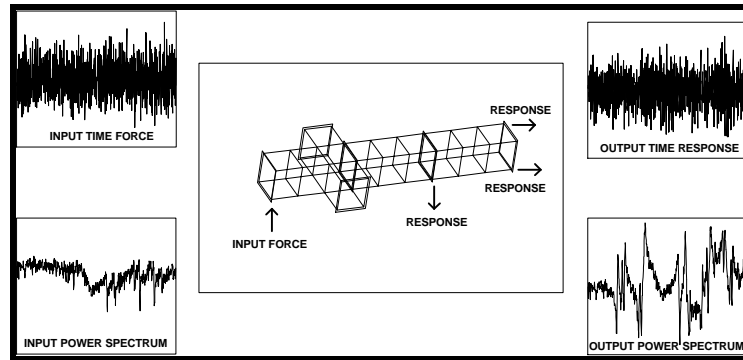
### Flattop Window with Non-Periodic Signal



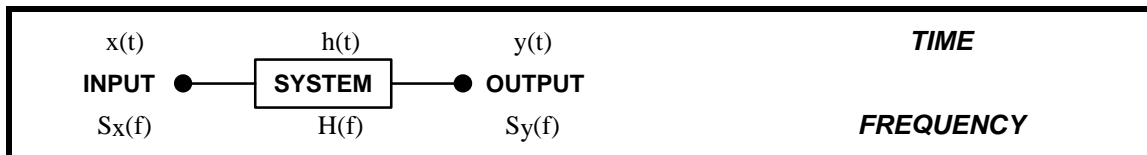


## Frequency Response Function Formulation

Several FRF formulations exist for the formulation of measured frequency response functions in the presence of noise. In all formulations of the frequency response function, if the noise is minimized then all the different forms of the measured frequency response function will approach the same value in the limit. While several approaches exist, two common approaches are identified below.



First, let's define an input-output model. If we define  $x(t)$  as the input signal and  $y(t)$  as the resulting output signal, then performing an FFT on these signals will produce



$S_x$  - linear Fourier spectrum of the input signal  $x(t)$

$S_y$  - linear Fourier spectrum of the input signal  $y(t)$

These frequency domain signals are related to the frequency response function as

$$S_y = H S_x$$

Generally, most analyzers will measure averaged power spectrum of time signals to minimize noise on the measurement. These computed power spectra are related to the linear spectra as



$G_{xx}$	- input power spectrum	- $S_x S_x^*$
$G_{yy}$	- output power spectrum	- $S_y S_y^*$
$G_{yx}$	- cross power spectrum	- $S_y S_x^*$

With these definitions, two relations can be written by post multiplying the input-output relationship by  $S_x^*$  in one case and by  $S_y^*$  in the other case to give

$$S_y S_x^* = H S_x S_x^* \Rightarrow H_1 = \frac{G_{yx}}{G_{xx}}$$

$$S_y S_y^* = H S_x S_y^* \Rightarrow H_2 = \frac{G_{yy}}{G_{xy}}$$

The first formulation of  $H$  tends to minimize noise on the output and is generally an underestimate of the measured frequency response function. The second formulation of  $H$  tends to minimize noise on the input and is generally an overestimate of the measured frequency response function. A third formulation, called  $H_V$ , is computed in a vector least squares sense and minimizes noise on both the input and output simultaneously and is a better approximation to the true  $H$  of the system.

The *coherence*, or ordinary coherence, function is defined as

$$\gamma^2 = \frac{G_{yx} G_{xy}}{G_{xx} G_{yy}} = \frac{H_1}{H_2}$$

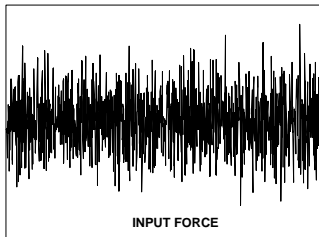
The coherence function is a scalar value which ranges between 0 and 1. When the coherence is zero, none of the output signal is coherently related to the input signal and there is no causal relationship; when the coherence is one, all of the measured output signal is coherently related to the input signal.



## Typical Measurement - Time Signal and Auto Power Functions

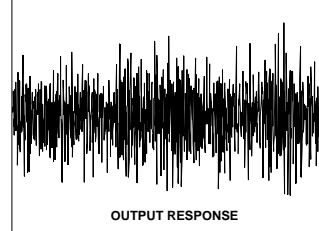
Both input and response time signals are captured in the FFT analyzer. If needed, windows are applied to the discretized data. Once this is done the signal is transformed to the frequency domain as linear Fourier spectra. These linear spectra are complex valued functions having real and imaginary part or magnitude and phase. In order to compute the auto-power spectra, the two signals are multiplied by their respective complex conjugates. Once these functions are changed from linear spectra to power spectra, the functions becomes real valued with no phase relationship.

INPUT TIME SIGNAL

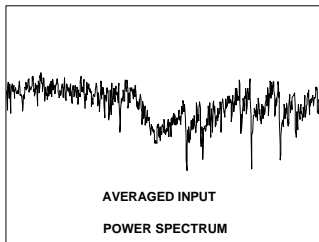


$x(t)$

RESPONSE TIME SIGNAL

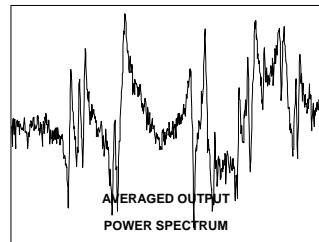


$y(t)$



$G_{xx}(f)$

INPUT POWER SPECTRUM



$G_{yy}(f)$

RESPONSE POWER SPECTRUM

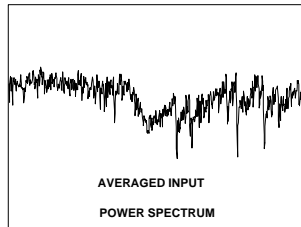


## Typical Measurement - Cross Power Function

Once the input and response linear Fourier spectra are computed, then the cross power spectrum can be computed.

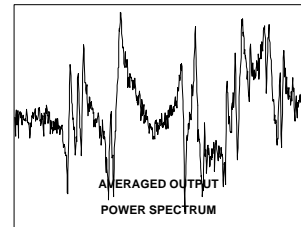
The cross power spectrum is a complex valued function having real and imaginary part or magnitude and phase

INPUT POWER SPECTRUM

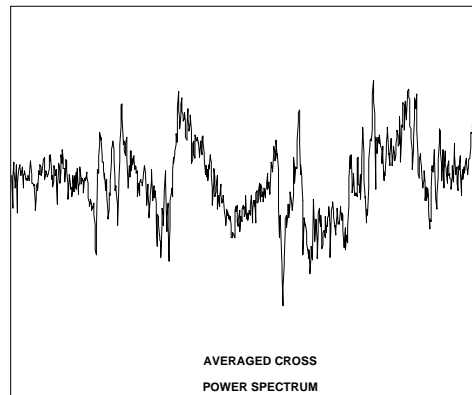


$$G_{xx}(f)$$

RESPONSE POWER SPECTRUM



$$G_{yy}(f)$$



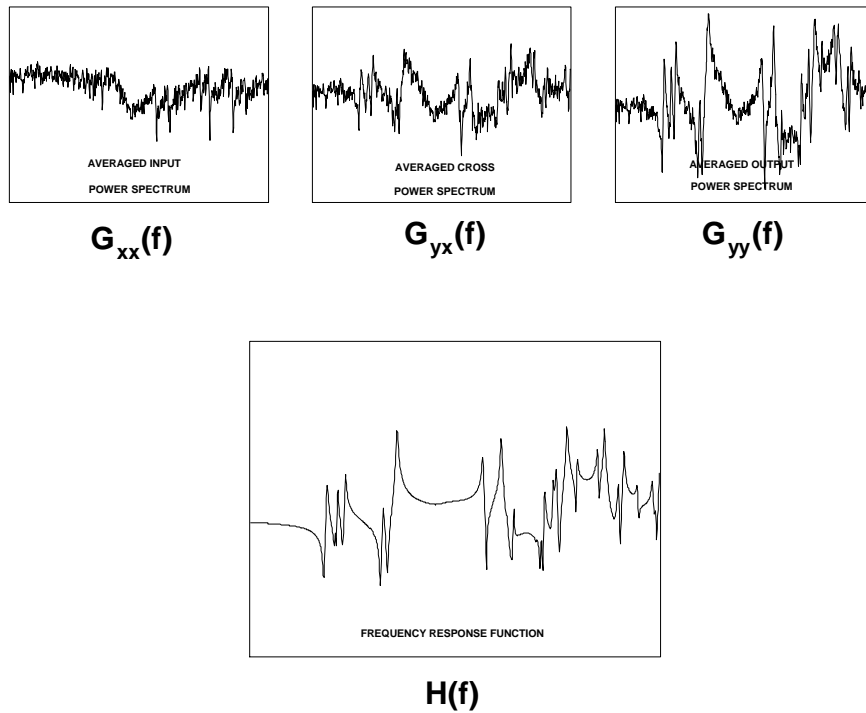
$$G_{yx}(f)$$

CROSS POWER SPECTRUM



## Typical Measurement - Frequency Response Function

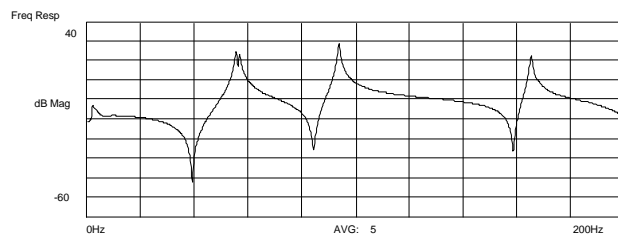
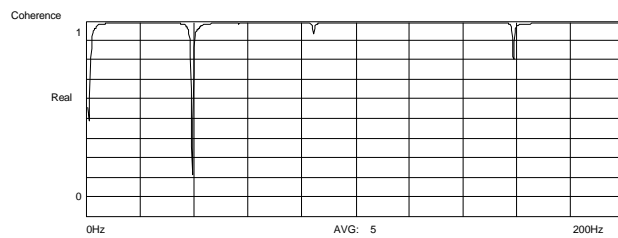
Once the input and response autopower spectra and the cross power spectrum are computed, then the frequency response function is generated from these spectra. The FRF is a complex valued function because in all of the formulations of  $H$ , the cross power spectrum is used.





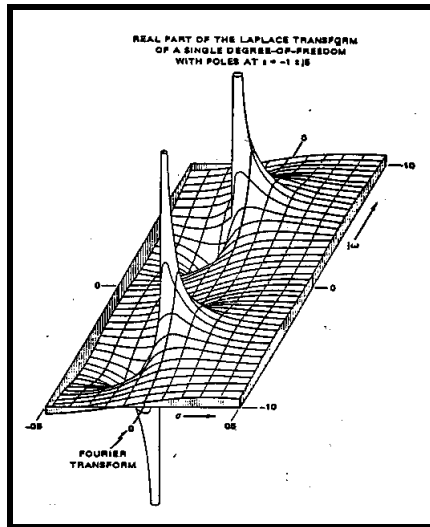
## Typical Measurement - Coherence Function

At the same time the FRF is computed,  $H$ , the coherence function is also evaluated. A typical coherence plot is shown below with the FRF. Notice that the coherence appears to be very good with values approaching 1.0. There are a few frequencies where the coherence drops most noticeably. These coherence drops occur close to anti-resonances which is not a problem since there is very little output if any at these locations. Thus it is expected for the coherence to drop here.

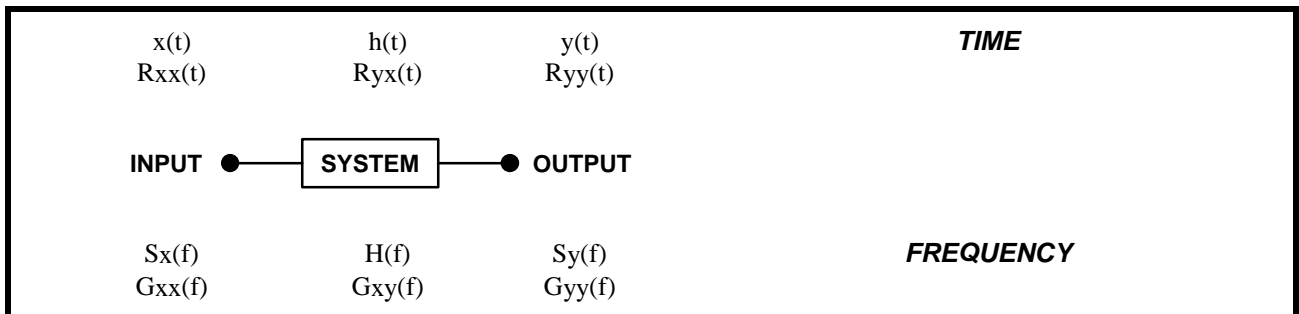




**Time and Frequency Relationship Definition** (put these in a box like a side bar to the text)



The input output model and definition of linear and square law relationships is



where

- |   |   |
|---|---|
| <ul style="list-style-type: none"> <li><math>x(t)</math> - time domain input to the system</li> <li><math>S_x(f)</math> - linear Fourier spectrum of <math>x(t)</math></li> <li><math>H(f)</math> - system transfer function</li> <li><math>R_{xx}(t)</math> - autocorrelation of the input signal <math>x(t)</math></li> <li><math>G_{xx}(f)</math> - autopower spectrum of <math>x(t)</math></li> <li><math>G_{yx}(f)</math> - cross power spectrum of <math>y(t)</math> and <math>x(t)</math></li> </ul> | <ul style="list-style-type: none"> <li><math>y(t)</math> - time domain output to the system</li> <li><math>S_y(f)</math> - linear Fourier spectrum of <math>y(t)</math></li> <li><math>h(t)</math> - system impulse response</li> <li><math>R_{yy}(t)</math> - autocorrelation of the output signal <math>y(t)</math></li> <li><math>G_{yy}(f)</math> - autopower spectrum of <math>y(t)</math></li> <li><math>R_{yx}(t)</math> - cross correlation of <math>y(t)</math> and <math>x(t)</math></li> </ul> |
|---|---|



**Time and Frequency Relationship Definition** (put these in a box like a side bar to the text)

$$x(t) = \int_{-\infty}^{+\infty} S_x(f) e^{j2\pi ft} df$$

$$S_x(f) = \int_{-\infty}^{+\infty} x(t) e^{-j2\pi ft} dt$$

$$y(t) = \int_{-\infty}^{+\infty} S_y(f) e^{j2\pi ft} df$$

$$S_y(f) = \int_{-\infty}^{+\infty} y(t) e^{-j2\pi ft} dt$$

$$h(t) = \int_{-\infty}^{+\infty} H(f) e^{j2\pi ft} df$$

$$H(f) = \int_{-\infty}^{+\infty} h(t) e^{-j2\pi ft} dt$$

$$R_{xx}(\tau) = E[x(t), x(t + \tau)] = \lim_{T \rightarrow \infty} \frac{1}{T} \int_T x(t) x(t + \tau) dt$$

$$G_{xx}(f) = \int_{-\infty}^{+\infty} R_{xx}(\tau) e^{-j2\pi ft} d\tau = S_x(f) \bullet S_x^*(f)$$

$$R_{yy}(\tau) = E[y(t), y(t + \tau)] = \lim_{T \rightarrow \infty} \frac{1}{T} \int_T y(t) y(t + \tau) dt$$

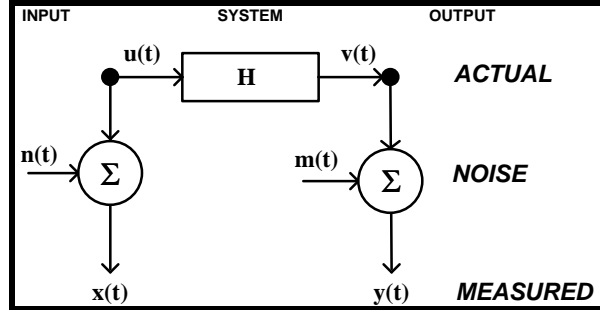
$$G_{yy}(f) = \int_{-\infty}^{+\infty} R_{yy}(\tau) e^{-j2\pi ft} d\tau = S_y(f) \bullet S_y^*(f)$$

$$R_{yx}(\tau) = E[y(t), x(t + \tau)] = \lim_{T \rightarrow \infty} \frac{1}{T} \int_T y(t) x(t + \tau) dt$$

$$G_{yx}(f) = \int_{-\infty}^{+\infty} R_{yx}(\tau) e^{-j2\pi ft} d\tau = S_y(f) \bullet S_x^*(f)$$



**Input-Output Model with Noise** (put these in a box like a side bar to the text)



Using the input-output noise model above, the formulation of H is as follows.

$$H = G_{uv} / G_{uu}$$

sensitive to noise on input  
underestimate of true H

sensitive to noise on output  
overestimate of true H

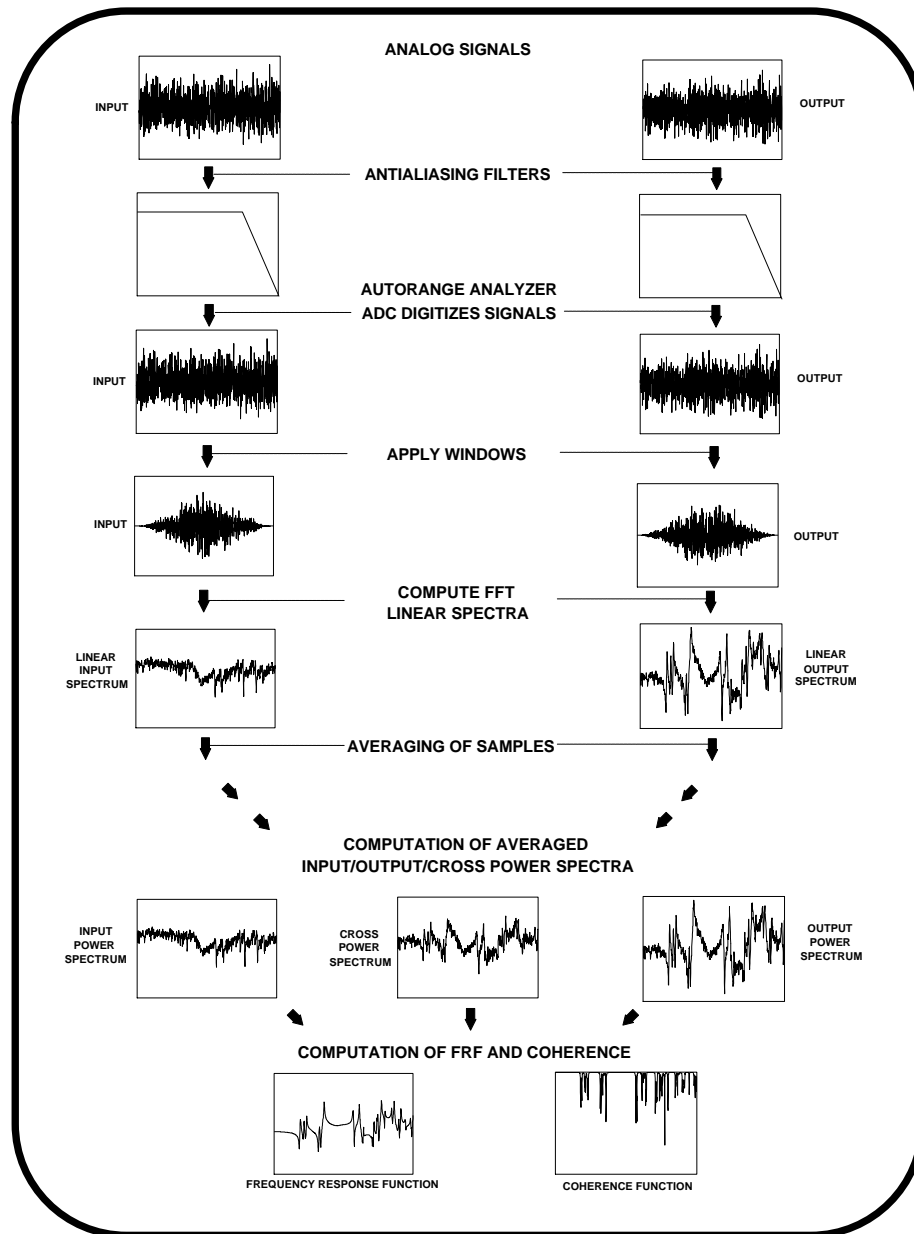
$$H_1 = H \left[ \frac{1}{1 + \frac{G_{nn}}{G_{uu}}} \right]$$

$$H_2 = H \left[ 1 + \frac{G_{mm}}{G_{vv}} \right]$$



## TYPICAL SCHEMATIC OF FFT ANALYZER OPERATION

(put these in a box like a side bar to the text)





## **H<sub>1</sub> Formulation - Output Noise Only**

Using the basic input-output model and adding noise  $S_m$  on the output, gives

$$S_m + S_v = H S_u$$

Post-multiplying by the conjugate of the input spectrum  $S_u^*$ , gives

$$(S_m + S_v) S_u^* = H_1 S_u S_u^*$$

$$S_m S_u^* + S_v S_u^* = H_1 S_u S_u^*$$

If the output noise is incoherent with input signal (uncorrelated), then  $S_m S_u^* = 0$  as more averages are taken. Then the following can be written

$$H_1 = S_v S_u^* / S_u S_u^* = G_{uv} / G_{uu}$$

## **H<sub>2</sub> Formulation - Output Noise Only**

Using the basic input-output model and adding noise  $S_m$  on the output, gives

$$S_m + S_v = H S_u$$

Post-multiplying by the conjugate of the output spectrum  $(S_m^* + S_v^*)$ , gives

$$(S_m + S_v) (S_m^* + S_v^*) = H_2 S_u (S_m^* + S_v^*)$$

$$S_m S_m^* + S_v S_v^* + S_v S_m^* + S_m S_v^* = H_2 S_u S_m^* + H_2 S_u S_v^*$$

If the output noise is incoherent with input and output signal (uncorrelated), then as more averages are taken, the following can be written

$$S_m S_m^* + S_v S_v^* = H_2 S_u S_v^*$$

$$G_{mm} + G_{vv} = H_2 G_{uv}$$

$$H_2 = (G_{mm} + G_{vv}) / G_{uv} = H + G_{mm} / G_{uv}$$

$$H_2 = H (1 + G_{mm} / G_{vv})$$



## **H<sub>1</sub> Formulation - Input Noise Only**

Using the basic input-output model and adding noise  $S_n$  on the input, gives

$$S_v = H (S_u + S_n)$$

Post-multiplying by the conjugate of the input spectrum ( $S_u^* + S_n^*$ ), gives

$$S_v (S_u^* + S_n^*) = H_1 (S_u + S_n) (S_u^* + S_n^*)$$

$$S_v S_u^* + S_v S_n^* = H_1 (S_u S_u^* + S_n S_n^* + S_n S_u^* + S_u S_n^*)$$

If the input noise is incoherent with input and output signal (uncorrelated), then as more averages are taken, the following can be written

$$S_v S_u^* = H_1 (S_u S_u^* + S_n S_n^*)$$

$$G_{vu} = H_1 (G_{uu} + G_{nn})$$

$$H_1 = G_{uv} / (G_{uu} + G_{nn}) = (G_{uv} / G_{uu}) / (1 + G_{nn} / G_{uu})$$

$$H_1 = H / (1 + G_{nn} / G_{uu})$$

## **H<sub>2</sub> Formulation - Input Noise Only**

Using the basic input-output model and adding noise  $S_n$  on the input, gives

$$S_v = H (S_u + S_n)$$

Post-multiplying by the conjugate of the output spectrum  $S_v^*$ , gives

$$S_v S_v^* = H_2 (S_u + S_n) S_v^*$$

$$S_v S_v^* = H_2 (S_u S_v^* + S_n S_v^*)$$

If the input noise is incoherent with input and output signal (uncorrelated), then as more averages are taken, the following can be written

$$H_2 = G_{vv} / G_{uv}$$



## Coherence - Output Noise

Using the basic input-output coherence model and adding noise  $S_m$  on the output, gives

$$\gamma^2 = (G_{yx}^2) / G_{xx} G_{yy}$$

$$\gamma^2 = (H G_{uu})^2 / [(S_u S_u^*) (S_v + S_m) (S_v^* + S_m^*)]$$

$$\gamma^2 = (H G_{uu})^2 / [(G_{uu}) (S_v S_v^* + S_m S_m^* + S_m S_v^* + S_v S_m^*)]$$

As more averages are taken, the following can be written

$$\gamma^2 = (H^2 G_{uu}^2) / [(G_{uu}) (G_{vv} + G_{mm})]$$

Recalling that

$$H^2 = G_{vv} / G_{uu} \quad (\text{since } S_v = H S_u)$$

the following can be written

$$\gamma^2 = G_{vv} / (G_{vv} + G_{mm})$$

$$\gamma^2 = 1 / (1 + G_{mm}/G_{vv})$$

## SUMMARY

Digital signal processing concepts were reviewed. Digitization, aliasing, quantization, sampling, and aliasing of measured signals were reviewed. The concept of leakage and the use of weighting functions (windows) was described. Different techniques for estimation of frequency response functions were discussed.



## **OVERVIEW OF EXPERIMENTAL MODAL ANALYSIS USING THE FREQUENCY RESPONSE METHOD**

### **PART 3 - EXCITATION TECHNIQUES**

#### **INTRODUCTION**

From the development of general modal theory, it is clear that measured frequency response functions are needed in order to extract a modal model. Several alternatives exist for exciting a structure to measure response characteristics. However, in order to obtain a set of calibrated measurements, the response of the system due to an applied known input force is required. This limits the type of excitation that can be used for obtaining frequency response functions. Generally, two categories of applied forcing functions are used for experimental modal testing - impact and shaker excitation. While there are numerous other types of excitation, generally they do not provide a known or measured input force. Therefore the discussions here will be limited to impact and shaker excitation methods.

The most common of the impact techniques involves the use of an impact hammer that is fitted with a force transducer at the head with a variety of tips that can be used to impart impulsive type of excitation to the structure. In regards to shaker testing, there are several commonly used techniques for the development of an experimental modal model using force shakers. The force inputs to the system can have two general categories of classification - random or deterministic. Each of these categories of signals can be used to determine the character of the system - both generation of the frequency response function as well as an assessment of the linearity of the system under test.

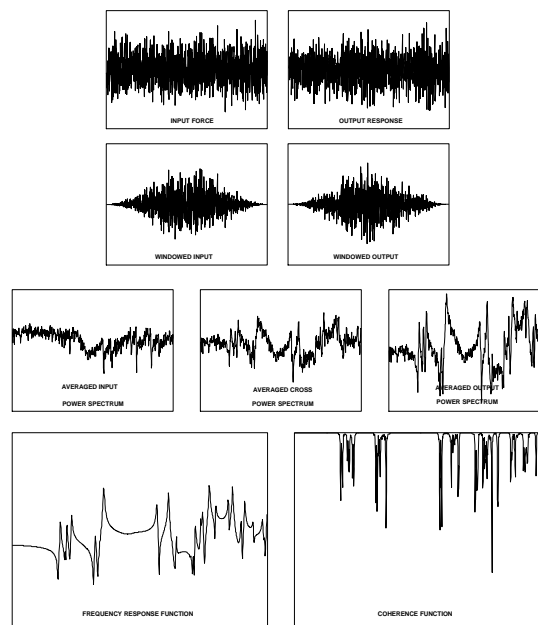
Random excitations have properties that can only be described by some statistical character of the signal. The signal can be described as having some overall level with some statistical confidence concerning the signal as time progresses. Generally, a mathematical relationship cannot be written to describe the signal at any point in time. These classification of signals generally have varying amplitude, phase and frequency content at any point in time. Some random signals commonly used in modal testing are pure random, pseudo random, periodic random, and burst random.

Deterministic signals on the other hand conform to a particular mathematical relationship and can be described exactly at any instant in time. As such, the response of the system can also be exactly defined if the system



character is known. Some deterministic signals commonly used in modal testing are swept sine, digital stepped sine and sine chirp.

As for all of the measurement techniques, the input/output signals are sampled and the time data is digitized. If necessary, these sampled signals are windowed to minimize leakage in the measured spectrum; some of the excitation techniques considered are specifically designed such that there will not be any leakage associated with the measurement process and therefore do not need a window weighting function to be applied to the signal. The resulting input power spectrum, output power spectrum and cross power spectrum are averaged in order to obtain confidence in the measured characteristic. These averaged functions are then used to compute frequency response functions. The overall measurement process is shown below for reference.



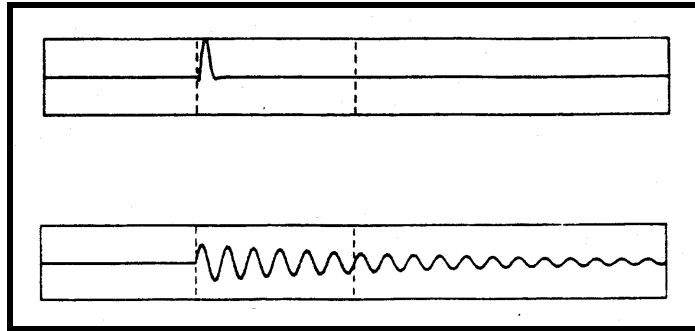
## THE OVERALL MEASUREMENT PROCESS

First we will discuss some of the aspects of impact testing and then shaker testing. Impact testing items are discussed followed by an example of some data collected on a simple structure to illustrate some key points. Shaker testing techniques are described followed by some typical data collected for a simple structure.



## IMPACT EXCITATION TECHNIQUE

Impact testing has become a very popular method of acquiring frequency response functions for experimental modal testing. The portability and simplicity of amount of equipment required lend it to be a valuable test technique for troubleshooting applications. Several issues need to be addressed concerning impact technique with regards to the input force and resulting output response of the system. A typical impact response measurement is shown below. Notice that while the input force is totally observable within one sample interval of the analyzer, the response of the system is not. This will introduce significant distortion of the signal due to leakage unless a window is used.

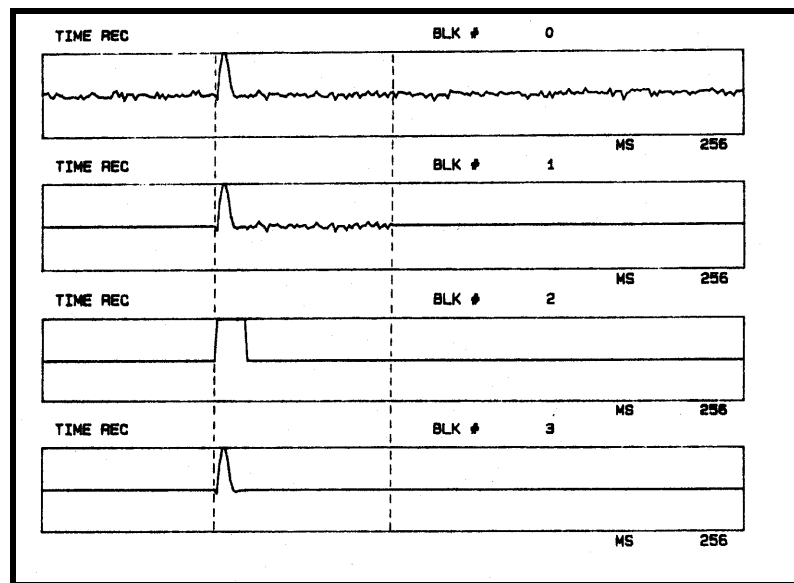


There are many items to discuss relative to impact testing. Aspects of hammer tip selection, use of force window, pretrigger delay, double impact and use of exponential response window are discussed next.



## Force Window for Impact Excitation

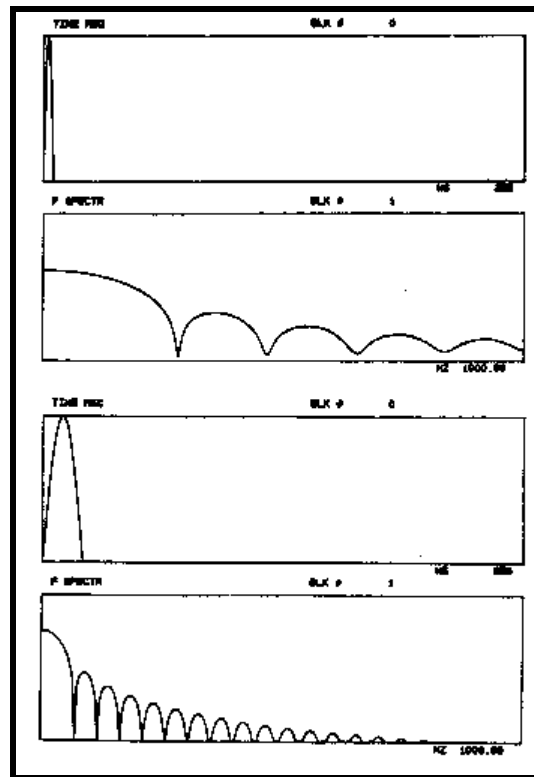
Since there may be some unwanted noise on the impact channel, the use of a force window may be needed to minimize this effect. The use of a force window is shown below. This window may be a rectangular window that exists over a portion of the block or may be a cosine wave taper on the input depending on the particular implementation. The main use of the force window is to minimize the effect of spurious noise on the input channel.





## Hammer Impact Tip Selection

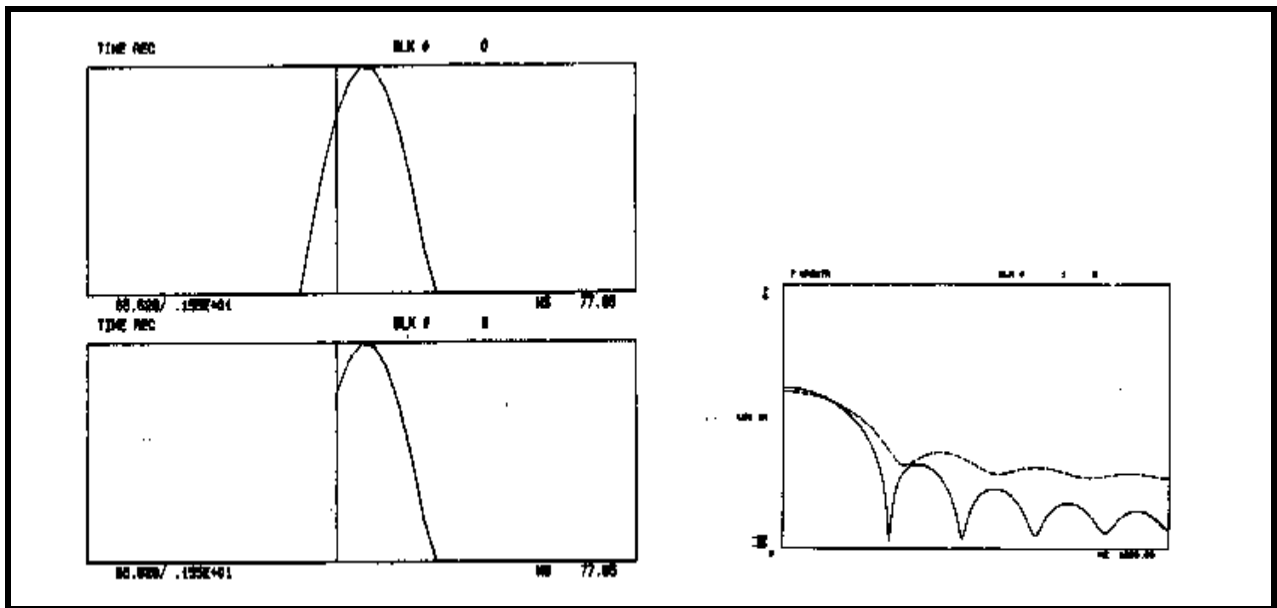
One very important area for consideration is that of the hammer tip selection. The input force spectrum frequency content is controlled by a large degree due to the length of the time pulse (time of duration of impact) applied to the system. This is controlled largely by the stiffness of the hammer tip (although the input force spectrum can at times be controlled mainly by the local flexibility of the structure under test). In general, the harder the tip, the wider the frequency spectrum that is excited; the softer the tip, the narrower the frequency spectrum that is excited. This is shown below for a hard tip time pulse and resulting frequency spectrum in the top two traces and a softer tip time pulse and resulting frequency spectrum in the lower two traces. Care must be exercised in impact testing to select the proper tip to excite the frequency range of interest.





## Pretrigger Delay

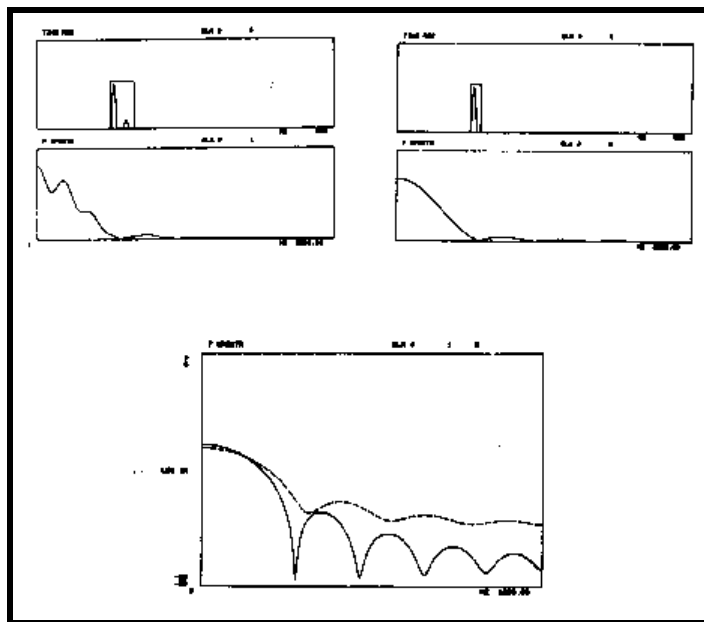
Another feature common to impact testing is the need for pretrigger delay in acquiring frequency response measurements. Since the analyzer needs to measure some voltage in order to impact, part of the impact measurement is lost if the zero time is set based on the trigger time (as depicted in the lower left trace). In actuality, the pulse that the system is exposed to can be significantly different (as depicted in the upper left trace). The resulting force spectrum can at times be substantially different (as depicted in the right trace). Pretrigger delay allows for the capturing of the entire force pulse in order to minimize any distortion that may result from this triggering problem.





## Double Impact

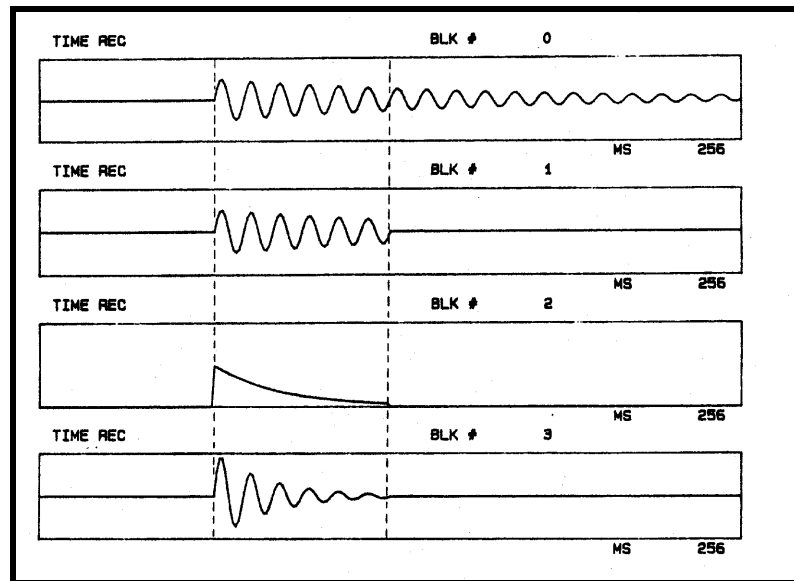
A common problem in impact testing is double impacts that often occur. Many times the double impact occurs due to improper excitation using the hammer. Other times, however, the structure may be very lightly damped and extremely responsive in certain locations. In these cases, the structure is excited with the impulsive excitation and responds such that the structure impacts the impact hammer before the hammer can be moved away from the structure. While double impacts are undesirable and should be avoided, there are situations where double impacts can not be prevented. This is only a serious situation when the resulting input force spectrum is distorted as a result of the double impact causing serious dropout of the force spectrum. However in no case should a force window be used to window out the effects of the double impact. The double impact is truly the input that is seen by the structure and the response of the system is due to all of the impacts that occur during the time sample.





## Response due to Impact

The response of the system due to the impact excitation will be the result of the damped exponential response of all of the modes that are activated by the input. For lightly damped structures, many times the response of the structure does not die out by the end of the sample interval and thus the signal is not totally observable within one sample interval. In this case leakage will be a serious concern and an exponential window may potentially be required as shown below. The use of the exponential window will minimize the effects of leakage but provides its own distortion of the signal. Two options to circumvent the need for the use of the window would be to lengthen the time block (by narrowing the bandwidth) or increasing the number of time samples to acquire data; both of these will have the effect of making the signal more observable within one sample of data and should be considered before an exponential window is used. In extremely lightly damped structures, however, this is not always possible or practical and the use of the exponential window cannot be avoided. The use of the exponential window can at times mask the presence of closely spaced modes and should be used cautiously.



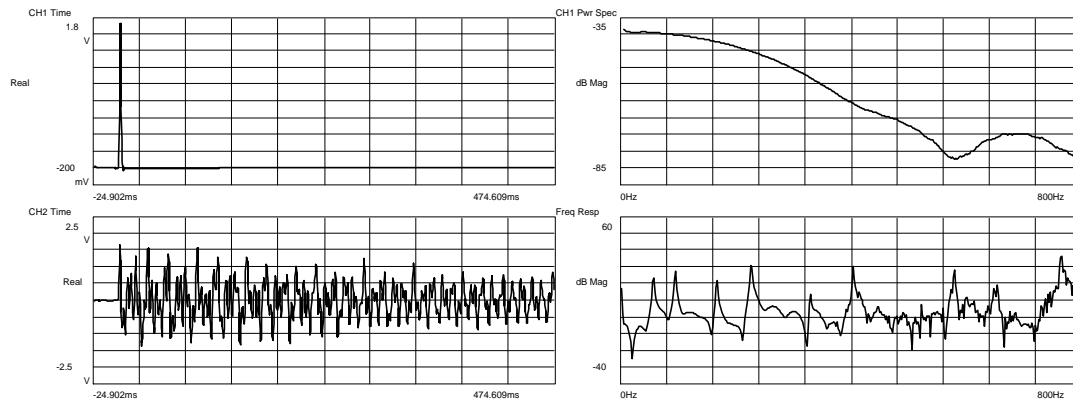


## IMPACT TESTING - AN EXAMPLE SET OF MEASUREMENTS

Now let's look at taking some measurements on a simple structure and look at the effects of different analyzer setting and their impact (no pun intended) on the resulting FRFs. We will look at frequency bandwidth, lines of resolution and different impact tips to make these measurements. (NOTE: Some of the FRFs were obtained by using HPGL output files for presentation and unfortunately suffer from some screen resolution problems.)

Now let's impact using the soft plastic tip first. We will use an 800 Hz BW with 400 spectral lines. Notice that the input is fairly sharp and that there is quite a bit of time response that does not decay by the end of the block. Clearly if no window is used then there will be leakage in this measurement.

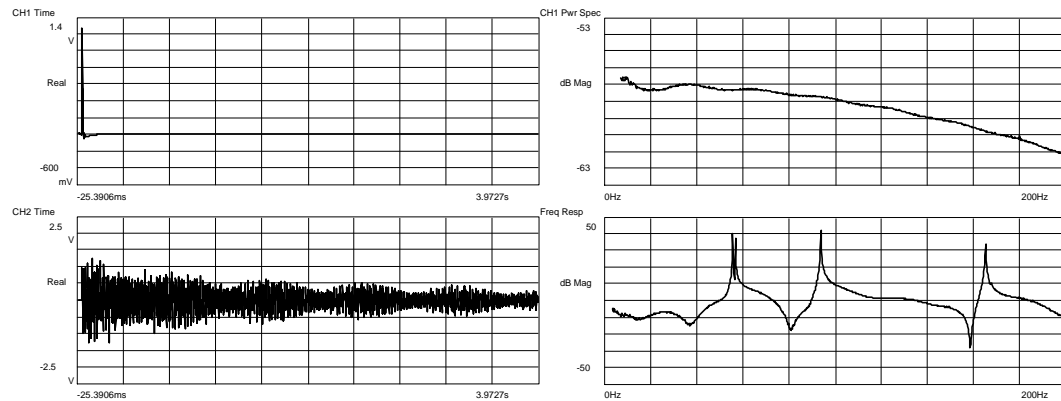
Now leakage can be seen in the measurement but I also notice at higher frequencies that the measurement does look particularly good either. This is because the input force spectrum drops off quite substantially by 400 Hz - this is due to the fact that the impact tip used does not excite this frequency range very well at all. I must select either a harder tip or a different frequency range.



Now still using the soft plastic tip, we will use a 200 Hz BW with 800 spectral lines. Notice that the input is fairly sharp and that there is quite a bit of time response. But notice that the time response tends to decay much closer to zero than in the previous case. This is because that time record is much longer than the previous case so that the time response has more time to naturally decay to zero but the signal does not decay enough to eliminate the leakage problem.



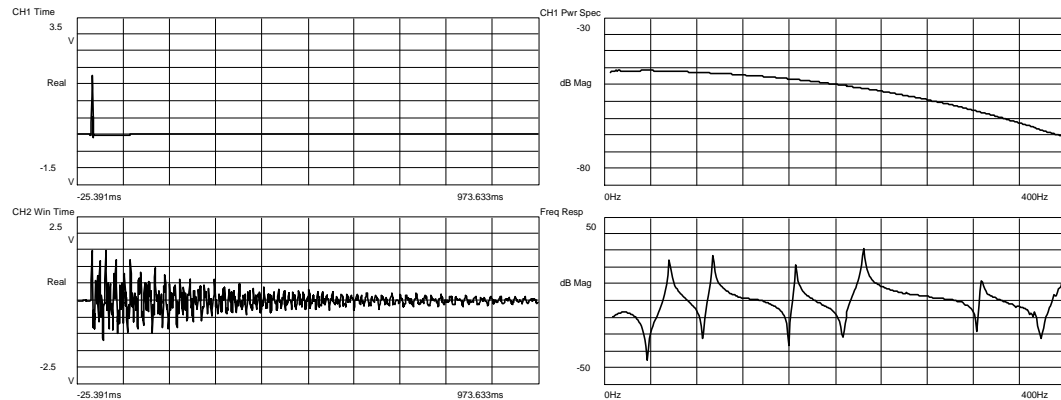
Now leakage can be seen in the measurement as a distortion of the FRF in the region at the base of the peaks of the FRF. It may not be clear just yet what a good FRF should look like so let's look at a few more parameters to change.



Now still using the soft plastic tip, we will use a 400 Hz BW with 400 spectral lines and we will now use a damping window on the time data. Notice that the input is fairly sharp and that the response seems to die out by the end of the time block. But because I now have a damping window applied to the data, you don't see the unwindowed data. We'll look at that in a moment but for now let's just realize that the signal appears to be totally observable within one sample interval of the analyzer.

Now this measurement looks fairly good. Notice that the input power spectrum is fairly flat but does have some rolloff by the end of the frequency block and I can see that the FRF also has some distortion at the end of the frequency block also. If I take a close look at the last measurement, I will notice that there appeared to be two closely spaced modes at that first frequency but I don't see them in this measurement. Let's look at this a little closer.

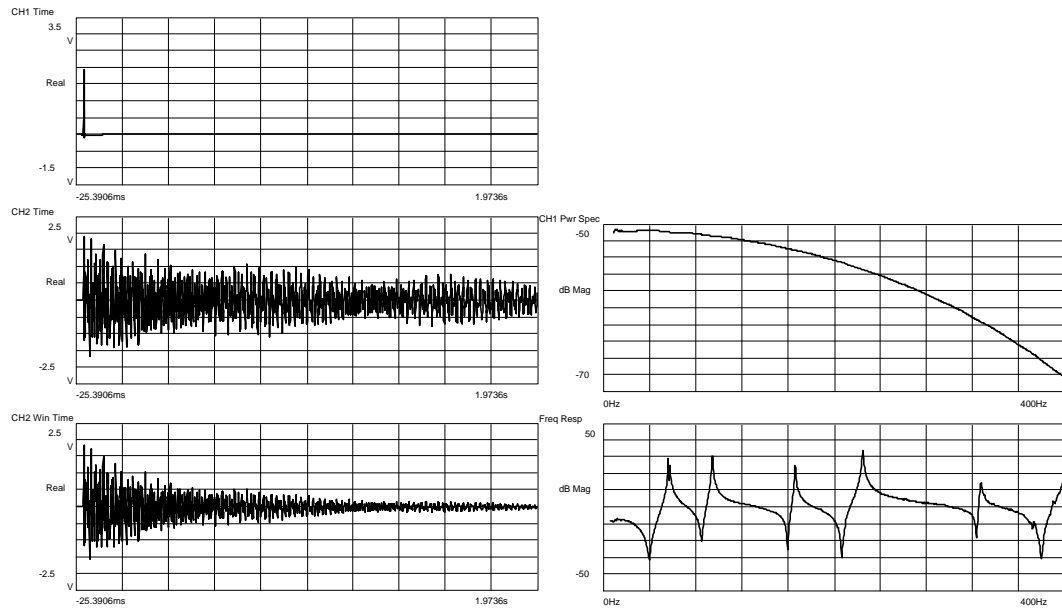




Now we are still using the soft plastic tip, but now we will use a 400 Hz BW with 800 spectral lines along with a damping window on the time data. We now see both the unwindowed time data and the windowed data so we can see what's going on. Notice that the time signal appears to be totally observable within one sample interval of the analyzer now.

Now this measurement looks fairly good. Notice that the input power spectrum is fairly flat but does have some rolloff by the end of the frequency block of approx 20dB and I can see that the FRF also has some distortion at the end of the frequency block also. Notice that there are two peaks at that first frequency now. That's because I used more lines of resolution which enabled me to use less damping window. In the last measurement I had to apply a fairly heavy damping window so I smeared the two peaks together in what looks like one peak when in fact there are two peaks. This is a very important concern when impact testing and the damping window.

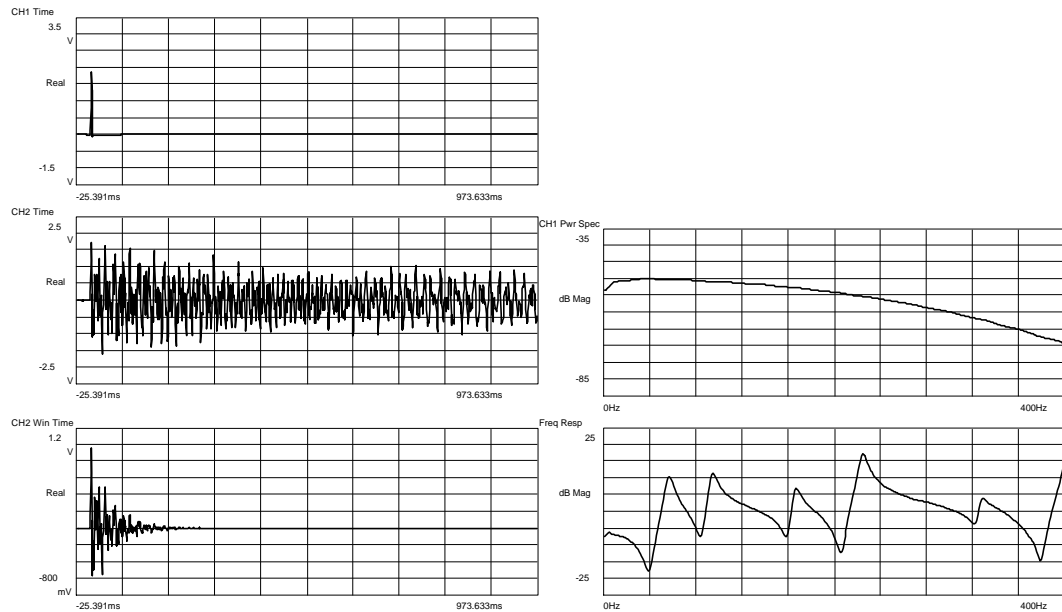




Now just to confirm what I think is happening, let's put on a very heavy damping window to see what happens. We are still using the soft plastic tip, but now we will use a 400 Hz BW with 400 spectral lines again along with a damping window on the time data. Again we see both the unwindowed time data and the windowed data so we can see what's going on. Notice that the time signal appears to be totally observable within one sample interval of the analyzer now but I also see that the damping applied to the signal is quite significant.

Now this measurement looks fairly good. Notice that the input power spectrum is fairly flat but does have some rolloff by the end of the frequency block. But I don't see those two closely spaced peaks at that first frequency. So that means that you can actually apply too much damping and you may not be able to see all of the modes of the system clearly. So what should I do when testing using impact? Generally I want to add as little damping to my system as possible - I can do this by adding more spectral lines or by changing the bandwidth. Let's do both of these next.

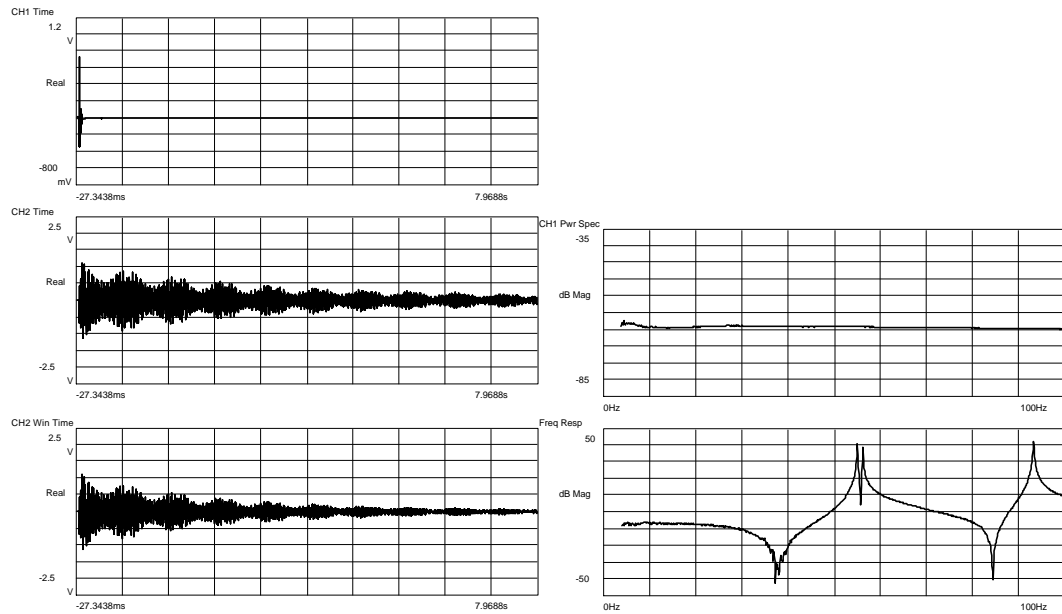




Now we are still using the soft plastic tip (I haven't changed the tip up to this point). Now we will use a 100 Hz BW with 800 spectral lines along with a very light damping window on the time data. We now see both the unwindowed time data and the windowed data so we can see what's going on. Notice that the time signal appears to be totally observable within one sample interval of the analyzer now but I do need to add a little bit of damping to the response signal.

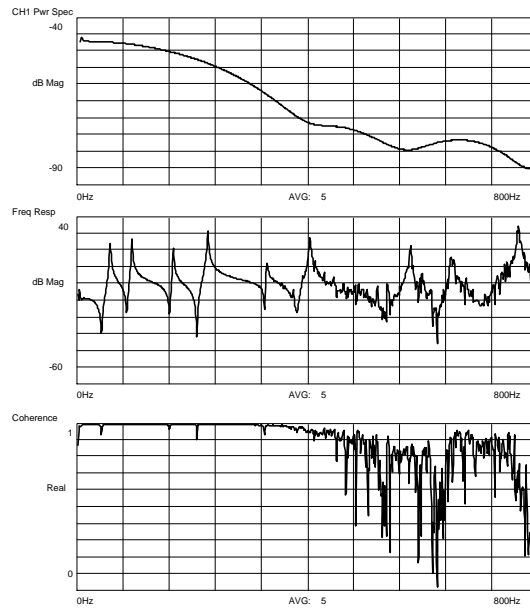
Now that FRF looks pretty good. Notice that there are two closely spaced modes in the 50 Hz range. If I wasn't paying attention to the data I may not have been able to clearly see those two modes depending on the analyzer setting that I used. You need to be very careful when taking these measurements. Now that we have a better handle on the technique, let's look at some different tips on the impact hammer.





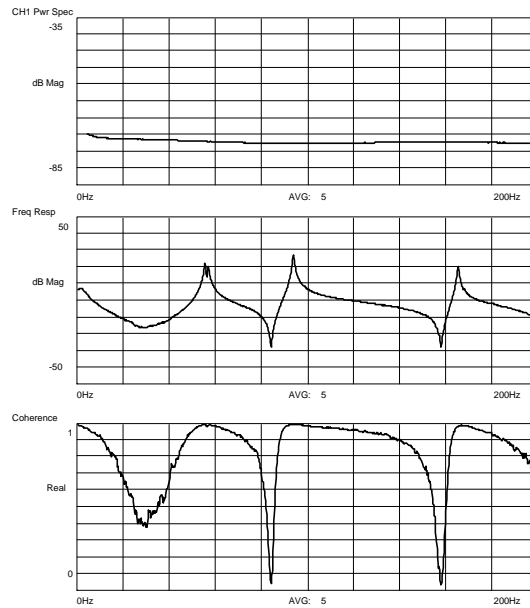
Now let's try using a soft eraser tip with a 800 Hz BW and 800 spectral lines. We will only look at the input power spectrum, FRF and coherence. Notice that the input force spectrum rolls of quite rapidly and there is not significant energy half way through the frequency range. The FRF also looks poor for the higher frequencies and if I look at the coherence function it is very obvious that the measurement does not seem adequate for the second half of the frequency block.



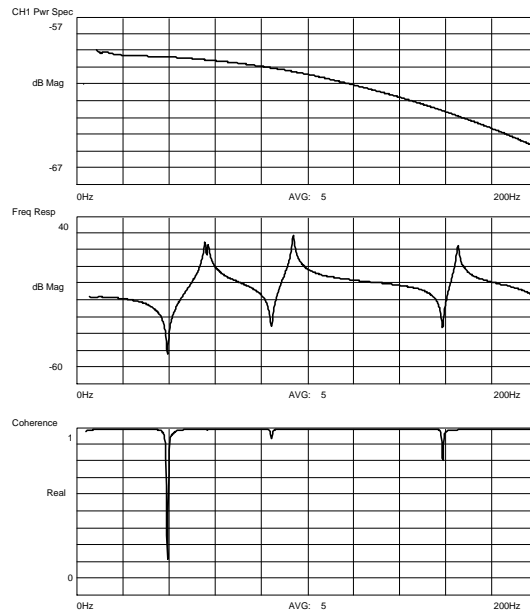


Now let's try using a hard metal tip with a 200 Hz BW and 800 spectral lines. Again I'll only show the input power spectrum, FRF and coherence. Now since I am using a hard tip I would expect a very flat input spectrum which is what I see. But the FRF and coherence don't seem to look too good. Why? Well the input certainly is flat - so flat that it excites many of modes well outside the frequency range of interest. Certainly the accelerometer measures that response and my ADC settings must be set up for that total energy that the accelerometer sees - even though I only use the energy associated with the lower frequencies. This is a quantization error here. I should always pick my hammer tip to excite just the right frequency range. Basically there is balancing act that needs to be done here - large hammer rolloff and lack of exciting modes vs. small hammer rolloff and exciting modes that aren't of interest.



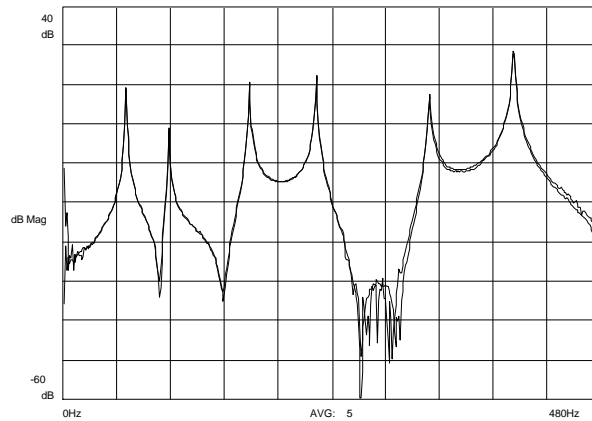


Now let's try using that soft tip again with a 200 Hz BW and 800 spectral lines. Again I'll only show the input power spectrum, FRF and coherence. Now there is slightly less than 10 dB rolloff in the input force spectrum for this condition. This is probably acceptable. The FRF is fairly good and I can see the closely spaced mode. The coherence function also looks very good with close to unity at all frequencies except some minor dropouts at the antiresonances which is expected and tolerable. This seems to be an acceptable measurement.





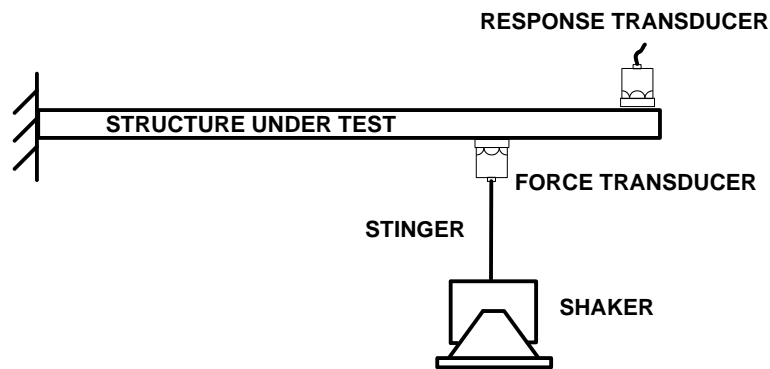
Now go back and look at all the steps we took to get to this point and all the things we did to get here. This is a typical measurement sequence that I will go through almost every time I run an impact test to make sure I don't miss anything. One last thing to check is the reciprocity of the system. The measurement below shows this check.





## HISTORICAL DEVELOPMENT OF SHAKER EXCITATION TECHNIQUES

Rather than describe each of the excitation techniques by category of deterministic vs. random, a clearer perspective can be obtained if each of the different excitation techniques is presented in chronological order as they were developed. But before we discuss the actual excitation techniques, let's describe a typical shaker test setup. A force shaker is usually attached to the structure through a long rod called a stinger or quill. This stinger is intended to transmit force only in the direction of thrust of the actuator and impose as little stiffness effect as possible in the other directions - the quill acts as a mechanical fuse. A force transducer is mounted on the structure side of the quill to measure the imparted force into the system. A response accelerometer is mounted at one or several locations on the structure to measure the frequency response function. The excitation signal is fed to the shaker system (shaker and amplifier) through the data acquisition system.



### Swept Sine Excitation

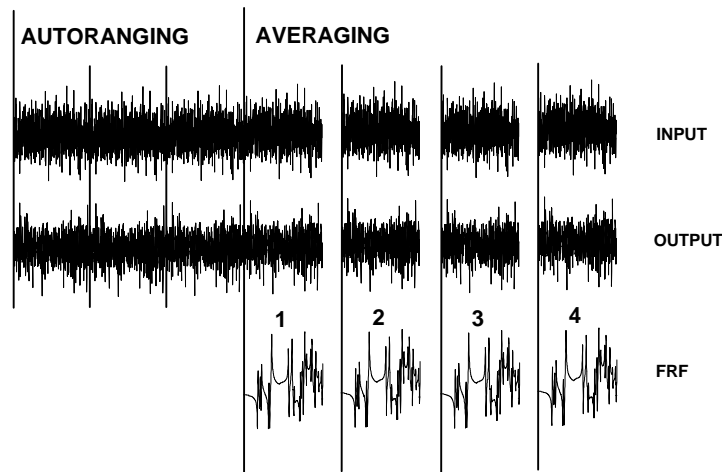
Historically, swept sine testing was used by the aerospace industry for ground vibration testing for many years. As a testing technique, it has a very long history of usage and is widely accepted by many in the industry. Basically, a sine wave is swept from a low frequency to a high frequency over a very long time. During the sweep, the output response is measured. This testing technique has very good signal to noise and overall rms levels are very good.

However, swept sine testing was developed for analog instrumentation applications and its direct application in standard form using digital signal processing techniques has some limitations. Due to the nature of the extremely slow sweep, the time for test is very long and does not take advantage of the speed and processing power of the FFT process and leakage is a very serious concern. The obvious advantages of this test technique is that the signals obtained are always very good with excellent signal to noise ratios and excellent overall rms level. Swept sine is excellent for characterizing nonlinear character of a system.



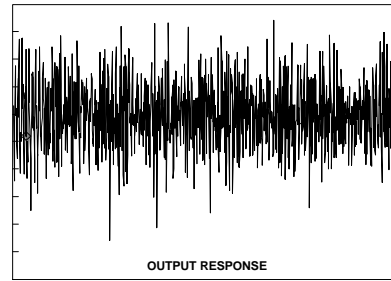
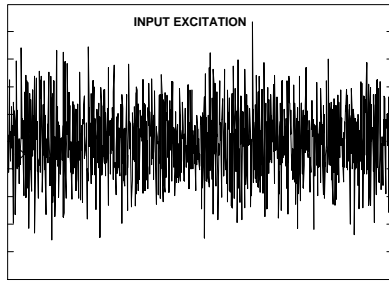
## Pure Random Excitation

One of the first shaker excitation techniques utilized for experimental modal testing was pure random excitation. Pure random excitation is a stationary, ergodic process. As such, the specific excitation cannot be defined at any instant in time but rather only statistical properties of the signal can be assessed. This signal has randomly varying amplitude and phase and is a good general purpose excitation method. The basic measurement process for acquiring frequency response functions is shown below.

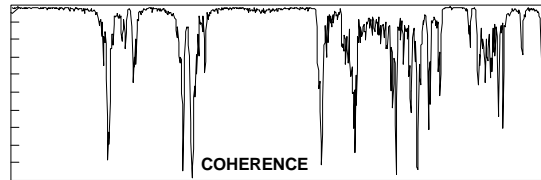


As a general test excitation technique, random was very easy to implement and was one of the first general excitation techniques used. However, a significant problem associated with a random excitation is that both the input and output response signals will always suffer from leakage. This is the most serious of all the signal processing errors associated with pure random excitation. The leakage error will cause a serious degradation of the quality of the measured frequency response function with significant error particularly at the resonant peaks of the system. The time domain input excitation and output response for a typical measurement is shown below.





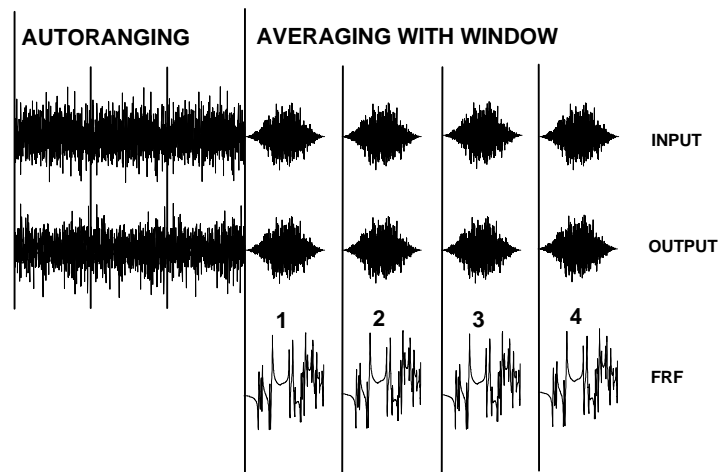
The frequency response function along with coherence for this measurement taken with pure random excitation is shown next. The coherence is poor at many frequencies and the frequency response function shows some variance on the data. This is a normal characteristic of a frequency response function acquired using pure random excitation. In general, the quality of the measurement will improve as more averages are acquired but when compared to other excitation techniques, no amount of averaging will improve the measurement to a point where pure random would be considered a viable technique for most modal testing performed today.



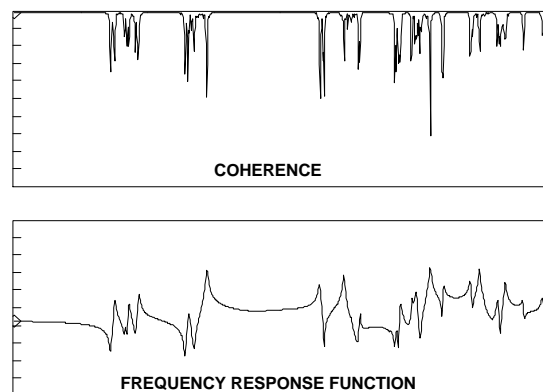


## Pure Random Excitation with Windows Applied

The data shown above was acquired with no window or weighting functions applied to the measured data. From digital signal processing consideration, a window is necessary in order to minimize the effects of this leakage phenomena. Now if a Hanning window is added to the same data, the window tends to make the signal appear to better meet the periodicity requirement of the FFT process. The measurement process is shown below for the same random excitation shown above except that a weighting function (in this case a Hanning window) was applied to the data.



The frequency response function appears much cleaner with dramatically improved coherence. While the measurement is generally much better with the use of a window on the measured data, leakage is still a concern and causes degradation of the measured frequency response function. Leakage is mostly a concern at resonances of the system.

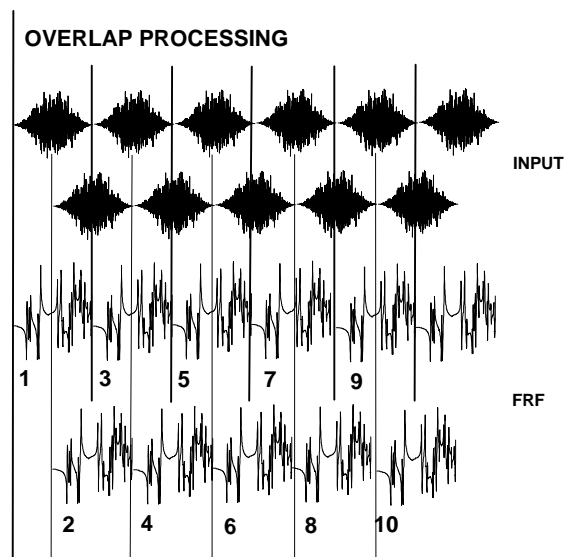




Due to the varying amplitude and phase of the input signal, generally system nonlinearities will be averaged out as more and more averages are taken. This is a very important advantage of using random excitation. Slight nonlinearities will tend to be averaged away with more averages. Due to leakage considerations and the fact that slight nonlinearities need to be averaged out of the measured frequency response function, many averages should routinely be acquired when using random excitation. This will tend to cause the test time to increase significantly.

### Pure Random Excitation with Overlap Processing

One method used to reduce test time with pure random excitations is to perform overlap processing. Since the Hanning window tends to weight the first and last quarter of the time block to zero, this data is not effectively used in the normal averaging process. Overlap processing effectively uses the portion of the block that has been heavily weighted to zero as a result of the application of the Hanning window. Overlap processing allows for almost twice as many averages with the same data when fifty percent overlap is used. The overlap process with 50% overlap is shown below to illustrate how averaged data is acquired. In this schematic, only six samples of data are acquired but with overlap processing eleven averages are computed from the measured data.





## **Pseudo Random Excitation**

Considering the leakage problem using a pure random excitation as described above, efforts were made to try to reduce the error associated with the measured frequency response function. Since the error described above is directly due to violation of the periodicity requirements of the FFT process, let's consider the development of a signal whose general characteristic does not violate the basic periodicity requirement of the FFT process.

If we look at a particular spectral line in the frequency domain and take the inverse FFT, then the resulting time response will be a sinusoid and the time signal will contain an integer number of cycles of the signal. Since this time signal does not violate the periodicity requirement of the FFT process, no windows are necessary in order to transform this signal without distortion. Now if we take a second spectral line at a different frequency and take its inverse FFT, the resulting time signal will also be a sinusoid with the same character as the previous signal described above. If these two sinusoids are added together, then the resulting time signal will also satisfy the periodicity requirement of the FFT process and no windows will be required in order to transform this data.

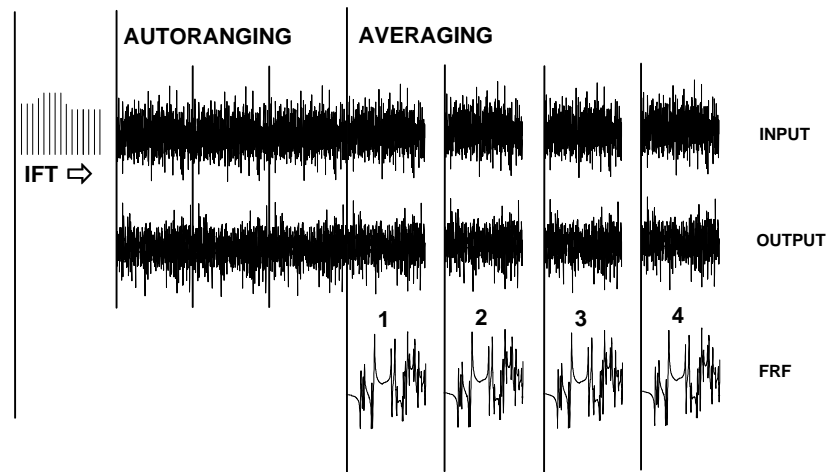
If we took each spectral line in the FFT analyzer and assigned a particular value, and an inverse FFT were taken, the resulting signal would be the summation of all the sinusoids making up the discrete spectral values of the signal in the frequency domain. The resulting time signal would look very much like a random signal but would be made up of the summation of sinusoids - this signal is referred to as a pseudo-random signal. It would also satisfy the periodicity requirement of the FFT process and no windows would be required in order to transform this data.

If this signal was used for excitation to the system, the response of the system would also satisfy the periodicity requirement of the FFT analyzer once the system reached steady state. This would occur since the response of the system is made up from basically sinusoidal response of many sinusoids. Since the basic signal would then contain an integer number of cycles of the signal over the sample interval, no window would be required on the input or output signals and leakage would not be a problem. This now eliminates one of the biggest contributors to the distortion of the measured frequency response function - leakage.

Of course, this comes with some side effects. Since the same signal is continually used as input to the system, the system will respond the exactly same way to each input block of data once steady state response is reached. Therefore, a serious disadvantage of using pseudo-random is that this excitation will not have the ability to average out any slight nonlinearities that may exist in the system. Therefore rattles and slight nonlinearities will not be averaged out of the data as more averages are acquired.



The pseudo random measurement process can be seen below. The excitation is input to the structure and the response is measured. The analyzer is set to autoranging such that optimal ADC settings can be achieved at the same time the structure is reaching steady state response. Once this is achieved, then averaging is initiated for the desired number of averages. Again it must be emphasized that the same excitation is used over and over and therefore the structural response will be the same once steady state response is achieved.



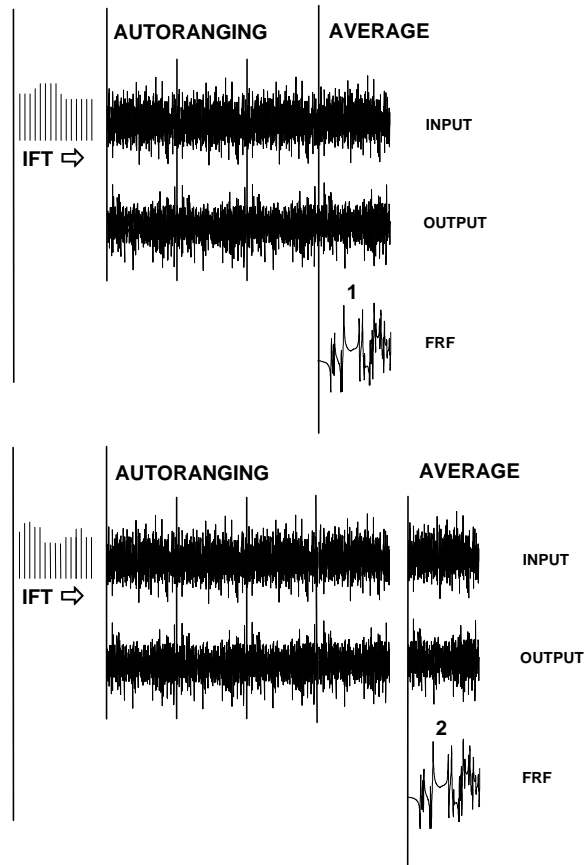
### Periodic Random Excitation

Considering the problems associated with pseudo-random excitation, further enhancements were made to this excitation technique with an excitation technique referred to as periodic random excitation. Basically, periodic random excitation is the same as pseudo random excitation except that for each measurement a new input spectrum is generated and an inverse FFT is taken to create a new time signal for each average of the measurement process. Again the signal is used to excite the system and the system is allowed to come to steady state response while the autoranging process of the acquisition is under way. Once this is achieved, then only one average is taken. At this point, another spectrum is generated (different from the first spectrum), inverse transformed to start the process again to acquire the next average of the frequency response function. In this way, each measurement will excite the structure differently and then with averaging, nonlinearities will be removed from the measurement as more and more averages are taken. As with pseudo random, no windows are necessary for this measurement process since the input excitation signals and the output response signals will all satisfy the periodicity requirement of the FFT



process. While very high quality frequency response functions are obtained from this approach, a significant amount of time and hardware is required to perform this measurement technique.

The basic measurement process for periodic random excitation is shown below.

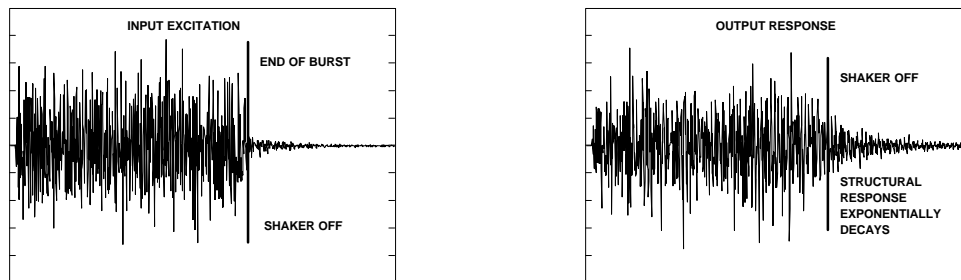




## Burst Random Excitation

Due to time and cost considerations of pseudo-random and periodic random excitation techniques, easier to implement techniques were needed in order to make the measurement of high quality frequency response functions feasible. Again realizing that the main concern was the distortion of the measure frequency response function due to leakage resulting from violation of the periodicity requirement of the FFT process, transient signals whose total duration could be observed within one sample interval of the block of data acquired were considered. One signal that offered great potential was that of burst random. Burst random excitation has become one of the more popular excitations available for experimental modal testing today. This special excitation technique offers all the advantages of random, pseudo-random and periodic random excitations without the disadvantages associated with these techniques.

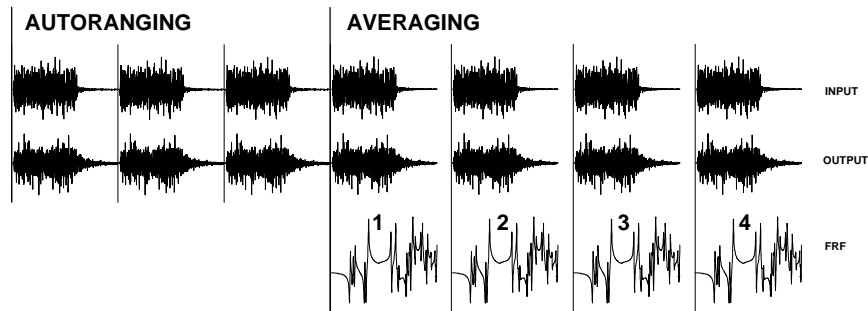
Burst random is formed as follows. A random excitation is generated but is only output for a portion of the data block. In this way, the excitation signal is totally observable within one sample interval of the FFT analyzer and there is no need for the use of windows since there is no leakage associated with the capture signal. In addition, a pretrigger delay is often used with this excitation so that there is no excitation signal within the first several time bins of the captured data.



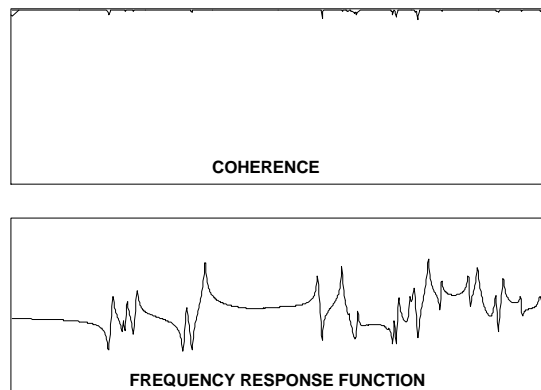
Providing that the response measured on the structure is also totally observable within one sample interval of the FFT analyzer then there is no need for the use of windows since there is no leakage associated with the captured signal. However, once the excitation is turned off, the structural response will die exponentially depending on the damping associated with the structure. If the response of the structure does not die out within one sample interval, then the burst should be shortened such that the response does end before the end of the sample interval. The burst can be controlled by specifying the percentage of the block over which the excitation is to be applied. Generally, this can be accomplished with most structures.



The burst random measurement process can be seen below. The excitation is input to the structure and the response is monitored to assure that the response dies out before the end of the sample interval. The burst length can be adjusted accordingly such that this is accomplished. During this time the analyzer can be autoranging such that optimal ADC settings can be achieved. Once this is achieved, then averaging is initiated for the desired number of averages.



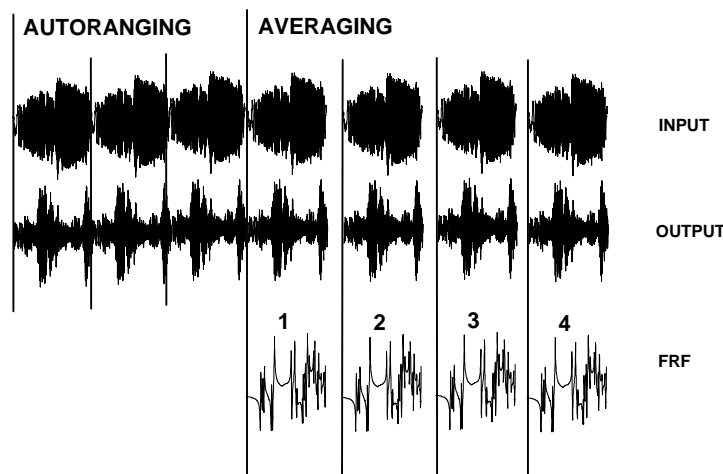
Since the basic excitation technique is comprised of a random function, all of the advantages of random excitation to linearize slight nonlinearities that exist in the data will be retained. In addition, none of the disadvantages associated with random excitation, namely leakage, are seen with burst random excitation since the transient nature of the signal prevents this from happening. The FRF and coherence functions for the measured time data are shown below and it is clearly seen that the measured FRF and coherence are greatly improved relative to the measurements previously shown that were acquired with random excitation.



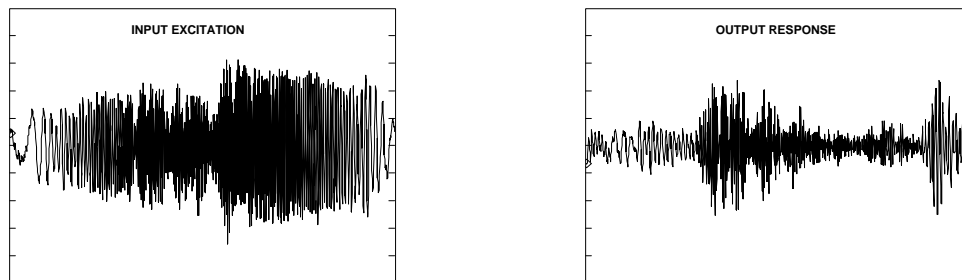


## Sine Chirp Excitation

Sine chirp excitation has become a very popular technique for efficient testing of linear structures for development of a modal model. Basically, the sine chirp is very similar to the traditional swept sine test performed for many years - the only difference is that one whole sweep of the frequency range occurs within one sample interval of the FFT analyzer. Since the input signal is totally observable from one sample of the signal, the periodicity requirement of the FFT process is not violated and no windows are required. The basic measurement process is shown below.



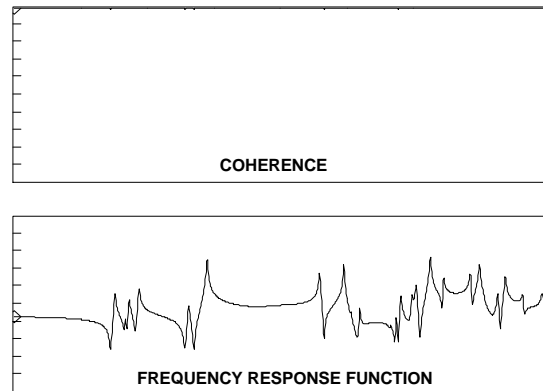
This signal is input to the structure and while the analyzer is autoranging, the system response will eventually reach steady state response. Therefore, the output response is also totally observable within one sample interval and no window is required for this excitation type.



Sine chirp provides all the advantages of traditional swept sine testing along with the speed of the FFT process. The resulting frequency response function is one of the best possible acquired measurements other than digital stepped



sine for linear systems. Also note the coherence values for this measurement. Sine chirp is also a good test technique for identifying nonlinear system character.

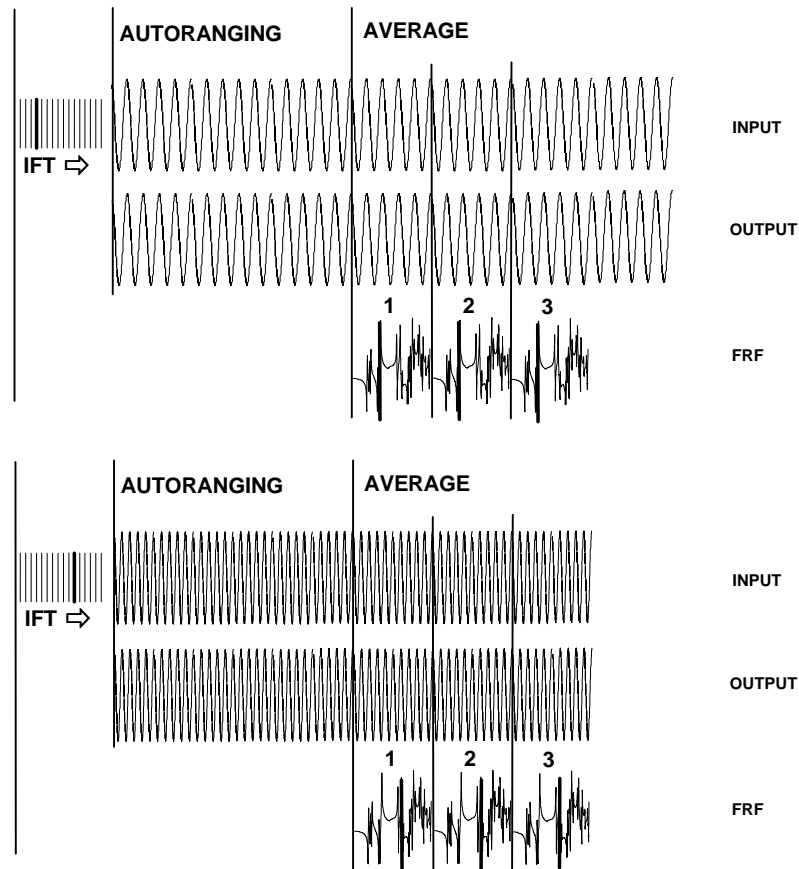


### **Digital Stepped Sine Excitation**

Due to the excellent nature of swept sine testing, an alternative technique which utilizes the speed of the FFT analyzer was developed and is referred to as digital stepped sine. Basically, sine waves are generated at discrete frequencies which correspond to the digital values of the FFT analyzer for the frequency resolution available.

The system is excited with a single sine wave and the steady state response is measured. Since the input frequency coincides with one discrete spectral line of the FFT analyzer, the measured time signal will always contain an integer number of cycles of the signal and is considered to satisfy the periodicity requirement of the FFT process.





Once an acceptable measurement is achieved, the excitation is digitally stepped to the next discrete frequency available in the FFT analyzer. This process is repeated until all discrete frequencies have been measured.

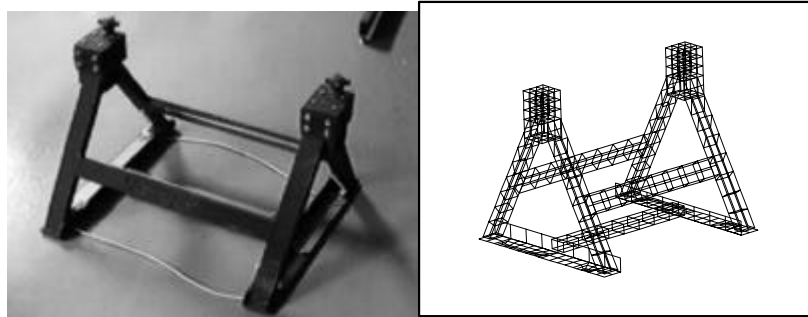
This test technique retains all the advantages of swept sine testing and combines all the advantages of the FFT analysis process. Obviously, the test time to acquire a wide frequency band with fine frequency resolution will require a significant amount of time but the accuracy and resolution of the data lend it to be an excellent test technique. Like swept sine, digital stepped sine is excellent for characterizing nonlinear character of a system.



## COMPARISON OF DIFFERENT EXCITATIONS FOR A WELDMENT STRUCTURE

Several of the more commonly used excitation techniques were used for the development of a frequency response function for a weldment structure are presented in this section for comparison purposes. In particular, random with and without a Hanning window, burst random and sine chirp were used on the same weldment structure. Also, a linearity check was performed using sine chirp to illustrate the effects of non-linearities in a structure. In this way, a clear assessment of the advantages and disadvantages of the different excitation techniques can be made.

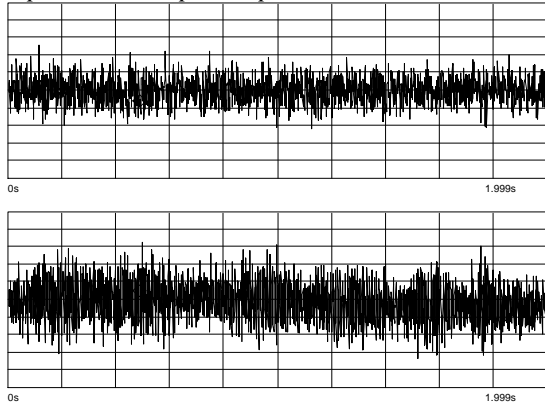
For all measurements made, a frequency range of 400 Hz was used with 800 spectral lines of resolution. Typically, 10 averages were made in order to compute the H1 frequency response function. Input and output time histories are shown along with the resulting frequency response function and coherence.



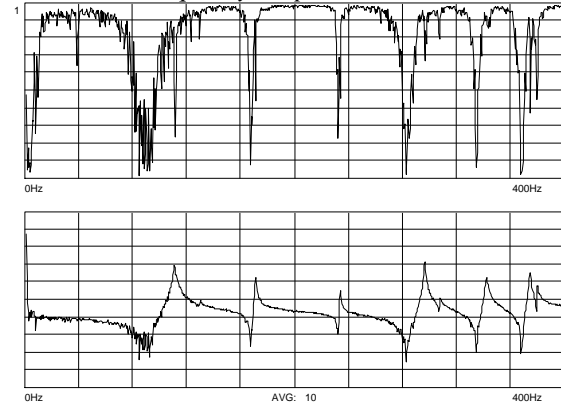


## Random Excitation With No Window

*Input Force/Output Response*



*Coherence/Frequency Response Function*

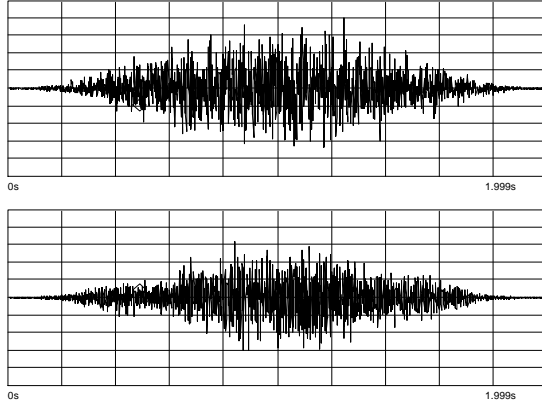


Shown above is the input/output time histories on the left and the coherence/frequency response on the right. Viewing the results in the time domain, the input and output signals are random in nature but there is no useful information that can easily be seen in the data. In the frequency domain, however, the frequency response function shows several modes that exist. The frequency response measurement shows quite a bit of variance on the measured function. Many more averages would be required in order to reduce the variance on this measurement. Even with excessive averaging and overlap processing, however, the variance would not be able to be reduced to acceptable levels. The main reason for the distortion of this measurement is leakage. This is always a problem with random excitation techniques.

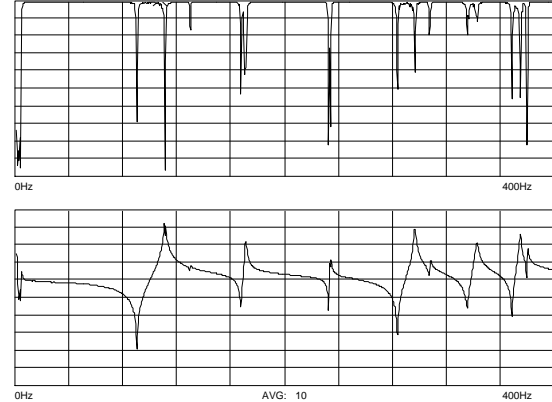


## Random Excitation With Hanning Window

*Input Force/Output Response*



*Coherence/Frequency Response Function*



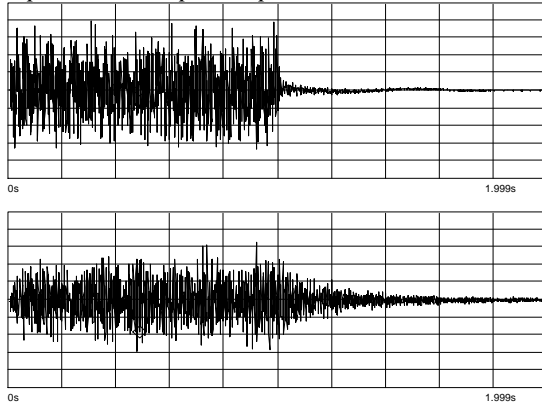
Shown above is the input/output time histories on the left and the coherence/frequency response on the right.

With a Hanning window applied the situation is somewhat improved. Viewing the results in the time domain, the input and output signals are again random in nature but there is no useful information that can easily be seen in the data; the effects of the Hanning window, however, are clearly seen on the data. In the frequency domain, the frequency response function shows several modes that exist. The frequency response measurement still shows quite a bit of variance on the measured function. Many more averages would be required in order to reduce the variance on this measurement. It is very important to note that the coherence function has fairly low values particularly at the resonant peaks. Even with the Hanning window applied, excessive averaging is still necessary in order to reduce the variance to acceptable levels. Again the main reason for the distortion of this measurement is leakage. This will always be a problem with random excitation techniques even with the Hanning window applied. The Hanning window reduces a good deal of the leakage but does not eliminate the problem.



## Burst Random Excitation With No Window

*Input Force/Output Response*



*Coherence/Frequency Response Function*

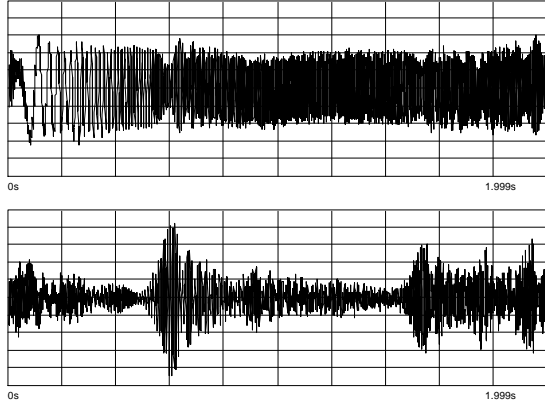


Shown above is the input/output time histories on the left and the coherence/frequency response on the right. Viewing the results in the time domain, the burst random excitation signals shown above still contain no useful information that can be easily seen. However, both the input and output signals are now completely observed within one sample interval of the time block. Since this is the case, the signal does not violate the basic periodicity requirement of the FFT process and there is no need to apply any window in this case. This will produce a leakage free measurement that will not be distorted by leakage. The frequency response function is considerably better than the random case with significantly improved coherence values particularly at the resonant peaks. Also note that the resonant peaks are much sharper than in the random case since leakage and windows tend to smear data causing an appearance of higher damping than what actually exists.

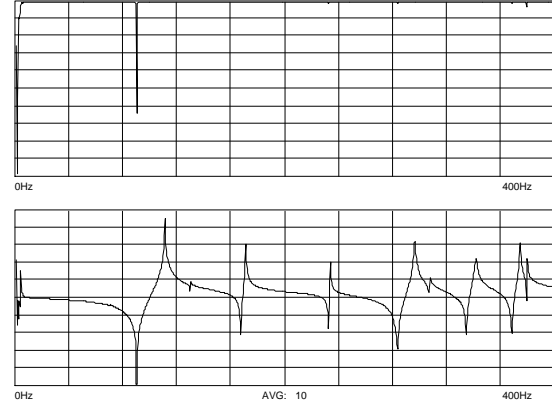


## Sine Chirp Excitation With No Window

*Input Force/Output Response*



*Coherence/Frequency Response Function*

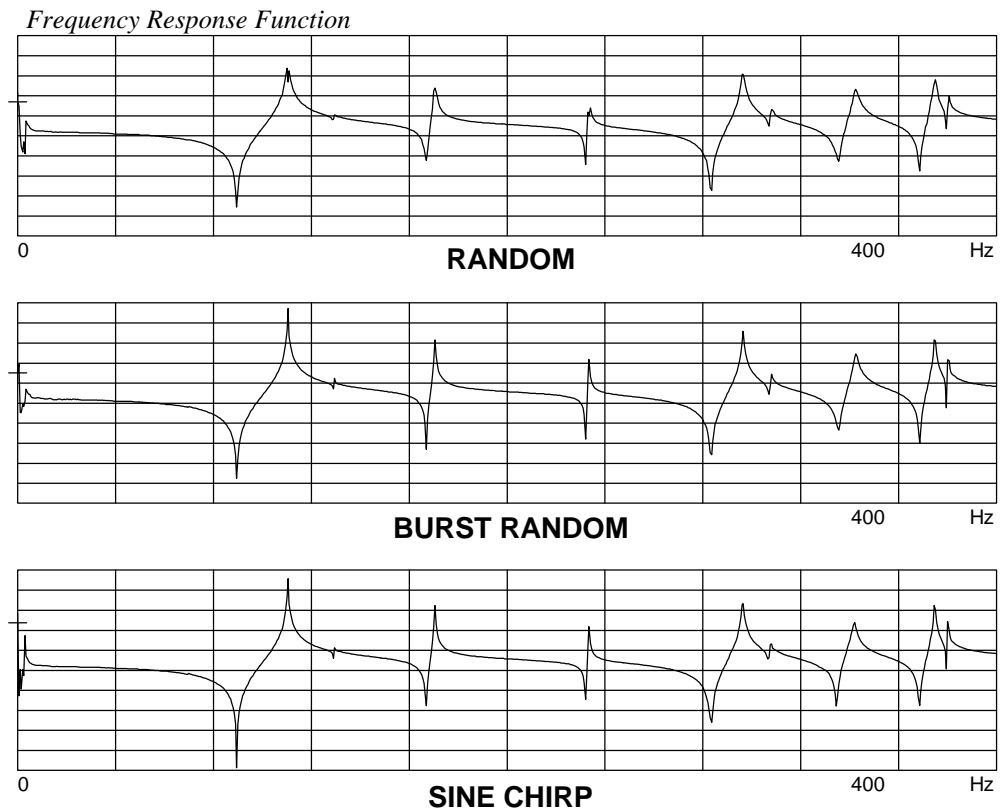


Shown above is the input/output time histories on the left and the coherence/frequency response on the right.

Viewing the results in the time domain, the sine chirp signals shown above show some useful information. Since the chirp sweeps from low to high frequency within one sample interval, the time response will contain amplification as the chirp sweeps through each of the resonant frequencies. Again, both the input and output signals are completely observed within one sample interval of the time block. Since this is the case, the signal does not violate the basic requirement of the FFT process and there is no need to apply any window in this case. This will produce a leakage free measurement that will not be distorted by leakage. The frequency response function is considerably better than the random case with significantly improved coherence values particularly at the resonant peaks. Also note that the resonant peaks are much sharper than in the random case since leakage and windows tend to smear data causing an appearance of higher damping than what actually exists.



## Comparison of Random, Burst Random and Sine Chirp

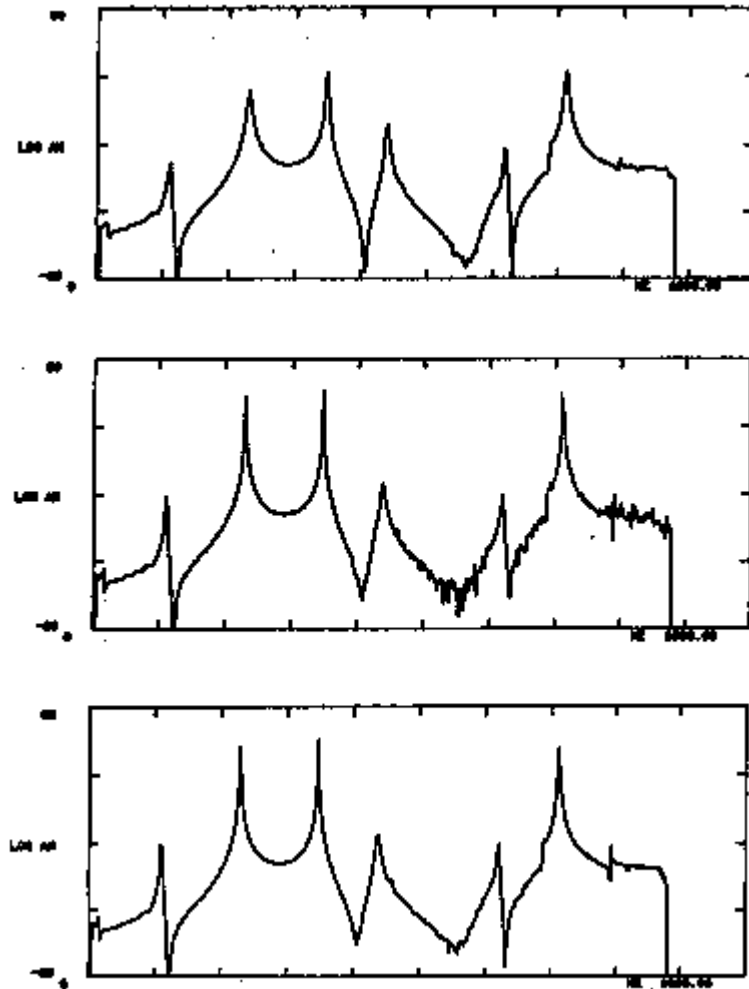


The burst random and sine chirp produce very similar results. The resonant peaks are well defined and there is very little variance on the measured data. Comparing these two results to the random measurement, it can be seen that the random measurement appears to have considerably more damping at the resonant peaks when looking at the burst random and sine chirp. Also notice that there appears to be a double peak at the first frequency in the random measurement; this is due to leakage and will be looked at closer.



## Comparison of Random, Pseudo Random and Periodic Random

*Frequency Response Function (scanned image)*



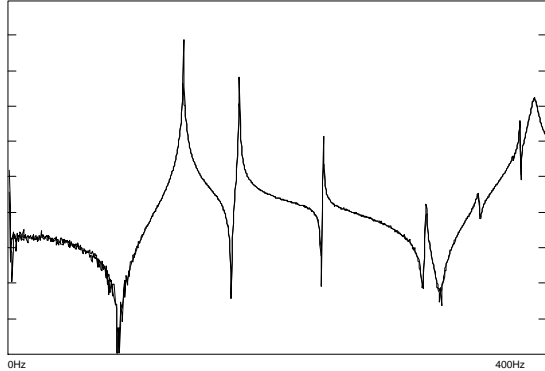
The results shown above are from a different structure than that used for the other results presented herein. From the results above, the random excitation produces results that will be affected by the Hanning window and leakage. The pseudo random results are improved over the random case mainly due to the fact that the input and output signals are periodic with respect to the sample block and will not be distorted by leakage without using a window. However, there exists some regions of the frequency response function that contain some variance which will not be averaged away by taking more averages; this is due to the fact that the same signal is repeated used for each average taken thereby preventing the removal of noise with averaging. However, the periodic random signal significantly improves this situation since a different signal is used for each average.



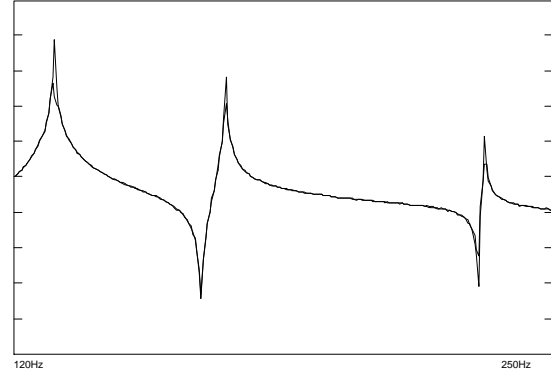
## Comparison of Random and Burst Random at Resonant Peaks

Let's compare the results of the random and burst random excitation.

*Frequency Response Function*

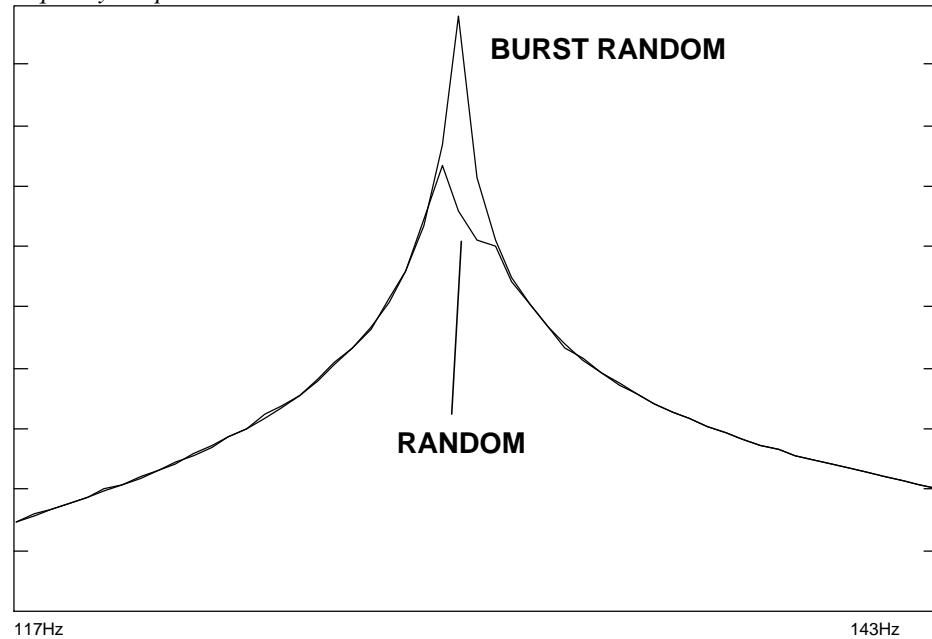


*Frequency Response Function*



On the surface, it appears that both measurements look the same on the left but as we take a closer look on the right, there appears to be some distortion at the peaks. As we take even a closer look below, it becomes very apparent that there is a severe distortion of the frequency response function particularly at the resonant peak. Even with the use of a Hanning window on the random data, there is still a serious effect from leakage !!!

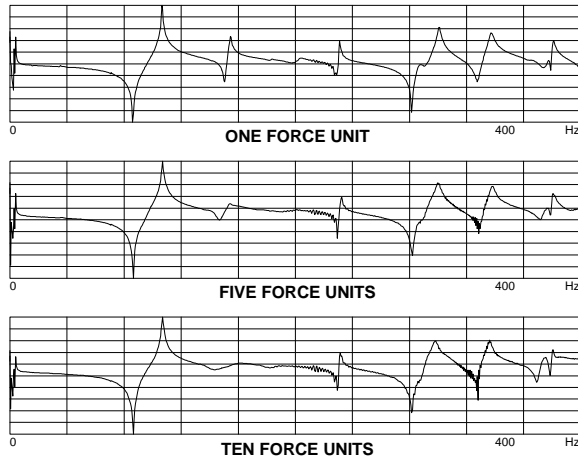
*Frequency Response Function*



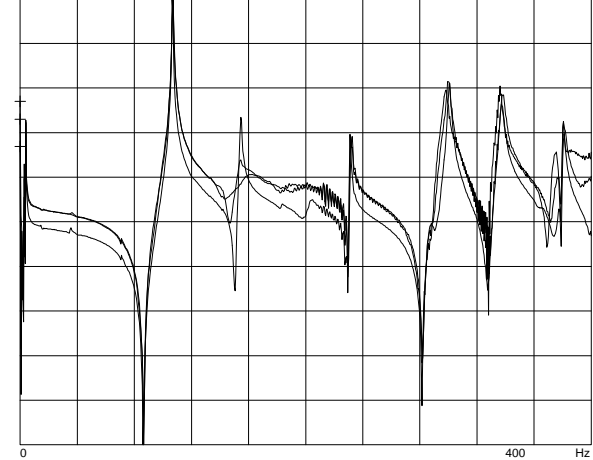


## Linearity Check Using Sine Chirp

*Frequency Response Function*



*Frequency Response Function*



The frequency response function was measured using different force levels with sine chirp excitation to document the linearity of the system. Clearly there is nonlinear behavior but not all of the modes are affected equally by whatever nonlinearity exists in the system. Some modes show very little change due to increase in force level, other modes show some slight differences due to increase in force level and a few other modes show a dramatic change in the dynamic characteristics of the system.



## MULTIPLE INPUT MULTIPLE OUTPUT MEASUREMENTS

Multiple input multiple output (MIMO) testing has become very popular over the past several years and offers several advantages over single input single output testing (SISO) methods. This technique allows for a better energy distribution to excite large structures more uniformly. The simultaneous input also allows for nonlinearities to be excited differently such that a better linear approximation of the system can be obtained. In addition, the simultaneous collection of multiple columns of the frequency response matrix allows for a more uniform and consistent definition of the frequency response functions which will be used to develop the experimental modal model of the system. The data collection time for MIMO is the same as SISO.

Instead of computing frequency response functions as scalar quantities, matrix processing of the data is required. The input output model is the same and is defined as

$$[G_{XF}] = [H][G_{FF}]$$

where

$$[H] = \begin{bmatrix} H_{11} & H_{12} & \cdots & H_{1,Ni} \\ H_{21} & H_{22} & \cdots & H_{2,Ni} \\ \vdots & \vdots & & \vdots \\ H_{No,1} & H_{No,2} & \cdots & H_{No,Ni} \end{bmatrix}$$

where No is the number of outputs and Ni is the number of inputs. Solving for [H] we get

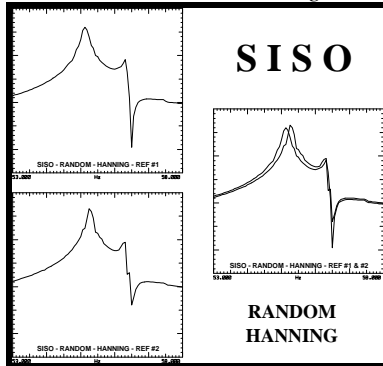
$$[H] = [G_{XF}][G_{FF}]^{-1}$$



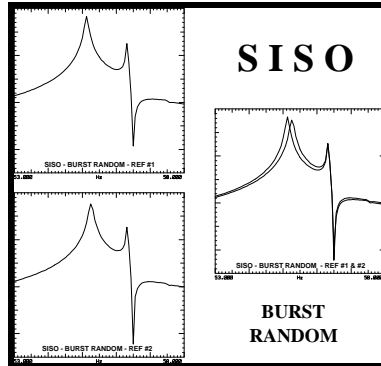
## Multiple Input vs Single Input Testing

Due to effects from shaker mass and stiffness, there may at times be differences between the results from several different single input tests. However, the theory of modal analysis implies that reciprocity must hold true. From a practical standpoint this is often not the case in an actual test condition. Using multiple input testing, the resulting data will better satisfy the reciprocity requirement as seen in the data below.

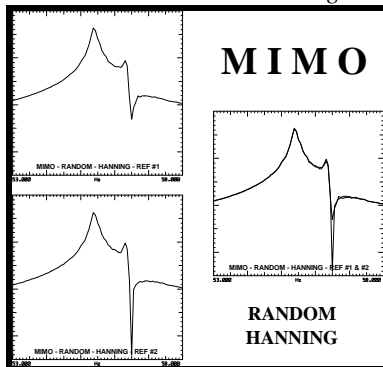
*SISO - Random with Hanning Window*



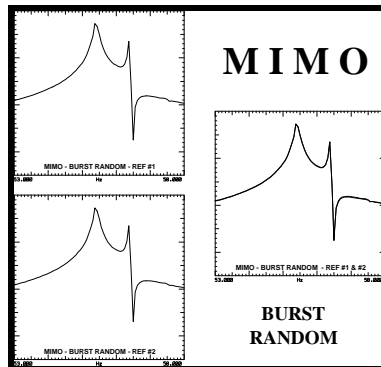
*SISO - Burst Random without Window*



*MIMO - Random with Hanning Window*



*MIMO - Burst Random without Window*

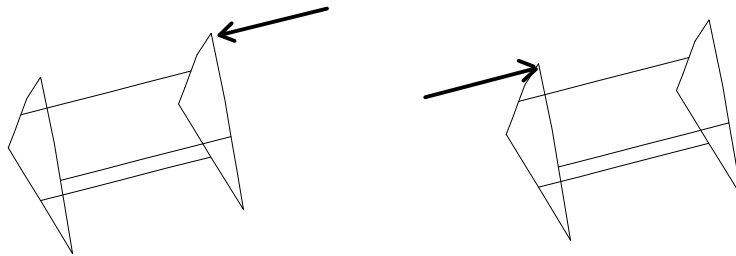




## MULTIPLE INPUT VS SINGLE INPUT FOR A WELDMENT STRUCTURE

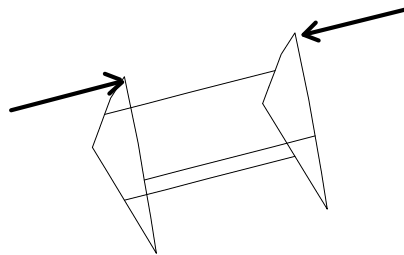
Due to effects from shaker mass and stiffness, there may at times be differences between the results from several different single input tests. Using the same structure used for demonstration of different excitation techniques, reciprocity measurements were made using single input vs multiple input for comparison.

### SINGLE INPUT CASE



### TWO SEPARATE TESTS

### MULTIPLE INPUT CASE

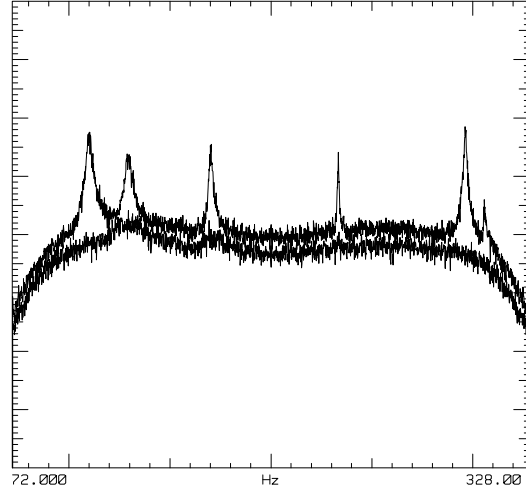




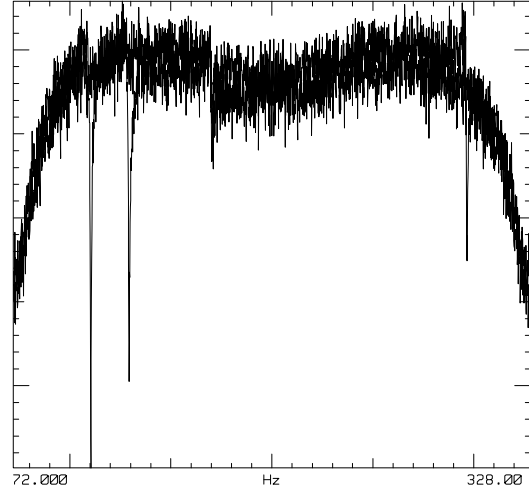
## Multiple Input vs Single Input Testing

For multiple input testing, each of the inputs must be uncorrelated from the other inputs to the system. Generally a principal component analysis is performed and the input power to all of the force shakers is checked to assure sufficient input to the system is available as shown below.

*Principal Component Analysis for 2 Inputs*

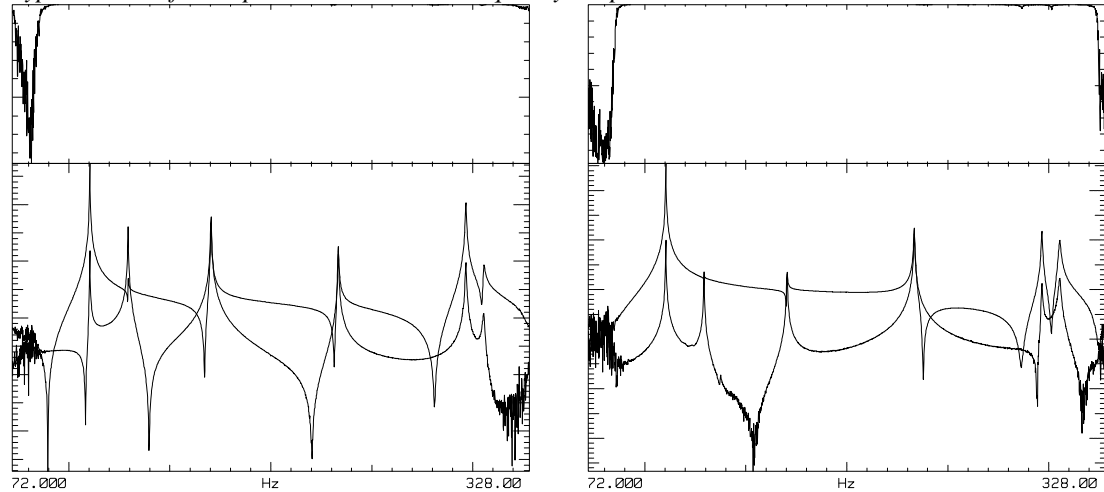


*Input Force Spectrum for 2 Shakers*



Once the inputs are checked for the system, then measurements are acquired in the usual fashion. Several typical measurements are shown below.

*Typical Plots of Multiple Coherence and Frequency Response Measurements*

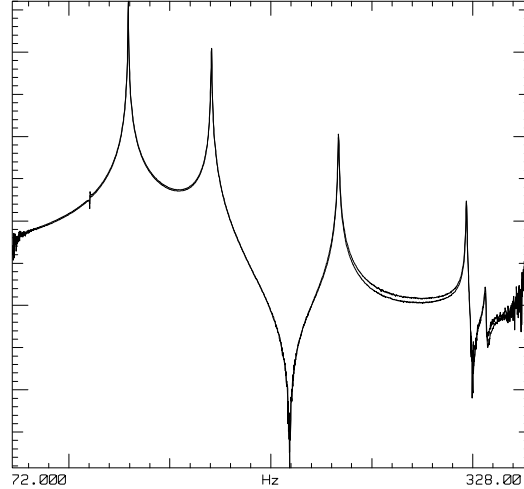




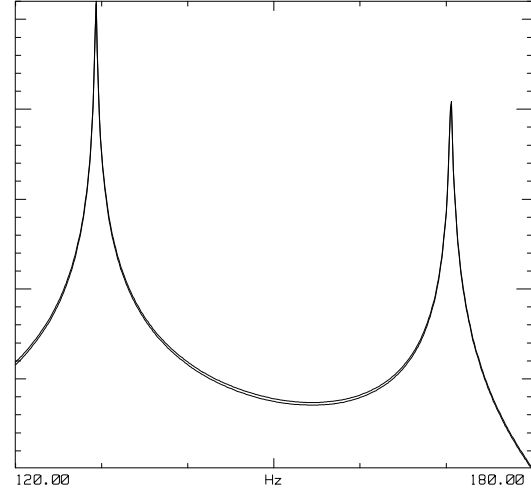
## Comparison of Multiple Input vs Single Input for Weldment Structure

While the particular structure under test is fairly linear, there is very little difference between the multiple input and single input cases. This is not generally the rule in most testing situations. However, some difference are noted in the comparison measurement below.

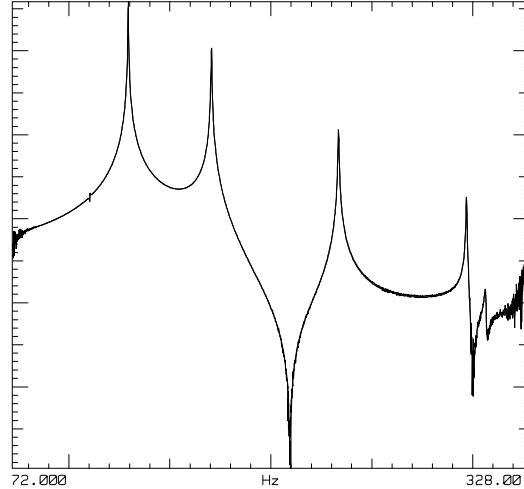
*SISO - Frequency Response Measurements*



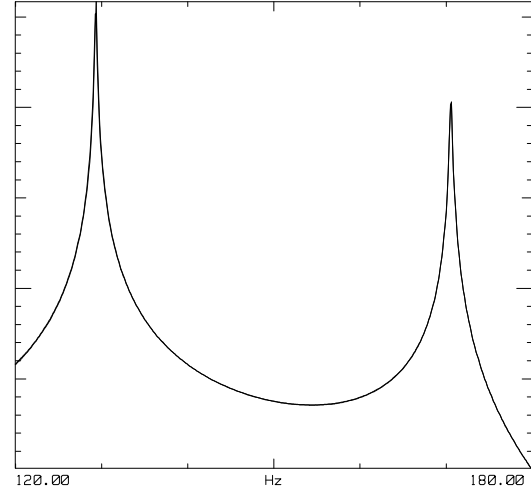
*SISO - Expanded for First 2 Modes*



*MIMO - Frequency Response Measurements*



*MIMO - Expanded for First 2 Modes*





## **SUMMARY**

Impact techniques for acquiring frequency response measurement were reviewed. Shaker excitation techniques using a variety of different excitation signals was also reviewed. Multiple input multiple output testing techniques were also included.



## OVERVIEW OF EXPERIMENTAL MODAL ANALYSIS USING THE FREQUENCY RESPONSE METHOD

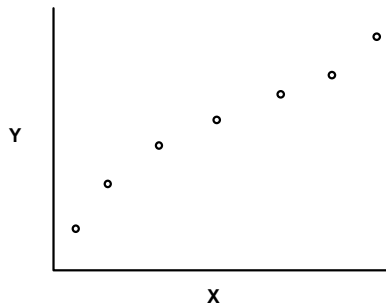
### PART 4 - MODAL PARAMETER ESTIMATION TECHNIQUES

#### INTRODUCTION

From the development of general modal theory, it is clear that all that is needed is the poles and residues of the system in order to generate frequency response function. It should be equally clear that if a point to point frequency response function is measured, then it should be possible to extract the system parameters of poles and residues from the measurement. The process of extracting this information is referred to as *modal parameter estimation*. Since a mathematical function expressing the frequency response function is used to fit the measured data to this relationship, the process is often referred to as *curvefitting*. The problem faced by the analyst is the determination of the order of the model (number of modes) and the form of the model (time or frequency domain). These are not trivial problems that are faced by the analyst especially when the data collected is not perfect. In the following sections some traditional approaches and definitions for estimating modal parameters will be addressed. However, before any in depth treatment of particular curvefitters is performed some simplistic concepts of least squares approximation of data will be discussed.

#### Least Squares Approximation of Data

At one time or another, we have all had to perform a least squares approximation for data probably utilizing a linear relationship to characterize the data set. Consider the figure below which shows some data collected for a force gage.

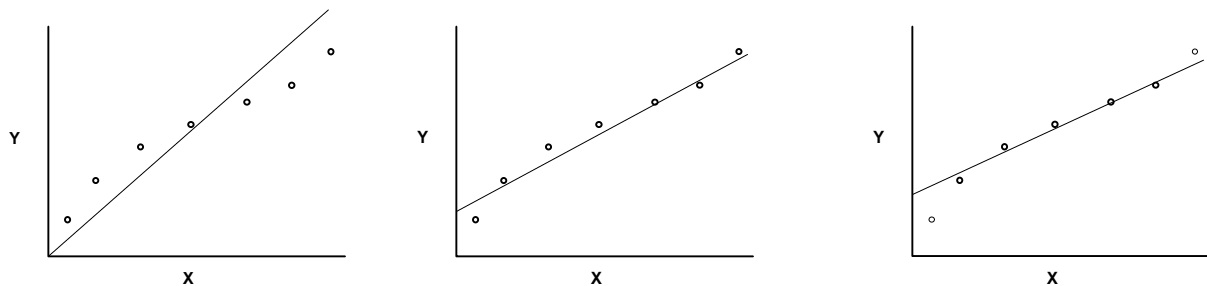




Assuming that there is no voltage when there is no force, then we know that the straight line describing the force transducer must pass through zero. The dotted line on the left figure below shows the best possible (minimization of error on a least squares basis) straight line to fit the data. However, looking at this straight line, we see a lot of variance between the measured data and the straight line describing the data and our confidence in the accuracy of the predicted line is not good.

Now let's suppose that we do not impose the restriction that the straight line pass through zero and fit the data again with the line shown in the middle figure below. This would assume that the force gage could actually have a load with no voltage reading; this could correspond to a preload situation for instance. While this curve appears to better fit the data, there is still some significant variance between the data and the straight line.

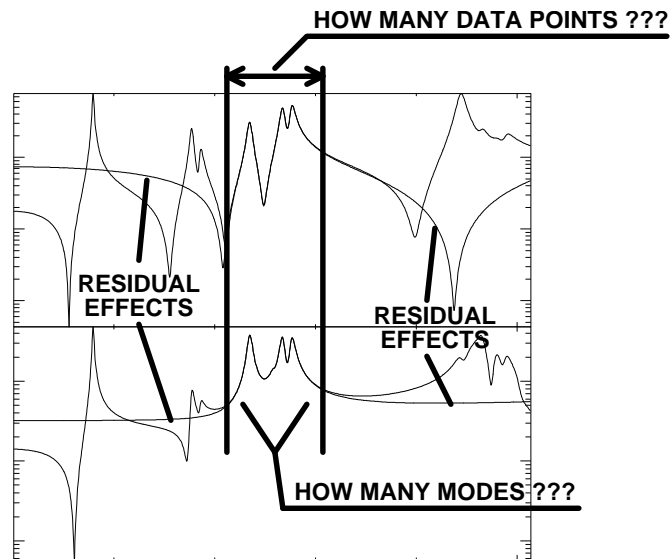
Now what if the fit were to exclude the lowest reading and the highest readings as shown in the right figure below; exclusion of these readings may be warranted if there were a minimum threshold voltage before a valid reading could be obtained as well as there being an upper end of useful obtained data from the transducer. This curve seems to even better yet fit the measured data. Notice that three different straight lines have been obtained from this estimation process all of which are approximations of the actual phenomena.



In fact, there is actually no basis for an assumption that the line is a first order mathematical relationship. The data could possibly be better identified with a higher order model to better describe the measured data. Notice that it is at the discretion of the analyst as to the order of the model, whether to allow for compensation for other effects and which data points are to be included in the estimation process. These judgments result in very different approximations of the system to be characterized. This will also be very true in modal parameter estimation.



The analyst must decide on several items pertinent to the extraction of modal data from the measured frequency response function as shown in the figure below. The analyst must decide on the *order of the model*, the *amount of data to be used*, and the need for *compensation for residuals*.



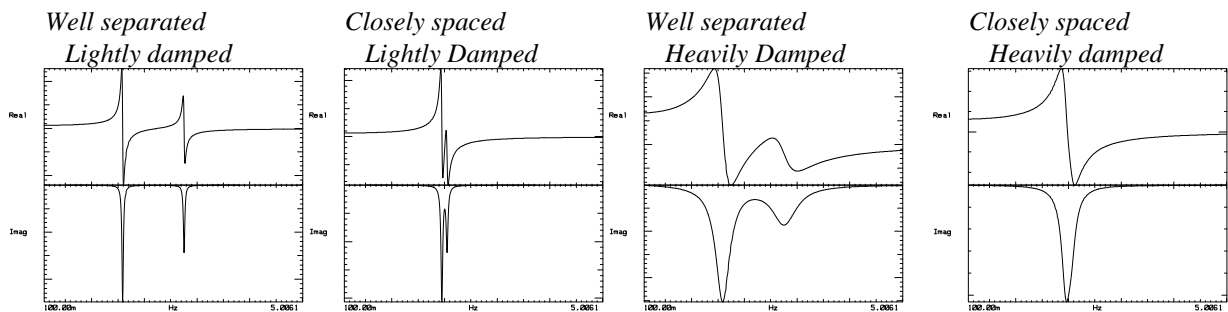


## Classification of Modal Parameter Estimation Techniques

The basic theory for development of the modal model can be written in many different forms but in essence all of the techniques are the same. Differences occur mainly due to numerical considerations of less than perfect measured data.

In the most basic approximation, a frequency response measurement can be broken down into the modal components that make up the measurement derived from equivalent single degree of freedom systems. Therefore it would stand to reason from an analytical standpoint that only a *sdof* approximation would be required. However, from a measurement standpoint, there may be significant modal overlap between two closely spaced modes that would prevent the accurate extraction of modal parameters using a *sdof* technique. Therefore many times it is necessary to utilize a multiple degree of freedom model in order to extract valid parameters when the modes are closely spaced with significant modal overlap. Thus, at a first level of approximation we see that there may be the need for both *sdof curvefitters* and *mdof curvefitters* in order to handle a range of situations.

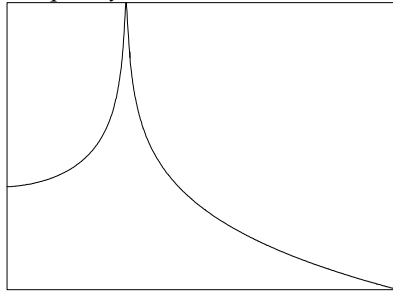
Below are four figures of a 2 dof system with different types of modal overlap due to different reasons. The first plot shows well separated lightly damped modes. The second plot shows two lightly damped modes with coupling that is a result of the closeness of the modes to each other. The third plot shows two heavily damped modes with coupling that results from the damping on the system as opposed to the closeness of modes in the previous case. The fourth plot shows two heavily damped closely spaced modes which could easily be misconstrued as a single dof system if the plot was not reviewed carefully.





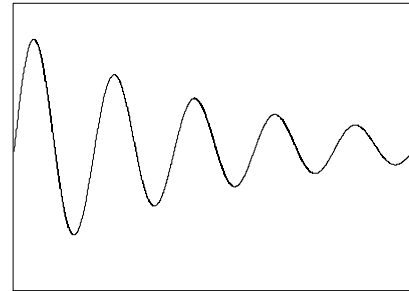
The next consideration would be as to whether the data is to be fit in the *time domain* or the *frequency domain*. Since the equations can be cast in either domain, the modal parameter estimation phase can be carried out in either domain and when using the frequency domain, the equations may be cast in partial fraction form, pole-zero form, polynomial form or some other equivalent form. Basically the equations will be cast into a form that offers some numerical advantage or mathematical "gimmick" that will enable the equations to be processed more efficiently or with greater speed. In both representations of the sdof system below, the system time or frequency characteristic can be defined by the pole and residue of the system regardless of the domain it is presented in.

*Frequency Domain*



$$h(j\omega) = \frac{a_1}{(j\omega - p_1)} + \frac{a_1^*}{(j\omega - p_1^*)}$$

*Time Domain*

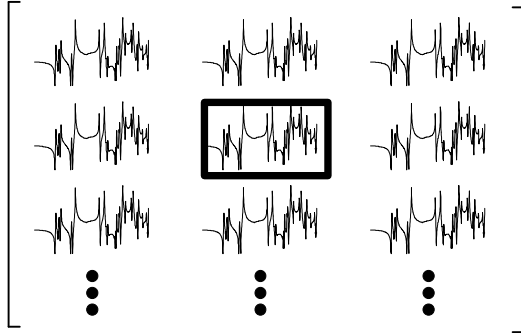


$$h(t) = \frac{1}{m\omega_d} e^{-\sigma t} \sin \omega_d t$$



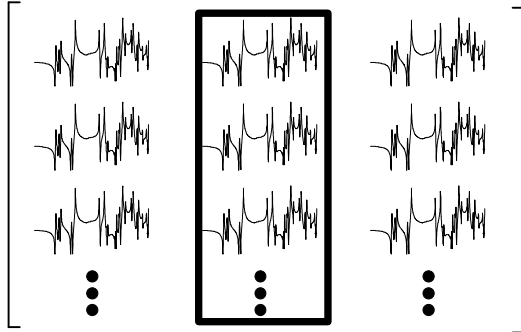
Additionally, the measured frequency response data can be measured one measurement at a time or one column of data at a time or several columns of data at a time and is referred to as *local*, *global* or *polyreference* curvefitting.

#### *Local Curvefitting*



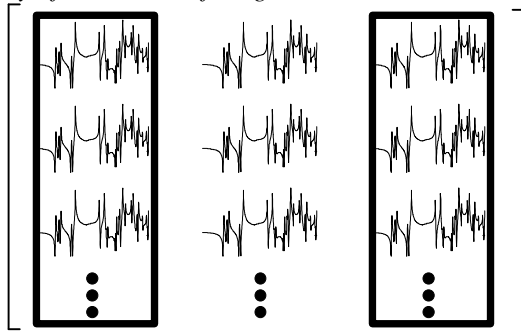
In *local curvefitting*, the pole and residue are extracted for each measurement independent of other measurements in the frf matrix. This is shown in the frf matrix on the left. This is useful when the frequency and damping are not constant from one measurement to the next.

#### *Global Curvefitting*



In *global curvefitting*, an estimate is made of the poles from a global standpoint using all or a selected set of measurements that are available from a single row or column of the frf matrix as shown on the left. The residues are then extracted in a second pass using the fixed global poles found in the first pass.

#### *Polyreference Curvefitting*



In *polyreference curvefitting*, an estimate is made of the poles from a global standpoint using all or a selected set of measurements that are available from a multiple rows or columns of the frf matrix as shown on the left. The residues are then extracted in a second pass using the fixed global poles found in the first pass.



## Extraction of Modal Parameters

With some of the basic terminology defined above, some of the more elementary techniques for estimation of parameters will now be addressed.

### Peak Picking Technique

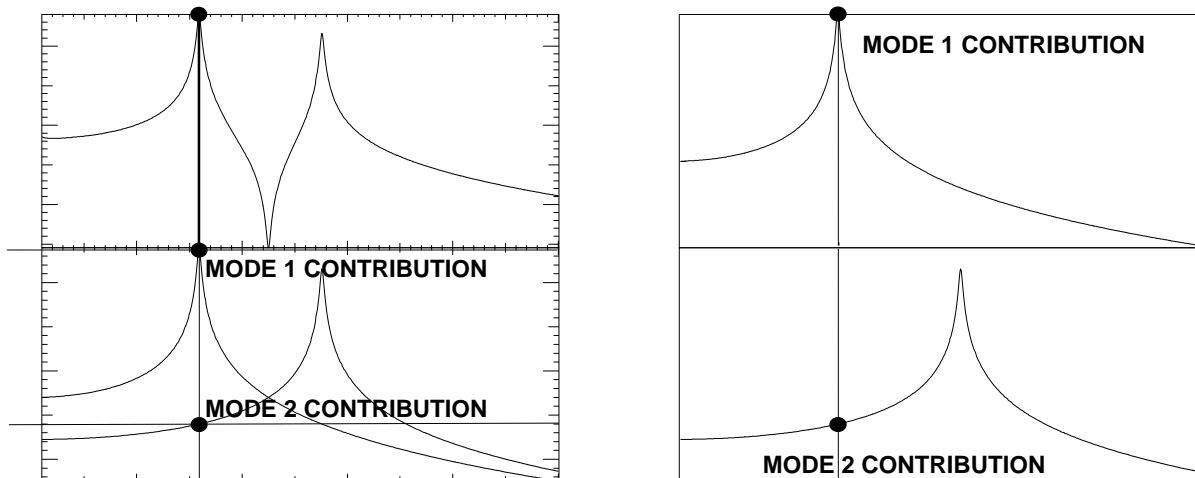
One of the first parameter estimation techniques involved the use of peak picking to obtain a rough estimate of the residue of the system. Providing there is sufficient separation between the modes of the system, this provided a reasonably good estimate of the residue of the system. The frequency was determined by the location of the peak and the damping was estimate by the half power method. If the frequency response function is evaluated at the natural frequency of the system, then the residue can be approximated for a sdof system by

$$h(j\omega) \Big|_{\omega \rightarrow \omega_n} = \frac{a_1}{(j\omega_n + \sigma - j\omega_d)} + \frac{a_1^*}{(j\omega_n + \sigma + j\omega_d)}$$

Realizing that the damped natural frequency and natural frequency are approximately equal for lightly damped systems, the residue can be approximated by

$$a_1 = \sigma h(j\omega) \Big|_{\omega \rightarrow \omega_n}$$

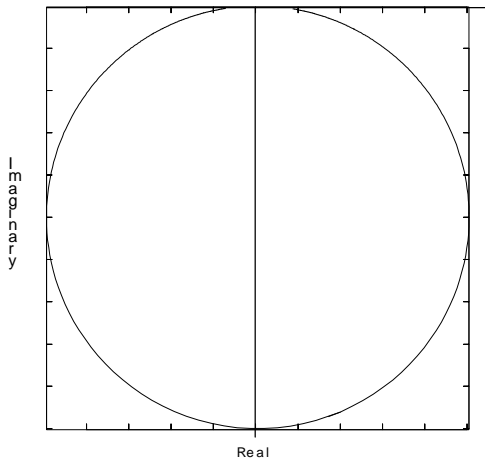
Basically this implies that the peak of the frequency response function is directly related to the residue (to within a scale constant of the damping of the system). The peak picking process is shown schematically below.





## Circle Fitting - Kennedy & Pancu

For lightly damped, well separated modes, a single degree of freedom approximation is accurate. If the frequency response function is cast in complex form, then in the complex plane (Nyquist plane), the frequency response function appears as a rotated circle. In this form the equation of a circle can be used in a least squares fashion to extract the parameters of interest, namely the pole and residue. The frequency can be found to be bounded by the two data points where the widest separation of data points exists when displayed in the Nyquist plot. The damping of the system can be determined by the half power point method. The residue can be approximated by the diameter of the circle as  $a_{ijk}/\sigma_k$ . Extensions of the circle fit can be made to account for some coupling from adjacent modes as well as complex mode characteristics.



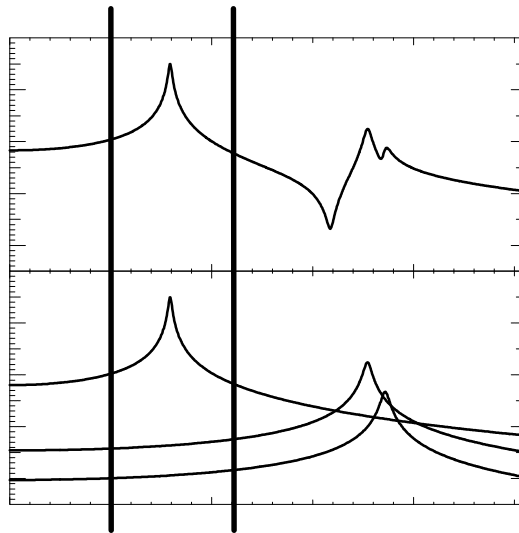


## SDOF Polynomial

An extension of the circle fit technique was the single dof polynomial frequency domain approach used to estimate parameters using

$$h(s) = \frac{1}{ms^2 + cs + k}$$

With this technique the parameters are again to extract the pole and residue but in this form, the residual effects of other adjacent modes can be included in the model as a mass effect of the lower modes and as a stiffness effect due to the higher modes. This is seen schematically in the figure below.



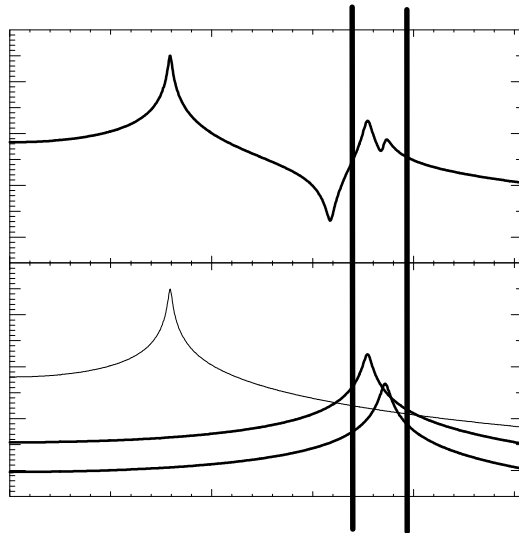


## MDOF Polynomial

An extension of the sdof polynomial technique where a number of modes are included to estimate parameters using

$$h_{ij}(j\omega) = \frac{a_{ij2}}{(j\omega - p_2)} + \frac{a_{ij2}^*}{(j\omega - p_2^*)} + \frac{a_{ij3}}{(j\omega - p_3)} + \frac{a_{ij3}^*}{(j\omega - p_3^*)}$$

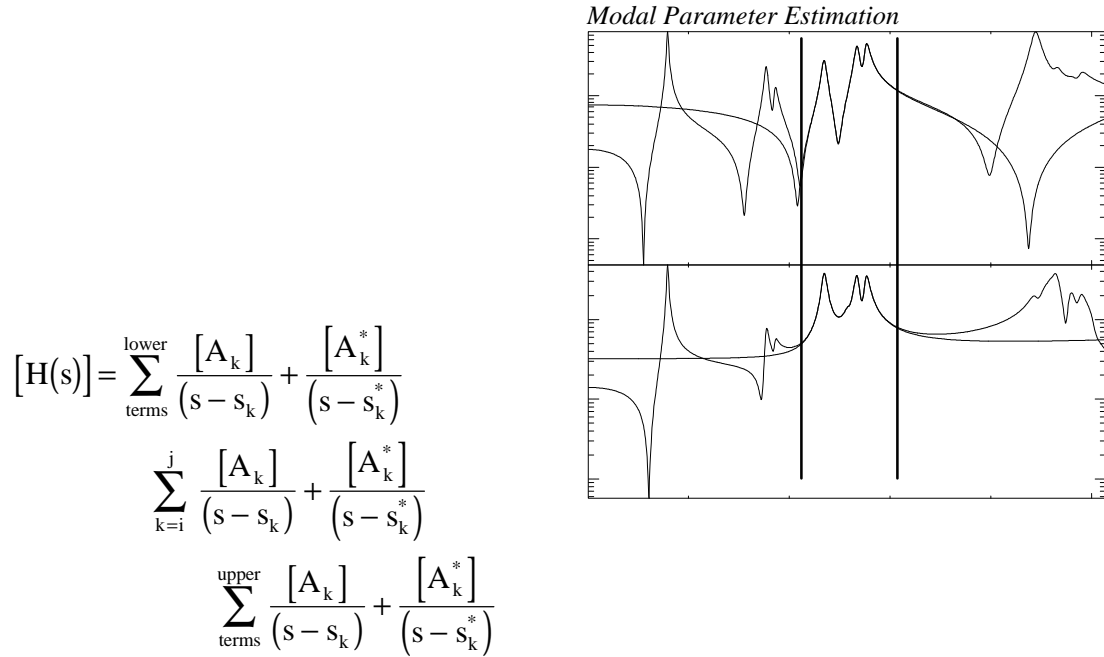
where the parameters to be extracted are for mode 2 and 3 for this case. Obviously this can be extended to a number of modes over a variety of different bands. Compensation of residual effects is discussed next.





## Compensation for Residual Effects

Usually modal parameters are extracted piecewise in narrow bands that generally does not contain all of the modes in the measured frequency response; several bands are evaluated in order to obtain all of the modes observed in the measured data. The mathematical model may be a partial fraction formulation, pole-zero formulation, polynomial formulation in the frequency domain or an impulse response formulation in the time domain. In partial fraction form, modes  $i$  through  $j$  for instance, are extracted but there is an effect of modes outside the band as shown



Since the narrow bands contain predominantly the modes in the band as well as the effects of modes outside the band, generally the modal parameter estimation algorithms include compensation for the *residual effects* of modes outside the band of interest.

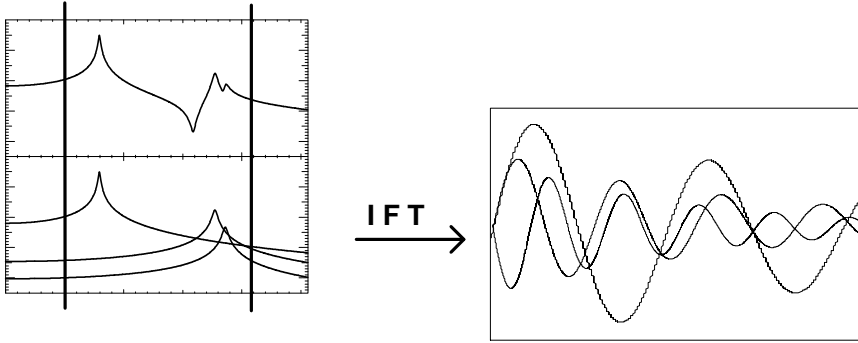
$$[H(s)] = \text{lower residuals} + \sum_{k=i}^j \frac{[A_k]}{(s - s_k)} + \frac{[A_k^*]}{(s - s_k^*)} + \text{upper residuals}$$



## Least Squares Complex Exponential

The *least squares complex exponential* can be written as

$$h(t) = \sum_{k=1}^m \frac{1}{m_k \omega_{dk}} e^{-\sigma_k t} \sin \omega_{dk} t$$



$$h(t) = \frac{1}{m_1 \omega_{d1}} e^{-\sigma_1 t} \sin \omega_{d1} t + \frac{1}{m_2 \omega_{d2}} e^{-\sigma_2 t} \sin \omega_{d2} t + \frac{1}{m_3 \omega_{d3}} e^{-\sigma_3 t} \sin \omega_{d3} t + \dots$$

Normally the complex exponential is written in exponential form. In this form with sampled data, the solution of this equation can be written as linear finite difference equations with constant real coefficients of order  $2m$ . The resulting characteristic equation can be solved using a least squares approach for the highly overdetermined set of equations. In the process of manipulating the equations into normal form, a compact coefficient matrix, the *Covariant Matrix*, is formed; the rank of this matrix is used to determine the number of modes using a *Least Squares Error Chart* or *Singular Values Diagram*.



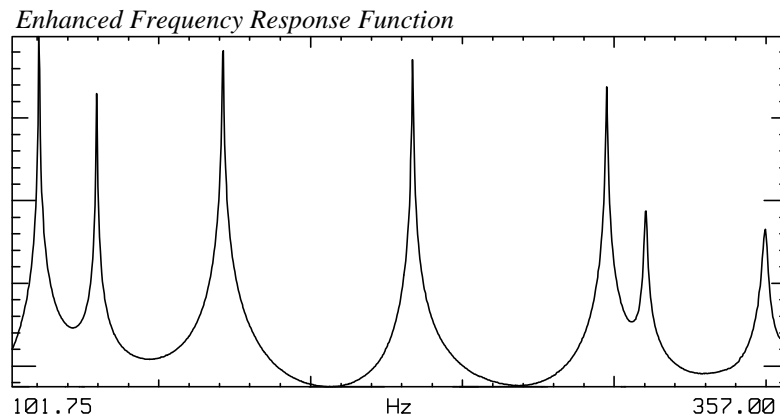
## Mode Identification Tools

Several tools exist to aid in the identification of number of modes that exist in a given frequency band.

### Summation Function

In terms of determining the number of poles to extract from the measured data, several indicator functions exist. The first approach is to generally review the measured frequency response functions and look for peaks in the measured data. However, the presence of closely spaced or repeated roots makes this difficult.

A summation of all the measured frequency response functions, referred to as the *enhanced frequency response function* or *summation function*, will tend to accentuate modal peaks that exist in the data. However, closely spaced or repeated roots will tend to add to the power of the summation function thereby lending this tool to only be useful when the modes are reasonably far spaced.





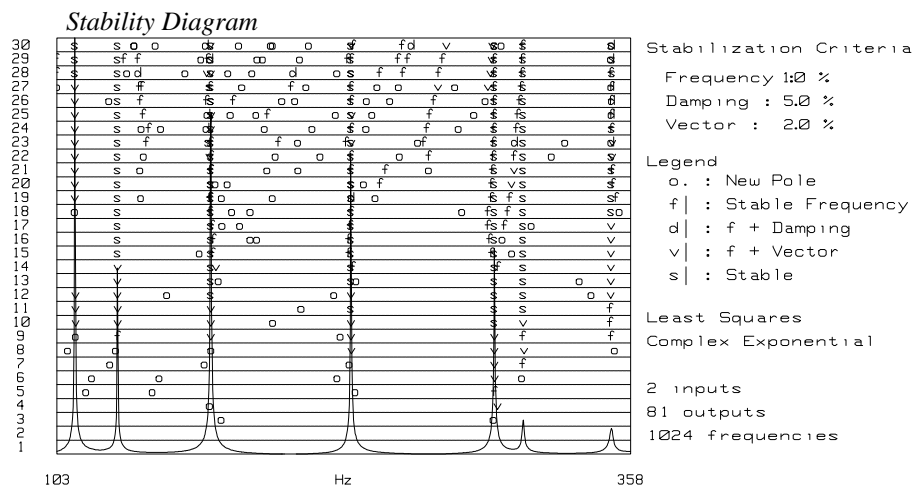




## Stability Diagram

Once the number of modes is estimated for a certain band then one of the tools available when fitting a mdof model in the time domain to the band of interest is the *Least Squares Error Chart*. As the number of modes assumed to exist in the model is increased, a least squares error can be observed as a function of the number of assumed modes in the model. The number of modes in the data is determined by the knee of the curve where there is a pronounced change in the number of modes vs. the error. The *Covariance Matrix* generated in this process can also be spectrally decomposed using singular valued decomposition to determine the rank of the set of equations and plotted either as an Error Chart or as a *Singular Values Diagram*. The interpretation of the singular values diagram is much more straightforward when compared to the error chart.

As higher and higher order models are assumed, the true structural modes will converge to a stable number whereas noise or computational modes will appear in an inconsistent or random fashion in the data. The *Stabilization Diagram* shows this information. Generally, a selection on the accuracy of the frequency, damping and vector can be selected. Usually the stabilization diagram is shown on the mode indicator function or enhanced frequency response function.





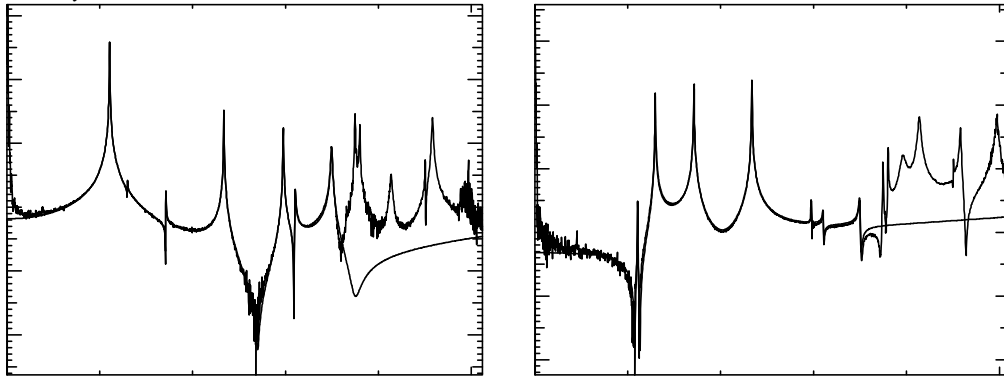
## Modal Model Validation Tools

Several techniques exist that aid in the validation of the modal model.

### Synthesis of Frequency Response Functions using Extracted Parameters

Once parameters are extracted over several smaller bands, then the extracted pole and residue information is used to synthesize a frequency response function and then compared to the actual measured data in order to assure that the extracted parameters are accurate.

*FRF Synthesis*





## Modal Assurance Criteria

Since different experimental modal vectors can be extracted from different modal parameter estimation techniques, or from different rows or columns of the frequency response matrix, or from entirely different modal tests, the *Modal Assurance Criteria (MAC)* was developed to determine the amount of correlation (or lack thereof) that exists between different modal vectors. The MAC is computed as

$$MAC_{ij} = \frac{\left[ \{e_i\}^T \{e_j\} \right]^2}{\left[ \{e_i\}^T \{e_i\} \right] \left[ \{e_j\}^T \{e_j\} \right]}$$

As the MAC approaches 1, there is a high indication that the two vectors are very correlated. As the MAC approaches 0, there is a high indication that the two vectors are very uncorrelated. Notice that the MAC is formulated the same as the coherence function.

## SUMMARY

Basic concepts of modal parameter estimation were introduced. Differences between single dof and multiple dof techniques were discussed by example for a simple 2 dof system. The similarity of using time and frequency domain representations were described along with a description of local, global and polyreference techniques. Finally, commonly used techniques were briefly described. Mode identification tools and model validation tools were also presented.



## LINEAR ALGEBRA - BASICS OPERATIONS NEEDED FOR MODAL ANALYSIS OPERATIONS

Let's just review some basic linear algebra material that we need to know for modal analysis.

### DEFINE A MATRIX

We can define a general matrix  $[A]$  to be of size  $n$  by  $m$  - meaning that it has  $n$  rows by  $m$  columns.

$$[A] = \begin{bmatrix} a_{11} & a_{12} & \cdots & a_{1m} \\ a_{21} & a_{22} & \cdots & a_{2m} \\ \vdots & \vdots & a_{ij} & \vdots \\ a_{n1} & a_{n2} & \cdots & a_{nm} \end{bmatrix}$$

The indices of the matrix indicate the specific row column. So that  $a_{ij}$  indicates the 'ith' row and 'jth' column of the matrix  $[A]$ . Typically we will use a capital letter to denote a matrix and a lower case letter to indicate a particular term of the matrix. This is called a rectangular matrix when  $n$  is not equal to  $m$ ; it is called a square matrix when  $n$  is equal to  $m$  meaning that you have as many rows as columns defining the matrix.

### DEFINE A COLUMN VECTOR

We can define a general column vector  $\{B\}$  to be of size  $n$  by 1 - meaning that it has  $n$  rows by one column.

$$\{B\} = \begin{Bmatrix} b_1 \\ b_2 \\ \vdots \\ b_i \\ \vdots \\ b_n \end{Bmatrix}$$

The indices of the vector indicate a specific row of the vector. So that  $b_i$  indicates the 'ith' row of the vector. Typically we use a capital letter to denote a vector and a lower case letter to indicate a particular term of the vector.



### DEFINE A ROW VECTOR

We can define a general row vector  $[C]$  to be of size 1 by m - meaning that it has one row by m columns.

$$[C] = [c_1 \quad c_2 \quad \cdots \quad c_j \quad \cdots \quad c_m]$$

The indices of the vector indicate a specific column of the vector. So that  $c_j$  indicates the 'jth' column of the vector.

Typically we use a capital letter to denote a vector and a lower case letter to indicate a particular term of the vector.

### DEFINE A DIAGONAL MATRIX

We can define a diagonal matrix  $[D]$  where non-zero terms exist only on the diagonal of the matrix.

$$[D] = \begin{bmatrix} d_{11} & & & & \\ & d_{22} & & & \\ & & \ddots & & \\ & & & d_{ii} & \\ & & & & \ddots \\ & & & & & d_{nn} \end{bmatrix} \quad \text{where } d_{ij} = 0 \quad \text{for } i \neq j$$

A diagonal matrix is square and a special form of this matrix is the Identity Matrix which has all diagonal terms equal to 1.

### DEFINE MATRIX ADDITION

We can add two matrices together but they must be the same size

$$[C] = [A] + [B] \Rightarrow c_{ij} = a_{ij} + b_{ij}$$

Each of the corresponding terms of the matrix  $[A]$  and  $[B]$  are added together to form the terms of matrix  $[C]$

#### Example

$$[A] = \begin{bmatrix} 2 & 3 \\ 1 & 4 \\ 3 & 2 \end{bmatrix} ; [B] = \begin{bmatrix} 1 & 0 \\ 0 & 1 \\ 1 & 1 \end{bmatrix} ; [C] = [A] + [B] = \begin{bmatrix} 2 & 3 \\ 1 & 4 \\ 3 & 2 \end{bmatrix} + \begin{bmatrix} 1 & 0 \\ 0 & 1 \\ 1 & 1 \end{bmatrix} = \begin{bmatrix} 3 & 3 \\ 1 & 5 \\ 4 & 3 \end{bmatrix}$$



### DEFINE MATRIX SCALAR MULTIPLY

We can scale the terms of a matrix by a scalar

$$[B] = s*[A] \Rightarrow b_{ij} = s*a_{ij}$$

Each term of the matrix [A] is multiplied by the scalar s to form matrix [B]

#### Example

$$s = 2 ; [A] = \begin{bmatrix} 2 & 3 \\ 1 & 4 \\ 3 & 2 \end{bmatrix} ; [B] = 2*[A] = \begin{bmatrix} 4 & 6 \\ 2 & 8 \\ 6 & 2 \end{bmatrix}$$

### DEFINE MATRIX MULTIPLY

We can multiply two matrices together. However, the number of columns of the matrix [A] must be the same as the number of rows of the matrix [B] in order to do this multiplication.

$$[C] = [A][B] \Rightarrow c_{ij} = [a_i] \{b_j\}$$
$$c_{ij} = \begin{bmatrix} a_{i1} & a_{i2} & \cdots & a_{ik} \end{bmatrix} \begin{bmatrix} b_{1j} \\ b_{2j} \\ \vdots \\ b_{kj} \end{bmatrix} \Rightarrow c_{ij} = \sum_k a_{ik} b_{kj}$$

Each term of the matrix [C] is made up of a row of the matrix [A] times a column of the matrix [B] which in essence is a dot product; an individual 'ij' term of the matrix [C] is formed from the summation of the multiplication of each sequential term of the row vector of the matrix [A] times each sequential term of the column vector of matrix [B].

#### Example

$$[A] = \begin{bmatrix} 1 & 2 & 3 \\ 0 & 1 & 0 \\ 1 & 0 & 1 \end{bmatrix} ; [B] = \begin{bmatrix} 1 & 0 & 0 & 0 & 1 \\ 0 & 1 & 0 & 1 & 0 \\ 0 & 0 & 1 & 0 & 0 \end{bmatrix}$$
$$[C] = [A][B] = \begin{bmatrix} 1 & 2 & 3 & 2 & 1 \\ 0 & 1 & 0 & 1 & 0 \\ 1 & 0 & 1 & 0 & 1 \end{bmatrix}$$



## MATRIX MULTIPLICATION RULES

The following rules of matrix multiplication apply

- ➔  $[A][B] = [C] \neq [B][A]$
- ➔  $[A]([B] + [C]) = [A][B] + [A][C]$
- ➔  $([A][B])[C] = [A]([B][C])$
- ➔  $[A][B] = [0]$  does not imply that  $[A] = [0]$  or  $[B] = [0]$  !!!
- ➔ Premultiplication of a matrix  $[A]$  by a diagonal matrix  $[D]$  multiplies the rows of matrix  $[A]$  by corresponding diagonal terms of the matrix  $[D]$

$$\begin{bmatrix} \ddots & & & & \\ & D & & & \\ & & \ddots & & \\ & & & \ddots & \\ & & & & \ddots \end{bmatrix} [A] = \begin{bmatrix} d_{11} [a_{11} \ a_{12} \ \cdots \ a_{1m}] \\ d_{22} [a_{21} \ a_{22} \ \cdots \ a_{2m}] \\ \vdots \\ d_{ii} [a_{i1} \ a_{i2} \ \cdots \ a_{im}] \\ \vdots \\ d_{nn} [a_{n1} \ a_{n2} \ \cdots \ a_{nm}] \end{bmatrix}$$

- ➔ Postmultiplication of a matrix  $[A]$  by a diagonal matrix  $[D]$  multiplies the columns of matrix  $[A]$  by corresponding diagonal terms of the matrix  $[D]$

$$[A] \begin{bmatrix} \ddots & & & & \\ & D & & & \\ & & \ddots & & \\ & & & \ddots & \\ & & & & \ddots \end{bmatrix} = \begin{bmatrix} \begin{Bmatrix} a_{11} \\ a_{21} \\ \vdots \\ a_{n1} \end{Bmatrix} \\ \begin{Bmatrix} a_{12} \\ a_{22} \\ \vdots \\ a_{n2} \end{Bmatrix} \\ \vdots \\ \begin{Bmatrix} a_{1i} \\ a_{2i} \\ \vdots \\ a_{ni} \end{Bmatrix} \end{bmatrix}$$

### Example

$$[A] = \begin{bmatrix} 1 & 2 & 3 \\ 2 & 4 & 6 \\ 3 & 6 & 9 \end{bmatrix} ; [D] = \begin{bmatrix} 3 & & \\ & 15 & \\ & & 1 \end{bmatrix}$$

$$[C] = [A][D] = \begin{bmatrix} 3 & 3 & 3 \\ 6 & 6 & 6 \\ 9 & 9 & 9 \end{bmatrix}$$



## TRANPOSE OF A MATRIX

We can define the tranpose of a matrix where the rows and columns are interchanged as follows

$$[A] = \begin{bmatrix} a_{11} & a_{12} \\ a_{21} & a_{22} \\ & & a_{ij} \end{bmatrix} \Rightarrow [B] = [A]^T = \begin{bmatrix} a_{11} & a_{21} \\ a_{12} & a_{22} \\ & & a_{ji} \end{bmatrix}$$

### Example

$$[A] = \begin{bmatrix} 1 & 2 \\ 3 & 4 \\ 5 & 6 \end{bmatrix} ; [A]^T = \begin{bmatrix} 1 & 3 & 5 \\ 2 & 4 & 6 \end{bmatrix}$$

## TRANSPOSITION RULES

The following rules of matrix transposition apply

- ➔  $([A] + [B])^T = [A]^T + [B]^T$
- ➔  $\left([A]^T\right)^T = [A]$
- ➔  $([A][B])^T = [B]^T[A]^T$
- ➔  $([A][B][C])^T = [C]^T[B]^T[A]^T$

## SYMMETRIC MATRIX RULES

The following rules apply for symmetric matrices; symmetric matrices are square and corresponding 'ij' terms are equal to 'ji' terms due to symmetry

- ➔  $[A] = [A]^T ; [B] = [B]^T ; [A][B] \neq ([A][B])^T$
- ➔  $[A] = [A]^T ; [C] = [B]^T[A][B] ; [C] = [C]^T$



## DEFINE A MATRIX INVERSE

We can define a matrix inverse as

$$[A]^{-1} = \frac{\text{Adj}[A]}{\det[A]} \quad ; \quad \text{Adj}[A] = [C]^T \quad \text{where } c_{ij} = (-1)^{(i+j)} \left| [M_{ij}] \right|$$

### Example

$$[A] = \begin{bmatrix} 2 & -1 \\ -1 & 1 \end{bmatrix} \Rightarrow [A]^{-1} = \begin{bmatrix} 1 & 1 \\ 1 & 2 \end{bmatrix}$$

## MATRIX INVERSE PROPERTIES

The following properties of matrix inverse apply

- ➔ If the inverse of  $[A]$  exists, then the matrix  $[A]$  is not singular
- ➔ If the inverse of  $[A]$  does not exist, the the matrix  $[A]$  is singular
- ➔  $\left[ [A]^{-1} \right]^{-1} = [A]$
- ➔  $([A][B])^{-1} = [B]^{-1}[A]^{-1}$

## DEFINE AN EIGENVALUE PROBLEM

We can decompose two square non-singular, symmetric matrices into their associated eigenvalues and eigenvectors using

$$[[A] - \lambda[B]]\{X\} = \{0\} \Rightarrow \omega_i^2; \{x_i\}$$

There will exist a pair of eigenvalue/eigenvector for as many equations as there are for the system

### Example

$$[A] = \begin{bmatrix} 2 & -1 \\ -1 & 1 \end{bmatrix} \quad ; \quad [B] = \begin{bmatrix} 1 & 0 \\ 0 & 1 \end{bmatrix} \Rightarrow \left[ \begin{bmatrix} 2 & -1 \\ -1 & 1 \end{bmatrix} - \lambda \begin{bmatrix} 1 & 0 \\ 0 & 1 \end{bmatrix} \right] \begin{Bmatrix} x_1 \\ x_2 \end{Bmatrix} = \begin{Bmatrix} 0 \\ 0 \end{Bmatrix}$$
$$\omega_1^2 = 0.382 \quad ; \quad \{x_1\} = \begin{Bmatrix} 0.5257 \\ 0.8507 \end{Bmatrix} \quad ; \quad \omega_2^2 = 2.618 \quad ; \quad \{x_1\} = \begin{Bmatrix} 0.8507 \\ -0.5257 \end{Bmatrix}$$



## GENERALIZED INVERSE

Any general rectangular matrix can be inverted, however when the number of rows or columns are not equal then the inverse is referred to as a generalized inverse

$$\begin{aligned}\{x\} &= [U]\{p\} \Rightarrow \{p\} = [U]^g \{x\} \\ [U]^g &= \left([U]^T [U]\right)^{-1} [U]^T\end{aligned}$$

The Moore-Penrose conditions of the generalized inverse are:

- ➔  $[U][U]^g[U] = [U]$
- ➔  $[U]^g[U][U]^g = [U]^g$
- ➔  $\left([U]^g[U]\right)^T = [U]^g[U]$
- ➔  $\left([U][U]^g\right)^T = [U][U]^g$

If all 4 of the Moore-Penrose conditions are met then this is a Pseudo Inverse

### Example

$$[x] = \begin{bmatrix} 1 & 2 \\ 3 & 4 \\ 5 & 6 \end{bmatrix} \Rightarrow [x]^g = \begin{bmatrix} -1.333 & -.333 & .667 \\ 1.083 & .333 & -.417 \end{bmatrix}$$



## SINGULAR VALUE DECOMPOSITION

Any matrix can be decomposed down into it's spectral parts (eigenvalues and eigenvectors)

$$[A] = [U][S][V]^T$$

$$[A] = \begin{bmatrix} \{u_1\} & \{u_2\} & \cdots \\ & s_1 & \\ & & s_2 \\ & & & \ddots \end{bmatrix} \begin{bmatrix} \{v_1\} & \{v_2\} & \cdots \end{bmatrix}^T$$

$$[A] = \{u_1\} s_1 \{v_1\}^T + \{u_2\} s_2 \{v_2\}^T + \cdots = \sum_{k=1}^n \{u_k\} s_k \{v_k\}^T$$

Example

$$\begin{bmatrix} 1 & 2 & 3 \\ 2 & 4 & 6 \\ 3 & 6 & 9 \end{bmatrix} = [A] = \{u_1\} s_1 \{u_1\}^T = \begin{bmatrix} 1 \\ 2 \\ 3 \end{bmatrix} \frac{1}{3} \begin{bmatrix} 1 & 2 & 3 \end{bmatrix}^T$$

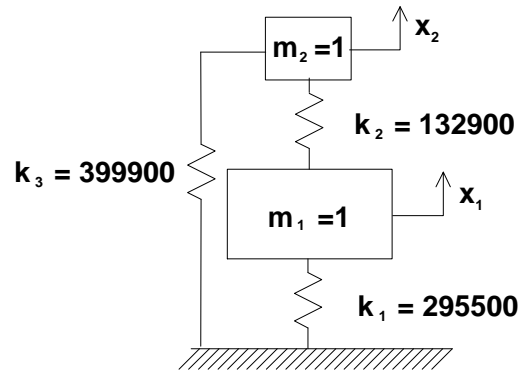
Example

$$\begin{bmatrix} 2 & 3 & 5 \\ 3 & 5 & 8 \\ 5 & 8 & 13 \end{bmatrix} = \{u_1\} s_1 \{v_1\}^T + \{u_2\} s_2 \{v_2\}^T = \begin{bmatrix} 1 \\ 2 \\ 3 \end{bmatrix} \frac{1}{3} \begin{bmatrix} 1 & 2 & 3 \end{bmatrix}^T + \begin{bmatrix} 1 \\ 1 \\ 2 \end{bmatrix} \frac{1}{2} \begin{bmatrix} 1 & 1 & 2 \end{bmatrix}^T$$

$$\begin{bmatrix} 1 & 2 & 3 \\ 2 & 4 & 6 \\ 3 & 6 & 9 \end{bmatrix} + \begin{bmatrix} 1 & 1 & 2 \\ 1 & 1 & 2 \\ 2 & 2 & 4 \end{bmatrix}$$



## EXAMPLE USING TWO DEGREE OF FREEDOM SYSTEM



Using the two degree of freedom system shown above, let's step through all the equations we have developed and compute the following items:

- Formulate the characteristic polynomial
- Find the eigenvalues
- Find the mode shape for mode 1 using BOTH equation 1 and 2 of the system
- Show that the modes are orthogonal wrt the system matrices
- Compute the modal mass and modal stiffness
- Normalize the mode shapes for unit modal mass

Performing a force balance for each mass in the system results in 2 equations which are

$$m_1 \ddot{x}_1 + k_1 x_1 - k_2 (x_2 - x_1) = f_1(t)$$

$$m_2 \ddot{x}_2 + k_3 x_2 + k_2 (x_2 - x_1) = f_2(t)$$

and when substituting in the values gives

$$\ddot{x}_1 + 428400x_1 - 132900x_2 = f_1(t)$$

$$\ddot{x}_2 - 132900x_1 + 532800x_2 = f_2(t)$$

This can be conveniently written in matrix form as

$$[M]\{\ddot{x}\} + [K]\{x\} = \begin{bmatrix} 1 & 0 \\ 0 & 1 \end{bmatrix} \begin{Bmatrix} \ddot{x}_1 \\ \ddot{x}_2 \end{Bmatrix} + \begin{bmatrix} 428400 & -132900 \\ -132900 & 532800 \end{bmatrix} \begin{Bmatrix} x_1 \\ x_2 \end{Bmatrix}$$



Now we recall that the eigen solution can be written as

$$[[\mathbf{K}] - \lambda[\mathbf{M}]]\{\mathbf{X}\} = \{0\} \quad \text{where } \lambda \text{ is the eigenvalue } \omega^2$$

If we substitute in the values for the mass and stiffness matrices for this equation we get

$$\begin{bmatrix} 428400 & -132900 \\ -132900 & 532800 \end{bmatrix} - \omega^2 \begin{bmatrix} 1 & 0 \\ 0 & 1 \end{bmatrix} \begin{Bmatrix} x_1 \\ x_2 \end{Bmatrix} = \begin{Bmatrix} 0 \\ 0 \end{Bmatrix}$$

Regrouping terms we get

$$\begin{bmatrix} (-\omega^2 + 428400) & -132900 \\ -132900 & (-\omega^2 + 532800) \end{bmatrix} \begin{Bmatrix} x_1 \\ x_2 \end{Bmatrix} = \begin{Bmatrix} 0 \\ 0 \end{Bmatrix}$$

Now the characteristic equation comes from

$$\det \begin{bmatrix} (-\omega^2 + 428400) & -132900 \\ -132900 & (-\omega^2 + 532800) \end{bmatrix} = 0$$

$$\text{which is } \omega^4 - 961200\omega^2 + 2.10588 \times 10^{11} = 0$$

Using the quadratic equation to solve this gives

$$\omega_1^2, \omega_2^2 = \frac{961200 \pm \sqrt{(961200)^2 - 4(1)(2.10588 \times 10^{11})}}{2}$$

which results in the eigenvalues of

$$\begin{aligned} \omega_1^2 = 337816 & \Rightarrow \omega_1 = 581 \text{ rad / sec} \Rightarrow f_1 = 92 \text{ Hz} \\ \omega_2^2 = 623384 & \Rightarrow \omega_2 = 790 \text{ rad / sec} \Rightarrow f_2 = 125 \text{ Hz} \end{aligned}$$



Now in order to find the mode shapes, let's write out the equation 1 and 2 from the system equation

$$(-\omega^2 + 428400)x_1 - 132900x_2 = 0 \quad \text{eq(1)}$$

$$-132900x_1 + (-\omega^2 + 532800)x_2 = 0 \quad \text{eq(2)}$$

Now in order to find the mode shape for mode 1, we can use either eq(1) or eq(2)

From eq(1), substitute in  $\omega_1$

$$(-337816 + 428400)x_1 - 132900x_2 = 0 \quad \Rightarrow \quad x_1 = 1.467x_2$$

From eq(2), substitute in  $\omega_1$

$$-132900x_1 + (-337816 + 532800)x_2 = 0 \quad \Rightarrow \quad x_1 = 1.467x_2$$

Now in order to find the mode shape for mode 2, we can use either eq(1) or eq(2)

From eq(1), substitute in  $\omega_2$

$$(-623384 + 428400)x_1 - 132900x_2 = 0 \quad \Rightarrow \quad x_1 = -0.682x_2$$

From eq(2), substitute in  $\omega_2$

$$-132900x_1 + (-623384 + 532800)x_2 = 0 \quad \Rightarrow \quad x_1 = -0.682x_2$$

So that the eigenvalues/vectors are

$$\begin{aligned} \begin{bmatrix} \omega_1^2 & \\ & \omega_2^2 \end{bmatrix} &= \begin{bmatrix} 337816 & 0 \\ 0 & 623384 \end{bmatrix} \\ \begin{bmatrix} u_1^{(1)} & u_1^{(2)} \\ u_2^{(1)} & u_2^{(2)} \end{bmatrix} &= \begin{bmatrix} 1 & 1 \\ 0.682 & -1.467 \end{bmatrix} \\ \left[ \begin{bmatrix} u_1 \\ u_2 \end{bmatrix} \right] &= \left[ \begin{bmatrix} u_1^{(1)} \\ u_2^{(1)} \end{bmatrix} \quad \begin{bmatrix} u_1^{(2)} \\ u_2^{(2)} \end{bmatrix} \right] = \left[ \begin{bmatrix} 1 \\ 0.682 \end{bmatrix} \quad \begin{bmatrix} 1 \\ -1.467 \end{bmatrix} \right] \end{aligned}$$



Now we recall that the 'ith' modal vector is orthogonal with respect to the 'jth' modal vector using the system matrices. Let's check this with the mass matrix.

$$\{u_j\}^T [M] \{u_i\} \stackrel{?}{=} 0 \Rightarrow \begin{Bmatrix} 1 & -1.467 \end{Bmatrix} \begin{bmatrix} 1 & 0 \\ 0 & 1 \end{bmatrix} \begin{Bmatrix} 1 \\ 0.682 \end{Bmatrix} \equiv 0$$

Now from the system equations we can write the modal mass and modal stiffness matrices

$$\begin{aligned} [U]^T [M] [U] &= \begin{bmatrix} 1 & 0.682 \\ 1 & -1.467 \end{bmatrix} \begin{bmatrix} 1 & 0 \\ 0 & 1 \end{bmatrix} \begin{bmatrix} 1 & 1 \\ 0.682 & -1.467 \end{bmatrix} = \begin{bmatrix} 1.465 & \\ & 3.152 \end{bmatrix} \\ [U]^T [K] [U] &= \begin{bmatrix} 1 & 0.682 \\ 1 & -1.467 \end{bmatrix} \begin{bmatrix} 428400 & -132900 \\ -132900 & 532800 \end{bmatrix} \begin{bmatrix} 1 & 1 \\ 0.682 & -1.467 \end{bmatrix} = \begin{bmatrix} 494900 & \\ & 1965000 \end{bmatrix} \end{aligned}$$

Now if I normalize the mode shapes to unit modal mass (recall that the normalized mode shapes are the original mode shapes post multiplied by one over the square root of the modal mass), then the mode shape matrix becomes

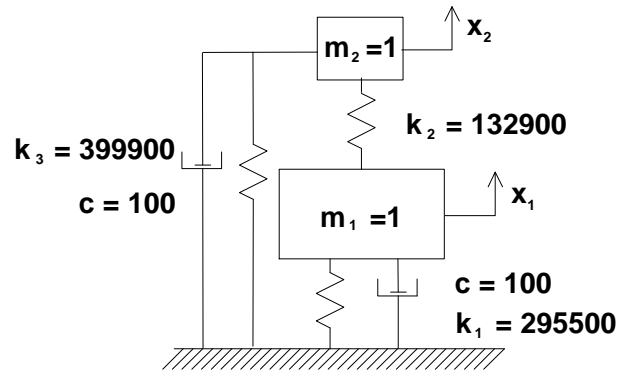
$$[U^n] = [U] [N] = \begin{bmatrix} 1 & 1 \\ 0.682 & -1.467 \end{bmatrix} \begin{bmatrix} \sqrt{\frac{1}{1.465}} & \\ & \sqrt{\frac{1}{3.152}} \end{bmatrix} = \begin{bmatrix} 0.826 & 0.563 \\ 0.563 & -0.826 \end{bmatrix}$$

and the modal mass and modal stiffness matrices become

$$\begin{aligned} [U^n]^T [M] [U^n] &= \begin{bmatrix} 0.826 & 0.563 \\ 0.563 & -0.826 \end{bmatrix} \begin{bmatrix} 1 & 0 \\ 0 & 1 \end{bmatrix} \begin{bmatrix} 0.826 & 0.563 \\ 0.563 & -0.826 \end{bmatrix} = \begin{bmatrix} 1 & \\ & 1 \end{bmatrix} \\ [U^n]^T [K] [U^n] &= \begin{bmatrix} 0.826 & 0.563 \\ 0.563 & -0.826 \end{bmatrix} \begin{bmatrix} 428400 & -132900 \\ -132900 & 532800 \end{bmatrix} \begin{bmatrix} 0.826 & 0.563 \\ 0.563 & -0.826 \end{bmatrix} = \begin{bmatrix} 337816 & \\ & 623384 \end{bmatrix} \end{aligned}$$



## EXAMPLE USING TWO DEGREE OF FREEDOM SYSTEM



Using the two degree of freedom system shown above (same as the one used previously but now damping has been added), let's step through rest of the equations we have developed and compute the following items:

- Formulate the characteristic polynomial and the resulting poles of the system
- Formulate the system transfer matrix the residue matrix and the frequency response matrix
- Compute the residues for the first column of the system matrix for mode 1 and 2
- Compute the modal mass, modal damping and modal stiffness matrices using the normalized mode shapes from the eigenvalue problem done previously

Performing a force balance for each mass in the system results in 2 equations which are shown below (written in matrix form)

$$[M]\{\ddot{x}\} + [C]\{\dot{x}\} + [K]\{x\} = \begin{bmatrix} 1 & 0 \\ 0 & 1 \end{bmatrix} \begin{Bmatrix} \ddot{x}_1 \\ \ddot{x}_2 \end{Bmatrix} + \begin{bmatrix} 100 & 0 \\ 0 & 100 \end{bmatrix} \begin{Bmatrix} \dot{x}_1 \\ \dot{x}_2 \end{Bmatrix} + \begin{bmatrix} 428400 & -132900 \\ -132900 & 532800 \end{bmatrix} \begin{Bmatrix} x_1 \\ x_2 \end{Bmatrix}$$



Now we can write the System Matrix as

$$[B(s)] = [M]s^2 + [C]s + [K] = \begin{bmatrix} 1 & 0 \\ 0 & 1 \end{bmatrix} s^2 + \begin{bmatrix} 100 & 0 \\ 0 & 100 \end{bmatrix} s + \begin{bmatrix} 428400 & -132900 \\ -132900 & 532800 \end{bmatrix}$$

Now the characteristic equation comes from

$$\det[B(s)] = 0 \Rightarrow \det \begin{bmatrix} (s^2 + 100s + 428400) & -132900 \\ -132900 & (s^2 + 100s + 532800) \end{bmatrix} = 0$$

$$(s^2 + 100s + 428400)(s^2 + 100s + 532800) - (132900)^2 = 0$$

$$s^4 + 200s^3 + 971200s^2 + 96120000s + 21058911000 = 0$$

Solving this gives the roots or poles of the system as

$$p_1 = -50 + j579, p_1^* = -50 - j579, p_2 = -50 + j788, p_2^* = -50 - j788$$

Now the System Transfer matrix is

$$[H(s)] = [B(s)]^{-1} = \frac{\text{Adj}[B(s)]}{\det[B(s)]} = \frac{\begin{bmatrix} (s^2 + 100s + 532800) & 132900 \\ 132900 & (s^2 + 100s + 428400) \end{bmatrix}}{\det[B(s)]}$$

or as

$$[H(s)] = [B(s)]^{-1} = \frac{\text{Adj}[B(s)]}{\det[B(s)]} = \frac{\begin{bmatrix} (s^2 + 100s + 532800) & 132900 \\ 132900 & (s^2 + 100s + 428400) \end{bmatrix}}{(s - p_1)(s - p_1^*)(s - p_2)(s - p_2^*)}$$



and we can write out each term of the System Transfer Matrix as

$$h_{11}(s) = \frac{(s^2 + 100s + 532800)}{\det[B(s)]}$$

$$h_{12}(s) = \frac{132900}{\det[B(s)]}$$

$$h_{21}(s) = \frac{132900}{\det[B(s)]}$$

$$h_{22}(s) = \frac{(s^2 + 100s + 428400)}{\det[B(s)]}$$

or as

$$h_{11}(s) = \frac{(s^2 + 100s + 532800)}{(s - p_1)(s - p_1^*)(s - p_2)(s - p_2^*)}$$

$$h_{12}(s) = \frac{132900}{(s - p_1)(s - p_1^*)(s - p_2)(s - p_2^*)}$$

$$h_{21}(s) = \frac{132900}{(s - p_1)(s - p_1^*)(s - p_2)(s - p_2^*)}$$

$$h_{22}(s) = \frac{(s^2 + 100s + 428400)}{(s - p_1)(s - p_1^*)(s - p_2)(s - p_2^*)}$$



Let's compute the residues for each mode of the system for the 1-1 term of the matrix

$$a_{11k}(s) = h_{11}(s)(s - p_k) \Big|_{s \rightarrow p_k} = \frac{(s^2 + 100s + 532800)}{(s - p_1)(s - p_1^*)(s - p_2)(s - p_2^*)} (s - p_k)$$

Now for pole 1,  $p_1 = -50 + j579$ , (and it's conjugate  $p_1^* = -50 - j579$ ), the residue for the 1-1 term becomes

$$a_{111}(p_1) = \frac{(p_1^2 + 100p_1 + 532800)}{(p_1 - p_1^*)(p_1 - p_2)(p_1 - p_2^*)} = 0.11791 \times 10^{-2} / 2j \quad a_{11k}^*(p_1^*) = -0.11791 \times 10^{-2} / 2j$$

and for pole 2,  $p_2 = -50 + j788$  (and it's conjugate  $p_2^* = -50 - j788$ ), the residue for the 1-1 term becomes

$$a_{112}(p_2) = \frac{(p_2^2 + 100p_2 + 532800)}{(p_2 - p_1)(p_2 - p_1^*)(p_2 - p_2^*)} = 0.4025 \times 10^{-3} / 2j \quad a_{112}^*(p_2^*) = -0.4025 \times 10^{-3} / 2j$$

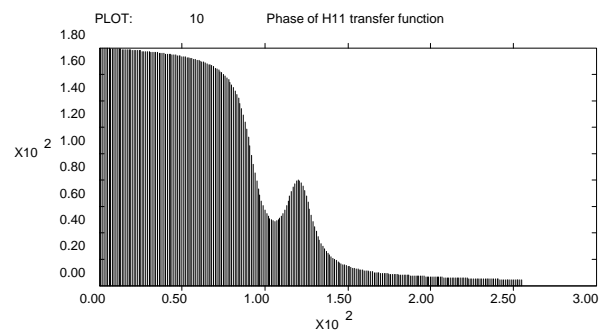
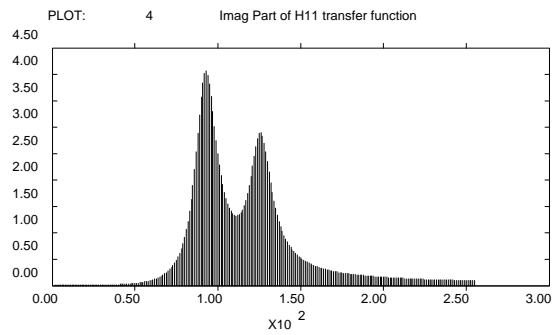
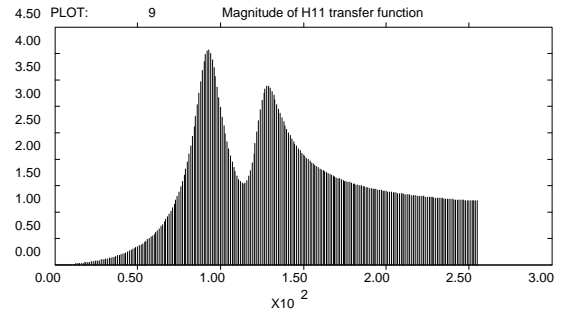
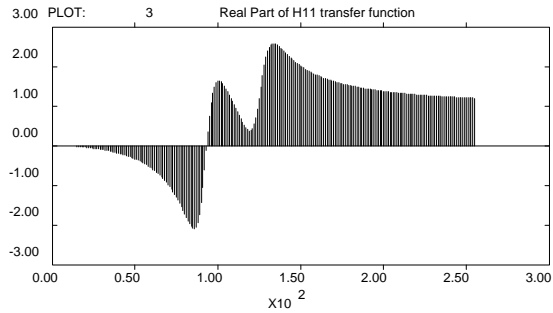
and now since we have the residues we can write the system transfer function for the 1-1 term as

$$h_{11}(s) = \sum_{k=1}^2 \left[ \frac{a_{11k}}{(s - p_k)} + \frac{a_{11k}^*}{(s - p_k^*)} \right] = \frac{a_{111}}{(s - p_1)} + \frac{a_{111}^*}{(s - p_1^*)} + \frac{a_{112}}{(s - p_2)} + \frac{a_{112}^*}{(s - p_2^*)}$$

$$h_{11}(s) = \frac{0.11791 \times 10^{-2} / 2j}{(s - (-50 + j579))} + \frac{-0.11791 \times 10^{-2} / 2j}{(s - (-50 - j579))} + \frac{0.4025 \times 10^{-3} / 2j}{(s - (-50 + j788))} + \frac{-0.4025 \times 10^{-3} / 2j}{(s - (-50 - j788))}$$



## MODEL TTA - FREQUENCY RESPONSE FUNCTION - H11





Let's compute the residues for each mode of the system for the 2-1 term of the matrix

$$a_{21k}(s) = h_{21}(s)(s - p_k) \Big|_{s \rightarrow p_k} = \frac{132900}{(s - p_1)(s - p_1^*)(s - p_2)(s - p_2^*)}(s - p_k)$$

Now for pole 1,  $p_1 = -50 + j579$ , (and it's conjugate  $p_1^* = -50 - j579$ ), the residue for the 2-1 term becomes

$$a_{211}(p_1) = \frac{(p_1^2 + 100p_1 + 532800)}{(p_1 - p_1^*)(p_1 - p_2)(p_1 - p_2^*)} = 0.8037 \times 10^{-3} / 2j \quad a_{211}^*(p_1^*) = -0.8037 \times 10^{-3} / 2j$$

and for pole 2,  $p_2 = -50 + j788$  (and it's conjugate  $p_2^* = -50 - j788$ ), the residue for the 2-1 term becomes

$$a_{212}(p_2) = \frac{(p_2^2 + 100p_2 + 532800)}{(p_2 - p_1)(p_2 - p_1^*)(p_2 - p_2^*)} = 0.5906 \times 10^{-3} / 2j \quad a_{212}^*(p_2^*) = -0.5906 \times 10^{-3} / 2j$$

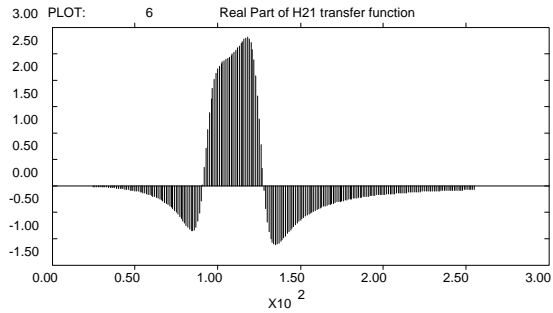
and now since we have the residues we can write the system transfer function for the 2-1 term as

$$h_{21}(s) = \sum_{k=1}^2 \left[ \frac{a_{21k}}{(s - p_k)} + \frac{a_{21k}^*}{(s - p_k^*)} \right] = \frac{a_{211}}{(s - p_1)} + \frac{a_{211}^*}{(s - p_1^*)} + \frac{a_{212}}{(s - p_2)} + \frac{a_{212}^*}{(s - p_2^*)}$$

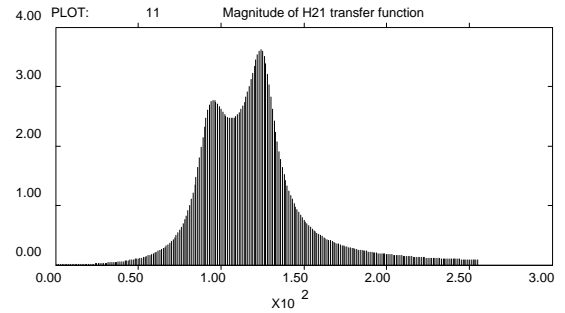
$$h_{21}(s) = \frac{0.8037 \times 10^{-3} / 2j}{(s - (-50 + j579))} + \frac{-0.8037 \times 10^{-3} / 2j}{(s - (-50 - j579))} + \frac{0.5906 \times 10^{-3} / 2j}{(s - (-50 + j788))} + \frac{-0.5906 \times 10^{-3} / 2j}{(s - (-50 - j788))}$$



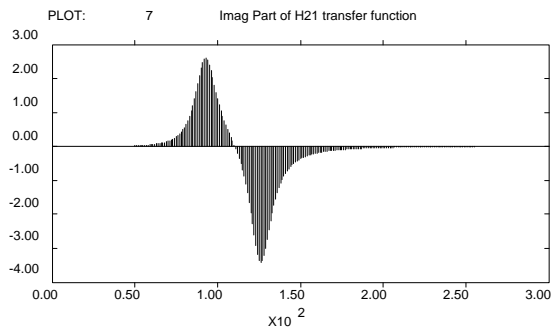
## MODEL TTA - FREQUENCY RESPONSE FUNCTION - H21



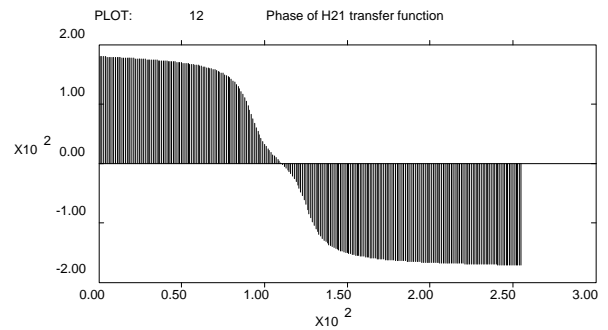
Two DOF system model, Frequency Response Functions



Two DOF system model, Frequency Response Functions



Two DOF system model, Frequency Response Functions



Two DOF system model, Frequency Response Functions



Recall that the eigenvalues/vectors from the undamped solution were

$$\begin{bmatrix} \omega_1^2 & \\ & \omega_2^2 \end{bmatrix} = \begin{bmatrix} 337816 & 0 \\ 0 & 623384 \end{bmatrix}$$

$$\begin{bmatrix} u_1^{(1)} & u_1^{(2)} \\ u_2^{(1)} & u_2^{(2)} \end{bmatrix} = \begin{bmatrix} 1 & 1 \\ 0.682 & -1.467 \end{bmatrix}$$

$$\left\{ \begin{bmatrix} u_1 \\ u_2 \end{bmatrix} \right\} = \left\{ \begin{bmatrix} u_1^{(1)} \\ u_2^{(1)} \end{bmatrix} \right\} \left\{ \begin{bmatrix} u_1^{(2)} \\ u_2^{(2)} \end{bmatrix} \right\} = \left\{ \begin{bmatrix} 1 \\ 0.682 \end{bmatrix} \right\} \left\{ \begin{bmatrix} 1 \\ -1.467 \end{bmatrix} \right\}$$

and the normalized mode shapes were

$$[U^n] = [U][N] = \begin{bmatrix} 1 & 1 \\ 0.682 & -1.467 \end{bmatrix} \begin{bmatrix} \sqrt{\frac{1}{1.465}} & \\ & \sqrt{\frac{1}{3.152}} \end{bmatrix} = \begin{bmatrix} 0.826 & 0.563 \\ 0.563 & -0.826 \end{bmatrix}$$

The modal mass and modal stiffness matrices written earlier are

$$[U^n]^T [M] [U^n] = \begin{bmatrix} 0.826 & 0.563 \\ 0.563 & -0.826 \end{bmatrix} \begin{bmatrix} 1 & 0 \\ 0 & 1 \end{bmatrix} \begin{bmatrix} 0.826 & 0.563 \\ 0.563 & -0.826 \end{bmatrix} = \begin{bmatrix} 1 & \\ & 1 \end{bmatrix}$$

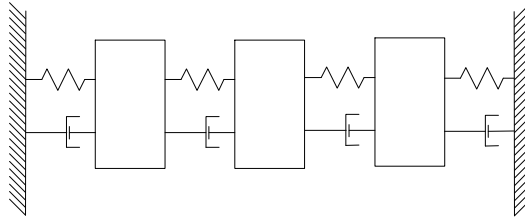
$$[U^n]^T [K] [U^n] = \begin{bmatrix} 0.826 & 0.563 \\ 0.563 & -0.826 \end{bmatrix} \begin{bmatrix} 428400 & -132900 \\ -132900 & 532800 \end{bmatrix} \begin{bmatrix} 0.826 & 0.563 \\ 0.563 & -0.826 \end{bmatrix} = \begin{bmatrix} 337816 & \\ & 623384 \end{bmatrix}$$

and now we can write the modal damping matrix as

$$[U^n]^T [C] [U^n] = \begin{bmatrix} 0.826 & 0.563 \\ 0.563 & -0.826 \end{bmatrix} \begin{bmatrix} 100 & 0 \\ 0 & 100 \end{bmatrix} \begin{bmatrix} 0.826 & 0.563 \\ 0.563 & -0.826 \end{bmatrix} = \begin{bmatrix} 100 & \\ & 100 \end{bmatrix}$$



## EXAMPLE USING THREE DEGREE OF FREEDOM SYSTEM



Using the three degree of freedom system shown above some additional equations will be written to illustrate some additional key points.

- Formulate the equations of motion of the system
- Formulate the eigensolution and find the eigenvalues/eigenvectors
- Formulate the equations of motion in modal space
- Compute the residue matrix and show the frequency response functions
- Compute the scaling factors using real normal modes
- Compute the scaling factors using complex modes (might be too much for them)

### Equations of Motion

$$[M]\{\ddot{x}\} + [C]\{\dot{x}\} + [K]\{x\} = [F(t)]$$

$$\begin{bmatrix} 1 & & \\ & 1 & \\ & & 1 \end{bmatrix} \begin{Bmatrix} \ddot{x}_1 \\ \ddot{x}_2 \\ \ddot{x}_3 \end{Bmatrix} + \begin{bmatrix} 0.2 & -0.1 & \\ -0.1 & 0.2 & -0.1 \\ & -0.1 & 0.2 \end{bmatrix} \begin{Bmatrix} \dot{x}_1 \\ \dot{x}_2 \\ \dot{x}_3 \end{Bmatrix} + \begin{bmatrix} 20000 & -10000 & \\ -10000 & 20000 & -10000 \\ & -10000 & 20000 \end{bmatrix} \begin{Bmatrix} x_1 \\ x_2 \\ x_3 \end{Bmatrix} = \begin{Bmatrix} f_1 \\ f_2 \\ f_3 \end{Bmatrix}$$

### Eigensolution

$$[[K] - \lambda[M]]\{X\} = \{0\}$$

$$[\Omega^2] = \begin{bmatrix} 5858 & & \\ & 20000 & \\ & & 34142 \end{bmatrix} ; [U] = [\{u_1\} \quad \{u_2\} \quad \{u_3\}] = \begin{bmatrix} \begin{Bmatrix} 0.500 \\ 0.707 \\ 0.500 \end{Bmatrix} & \begin{Bmatrix} 0.707 \\ 0 \\ -0.707 \end{Bmatrix} & \begin{Bmatrix} -0.500 \\ 0.707 \\ -0.500 \end{Bmatrix} \end{bmatrix}$$

### Equations of Motion - Modal Space

$$\begin{bmatrix} \ddots & & \\ & \bar{M} & \\ & & \ddots \end{bmatrix} \begin{Bmatrix} \ddot{p}_1 \\ \ddot{p}_2 \\ \ddot{p}_3 \end{Bmatrix} + \begin{bmatrix} \ddots & & \\ & \bar{C} & \\ & & \ddots \end{bmatrix} \begin{Bmatrix} \dot{p}_1 \\ \dot{p}_2 \\ \dot{p}_3 \end{Bmatrix} + \begin{bmatrix} \ddots & & \\ & \bar{K} & \\ & & \ddots \end{bmatrix} \begin{Bmatrix} p_1 \\ p_2 \\ p_3 \end{Bmatrix} = \begin{Bmatrix} \bar{f}_1 \\ \bar{f}_2 \\ \bar{f}_3 \end{Bmatrix}$$

$$\begin{bmatrix} 1 & & \\ & 1 & \\ & & 1 \end{bmatrix} \begin{Bmatrix} \ddot{p}_1 \\ \ddot{p}_2 \\ \ddot{p}_3 \end{Bmatrix} + \begin{bmatrix} 0.058 & & \\ & 0.200 & \\ & & 0.341 \end{bmatrix} \begin{Bmatrix} \dot{p}_1 \\ \dot{p}_2 \\ \dot{p}_3 \end{Bmatrix} + \begin{bmatrix} 5858 & & \\ & 20000 & \\ & & 34142 \end{bmatrix} \begin{Bmatrix} p_1 \\ p_2 \\ p_3 \end{Bmatrix} = \begin{Bmatrix} \bar{f}_1 \\ \bar{f}_2 \\ \bar{f}_3 \end{Bmatrix}$$



Now complex pole solution gives the following pole information

Mode	$\omega$ (Hz)	$\omega$ (Hz)	$\zeta$ % critical	Complex pole (rad/sec)
1	12.18	12.18	0.038%	$-0.029 \pm j 76.537$
2	22.51	22.51	0.071%	$-0.100 \pm j 141.42$
3	29.41	29.41	0.092%	$-0.171 \pm j 184.78$

Now the residues (note that these are R and not A) for the first column of the frequency response matrix is

	Mode 1	Mode 2	Mode 3
$h_{11}$	$0.003266 \pm j 0.0$	$0.003536 \pm j 0.0$	$0.001353 \pm j 0.0$
$h_{21}$	$0.004619 \pm j 0.0$	$0.0 \pm j 0.0$	$0.001913 \pm j 0.0$
$h_{31}$	$0.003266 \pm j 0.0$	$-0.003536 \pm j 0.0$	$0.001353 \pm j 0.0$

Now the residues for the first column of the frequency response matrix is

$$h_{11} = \frac{0.003266 + j0}{j\omega - (-0.029 + 76.537)} + \frac{0.003266 - j0}{j\omega - (-0.029 - 76.537)} + \frac{0.003536 + j0}{j\omega - (-0.100 + 141.42)} + \frac{0.003536 - j0}{j\omega - (-0.100 - 141.42)} + \frac{0.001353 + j0}{j\omega - (-0.171 + 184.78)} + \frac{0.001353 - j0}{j\omega - (-0.171 - 184.78)}$$

$$h_{21} = \frac{0.004619 + j0}{j\omega - (-0.029 + 76.537)} + \frac{0.004619 - j0}{j\omega - (-0.029 - 76.537)} + \frac{0.0 + j0}{j\omega - (-0.100 + 141.42)} + \frac{0.0 - j0}{j\omega - (-0.100 - 141.42)} + \frac{0.001913 + j0}{j\omega - (-0.171 + 184.78)} + \frac{0.001913 - j0}{j\omega - (-0.171 - 184.78)}$$

$$h_{31} = \frac{0.003266 + j0}{j\omega - (-0.029 + 76.537)} + \frac{0.003266 - j0}{j\omega - (-0.029 - 76.537)} + \frac{-0.003536 + j0}{j\omega - (-0.100 + 141.42)} + \frac{-0.003536 - j0}{j\omega - (-0.100 - 141.42)} + \frac{0.001353 + j0}{j\omega - (-0.171 + 184.78)} + \frac{0.001353 - j0}{j\omega - (-0.171 - 184.78)}$$



Now the residues can be computed using real normal modes as follows. Recall that the residue matrix is

$$\begin{bmatrix} r_{11} & r_{12} & r_{13} \\ r_{21} & r_{22} & r_{23} \\ r_{31} & r_{32} & r_{33} \end{bmatrix}^{(k)} = \frac{1}{\bar{m}_k \bar{\omega}_k} \begin{bmatrix} u_1 u_1 & u_1 u_2 & u_1 u_3 \\ u_2 u_1 & u_2 u_2 & u_2 u_3 \\ u_3 u_1 & u_3 u_2 & u_3 u_3 \end{bmatrix}^{(k)}$$

Recall for a drive point measurement, we can compute

- modal mass  $\bar{m}_k = \frac{1}{q_k \bar{\omega}_k}$
- modal damping  $\bar{c}_k = 2\sigma_k \bar{m}_k$
- modal stiffness  $\bar{k}_k = (\sigma_k^2 + \bar{\omega}_k^2) \bar{m}_k$

Now using unit modal mass scaling, the first column of the frequency response matrix can be written as

$$\begin{Bmatrix} r_{11} \\ r_{21} \\ r_{31} \end{Bmatrix}^{(k)} = q_k \begin{Bmatrix} u_1 u_1 \\ u_2 u_1 \\ u_3 u_1 \end{Bmatrix}^{(k)} = q_k u_1 \begin{Bmatrix} u_1 \\ u_2 \\ u_3 \end{Bmatrix}^{(k)}$$

For Mode 1,

$$\begin{Bmatrix} 0.32664E-2 \\ 0.46194E-2 \\ 0.32664E-2 \end{Bmatrix} = \begin{Bmatrix} r_{11} \\ r_{21} \\ r_{31} \end{Bmatrix}^{(1)} = q_1 u_1 \begin{Bmatrix} u_1 \\ u_2 \\ u_3 \end{Bmatrix}^{(1)} = \frac{1}{76.537} (0.500) \begin{Bmatrix} 0.500 \\ 0.707 \\ 0.500 \end{Bmatrix}$$

For Mode 2,

$$\begin{Bmatrix} 0.3536E-2 \\ 0.0 \\ -0.3536E-2 \end{Bmatrix} = \begin{Bmatrix} r_{11} \\ r_{21} \\ r_{31} \end{Bmatrix}^{(2)} = q_2 u_1 \begin{Bmatrix} u_1 \\ u_2 \\ u_3 \end{Bmatrix}^{(2)} = \frac{1}{141.42} (0.707) \begin{Bmatrix} 0.707 \\ 0.0 \\ 0.707 \end{Bmatrix}$$

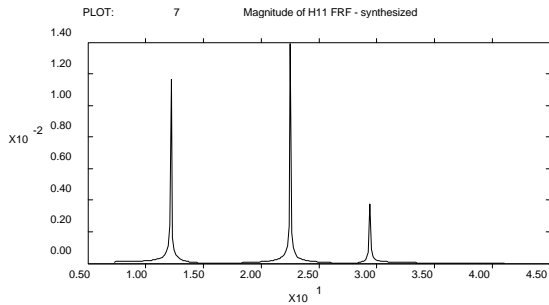
For Mode 3,

$$\begin{Bmatrix} 0.13530E-2 \\ -0.19134E-2 \\ 0.13530E-2 \end{Bmatrix} = \begin{Bmatrix} r_{11} \\ r_{21} \\ r_{31} \end{Bmatrix}^{(3)} = q_3 u_1 \begin{Bmatrix} u_1 \\ u_2 \\ u_3 \end{Bmatrix}^{(3)} = \frac{1}{184.78} (-0.500) \begin{Bmatrix} -0.500 \\ 0.707 \\ -0.500 \end{Bmatrix}$$

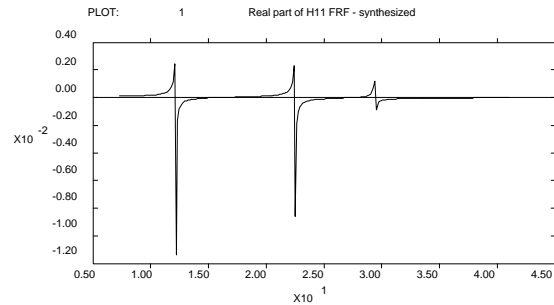


## MTU ANALOG - FREQUENCY RESPONSE FUNCTION - H11

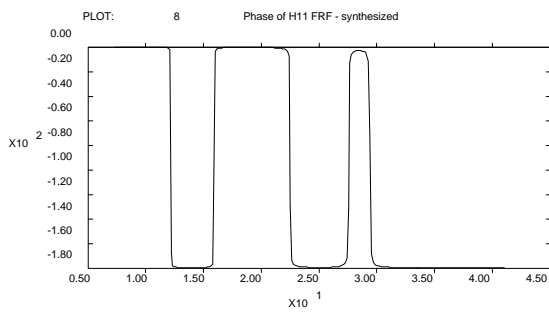
$$h_{11} = \frac{0.003266 + j0}{j\omega - (-0.029 + 76.537)} + \frac{0.003266 - j0}{j\omega - (-0.029 - 76.537)} \\ + \frac{0.003536 + j0}{j\omega - (-0.100 + 141.42)} + \frac{0.003536 - j0}{j\omega - (-0.100 - 141.42)} \\ + \frac{0.001353 + j0}{j\omega - (-0.171 + 184.78)} + \frac{0.001353 - j0}{j\omega - (-0.171 - 184.78)}$$



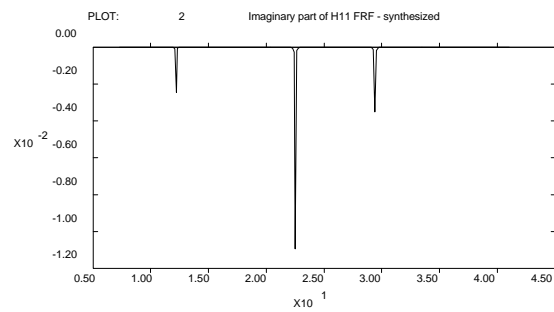
3 DOF ANALOG MODEL



3 DOF ANALOG MODEL



3 DOF ANALOG MODEL

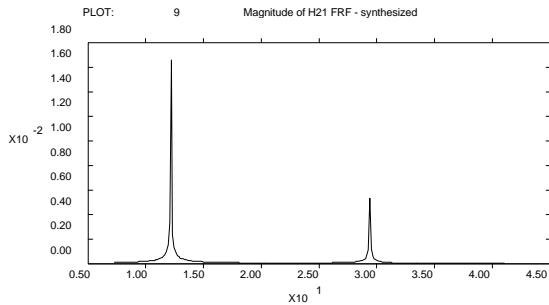


3 DOF ANALOG MODEL

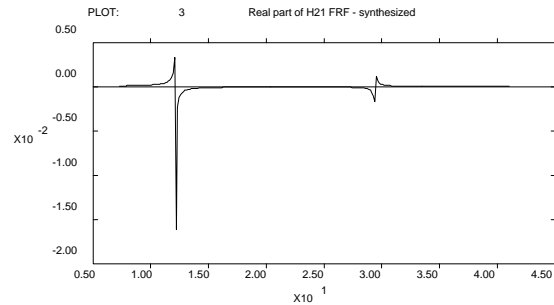


## MTU ANALOG - FREQUENCY RESPONSE FUNCTION - H21

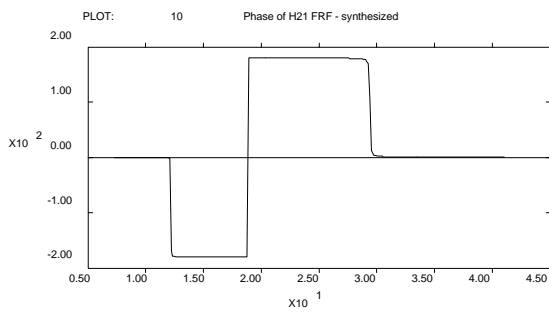
$$h_{21} = \frac{0.004619 + j0}{j\omega - (-0.029 + 76.537)} + \frac{0.004619 - j0}{j\omega - (-0.029 - 76.537)} + \frac{0.0 + j0}{j\omega - (-0.100 + 141.42)} + \frac{0.0 - j0}{j\omega - (-0.100 - 141.42)} + \frac{0.001913 + j0}{j\omega - (-0.171 + 184.78)} + \frac{0.001913 - j0}{j\omega - (-0.171 - 184.78)}$$



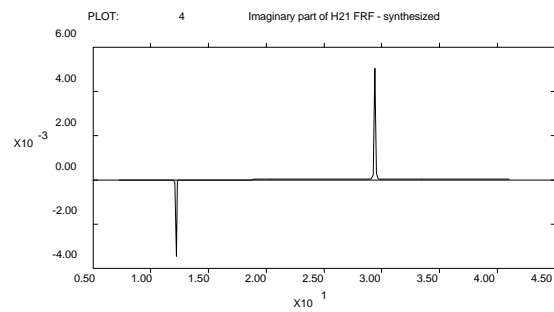
3 DOF ANALOG MODEL



3 DOF ANALOG MODEL



3 DOF ANALOG MODEL

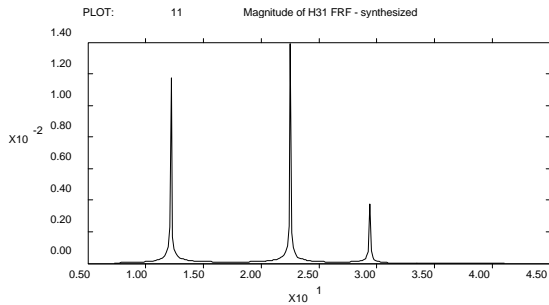


3 DOF ANALOG MODEL

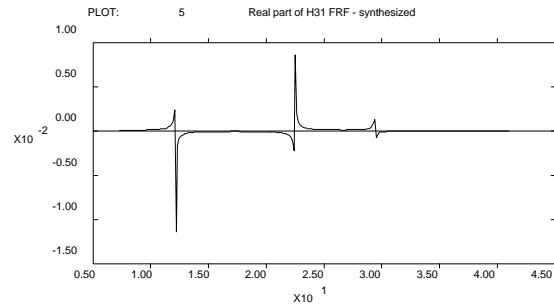


## MTU ANALOG - FREQUENCY RESPONSE FUNCTION - H31

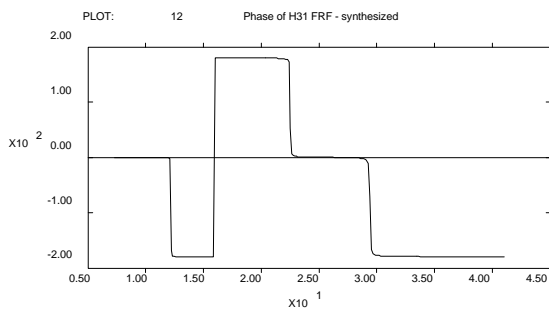
$$h_{31} = \frac{0.003266 + j0}{j\omega - (-0.029 + 76.537)} + \frac{0.003266 - j0}{j\omega - (-0.029 - 76.537)} \\ + \frac{-0.003536 + j0}{j\omega - (-0.100 + 141.42)} + \frac{-0.003536 - j0}{j\omega - (-0.100 - 141.42)} \\ + \frac{0.001353 + j0}{j\omega - (-0.171 + 184.78)} + \frac{0.001353 - j0}{j\omega - (-0.171 - 184.78)}$$



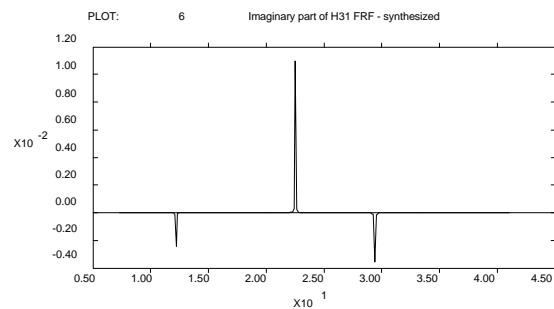
3 DOF ANALOG MODEL



3 DOF ANALOG MODEL



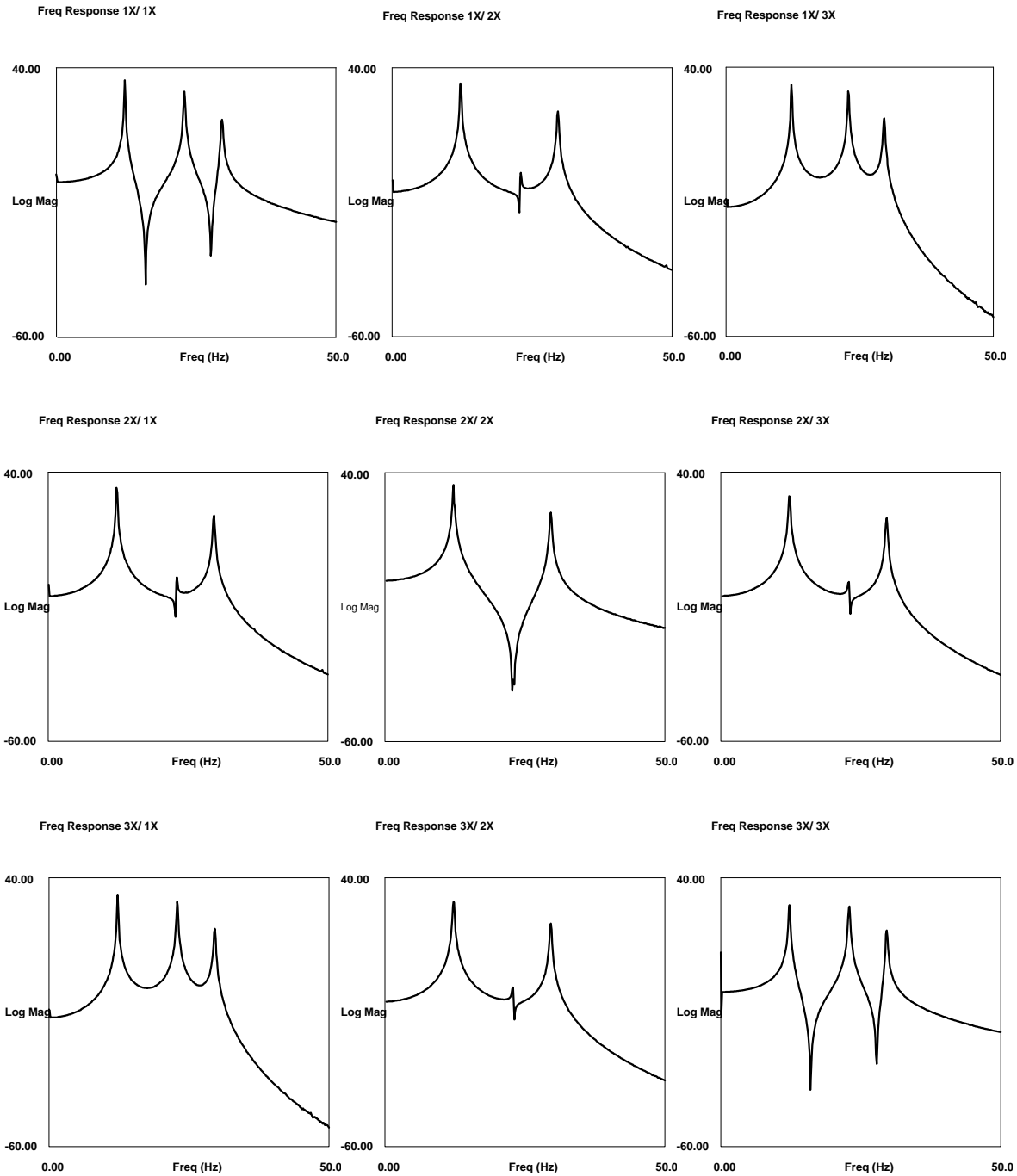
3 DOF ANALOG MODEL



3 DOF ANALOG MODEL



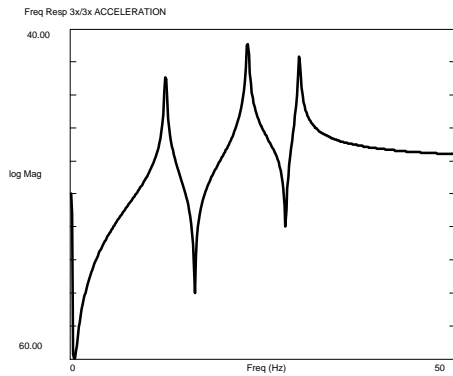
# MTU ANALOG - FREQUENCY RESPONSE FUNCTION MATRIX



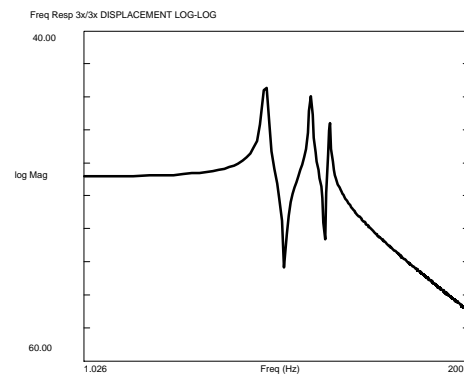
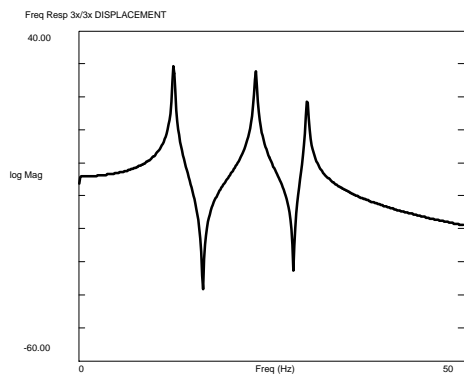
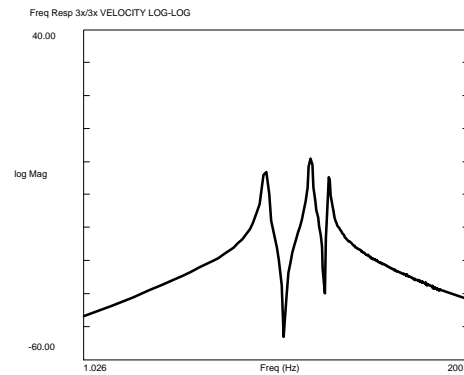
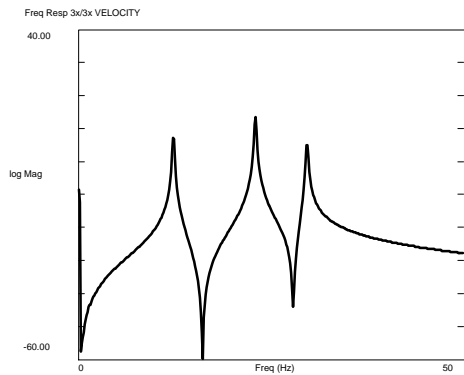
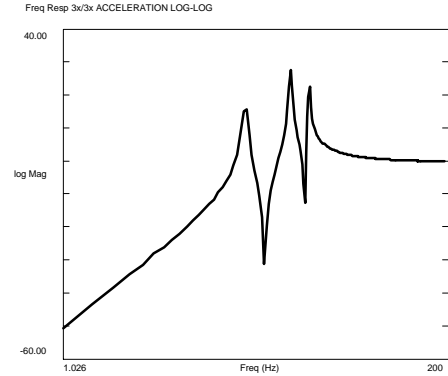


# MTU ANALOG - FREQUENCY RESPONSE FUNCTION ACCELERATION / VELOCITY / DISPLACEMENT PLOTS

## LOG AMP VS FREQUENCY

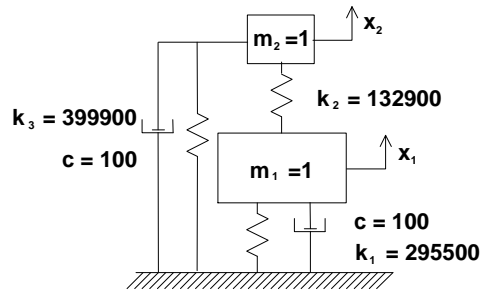


## LOG AMP VS LOG FREQUENCY





## EXAMPLE USING TWO DEGREE OF FREEDOM SYSTEM



Using FRF measurements from the two degree of freedom system shown above, let's step through the modal parameter estimation process and compute system poles and residues (the poles and residues are extracted from the measured FRFs). A summary of some of the pertinent equations previously computed from an analytical model are shown below for reference.

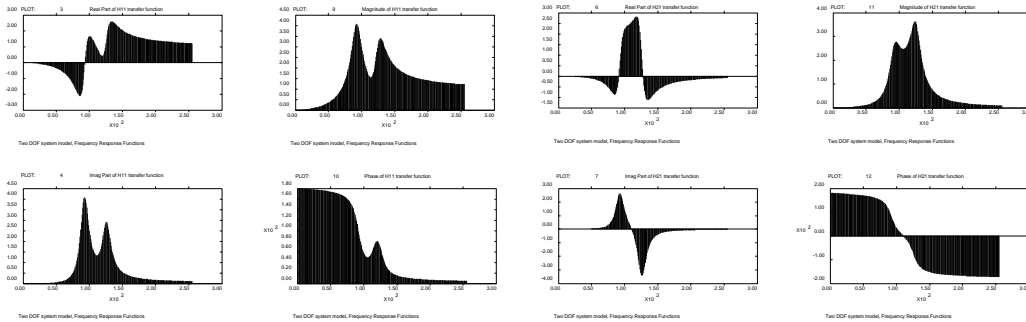
$$[B(s)] = [M]s^2 + [C]s + [K] = \begin{bmatrix} 1 & 0 \\ 0 & 1 \end{bmatrix} s^2 + \begin{bmatrix} 100 & 0 \\ 0 & 100 \end{bmatrix} s + \begin{bmatrix} 428400 & -132900 \\ -132900 & 532800 \end{bmatrix}$$

**H11**

$$h_{11}(s) = \frac{(s^2 + 100s + 532800)}{(s - p_1)(s - p_1^*)(s - p_2)(s - p_2^*)}$$

**H12**

$$h_{21}(s) = \frac{132900}{(s - p_1)(s - p_1^*)(s - p_2)(s - p_2^*)}$$



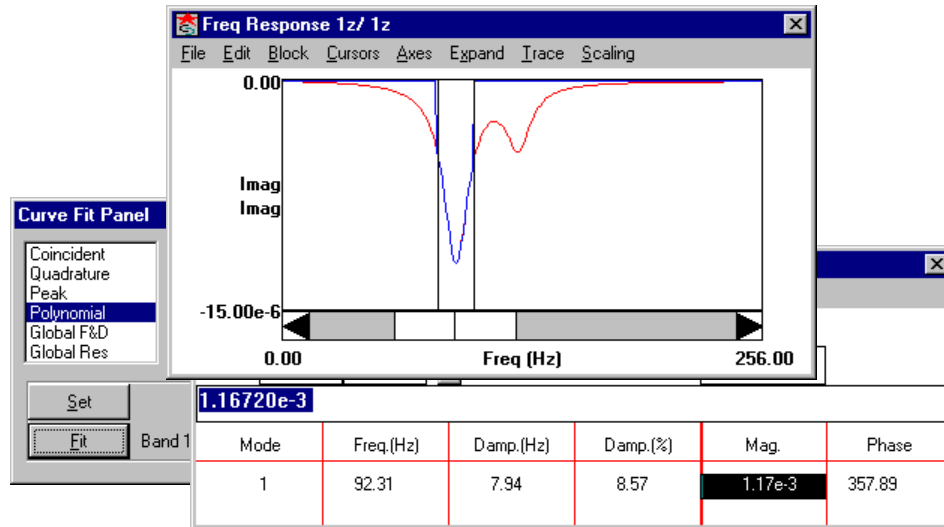
$$h_{11}(s) = \frac{0.11791 \times 10^{-2} / 2j}{(s - (-50 + j579))} + \frac{-0.11791 \times 10^{-2} / 2j}{(s - (-50 - j579))} + \frac{0.4025 \times 10^{-3} / 2j}{(s - (-50 + j788))} + \frac{-0.4025 \times 10^{-3} / 2j}{(s - (-50 - j788))}$$

$$h_{21}(s) = \frac{0.8037 \times 10^{-3} / 2j}{(s - (-50 + j579))} + \frac{-0.8037 \times 10^{-3} / 2j}{(s - (-50 - j579))} + \frac{0.5906 \times 10^{-3} / 2j}{(s - (-50 + j788))} + \frac{-0.5906 \times 10^{-3} / 2j}{(s - (-50 - j788))}$$



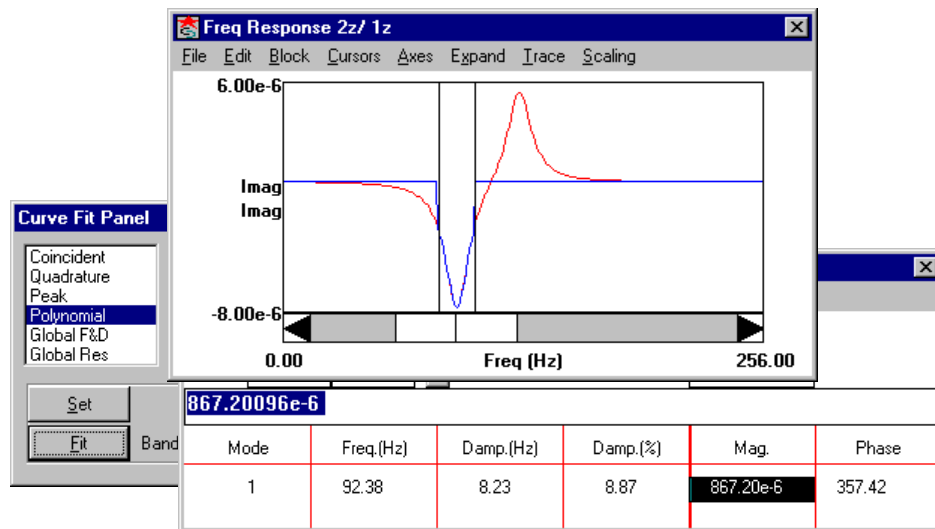
## H11 - Local SDOF Polynomial - Mode 1

Using the SDOF polynomial curvefitter process with the cursor band as shown, the estimated residue is 0.00117 which is very close to the analytical value.



## H21 - Local SDOF Polynomial - Mode 1

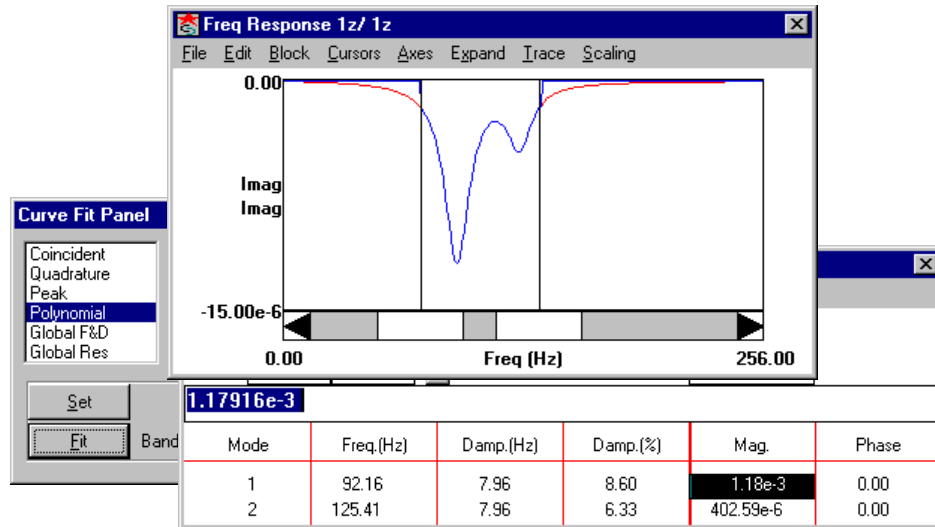
Using the SDOF polynomial curvefitter process with the cursor band as shown, the estimated residue is 0.000867 which is fairly close to the analytical value but shows some error which is likely due to insufficient compensation terms or slight errors in the local pole estimation.





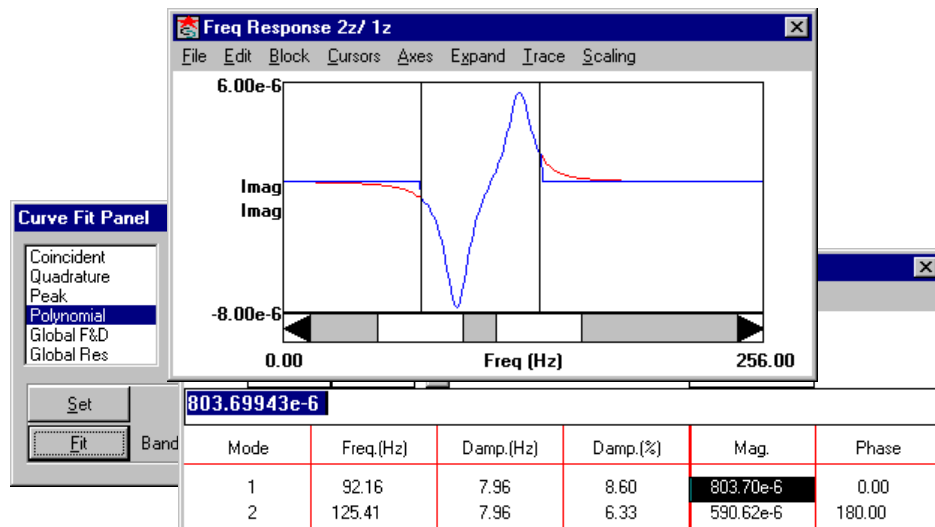
## H11 - Local MDOF Polynomial - Mode 1 & 2

Using the MDOF polynomial curvefitter process with the cursor band as shown, the estimated residue is 0.00118 for mode 1 and 0.000403 for mode 2 which is very close to the analytical value.



## H21 - Local MDOF Polynomial - Mode 1 & 2

Using the MDOF polynomial curvefitter process with the cursor band as shown, the estimated residue is 0.000804 for mode 1 and 0.000591 for mode 2 which is very close to the analytical value.





## H11 & H21 - Global MDOF Polynomial - Mode 1 & 2

Using the MDOF polynomial curvefitter process with the cursor band as shown, the estimated residue from H11 is 0.00118 for mode 1 and 0.000403 for mode 2 and from H21 is 0.000804 for mode 1 and 0.000591 for mode 2 which is very close to the analytical value.

The screenshot displays two overlapping software windows. The top window, titled "Frequency Results: Points", shows a table of modal data for H11. The bottom window, titled "Curve Fit Panel", shows a table of modal data for H21. Both windows include a "Curve Fit Panel" on the left with options like "Coincident", "Quadrature", "Peak", "Polynomial", "Global F&D", and "Global Res".

**Frequency Results: Points (H11)**

Mode	Freq.(Hz)	Damp.(Hz)	Damp.(%)	Mag.	Phase
1	92.16	7.96	8.60	0.00	0.00
2	125.41	7.96	6.33	0.00	0.00

**Curve Fit Panel (H21)**

Mode	Freq.(Hz)	Damp.(Hz)	Damp.(%)	Mag.	Phase
1	92.16	7.96	8.60	1.18e-3	0.00
2	125.41	7.96	6.33	402.58e-6	0.00